

INVESTIGATION OF GEOTHERMAL POWER PLANT PERFORMANCE USING
SEQUESTERED CARBON DIOXIDE AS A HEAT TRANSFER OR WORKING
FLUID

A THESIS
SUBMITTED TO THE FACULTY OF THE GRADUATE SCHOOL
OF THE UNIVERSITY OF MINNESOTA
BY

BRIAN D. JANKE

IN PARTIAL FULFILLMENT OF THE REQUIREMENTS
FOR THE DEGREE OF
MASTER OF SCIENCE

DR. THOMAS H. KUEHN

JULY 2011

© Brian D. Janke, 2011

Abstract

This study investigates the potential for combining carbon dioxide (CO₂) sequestration with geothermal power production in areas with low geothermal resource temperatures. Using sequestered CO₂ as the working fluid or heat transfer fluid, power production of a Direct Single-Loop System and Binary Organic Rankine Cycle (ORC) System were simulated using Engineering Equation Solver (EES) and the ASHRAE reference state for thermophysical properties. The two power plants were simulated under a variety of operating conditions, with the main variables being the reservoir temperature (100°C-150°C), the mass flow rate of the CO₂ (70kg/s, 90kg/s, 120kg/s, 140kg/s), the reservoir depth (2.5km, 3.1km, 3.6km), and the condensing temperature. The condensing temperature was taken as the monthly average ambient wet-bulb temperature for the summer months of April through September and dry-bulb temperature for the remaining months of the year at Minneapolis, Minnesota. Results showed that using CO₂ for geothermal power production is a viable possibility. Power production from the simulations matched or surpassed the power production of currently installed low-temperature water-based geothermal plants. A second-law analysis showed that for the Direct Single-Loop System the largest considerations needed to be put into turbine design, while for the Binary ORC System the CO₂ heat exchanger should receive the most attention. In addition to this, replacing the expansion valve in the Binary ORC System with a supplemental power-generating device, such as a screw or scroll expander, has the potential for additional power production.

Table of Contents

List of Tables	iv
List of Figures.....	xiv
Nomenclature	xix
1. Introduction.....	1
1.1. Motivation for Research.....	1
1.2. Previous Research (Benefits of using CO ₂).....	2
1.3. Research Goals.....	7
2. Power Plant System Design Considerations	8
2.1. Operating Conditions and the Base Case	8
2.2. Direct Single-Loop System Layout.....	10
2.3. Binary Organic Rankine Cycle System Layout	13
2.4. Compression Process Considerations for Sequestration.....	17
3. Simulation Considerations and Results	23
3.1. Simulation Considerations and Assumptions	23
3.2. Direct Single-Loop System Power Production under Various Operating Conditions.....	30
3.3. Binary Organic Rankine Cycle System Power Production under Various Operating Conditions.....	41
3.4. Accounting for System Losses through Exergy Analysis.....	54
4. Discussion and Conclusion	60
4.1. Comparison of Conventional Systems to CO ₂ Systems	60
4.2. Choosing an Ideal System for CO ₂ Geothermal Power Production.....	64
4.3. Next Steps and Additional Considerations for Expanding Research	65

5. References	68
Appendix A: Direct Single-Loop System Simulation Results	74
Appendix B: Direct Single-Loop System Thermodynamic Property Tables	98
Appendix C: Binary ORC System Simulation Results.....	170
Appendix D: Binary ORC System Thermodynamic Property Tables.....	182
Appendix E: Supplemental Diagrams.....	218
Appendix F: EES Codes for System Simulations.....	219

List of Tables

Table 3-1: State Point Properties for the Month of July.....	32
Table 3-2: State Point Properties for the Month of January.....	32
Table3-3: Monthly Average Ambient Temperatures (Winter DB, Summer WB).....	34
Table3-4: Monthly Average Ambient Temperatures (Dry Bulb Year-round).....	34
Table3-5: Direct Single-Loop System Monthly Average Power Production (Winter DB, Summer WB)	34
Table3-6: Direct Single-Loop System Monthly Average Power Production (Dry Bulb Year-round).	34
Table 3-7: Binary ORC System State Point Properties for the CO2 Loop (July).....	46
Table 3-8: Binary ORC System State Point Properties for the CO2 Loop (January).....	46
Table 3-9: Binary ORC System State Point Properties for the isobutane Loop (July).....	46
Table 3-10: Binary ORC System State Point Properties for the isobutane Loop (January).....	47
Table 3-11: Binary ORC System Monthly Average isobutane Boiling Temperatures.....	48
Table 3-12: Binary ORC System Monthly Average Power Production.....	49
Table 3-13: Exergy Destruction of the Direct Single-Loop System Components in July.....	57
Table 3-14: Exergy Destruction of the Direct Single-Loop System Components in January.....	57
Table 3-15: Exergy Destruction of the Binary ORC System Components in July.....	58
Table 3-16: Exergy Destruction of the Binary ORC System Components in January.....	58
TableA-1: Direct Single-Loop System Monthly Average Power Production (DTE=0.85) at 2.5km Depth.....	74
Table A-2: Direct Single-Loop System Monthly Average Power Production (DTE=0.85) at 3.1km Depth.....	75
Table A-3: Direct Single-Loop System Monthly Average Power Production (DTE=0.85) at 3.6km Depth.....	76
TableA-4: Direct Single-Loop System Monthly Average Power Production (DTE=0.50) at 2.5km Depth.....	77
Table A-5: Direct Single-Loop System Monthly Average Power Production (DTE=0.50) at 3.1km Depth.....	78

Table A-6: Direct Single-Loop System Monthly Average Power Production (DTE=0.50) at 3.6km	
Depth.....	79
Table A-7: Direct Single-Loop System Monthly Average System Efficiency (DTE=0.85) at 2.5km	
Depth.....	80
TableA-8: Direct Single-Loop System Monthly Average System Efficiency (DTE=0.85) at 3.1km	
Depth.....	81
Table A-9: Direct Single-Loop System Monthly Average System Efficiency (DTE=0.85) at 3.6km	
Depth.....	82
Table A-10: Direct Single-Loop System Monthly Average System Efficiency (DTE=0.50) at 2.5km	
Depth.....	83
TableA-11: Direct Single-Loop System Monthly Average System Efficiency (DTE=0.50) at 3.1km	
Depth.....	84
Table A-12: Direct Single-Loop System Monthly Average System Efficiency (DTE=0.50) at 3.6km	
Depth.....	85
Table B-1: Thermodynamic Properties for Direct Single-Loop System Simulations at 2.5km Depth, CO2 Mass Flow Rate of 70kg/s, and Reservoir Temperature of 100°C (DTE=0.85).	98
Table B-2: Thermodynamic Properties for Direct Single-Loop System Simulations at 2.5km Depth, CO2 Mass Flow Rate of 90kg/s, and Reservoir Temperature of 100°C (DTE=0.85).	99
Table B-3: Thermodynamic Properties for Direct Single-Loop System Simulations at 2.5km Depth, CO2 Mass Flow Rate of 120kg/s, and Reservoir Temperature of 100°C (DTE=0.85).	100
Table B-4: Thermodynamic Properties for Direct Single-Loop System Simulations at 2.5km Depth, CO2 Mass Flow Rate of 140kg/s, and Reservoir Temperature of 100°C (DTE=0.85).	101
Table B-5: Thermodynamic Properties for Direct Single-Loop System Simulations at 2.5km Depth, CO2 Mass Flow Rate of 70kg/s, and Reservoir Temperature of 125°C (DTE=0.85).	102
Table B-6: Thermodynamic Properties for Direct Single-Loop System Simulations at 2.5km Depth, CO2 Mass Flow Rate of 90kg/s, and Reservoir Temperature of 125°C (DTE=0.85).	103
Table B-7: Thermodynamic Properties for Direct Single-Loop System Simulations at 2.5km Depth, CO2 Mass Flow Rate of 120kg/s, and Reservoir Temperature of 125°C (DTE=0.85).	104

Table B-8: Thermodynamic Properties for Direct Single-Loop System Simulations at 2.5km Depth, CO2 Mass Flow Rate of 140kg/s, and Reservoir Temperature of 125°C (DTE=0.85).	105
Table B-9: Thermodynamic Properties for Direct Single-Loop System Simulations at 2.5km Depth, CO2 Mass Flow Rate of 70kg/s, and Reservoir Temperature of 150°C (DTE=0.85).	106
Table B-10: Thermodynamic Properties for Direct Single-Loop System Simulations at 2.5km Depth, CO2 Mass Flow Rate of 90kg/s, and Reservoir Temperature of 150°C (DTE=0.85).	107
Table B-11: Thermodynamic Properties for Direct Single-Loop System Simulations at 2.5km Depth, CO2 Mass Flow Rate of 120kg/s, and Reservoir Temperature of 150°C (DTE=0.85).	108
Table B-12: Thermodynamic Properties for Direct Single-Loop System Simulations at 2.5km Depth, CO2 Mass Flow Rate of 140kg/s, and Reservoir Temperature of 150°C (DTE=0.85).	109
Table B-13: Thermodynamic Properties for Direct Single-Loop System Simulations at 3.1km Depth, CO2 Mass Flow Rate of 70kg/s, and Reservoir Temperature of 100°C (DTE=0.85).	110
Table B-14: Thermodynamic Properties for Direct Single-Loop System Simulations at 3.1km Depth, CO2 Mass Flow Rate of 90kg/s, and Reservoir Temperature of 100°C (DTE=0.85).	111
Table B-15: Thermodynamic Properties for Direct Single-Loop System Simulations at 3.1km Depth, CO2 Mass Flow Rate of 120kg/s, and Reservoir Temperature of 100°C (DTE=0.85).	112
Table B-16: Thermodynamic Properties for Direct Single-Loop System Simulations at 3.1km Depth, CO2 Mass Flow Rate of 140kg/s, and Reservoir Temperature of 100°C (DTE=0.85).	113
Table B-17: Thermodynamic Properties for Direct Single-Loop System Simulations at 3.1km Depth, CO2 Mass Flow Rate of 70kg/s, and Reservoir Temperature of 125°C (DTE=0.85).	114
Table B-18: Thermodynamic Properties for Direct Single-Loop System Simulations at 3.1km Depth, CO2 Mass Flow Rate of 90kg/s, and Reservoir Temperature of 125°C (DTE=0.85).	115
Table B-19: Thermodynamic Properties for Direct Single-Loop System Simulations at 3.1km Depth, CO2 Mass Flow Rate of 120kg/s, and Reservoir Temperature of 125°C (DTE=0.85).	116
Table B-20: Thermodynamic Properties for Direct Single-Loop System Simulations at 3.1km Depth, CO2 Mass Flow Rate of 140kg/s, and Reservoir Temperature of 125°C (DTE=0.85).	117
Table B-21: Thermodynamic Properties for Direct Single-Loop System Simulations at 3.1km Depth, CO2 Mass Flow Rate of 70kg/s, and Reservoir Temperature of 150°C (DTE=0.85).	118

Table B-22: Thermodynamic Properties for Direct Single-Loop System Simulations at 3.1km Depth, CO2 Mass Flow Rate of 90kg/s, and Reservoir Temperature of 150°C (DTE=0.85).	119
Table B-23: Thermodynamic Properties for Direct Single-Loop System Simulations at 3.1km Depth, CO2 Mass Flow Rate of 120kg/s, and Reservoir Temperature of 150°C (DTE=0.85).	120
Table B-24: Thermodynamic Properties for Direct Single-Loop System Simulations at 3.1km Depth, CO2 Mass Flow Rate of 140kg/s, and Reservoir Temperature of 150°C (DTE=0.85).	121
Table B-25: Thermodynamic Properties for Direct Single-Loop System Simulations at 3.6km Depth, CO2 Mass Flow Rate of 70kg/s, and Reservoir Temperature of 100°C (DTE=0.85).	122
Table B-26: Thermodynamic Properties for Direct Single-Loop System Simulations at 3.6km Depth, CO2 Mass Flow Rate of 90kg/s, and Reservoir Temperature of 100°C (DTE=0.85).	123
Table B-27: Thermodynamic Properties for Direct Single-Loop System Simulations at 3.6km Depth, CO2 Mass Flow Rate of 120kg/s, and Reservoir Temperature of 100°C (DTE=0.85).	124
Table B-28: Thermodynamic Properties for Direct Single-Loop System Simulations at 3.6km Depth, CO2 Mass Flow Rate of 140kg/s, and Reservoir Temperature of 100°C (DTE=0.85).	125
Table B-29: Thermodynamic Properties for Direct Single-Loop System Simulations at 3.6km Depth, CO2 Mass Flow Rate of 70kg/s, and Reservoir Temperature of 125°C (DTE=0.85).	126
Table B-30: Thermodynamic Properties for Direct Single-Loop System Simulations at 3.6km Depth, CO2 Mass Flow Rate of 90kg/s, and Reservoir Temperature of 125°C (DTE=0.85).	127
Table B-31: Thermodynamic Properties for Direct Single-Loop System Simulations at 3.6km Depth, CO2 Mass Flow Rate of 120kg/s, and Reservoir Temperature of 125°C (DTE=0.85).	128
Table B-32: Thermodynamic Properties for Direct Single-Loop System Simulations at 3.6km Depth, CO2 Mass Flow Rate of 140kg/s, and Reservoir Temperature of 125°C (DTE=0.85).	129
Table B-33: Thermodynamic Properties for Direct Single-Loop System Simulations at 3.6km Depth, CO2 Mass Flow Rate of 70kg/s, and Reservoir Temperature of 150°C (DTE=0.85).	130
Table B-34: Thermodynamic Properties for Direct Single-Loop System Simulations at 3.6km Depth, CO2 Mass Flow Rate of 90kg/s, and Reservoir Temperature of 150°C (DTE=0.85).	131
Table B-35: Thermodynamic Properties for Direct Single-Loop System Simulations at 3.6km Depth, CO2 Mass Flow Rate of 120kg/s, and Reservoir Temperature of 150°C (DTE=0.85).	132

Table B-36: Thermodynamic Properties for Direct Single-Loop System Simulations at 3.6km Depth, CO2 Mass Flow Rate of 140kg/s, and Reservoir Temperature of 150°C (DTE=0.85).	133
Table B-37: Thermodynamic Properties for Direct Single-Loop System Simulations at 2.5km Depth, CO2 Mass Flow Rate of 70kg/s, and Reservoir Temperature of 100°C (DTE=0.50).	134
Table B-38: Thermodynamic Properties for Direct Single-Loop System Simulations at 2.5km Depth, CO2 Mass Flow Rate of 90kg/s, and Reservoir Temperature of 100°C (DTE=0.50).	135
Table B-39: Thermodynamic Properties for Direct Single-Loop System Simulations at 2.5km Depth, CO2 Mass Flow Rate of 120kg/s, and Reservoir Temperature of 100°C (DTE=0.50).	136
Table B-40: Thermodynamic Properties for Direct Single-Loop System Simulations at 2.5km Depth, CO2 Mass Flow Rate of 140kg/s, and Reservoir Temperature of 100°C (DTE=0.50).	137
Table B-41: Thermodynamic Properties for Direct Single-Loop System Simulations at 2.5km Depth, CO2 Mass Flow Rate of 70kg/s, and Reservoir Temperature of 125°C (DTE=0.50).	138
Table B-42: Thermodynamic Properties for Direct Single-Loop System Simulations at 2.5km Depth, CO2 Mass Flow Rate of 90kg/s, and Reservoir Temperature of 125°C (DTE=0.50).	139
Table B-43: Thermodynamic Properties for Direct Single-Loop System Simulations at 2.5km Depth, CO2 Mass Flow Rate of 120kg/s, and Reservoir Temperature of 125°C (DTE=0.50).	140
Table B-44: Thermodynamic Properties for Direct Single-Loop System Simulations at 2.5km Depth, CO2 Mass Flow Rate of 140kg/s, and Reservoir Temperature of 125°C (DTE=0.50).	141
Table B-45: Thermodynamic Properties for Direct Single-Loop System Simulations at 2.5km Depth, CO2 Mass Flow Rate of 70kg/s, and Reservoir Temperature of 150°C (DTE=0.50).	142
Table B-46: Thermodynamic Properties for Direct Single-Loop System Simulations at 2.5km Depth, CO2 Mass Flow Rate of 90kg/s, and Reservoir Temperature of 150°C (DTE=0.50).	143
Table B-47: Thermodynamic Properties for Direct Single-Loop System Simulations at 2.5km Depth, CO2 Mass Flow Rate of 120kg/s, and Reservoir Temperature of 150°C (DTE=0.50).	144
Table B-48: Thermodynamic Properties for Direct Single-Loop System Simulations at 2.5km Depth, CO2 Mass Flow Rate of 140kg/s, and Reservoir Temperature of 150°C (DTE=0.50).	145
Table B-49: Thermodynamic Properties for Direct Single-Loop System Simulations at 3.1km Depth, CO2 Mass Flow Rate of 70kg/s, and Reservoir Temperature of 100°C (DTE=0.50).	146

Table B-50: Thermodynamic Properties for Direct Single-Loop System Simulations at 3.1km Depth, CO2 Mass Flow Rate of 90kg/s, and Reservoir Temperature of 100°C (DTE=0.50).	147
Table B-51: Thermodynamic Properties for Direct Single-Loop System Simulations at 3.1km Depth, CO2 Mass Flow Rate of 120kg/s, and Reservoir Temperature of 100°C (DTE=0.50).	148
Table B-52: Thermodynamic Properties for Direct Single-Loop System Simulations at 3.1km Depth, CO2 Mass Flow Rate of 140kg/s, and Reservoir Temperature of 100°C (DTE=0.50).	149
Table B-53: Thermodynamic Properties for Direct Single-Loop System Simulations at 3.1km Depth, CO2 Mass Flow Rate of 70kg/s, and Reservoir Temperature of 125°C (DTE=0.50).	150
Table B-54: Thermodynamic Properties for Direct Single-Loop System Simulations at 3.1km Depth, CO2 Mass Flow Rate of 90kg/s, and Reservoir Temperature of 125°C (DTE=0.50).	151
Table B-55: Thermodynamic Properties for Direct Single-Loop System Simulations at 3.1km Depth, CO2 Mass Flow Rate of 120kg/s, and Reservoir Temperature of 125°C (DTE=0.50).	152
Table B-56: Thermodynamic Properties for Direct Single-Loop System Simulations at 3.1km Depth, CO2 Mass Flow Rate of 140kg/s, and Reservoir Temperature of 125°C (DTE=0.50).	153
Table B-57: Thermodynamic Properties for Direct Single-Loop System Simulations at 3.1km Depth, CO2 Mass Flow Rate of 70kg/s, and Reservoir Temperature of 150°C (DTE=0.50).	154
Table B-58: Thermodynamic Properties for Direct Single-Loop System Simulations at 3.1km Depth, CO2 Mass Flow Rate of 90kg/s, and Reservoir Temperature of 150°C (DTE=0.50).	155
Table B-59: Thermodynamic Properties for Direct Single-Loop System Simulations at 3.1km Depth, CO2 Mass Flow Rate of 120kg/s, and Reservoir Temperature of 150°C (DTE=0.50).	156
Table B-60: Thermodynamic Properties for Direct Single-Loop System Simulations at 3.1km Depth, CO2 Mass Flow Rate of 140kg/s, and Reservoir Temperature of 150°C (DTE=0.50).	157
Table B-61: Thermodynamic Properties for Direct Single-Loop System Simulations at 3.6km Depth, CO2 Mass Flow Rate of 70kg/s, and Reservoir Temperature of 100°C (DTE=0.50).	158
Table B-62: Thermodynamic Properties for Direct Single-Loop System Simulations at 3.6km Depth, CO2 Mass Flow Rate of 90kg/s, and Reservoir Temperature of 100°C (DTE=0.50).	159
Table B-63: Thermodynamic Properties for Direct Single-Loop System Simulations at 3.6km Depth, CO2 Mass Flow Rate of 120kg/s, and Reservoir Temperature of 100°C (DTE=0.50).	160

Table B-64: Thermodynamic Properties for Direct Single-Loop System Simulations at 3.6km Depth, CO2 Mass Flow Rate of 140kg/s, and Reservoir Temperature of 100°C (DTE=0.50).	161
Table B-65: Thermodynamic Properties for Direct Single-Loop System Simulations at 3.6km Depth, CO2 Mass Flow Rate of 70kg/s, and Reservoir Temperature of 125°C (DTE=0.50).	162
Table B-66: Thermodynamic Properties for Direct Single-Loop System Simulations at 3.6km Depth, CO2 Mass Flow Rate of 90kg/s, and Reservoir Temperature of 125°C (DTE=0.50).	163
Table B-67: Thermodynamic Properties for Direct Single-Loop System Simulations at 3.6km Depth, CO2 Mass Flow Rate of 120kg/s, and Reservoir Temperature of 125°C (DTE=0.50).	164
Table B-68: Thermodynamic Properties for Direct Single-Loop System Simulations at 3.6km Depth, CO2 Mass Flow Rate of 140kg/s, and Reservoir Temperature of 125°C (DTE=0.50).	165
Table B-69: Thermodynamic Properties for Direct Single-Loop System Simulations at 3.6km Depth, CO2 Mass Flow Rate of 70kg/s, and Reservoir Temperature of 150°C (DTE=0.50).	166
Table B-70: Thermodynamic Properties for Direct Single-Loop System Simulations at 3.6km Depth, CO2 Mass Flow Rate of 90kg/s, and Reservoir Temperature of 150°C (DTE=0.50).	167
Table B-71: Thermodynamic Properties for Direct Single-Loop System Simulations at 3.6km Depth, CO2 Mass Flow Rate of 120kg/s, and Reservoir Temperature of 150°C (DTE=0.50).	168
Table B-72: Thermodynamic Properties for Direct Single-Loop System Simulations at 3.6km Depth, CO2 Mass Flow Rate of 140kg/s, and Reservoir Temperature of 150°C (DTE=0.50).	169
Table C-1: Binary ORC System Monthly Average Power Production at 2.5km Depth	170
Table C-2: Binary ORC System Monthly Average Power Production at 3.1km Depth	171
Table C-3: Binary ORC System Monthly Average Power Production at 3.6km Depth	172
Table C-4: Binary ORC System Monthly Average System Efficiency at 2.5km Depth	173
Table C-5: Binary ORC System Monthly Average System Efficiency at 3.1km Depth	174
Table C-6: Binary ORC System Monthly Average System Efficiency at 3.6km Depth	175
Table D-1: Thermodynamic properties for Binary ORC System simulations at 2.5km depth with a CO2 mass flow rate of 70kg/s and a reservoir temperature of 100°C.	182
Table D-2: Thermodynamic properties for Binary ORC System simulations at 2.5km depth with a CO2 mass flow rate of 90kg/s and a reservoir temperature of 100°C.	183

Table D-3: Thermodynamic properties for Binary ORC System simulations at 2.5km depth with a CO2 mass flow rate of 120kg/s and a reservoir temperature of 100°C.	184
Table D-4: Thermodynamic properties for Binary ORC System simulations at 2.5km depth with a CO2 mass flow rate of 140kg/s and a reservoir temperature of 100°C.	185
Table D-5: Thermodynamic properties for Binary ORC System simulations at 2.5km depth with a CO2 mass flow rate of 70kg/s and a reservoir temperature of 125°C.	186
Table D-6: Thermodynamic properties for Binary ORC System simulations at 2.5km depth with a CO2 mass flow rate of 90kg/s and a reservoir temperature of 125°C.	187
Table D-7: Thermodynamic properties for Binary ORC System simulations at 2.5km depth with a CO2 mass flow rate of 120kg/s and a reservoir temperature of 125°C.	188
Table D-8: Thermodynamic properties for Binary ORC System simulations at 2.5km depth with a CO2 mass flow rate of 140kg/s and a reservoir temperature of 125°C.	189
Table D-9: Thermodynamic properties for Binary ORC System simulations at 2.5km depth with a CO2 mass flow rate of 70kg/s and a reservoir temperature of 150°C.	190
Table D-10: Thermodynamic properties for Binary ORC System simulations at 2.5km depth with a CO2 mass flow rate of 90kg/s and a reservoir temperature of 150°C.	191
Table D-11: Thermodynamic properties for Binary ORC System simulations at 2.5km depth with a CO2 mass flow rate of 120kg/s and a reservoir temperature of 150°C.	192
Table D-12: Thermodynamic properties for Binary ORC System simulations at 2.5km depth with a CO2 mass flow rate of 140kg/s and a reservoir temperature of 150°C.	193
Table D-13: Thermodynamic properties for Binary ORC System simulations at 3.1km depth with a CO2 mass flow rate of 70kg/s and a reservoir temperature of 100°C.	194
Table D-14: Thermodynamic properties for Binary ORC System simulations at 3.1km depth with a CO2 mass flow rate of 90kg/s and a reservoir temperature of 100°C.	195
Table D-15: Thermodynamic properties for Binary ORC System simulations at 3.1km depth with a CO2 mass flow rate of 120kg/s and a reservoir temperature of 100°C.	196
Table D-16: Thermodynamic properties for Binary ORC System simulations at 3.1km depth with a CO2 mass flow rate of 140kg/s and a reservoir temperature of 100°C.	197

Table D-17: Thermodynamic properties for Binary ORC System simulations at 3.1km depth with a CO2 mass flow rate of 70kg/s and a reservoir temperature of 125°C.	198
Table D-18: Thermodynamic properties for Binary ORC System simulations at 3.1km depth with a CO2 mass flow rate of 90kg/s and a reservoir temperature of 125°C.	199
Table D-19: Thermodynamic properties for Binary ORC System simulations at 3.1km depth with a CO2 mass flow rate of 120kg/s and a reservoir temperature of 125°C.	200
Table D-20: Thermodynamic properties for Binary ORC System simulations at 3.1km depth with a CO2 mass flow rate of 140kg/s and a reservoir temperature of 125°C.	201
Table D-21: Thermodynamic properties for Binary ORC System simulations at 3.1km depth with a CO2 mass flow rate of 70kg/s and a reservoir temperature of 150°C.	202
Table D-22: Thermodynamic properties for Binary ORC System simulations at 3.1km depth with a CO2 mass flow rate of 90kg/s and a reservoir temperature of 150°C.	203
Table D-23: Thermodynamic properties for Binary ORC System simulations at 3.1km depth with a CO2 mass flow rate of 120kg/s and a reservoir temperature of 150°C.	204
Table D-24: Thermodynamic properties for Binary ORC System simulations at 3.1km depth with a CO2 mass flow rate of 140kg/s and a reservoir temperature of 150°C.	205
Table D-25: Thermodynamic properties for Binary ORC System simulations at 3.6km depth with a CO2 mass flow rate of 70kg/s and a reservoir temperature of 100°C.	206
Table D-26: Thermodynamic properties for Binary ORC System simulations at 3.6km depth with a CO2 mass flow rate of 90kg/s and a reservoir temperature of 100°C.	207
Table D-27: Thermodynamic properties for Binary ORC System simulations at 3.6km depth with a CO2 mass flow rate of 120kg/s and a reservoir temperature of 100°C.	208
Table D-28: Thermodynamic properties for Binary ORC System simulations at 3.6km depth with a CO2 mass flow rate of 140kg/s and a reservoir temperature of 100°C.	209
Table D-29: Thermodynamic properties for Binary ORC System simulations at 3.6km depth with a CO2 mass flow rate of 70kg/s and a reservoir temperature of 125°C.	210
Table D-30: Thermodynamic properties for Binary ORC System simulations at 3.6km depth with a CO2 mass flow rate of 90kg/s and a reservoir temperature of 125°C.	211

Table D-31: Thermodynamic properties for Binary ORC System simulations at 3.6km depth with a CO2 mass flow rate of 120kg/s and a reservoir temperature of 125°C.	212
Table D-32: Thermodynamic properties for Binary ORC System simulations at 3.6km depth with a CO2 mass flow rate of 140kg/s and a reservoir temperature of 125°C.	213
Table D-33: Thermodynamic properties for Binary ORC System simulations at 3.6km depth with a CO2 mass flow rate of 70kg/s and a reservoir temperature of 150°C.	214
Table D-34: Thermodynamic properties for Binary ORC System simulations at 3.6km depth with a CO2 mass flow rate of 90kg/s and a reservoir temperature of 150°C.	215
Table D-35: Thermodynamic properties for Binary ORC System simulations at 3.6km depth with a CO2 mass flow rate of 120kg/s and a reservoir temperature of 150°C.	216
Table D-36: Thermodynamic properties for Binary ORC System simulations at 3.6km depth with a CO2 mass flow rate of 140kg/s and a reservoir temperature of 150°C.	217

List of Figures

Figure 1-1: Lines of constant mobility (ρ/μ) for CO ₂ in units of 10^6 s/m ² [3]	3
Figure 1-2: Lines of constant mobility (ρ/μ) for water in units of 10^6 s/m ² [3].....	4
Figure 1-3: Heat extraction rate of CO ₂ and water (blue) in MW vs. time for $T_{res}=200^\circ\text{C}$ at various pressures. [4]	5
Figure 1-4: Geothermal heat flow map of the United States in mW/m ² from 25 (blue) to 150 (red) [10]	7
Figure 2-1: Direct Single-Loop Power Plant Layout.....	11
Figure 2-2: Binary Organic Rankine Cycle Power Plant Layout	15
Figure 2-3: Isentropic Compression Process for Pre-treating CO ₂ prior to injection	18
Figure 2-4: Isentropic Compression Cycle with Intercooling for Pre-treating CO ₂ prior to injection	19
Figure 2-5: Isentropic Compression Cycle with Precooling for Pre-treating CO ₂ prior to injection .	21
Figure 2-6: T-s diagram of the four different compression cycles under winter operating conditions.	22
Figure 3-1: Diagram of a segment of the return line piping system showing thermal loss considerations.....	28
Figure 3-2: Direct Single-Loop System Layout w/ State Points	31
Figure 3-3: T-s Diagram for Base Case Simulation of the Direct Single-Loop System	33
Figure 3-4: Direct Single-Loop System Monthly Average Power Production for a Single Well	35
Figure 3-5: Direct Single-Loop Monthly Average System Efficiency.....	35
Figure 3-6: Direct Single-Loop System Power Production for a Single Well with Varying Mass Flow Rate	37
Figure 3-7: Direct Single-Loop System Power Production for a Single Well with Varying Reservoir Temperature.....	38
Figure3-8: Direct System Monthly Average Power Production for a Single Well Under Base Case Operating Conditions at Various Reservoir Depths.	39

Figure 3-9: Direct Single-Loop System Monthly Average Power Production for a Single Well with Mass Flow Rate 70kg/s with Varying Reservoir Temperatures and Depths.	40
Figure 3-10: Binary ORC System Layout w/ State Points	45
Figure 3-11: T-s Diagram for the Binary ORC System operating under Base Case conditions for the month of January. *State Points 1/1's/6s/9s. **State Points 1/1'w/6w/9w.	47
Figure 3-12: Base Case Binary ORC System Monthly Average Power Production for a Single Well.	49
Figure 3-13: Base Case Binary ORC System Monthly Average System Efficiency.	50
Figure 3-14: Binary ORC System Power Production for a Single Well with Varying Mass Flow Rate	51
Figure 3-15: Overlay Plot of Direct and Binary System Power Production for a Single Well with Varying Mass Flow Rates	52
Figure 3-16: Binary ORC System Power Production for a Single Well with Varying Reservoir Temperature.	53
Figure 3-17: Overlay Plot of the Direct and Binary System Power Production for a Single Well with Varying Reservoir Temperature.	53
Figure A-1: Direct Single-Loop System monthly average power production simulation results at 2.5km depth with CO2 mass flow rate of 70kg/s and DTE=0.85 for various reservoir temperatures.	86
Figure A-2: Direct Single-Loop System monthly average power production simulation results at 2.5km depth with CO2 mass flow rate of 90kg/s and DTE=0.85 for various reservoir temperatures.	86
Figure A-3: Direct Single-Loop System monthly average power production simulation results at 2.5km depth with CO2 mass flow rate of 120kg/s and DTE=0.85 for various reservoir temperatures.	87
Figure A-4: Direct Single-Loop System monthly average power production simulation results at 2.5km depth with CO2 mass flow rate of 140kg/s and DTE=0.85 for various reservoir temperatures.	87
Figure A-5: Direct Single-Loop System monthly average power production simulation results at 3.1km depth with CO2 mass flow rate of 70kg/s and DTE=0.85 for various reservoir temperatures.	88

Figure A-6: Direct Single-Loop System monthly average power production simulation results at 3.1km depth with CO2 mass flow rate of 90kg/s and DTE=0.85 for various reservoir temperatures. 88

Figure A-7: Direct Single-Loop System monthly average power production simulation results at 3.1km depth with CO2 mass flow rate of 120kg/s and DTE=0.85 for various reservoir temperatures. 89

Figure A-8: Direct Single-Loop System monthly average power production simulation results at 3.1km depth with CO2 mass flow rate of 140kg/s and DTE=0.85 for various reservoir temperatures. 89

Figure A-9: Direct Single-Loop System monthly average power production simulation results at 3.6km depth with CO2 mass flow rate of 70kg/s and DTE=0.85 for various reservoir temperatures. 90

Figure A-10: Direct Single-Loop System monthly average power production simulation results at 3.6km depth with CO2 mass flow rate of 90kg/s and DTE=0.85 for various reservoir temperatures. 90

Figure A-11: Direct Single-Loop System monthly average power production simulation results at 3.6km depth with CO2 mass flow rate of 120kg/s and DTE=0.85 for various reservoir temperatures. 91

Figure A-12: Direct Single-Loop System monthly average power production simulation results at 3.6km depth with CO2 mass flow rate of 140kg/s and DTE=0.85 for various reservoir temperatures. 91

Figure A-13: Direct Single-Loop System monthly average power production simulation results at 2.5km depth with CO2 mass flow rate of 70kg/s and DTE=0.50 for various reservoir temperatures. 92

Figure A-14: Direct Single-Loop System monthly average power production simulation results at 2.5km depth with CO2 mass flow rate of 90kg/s and DTE=0.50 for various reservoir temperatures. 92

Figure A-15: Direct Single-Loop System monthly average power production simulation results at 2.5km depth with CO2 mass flow rate of 120kg/s and DTE=0.50 for various reservoir temperatures. 93

Figure A-16: Direct Single-Loop System monthly average power production simulation results at 2.5km depth with CO2 mass flow rate of 140kg/s and DTE=0.50 for various reservoir temperatures. 93

Figure A-17: Direct Single-Loop System monthly average power production simulation results at 3.1km depth with CO2 mass flow rate of 70kg/s and DTE=0.50 for various reservoir temperatures.	94
Figure A-18: Direct Single-Loop System monthly average power production simulation results at 3.1km depth with CO2 mass flow rate of 90kg/s and DTE=0.50 for various reservoir temperatures.	94
Figure A-19: Direct Single-Loop System monthly average power production simulation results at 3.1km depth with CO2 mass flow rate of 120kg/s and DTE=0.50 for various reservoir temperatures.	95
Figure A-20: Direct Single-Loop System monthly average power production simulation results at 3.1km depth with CO2 mass flow rate of 140kg/s and DTE=0.50 for various reservoir temperatures.	95
Figure A-21: Direct Single-Loop System monthly average power production simulation results at 3.6km depth with CO2 mass flow rate of 70kg/s and DTE=0.50 for various reservoir temperatures.	96
Figure A-22: Direct Single-Loop System monthly average power production simulation results at 3.6km depth with CO2 mass flow rate of 90kg/s and DTE=0.50 for various reservoir temperatures.	96
Figure A-23: Direct Single-Loop System monthly average power production simulation results at 3.6km depth with CO2 mass flow rate of 120kg/s and DTE=0.50 for various reservoir temperatures.	97
Figure A-24: Direct Single-Loop System monthly average power production simulation results at 3.6km depth with CO2 mass flow rate of 140kg/s and DTE=0.50 for various reservoir temperatures.	97
Figure C-1: Binary ORC System monthly average power production simulation results at 2.5km depth with a CO2 mass flow rate of 70kg/s for various reservoir temperatures.	176
Figure C-2: Binary ORC System monthly average power production simulation results at 2.5km depth with a CO2 mass flow rate of 90kg/s for various reservoir temperatures.	176
Figure C-3: Binary ORC System monthly average power production simulation results at 2.5km depth with a CO2 mass flow rate of 120kg/s for various reservoir temperatures.	177
Figure C-4: Binary ORC System monthly average power production simulation results at 2.5km depth with a CO2 mass flow rate of 140kg/s for various reservoir temperatures.	177

Figure C-5: Binary ORC System monthly average power production simulation results at 3.1km depth with a CO2 mass flow rate of 70kg/s for various reservoir temperatures.....	178
Figure C-6: Binary ORC System monthly average power production simulation results at 3.1km depth with a CO2 mass flow rate of 90kg/s for various reservoir temperatures.....	178
Figure C-7: Binary ORC System monthly average power production simulation results at 3.1km depth with a CO2 mass flow rate of 120kg/s for various reservoir temperatures.....	179
Figure C-8: Binary ORC System monthly average power production simulation results at 3.1km depth with a CO2 mass flow rate of 140kg/s for various reservoir temperatures.....	179
Figure C-9: Binary ORC System monthly average power production simulation results at 3.6km depth with a CO2 mass flow rate of 70kg/s for various reservoir temperatures.....	180
Figure C-10: Binary ORC System monthly average power production simulation results at 3.6km depth with a CO2 mass flow rate of 90kg/s for various reservoir temperatures.....	180
Figure C-11: Binary ORC System monthly average power production simulation results at 3.6km depth with a CO2 mass flow rate of 120kg/s for various reservoir temperatures.....	181
Figure C-12: Binary ORC System monthly average power production simulation results at 3.6km depth with a CO2 mass flow rate of 140kg/s for various reservoir temperatures.....	181
Figure E-1: Moody Diagram [27] relating friction factor to Reynolds number for various ratios of pipe roughness coefficient to pipe diameter.....	218

Nomenclature

C = heat capacity rate

CCS = carbon capture and sequestration

c_p = specific heat

Comp. = compressor

D = pipe diameter

DB = dry bulb

DTE = direct system turbine efficiency

e = emissivity

e_f = exergy flow rate

\dot{E}_d = exergy destruction rate

EES = Engineering Equation Solver

EGS = enhanced geothermal system

f = friction factor

g = gravitational constant

Gr = Grashof number

h = convective heat transfer coefficient

h_l = headloss

h_o = dead state enthalpy

H = enthalpy

HX = heat exchanger

k = thermal conductivity

L = pipe segment length

\dot{m} = mass flow rate

NREL = National Renewable Energy Laboratory

NTU = number of transfer units

Nu = Nusselt number

ORC = Organic Rankine Cycle

p = pressure

Pr = Prandtl number

\dot{Q} = heat transfer rate

r = radius

Ra = Rayleigh number

Re = Reynolds number

s = entropy

s_o = dead state entropy

T = temperature

T_o = dead state temperature

v = mean velocity

V = velocity

\dot{W} = work rate

WB = wet bulb

Z = vertical elevation

greek variables

β = volumetric thermal expansion coefficient

ϵ = heat exchanger/condenser effectiveness

μ = dynamic viscosity

ν = kinematic viscosity

ρ = density

σ = Stefan-Boltzmann constant

subscripts

∞ = ambient value

CO₂ = carbon dioxide

c = cold fluid

conv = convection

D = diametric

e = exit

h = hot fluid

i = inlet

ins = insulation

iso = Isobutane

min = minimum

o = outlet

rad = radiation

res = reservoir

s = surface

t = turbine

1. Introduction

1.1. Motivation for Research

The development of alternative and renewable energy production in the United States continues to advance for a variety of reasons. Some push for advancements due to concerns about global climate change while others simply desire energy production that is independent of foreign influence and control. Regardless of the reasons, the continued growth of alternative energy production is a global trend that shows no signs of stopping. If the United States wishes to hold a stake in this developing market, it must continue to promote research that will improve the efficiency of older systems as well as increase the scope of developing new technologies. The combination of carbon sequestration and geothermal energy production has the potential to accomplish both of these objectives.

The United States has one of the largest surpluses of coal in the world, [1] accounting for a little over a quarter of the world's available coal. This fact, coupled with concerns about the impact of carbon emissions on the global climate, have increased demand for the development of clean coal technologies. This involves the separation of carbon dioxide from the exhaust gases of coal power plants to be injected and stored in large underground reservoirs and is also known as carbon capture and sequestration (CCS).

What this research proposes is that the geologically sequestered and geothermally heated CO₂ can then be used for electricity generation. Depending on the size and location of the reservoir and subsurface temperatures, the use of CO₂ for power production can be used to improve coal power plant efficiency by reducing the amount of coal necessary to

meet power production demands, to increase the scope of current geothermal power by allowing power production in regions where current geothermal power plants would be unable to perform, or to provide power for CO₂ injection. Though these developments may seem ambitious, extensive research on the thermophysical properties and fluid-dynamical behavior of CO₂ has been conducted prior to this study, including work on the feasibility of CO₂-based geothermal power plant implementations, as discussed in the next section.

1.2. Previous Research (Benefits of using CO₂)

The Los Alamos National Laboratory performed an initial study in 2000 [2] to specifically investigate and compare the thermophysical properties of both supercritical CO₂ and water under ideal reservoir conditions for geothermal power production. What the study found was that certain physical characteristics of CO₂ would not only allow for its use in geothermal power production, but would also allow for potential improvements over a traditional system. The larger density differential between the cold, injected CO₂ and the geothermally heated CO₂ produced, in comparison to water, results in a more pronounced thermosyphon that could greatly reduce the pumping power requirements necessary to circulate the heat transfer fluid through the reservoir [2]. In addition to this, the significantly lower viscosity of CO₂, compared to water, allows for greater fluid mobility (ρ/μ) in a system that uses CO₂ as the subsurface heat transfer or working fluid. This increased mobility of CO₂ allows for greater mass flow rates through a reservoir of given permeability, potentially increasing the heat extraction rate. A study done at Lawrence Berkeley National Laboratory [3] confirmed these results and expanded upon

them by investigating the mobility of CO₂ and water under a wide range of temperatures and pressures. The trends that arose from these investigations had large implications for the effects of reservoir conditions on the rate of heat extraction by CO₂ and water. It was found that the mobility of CO₂ was largely dependent on both temperature and pressure, whereas the mobility of water was primarily dependent on temperature and largely independent of pressure [3]. The trends can be seen in Figures 1-1 and 1-2 below.

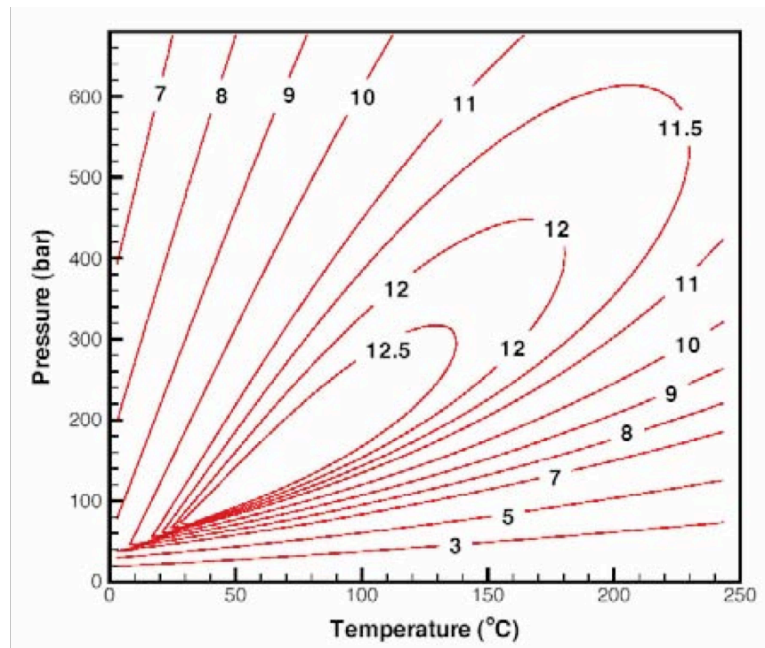


Figure 1-1: Lines of constant mobility (ρ/μ) for CO₂ in units of 10^6 s/m^2 [3]

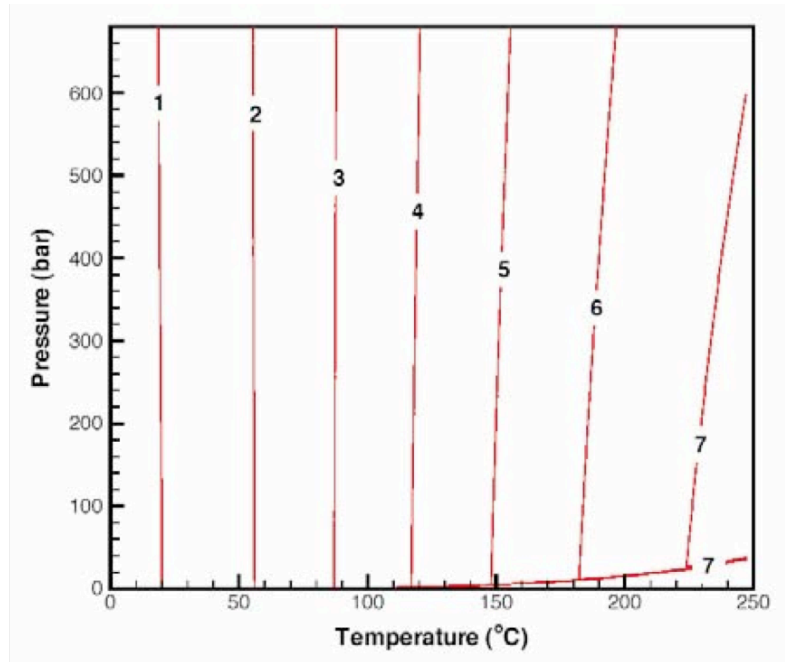


Figure 1-2: Lines of constant mobility (ρ/μ) for water in units of 10^6 s/m^2 [3]

A subsequent study [4] then investigated the actual heat extraction rates of CO₂ and water under a variety of reservoir conditions. Given the independence of the mobility of water with respect to pressure, a reservoir temperature (T_{res}) was set and the pressure varied to find the conditions necessary for a CO₂ system to surpass water in heat extraction. The results are shown in the figure below.

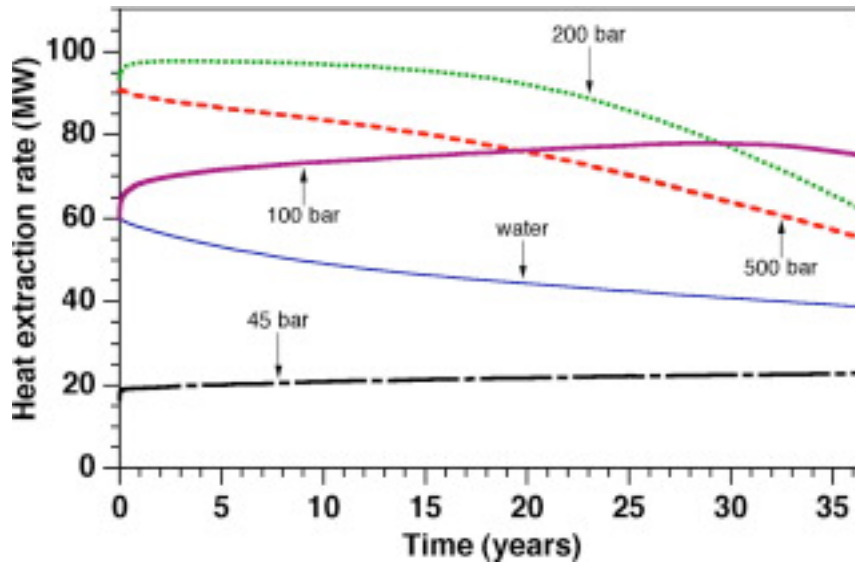


Figure 1-3: Heat extraction rate of CO₂ and water (blue) in MW vs. time for $T_{res}=200^{\circ}\text{C}$ at various pressures. [4]

The implications of the above studies on the potential for expanding the scope of geothermal power production are strong. The flexibility of CO₂ with respect to reservoir parameters, and their effects on mobility and heat extraction rate, is enough to indicate that it could be used under conditions where water would be unsuitable for heat extraction.

Even in areas where geothermal power production is currently being implemented, water use is coming under increased scrutiny. Current geothermal systems require large quantities of water for both operation and installation. During installation, water is injected into deep-ground reservoirs where it is flashed from a liquid to a gas. This phase change causes rapid expansion of the fluid, which fractures the reservoir rock, increasing reservoir volume. This process is known as hydrofracturing and the resultant geothermal system is commonly referred to as an enhanced geothermal system (EGS). In addition to the water needed for this process, large quantities of water are pumped through the

system for heat extraction and partially lost to the subsurface formations. Considering that most geothermal power systems in the United States are installed in dry arid regions where water resources are already strained and water conservation is becoming an increasingly high priority, the amount of water consumed by these systems is a very large drawback. In addition, numerous studies [5-9] have been completed investigating the tendency of injected fluids involved in deep-ground drilling and hydrofracturing to induce seismicity. For example, an incident involving an EGS project in Basel, Switzerland, caused an earthquake of magnitude 3.4 during drilling operations. However, using CO₂ as the geothermal fluid in naturally permeable and porous formations that do not require hydrofracturing has the potential to mitigate all of these drawbacks. The dependence of CO₂ on both temperature and pressure would allow for its use in much shallower depths, where larger naturally occurring reservoirs are available; reducing the necessity for hydrofracturing and greatly reducing induced seismicity. Water consumption could also be drastically reduced simply by replacing water with CO₂ as the geothermal fluid and any CO₂ “lost” to subsurface formations would constitute a form of geologic CO₂ sequestration – a process that is desired, in contrast to subsurface loss of water. Taking these considerations into account, not only could CO₂ potentially expand the areas available for geothermal power production, but it could also prove to be the ideal geothermal working fluid for use in current geothermal systems.

1.3. Research Goals

While considerable research has been performed to investigate the potential of CO₂ as a subsurface working fluid for geothermal applications, very little has been done to expand this work to investigate the mechanical power plant system at the surface and its potential for commercial implementation. This is the focus of the present study. Currently, the vast majority of geothermal electricity production within the United States is found in the tectonically and/or volcanically active western states.

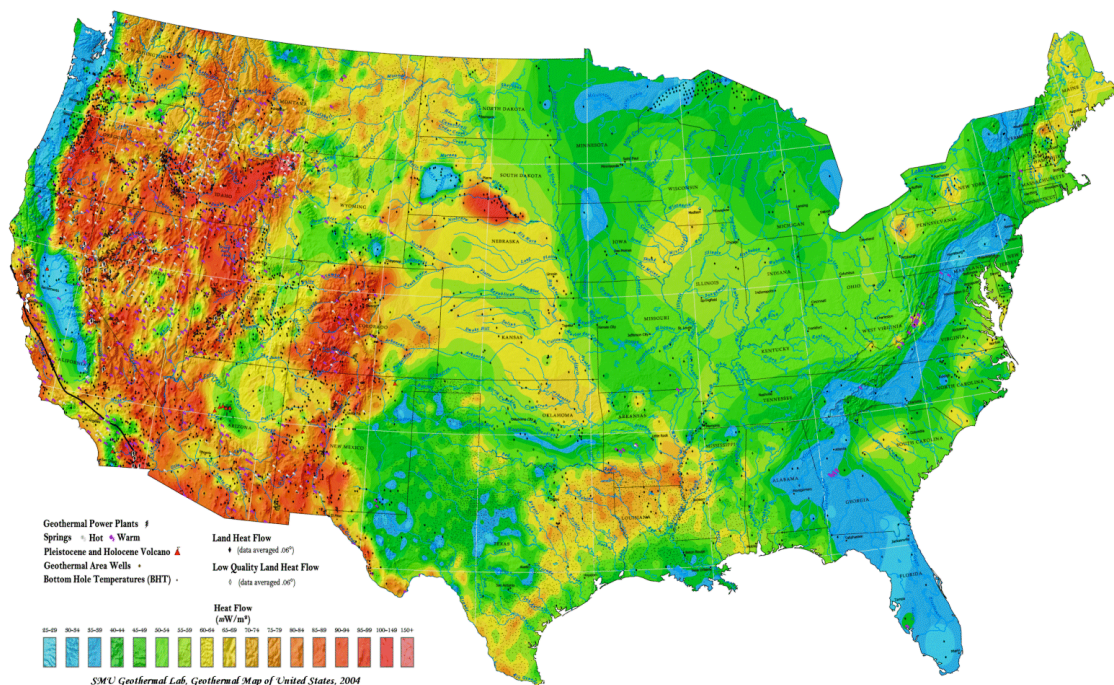


Figure 1-4: Geothermal heat flow map of the United States in mW/m^2 from 25 (blue) to 150 (red) [10]
Figure 1-4 illustrates why the majority of geothermal activities are being conducted in the western regions, as this is where relatively high subsurface temperatures and heat flow rates are reached at relatively shallow depths. Based on the conclusions reached by the above studies and current geothermal applications, this research investigates the potential to expand the scope of geothermal power production to include areas under operating conditions and reservoir parameters more typical of the Midwest (the green to yellow

regions in Figure 1-4). To fully investigate the potential for geothermal power production in these regions, a variety of operating conditions and design constraints were taken into account. This led to the design and simulation of two different geothermal systems; a Direct Single-Loop (DSL) system, where CO₂ is used as both the subsurface and the surface (i.e., power plant) working fluid, and a Binary Organic Rankine Cycle (ORC) system, where CO₂ is used as a heat transfer fluid to transfer the mined heat from the geothermal reservoir to a secondary working fluid through a heat exchanger. Both systems have their advantages and disadvantages, and both could be viewed as the superior system depending largely on the necessity of each for custom components, the costs associated with such components, and the potential power production. In the following chapter, the advantages and disadvantages of these two systems are investigated in further detail, taking into consideration design constraints and potential problems that could arise depending on operating conditions.

2. Power Plant System Design Considerations

2.1. Operating Conditions and the Base Case

As stated in the introduction, this research aims to investigate the potential for geothermal power production with CO₂ as the subsurface working fluid. An integral part of this analysis is the design of the power plant system and optimization of operating considerations. The two system layouts considered were a Direct Single-Loop (DSL) system and a Binary ORC system. The layouts for the geothermal portion of these two systems are largely identical, with the Binary ORC system using a heat exchanger and

expansion valve instead of a turbine in the geothermal loop. This means that the ideal operating conditions for the geothermal loops of both systems can be treated as identical. In the case of the Binary ORC, additional considerations surrounding the heat exchanger and the secondary working fluid must be taken into account in order to maximize heat extraction from the reservoir and will be discussed later in this chapter.

A base case scenario for the system operating conditions was established with the goal of investigating power production under non-ideal (i.e., low temperature) conditions for a traditional geothermal system in order to investigate the potential for using CO₂ as the geothermal working fluid to expand the scope of geothermal energy production to regions with relatively low subsurface temperatures and heat flow rates (green and yellow regions in Figure 4-1). The reservoir conditions for the base case scenario were taken from nationally averaged values from geologic CO₂ sequestration sites [11]. The reservoir depth was taken to be 2.5km, roughly half the depth of a typical EGS. The reservoir temperature and pressure were, respectively, 100°C and 25MPa and the mass flow rate of the CO₂ through the geothermal loop was taken to be 70kg/s. Under these reservoir conditions the CO₂ exits the production well and travels along the supply line as a supercritical gas before running through the turbine, in the case of the Direct Single-Loop system, or heat exchanger, in the case of the Binary ORC system. In order to maximize the density differential between the production and injection wells (to maximize the thermosyphon effect), it was assumed that the CO₂ was condensed to a saturated liquid state near ambient temperature before traveling along the return line and being injected into the reservoir. The ambient temperatures used were taken from the monthly averaged

temperatures for Minneapolis, MN [12]. Dry bulb (DB) temperatures were used for the months of October through March to simulate use of a dry cooling tower for winter operation and wet bulb (WB) temperatures were used for the months of April through September to simulate the use of a wet cooling tower for summer operation. The heat transfer fluid used for the cooling tower loops was a 40% water-ethylene glycol mixture. This mixture was chosen in order to ensure that no freezing would occur under the extreme cold temperatures experienced by the regions for which the power simulations were conducted (particularly in the upper Midwest).

2.2. Direct Single-Loop System Layout

The surface layout of the system assumes dimensions typical of a 5-spot arrangement used in many geothermal fields. This consists of four exterior production wells at the corners of a square area and one central injection well. In the case of this system, a subsurface system footprint area of 4km^2 is assumed. This study investigates one segment of this arrangement, simulating the performance of a single production well, where the distance between the production and injection wells is approximately 710m. The system was modeled using schedule 40 steel piping, with an injection pipe diameter of 0.254m and a production well diameter of 0.20m. This surface layout is used for both the Direct Single-Loop System and Binary ORC System.

The design and layout of the Direct Single-Loop system is fairly simple and is a design currently used by many traditional geothermal power plants. As stated above, CO₂ is injected as a saturated liquid at ambient temperature. The CO₂ is then heated to a

supercritical state inside of the reservoir before entering the production well. Upon exiting the production well, the supercritical CO₂ is run through a turbine. Depending on the temperature and pressure of the CO₂ exiting the production well, in addition to the turbine performance, the CO₂ exits the turbine as a mixture of saturated liquid and vapor. It is then run through a condenser where it is condensed to a saturated liquid before being re-injected into the reservoir. A layout of the system can be seen in Figure 2-1.

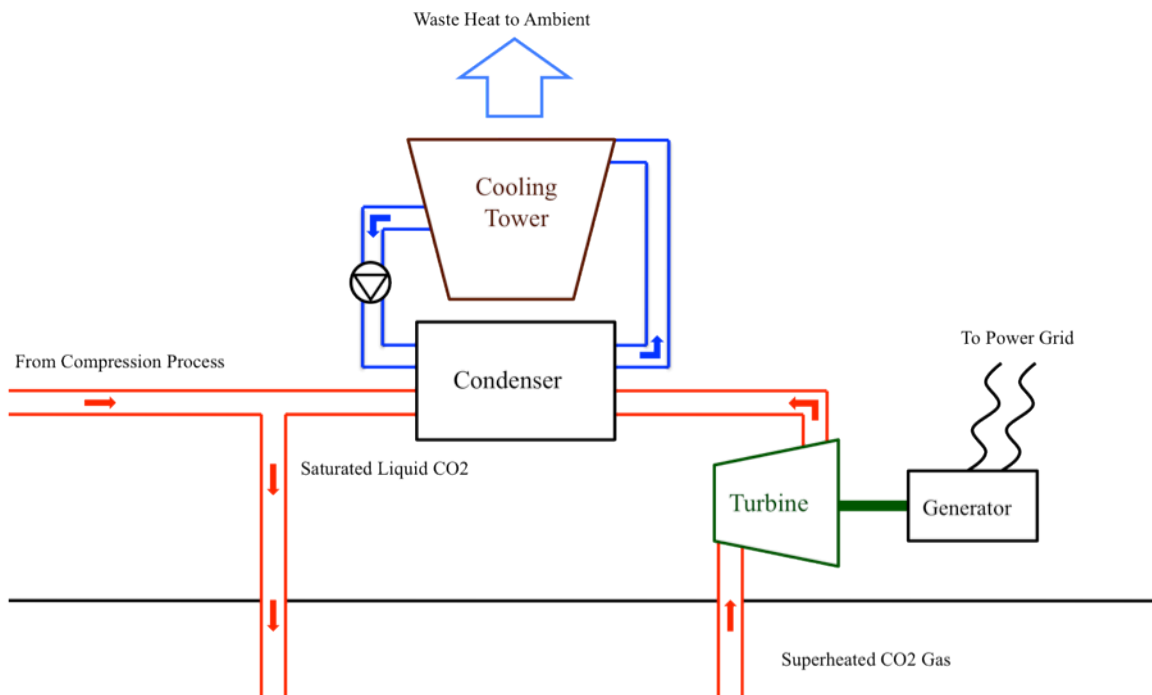


Figure 2-1: Direct Single-Loop Power Plant Layout

The main difference between this system layout and those of a traditional geothermal system is the lack of necessity for an injection pump, except for possibly having to initiate the thermosyphon circulation. Also note that if the system is coupled to a CO₂ sequestration site, much larger amounts of CO₂ are being injected into the subsurface formation than those that circulate through the power-generation cycle. In such cases, all of the injected CO₂ is geologically sequestered once the power production cycle has been initially filled with CO₂. The thermosyphon effect would not then be expected to be able

to draw down all the extra CO₂ but only the portion used in the pump-free circulation of the subsurface power cycle itself, so that pumps may be needed to inject the CO₂ for permanent geologic sequestration. However, the geothermal electricity produced could help provide the power necessary for continuous CO₂ sequestration, thereby facilitating economic implementation of CCS.

The above assumed design considerations, which maximize the change in density between the two wells, account for the variation in system design. This design reduces the parasitic power losses considerably and its functionality is verified in the results section. The simplicity of the Direct Single-Loop system design provides a large portion of its benefits. With fewer components, there are fewer places for the system to lose potential energy production. By running the supercritical CO₂ directly through the turbine, prior to any additional heat transfer processes, this system design allows for maximum energy production.

The Direct Single-Loop system is not without its drawbacks however. As stated above, the supercritical CO₂ entering the turbine changes to a mixture of saturated liquid and vapor inside of the turbine. The effect that this phase change has on the turbine performance is not inconsequential. Thorough investigation of the effects of this phase change on turbine performance has been done for many years. Several of these studies [13-15] have conducted extensive research on the negative impacts on turbine efficiency and turbine blade erosion-corrosion effects due to two-phase flow. The efficiency of the turbine can drop considerably depending on how much of the CO₂ in the turbine is in this

mixture region and how long it is in the turbine. Two-phase flow through a turbine can increase the deterioration rate of turbine blades in the transition zone, due to high-speed droplet deposition, and put a considerable strain on the life cycle of the system, increasing maintenance costs over the duration of power plant operation. It is also uncertain what the composition of the fluid exiting the reservoir could be, and depending on the water present in the CO₂, carbonic acid formation could occur further increasing corrosiveness. A study in 2002 [16] was conducted to investigate potential water-CO₂ mixtures in reservoirs under certain conditions. Based on the results, the issue associated with carbonic acid formation would be more likely at higher reservoir temperatures.

The complications surrounding the use of CO₂ as a working fluid in the Direct Single-Loop system can be seen. Custom components capable of handling CO₂ under the expected temperatures and pressures need to be designed with these considerations in mind. A custom-built turbine capable of handling the high absolute pressure of the CO₂ and the large pressure drops while operating under two-phase flow could have significant impacts on the efficiency of the turbine and could greatly reduce the potential power production. Such considerations need to be taken into account when choosing the operating conditions of the simulations in order to determine an appropriate range of potential power production.

2.3. Binary Organic Rankine Cycle System Layout

The geothermal portion of the design and layout of the Binary ORC system is similar to the Direct Single-Loop system. The main difference is that the turbine is replaced by a

heat exchanger and a throttling valve, where the heat exchanger is used to transfer heat to the power cycle of the Binary ORC system and the throttling valve is used to drop the pressure of the CO₂ exiting the heat exchanger back down to the saturation pressure near ambient temperature. As stated in the previous chapter, the ability of CO₂ to obtain higher density differentials between the injection and production wells has the potential to reduce, or even eliminate, pumping power requirements for the geothermal loop (excluding pumping power requirements for permanent CO₂ sequestration). A throttling process is used in order to maximize the density differential between the injection and production wells, thus ensuring that the change in density is large enough to drive the flow of the CO₂ through the geothermal loop regardless of the time of year, thus eliminating pumping power requirements all together. Other than these changes, the geothermal loop of the Binary ORC system operates in exactly the same way as the Direct Single-Loop system. The layout of the Binary ORC system can be seen in Figure 2-2.

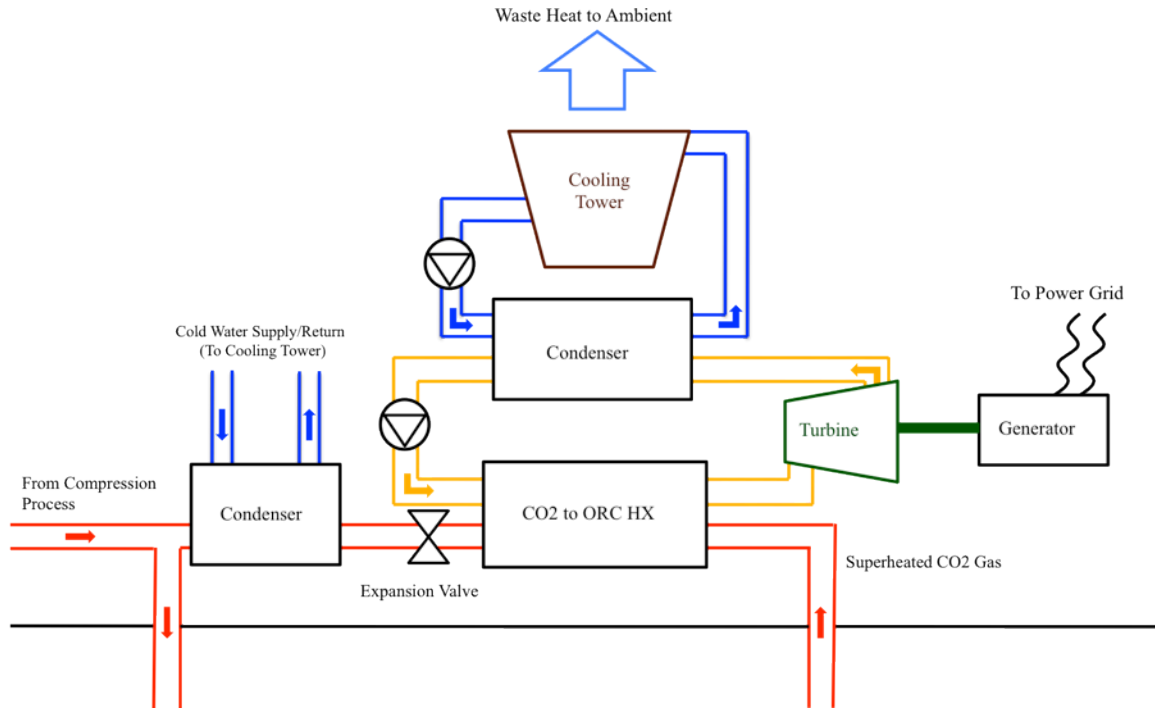


Figure 2-2: Binary Organic Rankine Cycle Power Plant Layout

The design considerations for this system are numerous in comparison to those of the direct system. This is largely due to the optimization of the power cycle, which revolves heavily around design considerations for the heat exchanger as well as choosing an appropriate secondary working fluid. Several studies [17-22] have been conducted investigating design optimization and system performance of geothermal ORC power plants and other binary geothermal systems. Several of these studies investigated the performance of different secondary working fluids in extensive detail. The working fluids were investigated not only based on their potential for heat extraction and power production, but also on the heat exchanger surface area necessary to attain these heat extraction and power production rates. While these studies give valuable insight into both economic and functional design considerations for the heat exchanger, they were done under reservoir and operating conditions typical of standard, water-based subsurface

geothermal systems. For this reason, some of the secondary working fluids may not be ideal for use in the CO₂-based geothermal system envisioned here. A critical part of the motivation to use a Binary ORC system is to avoid the complications involving the custom turbine design necessary in a Direct Single-Loop system. However, one of the better performing fluids found in the previous research, in terms of the ratio of power production to heat exchanger area, was isobutane. Due to the irregular thermophysical behavior of isobutane, it is capable of operating under lower temperatures without undergoing a phase transition inside the turbine, and for this reason appears to be an ideal fluid to consider in this research. This is one of the largest benefits to using a Binary ORC system because it greatly reduces the complications involved in designing custom components. The complications of designing a custom turbine capable of handling large pressure drops and operating under two-phase flow are far larger than the complications of designing a custom heat exchanger operating with high pressure CO₂ on one side and a lower pressure refrigerant on the other. The use of simpler custom components coupled with traditional ORC power plant design also gives the Binary ORC system the advantage of being capable of rapid commercialization, as it only requires a slight modification of off-the-shelf ORC power plant components.

The Binary ORC system does, however, have significant drawbacks in terms of its potential power production. The Binary ORC system has a considerably larger number of components than the Direct Single-Loop system, thereby greatly increasing the losses within the system. Parasitic power losses are also greater within the Binary ORC system. While the geothermal loop may not require a circulation pump if a thermosyphon is

established, the power cycle loop does require a pump in order to keep the isobutane moving through the system. In addition to this, there are two condensing phases; one for the CO₂ after it exits the throttling valve and one for isobutane after it exits the turbine in the power cycle. For these reasons, the benefits for using a Binary ORC system can be seen as largely economical. However, depending on the results of the simulations, using a Binary ORC system could still prove to be the superior choice.

2.4. Compression Process Considerations for Sequestration

Because the combination of geothermal energy production and carbon sequestration is largely theoretical at this point, there are no current policies in place to assign responsibility for the actual sequestration of CO₂. Depending on the potential for geothermal power production using CO₂, the demand for CO₂ as a geothermal fluid could increase. If the demand for CO₂ as a geothermal fluid is high enough, it could reduce the incentive of coal power plants to sequester the CO₂ themselves when they could sell it as a commodity to geothermal power companies. This would place the responsibility of sequestering CO₂ on the geothermal power companies. Since sequestration requires energy to compress the CO₂ for injection, optimization of the compression process, in order to minimize the energy consumption, needs to be taken into account. Because an ideal isothermal compression cycle would require the least amount of energy to prepare the CO₂ for injection, three different compression processes were considered and compared to an ideal isothermal compression process.

The first compression process considered was an isentropic cycle. This was considered first as it is one of the most basic and most commonly used compression processes. The layout and design of the system is identical to the ideal isothermal compression process, however the operating conditions are different. It is assumed that the CO₂ is supplied at ambient temperature and pressure. The CO₂ is then run through a compressor, or series of compressors if the pressure differential is too high, until it reaches the saturation pressure at ambient temperature. It is then run through a condenser until it reaches a saturated liquid state and is then injected into a reservoir for sequestration.

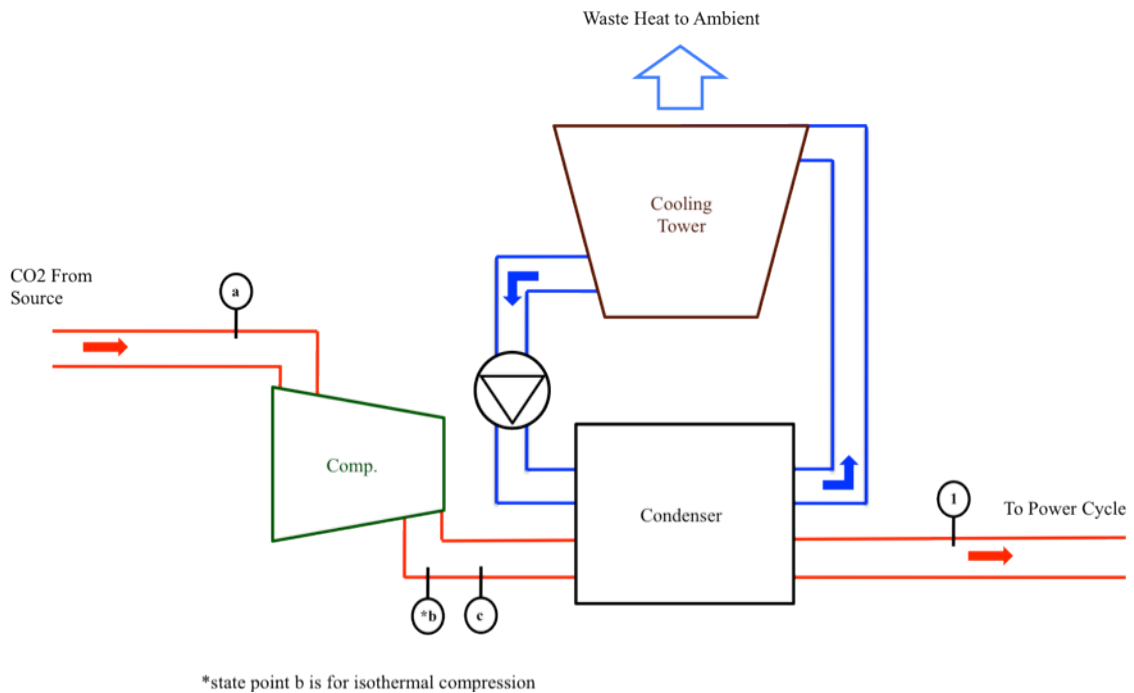


Figure 2-3: Isentropic Compression Process for Pre-treating CO₂ prior to injection

In Figure 2-3, the compression process of the isothermal and isentropic compression cycles are represented by state-points a, b, and c, where state point a represents the state of the CO₂ entering the system, state point b represents the state of the CO₂ exiting the compressor under isothermal conditions, and state point c represents the state of the CO₂ exiting the compressor under isentropic conditions. The main difference between state

points b and c is that state point c is at an elevated temperature while state point b is assumed to be at the same temperature as state point a. State point 1 represents the CO₂ as a saturated liquid at ambient temperature, ready for injection into the thermal reservoir.

The second compression process considered was a series of isentropic compressions with intercooling. This compression process was taken into consideration in order to reduce the amount of work required in a single isentropic compression without intercooling and is often used when large pressure changes are experienced through a compression process. Like the first process, the CO₂ is first run through an isentropic compressor. It is compressed to some intermediate pressure in between the ambient and saturation pressures. It is then cooled in a heat exchanger back down to the ambient temperature. The CO₂, now at the intermediate pressure and ambient temperature, is then run through a second isentropic compressor to the saturation pressure at ambient temperature. It is then cooled and condensed to a saturated liquid state for injection into the reservoir.

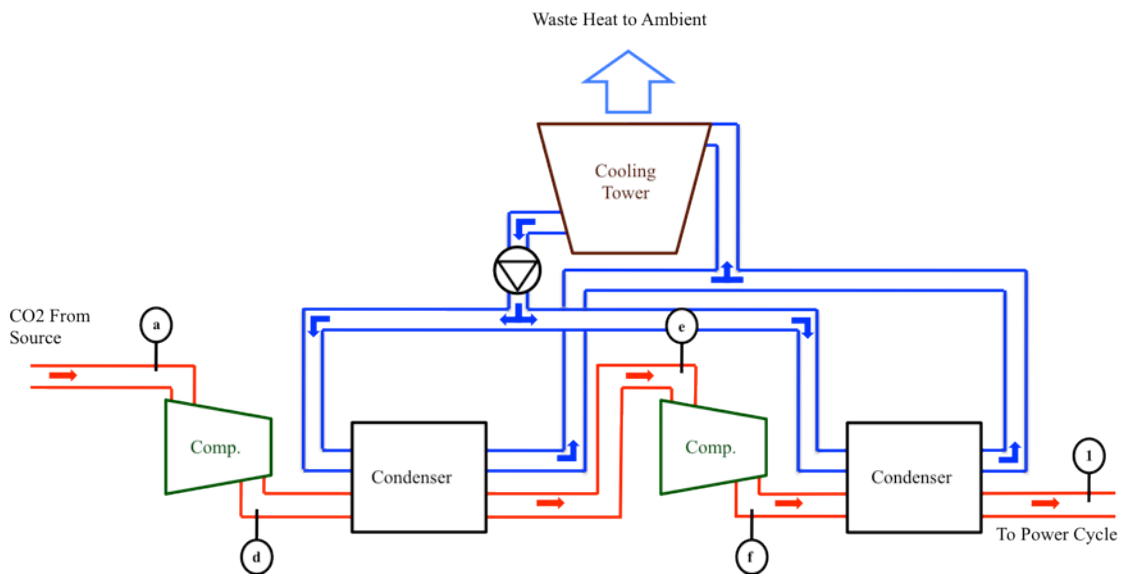


Figure 2-4: Isentropic Compression Cycle with Intercooling for Pre-treating CO₂ prior to injection

In Figure 2-4, state point a represents the CO₂ entering the compression cycle. State point d represents the state of the CO₂ exiting the first compressor after undergoing isentropic compression. State point e represents the CO₂ at the intermediate pressure and ambient temperature. State point f represents the CO₂ exiting the second compressor at an elevated temperature and the saturation pressure of the ambient conditions. Again, state point 1 represents the CO₂ as a saturated liquid at ambient temperature.

The third compression process taken into consideration was isentropic compression with precooling. This process had the largest potential to approach the ideal isothermal case. The layout of this option largely resembles the first process considered and would at first operate identically. CO₂ would be compressed isentropically to the saturation pressure at ambient temperature and would then be cooled and condensed to a saturated liquid. However, before injecting the saturated liquid into the reservoir, a portion of it would be redirected back to the beginning of the compression. This CO₂ would be used to pre-cool the CO₂ entering the compressor. The redirected CO₂ would be run through a throttling valve to flash-cool it even further. The flash-cooled CO₂ would then be sprayed into the supply stream of CO₂ just before entering the compressor to increase its density. In this way, the temperature would be dropped drastically and could greatly reduce the compression power requirement.

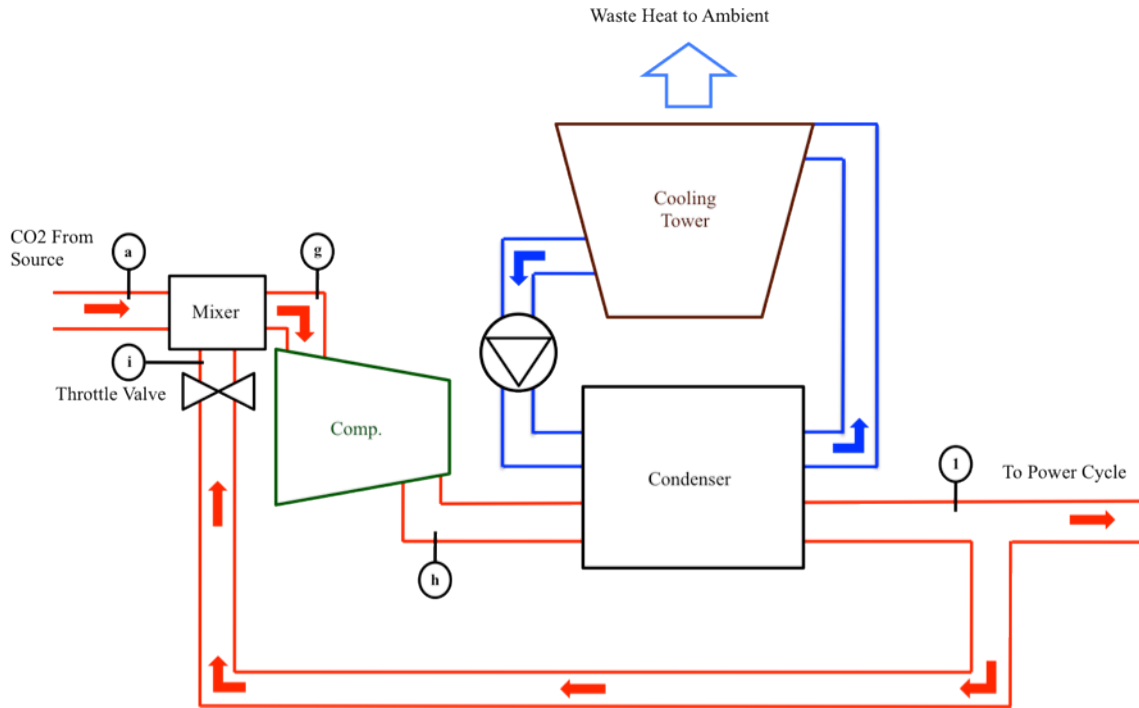


Figure 2-5: Isentropic Compression Cycle with Precooling for Pre-treating CO₂ prior to injection

The isentropic compression cycle with precooling is represented by state points a, g, h, and i in Figure 2-5. The same as the two previous compression processes, state point a represents the CO₂ entering the compression cycle and state point 1 represents the CO₂ exiting the cycle to be injected into the thermal reservoir. State point g represents the pre-cooled CO₂ entering the compressor. State point h represents the CO₂ exiting the compressor at the saturation pressure of the ambient conditions. State point i represents the redirected CO₂ that has been throttled back to a much lower temperature in order to precool the CO₂ entering the compression cycle.

In order to present the operation of the different compression cycles, a temperature-entropy ($T-s$) diagram was constructed under the operating assumptions made in order for the CO₂ to be injected as a saturated liquid at ambient temperature. Figure 2-6 shows an

overlay plot of the four different compression cycles. The expected operation of the compressors for each of the individual compression cycles under the assumed conditions are identified by the state points shown on the diagrams in the figures above. The red line (a-b-1) represents the ideal isothermal compression cycle and the green line (a-c-1) represents the basic isentropic compression cycle. The isentropic compression cycle with intercooling is identified by the purple line (a-d-e-f-1) and the isentropic compression cycle with precooling is identified by the teal line (a-1-i-g-h-1).

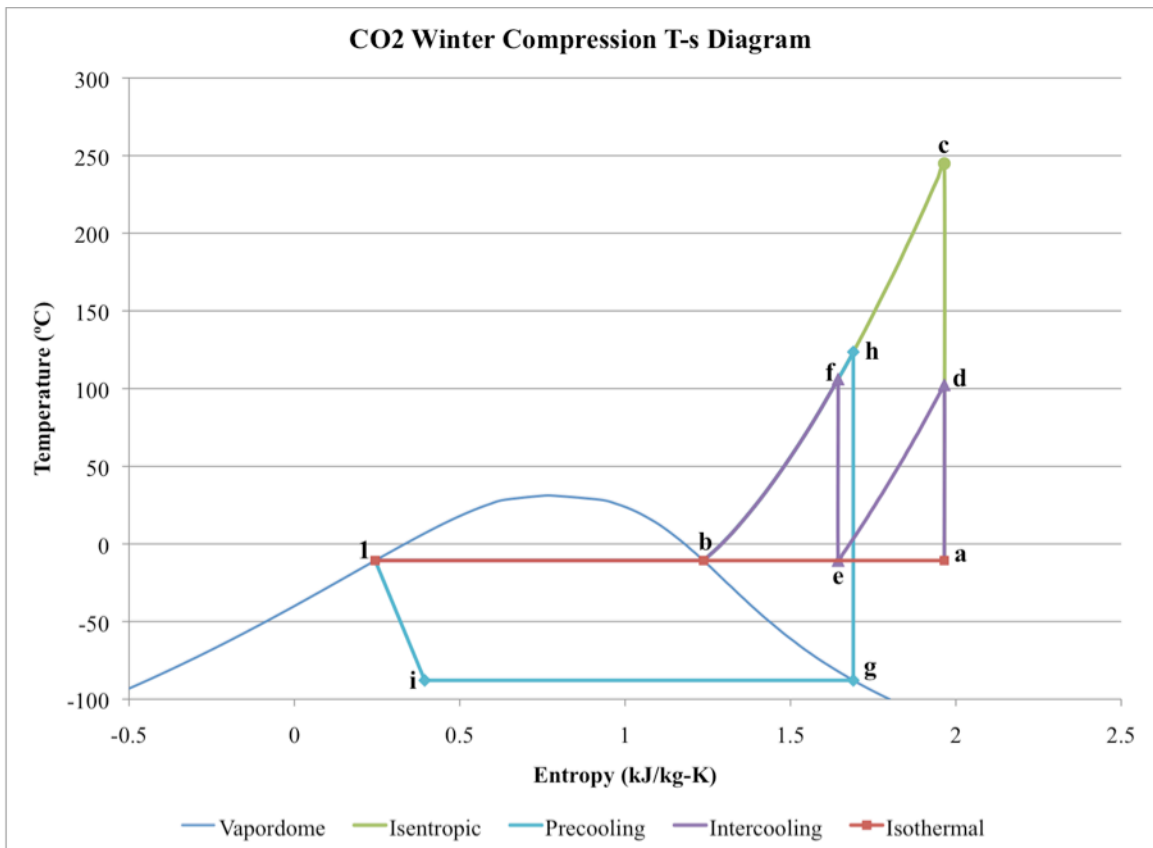


Figure 2-6: T-s diagram of the four different compression cycles under winter operating conditions.

While these compression processes are important to consider, until policies are in place to assign ownership of CO2 and responsibility for its sequestration, their impact on the

power production of a geothermal plant and payback period of its installation are uncertain. For this reason, further analysis will be left to future research.

3. Simulation Considerations and Results

3.1. Simulation Considerations and Assumptions

The system performance modeling was done using Engineering Equation Solver (EES); a simultaneous equation solver developed at The University of Wisconsin designed with the intent to simplify modeling of engineering systems for the advancement of research. EES has built in property tables, reference standards, and thermodynamic functions that greatly accelerate the simulation process for determining the outcome of mechanical systems. The reference standard used for this study was the ASHRAE standard for thermodynamic properties. Values were verified using those [24] provided in the ASHRAE Fundamentals Handbook tables for CO₂ and isobutane. While EES has many built in functions, it is also a simultaneous equation solver. If the necessary equations for simulating a specific process are known, or a different set of assumptions are being made, then a model can be built from the ground up without using all of the available built in functions. The flexibility and large number of available features of EES are what made it an ideal program for use in simulating the performance of the geothermal systems discussed in the previous chapter.

The assumptions made for the operation of the Direct Single-Loop system and the Binary ORC system were the same for the geothermal portion of the two systems. The reservoir parameters and the injection conditions were considered the same for both systems.

Pressure gains and losses through the injection and production wells, and the changes in thermodynamic properties associated with them, were calculated through hydrostatic head loss considerations and frictional losses based on the choice of piping discussed in the previous chapter. Flow through the system was assumed to have reached steady state, so no change in mass flow rate was considered. In addition to this, it was assumed that the processes through the injection and production wells were adiabatic, so no heat transfer was considered between the pipe walls and the rock. Very little change in entropy was observed due to the magnitude of the mass flow rates, resulting in near isentropic performance. To further simplify the momentum equation, flow was considered to be one-dimensional. Based on these assumptions, the change in pressure, temperature, and enthalpy were calculated using an iterative process in 10m intervals from the point of injection through the full length of pipe necessary to meet the specified depth of the reservoir. The equations used for flow through these pipes were taken from [25,26] and were simplified by the assumptions above. The reduced equations are

$$\frac{v^2}{2} + \frac{p}{\rho} + gZ = const \quad , \quad (3-1-1)$$

$$h_f = \frac{fL}{gD} \left(\frac{v^2}{2} \right) \quad , \quad (3-1-2)$$

$$\Delta p = \rho gL - \rho g h_f \quad , \quad (3-1-3)$$

$$\Delta H = \frac{\Delta p}{\rho} \quad , \quad (3-1-4)$$

and

$$Re_D = \frac{\rho v D}{\mu} \quad , \quad (3-1-5)$$

where, for a given pipe segment, v is the mean velocity, p is the pressure, ρ is the density, g is the gravitational constant, Z is the elevation, f is the friction factor, D is the diameter, L is the segment length, and μ is the dynamic viscosity. Equation (3-1-1) is the simple form of the Bernoulli Equation. This equation combined with Equation (3-1-2), which accounts for the frictional headloss of the flow through the pipes, gives an equation for the pressure change of the flow through the injection and production pipes (Equation 3-1-3). Equation (3-1-4) is a reduced form of the steady-state energy equation according to the assumptions made above and Equation (3-1-5) represents the general Reynolds Number, Re_D , used to distinguishing between laminar ($Re_D < 2000$) and turbulent ($Re_D > 2000$) flow through a pipe.

Based on the choice of base case operating conditions and piping size, the Reynolds number was calculated at the inlet and outlet of both the production and injection wells in order to determine the flow through the system. The flow was found to have been far into the turbulent region, which greatly simplified frictional loss considerations, as the friction factor, f , could be held constant throughout the injection and production wells. The friction factor used in the calculations was taken from a Moody diagram [27] based on the calculated Reynolds number and piping design considerations. The Moody diagram used can be found in the appendices.

Thermal losses to the ambient through the supply line and return line were also calculated, where the supply line is the segment of the pipe providing superheated CO₂ to the power plant and the return line is the segment of the pipe returning the condensed

CO₂ to the injection well. The lengths of these segments were chosen as 690m for the supply line and 20m for the return line coinciding with the total length assumed in the previous chapter. Once again, one-dimensional steady state assumptions were used for flow through the pipe and an iterative process was used with 10m segments to calculate the thermal and head losses. Due to the one-dimensional assumptions, internal contributions to the head losses were limited to frictional effects and were again calculated using Equation (3-1-2). The method used to calculate the external heat losses follows that used by [26], and accounts for the convection and radiation heat transfer from the surface of the piping. To reduce the impact of the external heat losses in the supply line, an insulation layer of 0.05m was used with an assumed thermal conductivity, k , of 0.042 W/m/°C. The conductive heat transfer through the insulation was calculated using Equation (3-1-6) using the thermal conductivity, the temperature differential between the CO₂ in the pipe, T_4 , and the surface of the insulation, T_s , and the ratio of the radius of the pipe and insulation, r_2 , to that of the pipe by itself, r_1 . The external convective heat transfer coefficient, h , was calculated using the Nusselt number, Nu, Rayleigh number, Ra, Grashof number, Gr, and the Prandtl number, Pr. This, combined with the temperature differential between the surface of the insulation, T_s , and the ambient air, T_∞ , as well as the surface area of the insulation, accounted for the convective heat losses and is expressed in Equation (3-1-11). The heat losses due to radiation were calculated with an assumed emissivity, e , of 0.90, again using the temperature differential and the surface area of the insulation, as well as the Stefan-Boltzmann constant, σ , and is expressed in Equation (3-1-12). The equations used to calculate the thermal losses are

$$\dot{Q}_{ins} = \frac{2\pi kL(T_4 - T_s)}{\ln(r_2/r_1)}, \quad (3-1-6)$$

$$Gr = \frac{g\beta(T_s - T_\infty)D^3}{\nu^2}, \quad (3-1-7)$$

$$Ra = GrPr, \quad (3-1-8)$$

$$Nu = \left(0.60 + \frac{0.387Ra^{1/6}}{\left(1 + (0.599/Pr)^{9/16}\right)^{8/27}} \right)^2, \quad (3-1-9)$$

$$h = \frac{kNu}{D}, \quad (3-1-10)$$

$$\dot{Q}_{conv} = h(2\pi r_2 L)(T_s - T_\infty), \quad (3-1-11)$$

$$\dot{Q}_{rad} = e2\pi r_2 L\sigma(T_s^4 - T_\infty^4), \quad (3-1-12)$$

and

$$\Delta H = \frac{\Delta p}{\rho} - \frac{\dot{Q}_{ins}}{\dot{m}_{CO_2}}. \quad (3-1-13)$$

The thermophysical properties used in the above equations were taken from the EES built-in property functions for air at ambient conditions, including the volumetric thermal expansion coefficient, β , and the kinematic viscosity, ν . In order to solve this series of equations, the temperature of the surface of the insulation was solved for using an iterative process until the conductive heat loss was equal to the combined value of the convective and radiation heat losses. With these values known, the change in pressure and enthalpy could be found using Equation (3-1-3), considering only the frictional losses, and Equation (3-1-13). With the pressure and enthalpy known, the temperature

and entropy were calculated as well, and the thermal losses to the ambient and the head losses were accounted for. To make the contribution of the thermal losses through the piping more apparent, Figure 3-1 shows a representative diagram of a segment of the pipe.

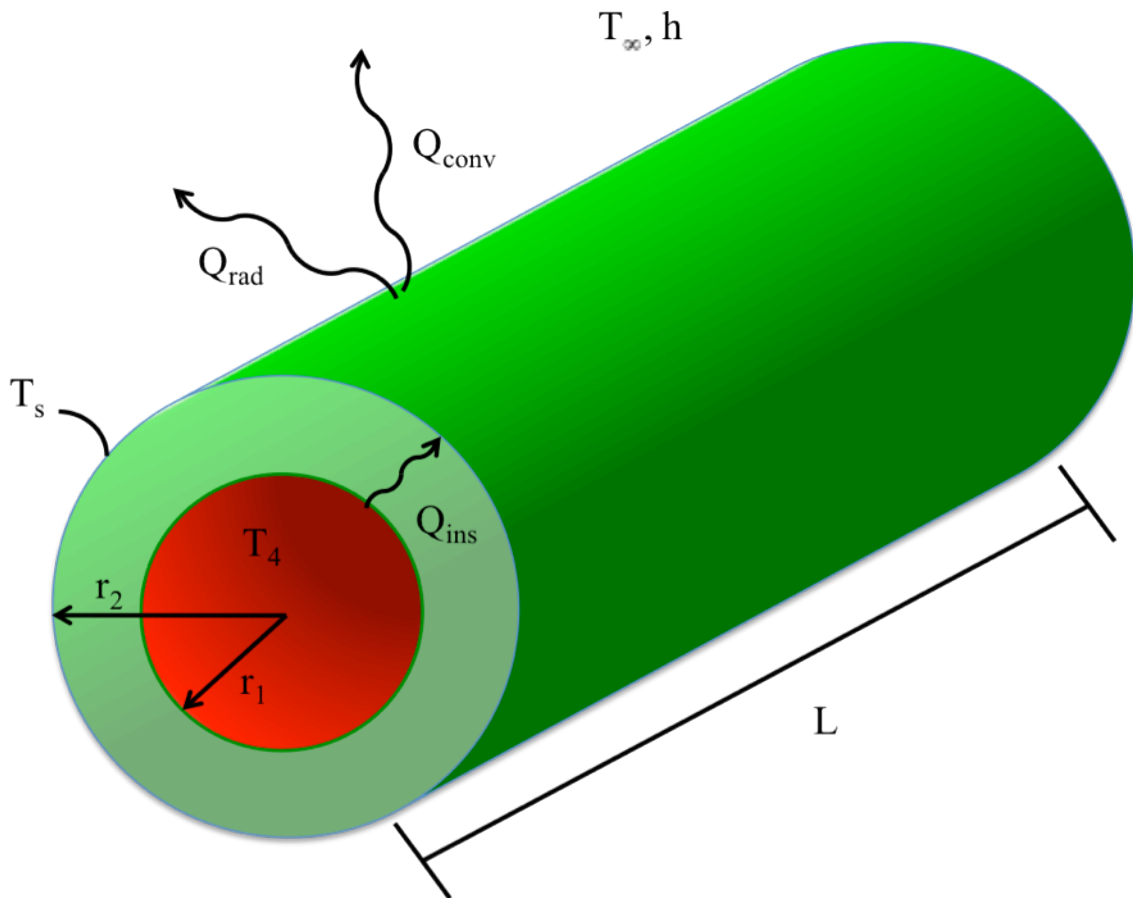


Figure 3-1: Diagram of a segment of the return line piping system showing thermal loss considerations.

Turbine operation between the two systems was also considered largely to be the same. The only difference between the simulation considerations was the efficiency of the turbines in the two systems and the working fluids used. Both systems used an initial turbine efficiency assumption of 85%. However, for the Direct Single-Loop the turbine

operates with a two-phase mixture of liquid CO₂ and CO₂ vapor. Because this can have a significant impact on custom turbine design considerations, which ultimately affect the efficiency of the turbine, a second simulation was done for the Direct Single-Loop system with a very low turbine efficiency of 50%. In the system models, the turbine performance was first calculated under ideal isentropic considerations to get theoretical values of the thermodynamic properties of the flow exiting the turbine. The assumed turbine efficiency was then used to find the actual thermodynamic properties of the flow exiting the turbine based on the theoretical values. The potential turbine power production for the two models was then calculated based on the resulting thermodynamic properties.

For both system models, the assumptions around both the heat exchanger and the condensers were considered the same. These components were assumed to operate under constant pressure, with a significantly higher pressure on the geothermal loop side of the heat exchanger and condensers. While this is a very ideal consideration, its effects on power production of the Direct Single-Loop are not of great concern, as the turbine power production occurs before the condensing process. This implies that while this assumption will have some impact on the parasitic power losses involved in the cooling tower operation, the simulations will still give a fairly good first estimate of the potential power production of these systems. Additional considerations for the heat exchanger in the Binary ORC System need to be made based on which month of the year the power production is to be optimized for. Further analysis of the heat exchanger will be discussed in the Binary ORC System Results section of this chapter.

3.2. Direct Single-Loop System Power Production under Various Operating Conditions

The Direct Single-Loop System is investigated first because it has a much simpler design layout. For this reason the simulation optimization for performance has far less variation in comparison to the Binary ORC System. The initial simulation of the system was done under the base case operating conditions with a CO₂ mass flow rate of 70kg/s and a reservoir temperature of 100°C. These values were used in conjunction with the monthly average ambient temperatures for Minneapolis, MN, in order to calculate the monthly average power production for the base case scenario. These ambient temperatures and reservoir conditions were chosen in order to simulate conditions typical of sites in the Upper Midwest United States. This was done in order to investigate the potential for geothermal power production in a region not suitable for power production with current geothermal systems.

To better understand the calculations of the system, a more in-depth analysis can be done by looking at the thermodynamic property values of the individual state points. Figure 3-2 shows the Direct Single-Loop System layout with the state points labeled.

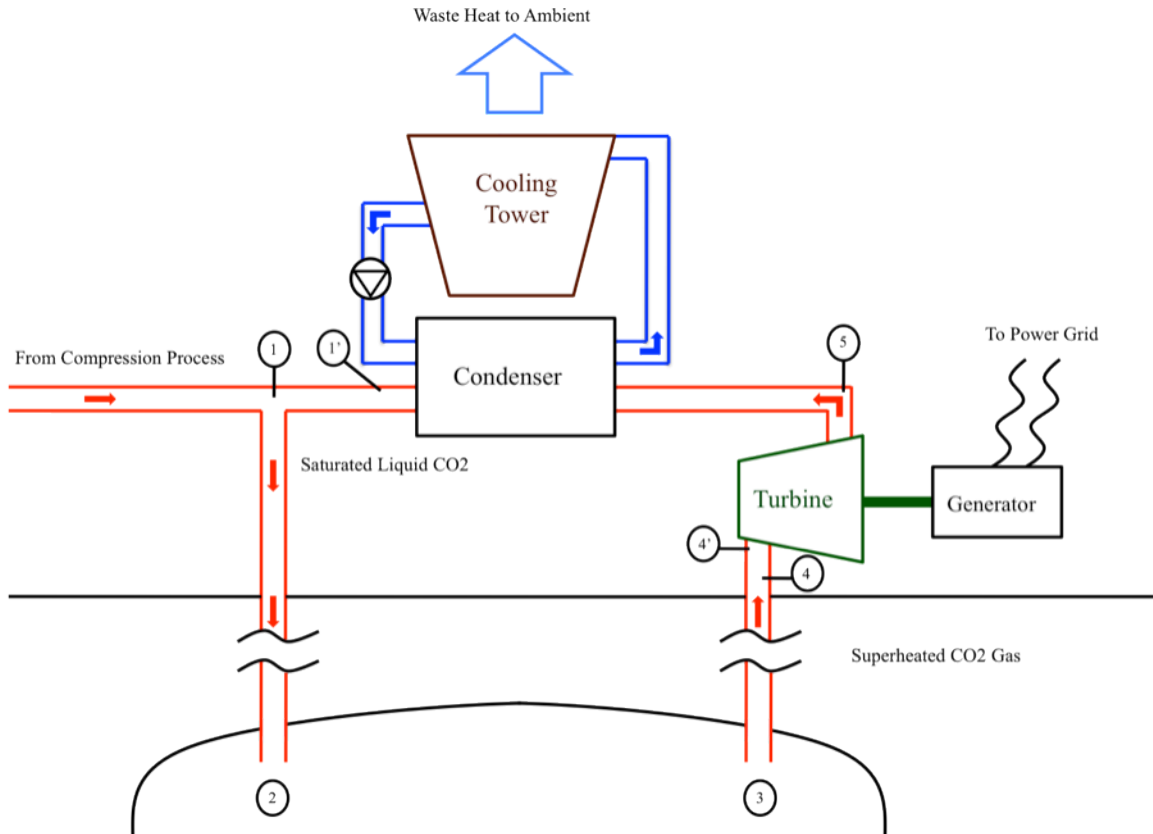


Figure 3-2: Direct Single-Loop System Layout w/ State Points

To simplify the analysis of the state points, a minimum and maximum system performance using a direct system turbine efficiency (DTE) of 85% is investigated by looking at the months of July (minimum) and January (maximum), with wet cooling tower operation for July and dry cooling tower operation for January. Tables containing the thermodynamic properties for all months can be found in the appendices. First the month of July is used to find the minimum performance of the system. The thermodynamic properties of the state points for July can be seen in Table 3-1.

Table 3-1: State Point Properties for the Month of July

State Point	T (°C)	P (kPa)	H (kJ/kg)	s (kJ/kg-K)
1'	23.21	6174	154.8	0.5601
1	23.2	6173	154.6	0.5595
2	49.36	25530	178.9	0.5595
3	100	25000	291.5	0.8858
4	55.9	11380	265.4	0.8859
4'	54.1	11107	262.6	0.8792
5	23.21	6174	251.3	0.8859

To compare the minimum and maximum performance of the system, the thermodynamic properties for January are listed in Table 3-2.

Table 3-2: State Point Properties for the Month of January

State Point	T (°C)	P (kPa)	H (kJ/kg)	s (kJ/kg-K)
1'	-5.717	2986	73.68	0.2867
1	-5.73	2985	73.46	0.2859
2	8.958	27072	97.82	0.2859
3	100	25000	291.5	0.8858
4	55.9	11380	265.4	0.8859
4'	53.79	11108	260.8	0.8738
5	-5.717	2986	235.2	0.8907

The thermodynamic properties listed in Tables 3-1 and 3-2, used in conjunction with the equations listed at the beginning of the chapter, allow for a comparison of the system's minimum and maximum power production. By using Equations (3-1-3) and (3-1-4) with the thermodynamic values of State Point 1, the values of State Point 2 can be verified. In the same way, the values of State Point 3 can be used to verify the values of State Point 4. This coupled with the assumption of constant pressure through the condenser allows determination of the pressure drop across the turbine, which in turn can be used to calculate the entropy and enthalpy changes across the turbine based on the turbine efficiency. The isentropic turbine power production can then be calculated by.

$$\dot{W}_t = \dot{m}_{CO_2} (H_{4'} - H_5) \quad . \quad (3-2-1)$$

The heat transfer rate into the system can be calculated in the same manner using

$$\dot{Q}_{res} = \dot{m}_{CO_2}(H_3 - H_2) . \quad (3-2-2)$$

Under these assumptions, the values for January and July in Table 3-5 can be confirmed. Taking the state point values for the temperature and entropy from both Table 3-1 and 3-2, a T-s diagram was created to provide a graphical comparison of the summer and winter performance of the system. The T-s diagram can be seen in the Figure 3-3.

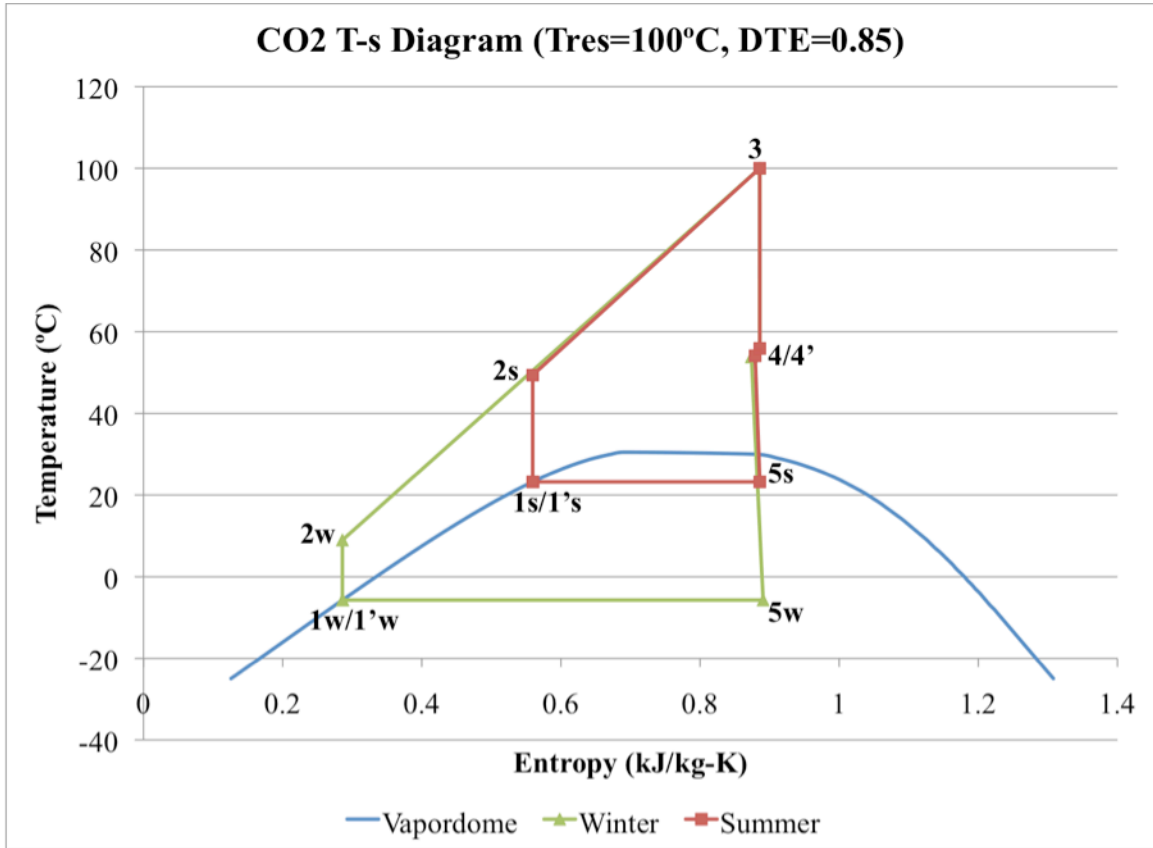


Figure 3-3: T-s Diagram for Base Case Simulation of the Direct Single-Loop System

Given the turbine performance is represented by the difference between state points four and five, where the summer and winter values are denoted by an s or w respectively, the magnitude of the difference between the minimum and maximum performance of the system can easily be seen on the T-s diagram.

In order to show the advantage of using a wet tower over a dry tower during summer operation, two simulations were done for the base case scenario; one using dry bulb (DB) temperatures year-round and one using dry bulb temperatures only for the winter months while using wet bulb (WB) temperatures for the summer months (April through September). The tables that follow show the monthly average ambient temperatures and monthly average power production, respectively, again noting that the power production is for a single production well.

Table3-3: Monthly Average Ambient Temperatures (Winter DB, Summer WB)

Month	Jan	Feb	Mar	Apr	May	June	July	Aug	Sept	Oct	Nov	Dec
Ave Temp (°C)	-10.73	-7.21	-2.23	4.16	10.23	15.79	18.20	17.30	12.19	10.39	0.58	-7.20

Table3-4: Monthly Average Ambient Temperatures (Dry Bulb Year-round)

Month	Jan	Feb	Mar	Apr	May	June	July	Aug	Sept	Oct	Nov	Dec
Ave Temp (°C)	-10.73	-7.21	-2.23	7.25	14.86	20.20	22.57	21.48	15.88	10.39	0.58	-7.20

Table3-5: Direct Single-Loop System Monthly Average Power Production (Winter DB, Summer WB)

Month	DTE	Jan	Feb	Mar	Apr	May	June	July	Aug	Sept	Oct	Nov	Dec
Ave. Power (kW)	0.85	1792	1656	1469	1242	1039	862	788	816	975	1033	1368	1655
Ave. Power (kW)	0.50	1054	974	864	731	611	507	464	480	574	608	805	974

Table3-6: Direct Single-Loop System Monthly Average Power Production (Dry Bulb Year-round)

Month	DTE	Jan	Feb	Mar	Apr	May	June	July	Aug	Sept	Oct	Nov	Dec
Ave. Power (kW)	0.85	1792	1656	1469	1137	891	728	659	691	859	1033	1368	1655
Ave. Power (kW)	0.50	1054	974	864	669	524	429	388	406	505	608	805	974

A graphical representation of the base case power production of the Direct Single-Loop System is also presented in Figure 3-4. Figure 3-5 shows the system efficiency of the two simulations run for the base case with direct system turbine efficiencies (DTE) of 85% and 50%.

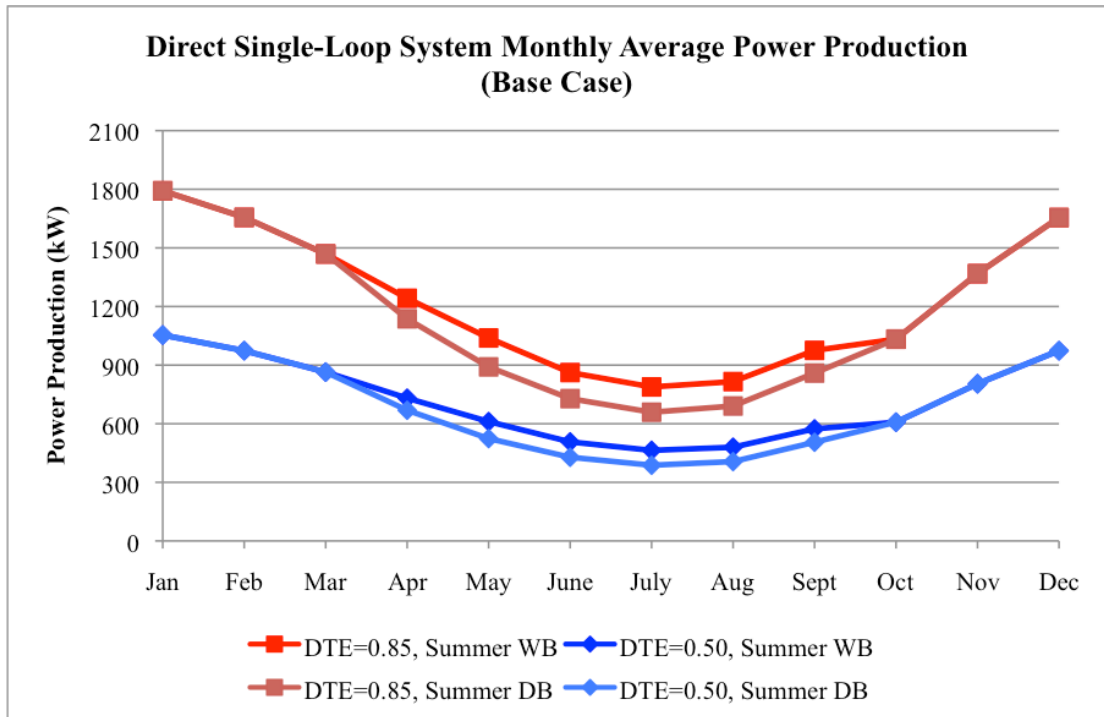


Figure 3-4: Direct Single-Loop System Monthly Average Power Production for a Single Well

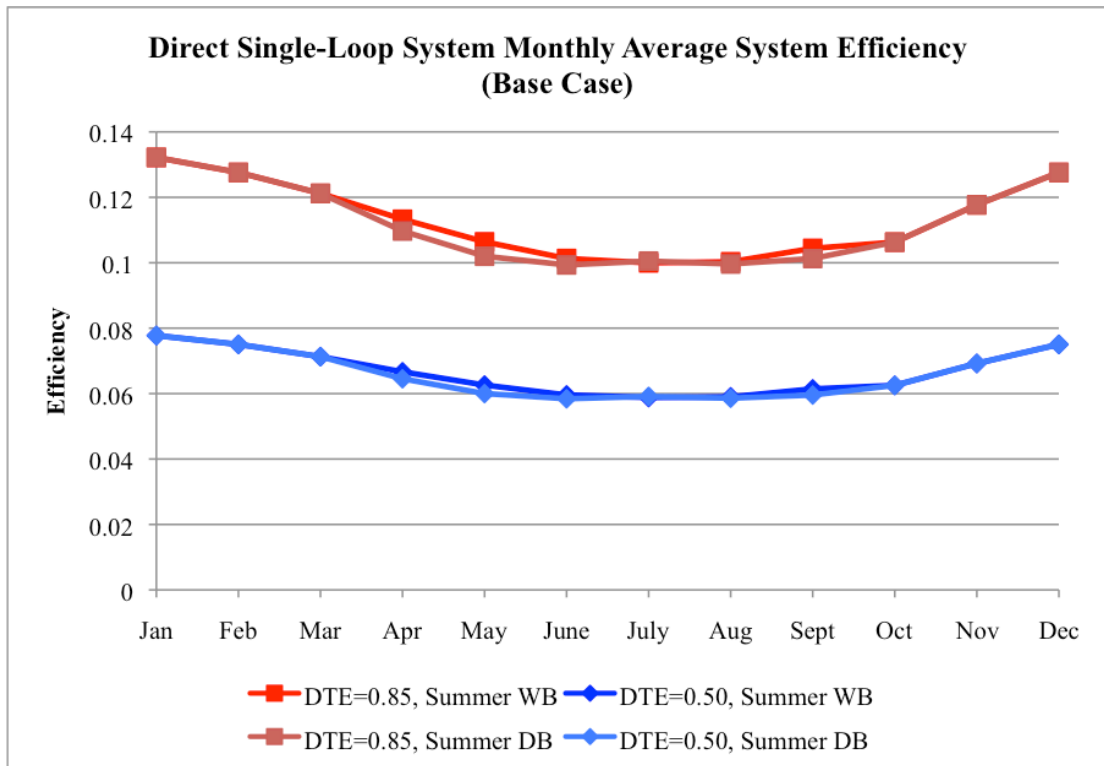


Figure 3-5: Direct Single-Loop Monthly Average System Efficiency

The improvement in summer power production using wet towers for summer operation is clear from the Figures 3-4 and 3-5, with the wet tower simulations approximately providing an additional 100-200kW of power over the dry tower simulations. With this in mind, the remaining simulations performed in this research used wet cooling tower operation for the summer months and dry cooling tower operation for the winter months. The significant difference in power production and system efficiency between the two simulations with turbine efficiencies of 85% and 50% is also apparent in Figure 3-4 and Figure 3-5. In the analysis that follows, the 50% turbine efficiency simulations are omitted to make the trends under investigation more apparent. Figures containing both the 85% and 50% turbine efficiency simulations are included in the appendix to allow further investigation of which systems are most suitable under variable conditions.

The above tables and figures outline in clear detail the analysis of the base case scenario and verify how the monthly average power production was calculated. These processes were repeated under various operating conditions to test the system performance with varying geologic locations in mind. The parameters whose values were changed to investigate their effect on the power production of the system were the mass flow rate of the system, the reservoir temperature, and the depth of the reservoir.

First the reservoir temperature was held constant at the base case value of 100°C while the mass flow rate was varied to values of 90kg/s, 120kg/s, and 140kg/s. In order to maintain the thermosyphon effect assumed under steady state conditions, for the higher mass flow rates of 120kg/s and 140kg/s, the injection pipe diameter was changed from

0.254m to 0.308m and the production pipe diameter was changed from 0.20m to 0.254m. This ensures that the headloss through the injection well allowed for a sufficiently high enough pressure to overcome the pressure inside the reservoir. The monthly average power production for a single well under these varying mass flow rates was calculated and can be seen in Figure 3-6.

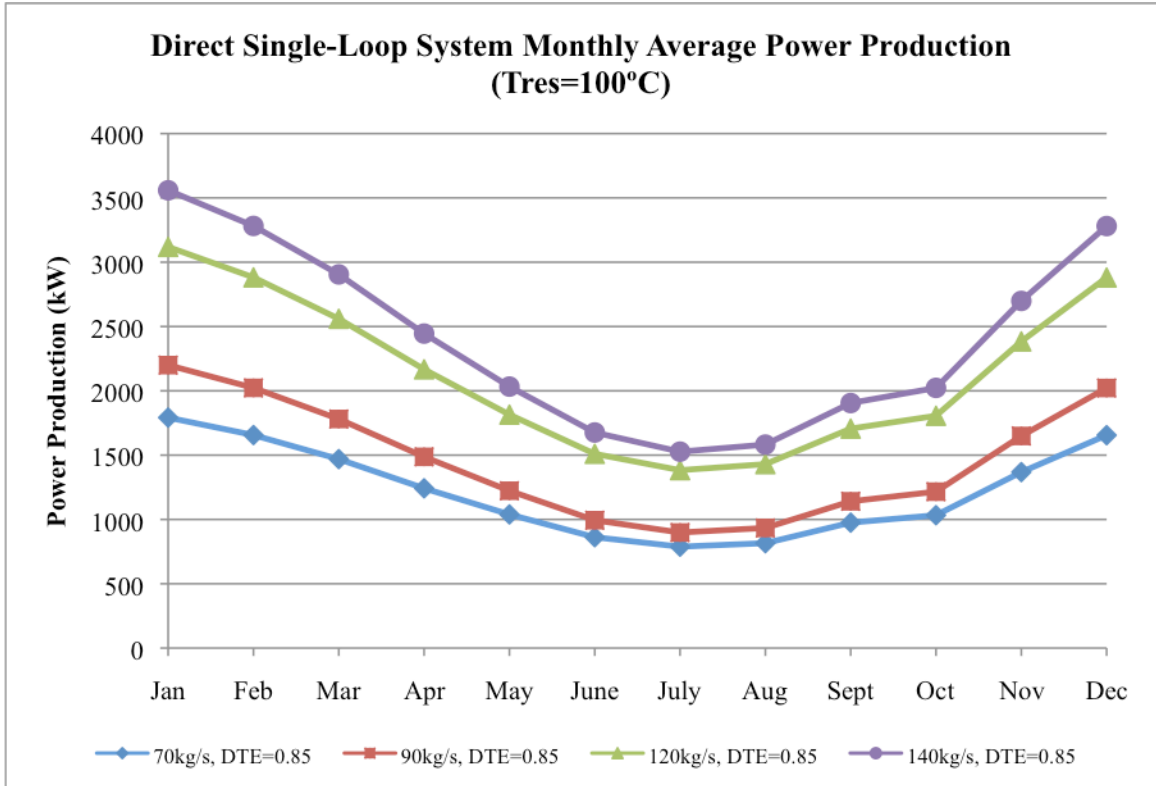


Figure 3-6: Direct Single-Loop System Power Production for a Single Well with Varying Mass Flow Rate
 Figure 3-6 shows the expected trend of increased power production with increased mass flow rate, based on Equation (3-2-1).

Next the mass flow rate was held constant at the base case value of 70kg/s while the reservoir temperature was changed to values of 100°C, 125°C, and 150°C. The monthly

average power production for a single well under these varying temperatures can be seen in Figure 3-7.

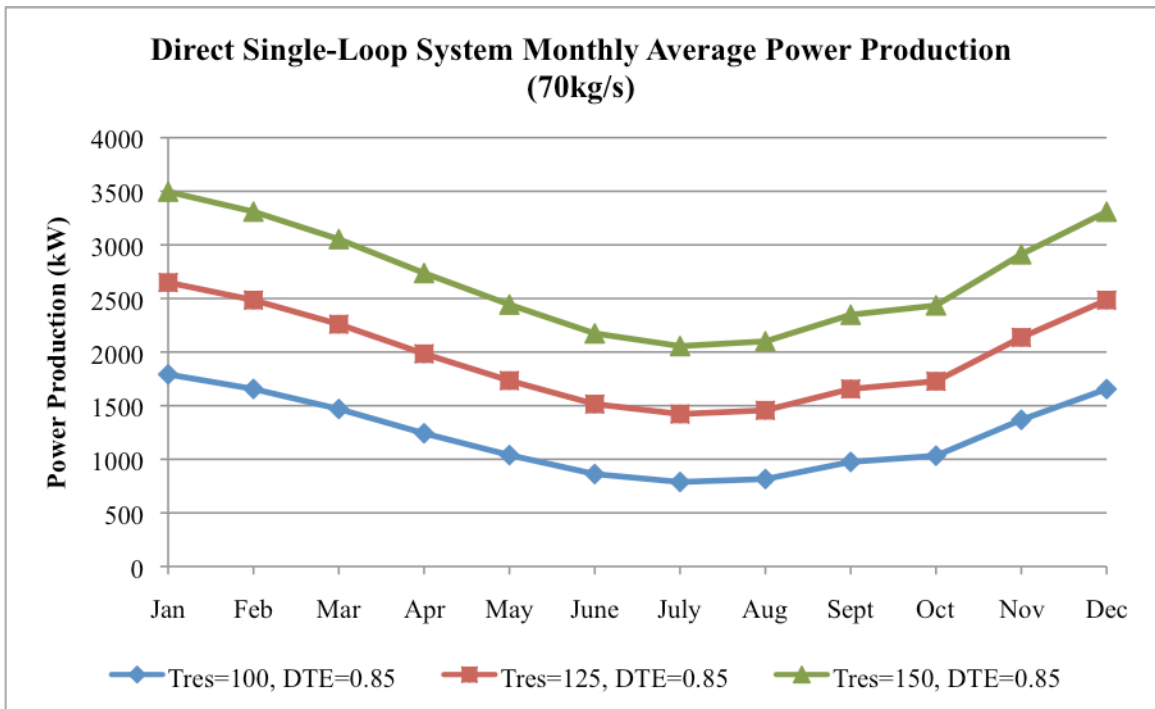


Figure 3-7: Direct Single-Loop System Power Production for a Single Well with Varying Reservoir Temperature

Figure 3-7 shows the general trend that should be expected with an increased reservoir temperature, in that the heat transfer into the system is also increased based on Equation (3-2-2).

Finally, the base case scenario was expanded to investigate its expected monthly average power production with varying reservoir depth. The various reservoir depths considered were 2.5km, 3.1km and 3.6km. In order to accommodate for appropriate headloss through the injection pipe to ensure a sustained thermosyphon effect without significantly altering the pressure differential through the reservoir, the injection pipe diameter for the simulations at a depth of 3.6km was set to 0.308m for mass flow rates of 70kg/s and

90kg/s, and 0.356m for mass flow rates of 120kg/s and 140kg/s, respectively. The results of the simulations with varying reservoir depth for the base case operating conditions can be seen in Figure 3-8.

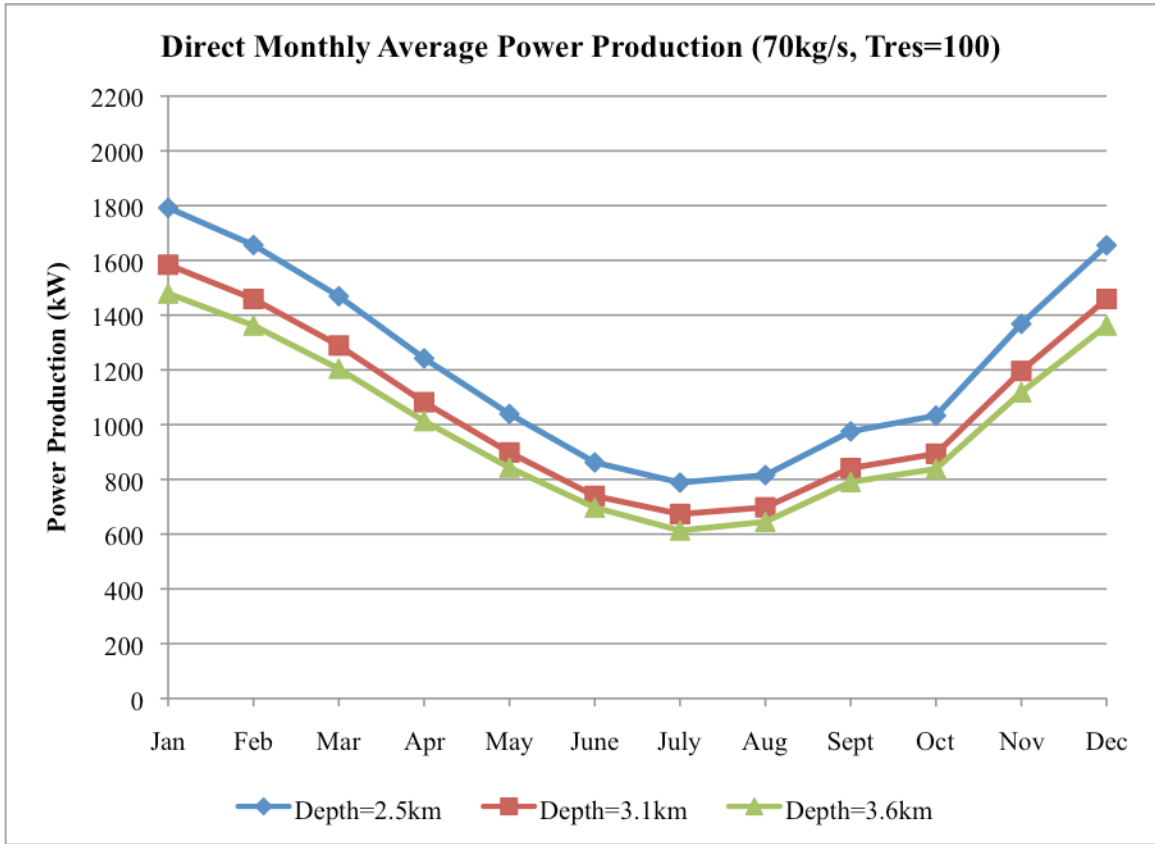


Figure3-8: Direct System Monthly Average Power Production for a Single Well Under Base Case Operating Conditions at Various Reservoir Depths.

Given the trends observed in the Figure 8, it can be determined that the losses through the injection and production pipes with the increased depth are considerable. This implies that drilling to the shallowest depths possible while still maintaining significant power production is ideal. However, for a given location, it can be assumed that the reservoir temperature would generally increase with reservoir depth. Therefore the expected change in power production with increased depth for a single geographic location would more likely resemble the trends seen in Figure 3-9.

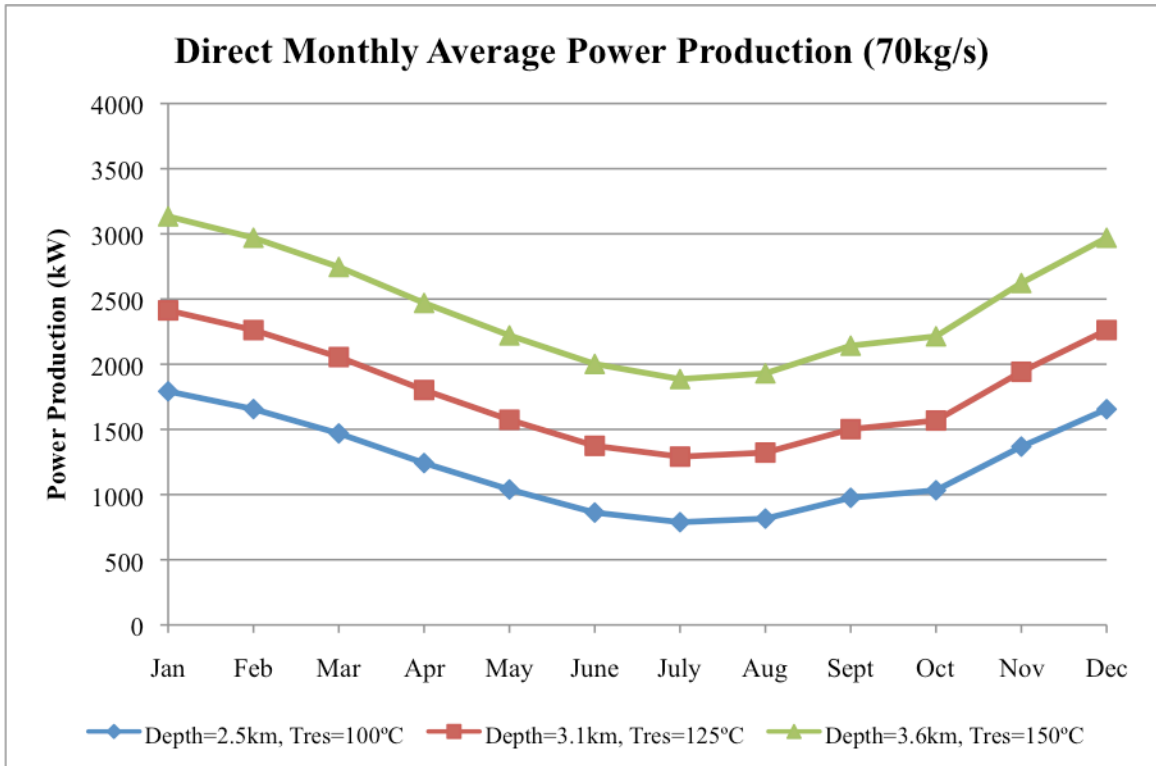


Figure 3-9: Direct Single-Loop System Monthly Average Power Production for a Single Well with Mass Flow Rate 70kg/s with Varying Reservoir Temperatures and Depths.

Comparing Figure 3-9 to Figure 3-7 shows the expected decrease in power production with increased reservoir depth that is made evident in Figure 3-8. However, the increase in reservoir temperature relative to increased reservoir depth in Figure 3-9 is likely more accurate for locations with high subsurface temperatures. Therefore the increase in power production with increased reservoir depth for the regions that this study is particularly interested in would be lower than those shown in Figure 3-9. Various additional figures can be found in the appendix investigating varying reservoir temperatures and mass flow rates at the selected depths. These figures give more insight into whether drilling to deeper depths at a given location would be worth it for the potential increase in power production.

From the above figures the general performance of the Direct Single-Loop System for various parameters can be seen. Simulations were done for all varying mass flow rates under each of the varied reservoir temperatures and figures for each can be found in the appendix. From this data, the expected system performance of the Direct Single-Loop System for numerous geographic locations can be extrapolated in order to determine whether a site is suitable for geothermal electricity production using CO₂ as a working fluid.

3.3. Binary Organic Rankine Cycle System Power Production under Various Operating Conditions

The Binary ORC System was significantly more complex to model in comparison to the Direct Single-Loop System. This was due to various changes in the system setup, including the use of two different fluids and the insertion of a heat exchanger and expansion valve in place of the turbine. In this system the CO₂ was used as a heat transfer fluid and operated under the same base case conditions as the CO₂ in the Direct Single-Loop System. Isobutane was used as the working fluid inside of the power cycle, operating under different conditions dependent on the operating conditions of the CO₂ loop as well as whether the heat transfer process was being optimized for power production during the winter or summer months. The same monthly average ambient air temperatures were used for the condensing process in the CO₂ and isobutane loops as were used in the Direct Single-Loop System.

As stated previously, optimization and simulation of the CO₂ to isobutane heat exchanger required far more complex considerations than any other component within the system. For the simulations, the heat exchanger was broken down into two components, a pre-heater and a boiler. This was done in order to deal with a phase change occurring on the isobutane side of the heat exchanger. By splitting the heat exchanger into two components, two different sets of operating assumptions were necessary to complete the simulation, including the type of heat exchange process and the effectiveness of that heat exchange process. Analysis of the boiler and pre-heater followed the Effectiveness-NTU method provided by [26].

The boiler was simulated as a simple counter-flow heat exchanger with an assumed effectiveness, ϵ , of 0.80 with both sides operating under constant pressure. The pressure on the CO₂ side of the heat exchanger was calculated after accounting for thermal losses to the ambient air after exiting the production well. This value was found to be relatively constant year round. The isobutane was assumed to enter the boiler as a saturated liquid and exit the boiler as a saturated vapor. Under these conditions the temperature, pressure, enthalpy, and entropy of the isobutane entering and exiting the boiler could be found. The boiling temperature of the isobutane was chosen in order to maximize the power production for a given month. This boiling temperature was found using an iterative process based on the condensing conditions for the month in question, as well as the properties of the CO₂ entering the boiler, in order to find the ideal pressure differential across the turbine and mass flow rate necessary to achieve it. In order to find the temperature, enthalpy and entropy of the CO₂ leaving the boiler, a relationship involving

the effectiveness of the boiler and the specific heat rates of the CO2 and isobutane was determined using

$$\varepsilon = \frac{C_h(T_{h,i} - T_{h,o})}{C_{\min}(T_{h,i} - T_{c,i})}, \quad (3-3-1)$$

$$C_h = \dot{m}_{CO_2} c_{p,CO_2}, \quad (3-3-2)$$

and

$$C_c = \dot{m}_{Iso} c_{p,Iso}. \quad (3-3-3)$$

The specific heat, c_p , values of the CO2 and isobutane through the boiler and preheater were calculated by taking the change in enthalpy and dividing it by the change in temperature using

$$c_{p,CO_2} = \frac{(H_{h,i} - H_{h,o})}{(T_{h,i} - T_{h,o})}, \quad (3-3-4)$$

and

$$c_{p,Iso} = \frac{(H_{c,o} - H_{c,i})}{(T_{c,o} - T_{c,i})}, \quad (3-3-5)$$

where Equation (3-3-4) is used to calculate the specific heat on the CO2 side of the boiler, and Equation (3-3-5) is used to calculate the specific heat on the isobutane side of the preheater. Since the isobutane in the boiler is always in a saturated state, the specific heat rate is infinitely large. This means that the specific heat rate of the CO2, C_h , is equal to C_{\min} . Applying this to Equation (3-3-1) and rearranging it can be used to find the temperature of the CO2 leaving the boiler using

$$T_{h,o} = T_{h,i} - \varepsilon(T_{h,i} - T_{c,i}). \quad (3-3-6)$$

With the temperature and the pressure of the CO2 exiting the boiler found, the enthalpy and entropy at this location can also be found using the EES property functions. With the

changes in the thermodynamic properties surrounding the boiler portion of the heat exchanger now known, the heat transfer rate through the boiler can be calculated using

$$\dot{Q}_{HX} = \varepsilon C_{\min}(T_{h,i} - T_{c,i}) \quad (3-3-7)$$

The mass flow rate of the isobutane can then be calculated using the heat transfer through the boiler as well as the enthalpy values of the isobutane entering and exiting the boiler and rearranging Equation (3-2-2). Once the mass flow rate is known, the power production of the turbine, the power consumption of the pump, and the heat transfer rate through the pre-heater can be determined.

Looking next at the pre-heater portion of the heat exchanger, the same considerations above can be used to find the heat transfer rate through the pre-heater. The pre-heater was simulated as a shell and tube heat exchanger with two passes. The pressure on both the CO₂ and isobutane sides of the heat exchanger were again assumed to be constant. For a given month, the isobutane was condensed to a saturated liquid at the temperatures listed in Table 3-1. This allows for the pressure, enthalpy, and entropy of the isobutane exiting the condenser to be found. Assuming a pump efficiency of 0.90 and assuming the pressure exiting the pump is the same as the pressure entering the pre-heater, the temperature, enthalpy, and entropy of the isobutane entering the pre-heater can be calculated as well. Given the change in the enthalpy of the isobutane entering and exiting the pre-heater, as well as the mass flow rate of the isobutane, Equation (3-2-2) can again be used to find the heat transfer rate through the pre-heater. This can then in turn be used to find the enthalpy of the CO₂ exiting the pre-heater. The enthalpy and pressure of the CO₂ can then be used to find the remaining thermodynamic properties of the CO₂ exiting

the pre-heater. Using Equations (3-3-4) and (3-3-5) the specific heat rates can again be calculated for the flows through the pre-heater and used to verify the heat transfer rate using Equation (3-3-7). The thermodynamic properties of the CO₂ leaving the pre-heater can then be used to find those of the CO₂ exiting the expansion valve and entering the condenser. The CO₂ is then condensed back to a saturated liquid at ambient temperature before being re-injected into the reservoir and the heat transfer process is complete.

To better understand the calculations surrounding the simulation of the Binary ORC System, the thermodynamic properties of the individual state points are again presented. Figure 3-10 shows the Binary ORC System layout with the state points labeled.

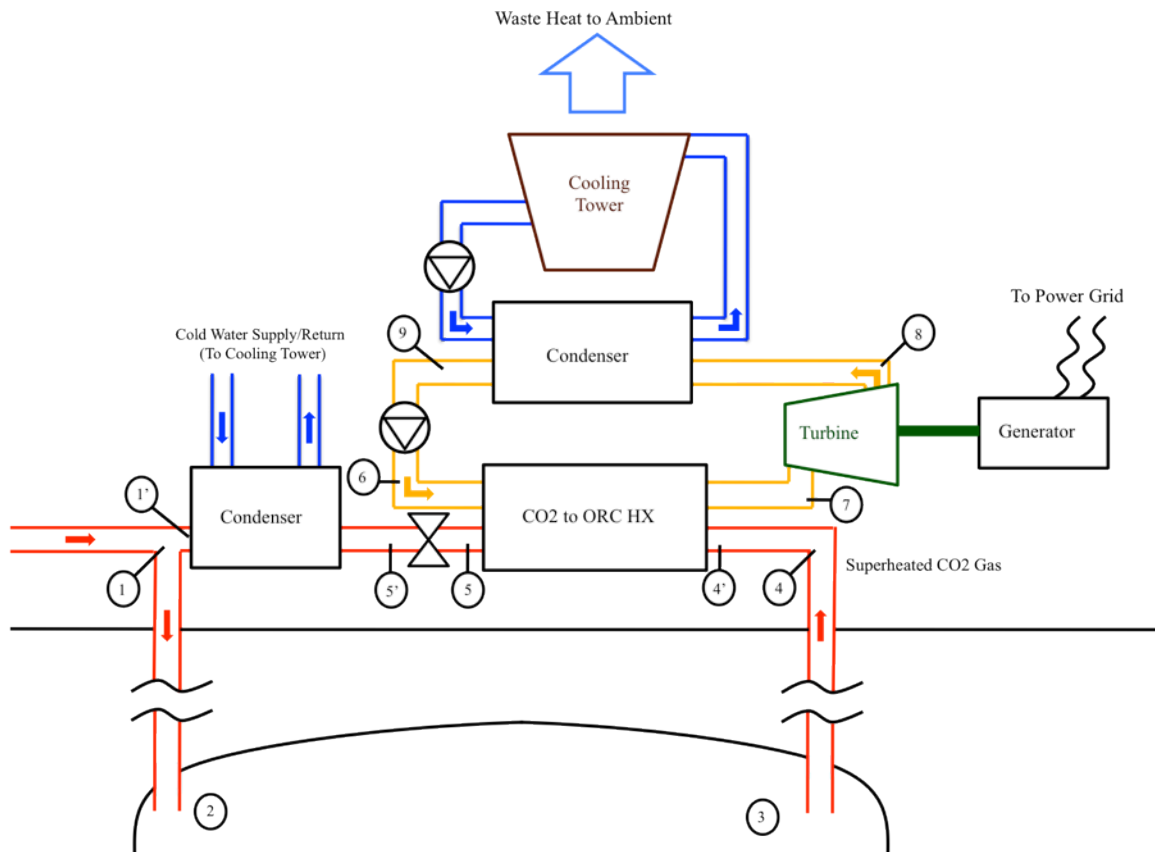


Figure 3-10: Binary ORC System Layout w/ State Points

The thermodynamic properties of the state points were calculated for all months using the above equations for the Binary ORC simulation and are presented in the appendices. To give a range of the thermodynamic properties encountered throughout the year, tables with the thermodynamic properties from the months of July and January are presented in Table 3-7 and Table 3-8 for the CO₂ loop, and Table 3-9 and Table 3-10 for the isobutane loop. Tables and figures containing data for all months can be found in the appendices.

Table 3-7: Binary ORC System State Point Properties for the CO₂ Loop (July)

State Point	T (°C)	P (kPa)	H (kJ/kg)	s (kJ/kg-K)
1	23.2	6173	154.6	0.5595
1'	23.21	6174	154.8	0.5601
2	49.36	25530	178.9	0.5595
3	100	25000	291.5	0.8858
4	55.9	11380	265.4	0.8859
4'	54.1	11107	262.6	0.8792
5	41.37	11107	194.1	0.666
5'	23.21	6174	194.1	0.6929

Table 3-8: Binary ORC System State Point Properties for the CO₂ Loop (January)

State Point	T (°C)	P (kPa)	H (kJ/kg)	s (kJ/kg-K)
1	-5.73	2985	73.46	0.2859
1'	-5.717	2986	73.68	0.2867
2	8.958	27072	97.82	0.2859
3	100	25000	291.5	0.8858
4	55.9	11380	265.4	0.8859
4'	53.79	11108	260.8	0.8738
5	26.86	11108	146.1	0.51
5'	-5.717	2986	146.1	0.5575

Table 3-9: Binary ORC System State Point Properties for the isobutane Loop (July)

State Point	T (°C)	P (kPa)	H (kJ/kg)	s (kJ/kg-K)
6	23.3	537.9	143	0.5359
7	40.5	537.9	496.5	1.668
8	27.05	332.3	480.6	1.678
9	23.2	332.3	142.3	0.5362

Table 3-10: Binary ORC System State Point Properties for the isobutane Loop (January)

State Point	T (°C)	P (kPa)	H (kJ/kg)	s (kJ/kg-K)
6	-5.566	404.5	74.99	0.2971
7	30	404.5	482.5	1.659
8	0.7567	127.2	445.3	1.683
9	-5.73	127.2	74.57	0.2973

Taking the temperatures and entropies from Tables 3-7 through 3-10, a T-s diagram for the Binary ORC System was constructed. Figure 3-11 shows this diagram.

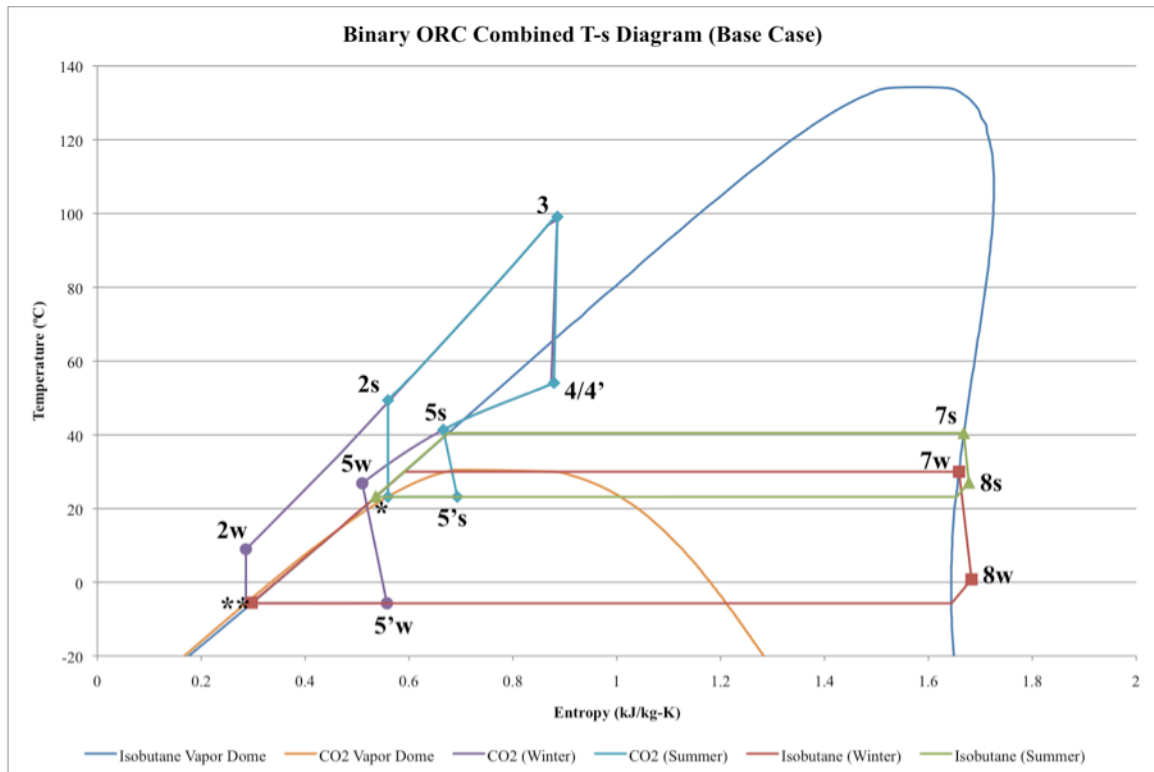


Figure 3-11: T-s Diagram for the Binary ORC System operating under Base Case conditions for the month of January. *State Points 1/1's/6s/9s. **State Points 1/1'w/6w/9w.

The CO2 loop for the summer and winter operation of the Binary ORC system are represented by the teal and purple lines, respectively. The CO2 is injected as a saturated liquid (1) into the thermal reservoir (2). After being heated to the reservoir temperature (3), the CO2 rises through the production well (4) and then travels through the supply line before entering the heat exchanger (4'). The CO2 then exits the heat exchanger (5) and is

throttled back down to the saturation pressure (5') before being condensed back to the injection conditions (1'). The isobutane loop for the summer and winter operation of the Binary ORC system are represented by the green and red lines, respectively. The isobutane is pumped from a saturated liquid state (9) into the heat exchanger (6). It is then heated to a saturated vapor state (7) before entering the turbine for power production. After exiting the turbine (8), the isobutane is once again condensed to a saturated liquid state. In this diagram, the turbine performance is represented by the change between State Points 7 and 8, where summer and winter performance are represented by s and w respectively. The difference in summer and winter turbine performance can clearly be seen in Figure 3-11 and the trend is similar to that seen in Figure 3-3.

To calculate the power production of the Binary ORC system, the heat exchange process needed to be simulated so that the mass flow rate of the isobutane could be found and so that the pressure drop across the turbine could be known. This pressure drop is found by again assuming a constant pressure through the condenser inside of the isobutane loop. The pressure drop, coupled with a turbine efficiency of 85% and the calculated mass flow rate, could then be used to calculate the monthly average power production for a single well. The monthly average power production and monthly average isobutane boiling temperatures for the Binary ORC System operating under the base case conditions used in the Direct Single-Loop System can be found below in Table 3-11 and Table 3-12.

Table 3-11: Binary ORC System Monthly Average isobutane Boiling Temperatures

Month	Jan	Feb	Mar	Apr	May	June	July	Aug	Sept	Oct	Nov	Dec
Boiling Temp (C°)	30	31	33	35.5	37.5	39.5	40.5	40	38	37.5	34	31

Table 3-12: Binary ORC System Monthly Average Power Production

Month	Jan	Feb	Mar	Apr	May	June	July	Aug	Sept	Oct	Nov	Dec
Ave. Power (kW)	725	649	546	427	326	244	205	217	296	323	492	648

A graphical representation of the Binary ORC System monthly average power production of a single well for the base case scenario can also be seen in Figure 3-12. Figure 3-13 shows the results of the monthly average system efficiency calculated for the Binary ORC System under base case operating conditions.

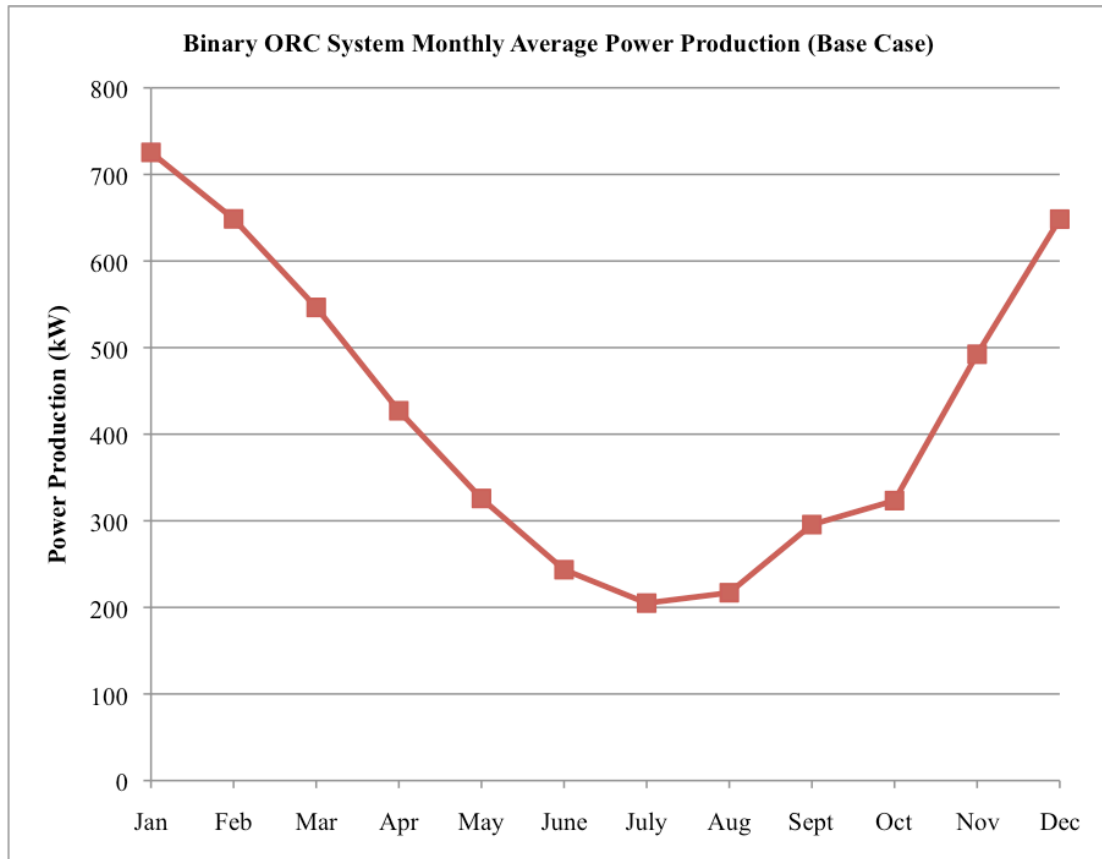


Figure 3-12: Base Case Binary ORC System Monthly Average Power Production for a Single Well.

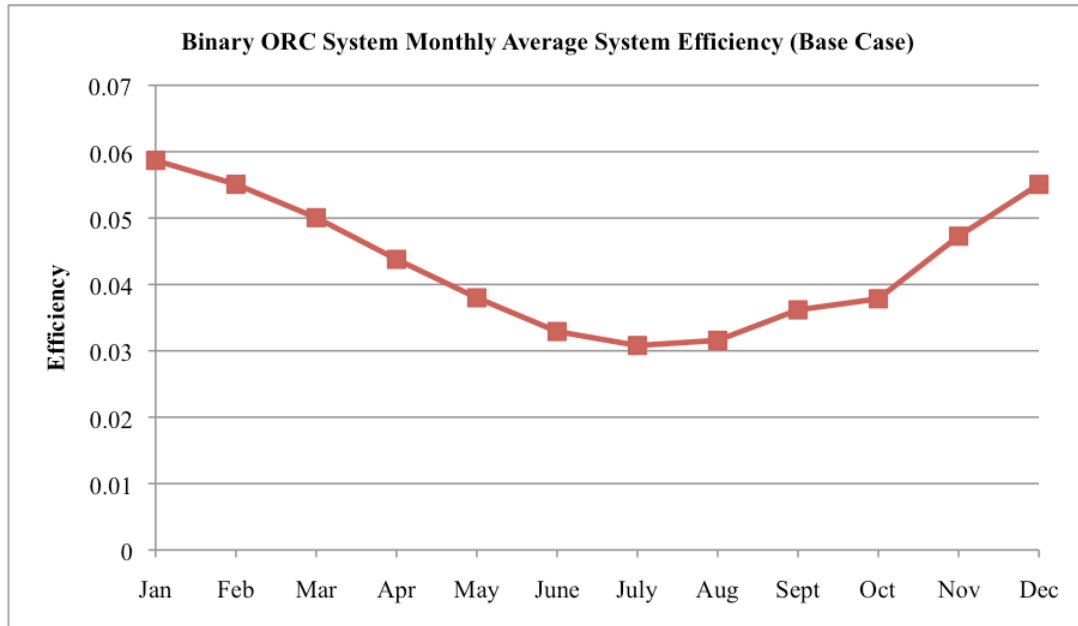


Figure 3-13: Base Case Binary ORC System Monthly Average System Efficiency.

Comparing the range of the values in Figures 3-12 and 3-13 to those of Figures 3-4 and 3-5, the discrepancy in system performance is apparent. In order to fully understand the magnitude of this discrepancy, however, simulations outside of the base case scenario need to be investigated.

The above in depth analysis clearly outlines the simulation of the base case scenario for the Binary ORC System. In the same way as the Direct Single-Loop System, the Binary ORC System was simulated to investigate power production under various sets of operating conditions. In order to be able to compare the performance of the two systems, the Binary ORC System was simulated with the same varying parameters as the Direct Single-Loop System. First, the reservoir temperature was fixed at 100°C with the mass flow rate being set to 70kg/s, 90kg/s, 120kg/s, and 140kg/s. Again for the higher mass flow rate simulations the injection pipe diameter was changed from 0.254m to 0.308m and the production pipe diameter was increased from 0.20m to 0.254m in order to

maintain the thermosyphon effect. The monthly average power production for a single well of the Binary ORC System under these varying mass flow rates can be seen in

Figure 3-14.

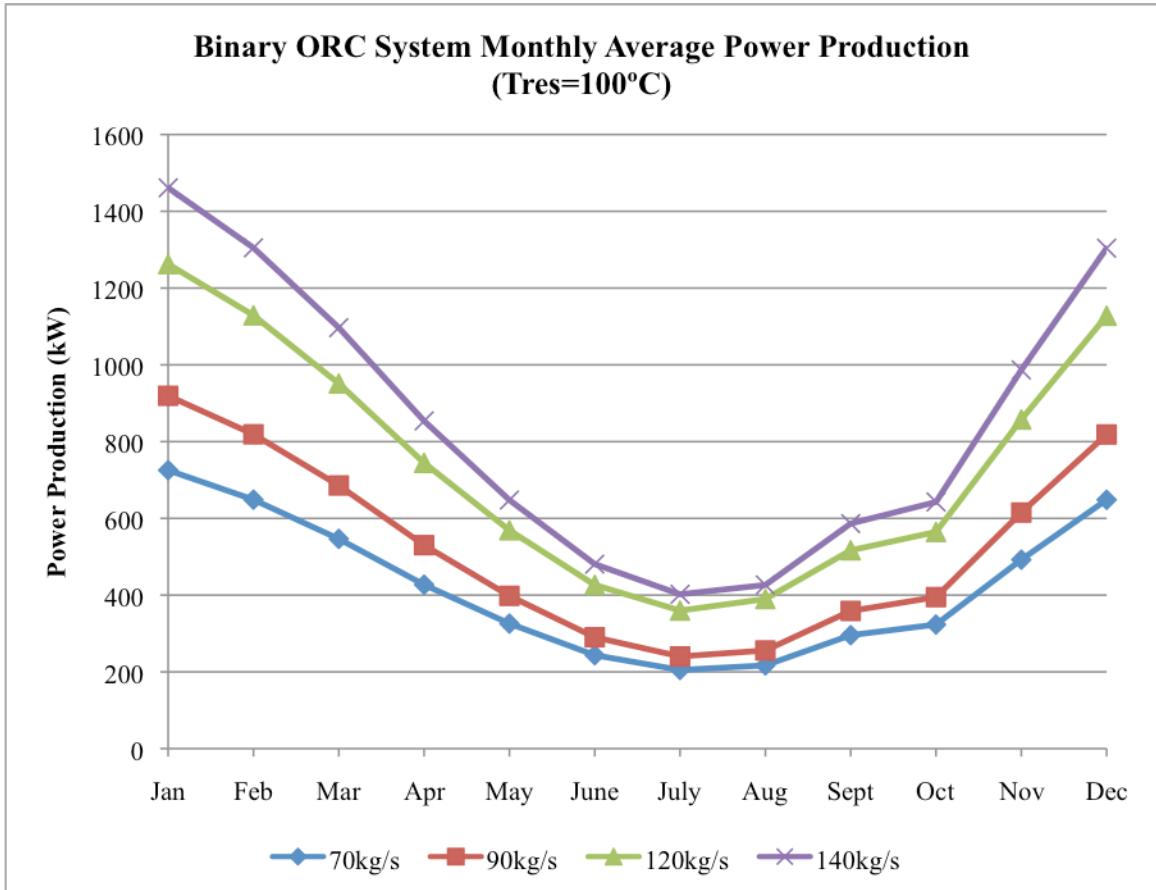


Figure 3-14: Binary ORC System Power Production for a Single Well with Varying Mass Flow Rate
 The same general trends can be seen in Figure 3-14 for the Binary ORC System as were seen for the Direct Single-Loop System in Figure 3-6. An overlaying comparison of the two systems can be seen in Figure 3-15.

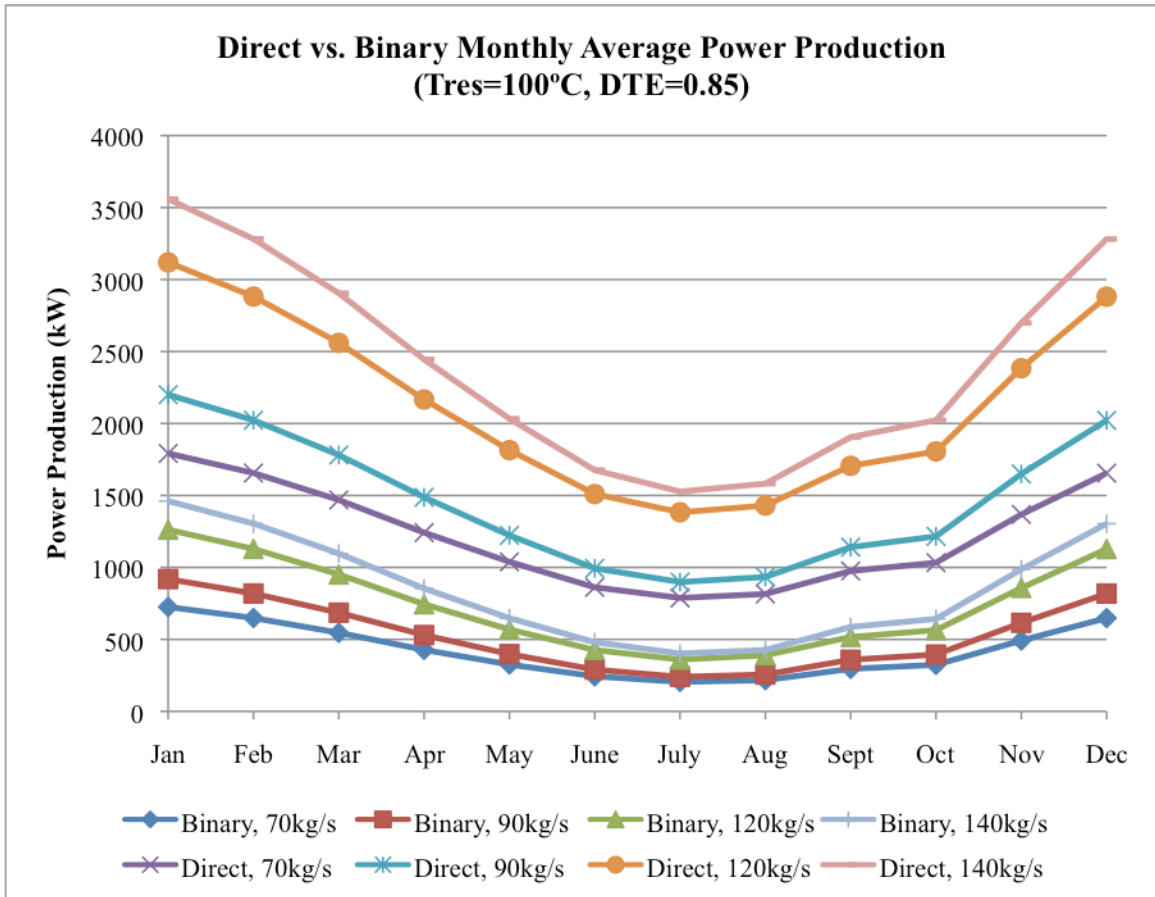


Figure 3-15: Overlay Plot of Direct and Binary System Power Production for a Single Well with Varying Mass Flow Rates

Figure 3-15 shows that in order for the Binary ORC System to approach the same level of power production as the Direct Single-Loop System, additional Binary ORC units would need to be installed in the same location. This provides insight into whether a Direct Single-Loop System or Binary ORC System is more suitable to a given site based on reservoir size and available geothermal heat capacity.

Simulations were also run fixing the mass flow rate at 70kg/s while changing the reservoir temperature to values of 100°C, 125°C, and 150°C. The monthly average power production for a single well under these simulations is presented in Figure 3-16.

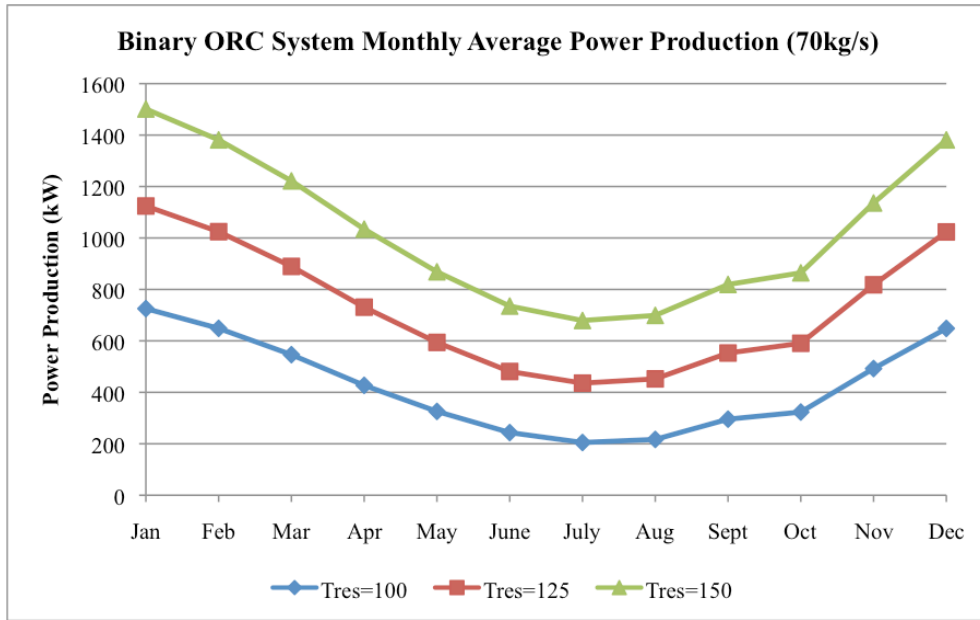


Figure 3-16: Binary ORC System Power Production for a Single Well with Varying Reservoir Temperature. Again similar trends can be seen in Figure 3-16 as are seen in Figure 3-7. An overlaying plot of the monthly average power production for the two systems is seen in Figure 3-17.

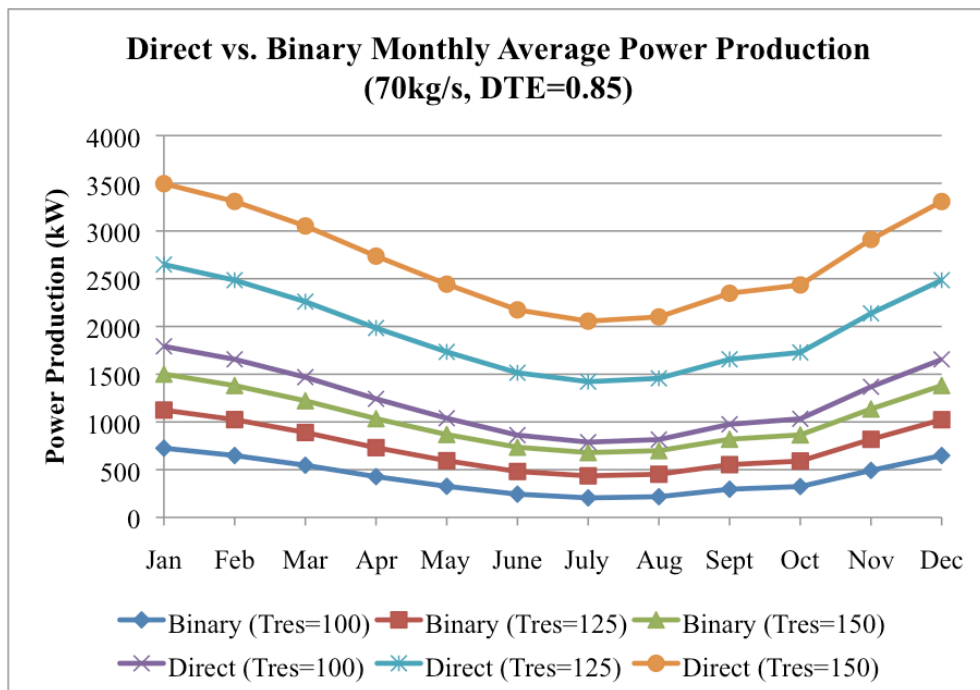


Figure 3-17: Overlay Plot of the Direct and Binary System Power Production for a Single Well with Varying Reservoir Temperature.

Similar conclusions can be drawn from Figure 3-17 as in Figure 3-15 and helps to identify site-specific qualifications of the two systems.

3.4. Accounting for System Losses through Exergy Analysis

A second law analysis was conducted in order to investigate and locate inefficiencies within the design of the two geothermal systems. This was done through an exergy analysis to identify the loss of potential energy due to irreversibilities in the individual components of both the Direct Single-Loop System and the Binary ORC System. The method used to conduct the second law analysis in this study follows the method provided by [28]. The exergetic losses were calculated by finding the specific flow exergy of each of the individual state points identified in the previous sections of this chapter. Equation (3-4-1) shows the formula used for calculating the specific flow exergy as

$$e_f = h - h_o - T_o(s - s_o) + \frac{V^2}{2} + gz \quad (3-4-1)$$

In Equation (3-4-1), reference values are denoted with the subscript o. The specific exergy flow values for the specific state points were calculated using the enthalpy and entropy values and using the ambient temperature as the reference temperature. To further simplify the calculations involved, the kinetic and potential energy portions of Equation (3-4-1) are assumed to be negligible, resulting in

$$e_f = h - h_o - T_o(s - s_o), \quad (3-4-2)$$

the only exceptions being the injection and production wells, where it is necessary to incorporate the potential energy effects due to the large vertical pipe lengths involved. Given that the simulations for the two systems were done under steady-state conditions, a steady-state form of the exergy rate balance equation results in

$$0 = \sum_j \left(1 - \frac{T_o}{T_j}\right) \dot{Q}_j - \dot{W}_j + \sum_i \dot{m}_i e_{fi} - \sum_e \dot{m}_e e_{fe} - \dot{E}_d \quad (3-4-3)$$

Furthermore, many components of the two systems were assumed to operate under adiabatic conditions with no work being done to or by the control volume. With these assumptions, Equation (3-4-3) can be rearranged to find the rate of exergy destruction, or the losses due to irreversibilities, and is represented by

$$\dot{E}_d = \dot{m}(e_{f1} - e_{f2}) \quad (3-4-4)$$

This equation was largely used to find the losses in the individual components of the two systems, with the exception of the turbine, pump, and reservoir, which incorporated the work and heat transfer terms from Equation (3-4-3). In this equation, the subscripts 1 and 2 denote the inlet and outlet of the flow through a given component. The total exergy destruction through the heat exchanger and condensers was calculated by taking the difference in exergy destruction of the flow through either side of the heat exchanger or condenser.

Due to the fact that the brine properties of the functions in EES could not be set to the same reference standards as the rest of the functions, the change in properties for the condensers had to be calculated separately. First, a temperature differential of 5°C between the ethylene-glycol and the condensed CO₂ or isobutane was assumed. This temperature was then used to find the specific heat capacity of the ethylene-glycol [29] calculated by M. Conde Engineering. These values were verified with the ASHRAE Fundamentals Handbook [24] to ensure they used the same ASHRAE reference standard as the other fluids. Assuming an effectiveness of 0.80 for the condenser, the exiting temperature of the ethylene-glycol was calculated in the same manner as for the heat exchanger. With the specific heat capacity and temperature differential known, the change in enthalpy for the ethylene-glycol was calculated. The mass flow rate of the ethylene-glycol could then be calculated using the heat transfer through the condenser. Given that the condensing pressure was assumed to be constant and the change in temperature for the ethylene-glycol was found, the change in entropy was next calculated using

$$s_2 - s_1 = c \ln\left(\frac{T_2}{T_1}\right) \quad (3-4-5)$$

With the mass flow rate, change in enthalpy, and change in entropy of the ethylene-glycol found, the exergy destruction through the tower side of the condensers could be calculated and the total exergy destruction through the condensers could be found.

The efficiency of the systems could be improved by focusing on optimizing the design constraints around the individual components with the largest exergy losses. By

identifying these components, it can be seen which components would require the most intensive design considerations, what impacts those considerations would have on the power production of the systems, and whether or not the additional power production would be worth the expenses involved in achieving those design considerations.

The above set of equations was used to perform a second law analysis for both the Direct Single-Loop System and the Binary ORC System. Analysis was first conducted for the Direct Single-Loop System. Similarly to the analysis of the power production, in order to get a range of the potential losses throughout the year, the exergy analysis was done for the months of July and January. Tables 3-13 and 3-14 below show the losses of the individual components for the Direct Single-Loop System.

Table 3-13: Exergy Destruction of the Direct Single-Loop System Components in July

Ed (kW)	Turbine	Condenser	Return	Supply	Injection	Production	Reservoir	Total
July	137	61	1.770	59.4	14	112	2951	3336

Table 3-14: Exergy Destruction of the Direct Single-Loop System Components in January

Ed (kW)	Turbine	Condenser	Return	Supply	Injection	Production	Reservoir	Total
Jan	311	120	0.713	99.9	10	112	6553	7206

From the above tables, it can be seen that heating the CO₂ in the thermal reservoir provides the largest losses due to irreversibilities. The exergy destruction in the reservoir represents the extra power that could be provided were the heat transfer process reversible. Since all available energy for use by the system is provided by the reservoir, it makes sense that the largest exergy destruction occurs in the reservoir as well. Outside of this, the largest exergy destruction is present in the turbine. This shows the potential additional energy production that would be available were it possible to obtain a perfectly

isentropic turbine. It also shows the importance of turbine design in terms of maximizing the isentropic turbine efficiency.

Next, the second law losses were found for the Binary ORC system. Again, an exergy analysis was conducted for the months of July and January to get a range of the potential losses throughout the year for comparison with the Direct Single-Loop System. Tables 3-15 and 3-16 show the exergetic losses of the Binary ORC System for the months of July and January, respectively.

Table 3-15: Exergy Destruction of the Binary ORC System Components in July

Ed (kW)	Turbine	Pump	Heat Ex.	Exp. Valve	Cond. (Iso)	Cond. (CO2)
July	39.5	0.018	125	549	35	23
Ed (kW)	Return	Supply	Injection	Production	Reservoir	Total
July	1.770	59.4	14	112	2951	3908

Table 3-16: Exergy Destruction of the Binary ORC System Components in January

Ed (kW)	Turbine	Pump	Heat Ex.	Exp. Valve	Cond. (Iso)	Cond. (CO2)
Jan	123	0.936	358	873	60	54
Ed (kW)	Return	Supply	Injection	Production	Reservoir	Total
Jan	0.713	99.9	10	112	6553	8245

The exergy destruction in the return line, supply line, injection well, production well, and the reservoir of the Binary ORC System were found to be identical to those of the Direct Single-Loop System, as should be expected since these components deal with the process of extracting heat from the geologic formation and not its incorporation into actual power production. Comparing the total exergy destruction of the two condensers in the Binary ORC System to the exergy destruction of the condenser in the Direct Single-Loop System shows similar values. This indicates that there are not considerable changes to the exergetic losses in the condensing processes of the Binary ORC System, but rather that the exergy destruction is shifted between the two condensers based on time of year. Comparing the exergy destruction between the turbines of the two systems shows

considerably larger losses in the Direct Single-Loop System. This should be expected, as the Direct Single-Loop System produces considerably more power and deals with larger thermodynamic property changes across its turbine. The exergy destruction in the pump in the Binary ORC system is largely negligible and relatively constant year round with fluctuations due to changes in the isobutane mass flow rate and pressure drop through the system.

The largest additional exergetic losses between the two systems are present in the CO₂ to isobutane heat exchanger and the expansion valve. The losses through the heat exchanger in the Binary ORC System exceed those of the turbine in the Direct Single-Loop System. This alone shows how the incorporation of a heat exchanger can decrease the efficiency of the system. The expansion valve accounts for the largest exergy destruction of the additional components in the Binary ORC System. This is due to the fact that the expansion valve acts as a pressure release for the pressure drop that would otherwise be experienced across the turbine in the Direct Single-Loop System.

Comparing the exergy destruction of the heat exchanger and expansion valve in the Binary ORC System to the turbine in the Direct Single-Loop System shows just how much of the potential usable energy is lost by changing from the Direct Single-Loop System to the Binary ORC System. This helps explain why there is such a large energy production gap between the two systems. It also shows why optimization of heat exchanger performance is paramount to the effectiveness of the Binary ORC System.

Previous studies [17,30,31] analyzing the second law performance of like cycles show similar trends in terms of component contribution to the overall exergy destruction. The main differences arise from the fact that [30] analyzes a compression cycle as opposed to a power cycle, while [31] shows the analysis of a Binary ORC System with an air-cooled condenser instead of a cooling tower. The second law analysis conducted by [17] largely agrees with the trends of the results obtained in this study. In terms of improving the Binary ORC System's performance, the clear area to focus on would be the expansion valve. If some additional design considerations were able to utilize even a portion of the losses through the expansion valve for additional energy production, they could significantly improve the Binary ORC System's overall efficiency, though these solutions would likely encounter the same problems surrounding the turbine in the Direct Single-Loop system.

4. Discussion and Conclusion

4.1. Comparison of Conventional Systems to CO₂ Systems

The research conducted in this study was done with the intention to investigate the potential for using CO₂ as either a working fluid or heat transfer fluid for geothermal power production, where it is used as a working fluid in the Direct Single-Loop System to perform actual turbine work and as a heat transfer fluid in the Binary ORC System to transfer the thermal energy to a secondary power cycle. In order to validate the use of CO₂ in geothermal systems, the potential power production of the two systems investigated in this study needs to be compared to the power production of current conventional geothermal systems. The potential for small-scale geothermal power plants

has been under investigation for a long time. A study conducted by NREL in 2000 [32] investigated the potential for geothermal power production of numerous locations in the Western United States using small-scale binary plants. All of the sites under investigation had resource temperatures below 150°C with some temperatures as low as 85°C. The study found the potential for geothermal power plants ranging in size from 249kW to 1MW, with a per well power production ranging from approximately 100kW to 900kW depending on reservoir temperature and mass flow rate. The mass flow rates of these plants ranged from 10kg/s to 90kg/s, depending on the pipe diameter. The power plant performance was generally investigated for locations with reservoir depths of less than 1km, though a few sites looked at reservoirs as deep as 3.5km. In Turkey, a study was done to investigate the potential power production of binary systems in the Simav region [33]. The results showed that the Turkey plant had the potential to generate approximately 1.1MW from a single well. While this is slightly more than the potential power production of the Binary ORC System in this study, this is largely due to the fact that the resource temperature is 162°C with a very shallow reservoir depth of 457m. Conventional geothermal systems installed worldwide [34-37] have been found to have a wide range of potential power production. Small-scale single-well binary power plants for use in areas with low geothermal resource temperatures were found to range in size from 180kW to 3.8MW. This includes an installation in Chena Hot Springs, Alaska, where two 200kW single-well binary units were installed. The design chosen for the Chena Hot Springs plant was taken from a study done in 2005 [38]. The site intends to install a total of 4 units for a total of 800kW of power production. These studies give a good approximation for the range of power production of currently installed single-well

binary power plants. The installations at the lower end of the power production range were generally at much shallower depths with lower reservoir temperatures, while the installations at the upper end were generally at much deeper depths with reservoir temperatures near 150°C. Larger plants constructed using multiple binary units were found to generate as much as 25MW, as in the case of the Richard Burdette Geothermal Plant in Nevada, where a per well production rate of 5MW was obtained [39], though this is in a region with slightly higher reservoir temperatures. Still larger direct plants, using flash technologies where high pressure steam is separated from brine, were found in areas with much larger geothermal resource temperatures generating as much as 110MW of electricity. Two such units installed in Indonesia at the Wayang Windu geothermal fields, where reservoir temperatures exceed 250°C, were found to have a gross power production of 227MW [40] with an average per well production rate of approximately 13MW. While these two geothermal plants operate under conditions far exceeding those simulated in this research, they are still worth noting as they represent two of the largest geothermal installations in the world.

To compare the potential power production of the Direct Single-Loop and Binary ORC Systems to that of conventional systems under comparable operating conditions, a range of power production for the two systems was determined from the results of the simulations run for all variations of the parameters discussed in the previous chapters. This accounts for all combinations of the varying reservoir temperatures and CO₂ mass flow rates. Three different ranges of power production were found for the simulations of the two systems, one for the Binary ORC System and one for each of the turbine

efficiency simulations of the Direct Single-Loop System. For the Binary ORC System, this resulted in a range of 205kW to 3.0MW of potential power production from a single well. For the Direct Single-Loop System, the simulation with turbine efficiency of 0.85 resulted in potential per well power production ranging from 788kW to 7.0MW while the simulation with turbine efficiency of 0.50 resulted in potential per well power production ranging from 464kW to 4.1MW.

While these simulations were run under ideal assumptions, the range of potential power production for the various potential site conditions still provides a good first estimate of what sort of power production could be expected when coupling geothermal energy production with CO₂ sequestration. Comparing the simulation results to the range of plant sizes already installed worldwide, the potential for geothermal energy production using CO₂ is apparent. Based on the site in question, an appropriate decision could be made on whether the Direct Single-Loop System or Binary ORC System would be more suitable for installation and could easily match the power production of currently installed systems. In many cases, an installation of either of the simulated systems could surpass the expected power production of a conventional system, since either the resource temperatures are lower or the reservoir depths are greater for the simulations than for the installed systems. While the maximum power production of the simulations would not likely be attainable due to seasonal variability of the pressure drop across the turbine, with appropriate design considerations a large enough portion of the power production could still be met. Such considerations could include the use of a multi-stage turbine or installation of multiple turbines in series. With all of this taken into account, using CO₂

for geothermal power production is clearly competitive with conventional systems, and given that the simulations were run with lower resource temperatures, the implications of using CO₂ to expand the scope of geothermal power production are strong.

4.2. Choosing an Ideal System for CO₂ Geothermal Power Production

Choosing an ideal system for geothermal power production using CO₂ is largely dependent on the site in question. Depending on the size, temperature, and pressure of the geothermal reservoir, as well as the mass flow rate of the CO₂ and the power demand of the region, both the Direct Single-Loop System and the Binary ORC System could be suitable choices. Under base case operating conditions, it is likely that the Direct Single-Loop System would be a better choice for installation. The reason for this is because the Binary ORC System under these operating conditions does not have significant power production year round. Thus, unless the system was only to be used in the winter months for supplemental power for heating, or unless the required power production was sufficiently low, the Direct Single-Loop System is the superior choice. Installing a system under these conditions could turn out to be an expensive endeavor, however, depending on the costs associated with designing a custom turbine capable of handling the pressure drop and phase change that it would encounter. This could mean that installing a system under these operating conditions would not be feasible without some kind of government incentive program similar to those associated with installation of wind turbines or solar panels. However, this issue diminishes as the reservoir temperature and CO₂ mass flow rate increase. Choosing a system then becomes far more dependent on the power demand of the region and the size of the reservoir, as well as

whether it is more expensive to install a larger number Binary ORC units to meet the same power production provided by fewer Direct Single-Loop units. In either case, both systems are capable of providing the necessary power to meet the demands of a given region under the operating conditions discussed in this paper and an intelligent decision can be made about which system is the ideal choice based on the results available in the appendices.

4.3. Next Steps and Additional Considerations for Expanding Research

The ideal assumptions made in this analysis restrict the results and a more refined model would likely yield more accurate projections of the potential power production of the systems. There are many considerations that could be taken into account that could help improve the model and provide more accurate results. The analysis conducted in this research used assumptions such as constant pressure through the heat exchangers and condensers, as well as ideal condensing temperatures and pressures, which would not likely be reached without using unnecessarily large condensers. The system was also assumed to operate at steady state, without accounting for the amount of time it would take for the system to reach steady state. Prior to this, there would be heat losses through both the injection and production well walls, which were not accounted for. A pump would be required to circulate the CO₂ until the heat losses through these walls became negligible, at which point a thermosyphon could be established. Another consideration that could be used to expand this research would be to investigate how continuous sequestration of CO₂ during system operation would affect the performance of the system, and what additional condensing and pumping considerations would need to be

met in order to match the injection pressures and mass flow rates of typical sequestered CO₂, which could have adverse effects on the thermosyphon.

In regards to the thermosyphon, there are many aspects of the systems that are either affected by it or could potentially have effects on it. The degree to which the thermosyphon is established and the changes it might go through throughout the year need to be investigated. Installation of a pilot plant could be used to measure the effect of the thermosyphon. If the ambient air temperature is found to have a significant impact on the thermosyphon, the mass flow rate through the CO₂ loop could vary throughout the year. This could have a significant impact on the yearly power production, indicating that the use of a pump may be necessary during summer operation. In addition to this, the effects of the lifespan of the geothermal reservoir need to be investigated. Over time the geothermal resource available to the plant diminishes and the reservoir temperature drops. This would also affect the thermosyphon and reduce the power generated by the plant unless a pump was used to increase the heat extraction rate from the reservoir, which would accelerate the reservoir depletion.

As stated in the second law analysis, the Binary ORC system contains large losses over the Direct Single-Loop system due to the incorporation of a heat exchanger and expansion valve. The expansion valve losses clearly show a missed opportunity for additional energy production. However, installation of a turbine in this location would suffer from the same difficulties encountered in the Direct Single-Loop system. Installation of other alternative power producing devices, such as scroll or rotary screw

expanders, could be considered though. Previous studies [41-44] have shown these devices to be suitable for use with ORC systems. The isentropic efficiencies have been found to vary from 0.20-0.60, with pressure ratios of around 2:1. These pressure ratios are similar to those found across the expansion valve for summer operation, but only about half of what is experienced during winter operation. The mass flow rate of the CO₂ in the Binary ORC system, however, is significantly greater than the mass flow rate of these previous studies, and its effect on the forces experienced by the expander would need to be taken into account when designing or sizing the expander. With appropriate design considerations, an expander or series of expanders could be used in place of the expansion valve to generate additional power.

All of these considerations could be used to improve the simulations. Reducing the number of ideal assumptions in the system would provide a more accurate level of power production. Investigation of the ramp up time necessary to reach steady state would show how long the system would need to run before it reaches the necessary operating conditions to maximize power production. An investigation of the behavior of the thermosyphon would help to show more realistic pumping requirements and under what conditions they would be necessary for additional energy production. An investigation of the lifespan of the geothermal reservoir and its effect on the thermosyphon would help identify an appropriate time to change to an alternate source to meet the power generation provided by the geothermal system. Incorporating alternative components, such as expanders, could also be used to increase power production. In these ways, this research can be expanded upon to discover the full potential of combining CO₂ sequestration with

geothermal energy production and potentially bring it closer to commercial implementation.

5. References

- [1] International Energy Statistics, Coal Reserve Index, Energy Information Administration, U.S. Department of Energy, www.eia.gov/cfapps/ipdbproject/IEDindex3.cfm, accessed 27, February, 2010.
- [2] Brown, D. W., 2000, “ A Hot Dry Rock Geothermal Energy Concept Utilizing Supercritical CO₂ Instead of Water,” Proc. Twenty-Fifth Workshop on Geothermal Reservoir Engineering, Stanford University, Stanford, CA, pp.233-238.
- [3] Pruess, K., and Azaroual, M., 2006, “On the Feasibility of Using Supercritical CO₂ as Heat Transmission Fluid in an Engineering Hot Dry Rock Geothermal System,” Proc. Thirty-First Workshop on Geothermal Reservoir Engineering, Stanford University, Stanford, CA.
- [4] Pruess, K., 2008, “On the Production Behavior of Enhanced Geothermal Systems with CO₂ as Working Fluid.” Lawrence Berkeley National Laboratory, University of California, Berkeley, CA.
- [5] Henderseon, J.R., Barton, D. J., Foulger, G. R., 1999, “Fractal clustering of induced seismicity in The Geysers geothermal area, California,” *Geophysical Journal International*, 139, pp.317-324.
- [6] Tadokoro, K., Nishigami, K., Ando, M., Hirata, N., Iidaka, T., Hashida, Y., Shimuzaki, K., Ohmi, S., Kano, Y., Koizumi, M., Matsuo, S., Wada, H., 2001, “Seismicity changes related to a water injection experiment in Nojima Fault Zone,” *The Island*, 10, pp.235-243.

- [7] Baisch, S., Harjes, H.-P., 2003, "A model for fluid-injection-induced seismicity at KTB, Germany," *Geophysical Journal International*, 152, pp.160-170
- [8] Bourouis, S., Bernard, P., 2007, "Evidence for coupled seismic and aseismic fault slip during water injection in the geothermal site of Soultz (France), and implications for seismogenic transients," *Geophysical Journal International*, 169, pp.723-732.
- [9] Shapiro, S.A., Dinske, C., 2009, "Fluid-induced seismicity: Pressure diffusion and hydraulic fracturing," *Geophysical Prospecting*, 57, pp.301-310.
- [10] Blackwell, D. D., Richards, M., 2004, *Geothermal Map of North America*, American Association of Petroleum Geologists (AAPG), Dallas, TX, April 17-20, 2004.
- [11] Steadman, E. N., Daly, D. J., de Silve, L. L., Harju, J. A., Jensen, M. D., O'Leary, E. M., Peck, W. D., Smith, S. A., Sorensen, J. A., 2006, "Plains CO2 Reduction (PCOR) Partnership (Phase I) Final Report," Final Report, Energy & Environmental Research Center, University of North Dakota, Grand Forks, ND.
- [12] Kuehn, T. H., Ramsey, J. W., Threlkeld, J. L., 1998, *Thermal Environmental Engineering Third Edition*, Prentice Hall, pp.723-725, App. B.
- [13] Kleitz, A., Dorey, J. M., 2004, "Instrumentation for wet steam," *Proc. Institution of Mechanical Engineering Part C: Journal of Mechanical Engineering*, 218, pp.811-842.
- [14] Kreitmeier, F., Greim, R., Congin, F., Faelling, J., 2005, "Experimental and numerical analysis of relaxation processing in LP steam turbines," *Proc. Institution of Mechanical Engineering Part C: Journal of Mechanical Engineering*, 219, pp.1411-1436
- [15] Hesketh, J. A., Walker, P. J., 2005, "Effects of wetness in steam turbines," *Proc. Institution of Mechanical Engineering Part C: Journal of Mechanical Engineering*, 219, pp.1301-1314.

- [16] Spycher, N., Pruess, K., Ennis-King, J., 2003, "CO₂-H₂O mixtures in the geological sequestration of CO₂. I. Assessment and calculation of mutual solubilities from 12 to 100°C and up to 600 bar," *Geochimica et Cosmochimica Acta*, Vol. 67, No. 16, pp.3015-3031.
- [17] Lukawski, M., 2009, "Design and Optimization of Standardized Organic Rankine Cycle Power Plant for European Conditions," Master's Thesis, The School for Renewable Energy Science, Akureyri, Iceland.
- [18] Hettiarachchi, H. D. M., Golubovic, M., Worek, W. M., Ikegami, Y., 2007, "Optimum Design Criteria for an Organic Rankine Cycle Using Low-Temperature Geothermal Heat Sources," *Energy*, 32, pp.1698-1706.
- [19] Hettiarachchi, H. D. M., Golubovic, M., Worek, W. M., Ikegami, Y., 2007, "A Study of the Kalina Cycle System 11 (KCS-11) for Low-Temperature Heat Sources," *ASME Journal of Energy Resources and Technology*, 129, 3, pp.243-247.
- [20] Borsukiewicz-Gozdur, A., Nowak, W., 2007, "Comparative analysis of natural and synthetic refrigerants in application to low temperature Clausius-Rankine cycle," *Energy*, 32, pp. 344-352.
- [21] Saleh, B., Koglbauer, G., Wendland, M., Fischer, J., 2007, "Working fluids for low-temperature organic Rankine cycles," *Energy*, 32, pp.1210-1221.
- [22] Franco, A., Villani, M., 2009. "Optimal design of binary cycle power plants for water-dominated, medium temperature geothermal fluids," *Geothermics*, 38, pp.379-391.
- [23] Frick, S., Kaltschmitt, M., Schröder, G., 2010, "Life cycle assessment of geothermal binary power plants using enhanced low-temperature reservoirs," *Energy*, 35, 5, pp.2281-2294.

- [24] 2009, *2009 ASHRAE Handbook: Fundamentals*, American Society of Heating Refrigerating and Air-Conditioning Engineers, Inc, Atlanta, GA, “Chap. 30: Thermophysical Properties of Refrigerants”, “Chap. 31: Physical Properties of Secondary Coolants (Brines).”
- [25] Panton, R. L., 2005, *Incompressible Flow*, John Wiley & Sons, Inc, Hoboken, NJ, pp.126-132, “Chap. 7.2: Mechanical Energy, Head Loss, and Bernoulli Equations.”
- [26] Incropera, F. P., Dewitt, D. P., 2002, *Fundamentals of Heat and Mass Transfer*, John Wiley & Sons, Inc, New York, NY, pp.539-556,659-665, “Chap. 9: Free Convection”, “Chap. 11: Heat Exchangers.”
- [27] Faculty of Engineering, “Pipe Friction Chart Applicable to Circular Pipes Running Full,” Glasgow College of Nautical Studies,
www.engineeringtoolbox.com/docs/documents/618/pipefric.pdf, accessed 5 April, 2010.
- [28] Moran, M. J., Shapiro, H. N., 2000, *Fundamentals of Engineering Thermodynamics*, John Wiley & Sons, Inc, New York, NY, pp.250, 332-346, “Chap. 6: Using Entropy”, “Chap. 7: Exergy (Availability) Analysis.”
- [29] M. Conde Engineering, 2002, “Thermophysical Properties of Brines,” www.mrc-eng.com/Downloads/Brine%20Properties.pdf, accessed 8 November, 2010.
- [30] Liang, H., Kuehn, T. H., 1988, “Irreversibility Analysis of a Water to Water Mechanical Compression Heat Pump,” Proc. The Winter Annual Meeting of the American Society of Mechanical Engineers, Chicago, IL, pp.31-36.
- [31] Kanoglu, M., Bolatturk, A., 2008, “Performance and parametric investigation of a binary geothermal power plant by exergy,” *Renewable Energy*, 33, pp.2366-2374.

- [32] Gawlik, K., Kutscher, C., 2000, "Investigation of the Opportunity for Small-Scale Geothermal Power Plants in the Western United States," National Renewable Energy Laboratory (NREL), Golden, CO.
- [33] Köse, R., 2005, "Research on the generation of electricity from the geothermal resources in Simav region, Turkey," *Renewable Energy*, 30, pp.67-79
- [34] Hammons, T. J., 2004, "Geothermal Power Generation Worldwide: Global Perspective, Technology, Field Experience, and Research and Development," *Electric Power Components and Systems*, 32, pp.529-553.
- [35] Lund, J. W., 2004, "100 Years of Geothermal Power Production," *Renewable Energy World*, vol. 7, no. 4, pp.11-19.
- [36] Lund, J. W., 2007, "Characteristics, Development and Utilization of Geothermal Resources," *Geo-Heat Center Quarterly Bulletin*, vol. 28, no. 2, (June), Klamath Falls, OR, pp. 1-9.
- [37] Bertani, R., 2007, "World Geothermal Generation in 2007," *Proc. European Geothermal Congress 2007*, pp.1-11, Unterhaching, Germany, May 20 – June 1.
- [38] Brasz, J. J., Biederman, B. P., Holdmann, G., 2005, "Power Production from a Moderate-Temperature Geothermal Resource," *GRC Annual Meeting*, Reno, NV, September 25-28.
- [39] Fleischmann, D. J., 2006, "Geothermal Resource Development in Nevada -2006," *Geothermal Energy Association*, <http://www.geothermalenergy.org/reports/Geothermal%20Resource%20Development%20in%20Nevada%202006.pdf>, accessed 1 July, 2011.

- [40] Mulyadi, Ashat, A., 2011, "Reservoir Modeling of the Northern Vapor-Dominated Two-Phase Zone of the Wayang Windu Geothermal Field, Java, Indonesia," Proc. Thirty-Sixth Workshop on Geothermal Reservoir Engineering, Stanford University, Stanford, CA.
- [41] Hiwata, A., Ikeda, A., Morimoto, T., Kosuda, O., Matsui, M., 2009, "Axial and Radial Force Control for a CO₂ Scroll Expander," HVAC&R Research, Vol. 15, No. 4, pp.759-770.
- [42] Matsui, M., Ogata, T., Wada, M., Hasegawa, H., 2009, "Development of the High-Efficiency Technology of a CO₂ Two-Stage Rotary Expander," HVAC&R Research Vol. 15, No. 4, pp.743-758.
- [43] Yang, B., Peng, PhD X., Sun, S., Guo, PhD B., Xing, PhD Z., 2009, "Study of a Rotary Vane Expander for the Transcritical CO₂ Cycle Part I: Experimental Investigation," HVAC&R Research, Vol. 15, No. 4, pp.673-688.
- [44] Jia, X., Yang, B., Peng, PhD X., Zhang, B., 2009, "Study of a Rotary Vane Expander for the Transcritical CO₂ Cycle Part II: Theoretical Modeling," HVAC&R Research, Vol. 15, No. 4, pp.689-707.

Appendix A: Direct Single-Loop System Simulation Results

A.1: Direct Single-Loop System Monthly Average Power Production Tables

TableA-1: Direct Single-Loop System Monthly Average Power Production (DTE=0.85) at 2.5km Depth

Direct Single-Loop System Power Production (DTE=0.85)					
Well Depth	2.5km				
CO2 Mass Flow		70 kg/s	90 kg/s	120 kg/s	140 kg/s
Tres		100°C			
Jan		1792 kW	2200 kW	3119 kW	3559 kW
Feb		1656 kW	2023 kW	2882 kW	3282 kW
Mar		1469 kW	1781 kW	2560 kW	2905 kW
Apr		1242 kW	1487 kW	2167 kW	2445 kW
May		1039 kW	1223 kW	1815 kW	2033 kW
June		862.0 kW	994.0 kW	1510 kW	1676 kW
July		788.3 kW	898.5 kW	1383 kW	1527 kW
Aug		815.6 kW	933.9 kW	1430 kW	1582 kW
Sept		975.3 kW	1141 kW	1706 kW	1905 kW
Oct		1033 kW	1216 kW	1806 kW	2023 kW
Nov		1368 kW	1649 kW	2384 kW	2699 kW
Dec		1655 kW	2022 kW	2881 kW	3281 kW
Total Power		14695 kW	17568 kW	25643 kW	28917 kW
Tres		125°C			
Jan		2649 kW	3251 kW	4615 kW	5268 kW
Feb		2485 kW	3039 kW	4332 kW	4937 kW
Mar		2260 kW	2747 kW	3943 kW	4480 kW
Apr		1984 kW	2389 kW	3465 kW	3921 kW
May		1734 kW	2064 kW	3032 kW	3413 kW
June		1515 kW	1780 kW	2652 kW	2969 kW
July		1422 kW	1660 kW	2493 kW	2782 kW
Aug		1457 kW	1705 kW	2552 kW	2852 kW
Sept		1656 kW	1963 kW	2896 kW	3255 kW
Oct		1728 kW	2056 kW	3021 kW	3400 kW
Nov		2137 kW	2588 kW	3730 kW	4231 kW
Dec		2485 kW	3038 kW	4331 kW	4935 kW
Total Power		23512 kW	28280 kW	41062 kW	46443 kW
Tres		150°C			
Jan		3496 kW	4283 kW	6102 kW	6961 kW
Feb		3310 kW	4042 kW	5780 kW	6583 kW
Mar		3053 kW	3709 kW	5335 kW	6062 kW
Apr		2737 kW	3297 kW	4786 kW	5419 kW
May		2443 kW	2915 kW	4276 kW	4821 kW
June		2174 kW	2565 kW	3809 kW	4272 kW
July		2056 kW	2412 kW	3605 kW	4033 kW
Aug		2100 kW	2469 kW	3681 kW	4123 kW
Sept		2348 kW	2792 kW	4112 kW	4628 kW
Oct		2435 kW	2905 kW	4263 kW	4805 kW
Nov		2912 kW	3525 kW	5091 kW	5776 kW
Dec		3309 kW	4041 kW	5779 kW	6582 kW
Total Power		32373 kW	38955 kW	56619 kW	64065 kW

Table A-2: Direct Single-Loop System Monthly Average Power Production (DTE=0.85) at 3.1km Depth

Direct Single-Loop System Power Production (DTE=0.85)					
Well Depth 3.1km					
CO2 Mass Flow		70 kg/s	90 kg/s	120 kg/s	140 kg/s
Tres		100°C			
Jan		1584 kW	1941 kW	2758 kW	3145 kW
Feb		1459 kW	1779 kW	2541 kW	2891 kW
Mar		1289 kW	1558 kW	2246 kW	2545 kW
Apr		1082 kW	1290 kW	1890 kW	2127 kW
May		898.3 kW	1051 kW	1571 kW	1755 kW
June		739.5 kW	845.5 kW	1297 kW	1434 kW
July		673.5 kW	760.1 kW	1183 kW	1300 kW
Aug		697.9 kW	791.7 kW	1225 kW	1350 kW
Sept		841.2 kW	977.4 kW	1473 kW	1639 kW
Oct		893.6 kW	1045 kW	1563 kW	1745 kW
Nov		1196 kW	1438 kW	2087 kW	2358 kW
Dec		1459 kW	1778 kW	2540 kW	2890 kW
Total Power		12813 kW	15255 kW	22374 kW	25179 kW
Tres		125°C			
Jan		2413 kW	2970 kW	4203 kW	4802 kW
Feb		2262 kW	2774 kW	3941 kW	4496 kW
Mar		2055 kW	2505 kW	3583 kW	4076 kW
Apr		1802 kW	2177 kW	3144 kW	3563 kW
May		1574 kW	1880 kW	2749 kW	3099 kW
June		1374 kW	1622 kW	2404 kW	2695 kW
July		1291 kW	1513 kW	2259 kW	2526 kW
Aug		1322 kW	1554 kW	2313 kW	2589 kW
Sept		1502 kW	1788 kW	2625 kW	2955 kW
Oct		1568 kW	1873 kW	2739 kW	3087 kW
Nov		1942 kW	2358 kW	3387 kW	3847 kW
Dec		2262 kW	2773 kW	3940 kW	4495 kW
Total Power		21367 kW	25787 kW	37287 kW	42230 kW
Tres		150°C			
Jan		3276 kW	4036 kW	5713 kW	6532 kW
Feb		3103 kW	3811 kW	5412 kW	6179 kW
Mar		2864 kW	3501 kW	4998 kW	5695 kW
Apr		2570 kW	3119 kW	4489 kW	5098 kW
May		2303 kW	2773 kW	4027 kW	4556 kW
June		2067 kW	2466 kW	3617 kW	4076 kW
July		1965 kW	2332 kW	3439 kW	3867 kW
Aug		2003 kW	2382 kW	3505 kW	3945 kW
Sept		2219 kW	2664 kW	3881 kW	4386 kW
Oct		2296 kW	2764 kW	4015 kW	4542 kW
Nov		2733 kW	3331 kW	4771 kW	5429 kW
Dec		3102 kW	3810 kW	5411 kW	6178 kW
Total Power		30501 kW	36989 kW	53278 kW	60483 kW

Table A-3: Direct Single-Loop System Monthly Average Power Production (DTE=0.85) at 3.6km Depth

Direct Single-Loop System Power Production (DTE=0.85)					
Well Depth	3.6km				
CO2 Mass Flow	70 kg/s	90 kg/s	120 kg/s	140 kg/s	
Tres	100°C				
Jan	1479 kW	1812 kW	2576 kW	2937 kW	
Feb	1362 kW	1661 kW	2373 kW	2700 kW	
Mar	1204 kW	1455 kW	2099 kW	2378 kW	
Apr	1013 kW	1207 kW	1768 kW	1991 kW	
May	842.9 kW	987.1 kW	1474 kW	1647 kW	
June	697.3 kW	798.4 kW	1223 kW	1352 kW	
July	613.3 kW	689.8 kW	1078 kW	1183 kW	
Aug	645.3 kW	731.2 kW	1133 kW	1247 kW	
Sept	790.5 kW	919.1 kW	1384 kW	1541 kW	
Oct	838.6 kW	981.5 kW	1467 kW	1638 kW	
Nov	1118 kW	1344 kW	1950 kW	2204 kW	
Dec	1362 kW	1660 kW	2372 kW	2699 kW	
Total Power	11966 kW	14246 kW	20897 kW	23517 kW	
Tres	125°C				
Jan	2278 kW	2811 kW	3966 kW	4537 kW	
Feb	2136 kW	2628 kW	3721 kW	4250 kW	
Mar	1943 kW	2377 kW	3385 kW	3857 kW	
Apr	1707 kW	2071 kW	2977 kW	3379 kW	
May	1495 kW	1796 kW	2610 kW	2949 kW	
June	1311 kW	1556 kW	2291 kW	2575 kW	
July	1210 kW	1426 kW	2117 kW	2372 kW	
Aug	1249 kW	1476 kW	2183 kW	2449 kW	
Sept	1429 kW	1710 kW	2496 kW	2815 kW	
Oct	1490 kW	1788 kW	2601 kW	2938 kW	
Nov	1838 kW	2240 kW	3203 kW	3644 kW	
Dec	2136 kW	2627 kW	3720 kW	4249 kW	
Total Power	20222 kW	24506 kW	35270 kW	40014 kW	
Tres	150°C				
Jan	3134 kW	3879 kW	5460 kW	6256 kW	
Feb	2970 kW	3666 kW	5177 kW	5924 kW	
Mar	2746 kW	3375 kW	4788 kW	5468 kW	
Apr	2470 kW	3017 kW	4310 kW	4908 kW	
May	2221 kW	2693 kW	3877 kW	4401 kW	
June	2002 kW	2409 kW	3498 kW	3957 kW	
July	1886 kW	2259 kW	3298 kW	3722 kW	
Aug	1930 kW	2316 kW	3374 kW	3811 kW	
Sept	2142 kW	2591 kW	3742 kW	4242 kW	
Oct	2214 kW	2685 kW	3866 kW	4388 kW	
Nov	2623 kW	3215 kW	4575 kW	5218 kW	
Dec	2970 kW	3666 kW	5176 kW	5922 kW	
Total Power	29308 kW	35771 kW	51141 kW	58217 kW	

TableA-4: Direct Single-Loop System Monthly Average Power Production (DTE=0.50) at 2.5km Depth

Direct Single-Loop System Power Production (DTE=0.50)					
Well Depth	2.5km				
CO2 Mass Flow		70 kg/s	90 kg/s	120 kg/s	140 kg/s
Tres		100°C			
Jan		1054 kW	1294 kW	1834 kW	2094 kW
Feb		973.9 kW	1190 kW	1696 kW	1931 kW
Mar		864.3 kW	1048 kW	1506 kW	1709 kW
Apr		730.8 kW	874.6 kW	1275 kW	1438 kW
May		611.0 kW	719.3 kW	1068 kW	1196 kW
June		507.1 kW	584.7 kW	888.4 kW	985.9 kW
July		463.7 kW	528.5 kW	813.6 kW	898.3 kW
Aug		479.8 kW	549.3 kW	841.3 kW	930.8 kW
Sept		573.7 kW	671.0 kW	1004 kW	1121 kW
Oct		607.9 kW	715.3 kW	1063 kW	1190 kW
Nov		804.6 kW	970.2 kW	1403 kW	1588 kW
Dec		973.7 kW	1189 kW	1695 kW	1930 kW
Total Power		8645 kW	10334 kW	15087 kW	17012 kW
Tres		125°C			
Jan		1558 kW	1913 kW	2715 kW	3099 kW
Feb		1462 kW	1788 kW	2548 kW	2904 kW
Mar		1330 kW	1616 kW	2319 kW	2636 kW
Apr		1167 kW	1405 kW	2038 kW	2306 kW
May		1020 kW	1214 kW	1783 kW	2008 kW
June		891.0 kW	1047 kW	1560 kW	1746 kW
July		836.7 kW	976.7 kW	1466 kW	1637 kW
Aug		856.9 kW	1003 kW	1501 kW	1677 kW
Sept		973.9 kW	1155 kW	1704 kW	1914 kW
Oct		1016 kW	1209 kW	1777 kW	2000 kW
Nov		1257 kW	1522 kW	2194 kW	2489 kW
Dec		1462 kW	1787 kW	2548 kW	2903 kW
Total Power		13831 kW	16636 kW	24153 kW	27319 kW
Tres		150°C			
Jan		2057 kW	2520 kW	3590 kW	4095 kW
Feb		1947 kW	2378 kW	3400 kW	3873 kW
Mar		1796 kW	2182 kW	3138 kW	3566 kW
Apr		1610 kW	1940 kW	2816 kW	3188 kW
May		1437 kW	1715 kW	2516 kW	2836 kW
June		1279 kW	1509 kW	2240 kW	2513 kW
July		1210 kW	1419 kW	2121 kW	2373 kW
Aug		1235 kW	1452 kW	2165 kW	2425 kW
Sept		1381 kW	1642 kW	2419 kW	2722 kW
Oct		1433 kW	1709 kW	2508 kW	2827 kW
Nov		1713 kW	2074 kW	3001 kW	3398 kW
Dec		1947 kW	2377 kW	3399 kW	3872 kW
Total Power		19045 kW	22917 kW	33313 kW	37688 kW

Table A-5: Direct Single-Loop System Monthly Average Power Production (DTE=0.50) at 3.1km Depth

Direct Single-Loop System Power Production (DTE=0.50)					
Well Depth 3.1km					
CO2 Mass Flow		70 kg/s	90 kg/s	120 kg/s	140 kg/s
Tres		100°C			
Jan		932.0 kW	1142 kW	1622 kW	1850 kW
Feb		858.4 kW	1046 kW	1495 kW	1700 kW
Mar		758.1 kW	916.2 kW	1321 kW	1497 kW
Apr		636.7 kW	758.8 kW	1112 kW	1251 kW
May		528.4 kW	618.4 kW	924.2 kW	1032 kW
June		435.0 kW	497.4 kW	762.9 kW	843.4 kW
July		396.2 kW	447.1 kW	695.9 kW	765.0 kW
Aug		410.6 kW	465.7 kW	720.7 kW	794.0 kW
Sept		494.8 kW	574.9 kW	866.3 kW	964.3 kW
Oct		525.6 kW	614.8 kW	919.5 kW	1027 kW
Nov		703.8 kW	845.7 kW	1227 kW	1387 kW
Dec		858.1 kW	1046 kW	1494 kW	1700 kW
Total Power		7538 kW	8973 kW	13161 kW	14811 kW
Tres		125°C			
Jan		1419 kW	1747 kW	2472 kW	2825 kW
Feb		1331 kW	1632 kW	2318 kW	2645 kW
Mar		1209 kW	1474 kW	2107 kW	2398 kW
Apr		1060 kW	1280 kW	1850 kW	2096 kW
May		925.7 kW	1106 kW	1617 kW	1823 kW
June		808.4 kW	953.9 kW	1414 kW	1586 kW
July		759.2 kW	890.2 kW	1329 kW	1486 kW
Aug		777.5 kW	913.8 kW	1361 kW	1523 kW
Sept		883.7 kW	1052 kW	1544 kW	1738 kW
Oct		922.2 kW	1102 kW	1611 kW	1816 kW
Nov		1142 kW	1387 kW	1992 kW	2263 kW
Dec		1330 kW	1631 kW	2318 kW	2644 kW
Total Power		12568 kW	15169 kW	21933 kW	24843 kW
Tres		150°C			
Jan		1927 kW	2374 kW	3360 kW	3842 kW
Feb		1825 kW	2242 kW	3184 kW	3635 kW
Mar		1685 kW	2059 kW	2940 kW	3350 kW
Apr		1512 kW	1835 kW	2641 kW	2999 kW
May		1355 kW	1631 kW	2369 kW	2680 kW
June		1216 kW	1450 kW	2128 kW	2397 kW
July		1156 kW	1372 kW	2023 kW	2275 kW
Aug		1178 kW	1401 kW	2062 kW	2321 kW
Sept		1306 kW	1567 kW	2283 kW	2580 kW
Oct		1351 kW	1626 kW	2362 kW	2672 kW
Nov		1608 kW	1959 kW	2807 kW	3193 kW
Dec		1825 kW	2241 kW	3183 kW	3634 kW
Total Power		17944 kW	21757 kW	31342 kW	35578 kW

Table A-6: Direct Single-Loop System Monthly Average Power Production (DTE=0.50) at 3.6km Depth

Direct Single-Loop System Power Production (DTE=0.50)					
Well Depth 3.6km					
CO2 Mass Flow		70 kg/s	90 kg/s	120 kg/s	140 kg/s
Tres		100°C			
Jan		870.1 kW	1066 kW	1515 kW	1727 kW
Feb		801.4 kW	977.0 kW	1396 kW	1588 kW
Mar		708.1 kW	856.0 kW	1235 kW	1399 kW
Apr		595.7 kW	710.1 kW	1040 kW	1171 kW
May		495.8 kW	580.6 kW	867.2 kW	968.7 kW
June		410.2 kW	469.6 kW	719.3 kW	795.4 kW
July		350.9 kW	393.2 kW	617.3 kW	676.2 kW
Aug		373.8 kW	422.7 kW	656.7 kW	722.2 kW
Sept		465.0 kW	540.7 kW	814.0 kW	906.3 kW
Oct		493.3 kW	577.3 kW	862.9 kW	963.5 kW
Nov		657.7 kW	790.5 kW	1147 kW	1297 kW
Dec		801.1 kW	976.6 kW	1396 kW	1587 kW
Total Power		7023 kW	8360 kW	12266 kW	13801 kW
Tres		125°C			
Jan		1340 kW	1654 kW	2333 kW	2669 kW
Feb		1257 kW	1546 kW	2189 kW	2500 kW
Mar		1143 kW	1398 kW	1991 kW	2269 kW
Apr		1004 kW	1218 kW	1751 kW	1988 kW
May		879.6 kW	1056 kW	1535 kW	1735 kW
June		771.2 kW	915.6 kW	1348 kW	1515 kW
July		702.1 kW	826.2 kW	1229 kW	1376 kW
Aug		728.7 kW	860.6 kW	1274 kW	1429 kW
Sept		840.8 kW	1006 kW	1468 kW	1656 kW
Oct		876.4 kW	1052 kW	1530 kW	1728 kW
Nov		1081 kW	1318 kW	1884 kW	2143 kW
Dec		1256 kW	1545 kW	2188 kW	2499 kW
Total Power		11880 kW	14395 kW	20720 kW	23507 kW
Tres		150°C			
Jan		1843 kW	2282 kW	3212 kW	3680 kW
Feb		1747 kW	2157 kW	3045 kW	3485 kW
Mar		1615 kW	1985 kW	2816 kW	3216 kW
Apr		1453 kW	1775 kW	2535 kW	2887 kW
May		1306 kW	1584 kW	2281 kW	2589 kW
June		1178 kW	1417 kW	2058 kW	2327 kW
July		1100 kW	1316 kW	1923 kW	2170 kW
Aug		1130 kW	1355 kW	1975 kW	2230 kW
Sept		1260 kW	1524 kW	2201 kW	2495 kW
Oct		1303 kW	1579 kW	2274 kW	2581 kW
Nov		1543 kW	1891 kW	2691 kW	3069 kW
Dec		1747 kW	2156 kW	3044 kW	3484 kW
Total Power		17225 kW	21021 kW	30055 kW	34213 kW

A.2 Direct Single-Loop System Monthly Average System Efficiency

Table A-7: Direct Single-Loop System Monthly Average System Efficiency (DTE=0.85) at 2.5km Depth

Direct Single-Loop System Efficiency (DTE=0.85)					
Well Depth	2.5km				
CO2 Mass Flow		70 kg/s	90 kg/s	120 kg/s	140 kg/s
Tres		100°C			
Jan		0.13220	0.12610	0.13420	0.13120
Feb		0.12760	0.12120	0.12960	0.12640
Mar		0.12120	0.11420	0.12320	0.11970
Apr		0.11330	0.10540	0.11530	0.11150
May		0.10640	0.09739	0.10850	0.10410
June		0.10130	0.09076	0.10350	0.09841
July		0.09996	0.08851	0.10230	0.09673
Aug		0.10030	0.08922	0.10260	0.09721
Sept		0.10440	0.09493	0.10660	0.10190
Oct		0.10630	0.09719	0.10840	0.10390
Nov		0.11770	0.11030	0.11960	0.11610
Dec		0.12760	0.12110	0.12950	0.12640
Tres		125°C			
Jan		0.15380	0.14670	0.15630	0.15290
Feb		0.14930	0.14190	0.15180	0.14820
Mar		0.14310	0.13520	0.14560	0.14180
Apr		0.13560	0.12690	0.13810	0.13390
May		0.12910	0.11950	0.13170	0.12700
June		0.12440	0.11360	0.12700	0.12180
July		0.12310	0.11170	0.12580	0.12030
Aug		0.12340	0.11230	0.12610	0.12070
Sept		0.12730	0.11730	0.12990	0.12500
Oct		0.12900	0.11930	0.13150	0.12690
Nov		0.13980	0.13150	0.14230	0.13830
Dec		0.14930	0.14190	0.15180	0.14820
Tres		150°C			
Jan		0.17070	0.16260	0.17380	0.16990
Feb		0.16630	0.15790	0.16940	0.16530
Mar		0.16030	0.15140	0.16340	0.15910
Apr		0.15300	0.14330	0.15610	0.15140
May		0.14640	0.13590	0.14950	0.14440
June		0.14080	0.12920	0.14390	0.13830
July		0.13880	0.12660	0.14200	0.13610
Aug		0.13950	0.12750	0.14260	0.13680
Sept		0.14440	0.13350	0.14750	0.14220
Oct		0.14630	0.13570	0.14930	0.14420
Nov		0.15700	0.14780	0.16010	0.15560
Dec		0.16630	0.15790	0.16940	0.16530

TableA-8: Direct Single-Loop System Monthly Average System Efficiency (DTE=0.85) at 3.1km Depth

Direct Single-Loop System Efficiency (DTE=0.85)					
Well Depth 3.1km					
CO2 Mass Flow		70 kg/s	90 kg/s	120 kg/s	140 kg/s
Tres		100°C			
Jan		0.12920	0.12300	0.13120	0.12810
Feb		0.12490	0.11830	0.12690	0.12370
Mar		0.11900	0.11180	0.12100	0.11750
Apr		0.11200	0.10370	0.11400	0.10990
May		0.10610	0.09649	0.10830	0.10360
June		0.10250	0.09101	0.10480	0.09923
July		0.10220	0.08952	0.10460	0.09849
Aug		0.10210	0.08991	0.10450	0.09856
Sept		0.10460	0.09438	0.10680	0.10180
Oct		0.10600	0.09632	0.10810	0.10340
Nov		0.11580	0.10820	0.11780	0.11410
Dec		0.12490	0.11830	0.12690	0.12360
Tres		125°C			
Jan		0.15320	0.14650	0.15560	0.15230
Feb		0.14910	0.14210	0.15150	0.14810
Mar		0.14350	0.13600	0.14590	0.14220
Apr		0.13690	0.12860	0.13940	0.13530
May		0.13160	0.12220	0.13410	0.12950
June		0.12830	0.11770	0.13090	0.12580
July		0.12800	0.11660	0.13070	0.12510
Aug		0.12790	0.11680	0.13060	0.12520
Sept		0.13020	0.12040	0.13270	0.12800
Oct		0.13150	0.12210	0.13400	0.12940
Nov		0.14050	0.13260	0.14290	0.13910
Dec		0.14910	0.14210	0.15150	0.14810
Tres		150°C			
Jan		0.17240	0.16510	0.17530	0.17180
Feb		0.16840	0.16080	0.17130	0.16760
Mar		0.16300	0.15490	0.16590	0.16200
Apr		0.15660	0.14780	0.15950	0.15520
May		0.15150	0.14170	0.15440	0.14970
June		0.14810	0.13730	0.15110	0.14590
July		0.14730	0.13590	0.15040	0.14490
Aug		0.14750	0.13630	0.15050	0.14510
Sept		0.15010	0.14000	0.15310	0.14820
Oct		0.15130	0.14160	0.15430	0.14960
Nov		0.16010	0.15170	0.16300	0.15890
Dec		0.16840	0.16080	0.17130	0.16760

Table A-9: Direct Single-Loop System Monthly Average System Efficiency (DTE=0.85) at 3.6km Depth

Direct Single-Loop System Efficiency (DTE=0.85)					
Well Depth 3.6km					
CO2 Mass Flow		70 kg/s	90 kg/s	120 kg/s	140 kg/s
Tres		100°C			
Jan		0.13010	0.12400	0.13210	0.12910
Feb		0.12630	0.11970	0.12830	0.12510
Mar		0.12120	0.11390	0.12320	0.11970
Apr		0.11550	0.10700	0.11750	0.11340
May		0.11140	0.10140	0.11360	0.10870
June		0.11040	0.09825	0.11290	0.10690
July		0.10820	0.09456	0.11090	0.10420
Aug		0.10890	0.09592	0.11150	0.10520
Sept		0.11060	0.09999	0.11290	0.10770
Oct		0.11130	0.10130	0.11360	0.10870
Nov		0.11850	0.11080	0.12060	0.11680
Dec		0.12630	0.11970	0.12830	0.12510
Tres		125°C			
Jan		0.15500	0.14870	0.15740	0.15430
Feb		0.15130	0.14470	0.15370	0.15050
Mar		0.14650	0.13930	0.14890	0.14540
Apr		0.14110	0.13300	0.14350	0.13950
May		0.13720	0.12810	0.13970	0.13520
June		0.13590	0.12540	0.13850	0.13340
July		0.13450	0.12320	0.13720	0.13170
Aug		0.13490	0.12390	0.13760	0.13220
Sept		0.13640	0.12690	0.13890	0.13430
Oct		0.13720	0.12800	0.13960	0.13520
Nov		0.14400	0.13650	0.14640	0.14270
Dec		0.15130	0.14470	0.15370	0.15050
Tres		150°C			
Jan		0.17530	0.16870	0.17810	0.17490
Feb		0.17170	0.16480	0.17460	0.17120
Mar		0.16700	0.15960	0.16980	0.16620
Apr		0.16170	0.15350	0.16450	0.16050
May		0.15780	0.14870	0.16060	0.15620
June		0.15610	0.14600	0.15900	0.15410
July		0.15490	0.14420	0.15790	0.15270
Aug		0.15520	0.14480	0.15820	0.15310
Sept		0.15690	0.14750	0.15980	0.15520
Oct		0.15770	0.14860	0.16060	0.15620
Nov		0.16450	0.15680	0.16740	0.16360
Dec		0.17170	0.16480	0.17450	0.17120

Table A-10: Direct Single-Loop System Monthly Average System Efficiency (DTE=0.50) at 2.5km Depth

Direct Single-Loop System Efficiency (DTE=0.50)					
Well Depth	2.5km				
CO2 Mass Flow		70 kg/s	90 kg/s	120 kg/s	140 kg/s
Tres		100°C			
Jan		0.07775	0.07419	0.07892	0.07718
Feb		0.07505	0.07127	0.07621	0.07436
Mar		0.07129	0.06717	0.07245	0.07044
Apr		0.06666	0.06201	0.06783	0.06557
May		0.06261	0.05729	0.06383	0.06124
June		0.05959	0.05339	0.06090	0.05789
July		0.05880	0.05206	0.06017	0.05690
Aug		0.05900	0.05248	0.06034	0.05718
Sept		0.06144	0.05584	0.06268	0.05996
Oct		0.06252	0.05717	0.06374	0.06114
Nov		0.06922	0.06488	0.07038	0.06827
Dec		0.07504	0.07127	0.07620	0.07435
Tres		125°C			
Jan		0.09045	0.08632	0.09192	0.08992
Feb		0.08782	0.08349	0.08929	0.08719
Mar		0.08420	0.07956	0.08566	0.08341
Apr		0.07978	0.07467	0.08125	0.07878
May		0.07596	0.07030	0.07747	0.07473
June		0.07316	0.06682	0.07472	0.07166
July		0.07241	0.06568	0.07401	0.07076
Aug		0.07261	0.06604	0.07419	0.07103
Sept		0.07487	0.06899	0.07639	0.07355
Oct		0.07587	0.07019	0.07738	0.07463
Nov		0.08221	0.07738	0.08368	0.08134
Dec		0.08781	0.08348	0.08928	0.08718
Tres		150°C			
Jan		0.10040	0.09564	0.10220	0.09993
Feb		0.09783	0.09288	0.09964	0.09726
Mar		0.09429	0.08904	0.09610	0.09358
Apr		0.08999	0.08430	0.09181	0.08908
May		0.08614	0.07991	0.08795	0.08496
June		0.08284	0.07598	0.08466	0.08137
July		0.08167	0.07446	0.08351	0.08005
Aug		0.08205	0.07498	0.08388	0.08049
Sept		0.08494	0.07850	0.08675	0.08366
Oct		0.08604	0.07980	0.08785	0.08485
Nov		0.09236	0.08693	0.09437	0.09156
Dec		0.09782	0.09287	0.09964	0.09725

TableA-11: Direct Single-Loop System Monthly Average System Efficiency (DTE=0.50) at 3.1km Depth

Direct Single-Loop System Efficiency (DTE=0.50)					
Well Depth 3.1km					
CO2 Mass Flow		70 kg/s	90 kg/s	120 kg/s	140 kg/s
Tres		100°C			
Jan		0.07599	0.07236	0.07716	0.07538
Feb		0.07347	0.06960	0.07463	0.07274
Mar		0.07001	0.06576	0.07118	0.06909
Apr		0.06586	0.06099	0.06705	0.06467
May		0.06243	0.05676	0.06368	0.06092
June		0.06029	0.05353	0.06166	0.05837
July		0.06009	0.05266	0.06156	0.05794
Aug		0.06004	0.05289	0.06146	0.05798
Sept		0.06152	0.05552	0.06281	0.05988
Oct		0.06235	0.05666	0.06361	0.06083
Nov		0.06813	0.06363	0.06931	0.06710
Dec		0.07346	0.06959	0.07462	0.07273
Tres		125°C			
Jan		0.09009	0.08618	0.09151	0.08960
Feb		0.08769	0.08358	0.08910	0.08710
Mar		0.08442	0.07998	0.08583	0.08367
Apr		0.08055	0.07562	0.08197	0.07957
May		0.07742	0.07189	0.07888	0.07619
June		0.07549	0.06922	0.07702	0.07398
July		0.07528	0.06858	0.07686	0.07361
Aug		0.07526	0.06873	0.07681	0.07364
Sept		0.07660	0.07084	0.07808	0.07528
Oct		0.07735	0.07180	0.07881	0.07611
Nov		0.08266	0.07802	0.08408	0.08182
Dec		0.08768	0.08357	0.08910	0.08709
Tres		150°C			
Jan		0.10140	0.09710	0.10310	0.10100
Feb		0.09905	0.09457	0.10080	0.09860
Mar		0.09588	0.09110	0.09759	0.09528
Apr		0.09213	0.08691	0.09385	0.09132
May		0.08909	0.08336	0.09084	0.08807
June		0.08711	0.08075	0.08890	0.08582
July		0.08666	0.07995	0.08847	0.08522
Aug		0.08675	0.08018	0.08855	0.08537
Sept		0.08829	0.08236	0.09005	0.08719
Oct		0.08902	0.08328	0.09078	0.08799
Nov		0.09417	0.08921	0.09589	0.09349
Dec		0.09904	0.09457	0.10080	0.09859

Table A-12: Direct Single-Loop System Monthly Average System Efficiency (DTE=0.50) at 3.6km Depth

Direct Single-Loop System Efficiency (DTE=0.50)					
Well Depth 3.6km					
CO2 Mass Flow		70 kg/s	90 kg/s	120 kg/s	140 kg/s
Tres		100°C			
Jan		0.07654	0.07293	0.07773	0.07595
Feb		0.07430	0.07043	0.07549	0.07358
Mar		0.07130	0.06701	0.07250	0.07039
Apr		0.06792	0.06294	0.06915	0.06671
May		0.06554	0.05966	0.06685	0.06397
June		0.06495	0.05780	0.06640	0.06291
July		0.06191	0.05390	0.06349	0.05957
Aug		0.06310	0.05545	0.06462	0.06089
Sept		0.06508	0.05882	0.06643	0.06337
Oct		0.06550	0.05959	0.06681	0.06392
Nov		0.06973	0.06517	0.07094	0.06870
Dec		0.07429	0.07042	0.07548	0.07357
Tres		125°C			
Jan		0.09116	0.08749	0.09257	0.09076
Feb		0.08902	0.08514	0.09042	0.08852
Mar		0.08618	0.08197	0.08758	0.08551
Apr		0.08299	0.07826	0.08440	0.08209
May		0.08073	0.07536	0.08217	0.07955
June		0.07995	0.07379	0.08147	0.07847
July		0.07802	0.07137	0.07961	0.07637
Aug		0.07873	0.07228	0.08029	0.07715
Sept		0.08026	0.07464	0.08173	0.07899
Oct		0.08068	0.07530	0.08213	0.07950
Nov		0.08470	0.08027	0.08610	0.08393
Dec		0.08902	0.08513	0.09042	0.08851
Tres		150°C			
Jan		0.10310	0.09923	0.10480	0.10290
Feb		0.10100	0.09696	0.10270	0.10070
Mar		0.09823	0.09389	0.09990	0.09777
Apr		0.09509	0.09031	0.09676	0.09442
May		0.09280	0.08750	0.09449	0.09191
June		0.09181	0.08589	0.09355	0.09067
July		0.09029	0.08401	0.09208	0.08902
Aug		0.09083	0.08470	0.09261	0.08962
Sept		0.09229	0.08679	0.09399	0.09132
Oct		0.09275	0.08744	0.09445	0.09186
Nov		0.09678	0.09225	0.09844	0.09623
Dec		0.10100	0.09695	0.10270	0.10070

A.3 Direct Single-Loop System Monthly Average Power Production Plots (DTE=0.85)

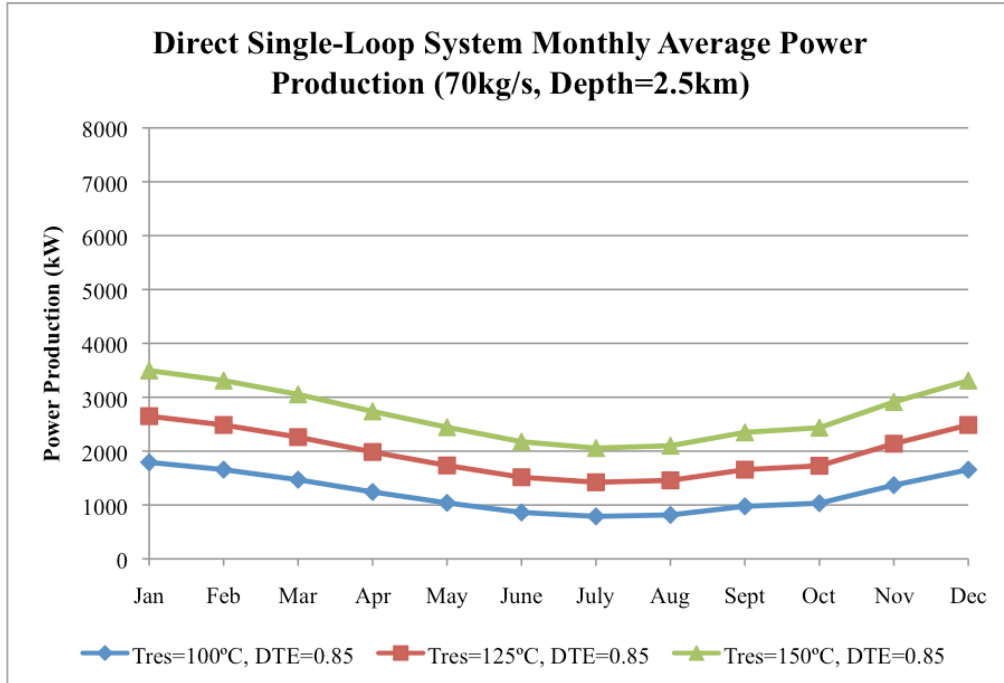


Figure A-1: Direct Single-Loop System monthly average power production simulation results at 2.5km depth with CO₂ mass flow rate of 70kg/s and DTE=0.85 for various reservoir temperatures.

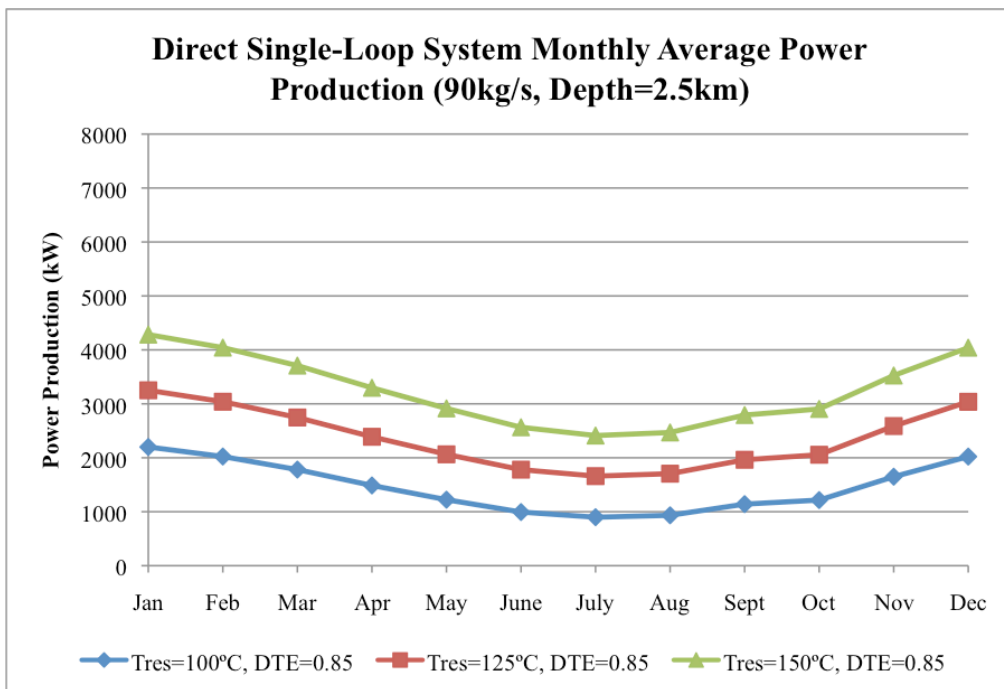


Figure A-2: Direct Single-Loop System monthly average power production simulation results at 2.5km depth with CO₂ mass flow rate of 90kg/s and DTE=0.85 for various reservoir temperatures.

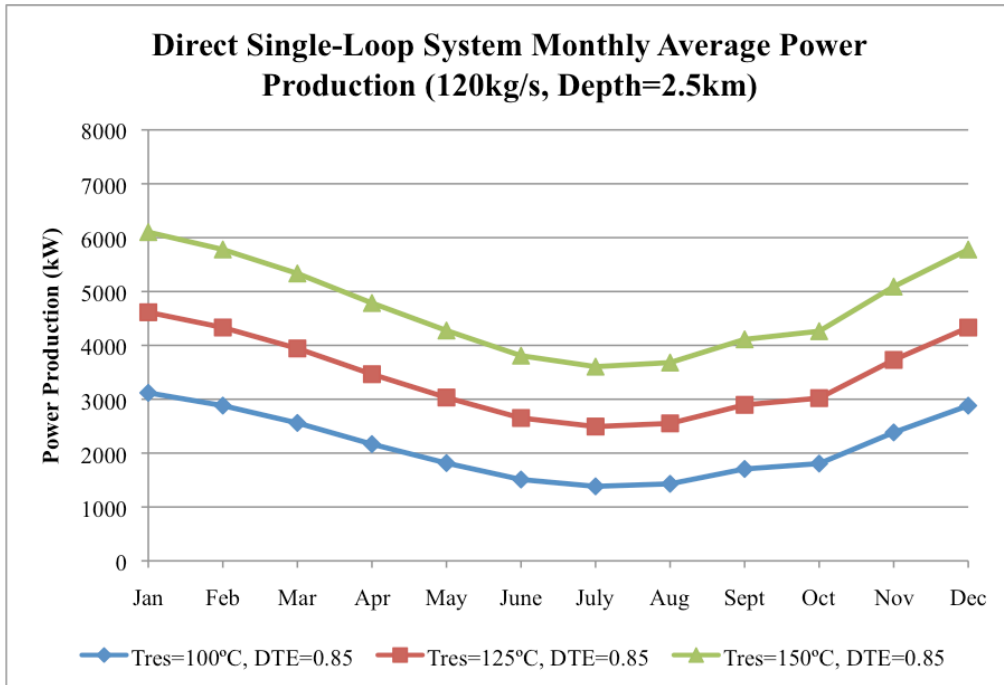


Figure A-3: Direct Single-Loop System monthly average power production simulation results at 2.5km depth with CO2 mass flow rate of 120kg/s and DTE=0.85 for various reservoir temperatures.

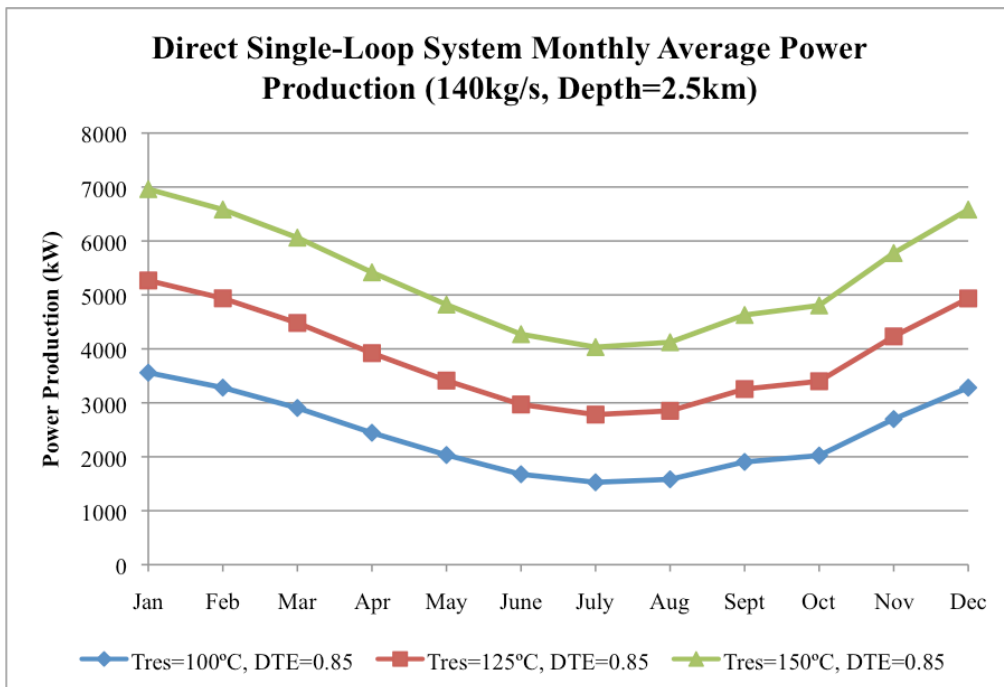


Figure A-4: Direct Single-Loop System monthly average power production simulation results at 2.5km depth with CO2 mass flow rate of 140kg/s and DTE=0.85 for various reservoir temperatures.

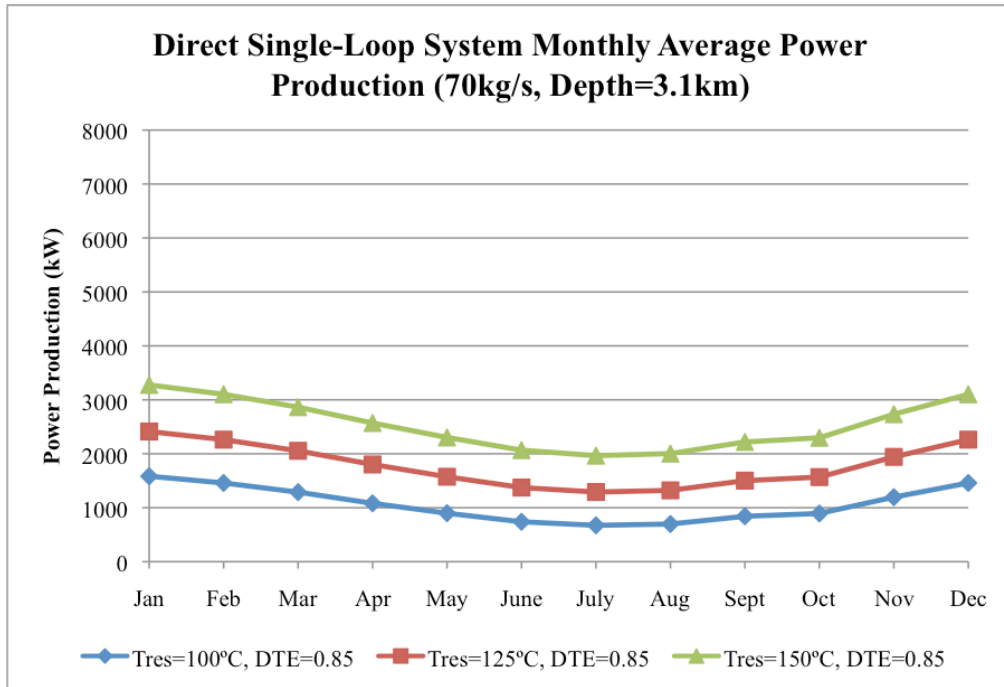


Figure A-5: Direct Single-Loop System monthly average power production simulation results at 3.1km depth with CO₂ mass flow rate of 70kg/s and DTE=0.85 for various reservoir temperatures.

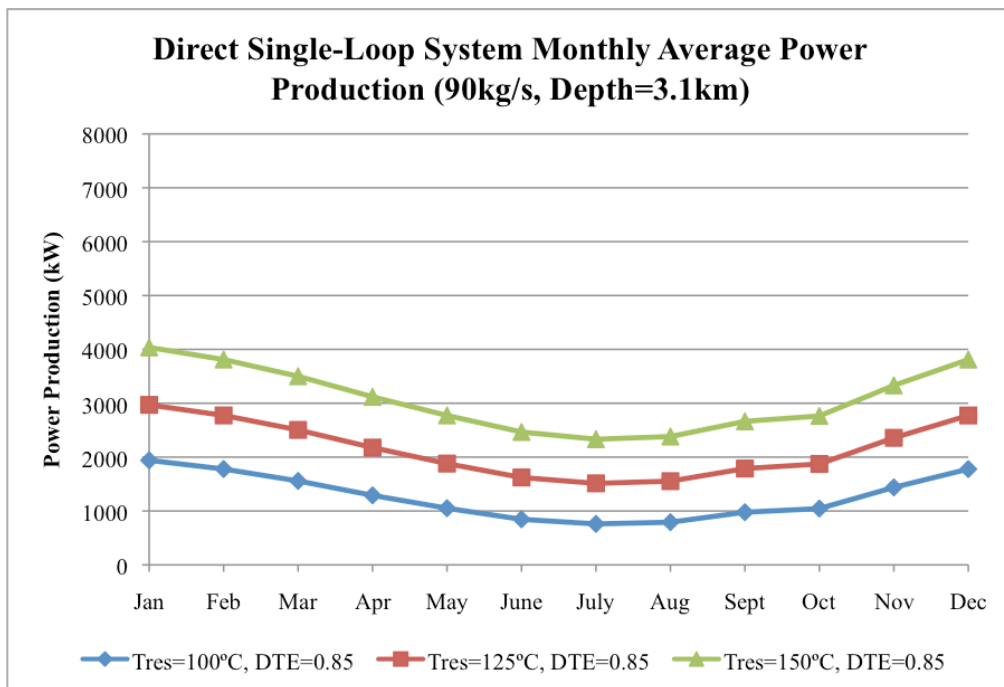


Figure A-6: Direct Single-Loop System monthly average power production simulation results at 3.1km depth with CO₂ mass flow rate of 90kg/s and DTE=0.85 for various reservoir temperatures.

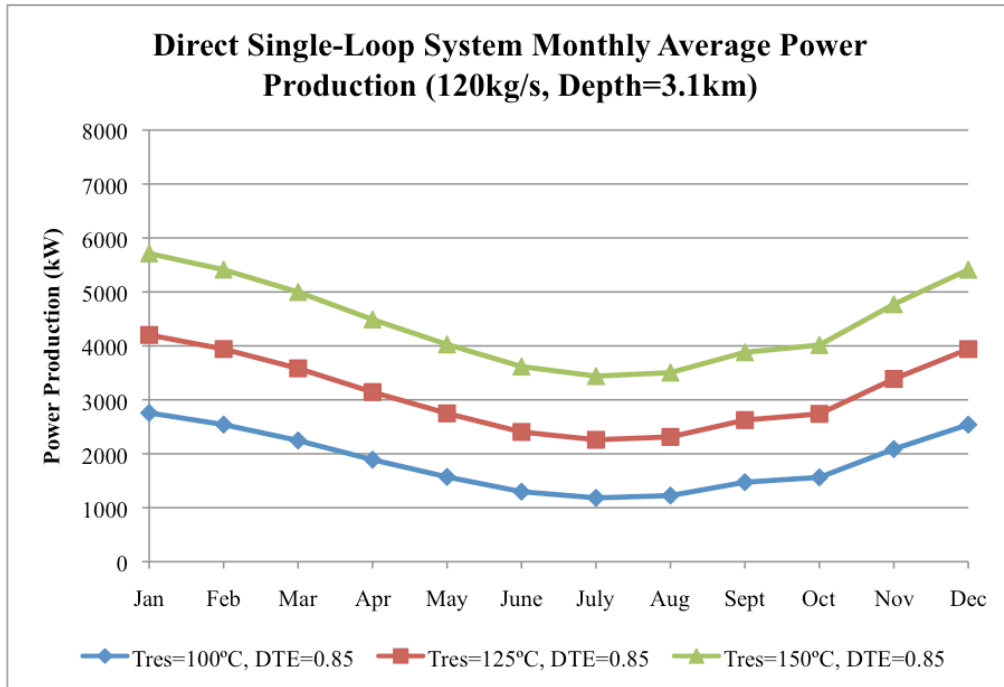


Figure A-7: Direct Single-Loop System monthly average power production simulation results at 3.1km depth with CO2 mass flow rate of 120kg/s and DTE=0.85 for various reservoir temperatures.

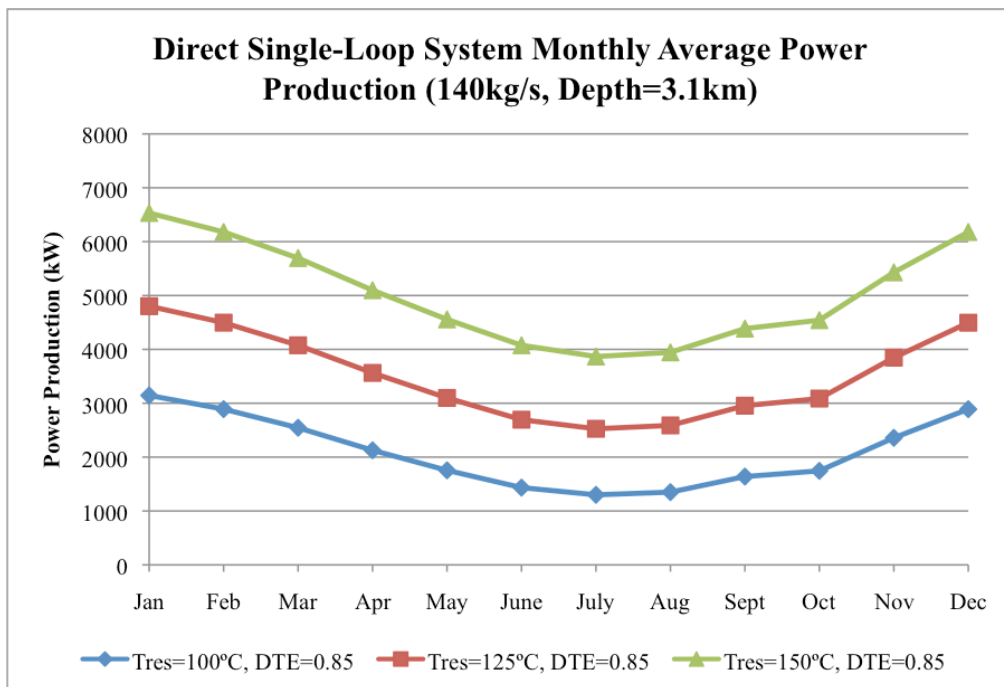


Figure A-8: Direct Single-Loop System monthly average power production simulation results at 3.1km depth with CO2 mass flow rate of 140kg/s and DTE=0.85 for various reservoir temperatures.

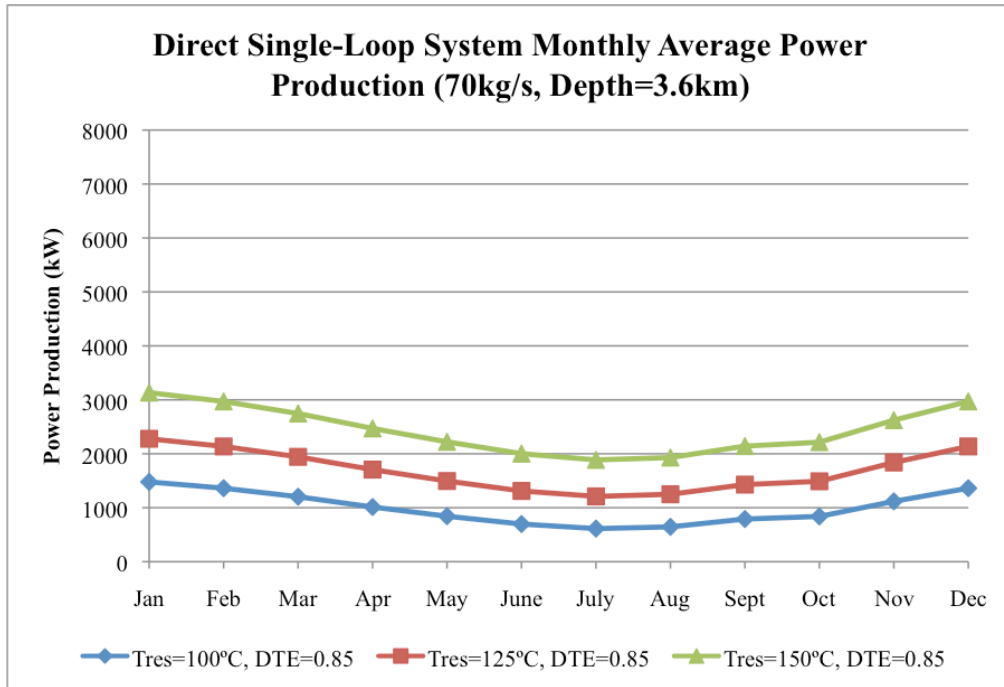


Figure A-9: Direct Single-Loop System monthly average power production simulation results at 3.6km depth with CO2 mass flow rate of 70kg/s and DTE=0.85 for various reservoir temperatures.

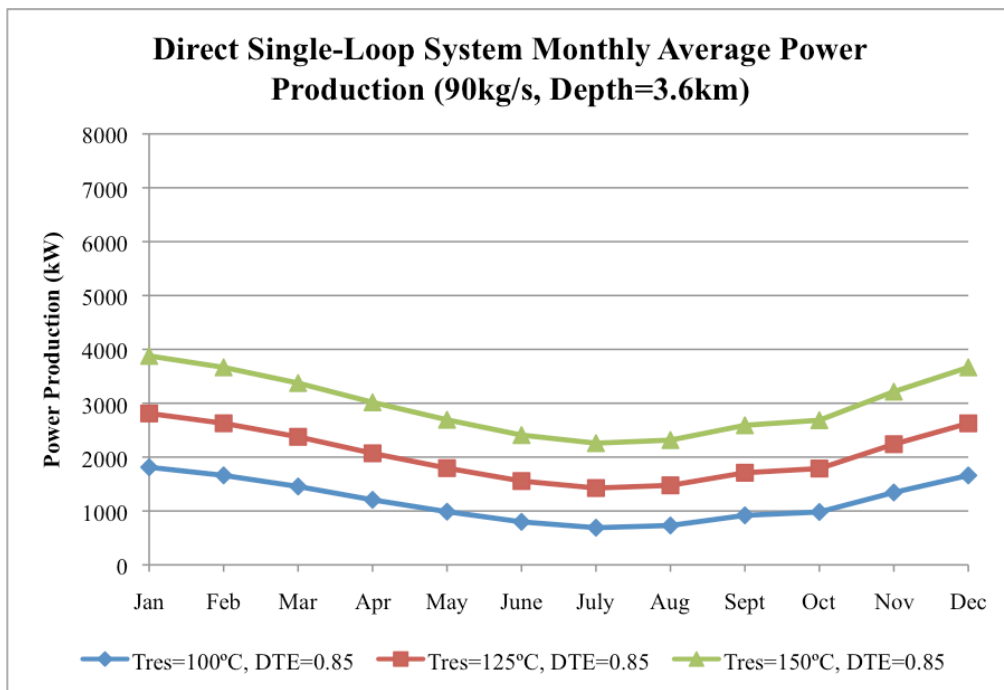


Figure A-10: Direct Single-Loop System monthly average power production simulation results at 3.6km depth with CO2 mass flow rate of 90kg/s and DTE=0.85 for various reservoir temperatures.

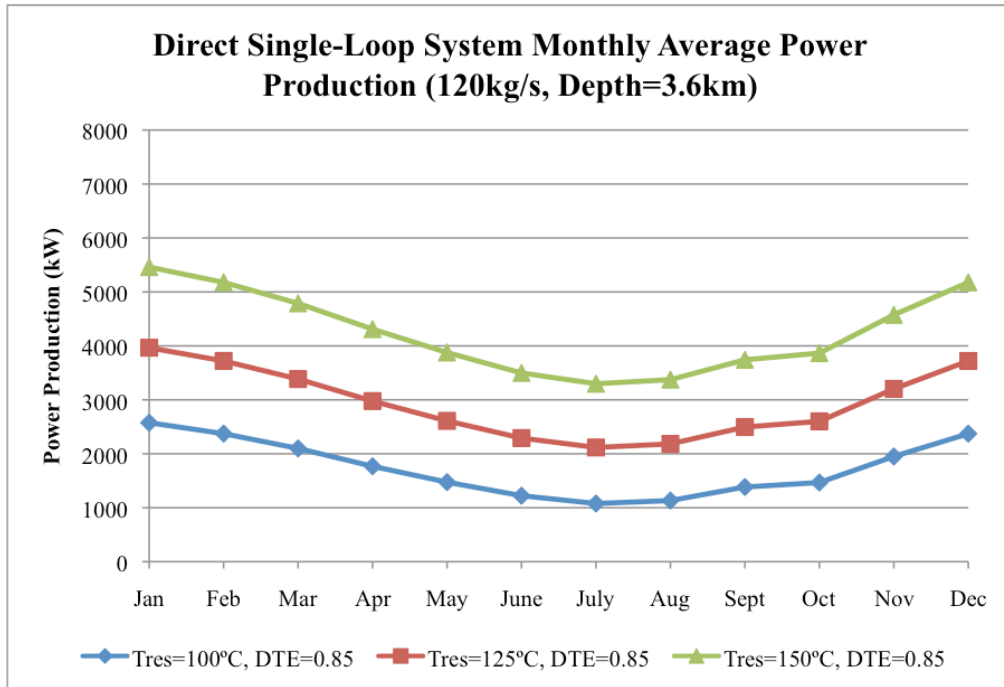


Figure A-11: Direct Single-Loop System monthly average power production simulation results at 3.6km depth with CO2 mass flow rate of 120kg/s and DTE=0.85 for various reservoir temperatures.

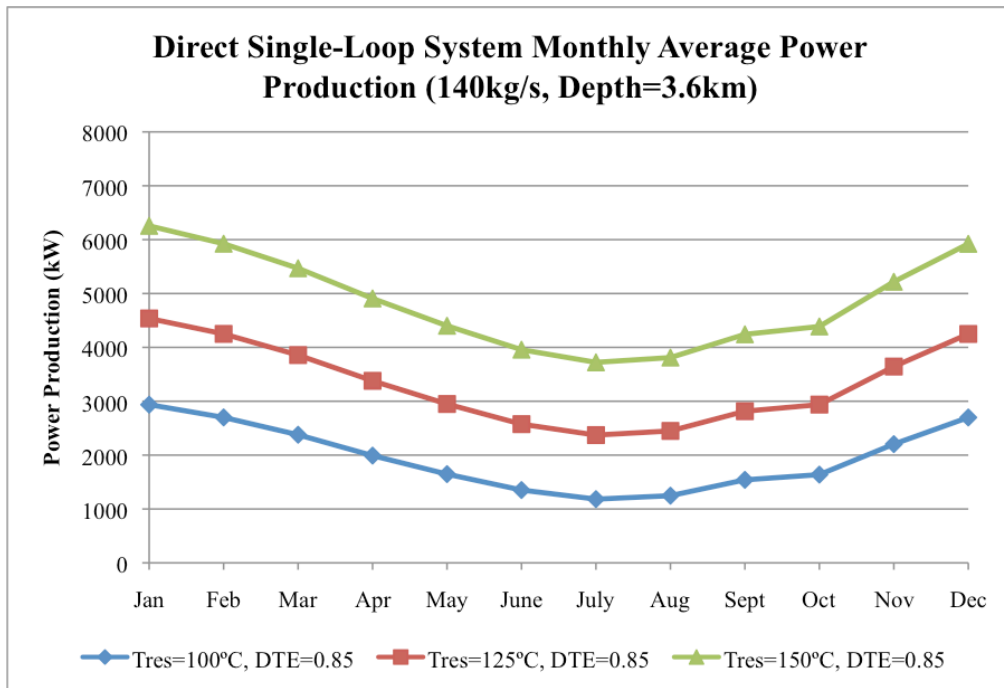


Figure A-12: Direct Single-Loop System monthly average power production simulation results at 3.6km depth with CO2 mass flow rate of 140kg/s and DTE=0.85 for various reservoir temperatures.

A.4 Direct Single-Loop System Monthly Average Power Production Plots (DTE=0.50)

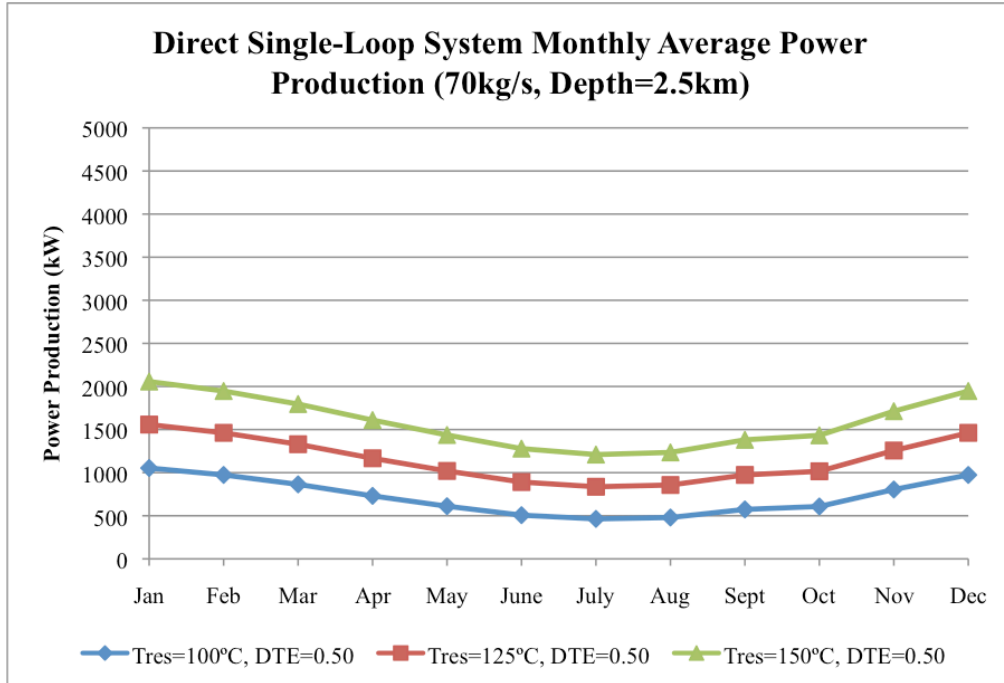


Figure A-13: Direct Single-Loop System monthly average power production simulation results at 2.5km depth with CO₂ mass flow rate of 70kg/s and DTE=0.50 for various reservoir temperatures.

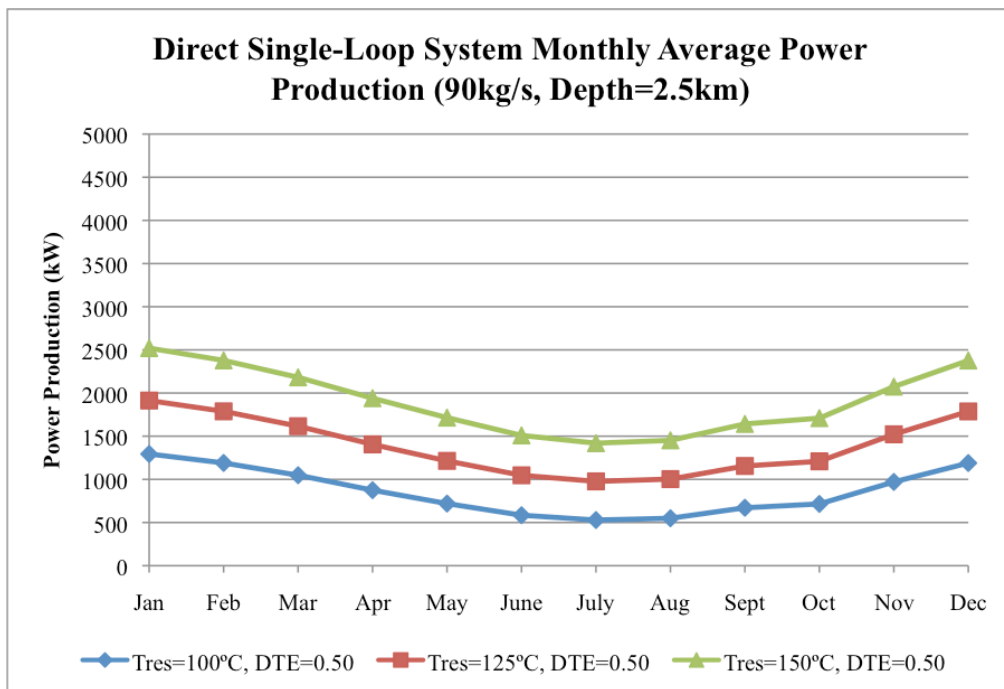


Figure A-14: Direct Single-Loop System monthly average power production simulation results at 2.5km depth with CO₂ mass flow rate of 90kg/s and DTE=0.50 for various reservoir temperatures.

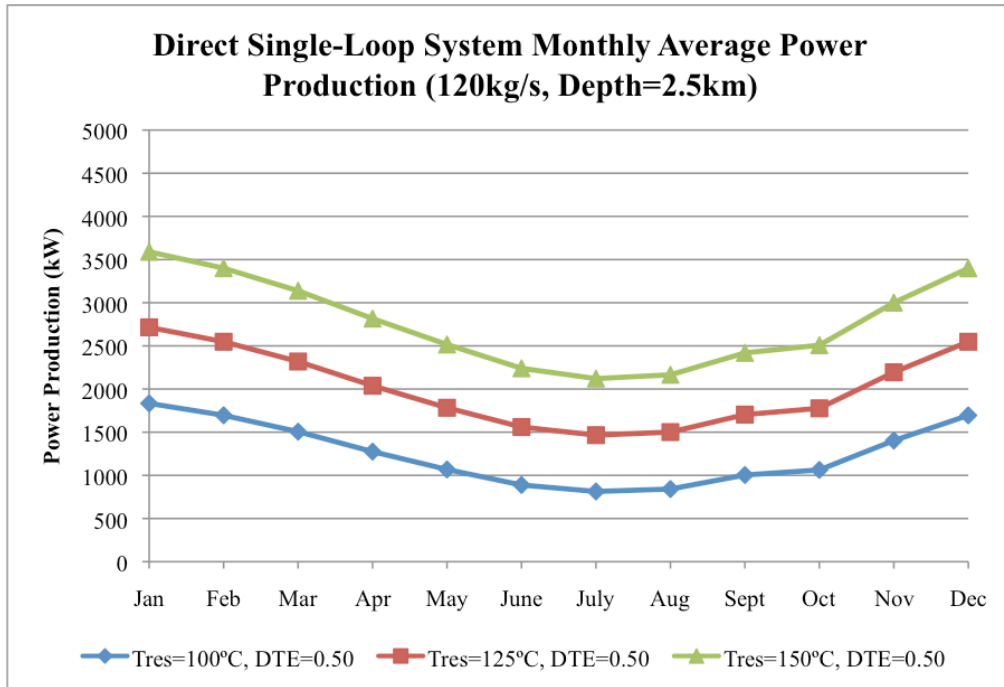


Figure A-15: Direct Single-Loop System monthly average power production simulation results at 2.5km depth with CO2 mass flow rate of 120kg/s and DTE=0.50 for various reservoir temperatures.

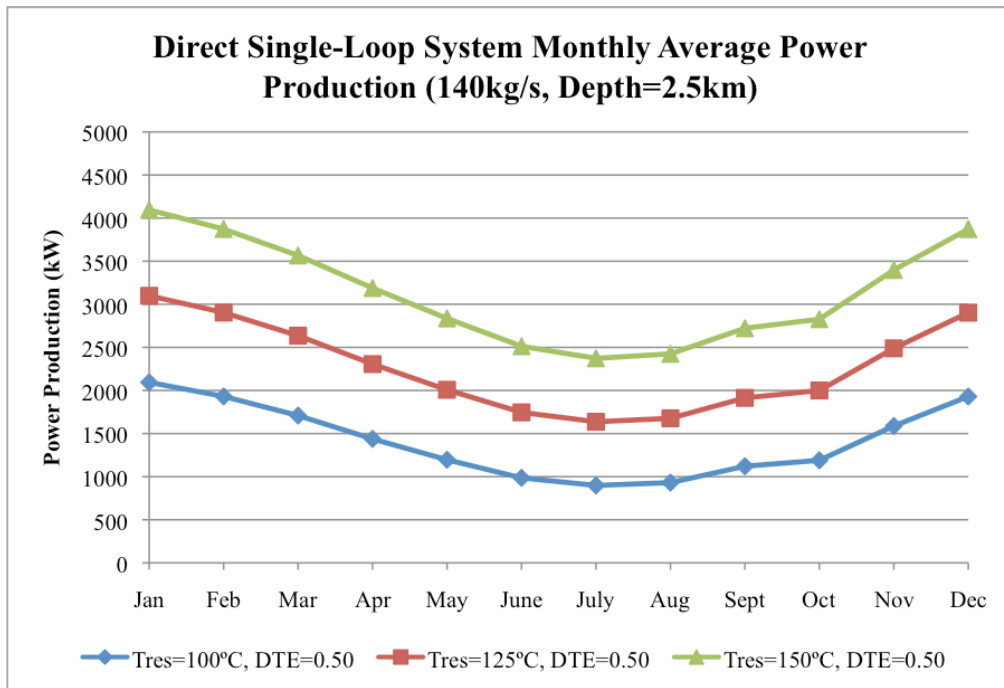


Figure A-16: Direct Single-Loop System monthly average power production simulation results at 2.5km depth with CO2 mass flow rate of 140kg/s and DTE=0.50 for various reservoir temperatures.

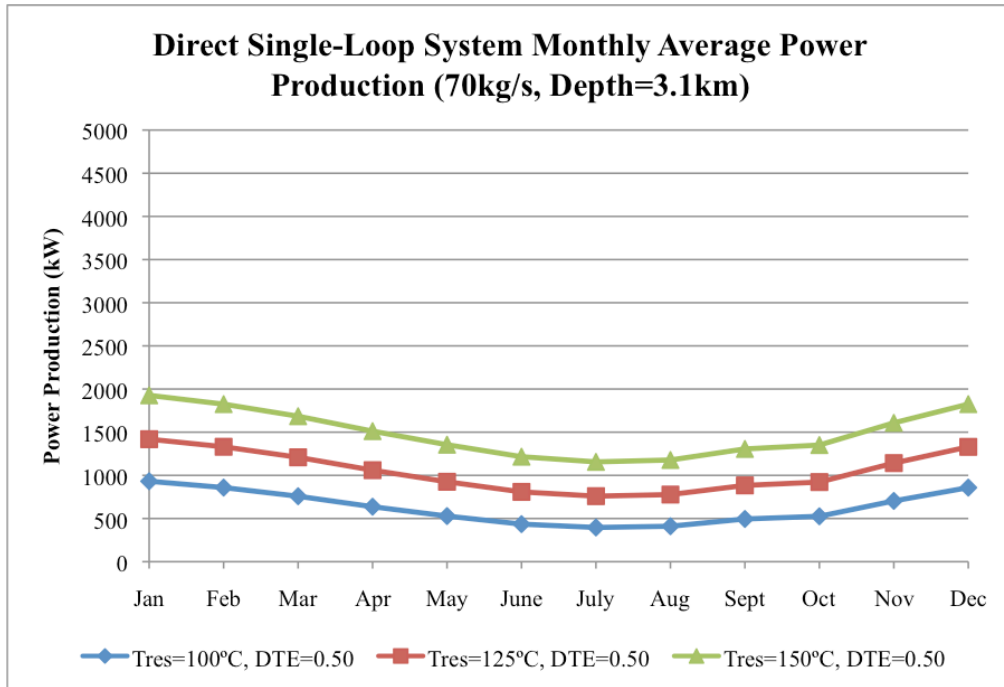


Figure A-17: Direct Single-Loop System monthly average power production simulation results at 3.1km depth with CO2 mass flow rate of 70kg/s and DTE=0.50 for various reservoir temperatures.

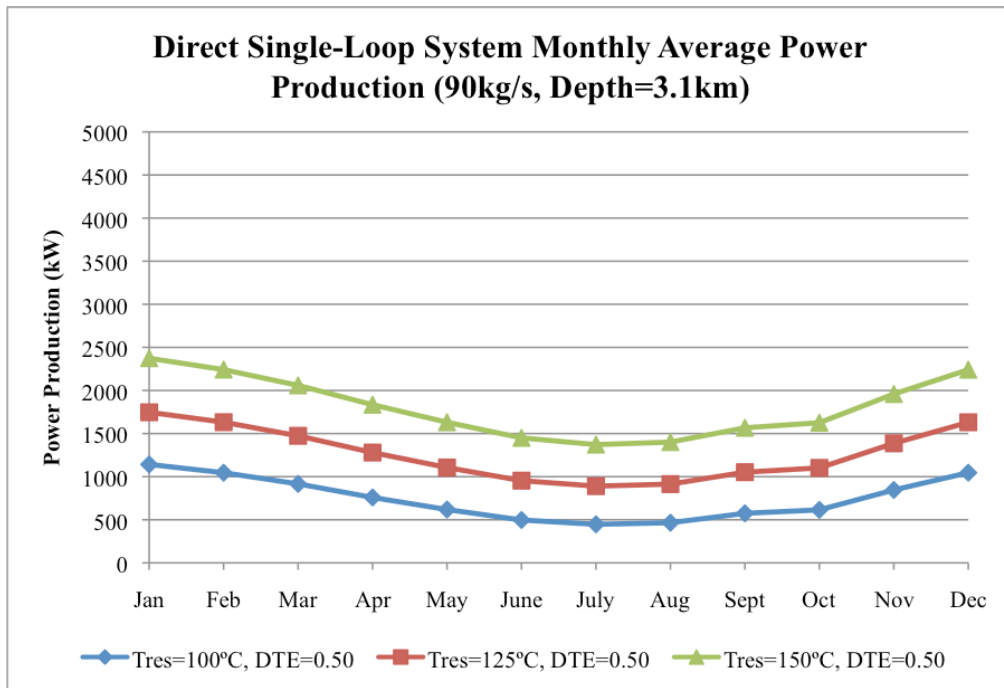


Figure A-18: Direct Single-Loop System monthly average power production simulation results at 3.1km depth with CO2 mass flow rate of 90kg/s and DTE=0.50 for various reservoir temperatures.

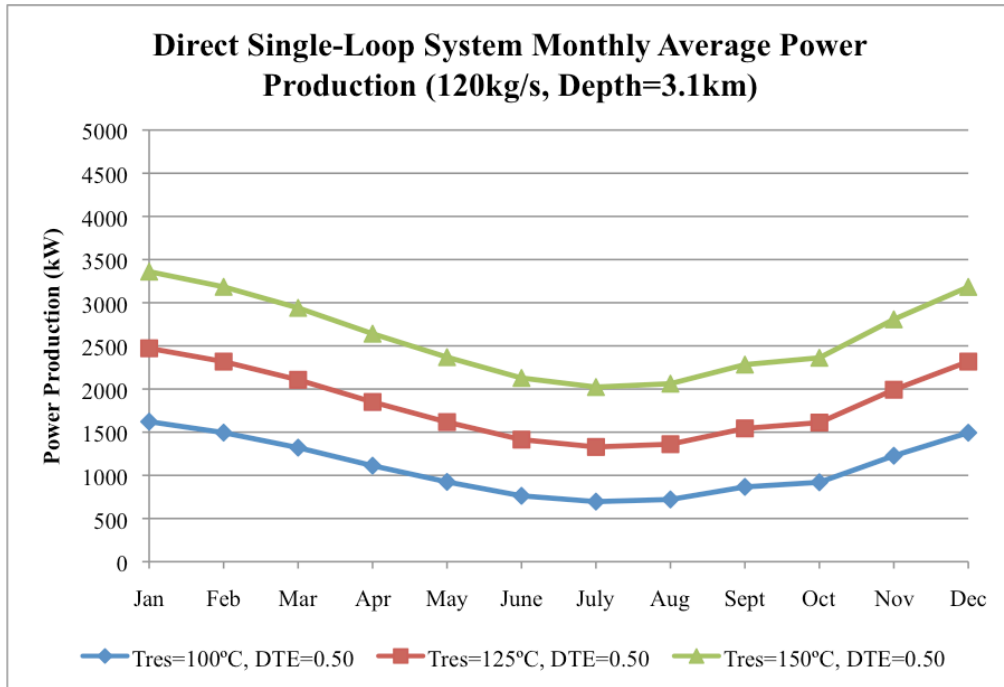


Figure A-19: Direct Single-Loop System monthly average power production simulation results at 3.1km depth with CO2 mass flow rate of 120kg/s and DTE=0.50 for various reservoir temperatures.

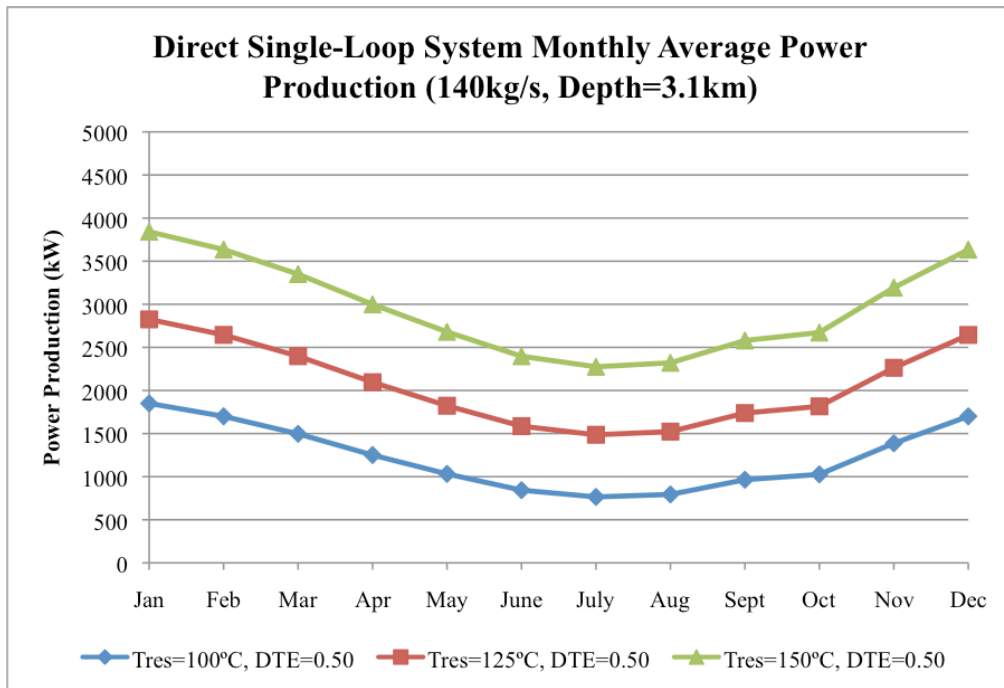


Figure A-20: Direct Single-Loop System monthly average power production simulation results at 3.1km depth with CO2 mass flow rate of 140kg/s and DTE=0.50 for various reservoir temperatures.

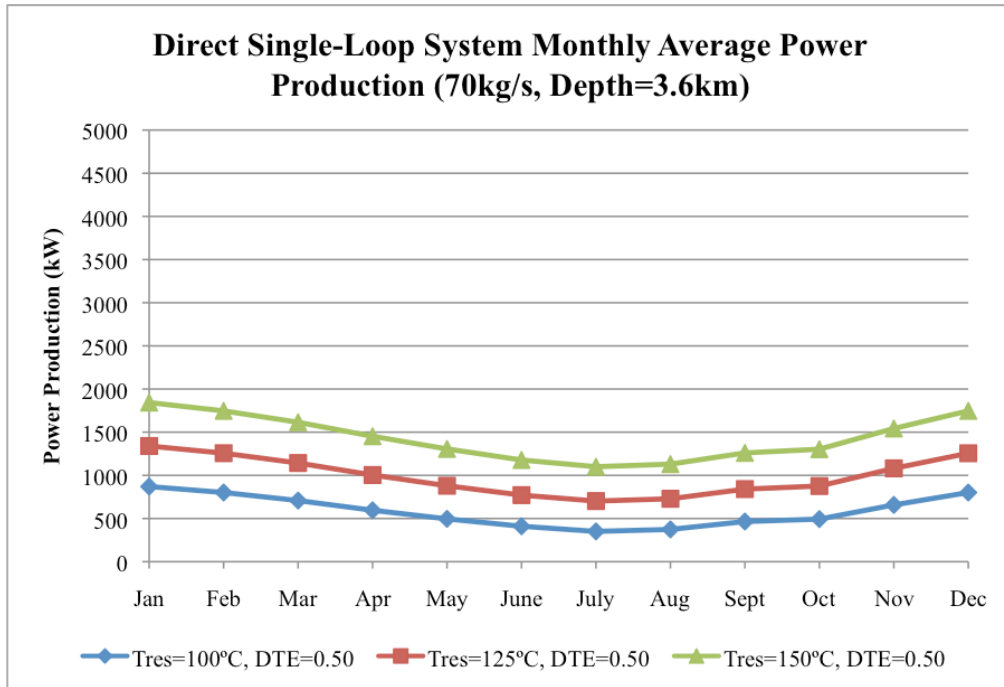


Figure A-21: Direct Single-Loop System monthly average power production simulation results at 3.6km depth with CO₂ mass flow rate of 70kg/s and DTE=0.50 for various reservoir temperatures.

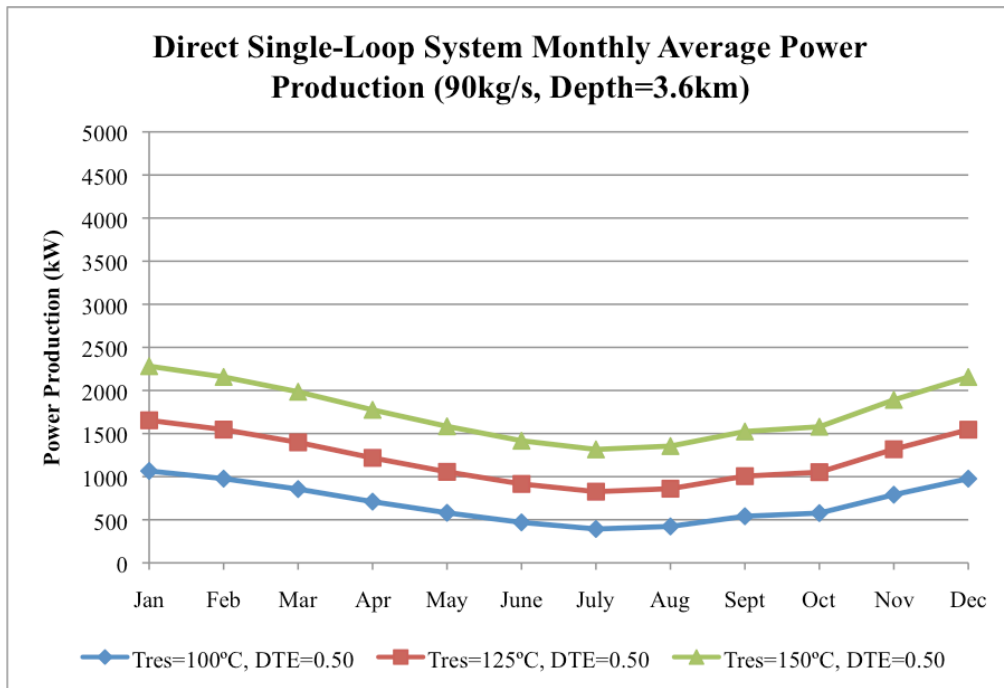


Figure A-22: Direct Single-Loop System monthly average power production simulation results at 3.6km depth with CO₂ mass flow rate of 90kg/s and DTE=0.50 for various reservoir temperatures.

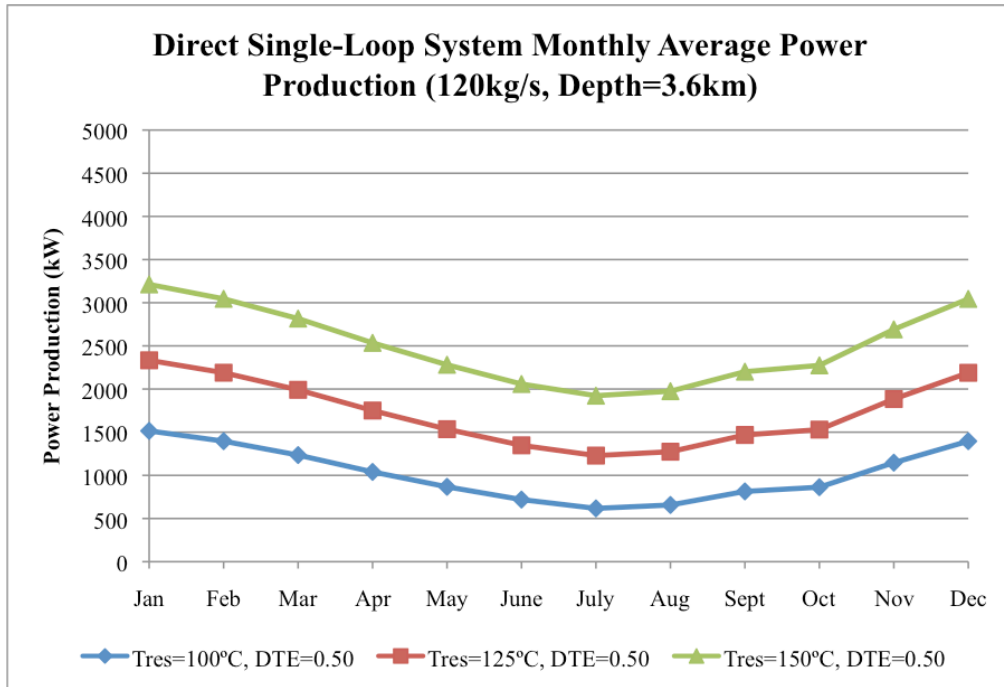


Figure A-23: Direct Single-Loop System monthly average power production simulation results at 3.6km depth with CO2 mass flow rate of 120kg/s and DTE=0.50 for various reservoir temperatures.

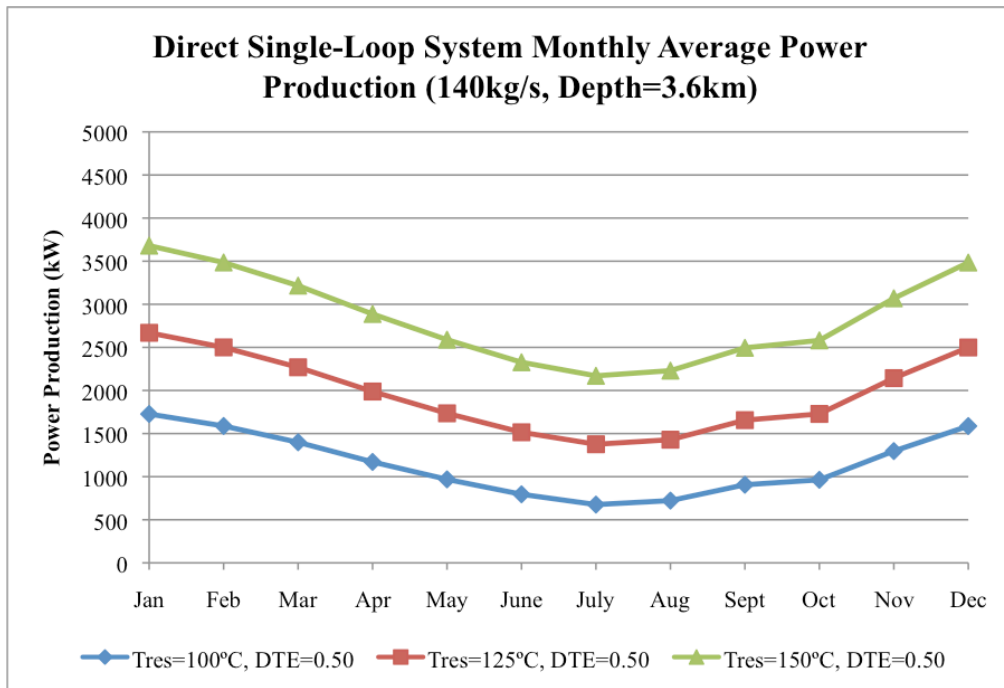


Figure A-24: Direct Single-Loop System monthly average power production simulation results at 3.6km depth with CO2 mass flow rate of 140kg/s and DTE=0.50 for various reservoir temperatures.

Appendix B: Direct Single-Loop System Thermodynamic Property Tables

State points listed in the tables refer to those labeled in Figure 3-2.

Table B-1: Thermodynamic Properties for Direct Single-Loop System Simulations at 2.5km Depth, CO₂ Mass Flow Rate of 70kg/s, and Reservoir Temperature of 100°C (DTE=0.85).

Tres	100°C						
Well Depth	2.5 km						
CO₂ Mass Flow	70 kg/s						
	Pressure (kPa)						
State Point	1'	1	2	3	4	4'	5
Jan	2986	2985	27072	25000	11380	11108	2986
Feb	3286	3285	26933	25000	11380	11108	3286
Mar	3749	3748	26736	25000	11380	11108	3749
Apr	4410	4409	26468	25000	11380	11107	4410
May	5117	5116	26164	25000	11380	11107	5117
June	5838	5836	25776	25000	11380	11107	5838
July	6174	6173	25530	25000	11380	11107	6174
Aug	6047	6045	25636	25000	11380	11107	6047
Sept	5362	5361	26044	25000	11380	11107	5362
Oct	5137	5135	26154	25000	11380	11107	5137
Nov	4030	4029	26622	25000	11380	11108	4030
Dec	3288	3286	26932	25000	11380	11108	3288
	Temperature (°C)						
State Point	1'	1	2	3	4	4'	5
Jan	-5.717	-5.73	8.958	100	55.9	53.79	-5.717
Feb	-2.201	-2.214	13.29	100	55.9	53.83	-2.201
Mar	2.785	2.773	19.6	100	55.9	53.88	2.785
Apr	9.17	9.159	28.02	100	55.9	53.95	9.17
May	15.24	15.23	36.57	100	55.9	54.02	15.24
June	20.8	20.79	45.18	100	55.9	54.08	20.8
July	23.21	23.2	49.36	100	55.9	54.1	23.21
Aug	22.31	22.3	47.72	100	55.9	54.09	22.31
Sept	17.2	17.19	39.5	100	55.9	54.04	17.2
Oct	15.4	15.39	36.81	100	55.9	54.02	15.4
Nov	5.595	5.583	23.25	100	55.9	53.91	5.595
Dec	-2.186	-2.199	13.32	100	55.9	53.83	-2.186
	Enthalpy (kJ/kg)						
State Point	1'	1	2	3	4	4'	5
Jan	73.68	73.46	97.82	291.5	265.4	260.8	235.2
Feb	81.98	81.77	106.1	291.5	265.4	261	237.4
Mar	94.19	93.98	118.3	291.5	265.4	261.3	240.3
Apr	110.8	110.6	134.9	291.5	265.4	261.7	244
May	128	127.8	152.1	291.5	265.4	262.1	247.2
June	145.8	145.7	170	291.5	265.4	262.4	250.1
July	154.8	154.6	178.9	291.5	265.4	262.6	251.3
Aug	151.2	151.1	175.3	291.5	265.4	262.5	250.9
Sept	134	133.8	158.1	291.5	265.4	262.2	248.3
Oct	128.5	128.3	152.6	291.5	265.4	262.1	247.3
Nov	101.3	101.1	125.5	291.5	265.4	261.5	242
Dec	82.02	81.81	106.2	291.5	265.4	261	237.4
	Entropy (kJ/kg-K)						
State Point	1'	1	2	3	4	4'	5
Jan	0.2867	0.2859	0.2859	0.8858	0.8859	0.8738	0.8907
Feb	0.3164	0.3156	0.3156	0.8858	0.8859	0.8745	0.8899
Mar	0.3592	0.3584	0.3584	0.8858	0.8859	0.8754	0.8888
Apr	0.4159	0.4152	0.4152	0.8858	0.8859	0.8766	0.8877
May	0.4733	0.4726	0.4726	0.8858	0.8859	0.8777	0.8868
June	0.5315	0.5308	0.5308	0.8858	0.8859	0.8787	0.8861
July	0.5601	0.5595	0.5595	0.8858	0.8859	0.8792	0.8859
Aug	0.5488	0.5482	0.5482	0.8858	0.8859	0.879	0.8859
Sept	0.493	0.4923	0.4923	0.8858	0.8859	0.878	0.8865
Oct	0.4749	0.4742	0.4742	0.8858	0.8859	0.8777	0.8867
Nov	0.3838	0.383	0.383	0.8858	0.8859	0.8759	0.8883
Dec	0.3165	0.3157	0.3157	0.8858	0.8859	0.8745	0.8899

Table B-2: Thermodynamic Properties for Direct Single-Loop System Simulations at 2.5km Depth, CO2 Mass Flow Rate of 90kg/s, and Reservoir Temperature of 100°C (DTE=0.85).

Tres	100°C						
Well Depth	2.5 km						
CO2 Mass Flow	90 kg/s						
Pressure (kPa)							
State Point	1'	1	2	3	4	4'	5
Jan	2987	2985	26983	25000	10901	10438	2987
Feb	3287	3285	26843	25000	10901	10438	3287
Mar	3750	3748	26642	25000	10901	10437	3750
Apr	4411	4409	26370	25000	10901	10437	4411
May	5118	5116	26060	25000	10901	10436	5118
June	5839	5836	25665	25000	10901	10436	5839
July	6175	6173	25416	25000	10901	10436	6175
Aug	6048	6045	25523	25000	10901	10436	6048
Sept	5363	5361	25938	25000	10901	10436	5363
Oct	5137	5135	26050	25000	10901	10436	5137
Nov	4031	4029	26527	25000	10901	10437	4031
Dec	3288	3286	26842	25000	10901	10438	3288
Temperature (°C)							
State Point	1'	1	2	3	4	4'	5
Jan	-5.708	-5.73	8.912	100	53.46	50.51	-5.708
Feb	-2.193	-2.214	13.24	100	53.46	50.53	-2.193
Mar	2.793	2.773	19.54	100	53.46	50.57	2.793
Apr	9.177	9.159	27.95	100	53.46	50.62	9.177
May	15.25	15.23	36.49	100	53.46	50.66	15.25
June	20.81	20.79	45.08	100	53.46	50.7	20.81
July	23.22	23.2	49.24	100	53.46	50.72	23.22
Aug	22.32	22.3	47.61	100	53.46	50.71	22.32
Sept	17.21	17.19	39.41	100	53.46	50.67	17.21
Oct	15.41	15.39	36.73	100	53.46	50.66	15.41
Nov	5.602	5.583	23.19	100	53.46	50.59	5.602
Dec	-2.178	-2.199	13.26	100	53.46	50.53	-2.178
Enthalpy (kJ/kg)							
State Point	1'	1	2	3	4	4'	5
Jan	73.63	73.46	97.73	291.5	264.3	260.3	235.8
Feb	81.94	81.77	106	291.5	264.3	260.4	237.9
Mar	94.15	93.98	118.2	291.5	264.3	260.7	240.9
Apr	110.7	110.6	134.8	291.5	264.3	261	244.4
May	128	127.8	152	291.5	264.3	261.2	247.7
June	145.8	145.7	169.8	291.5	264.3	261.5	250.5
July	154.7	154.6	178.7	291.5	264.3	261.6	251.6
Aug	151.2	151.1	175.2	291.5	264.3	261.6	251.2
Sept	134	133.8	158	291.5	264.3	261.3	248.7
Oct	128.4	128.3	152.5	291.5	264.3	261.2	247.7
Nov	101.3	101.1	125.4	291.5	264.3	260.8	242.5
Dec	81.98	81.81	106.1	291.5	264.3	260.4	238
Entropy (kJ/kg-K)							
State Point	1'	1	2	3	4	4'	5
Jan	0.2865	0.2859	0.2859	0.8858	0.8859	0.8768	0.893
Feb	0.3162	0.3156	0.3156	0.8858	0.8859	0.8773	0.892
Mar	0.359	0.3584	0.3584	0.8858	0.8859	0.8781	0.8907
Apr	0.4157	0.4152	0.4152	0.8858	0.8859	0.879	0.8893
May	0.4731	0.4726	0.4726	0.8858	0.8859	0.8799	0.8882
June	0.5313	0.5308	0.5308	0.8858	0.8859	0.8807	0.8873
July	0.56	0.5595	0.5595	0.8858	0.8859	0.881	0.887
Aug	0.5487	0.5482	0.5482	0.8858	0.8859	0.8809	0.8871
Sept	0.4928	0.4923	0.4923	0.8858	0.8859	0.8802	0.8879
Oct	0.4747	0.4742	0.4742	0.8858	0.8859	0.8799	0.8882
Nov	0.3836	0.383	0.383	0.8858	0.8859	0.8785	0.8901
Dec	0.3163	0.3157	0.3157	0.8858	0.8859	0.8773	0.892

Table B-3: Thermodynamic Properties for Direct Single-Loop System Simulations at 2.5km Depth, CO2

Mass Flow Rate of 120kg/s, and Reservoir Temperature of 100°C (DTE=0.85).

Tres	100°C						
Well Depth	2.5 km						
CO2 Mass Flow	120 kg/s						
Pressure (kPa)							
State Point	1'	1	2	3	4	4'	5
Jan	2986	2985	27055	25000	11461	11219	2986
Feb	3286	3285	26917	25000	11461	11219	3286
Mar	3749	3748	26719	25000	11461	11219	3749
Apr	4410	4409	26450	25000	11461	11218	4410
May	5117	5116	26144	25000	11461	11218	5117
June	5838	5836	25755	25000	11461	11218	5838
July	6174	6173	25509	25000	11461	11218	6174
Aug	6047	6045	25615	25000	11461	11218	6047
Sept	5363	5361	26024	25000	11461	11218	5363
Oct	5137	5135	26135	25000	11461	11218	5137
Nov	4030	4029	26605	25000	11461	11219	4030
Dec	3288	3286	26916	25000	11461	11219	3288
Temperature (°C)							
State Point	1'	1	2	3	4	4'	5
Jan	-5.715	-5.73	8.95	100	56.3	54.55	-5.715
Feb	-2.2	-2.214	13.28	100	56.3	54.57	-2.2
Mar	2.786	2.773	19.59	100	56.3	54.61	2.786
Apr	9.171	9.159	28.01	100	56.3	54.67	9.171
May	15.24	15.23	36.56	100	56.3	54.71	15.24
June	20.8	20.79	45.16	100	56.3	54.76	20.8
July	23.21	23.2	49.34	100	56.3	54.78	23.21
Aug	22.31	22.3	47.7	100	56.3	54.77	22.31
Sept	17.2	17.19	39.48	100	56.3	54.73	17.2
Oct	15.4	15.39	36.8	100	56.3	54.72	15.4
Nov	5.596	5.583	23.24	100	56.3	54.64	5.596
Dec	-2.185	-2.199	13.31	100	56.3	54.57	-2.185
Enthalpy (kJ/kg)							
State Point	1'	1	2	3	4	4'	5
Jan	73.61	73.46	97.81	291.5	265.6	262.2	236.2
Feb	81.92	81.77	106.1	291.5	265.6	262.3	238.3
Mar	94.13	93.98	118.3	291.5	265.6	262.5	241.2
Apr	110.7	110.6	134.9	291.5	265.6	262.8	244.8
May	127.9	127.8	152.1	291.5	265.6	263.1	248
June	145.8	145.7	169.9	291.5	265.6	263.3	250.7
July	154.7	154.6	178.8	291.5	265.6	263.4	251.9
Aug	151.2	151.1	175.3	291.5	265.6	263.4	251.5
Sept	133.9	133.8	158.1	291.5	265.6	263.2	249
Oct	128.4	128.3	152.6	291.5	265.6	263.1	248
Nov	101.3	101.1	125.5	291.5	265.6	262.7	242.8
Dec	81.96	81.81	106.2	291.5	265.6	262.3	238.3
Entropy (kJ/kg-K)							
State Point	1'	1	2	3	4	4'	5
Jan	0.2865	0.2859	0.2859	0.8858	0.8859	0.8772	0.8944
Feb	0.3161	0.3156	0.3156	0.8858	0.8859	0.8777	0.8933
Mar	0.3589	0.3584	0.3584	0.8858	0.8859	0.8783	0.892
Apr	0.4157	0.4152	0.4152	0.8858	0.8859	0.8792	0.8905
May	0.4731	0.4726	0.4726	0.8858	0.8859	0.88	0.8892
June	0.5313	0.5308	0.5308	0.8858	0.8859	0.8807	0.8883
July	0.5599	0.5595	0.5595	0.8858	0.8859	0.881	0.8879
Aug	0.5483	0.5482	0.5482	0.8858	0.8859	0.8809	0.888
Sept	0.4928	0.4923	0.4923	0.8858	0.8859	0.8802	0.8889
Oct	0.4747	0.4742	0.4742	0.8858	0.8859	0.88	0.8892
Nov	0.3836	0.383	0.383	0.8858	0.8859	0.8787	0.8913
Dec	0.3163	0.3157	0.3157	0.8858	0.8859	0.8777	0.8933

Table B-4: Thermodynamic Properties for Direct Single-Loop System Simulations at 2.5km Depth, CO2

Mass Flow Rate of 140kg/s, and Reservoir Temperature of 100°C (DTE=0.85).

Tres	100°C						
Well Depth	2.5 km						
CO2 Mass Flow	140 kg/s						
Pressure (kPa)							
State Point	1'	1	2	3	4	4'	5
Jan	2987	2985	27000	25000	11226	10892	2987
Feb	3287	3285	26860	25000	11226	10892	3287
Mar	3750	3748	26661	25000	11226	10892	3750
Apr	4411	4409	26389	25000	11226	10892	4411
May	5117	5116	26080	25000	11226	10892	5117
June	5838	5836	25687	25000	11226	10891	5838
July	6175	6173	25438	25000	11226	10891	6175
Aug	6047	6045	25545	25000	11226	10891	6047
Sept	5363	5361	25959	25000	11226	10891	5363
Oct	5137	5135	26070	25000	11226	10892	5137
Nov	4031	4029	26545	25000	11226	10892	4031
Dec	3288	3286	26859	25000	11226	10892	3288
Temperature (°C)							
State Point	1'	1	2	3	4	4'	5
Jan	-5.71	-5.73	8.921	100	55.12	52.98	-5.71
Feb	-2.195	-2.214	13.25	100	55.12	53	-2.195
Mar	2.791	2.773	19.55	100	55.12	53.04	2.791
Apr	9.176	9.159	27.97	100	55.12	53.08	9.176
May	15.25	15.23	36.51	100	55.12	53.12	15.25
June	20.81	20.79	45.1	100	55.12	53.15	20.81
July	23.22	23.2	49.27	100	55.12	53.17	23.22
Aug	22.32	22.3	47.64	100	55.12	53.16	22.32
Sept	17.21	17.19	39.43	100	55.12	53.13	17.21
Oct	15.41	15.39	36.74	100	55.12	53.12	15.41
Nov	5.601	5.583	23.2	100	55.12	53.05	5.601
Dec	-2.18	-2.199	13.27	100	55.12	53.01	-2.18
Enthalpy (kJ/kg)							
State Point	1'	1	2	3	4	4'	5
Jan	73.59	73.46	97.75	291.5	265	261.9	236.5
Feb	81.9	81.77	106.1	291.5	265	262	238.6
Mar	94.11	93.98	118.3	291.5	265	262.2	241.4
Apr	110.7	110.6	134.8	291.5	265	262.4	245
May	127.9	127.8	152	291.5	265	262.7	248.1
June	145.8	145.7	169.9	291.5	265	262.9	250.9
July	154.7	154.6	178.7	291.5	265	262.9	252
Aug	151.2	151.1	175.2	291.5	265	262.9	251.6
Sept	133.9	133.8	158	291.5	265	262.7	249.1
Oct	128.4	128.3	152.5	291.5	265	262.7	248.2
Nov	101.3	101.1	125.4	291.5	265	262.3	243
Dec	81.94	81.81	106.1	291.5	265	262	238.6
Entropy (kJ/kg-K)							
State Point	1'	1	2	3	4	4'	5
Jan	0.2864	0.2859	0.2859	0.8858	0.8859	0.8786	0.8954
Feb	0.316	0.3156	0.3156	0.8858	0.8859	0.879	0.8943
Mar	0.3589	0.3584	0.3584	0.8858	0.8859	0.8796	0.8928
Apr	0.4156	0.4152	0.4152	0.8858	0.8859	0.8803	0.8912
May	0.473	0.4726	0.4726	0.8858	0.8859	0.881	0.8899
June	0.5312	0.5308	0.5308	0.8858	0.8859	0.8816	0.8888
July	0.5599	0.5595	0.5595	0.8858	0.8859	0.8819	0.8884
Aug	0.5484	0.5482	0.5482	0.8858	0.8859	0.8818	0.8885
Sept	0.4927	0.4923	0.4923	0.8858	0.8859	0.8812	0.8895
Oct	0.4746	0.4742	0.4742	0.8858	0.8859	0.881	0.8898
Nov	0.3835	0.383	0.383	0.8858	0.8859	0.8799	0.8921
Dec	0.3162	0.3157	0.3157	0.8858	0.8859	0.879	0.8943

Table B-5: Thermodynamic Properties for Direct Single-Loop System Simulations at 2.5km Depth, CO2

Mass Flow Rate of 70kg/s, and Reservoir Temperature of 125°C (DTE=0.85).

Tres	125°C						
Well Depth	2.5 km						
CO2 Mass Flow	70 kg/s						
Pressure (kPa)							
State Point	1'	1	2	3	4	4'	5
Jan	2986	2985	27072	25000	13488	13158	2986
Feb	3286	3285	26933	25000	13488	13158	3286
Mar	3749	3748	26736	25000	13488	13157	3749
Apr	4410	4409	26468	25000	13488	13157	4410
May	5117	5116	26164	25000	13488	13157	5117
June	5838	5836	25776	25000	13488	13156	5838
July	6174	6173	25530	25000	13488	13156	6174
Aug	6047	6045	25636	25000	13488	13156	6047
Sept	5362	5361	26044	25000	13488	13156	5362
Oct	5137	5135	26154	25000	13488	13157	5137
Nov	4030	4029	26622	25000	13488	13157	4030
Dec	3288	3286	26932	25000	13488	13158	3288
Temperature (°C)							
State Point	1'	1	2	3	4	4'	5
Jan	-5.717	-5.73	8.958	125	80.05	76.32	-5.717
Feb	-2.201	-2.214	13.29	125	80.05	76.39	-2.201
Mar	2.785	2.773	19.6	125	80.05	76.5	2.785
Apr	9.17	9.159	28.02	125	80.05	76.63	9.17
May	15.24	15.23	36.57	125	80.05	76.76	15.24
June	20.8	20.79	45.18	125	80.05	76.87	20.8
July	24.09	23.2	49.36	125	80.05	76.92	24.09
Aug	22.68	22.3	47.72	125	80.05	76.9	22.68
Sept	17.2	17.19	39.5	125	80.05	76.8	17.2
Oct	15.4	15.39	36.81	125	80.05	76.76	15.4
Nov	5.595	5.583	23.25	125	80.05	76.55	5.595
Dec	-2.186	-2.199	13.32	125	80.05	76.39	-2.186
Enthalpy (kJ/kg)							
State Point	1'	1	2	3	4	4'	5
Jan	73.68	73.46	97.82	343.9	317	310.7	272.9
Feb	81.98	81.77	106.1	343.9	317	310.9	275.4
Mar	94.19	93.98	118.3	343.9	317	311.2	279
Apr	110.8	110.6	134.9	343.9	317	311.6	283.3
May	128	127.8	152.1	343.9	317	312	287.2
June	145.8	145.7	170	343.9	317	312.3	290.7
July	154.8	154.6	178.9	343.9	317	312.5	292.2
Aug	151.2	151.1	175.3	343.9	317	312.4	291.6
Sept	134	133.8	158.1	343.9	317	312.1	288.5
Oct	128.5	128.3	152.6	343.9	317	312	287.3
Nov	101.3	101.1	125.5	343.9	317	311.4	280.9
Dec	82.02	81.81	106.2	343.9	317	310.9	275.5
Entropy (kJ/kg-K)							
State Point	1'	1	2	3	4	4'	5
Jan	0.2867	0.2859	0.2859	1.022	1.022	1.007	1.032
Feb	0.3164	0.3156	0.3156	1.022	1.022	1.007	1.03
Mar	0.3592	0.3584	0.3584	1.022	1.022	1.008	1.029
Apr	0.4159	0.4152	0.4152	1.022	1.022	1.009	1.027
May	0.4733	0.4726	0.4726	1.022	1.022	1.01	1.025
June	0.5315	0.5308	0.5308	1.022	1.022	1.011	1.024
July	0.5601	0.5595	0.5595	1.022	1.022	1.012	1.024
Aug	0.5488	0.5482	0.5482	1.022	1.022	1.011	1.024
Sept	0.493	0.4923	0.4923	1.022	1.022	1.011	1.025
Oct	0.4749	0.4742	0.4742	1.022	1.022	1.01	1.025
Nov	0.3838	0.383	0.383	1.022	1.022	1.009	1.028
Dec	0.3165	0.3157	0.3157	1.022	1.022	1.007	1.03

Table B-6: Thermodynamic Properties for Direct Single-Loop System Simulations at 2.5km Depth, CO2

Mass Flow Rate of 90kg/s, and Reservoir Temperature of 125°C (DTE=0.85).

Tres	125°C						
Well Depth	2.5 km						
CO2 Mass Flow	90 kg/s						
Pressure (kPa)							
State Point	1'	1	2	3	4	4'	5
Jan	2987	2985	26983	25000	12893	12328	2987
Feb	3287	3285	26843	25000	12893	12328	3287
Mar	3750	3748	26642	25000	12893	12328	3750
Apr	4411	4409	26370	25000	12893	12327	4411
May	5118	5116	26060	25000	12893	12327	5118
June	5839	5836	25665	25000	12893	12326	5839
July	6175	6173	25416	25000	12893	12326	6175
Aug	6048	6045	25523	25000	12893	12326	6048
Sept	5363	5361	25938	25000	12893	12326	5363
Oct	5137	5135	26050	25000	12893	12327	5137
Nov	4031	4029	26527	25000	12893	12327	4031
Dec	3288	3286	26842	25000	12893	12328	3288
Temperature (°C)							
State Point	1'	1	2	3	4	4'	5
Jan	-5.708	-5.73	8.912	125	76.75	72.1	-5.708
Feb	-2.193	-2.214	13.24	125	76.75	72.16	-2.193
Mar	2.793	2.773	19.54	125	76.75	72.23	2.793
Apr	9.177	9.159	27.95	125	76.75	72.33	9.177
May	15.25	15.23	36.49	125	76.75	72.43	15.25
June	20.81	20.79	45.08	125	76.75	72.51	20.81
July	23.22	23.2	49.24	125	76.75	72.55	24.2
Aug	22.32	22.3	47.61	125	76.75	72.54	22.78
Sept	17.21	17.19	39.41	125	76.75	72.46	17.21
Oct	15.41	15.39	36.73	125	76.75	72.43	15.41
Nov	5.602	5.583	23.19	125	76.75	72.28	5.602
Dec	-2.178	-2.199	13.26	125	76.75	72.16	-2.178
Enthalpy (kJ/kg)							
State Point	1'	1	2	3	4	4'	5
Jan	73.63	73.46	97.73	343.9	315.3	309.7	273.6
Feb	81.94	81.77	106	343.9	315.3	309.9	276.1
Mar	94.15	93.98	118.2	343.9	315.3	310.1	279.6
Apr	110.7	110.6	134.8	343.9	315.3	310.4	283.9
May	128	127.8	152	343.9	315.3	310.7	287.8
June	145.8	145.7	169.8	343.9	315.3	311	291.2
July	154.7	154.6	178.7	343.9	315.3	311.1	292.6
Aug	151.2	151.1	175.2	343.9	315.3	311	292.1
Sept	134	133.8	158	343.9	315.3	310.8	289
Oct	128.4	128.3	152.5	343.9	315.3	310.7	287.9
Nov	101.3	101.1	125.4	343.9	315.3	310.3	281.5
Dec	81.98	81.81	106.1	343.9	315.3	309.9	276.1
Entropy (kJ/kg-K)							
State Point	1'	1	2	3	4	4'	5
Jan	0.2865	0.2859	0.2859	1.022	1.022	1.01	1.034
Feb	0.3162	0.3156	0.3156	1.022	1.022	1.011	1.033
Mar	0.359	0.3584	0.3584	1.022	1.022	1.012	1.031
Apr	0.4157	0.4152	0.4152	1.022	1.022	1.012	1.029
May	0.4731	0.4726	0.4726	1.022	1.022	1.013	1.027
June	0.5313	0.5308	0.5308	1.022	1.022	1.014	1.026
July	0.56	0.5595	0.5595	1.022	1.022	1.014	1.025
Aug	0.5487	0.5482	0.5482	1.022	1.022	1.014	1.026
Sept	0.4928	0.4923	0.4923	1.022	1.022	1.014	1.027
Oct	0.4747	0.4742	0.4742	1.022	1.022	1.013	1.027
Nov	0.3836	0.383	0.383	1.022	1.022	1.012	1.03
Dec	0.3163	0.3157	0.3157	1.022	1.022	1.011	1.033

Table B-7: Thermodynamic Properties for Direct Single-Loop System Simulations at 2.5km Depth, CO2

Mass Flow Rate of 120kg/s, and Reservoir Temperature of 125°C (DTE=0.85).

Tres	125°C						
Well Depth	2.5 km						
CO2 Mass Flow	120 kg/s						
Pressure (kPa)							
State Point	1'	1	2	3	4	4'	5
Jan	2986	2985	27055	25000	13587	13294	2986
Feb	3286	3285	26917	25000	13587	13294	3286
Mar	3749	3748	26719	25000	13587	13294	3749
Apr	4410	4409	26450	25000	13587	13293	4410
May	5117	5116	26144	25000	13587	13293	5117
June	5838	5836	25755	25000	13587	13293	5838
July	6174	6173	25509	25000	13587	13293	6174
Aug	6047	6045	25615	25000	13587	13293	6047
Sept	5363	5361	26024	25000	13587	13293	5363
Oct	5137	5135	26135	25000	13587	13293	5137
Nov	4030	4029	26605	25000	13587	13294	4030
Dec	3288	3286	26916	25000	13587	13294	3288
Temperature (°C)							
State Point	1'	1	2	3	4	4'	5
Jan	-5.715	-5.73	8.95	125	80.59	77.59	-5.715
Feb	-2.2	-2.214	13.28	125	80.59	77.65	-2.2
Mar	2.786	2.773	19.59	125	80.59	77.72	2.786
Apr	9.171	9.159	28.01	125	80.59	77.82	9.171
May	15.24	15.23	36.56	125	80.59	77.91	15.24
June	20.8	20.79	45.16	125	80.59	78	20.8
July	23.21	23.2	49.34	125	80.59	78.03	24.28
Aug	22.31	22.3	47.7	125	80.59	78.02	22.87
Sept	17.2	17.19	39.48	125	80.59	77.94	17.2
Oct	15.4	15.39	36.8	125	80.59	77.91	15.4
Nov	5.596	5.583	23.24	125	80.59	77.76	5.596
Dec	-2.185	-2.199	13.31	125	80.59	77.65	-2.185
Enthalpy (kJ/kg)							
State Point	1'	1	2	3	4'	4	5
Jan	73.61	73.46	97.81	343.9	317.3	312.6	274.2
Feb	81.92	81.77	106.1	343.9	317.3	312.8	276.7
Mar	94.13	93.98	118.3	343.9	317.3	313	280.1
Apr	110.7	110.6	134.9	343.9	317.3	313.3	284.4
May	127.9	127.8	152.1	343.9	317.3	313.5	288.3
June	145.8	145.7	169.9	343.9	317.3	313.8	291.7
July	154.7	154.6	178.8	343.9	317.3	313.9	293.1
Aug	151.2	151.1	175.3	343.9	317.3	313.8	292.6
Sept	133.9	133.8	158.1	343.9	317.3	313.6	289.5
Oct	128.4	128.3	152.6	343.9	317.3	313.5	288.4
Nov	101.3	101.1	125.5	343.9	317.3	313.1	282
Dec	81.96	81.81	106.2	343.9	317.3	312.8	276.7
Entropy (kJ/kg-K)							
State Point	1'	1	2	3	4	4'	5
Jan	0.2865	0.2859	0.2859	1.022	1.022	1.011	1.036
Feb	0.3161	0.3156	0.3156	1.022	1.022	1.011	1.035
Mar	0.3589	0.3584	0.3584	1.022	1.022	1.012	1.033
Apr	0.4157	0.4152	0.4152	1.022	1.022	1.013	1.031
May	0.4731	0.4726	0.4726	1.022	1.022	1.014	1.029
June	0.5313	0.5308	0.5308	1.022	1.022	1.014	1.027
July	0.5599	0.5595	0.5595	1.022	1.022	1.015	1.027
Aug	0.5483	0.5482	0.5482	1.022	1.022	1.014	1.027
Sept	0.4928	0.4923	0.4923	1.022	1.022	1.014	1.028
Oct	0.4747	0.4742	0.4742	1.022	1.022	1.014	1.029
Nov	0.3836	0.383	0.383	1.022	1.022	1.012	1.032
Dec	0.3163	0.3157	0.3157	1.022	1.022	1.011	1.035

Table B-8: Thermodynamic Properties for Direct Single-Loop System Simulations at 2.5km Depth, CO2

Mass Flow Rate of 140kg/s, and Reservoir Temperature of 125°C (DTE=0.85).

Tres	125°C						
Well Depth	2.5 km						
CO2 Mass Flow	140 kg/s						
Pressure (kPa)							
State Point	1'	1	2	3	4	4'	5
Jan	2987	2985	27000	25000	13297	12891	2987
Feb	3287	3285	26860	25000	13297	12891	3287
Mar	3750	3748	26661	25000	13297	12891	3750
Apr	4411	4409	26389	25000	13297	12891	4411
May	5117	5116	26080	25000	13297	12890	5117
June	5838	5836	25687	25000	13297	12890	5838
July	6175	6173	25438	25000	13297	12890	6175
Aug	6047	6045	25545	25000	13297	12890	6047
Sept	5363	5361	25959	25000	13297	12890	5363
Oct	5137	5135	26070	25000	13297	12890	5137
Nov	4031	4029	26545	25000	13297	12891	4031
Dec	3288	3286	26859	25000	13297	12891	3288
Temperature (°C)							
State Point	1'	1	2	3	4	4'	5
Jan	-5.71	-5.73	8.921	125	79.01	75.59	-5.71
Feb	-2.195	-2.214	13.25	125	79.01	75.63	-2.195
Mar	2.791	2.773	19.55	125	79.01	75.7	2.791
Apr	9.176	9.159	27.97	125	79.01	75.78	9.176
May	15.25	15.23	36.51	125	79.01	75.85	15.25
June	20.81	20.79	45.1	125	79.01	75.93	20.81
July	23.22	23.2	49.27	125	79.01	75.96	24.33
Aug	22.32	22.3	47.64	125	79.01	75.95	22.91
Sept	17.21	17.19	39.43	125	79.01	75.88	17.21
Oct	15.41	15.39	36.74	125	79.01	75.86	15.41
Nov	5.601	5.583	23.2	125	79.01	75.73	5.601
Dec	-2.18	-2.199	13.27	125	79.01	75.63	-2.18
Enthalpy (kJ/kg)							
State Point	1'	1	2	3	4	4'	5
Jan	73.59	73.46	97.75	343.9	316.5	312.1	274.5
Feb	81.9	81.77	106.1	343.9	316.5	312.2	277
Mar	94.11	93.98	118.3	343.9	316.5	312.4	280.4
Apr	110.7	110.6	134.8	343.9	316.5	312.7	284.7
May	127.9	127.8	152	343.9	316.5	312.9	288.5
June	145.8	145.7	169.9	343.9	316.5	313.1	291.9
July	154.7	154.6	178.7	343.9	316.5	313.2	293.3
Aug	151.2	151.1	175.2	343.9	316.5	313.1	292.8
Sept	133.9	133.8	158	343.9	316.5	313	289.7
Oct	128.4	128.3	152.5	343.9	316.5	312.9	288.6
Nov	101.3	101.1	125.4	343.9	316.5	312.5	282.3
Dec	81.94	81.81	106.1	343.9	316.5	312.2	277
Entropy (kJ/kg-K)							
State Point	1'	1	2	3	4	4'	5
Jan	0.2864	0.2859	0.2859	1.022	1.022	1.013	1.038
Feb	0.316	0.3156	0.3156	1.022	1.022	1.013	1.036
Mar	0.3589	0.3584	0.3584	1.022	1.022	1.014	1.034
Apr	0.4156	0.4152	0.4152	1.022	1.022	1.014	1.032
May	0.473	0.4726	0.4726	1.022	1.022	1.015	1.03
June	0.5312	0.5308	0.5308	1.022	1.022	1.015	1.028
July	0.5599	0.5595	0.5595	1.022	1.022	1.016	1.028
Aug	0.5484	0.5482	0.5482	1.022	1.022	1.016	1.028
Sept	0.4927	0.4923	0.4923	1.022	1.022	1.015	1.029
Oct	0.4746	0.4742	0.4742	1.022	1.022	1.015	1.03
Nov	0.3835	0.383	0.383	1.022	1.022	1.014	1.033
Dec	0.3162	0.3157	0.3157	1.022	1.022	1.013	1.036

Table B-9: Thermodynamic Properties for Direct Single-Loop System Simulations at 2.5km Depth, CO2

Mass Flow Rate of 70kg/s, and Reservoir Temperature of 150°C (DTE=0.85).

Tres	150°C						
Well Depth	2.5 km						
CO2 Mass Flow	70 kg/s						
	Pressure (kPa)						
State Point	1'	1	2	3	4	4'	5
Jan	2986	2985	27072	25000	14868	14484	2986
Feb	3286	3285	26933	25000	14868	14484	3286
Mar	3749	3748	26736	25000	14868	14483	3749
Apr	4410	4409	26468	25000	14868	14483	4410
May	5117	5116	26164	25000	14868	14483	5117
June	5838	5836	25776	25000	14868	14482	5838
July	6174	6173	25530	25000	14868	14482	6174
Aug	6047	6045	25636	25000	14868	14482	6047
Sept	5362	5361	26044	25000	14868	14483	5362
Oct	5137	5135	26154	25000	14868	14483	5137
Nov	4030	4029	26622	25000	14868	14483	4030
Dec	3288	3286	26932	25000	14868	14484	3288
	Temperature (°C)						
State Point	1'	1	2	3	4	4'	5
Jan	-5.717	-5.73	8.958	150	106.2	100.5	-5.717
Feb	-2.201	-2.214	13.29	150	106.2	100.6	-2.201
Mar	2.785	2.773	19.6	150	106.2	100.8	2.785
Apr	9.17	9.159	28.02	150	106.2	101	11.5
May	15.24	15.23	36.57	150	106.2	101.1	21.92
June	20.8	20.79	45.18	150	106.2	101.3	31.46
July	23.21	23.2	49.36	150	106.2	101.4	35.6
Aug	22.31	22.3	47.72	150	106.2	101.4	34.05
Sept	17.2	17.19	39.5	150	106.2	101.2	25.29
Oct	15.4	15.39	36.81	150	106.2	101.2	22.2
Nov	5.595	5.583	23.25	150	106.2	100.9	5.595
Dec	-2.186	-2.199	13.32	150	106.2	100.6	-2.186
	Enthalpy (kJ/kg)						
State Point	1'	1	2	3	4	4'	5
Jan	73.68	73.46	97.82	390.4	362.6	354.5	304.5
Feb	81.98	81.77	106.1	390.4	362.6	354.7	307.4
Mar	94.19	93.98	118.3	390.4	362.6	355	311.4
Apr	110.8	110.6	134.9	390.4	362.6	355.4	316.3
May	128	127.8	152.1	390.4	362.6	355.7	320.8
June	145.8	145.7	170	390.4	362.6	356.1	325
July	154.8	154.6	178.9	390.4	362.6	356.2	326.8
Aug	151.2	151.1	175.3	390.4	362.6	356.2	326.2
Sept	134	133.8	158.1	390.4	362.6	355.8	322.3
Oct	128.5	128.3	152.6	390.4	362.6	355.7	320.9
Nov	101.3	101.1	125.5	390.4	362.6	355.2	313.5
Dec	82.02	81.81	106.2	390.4	362.6	354.7	307.4
	Entropy (kJ/kg-K)						
State Point	1'	1	2	3	4	4'	5
Jan	0.2867	0.2859	0.2859	1.135	1.135	1.117	1.15
Feb	0.3164	0.3156	0.3156	1.135	1.135	1.118	1.148
Mar	0.3592	0.3584	0.3584	1.135	1.135	1.118	1.146
Apr	0.4159	0.4152	0.4152	1.135	1.135	1.119	1.144
May	0.4733	0.4726	0.4726	1.135	1.135	1.12	1.141
June	0.5315	0.5308	0.5308	1.135	1.135	1.121	1.139
July	0.5601	0.5595	0.5595	1.135	1.135	1.122	1.138
Aug	0.5488	0.5482	0.5482	1.135	1.135	1.121	1.139
Sept	0.493	0.4923	0.4923	1.135	1.135	1.121	1.141
Oct	0.4749	0.4742	0.4742	1.135	1.135	1.12	1.141
Nov	0.3838	0.383	0.383	1.135	1.135	1.119	1.145
Dec	0.3165	0.3157	0.3157	1.135	1.135	1.118	1.148

Table B-10: Thermodynamic Properties for Direct Single-Loop System Simulations at 2.5km Depth, CO2 Mass Flow Rate of 90kg/s, and Reservoir Temperature of 150°C (DTE=0.85).

Tres	150°C						
Well Depth	2.5 km						
CO2 Mass Flow	90 kg/s						
Pressure (kPa)							
State Point	1'	1	2	3	4	4'	5
Jan	2987	2985	26983	25000	14157	13495	2987
Feb	3287	3285	26843	25000	14157	13495	3287
Mar	3750	3748	26642	25000	14157	13494	3750
Apr	4411	4409	26370	25000	14157	13494	4411
May	5118	5116	26060	25000	14157	13493	5118
June	5839	5836	25665	25000	14157	13493	5839
July	6175	6173	25416	25000	14157	13493	6175
Aug	6048	6045	25523	25000	14157	13493	6048
Sept	5363	5361	25938	25000	14157	13493	5363
Oct	5137	5135	26050	25000	14157	13493	5137
Nov	4031	4029	26527	25000	14157	13494	4031
Dec	3288	3286	26842	25000	14157	13495	3288
Temperature (°C)							
State Point	1'	1	2	3	4	4'	5
Jan	-5.708	-5.73	8.912	150	102.1	95.52	-5.708
Feb	-2.193	-2.214	13.24	150	102.1	95.6	-2.193
Mar	2.793	2.773	19.54	150	102.1	95.71	2.793
Apr	9.177	9.159	27.95	150	102.1	95.86	11.83
May	15.25	15.23	36.49	150	102.1	95.99	22.24
June	20.81	20.79	45.08	150	102.1	96.12	31.77
July	23.22	23.2	49.24	150	102.1	96.17	35.9
Aug	22.32	22.3	47.61	150	102.1	96.15	34.36
Sept	17.21	17.19	39.41	150	102.1	96.04	25.6
Oct	15.41	15.39	36.73	150	102.1	96	22.52
Nov	5.602	5.583	23.19	150	102.1	95.78	5.675
Dec	-2.178	-2.199	13.26	150	102.1	95.6	-2.178
Enthalpy (kJ/kg)							
State Point	1'	1	2	3	4	4'	5
Jan	73.63	73.46	97.73	390.4	360.3	352.9	305.3
Feb	81.94	81.77	106	390.4	360.3	353.1	308.2
Mar	94.15	93.98	118.2	390.4	360.3	353.3	312.1
Apr	110.7	110.6	134.8	390.4	360.3	353.6	317
May	128	127.8	152	390.4	360.3	353.9	321.5
June	145.8	145.7	169.8	390.4	360.3	354.2	325.7
July	154.7	154.6	178.7	390.4	360.3	354.3	327.5
Aug	151.2	151.1	175.2	390.4	360.3	354.2	326.8
Sept	134	133.8	158	390.4	360.3	354	323
Oct	128.4	128.3	152.5	390.4	360.3	353.9	321.6
Nov	101.3	101.1	125.4	390.4	360.3	353.4	314.3
Dec	81.98	81.81	106.1	390.4	360.3	353.1	308.2
Entropy (kJ/kg-K)							
State Point	1'	1	2	3	4	4'	5
Jan	0.2865	0.2859	0.2859	1.135	1.135	1.121	1.153
Feb	0.3162	0.3156	0.3156	1.135	1.135	1.122	1.151
Mar	0.359	0.3584	0.3584	1.135	1.135	1.123	1.149
Apr	0.4157	0.4152	0.4152	1.135	1.135	1.123	1.146
May	0.4731	0.4726	0.4726	1.135	1.135	1.124	1.144
June	0.5313	0.5308	0.5308	1.135	1.135	1.125	1.141
July	0.56	0.5595	0.5595	1.135	1.135	1.125	1.14
Aug	0.5487	0.5482	0.5482	1.135	1.135	1.125	1.141
Sept	0.4928	0.4923	0.4923	1.135	1.135	1.124	1.143
Oct	0.4747	0.4742	0.4742	1.135	1.135	1.124	1.143
Nov	0.3836	0.383	0.383	1.135	1.135	1.123	1.148
Dec	0.3163	0.3157	0.3157	1.135	1.135	1.122	1.151

Table B-11: Thermodynamic Properties for Direct Single-Loop System Simulations at 2.5km Depth, CO₂

Mass Flow Rate of 120kg/s, and Reservoir Temperature of 150°C (DTE=0.85).

Tres	150°C						
Well Depth	2.5 km						
CO₂ Mass Flow	120 kg/s						
	Pressure (kPa)						
State Point	1'	1	2	3	4	4'	5
Jan	2986	2985	27055	25000	14987	14645	2986
Feb	3286	3285	26917	25000	14987	14645	3286
Mar	3749	3748	26719	25000	14987	14645	3749
Apr	4410	4409	26450	25000	14987	14645	4410
May	5117	5116	26144	25000	14987	14645	5117
June	5838	5836	25755	25000	14987	14644	5838
July	6174	6173	25509	25000	14987	14644	6174
Aug	6047	6045	25615	25000	14987	14644	6047
Sept	5363	5361	26024	25000	14987	14645	5363
Oct	5137	5135	26135	25000	14987	14645	5137
Nov	4030	4029	26605	25000	14987	14645	4030
Dec	3288	3286	26916	25000	14987	14645	3288
	Temperature (°C)						
State Point	1'	1	2	3	4	4'	5
Jan	-5.715	-5.73	8.95	150	106.8	102.4	-5.715
Feb	-2.2	-2.214	13.28	150	106.8	102.5	-2.2
Mar	2.786	2.773	19.59	150	106.8	102.6	2.786
Apr	9.171	9.159	28.01	150	106.8	102.7	12.15
May	15.24	15.23	36.56	150	106.8	102.9	22.56
June	20.8	20.79	45.16	150	106.8	103	32.08
July	23.21	23.2	49.34	150	106.8	103	36.2
Aug	22.31	22.3	47.7	150	106.8	103	34.66
Sept	17.2	17.19	39.48	150	106.8	102.9	25.91
Oct	15.4	15.39	36.8	150	106.8	102.9	22.83
Nov	5.596	5.583	23.24	150	106.8	102.7	6.001
Dec	-2.185	-2.199	13.31	150	106.8	102.5	-2.185
	Enthalpy (kJ/kg)						
State Point	1'	1	2	3	4	4'	5
Jan	73.61	73.46	97.81	390.4	363	356.9	306.1
Feb	81.92	81.77	106.1	390.4	363	357.1	308.9
Mar	94.13	93.98	118.3	390.4	363	357.3	312.8
Apr	110.7	110.6	134.9	390.4	363	357.6	317.7
May	127.9	127.8	152.1	390.4	363	357.8	322.2
June	145.8	145.7	169.9	390.4	363	358.1	326.3
July	154.7	154.6	178.8	390.4	363	358.2	328.1
Aug	151.2	151.1	175.3	390.4	363	358.1	327.5
Sept	133.9	133.8	158.1	390.4	363	357.9	323.7
Oct	128.4	128.3	152.6	390.4	363	357.8	322.3
Nov	101.3	101.1	125.5	390.4	363	357.4	315
Dec	81.96	81.81	106.2	390.4	363	357.1	308.9
	Entropy (kJ/kg-K)						
State Point	1'	1	2	3	4	4'	5
Jan	0.2865	0.2859	0.2859	1.135	1.135	1.122	1.156
Feb	0.3161	0.3156	0.3156	1.135	1.135	1.123	1.154
Mar	0.3589	0.3584	0.3584	1.135	1.135	1.123	1.152
Apr	0.4157	0.4152	0.4152	1.135	1.135	1.124	1.149
May	0.4731	0.4726	0.4726	1.135	1.135	1.125	1.146
June	0.5313	0.5308	0.5308	1.135	1.135	1.125	1.144
July	0.5599	0.5595	0.5595	1.135	1.135	1.125	1.143
Aug	0.5483	0.5482	0.5482	1.135	1.135	1.125	1.143
Sept	0.4928	0.4923	0.4923	1.135	1.135	1.125	1.145
Oct	0.4747	0.4742	0.4742	1.135	1.135	1.125	1.146
Nov	0.3836	0.383	0.383	1.135	1.135	1.123	1.15
Dec	0.3163	0.3157	0.3157	1.135	1.135	1.123	1.154

Table B-12: Thermodynamic Properties for Direct Single-Loop System Simulations at 2.5km Depth, CO2 Mass Flow Rate of 140kg/s, and Reservoir Temperature of 150°C (DTE=0.85).

Tres	150°C						
Well Depth	2.5 km						
CO2 Mass Flow	140 kg/s						
Pressure (kPa)							
State Point	1'	1	2	3	4	4'	5
Jan	2987	2985	27000	25000	14640	14167	2987
Feb	3287	3285	26860	25000	14640	14167	3287
Mar	3750	3748	26661	25000	14640	14166	3750
Apr	4411	4409	26389	25000	14640	14166	4411
May	5117	5116	26080	25000	14640	14166	5117
June	5838	5836	25687	25000	14640	14166	5838
July	6175	6173	25438	25000	14640	14166	6175
Aug	6047	6045	25545	25000	14640	14166	6047
Sept	5363	5361	25959	25000	14640	14166	5363
Oct	5137	5135	26070	25000	14640	14166	5137
Nov	4031	4029	26545	25000	14640	14166	4031
Dec	3288	3286	26859	25000	14640	14167	3288
Temperature (°C)							
State Point	1'	1	2	3	4	4'	5
Jan	-5.71	-5.73	8.921	150	104.9	100	-5.71
Feb	-2.195	-2.214	13.25	150	104.9	100.1	-2.195
Mar	2.791	2.773	19.55	150	104.9	100.2	2.791
Apr	9.176	9.159	27.97	150	104.9	100.3	12.3
May	15.25	15.23	36.51	150	104.9	100.4	22.7
June	20.81	20.79	45.1	150	104.9	100.5	32.21
July	23.22	23.2	49.27	150	104.9	100.6	36.34
Aug	22.32	22.3	47.64	150	104.9	100.5	34.8
Sept	17.21	17.19	39.43	150	104.9	100.5	26.05
Oct	15.41	15.39	36.74	150	104.9	100.4	22.97
Nov	5.601	5.583	23.2	150	104.9	100.2	6.155
Dec	-2.18	-2.199	13.27	150	104.9	100.1	-2.18
Enthalpy (kJ/kg)							
State Point	1'	1	2	3	4	4'	5
Jan	73.59	73.46	97.75	390.4	361.9	356.2	306.4
Feb	81.9	81.77	106.1	390.4	361.9	356.3	309.3
Mar	94.11	93.98	118.3	390.4	361.9	356.5	313.2
Apr	110.7	110.6	134.8	390.4	361.9	356.7	318
May	127.9	127.8	152	390.4	361.9	356.9	322.5
June	145.8	145.7	169.9	390.4	361.9	357.1	326.6
July	154.7	154.6	178.7	390.4	361.9	357.2	328.4
Aug	151.2	151.1	175.2	390.4	361.9	357.2	327.7
Sept	133.9	133.8	158	390.4	361.9	357	323.9
Oct	128.4	128.3	152.5	390.4	361.9	356.9	322.6
Nov	101.3	101.1	125.4	390.4	361.9	356.6	315.3
Dec	81.94	81.81	106.1	390.4	361.9	356.3	309.3
Entropy (kJ/kg-K)							
State Point	1'	1	2	3	4	4'	5
Jan	0.2864	0.2859	0.2859	1.135	1.135	1.124	1.157
Feb	0.316	0.3156	0.3156	1.135	1.135	1.125	1.155
Mar	0.3589	0.3584	0.3584	1.135	1.135	1.125	1.153
Apr	0.4156	0.4152	0.4152	1.135	1.135	1.126	1.15
May	0.473	0.4726	0.4726	1.135	1.135	1.126	1.147
June	0.5312	0.5308	0.5308	1.135	1.135	1.127	1.144
July	0.5599	0.5595	0.5595	1.135	1.135	1.127	1.144
Aug	0.5484	0.5482	0.5482	1.135	1.135	1.127	1.144
Sept	0.4927	0.4923	0.4923	1.135	1.135	1.126	1.146
Oct	0.4746	0.4742	0.4742	1.135	1.135	1.126	1.147
Nov	0.3835	0.383	0.383	1.135	1.135	1.125	1.151
Dec	0.3162	0.3157	0.3157	1.135	1.135	1.125	1.155

Table B-13: Thermodynamic Properties for Direct Single-Loop System Simulations at 3.1km Depth, CO2 Mass Flow Rate of 70kg/s, and Reservoir Temperature of 100°C (DTE=0.85).

Tres	100°C						
Well Depth	3.1 km						
CO2 Mass Flow	70 kg/s						
Pressure (kPa)							
State Point	1'	1	2	3	4	4'	5
Jan	2986	2985	33030	30000	11189	10946	2986
Feb	3286	3285	32796	30000	11189	10946	3286
Mar	3749	3748	32456	30000	11189	10945	3749
Apr	4410	4409	31989	30000	11189	10945	4410
May	5117	5116	31471	30000	11189	10945	5117
June	5838	5836	30853	30000	11189	10944	5838
July	6174	6173	30488	30000	11189	10944	6174
Aug	6047	6045	30641	30000	11189	10944	6047
Sept	5362	5361	31275	30000	11189	10945	5362
Oct	5137	5135	31455	30000	11189	10945	5137
Nov	4030	4029	32257	30000	11189	10945	4030
Dec	3288	3286	32794	30000	11189	10946	3288
Temperature (°C)							
State Point	1'	1	2	3	4	4'	5
Jan	-5.717	-5.73	11.98	100	51.67	49.98	-5.717
Feb	-2.201	-2.214	16.45	100	51.67	50.02	-2.201
Mar	2.785	2.773	22.96	100	51.67	50.07	2.785
Apr	9.17	9.159	31.7	100	51.67	50.13	9.17
May	15.24	15.23	40.6	100	51.67	50.19	15.24
June	20.8	20.79	49.63	100	51.67	50.24	20.8
July	23.21	23.2	54.03	100	51.67	50.26	23.21
Aug	22.31	22.3	52.3	100	51.67	50.25	22.31
Sept	17.2	17.19	43.66	100	51.67	50.2	17.2
Oct	15.4	15.39	40.85	100	51.67	50.19	15.4
Nov	5.595	5.583	26.74	100	51.67	50.09	5.595
Dec	-2.186	-2.199	16.47	100	51.67	50.02	-2.186
Enthalpy (kJ/kg)							
State Point	1'	1	2	3	4	4'	5
Jan	73.68	73.46	103.7	278.9	246.9	242.7	220.1
Feb	81.98	81.77	112	278.9	246.9	242.9	222.1
Mar	94.19	93.98	124.2	278.9	246.9	243.2	224.8
Apr	110.8	110.6	140.8	278.9	246.9	243.6	228.1
May	128	127.8	158	278.9	246.9	244	231.1
June	145.8	145.7	175.8	278.9	246.9	244.3	233.7
July	154.8	154.6	184.7	278.9	246.9	244.4	234.8
Aug	151.2	151.1	181.2	278.9	246.9	244.4	234.4
Sept	134	133.8	164	278.9	246.9	244.1	232.1
Oct	128.5	128.3	158.4	278.9	246.9	244	231.2
Nov	101.3	101.1	131.3	278.9	246.9	243.4	226.3
Dec	82.02	81.81	112	278.9	246.9	242.9	222.1
Entropy (kJ/kg-K)							
State Point	1'	1	2	3	4	4'	5
Jan	0.2867	0.2859	0.2859	0.8306	0.8306	0.8191	0.8341
Feb	0.3164	0.3156	0.3156	0.8306	0.8306	0.8198	0.8334
Mar	0.3592	0.3584	0.3584	0.8306	0.8306	0.8207	0.8325
Apr	0.4159	0.4152	0.4152	0.8306	0.8306	0.8219	0.8316
May	0.4733	0.4726	0.4726	0.8306	0.8306	0.8231	0.8309
June	0.5315	0.5308	0.5308	0.8306	0.8306	0.8241	0.8304
July	0.5601	0.5595	0.5595	0.8306	0.8306	0.8246	0.8303
Aug	0.5488	0.5482	0.5482	0.8306	0.8306	0.8244	0.8303
Sept	0.493	0.4923	0.4923	0.8306	0.8306	0.8234	0.8307
Oct	0.4749	0.4742	0.4742	0.8306	0.8306	0.8231	0.8309
Nov	0.3838	0.383	0.3831	0.8306	0.8306	0.8213	0.8321
Dec	0.3165	0.3157	0.3157	0.8306	0.8306	0.8198	0.8334

Table B-14: Thermodynamic Properties for Direct Single-Loop System Simulations at 3.1km Depth, CO2 Mass Flow Rate of 90kg/s, and Reservoir Temperature of 100°C (DTE=0.85).

Tres	100°C						
Well Depth	3.1 km						
CO2 Mass Flow	90 kg/s						
Pressure (kPa)							
State Point	1'	1	2	3	4	4'	5
Jan	2987	2985	32919	30000	10669	10257	2987
Feb	3287	3285	32683	30000	10669	10257	3287
Mar	3750	3748	32339	30000	10669	10256	3750
Apr	4411	4409	31867	30000	10669	10256	4411
May	5118	5116	31343	30000	10669	10255	5118
June	5839	5836	30716	30000	10669	10255	5839
July	6175	6173	30347	30000	10669	10255	6175
Aug	6048	6045	30502	30000	10669	10255	6048
Sept	5363	5361	31144	30000	10669	10255	5363
Oct	5137	5135	31327	30000	10669	10255	5137
Nov	4031	4029	32138	30000	10669	10256	4031
Dec	3288	3286	32682	30000	10669	10257	3288
Temperature (°C)							
State Point	1'	1	2	3	4	4'	5
Jan	-5.708	-5.73	11.92	100	49.33	47.01	-5.708
Feb	-2.193	-2.214	16.39	100	49.33	47.03	-2.193
Mar	2.793	2.773	22.9	100	49.33	47.06	2.793
Apr	9.177	9.159	31.62	100	49.33	47.1	9.177
May	15.25	15.23	40.51	100	49.33	47.14	15.25
June	20.81	20.79	49.51	100	49.33	47.17	20.81
July	23.22	23.2	53.9	100	49.33	47.18	23.22
Aug	22.32	22.3	52.18	100	49.33	47.18	22.32
Sept	17.21	17.19	43.56	100	49.33	47.15	17.21
Oct	15.41	15.39	40.76	100	49.33	47.14	15.41
Nov	5.602	5.583	26.67	100	49.33	47.08	5.602
Dec	-2.178	-2.199	16.41	100	49.33	47.03	-2.178
Enthalpy (kJ/kg)							
State Point	1'	1	2	3	4	4'	5
Jan	73.63	73.46	103.6	278.9	245.8	242.2	220.6
Feb	81.94	81.77	111.9	278.9	245.8	242.4	222.6
Mar	94.15	93.98	124.1	278.9	245.8	242.6	225.3
Apr	110.7	110.6	140.6	278.9	245.8	242.9	228.6
May	128	127.8	157.8	278.9	245.8	243.2	231.5
June	145.8	145.7	175.6	278.9	245.8	243.5	234.1
July	154.7	154.6	184.5	278.9	245.8	243.6	235.1
Aug	151.2	151.1	181	278.9	245.8	243.5	234.7
Sept	134	133.8	163.8	278.9	245.8	243.3	232.4
Oct	128.4	128.3	158.3	278.9	245.8	243.2	231.6
Nov	101.3	101.1	131.2	278.9	245.8	242.7	226.8
Dec	81.98	81.81	111.9	278.9	245.8	242.4	222.6
Entropy (kJ/kg-K)							
State Point	1'	1	2	3	4	4'	5
Jan	0.2865	0.2859	0.2859	0.8306	0.8306	0.822	0.8362
Feb	0.3162	0.3156	0.3156	0.8306	0.8306	0.8225	0.8354
Mar	0.359	0.3584	0.3584	0.8306	0.8306	0.8233	0.8343
Apr	0.4157	0.4152	0.4152	0.8306	0.8306	0.8242	0.8332
May	0.4731	0.4726	0.4726	0.8306	0.8306	0.8251	0.8322
June	0.5313	0.5308	0.5308	0.8306	0.8306	0.8259	0.8316
July	0.56	0.5595	0.5595	0.8306	0.8306	0.8263	0.8313
Aug	0.5487	0.5482	0.5482	0.8306	0.8306	0.8261	0.8314
Sept	0.4928	0.4923	0.4923	0.8306	0.8306	0.8254	0.832
Oct	0.4747	0.4742	0.4742	0.8306	0.8306	0.8251	0.8322
Nov	0.3836	0.383	0.3831	0.8306	0.8306	0.8237	0.8338
Dec	0.3163	0.3157	0.3157	0.8306	0.8306	0.8225	0.8354

Table B-15: Thermodynamic Properties for Direct Single-Loop System Simulations at 3.1km Depth, CO2 Mass Flow Rate of 120kg/s, and Reservoir Temperature of 100°C (DTE=0.85).

Tres	100°C						
Well Depth	3.1 km						
CO2 Mass Flow	120 kg/s						
Pressure (kPa)							
State Point	1'	1	2	3	4	4'	5
Jan	2986	2985	33009	30000	11276	11060	2986
Feb	3286	3285	32775	30000	11276	11060	3286
Mar	3749	3748	32434	30000	11276	11060	3749
Apr	4410	4409	31966	30000	11276	11060	4410
May	5117	5116	31447	30000	11276	11059	5117
June	5838	5836	30827	30000	11276	11059	5838
July	6174	6173	30462	30000	11276	11059	6174
Aug	6047	6045	30615	30000	11276	11059	6047
Sept	5363	5361	31251	30000	11276	11059	5363
Oct	5137	5135	31431	30000	11276	11059	5137
Nov	4030	4029	32235	30000	11276	11060	4030
Dec	3288	3286	32773	30000	11276	11060	3288
Temperature (°C)							
State Point	1'	1	2	3	4	4'	5
Jan	-5.715	-5.73	11.97	100	52.05	50.65	-5.715
Feb	-2.2	-2.214	16.44	100	52.05	50.68	-2.2
Mar	2.786	2.773	22.95	100	52.05	50.71	2.786
Apr	9.171	9.159	31.68	100	52.05	50.76	9.171
May	15.24	15.23	40.59	100	52.05	50.8	15.24
June	20.8	20.79	49.61	100	52.05	50.84	20.8
July	23.21	23.2	54	100	52.05	50.86	23.21
Aug	22.31	22.3	52.28	100	52.05	50.85	22.31
Sept	17.2	17.19	43.65	100	52.05	50.82	17.2
Oct	15.4	15.39	40.83	100	52.05	50.8	15.4
Nov	5.596	5.583	26.73	100	52.05	50.73	5.596
Dec	-2.185	-2.199	16.46	100	52.05	50.68	-2.185
Enthalpy (kJ/kg)							
State Point	1'	1	2	3	4	4'	5
Jan	73.61	73.46	103.7	278.9	247.1	244	221
Feb	81.92	81.77	112	278.9	247.1	244.1	223
Mar	94.13	93.98	124.2	278.9	247.1	244.3	225.6
Apr	110.7	110.6	140.7	278.9	247.1	244.6	228.9
May	127.9	127.8	157.9	278.9	247.1	244.9	231.8
June	145.8	145.7	175.8	278.9	247.1	245.1	234.3
July	154.7	154.6	184.7	278.9	247.1	245.2	235.4
Aug	151.2	151.1	181.2	278.9	247.1	245.2	235
Sept	133.9	133.8	163.9	278.9	247.1	245	232.7
Oct	128.4	128.3	158.4	278.9	247.1	244.9	231.9
Nov	101.3	101.1	131.3	278.9	247.1	244.5	227.1
Dec	81.96	81.81	112	278.9	247.1	244.1	223
Entropy (kJ/kg-K)							
State Point	1'	1	2	3	4	4'	5
Jan	0.2865	0.2859	0.2859	0.8306	0.8306	0.8224	0.8376
Feb	0.3161	0.3156	0.3156	0.8306	0.8306	0.8229	0.8367
Mar	0.3589	0.3584	0.3584	0.8306	0.8306	0.8235	0.8355
Apr	0.4157	0.4152	0.4152	0.8306	0.8306	0.8244	0.8342
May	0.4731	0.4726	0.4726	0.8306	0.8306	0.8252	0.8332
June	0.5313	0.5308	0.5308	0.8306	0.8306	0.8259	0.8324
July	0.5599	0.5595	0.5595	0.8306	0.8306	0.8262	0.8321
Aug	0.5483	0.5482	0.5482	0.8306	0.8306	0.8261	0.8322
Sept	0.4928	0.4923	0.4923	0.8306	0.8306	0.8254	0.8329
Oct	0.4747	0.4742	0.4742	0.8306	0.8306	0.8252	0.8332
Nov	0.3836	0.383	0.3831	0.8306	0.8306	0.8239	0.8349
Dec	0.3163	0.3157	0.3157	0.8306	0.8306	0.8229	0.8366

Table B-16: Thermodynamic Properties for Direct Single-Loop System Simulations at 3.1km Depth, CO2 Mass Flow Rate of 140kg/s, and Reservoir Temperature of 100°C (DTE=0.85).

Tres	100°C						
Well Depth	3.1 km						
CO2 Mass Flow	140 kg/s						
Pressure (kPa)							
State Point	1'	1	2	3	4	4'	5
Jan	2987	2985	32941	30000	11022	10724	2987
Feb	3287	3285	32705	30000	11022	10724	3287
Mar	3750	3748	32362	30000	11022	10723	3750
Apr	4411	4409	31891	30000	11022	10723	4411
May	5117	5116	31368	30000	11022	10723	5117
June	5838	5836	30743	30000	11022	10723	5838
July	6175	6173	30374	30000	11022	10723	6175
Aug	6047	6045	30529	30000	11022	10723	6047
Sept	5363	5361	31170	30000	11022	10723	5363
Oct	5137	5135	31352	30000	11022	10723	5137
Nov	4031	4029	32161	30000	11022	10723	4031
Dec	3288	3286	32704	30000	11022	10724	3288
Temperature (°C)							
State Point	1'	1	2	3	4	4'	5
Jan	-5.71	-5.73	11.93	100	50.93	49.23	-5.71
Feb	-2.195	-2.214	16.4	100	50.93	49.25	-2.195
Mar	2.791	2.773	22.91	100	50.93	49.28	2.791
Apr	9.176	9.159	31.63	100	50.93	49.32	9.176
May	15.25	15.23	40.53	100	50.93	49.35	15.25
June	20.81	20.79	49.53	100	50.93	49.38	20.81
July	23.22	23.2	53.92	100	50.93	49.4	23.22
Aug	22.32	22.3	52.2	100	50.93	49.39	22.32
Sept	17.21	17.19	43.58	100	50.93	49.36	17.21
Oct	15.41	15.39	40.78	100	50.93	49.35	15.41
Nov	5.601	5.583	26.68	100	50.93	49.3	5.601
Dec	-2.18	-2.199	16.42	100	50.93	49.25	-2.18
Enthalpy (kJ/kg)							
State Point	1'	1	2	3	4	4'	5
Jan	73.59	73.46	103.6	278.9	246.6	243.7	221.3
Feb	81.9	81.77	111.9	278.9	246.6	243.8	223.2
Mar	94.11	93.98	124.1	278.9	246.6	244	225.8
Apr	110.7	110.6	140.6	278.9	246.6	244.3	229.1
May	127.9	127.8	157.8	278.9	246.6	244.5	232
June	145.8	145.7	175.7	278.9	246.6	244.7	234.5
July	154.7	154.6	184.6	278.9	246.6	244.8	235.5
Aug	151.2	151.1	181.1	278.9	246.6	244.8	235.1
Sept	133.9	133.8	163.8	278.9	246.6	244.6	232.9
Oct	128.4	128.3	158.3	278.9	246.6	244.5	232
Nov	101.3	101.1	131.2	278.9	246.6	244.1	227.3
Dec	81.94	81.81	111.9	278.9	246.6	243.8	223.2
Entropy (kJ/kg-K)							
State Point	1'	1	2	3	4	4'	5
Jan	0.2864	0.2859	0.2859	0.8306	0.8306	0.8237	0.8385
Feb	0.316	0.3156	0.3156	0.8306	0.8306	0.8241	0.8375
Mar	0.3589	0.3584	0.3584	0.8306	0.8306	0.8247	0.8363
Apr	0.4156	0.4152	0.4152	0.8306	0.8306	0.8254	0.8349
May	0.473	0.4726	0.4726	0.8306	0.8306	0.8261	0.8338
June	0.5312	0.5308	0.5308	0.8306	0.8306	0.8267	0.8329
July	0.5599	0.5595	0.5595	0.8306	0.8306	0.827	0.8325
Aug	0.5484	0.5482	0.5482	0.8306	0.8306	0.8269	0.8327
Sept	0.4927	0.4923	0.4923	0.8306	0.8306	0.8263	0.8334
Oct	0.4746	0.4742	0.4742	0.8306	0.8306	0.8261	0.8337
Nov	0.3835	0.383	0.3831	0.8306	0.8306	0.825	0.8356
Dec	0.3162	0.3157	0.3157	0.8306	0.8306	0.8241	0.8375

Table B-17: Thermodynamic Properties for Direct Single-Loop System Simulations at 3.1km Depth, CO2 Mass Flow Rate of 70kg/s, and Reservoir Temperature of 125°C (DTE=0.85).

Tres	125°C						
Well Depth	3.1 km						
CO2 Mass Flow	70 kg/s						
Pressure (kPa)							
State Point	1'	1	2	3	4	4'	5
Jan	2986	2985	33030	30000	13797	13508	2986
Feb	3286	3285	32796	30000	13797	13508	3286
Mar	3749	3748	32456	30000	13797	13508	3749
Apr	4410	4409	31989	30000	13797	13507	4410
May	5117	5116	31471	30000	13797	13507	5117
June	5838	5836	30853	30000	13797	13507	5838
July	6174	6173	30488	30000	13797	13507	6174
Aug	6047	6045	30641	30000	13797	13507	6047
Sept	5362	5361	31275	30000	13797	13507	5362
Oct	5137	5135	31455	30000	13797	13507	5137
Nov	4030	4029	32257	30000	13797	13508	4030
Dec	3288	3286	32794	30000	13797	13508	3288
Temperature (°C)							
State Point	1'	1	2	3	4	4'	5
Jan	-5.717	-5.73	11.98	125	74.18	71.25	-5.717
Feb	-2.201	-2.214	16.45	125	74.18	71.31	-2.201
Mar	2.785	2.773	22.96	125	74.18	71.4	2.785
Apr	9.17	9.159	31.7	125	74.18	71.52	9.17
May	15.24	15.23	40.6	125	74.18	71.63	15.24
June	20.8	20.79	49.63	125	74.18	71.73	20.8
July	23.21	23.2	54.03	125	74.18	71.77	23.21
Aug	22.31	22.3	52.3	125	74.18	71.76	22.31
Sept	17.2	17.19	43.66	125	74.18	71.66	17.2
Oct	15.4	15.39	40.85	125	74.18	71.63	15.4
Nov	5.595	5.583	26.74	125	74.18	71.45	5.595
Dec	-2.186	-2.199	16.47	125	74.18	71.31	-2.186
Enthalpy (kJ/kg)							
State Point	1'	1	2	3	4	4'	5
Jan	73.68	73.46	103.7	328.8	296.2	290.4	255.9
Feb	81.98	81.77	112	328.8	296.2	290.6	258.3
Mar	94.19	93.98	124.2	328.8	296.2	290.9	261.6
Apr	110.8	110.6	140.8	328.8	296.2	291.3	265.6
May	128	127.8	158	328.8	296.2	291.7	269.2
June	145.8	145.7	175.8	328.8	296.2	292	272.4
July	154.8	154.6	184.7	328.8	296.2	292.2	273.7
Aug	151.2	151.1	181.2	328.8	296.2	292.1	273.2
Sept	134	133.8	164	328.8	296.2	291.8	270.3
Oct	128.5	128.3	158.4	328.8	296.2	291.7	269.3
Nov	101.3	101.1	131.3	328.8	296.2	291.1	263.3
Dec	82.02	81.81	112	328.8	296.2	290.6	258.3
Entropy (kJ/kg-K)							
State Point	1'	1	2	3	4	4'	5
Jan	0.2867	0.2859	0.2859	0.96	0.9601	0.9455	0.9682
Feb	0.3164	0.3156	0.3156	0.96	0.9601	0.9461	0.9671
Mar	0.3592	0.3584	0.3584	0.96	0.9601	0.947	0.9657
Apr	0.4159	0.4152	0.4152	0.96	0.9601	0.9481	0.9642
May	0.4733	0.4726	0.4726	0.96	0.9601	0.9491	0.9629
June	0.5315	0.5308	0.5308	0.96	0.9601	0.9501	0.9619
July	0.5601	0.5595	0.5595	0.96	0.9601	0.9505	0.9615
Aug	0.5488	0.5482	0.5482	0.96	0.9601	0.9504	0.9617
Sept	0.493	0.4923	0.4923	0.96	0.9601	0.9495	0.9625
Oct	0.4749	0.4742	0.4742	0.96	0.9601	0.9492	0.9629
Nov	0.3838	0.383	0.3831	0.96	0.9601	0.9475	0.965
Dec	0.3165	0.3157	0.3157	0.96	0.9601	0.9461	0.9671

Table B-18: Thermodynamic Properties for Direct Single-Loop System Simulations at 3.1km Depth, CO2 Mass Flow Rate of 90kg/s, and Reservoir Temperature of 125°C (DTE=0.85).

Tres	125°C						
Well Depth	3.1 km						
CO2 Mass Flow	90 kg/s						
	Pressure (kPa)						
State Point	1'	1	2	3	4	4'	5
Jan	2987	2985	32919	30000	13175	12683	2987
Feb	3287	3285	32683	30000	13175	12683	3287
Mar	3750	3748	32339	30000	13175	12683	3750
Apr	4411	4409	31867	30000	13175	12682	4411
May	5118	5116	31343	30000	13175	12682	5118
June	5839	5836	30716	30000	13175	12681	5839
July	6175	6173	30347	30000	13175	12681	6175
Aug	6048	6045	30502	30000	13175	12681	6048
Sept	5363	5361	31144	30000	13175	12682	5363
Oct	5137	5135	31327	30000	13175	12682	5137
Nov	4031	4029	32138	30000	13175	12683	4031
Dec	3288	3286	32682	30000	13175	12683	3288
	Temperature (°C)						
State Point	1'	1	2	3	4	4'	5
Jan	-5.708	-5.73	11.92	125	71.14	67.55	-5.708
Feb	-2.193	-2.214	16.39	125	71.14	67.6	-2.193
Mar	2.793	2.773	22.9	125	71.14	67.66	2.793
Apr	9.177	9.159	31.62	125	71.14	67.75	9.177
May	15.25	15.23	40.51	125	71.14	67.82	15.25
June	20.81	20.79	49.51	125	71.14	67.9	20.81
July	23.22	23.2	53.9	125	71.14	67.93	23.22
Aug	22.32	22.3	52.18	125	71.14	67.92	22.32
Sept	17.21	17.19	43.56	125	71.14	67.85	17.21
Oct	15.41	15.39	40.76	125	71.14	67.83	15.41
Nov	5.602	5.583	26.67	125	71.14	67.7	5.602
Dec	-2.178	-2.199	16.41	125	71.14	67.6	-2.178
	Enthalpy (kJ/kg)						
State Point	1'	1	2	3	4	4'	5
Jan	73.63	73.46	103.6	328.8	294.6	289.6	256.6
Feb	81.94	81.77	111.9	328.8	294.6	289.8	259
Mar	94.15	93.98	124.1	328.8	294.6	290	262.2
Apr	110.7	110.6	140.6	328.8	294.6	290.3	266.2
May	128	127.8	157.8	328.8	294.6	290.6	269.7
June	145.8	145.7	175.6	328.8	294.6	290.9	272.9
July	154.7	154.6	184.5	328.8	294.6	291	274.2
Aug	151.2	151.1	181	328.8	294.6	291	273.7
Sept	134	133.8	163.8	328.8	294.6	290.7	270.9
Oct	128.4	128.3	158.3	328.8	294.6	290.6	269.8
Nov	101.3	101.1	131.2	328.8	294.6	290.2	264
Dec	81.98	81.81	111.9	328.8	294.6	289.8	259
	Entropy (kJ/kg-K)						
State Point	1'	1	2	3	4	4'	5
Jan	0.2865	0.2859	0.2859	0.96	0.9601	0.9491	0.9708
Feb	0.3162	0.3156	0.3156	0.96	0.9601	0.9496	0.9696
Mar	0.359	0.3584	0.3584	0.96	0.9601	0.9502	0.9681
Apr	0.4157	0.4152	0.4152	0.96	0.9601	0.9511	0.9662
May	0.4731	0.4726	0.4726	0.96	0.9601	0.952	0.9648
June	0.5313	0.5308	0.5308	0.96	0.9601	0.9527	0.9636
July	0.56	0.5595	0.5595	0.96	0.9601	0.9531	0.9631
Aug	0.5487	0.5482	0.5482	0.96	0.9601	0.9529	0.9633
Sept	0.4928	0.4923	0.4923	0.96	0.9601	0.9522	0.9643
Oct	0.4747	0.4742	0.4742	0.96	0.9601	0.952	0.9647
Nov	0.3836	0.383	0.3831	0.96	0.9601	0.9506	0.9672
Dec	0.3163	0.3157	0.3157	0.96	0.9601	0.9496	0.9696

Table B-19: Thermodynamic Properties for Direct Single-Loop System Simulations at 3.1km Depth, CO2 Mass Flow Rate of 120kg/s, and Reservoir Temperature of 125°C (DTE=0.85).

Tres	125°C						
Well Depth	3.1 km						
CO2 Mass Flow	120 kg/s						
Pressure (kPa)							
State Point	1'	1	2	3	4	4'	5
Jan	2986	2985	33009	30000	13901	13644	2986
Feb	3286	3285	32775	30000	13901	13644	3286
Mar	3749	3748	32434	30000	13901	13644	3749
Apr	4410	4409	31966	30000	13901	13644	4410
May	5117	5116	31447	30000	13901	13644	5117
June	5838	5836	30827	30000	13901	13644	5838
July	6174	6173	30462	30000	13901	13644	6174
Aug	6047	6045	30615	30000	13901	13644	6047
Sept	5363	5361	31251	30000	13901	13644	5363
Oct	5137	5135	31431	30000	13901	13644	5137
Nov	4030	4029	32235	30000	13901	13644	4030
Dec	3288	3286	32773	30000	13901	13644	3288
Temperature (°C)							
State Point	1'	1	2	3	4	4'	5
Jan	-5.715	-5.73	11.97	125	74.68	72.33	-5.715
Feb	-2.2	-2.214	16.44	125	74.68	72.38	-2.2
Mar	2.786	2.773	22.95	125	74.68	72.44	2.786
Apr	9.171	9.159	31.68	125	74.68	72.52	9.171
May	15.24	15.23	40.59	125	74.68	72.6	15.24
June	20.8	20.79	49.61	125	74.68	72.68	20.8
July	23.21	23.2	54	125	74.68	72.71	23.21
Aug	22.31	22.3	52.28	125	74.68	72.7	22.31
Sept	17.2	17.19	43.65	125	74.68	72.63	17.2
Oct	15.4	15.39	40.83	125	74.68	72.61	15.4
Nov	5.596	5.583	26.73	125	74.68	72.48	5.596
Dec	-2.185	-2.199	16.46	125	74.68	72.38	-2.185
Enthalpy (kJ/kg)							
State Point	1'	1	2	3	4	4'	5
Jan	73.61	73.46	103.7	328.8	296.4	292.2	257.1
Feb	81.92	81.77	112	328.8	296.4	292.3	259.5
Mar	94.13	93.98	124.2	328.8	296.4	292.5	262.7
Apr	110.7	110.6	140.7	328.8	296.4	292.8	266.6
May	127.9	127.8	157.9	328.8	296.4	293.1	270.2
June	145.8	145.7	175.8	328.8	296.4	293.3	273.3
July	154.7	154.6	184.7	328.8	296.4	293.4	274.6
Aug	151.2	151.1	181.2	328.8	296.4	293.4	274.1
Sept	133.9	133.8	163.9	328.8	296.4	293.2	271.3
Oct	128.4	128.3	158.4	328.8	296.4	293.1	270.3
Nov	101.3	101.1	131.3	328.8	296.4	292.7	264.4
Dec	81.96	81.81	112	328.8	296.4	292.3	259.5
Entropy (kJ/kg-K)							
State Point	1'	1	2	3	4	4'	5
Jan	0.2865	0.2859	0.2859	0.96	0.9601	0.9496	0.9727
Feb	0.3161	0.3156	0.3156	0.96	0.9601	0.95	0.9714
Mar	0.3589	0.3584	0.3584	0.96	0.9601	0.9507	0.9698
Apr	0.4157	0.4152	0.4152	0.96	0.9601	0.9515	0.9678
May	0.4731	0.4726	0.4726	0.96	0.9601	0.9522	0.9662
June	0.5313	0.5308	0.5308	0.96	0.9601	0.9529	0.9649
July	0.5599	0.5595	0.5595	0.96	0.9601	0.9532	0.9644
Aug	0.5483	0.5482	0.5482	0.96	0.9601	0.9531	0.9646
Sept	0.4928	0.4923	0.4923	0.96	0.9601	0.9525	0.9658
Oct	0.4747	0.4742	0.4742	0.96	0.9601	0.9522	0.9662
Nov	0.3836	0.383	0.3831	0.96	0.9601	0.951	0.9689
Dec	0.3163	0.3157	0.3157	0.96	0.9601	0.95	0.9714

Table B-20: Thermodynamic Properties for Direct Single-Loop System Simulations at 3.1km Depth, CO2 Mass Flow Rate of 140kg/s, and Reservoir Temperature of 125°C (DTE=0.85).

Tres	125°C						
Well Depth	3.1 km						
CO2 Mass Flow	140 kg/s						
	Pressure (kPa)						
State Point	1'	1	2	3	4	4'	5
Jan	2987	2985	32941	30000	13597	13243	2987
Feb	3287	3285	32705	30000	13597	13243	3287
Mar	3750	3748	32362	30000	13597	13242	3750
Apr	4411	4409	31891	30000	13597	13242	4411
May	5117	5116	31368	30000	13597	13242	5117
June	5838	5836	30743	30000	13597	13242	5838
July	6175	6173	30374	30000	13597	13242	6175
Aug	6047	6045	30529	30000	13597	13242	6047
Sept	5363	5361	31170	30000	13597	13242	5363
Oct	5137	5135	31352	30000	13597	13242	5137
Nov	4031	4029	32161	30000	13597	13242	4031
Dec	3288	3286	32704	30000	13597	13243	3288
	Temperature (°C)						
State Point	1'	1	2	3	4	4'	5
Jan	-5.71	-5.73	11.93	125	73.22	70.56	-5.71
Feb	-2.195	-2.214	16.4	125	73.22	70.6	-2.195
Mar	2.791	2.773	22.91	125	73.22	70.66	2.791
Apr	9.176	9.159	31.63	125	73.22	70.73	9.176
May	15.25	15.23	40.53	125	73.22	70.79	15.25
June	20.81	20.79	49.53	125	73.22	70.85	20.81
July	23.22	23.2	53.92	125	73.22	70.88	23.22
Aug	22.32	22.3	52.2	125	73.22	70.87	22.32
Sept	17.21	17.19	43.58	125	73.22	70.81	17.21
Oct	15.41	15.39	40.78	125	73.22	70.79	15.41
Nov	5.601	5.583	26.68	125	73.22	70.69	5.601
Dec	-2.18	-2.199	16.42	125	73.22	70.6	-2.18
	Enthalpy (kJ/kg)						
State Point	1'	1	2	3	4	4'	5
Jan	73.59	73.46	103.6	328.8	295.7	291.8	257.5
Feb	81.9	81.77	111.9	328.8	295.7	291.9	259.8
Mar	94.11	93.98	124.1	328.8	295.7	292.1	263
Apr	110.7	110.6	140.6	328.8	295.7	292.3	266.9
May	127.9	127.8	157.8	328.8	295.7	292.5	270.4
June	145.8	145.7	175.7	328.8	295.7	292.7	273.5
July	154.7	154.6	184.6	328.8	295.7	292.8	274.8
Aug	151.2	151.1	181.1	328.8	295.7	292.8	274.3
Sept	133.9	133.8	163.8	328.8	295.7	292.6	271.5
Oct	128.4	128.3	158.3	328.8	295.7	292.5	270.5
Nov	101.3	101.1	131.2	328.8	295.7	292.2	264.7
Dec	81.94	81.81	111.9	328.8	295.7	291.9	259.8
	Entropy (kJ/kg-K)						
State Point	1'	1	2	3	4	4'	5
Jan	0.2864	0.2859	0.2859	0.96	0.9601	0.9512	0.9739
Feb	0.316	0.3156	0.3156	0.96	0.9601	0.9516	0.9725
Mar	0.3589	0.3584	0.3584	0.96	0.9601	0.9521	0.9708
Apr	0.4156	0.4152	0.4152	0.96	0.9601	0.9528	0.9687
May	0.473	0.4726	0.4726	0.96	0.9601	0.9535	0.967
June	0.5312	0.5308	0.5308	0.96	0.9601	0.9541	0.9656
July	0.5599	0.5595	0.5595	0.96	0.9601	0.9543	0.9651
Aug	0.5484	0.5482	0.5482	0.96	0.9601	0.9542	0.9653
Sept	0.4927	0.4923	0.4923	0.96	0.9601	0.9537	0.9665
Oct	0.4746	0.4742	0.4742	0.96	0.9601	0.9535	0.967
Nov	0.3835	0.383	0.3831	0.96	0.9601	0.9525	0.9698
Dec	0.3162	0.3157	0.3157	0.96	0.9601	0.9516	0.9725

Table B-21: Thermodynamic Properties for Direct Single-Loop System Simulations at 3.1km Depth, CO2 Mass Flow Rate of 70kg/s, and Reservoir Temperature of 150°C (DTE=0.85).

Tres	150°C						
Well Depth	3.1 km						
CO2 Mass Flow	70 kg/s						
Pressure (kPa)							
State Point	1'	1	2	3	4	4'	5
Jan	2986	2985	33030	30000	15710	15377	2986
Feb	3286	3285	32796	30000	15710	15377	3286
Mar	3749	3748	32456	30000	15710	15377	3749
Apr	4410	4409	31989	30000	15710	15376	4410
May	5117	5116	31471	30000	15710	15376	5117
June	5838	5836	30853	30000	15710	15376	5838
July	6174	6173	30488	30000	15710	15376	6174
Aug	6047	6045	30641	30000	15710	15376	6047
Sept	5362	5361	31275	30000	15710	15376	5362
Oct	5137	5135	31455	30000	15710	15376	5137
Nov	4030	4029	32257	30000	15710	15377	4030
Dec	3288	3286	32794	30000	15710	15377	3288
Temperature (°C)							
State Point	1'	1	2	3	4	4'	5
Jan	-5.717	-5.73	11.98	150	99.35	94.78	-5.717
Feb	-2.201	-2.214	16.45	150	99.35	94.88	-2.201
Mar	2.785	2.773	22.96	150	99.35	95.01	2.785
Apr	9.17	9.159	31.7	150	99.35	95.17	9.17
May	15.24	15.23	40.6	150	99.35	95.33	15.24
June	20.8	20.79	49.63	150	99.35	95.48	24.23
July	23.21	23.2	54.03	150	99.35	95.54	28.22
Aug	22.31	22.3	52.3	150	99.35	95.52	26.73
Sept	17.2	17.19	43.66	150	99.35	95.38	18.28
Oct	15.4	15.39	40.85	150	99.35	95.34	15.4
Nov	5.595	5.583	26.74	150	99.35	95.08	5.595
Dec	-2.186	-2.199	16.47	150	99.35	94.88	-2.186
Enthalpy (kJ/kg)							
State Point	1'	1	2	3	4	4'	5
Jan	73.68	73.46	103.7	375.2	341.8	334.4	287.6
Feb	81.98	81.77	112	375.2	341.8	334.6	290.3
Mar	94.19	93.98	124.2	375.2	341.8	334.9	294
Apr	110.8	110.6	140.8	375.2	341.8	335.3	298.5
May	128	127.8	158	375.2	341.8	335.6	302.7
June	145.8	145.7	175.8	375.2	341.8	336	306.4
July	154.8	154.6	184.7	375.2	341.8	336.1	308
Aug	151.2	151.1	181.2	375.2	341.8	336.1	307.4
Sept	134	133.8	164	375.2	341.8	335.7	304
Oct	128.5	128.3	158.4	375.2	341.8	335.6	302.8
Nov	101.3	101.1	131.3	375.2	341.8	335.1	296
Dec	82.02	81.81	112	375.2	341.8	334.6	290.3
Entropy (kJ/kg-K)							
State Point	1'	1	2	3	4	4'	5
Jan	0.2867	0.2859	0.2859	1.073	1.073	1.056	1.086
Feb	0.3164	0.3156	0.3156	1.073	1.073	1.056	1.085
Mar	0.3592	0.3584	0.3584	1.073	1.073	1.057	1.083
Apr	0.4159	0.4152	0.4152	1.073	1.073	1.058	1.081
May	0.4733	0.4726	0.4726	1.073	1.073	1.059	1.079
June	0.5315	0.5308	0.5308	1.073	1.073	1.06	1.078
July	0.5601	0.5595	0.5595	1.073	1.073	1.06	1.077
Aug	0.5488	0.5482	0.5482	1.073	1.073	1.06	1.077
Sept	0.493	0.4923	0.4923	1.073	1.073	1.059	1.079
Oct	0.4749	0.4742	0.4742	1.073	1.073	1.059	1.079
Nov	0.3838	0.383	0.3831	1.073	1.073	1.057	1.082
Dec	0.3165	0.3157	0.3157	1.073	1.073	1.056	1.085

Table B-22: Thermodynamic Properties for Direct Single-Loop System Simulations at 3.1km Depth, CO2 Mass Flow Rate of 90kg/s, and Reservoir Temperature of 150°C (DTE=0.85).

Tres	150°C						
Well Depth	3.1 km						
CO2 Mass Flow	90 kg/s						
Pressure (kPa)							
State Point	1'	1	2	3	4	4'	5
Jan	2987	2985	32919	30000	14977	14407	2987
Feb	3287	3285	32683	30000	14977	14407	3287
Mar	3750	3748	32339	30000	14977	14407	3750
Apr	4411	4409	31867	30000	14977	14406	4411
May	5118	5116	31343	30000	14977	14406	5118
June	5839	5836	30716	30000	14977	14406	5839
July	6175	6173	30347	30000	14977	14406	6175
Aug	6048	6045	30502	30000	14977	14406	6048
Sept	5363	5361	31144	30000	14977	14406	5363
Oct	5137	5135	31327	30000	14977	14406	5137
Nov	4031	4029	32138	30000	14977	14407	4031
Dec	3288	3286	32682	30000	14977	14407	3288
Temperature (°C)							
State Point	1'	1	2	3	4	4'	5
Jan	-5.708	-5.73	11.92	150	95.61	90.45	-5.708
Feb	-2.193	-2.214	16.39	150	95.61	90.52	-2.193
Mar	2.793	2.773	22.9	150	95.61	90.62	2.793
Apr	9.177	9.159	31.62	150	95.61	90.75	9.177
May	15.25	15.23	40.51	150	95.61	90.87	15.25
June	20.81	20.79	49.51	150	95.61	90.98	24.44
July	23.22	23.2	53.9	150	95.61	91.03	28.43
Aug	22.32	22.3	52.18	150	95.61	91.01	26.94
Sept	17.21	17.19	43.56	150	95.61	90.91	18.5
Oct	15.41	15.39	40.76	150	95.61	90.87	15.52
Nov	5.602	5.583	26.67	150	95.61	90.68	5.602
Dec	-2.178	-2.199	16.41	150	95.61	90.52	-2.178
Enthalpy (kJ/kg)							
State Point	1'	1	2	3	4	4'	5
Jan	73.63	73.46	103.6	375.2	339.7	333.2	288.4
Feb	81.94	81.77	111.9	375.2	339.7	333.4	291
Mar	94.15	93.98	124.1	375.2	339.7	333.6	294.7
Apr	110.7	110.6	140.6	375.2	339.7	333.9	299.3
May	128	127.8	157.8	375.2	339.7	334.2	303.4
June	145.8	145.7	175.6	375.2	339.7	334.5	307.1
July	154.7	154.6	184.5	375.2	339.7	334.6	308.7
Aug	151.2	151.1	181	375.2	339.7	334.5	308.1
Sept	134	133.8	163.8	375.2	339.7	334.3	304.7
Oct	128.4	128.3	158.3	375.2	339.7	334.2	303.5
Nov	101.3	101.1	131.2	375.2	339.7	333.8	296.7
Dec	81.98	81.81	111.9	375.2	339.7	333.4	291.1
Entropy (kJ/kg-K)							
State Point	1'	1	2	3	4	4'	5
Jan	0.2865	0.2859	0.2859	1.073	1.073	1.06	1.089
Feb	0.3162	0.3156	0.3156	1.073	1.073	1.06	1.088
Mar	0.359	0.3584	0.3584	1.073	1.073	1.061	1.086
Apr	0.4157	0.4152	0.4152	1.073	1.073	1.062	1.083
May	0.4731	0.4726	0.4726	1.073	1.073	1.063	1.081
June	0.5313	0.5308	0.5308	1.073	1.073	1.063	1.08
July	0.56	0.5595	0.5595	1.073	1.073	1.064	1.079
Aug	0.5487	0.5482	0.5482	1.073	1.073	1.064	1.079
Sept	0.4928	0.4923	0.4923	1.073	1.073	1.063	1.081
Oct	0.4747	0.4742	0.4742	1.073	1.073	1.063	1.081
Nov	0.3836	0.383	0.3831	1.073	1.073	1.061	1.085
Dec	0.3163	0.3157	0.3157	1.073	1.073	1.06	1.088

Table B-23: Thermodynamic Properties for Direct Single-Loop System Simulations at 3.1km Depth, CO2 Mass Flow Rate of 120kg/s, and Reservoir Temperature of 150°C (DTE=0.85).

Tres	150°C						
Well Depth	3.1 km						
CO2 Mass Flow	120 kg/s						
Pressure (kPa)							
State Point	1'	1	2	3	4	4'	5
Jan	2986	2985	33009	30000	15832	15537	2986
Feb	3286	3285	32775	30000	15832	15537	3286
Mar	3749	3748	32434	30000	15832	15536	3749
Apr	4410	4409	31966	30000	15832	15536	4410
May	5117	5116	31447	30000	15832	15536	5117
June	5838	5836	30827	30000	15832	15536	5838
July	6174	6173	30462	30000	15832	15536	6174
Aug	6047	6045	30615	30000	15832	15536	6047
Sept	5363	5361	31251	30000	15832	15536	5363
Oct	5137	5135	31431	30000	15832	15536	5137
Nov	4030	4029	32235	30000	15832	15536	4030
Dec	3288	3286	32773	30000	15832	15537	3288
Temperature (°C)							
State Point	1'	1	2	3	4	4'	5
Jan	-5.715	-5.73	11.97	150	99.96	96.39	-5.715
Feb	-2.2	-2.214	16.44	150	99.96	96.45	-2.2
Mar	2.786	2.773	22.95	150	99.96	96.55	2.786
Apr	9.171	9.159	31.68	150	99.96	96.67	9.171
May	15.24	15.23	40.59	150	99.96	96.78	15.43
June	20.8	20.79	49.61	150	99.96	96.89	24.63
July	23.21	23.2	54	150	99.96	96.93	28.61
Aug	22.31	22.3	52.28	150	99.96	96.92	27.12
Sept	17.2	17.19	43.65	150	99.96	96.82	18.67
Oct	15.4	15.39	40.83	150	99.96	96.79	15.7
Nov	5.596	5.583	26.73	150	99.96	96.6	5.596
Dec	-2.185	-2.199	16.46	150	99.96	96.45	-2.185
Enthalpy (kJ/kg)							
State Point	1'	1	2	3	4	4'	5
Jan	73.61	73.46	103.7	375.2	342.2	336.7	289
Feb	81.92	81.77	112	375.2	342.2	336.8	291.7
Mar	94.13	93.98	124.2	375.2	342.2	337	295.4
Apr	110.7	110.6	140.7	375.2	342.2	337.3	299.9
May	127.9	127.8	157.9	375.2	342.2	337.6	304
June	145.8	145.7	175.8	375.2	342.2	337.8	307.7
July	154.7	154.6	184.7	375.2	342.2	337.9	309.2
Aug	151.2	151.1	181.2	375.2	342.2	337.9	308.6
Sept	133.9	133.8	163.9	375.2	342.2	337.6	305.3
Oct	128.4	128.3	158.4	375.2	342.2	337.6	304.1
Nov	101.3	101.1	131.3	375.2	342.2	337.1	297.4
Dec	81.96	81.81	112	375.2	342.2	336.8	291.7
Entropy (kJ/kg-K)							
State Point	1'	1	2	3	4	4'	5
Jan	0.2865	0.2859	0.2859	1.073	1.073	1.061	1.092
Feb	0.3161	0.3156	0.3156	1.073	1.073	1.061	1.09
Mar	0.3589	0.3584	0.3584	1.073	1.073	1.062	1.088
Apr	0.4157	0.4152	0.4152	1.073	1.073	1.062	1.086
May	0.4731	0.4726	0.4726	1.073	1.073	1.063	1.084
June	0.5313	0.5308	0.5308	1.073	1.073	1.064	1.082
July	0.5599	0.5595	0.5595	1.073	1.073	1.064	1.081
Aug	0.5483	0.5482	0.5482	1.073	1.073	1.064	1.081
Sept	0.4928	0.4923	0.4923	1.073	1.073	1.063	1.083
Oct	0.4747	0.4742	0.4742	1.073	1.073	1.063	1.084
Nov	0.3836	0.383	0.3831	1.073	1.073	1.062	1.087
Dec	0.3163	0.3157	0.3157	1.073	1.073	1.061	1.09

Table B-24: Thermodynamic Properties for Direct Single-Loop System Simulations at 3.1km Depth, CO2 Mass Flow Rate of 140kg/s, and Reservoir Temperature of 150°C (DTE=0.85).

Tres	150°C						
Well Depth	3.1 km						
CO2 Mass Flow	140 kg/s						
Pressure (kPa)							
State Point	1'	1	2	3	4	4'	5
Jan	2987	2985	32941	30000	15475	15066	2987
Feb	3287	3285	32705	30000	15475	15066	3287
Mar	3750	3748	32362	30000	15475	15065	3750
Apr	4411	4409	31891	30000	15475	15065	4411
May	5117	5116	31368	30000	15475	15065	5117
June	5838	5836	30743	30000	15475	15065	5838
July	6175	6173	30374	30000	15475	15065	6175
Aug	6047	6045	30529	30000	15475	15065	6047
Sept	5363	5361	31170	30000	15475	15065	5363
Oct	5137	5135	31352	30000	15475	15065	5137
Nov	4031	4029	32161	30000	15475	15065	4031
Dec	3288	3286	32704	30000	15475	15066	3288
Temperature (°C)							
State Point	1'	1	2	3	4	4'	5
Jan	-5.71	-5.73	11.93	150	98.17	94.32	-5.71
Feb	-2.195	-2.214	16.4	150	98.17	94.38	-2.195
Mar	2.791	2.773	22.91	150	98.17	94.46	2.791
Apr	9.176	9.159	31.63	150	98.17	94.56	9.176
May	15.25	15.23	40.53	150	98.17	94.66	15.53
June	20.81	20.79	49.53	150	98.17	94.75	24.72
July	23.22	23.2	53.92	150	98.17	94.79	28.7
Aug	22.32	22.3	52.2	150	98.17	94.77	27.22
Sept	17.21	17.19	43.58	150	98.17	94.69	18.77
Oct	15.41	15.39	40.78	150	98.17	94.66	15.79
Nov	5.601	5.583	26.68	150	98.17	94.5	5.601
Dec	-2.18	-2.199	16.42	150	98.17	94.38	-2.18
Enthalpy (kJ/kg)							
State Point	1'	1	2	3	4	4'	5
Jan	73.59	73.46	103.6	375.2	341.2	336.1	289.4
Feb	81.9	81.77	111.9	375.2	341.2	336.2	292.1
Mar	94.11	93.98	124.1	375.2	341.2	336.4	295.7
Apr	110.7	110.6	140.6	375.2	341.2	336.6	300.2
May	127.9	127.8	157.8	375.2	341.2	336.8	304.3
June	145.8	145.7	175.7	375.2	341.2	337	307.9
July	154.7	154.6	184.6	375.2	341.2	337.1	309.5
Aug	151.2	151.1	181.1	375.2	341.2	337.1	308.9
Sept	133.9	133.8	163.8	375.2	341.2	336.9	305.6
Oct	128.4	128.3	158.3	375.2	341.2	336.8	304.4
Nov	101.3	101.1	131.2	375.2	341.2	336.5	297.7
Dec	81.94	81.81	111.9	375.2	341.2	336.2	292.1
Entropy (kJ/kg-K)							
State Point	1'	1	2	3	4	4'	5
Jan	0.2864	0.2859	0.2859	1.073	1.073	1.063	1.093
Feb	0.316	0.3156	0.3156	1.073	1.073	1.063	1.092
Mar	0.3589	0.3584	0.3584	1.073	1.073	1.063	1.089
Apr	0.4156	0.4152	0.4152	1.073	1.073	1.064	1.087
May	0.473	0.4726	0.4726	1.073	1.073	1.065	1.085
June	0.5312	0.5308	0.5308	1.073	1.073	1.065	1.083
July	0.5599	0.5595	0.5595	1.073	1.073	1.065	1.082
Aug	0.5484	0.5482	0.5482	1.073	1.073	1.065	1.082
Sept	0.4927	0.4923	0.4923	1.073	1.073	1.065	1.084
Oct	0.4746	0.4742	0.4742	1.073	1.073	1.065	1.085
Nov	0.3835	0.383	0.3831	1.073	1.073	1.064	1.088
Dec	0.3162	0.3157	0.3157	1.073	1.073	1.063	1.092

Table B-25: Thermodynamic Properties for Direct Single-Loop System Simulations at 3.6km Depth, CO2 Mass Flow Rate of 70kg/s, and Reservoir Temperature of 100°C (DTE=0.85).

Tres	100°C						
Well Depth	3.6 km						
CO2 Mass Flow	70 kg/s						
Pressure (kPa)							
State Point	1'	1	2	3	4	4'	5
Jan	2986	2985	38160	35000	11398	11176	2986
Feb	3286	3285	37851	35000	11398	11176	3286
Mar	3748	3748	37399	35000	11398	11176	3748
Apr	4410	4409	36777	35000	11398	11175	4410
May	5116	5116	36094	35000	11398	11175	5116
June	5837	5836	35299	35000	11398	11175	5837
July	6173	6423	35139	35000	11398	11175	6173
Aug	6046	6195	35208	35000	11398	11175	6046
Sept	5362	5361	35839	35000	11398	11175	5362
Oct	5136	5135	36073	35000	11398	11175	5136
Nov	4029	4029	37134	35000	11398	11175	4029
Dec	3287	3286	37849	35000	11398	11176	3287
Temperature (°C)							
State Point	1'	1	2	3	4	4'	5
Jan	-5.725	-5.73	14.45	100	50.22	48.74	-5.725
Feb	-2.209	-2.214	19.03	100	50.22	48.78	-2.209
Mar	2.778	2.773	25.71	100	50.22	48.83	2.778
Apr	9.163	9.159	34.69	100	50.22	48.89	9.163
May	15.23	15.23	43.88	100	50.22	48.96	15.23
June	20.79	20.79	53.22	100	50.22	49.01	20.79
July	23.2	23.76	58.05	100	50.22	49.04	23.2
Aug	22.3	22.6	56.15	100	50.22	49.03	22.3
Sept	17.19	17.19	47.04	100	50.22	48.98	17.19
Oct	15.39	15.39	44.13	100	50.22	48.96	15.39
Nov	5.588	5.583	29.59	100	50.22	48.86	5.588
Dec	-2.194	-2.199	19.05	100	50.22	48.78	-2.194
Enthalpy (kJ/kg)							
State Point	1'	1	2	3	4	4'	5
Jan	73.72	73.46	108.7	271.1	234.2	230.2	209
Feb	82.03	81.77	117	271.1	234.2	230.4	210.9
Mar	94.24	93.98	129.2	271.1	234.2	230.7	213.5
Apr	110.8	110.6	145.8	271.1	234.2	231.1	216.6
May	128	127.8	163	271.1	234.2	231.4	219.4
June	145.9	145.7	180.8	271.1	234.2	231.8	221.8
July	154.8	154.9	190.1	271.1	234.2	231.9	222.8
Aug	151.3	151.3	186.4	271.1	234.2	231.9	222.5
Sept	134	133.8	169	271.1	234.2	231.6	220.3
Oct	128.5	128.3	163.5	271.1	234.2	231.5	219.5
Nov	101.4	101.1	136.3	271.1	234.2	230.9	214.9
Dec	82.07	81.81	117	271.1	234.2	230.4	210.9
Entropy (kJ/kg-K)							
State Point	1'	1	2	3	4	4'	5
Jan	0.2869	0.2859	0.2859	0.7902	0.7902	0.7789	0.7929
Feb	0.3165	0.3156	0.3156	0.7902	0.7902	0.7796	0.7923
Mar	0.3593	0.3584	0.3584	0.7902	0.7902	0.7805	0.7915
Apr	0.416	0.4152	0.4152	0.7902	0.7902	0.7817	0.7908
May	0.4734	0.4726	0.4726	0.7902	0.7902	0.7829	0.7903
June	0.5316	0.5308	0.5308	0.7902	0.7902	0.7839	0.7899
July	0.5602	0.5595	0.5595	0.7902	0.7902	0.7844	0.7898
Aug	0.5489	0.5482	0.5482	0.7902	0.7902	0.7842	0.7898
Sept	0.4931	0.4923	0.4923	0.7902	0.7902	0.7833	0.7901
Oct	0.475	0.4742	0.4742	0.7902	0.7902	0.7829	0.7902
Nov	0.3839	0.383	0.3831	0.7902	0.7902	0.7811	0.7912
Dec	0.3167	0.3157	0.3157	0.7902	0.7902	0.7796	0.7923

Table B-26: Thermodynamic Properties for Direct Single-Loop System Simulations at 3.6km Depth, CO2 Mass Flow Rate of 90kg/s, and Reservoir Temperature of 100°C (DTE=0.85).

Tres	100°C						
Well Depth	3.6 km						
CO2 Mass Flow	90 kg/s						
Pressure (kPa)							
State Point	1'	1	2	3	4	4'	5
Jan	2986	2985	38111	35000	10844	10469	2986
Feb	3286	3285	37801	35000	10844	10469	3286
Mar	3749	3748	37348	35000	10844	10468	3749
Apr	4410	4409	36724	35000	10844	10468	4410
May	5116	5116	36037	35000	10844	10468	5116
June	5837	5836	35239	35000	10844	10467	5837
July	6174	6423	35077	35000	10844	10467	6174
Aug	6046	6195	35147	35000	10844	10467	6046
Sept	5362	5361	35781	35000	10844	10468	5362
Oct	5136	5135	36017	35000	10844	10468	5136
Nov	4030	4029	37082	35000	10844	10468	4030
Dec	3287	3286	37800	35000	10844	10469	3287
Temperature (°C)							
State Point	1'	1	2	3	4	4'	5
Jan	-5.722	-5.73	14.42	100	48.06	46.14	-5.722
Feb	-2.206	-2.214	19	100	48.06	46.16	-2.206
Mar	2.78	2.773	25.68	100	48.06	46.19	2.78
Apr	9.166	9.159	34.65	100	48.06	46.24	9.166
May	15.24	15.23	43.84	100	48.06	46.28	15.24
June	20.8	20.79	53.18	100	48.06	46.31	20.8
July	23.21	23.76	58	100	48.06	46.33	23.21
Aug	22.31	22.6	56.1	100	48.06	46.32	22.31
Sept	17.2	17.19	47	100	48.06	46.29	17.2
Oct	15.4	15.39	44.09	100	48.06	46.28	15.4
Nov	5.591	5.583	29.56	100	48.06	46.21	5.591
Dec	-2.191	-2.199	19.02	100	48.06	46.16	-2.191
Enthalpy (kJ/kg)							
State Point	1'	1	2	3	4	4'	5
Jan	73.66	73.46	108.6	271.1	233.2	229.8	209.6
Feb	81.97	81.77	116.9	271.1	233.2	229.9	211.5
Mar	94.18	93.98	129.1	271.1	233.2	230.2	214
Apr	110.8	110.6	145.7	271.1	233.2	230.5	217
May	128	127.8	162.9	271.1	233.2	230.7	219.8
June	145.8	145.7	180.8	271.1	233.2	231	222.1
July	154.7	154.9	190	271.1	233.2	231.1	223.1
Aug	151.2	151.3	186.4	271.1	233.2	231.1	222.8
Sept	134	133.8	168.9	271.1	233.2	230.8	220.6
Oct	128.5	128.3	163.4	271.1	233.2	230.8	219.8
Nov	101.3	101.1	136.3	271.1	233.2	230.3	215.4
Dec	82.01	81.81	117	271.1	233.2	229.9	211.5
Entropy (kJ/kg-K)							
State Point	1'	1	2	3	4	4'	5
Jan	0.2866	0.2859	0.2859	0.7902	0.7902	0.7817	0.795
Feb	0.3163	0.3156	0.3156	0.7902	0.7902	0.7823	0.7943
Mar	0.3591	0.3584	0.3584	0.7902	0.7902	0.783	0.7933
Apr	0.4158	0.4152	0.4152	0.7902	0.7902	0.7839	0.7923
May	0.4732	0.4726	0.4726	0.7902	0.7902	0.7848	0.7915
June	0.5314	0.5308	0.5308	0.7902	0.7902	0.7857	0.791
July	0.5601	0.5595	0.5595	0.7902	0.7902	0.786	0.7908
Aug	0.5488	0.5482	0.5482	0.7902	0.7902	0.7859	0.7909
Sept	0.4929	0.4923	0.4923	0.7902	0.7902	0.7851	0.7913
Oct	0.4748	0.4742	0.4742	0.7902	0.7902	0.7849	0.7915
Nov	0.3837	0.383	0.3831	0.7902	0.7902	0.7834	0.7929
Dec	0.3165	0.3157	0.3157	0.7902	0.7902	0.7823	0.7943

Table B-27: Thermodynamic Properties for Direct Single-Loop System Simulations at 3.6km Depth, CO₂

Mass Flow Rate of 120kg/s, and Reservoir Temperature of 100°C (DTE=0.85).

Tres	100°C						
Well Depth	3.6 km						
CO₂ Mass Flow	120 kg/s						
	Pressure (kPa)						
State Point	1'	1	2	3	4	4'	5
Jan	2986	2985	38129	35000	11491	11294	2986
Feb	3286	3285	37819	35000	11491	11294	3286
Mar	3749	3748	37366	35000	11491	11294	3749
Apr	4410	4409	36742	35000	11491	11293	4410
May	5116	5116	36057	35000	11491	11293	5116
June	5837	5836	35260	35000	11491	11293	5837
July	6173	6423	35098	35000	11491	11293	6173
Aug	6046	6195	35169	35000	11491	11293	6046
Sept	5362	5361	35802	35000	11491	11293	5362
Oct	5136	5135	36037	35000	11491	11293	5136
Nov	4030	4029	37100	35000	11491	11294	4030
Dec	3287	3286	37817	35000	11491	11294	3287
	Temperature (°C)						
State Point	1'	1	2	3	4	4'	5
Jan	-5.723	-5.73	14.43	100	50.57	49.36	-5.723
Feb	-2.207	-2.214	19.01	100	50.57	49.39	-2.207
Mar	2.779	2.773	25.69	100	50.57	49.43	2.779
Apr	9.165	9.159	34.67	100	50.57	49.47	9.165
May	15.24	15.23	43.85	100	50.57	49.52	15.24
June	20.8	20.79	53.19	100	50.57	49.56	20.8
July	23.21	23.76	58.02	100	50.57	49.58	23.21
Aug	22.31	22.6	56.12	100	50.57	49.57	22.31
Sept	17.2	17.19	47.01	100	50.57	49.53	17.2
Oct	15.4	15.39	44.11	100	50.57	49.52	15.4
Nov	5.59	5.583	29.57	100	50.57	49.45	5.59
Dec	-2.192	-2.199	19.03	100	50.57	49.39	-2.192
	Enthalpy (kJ/kg)						
State Point	1'	1	2	3	4	4'	5
Jan	73.64	73.46	108.6	271.1	234.4	231.4	210
Feb	81.94	81.77	116.9	271.1	234.4	231.6	211.8
Mar	94.15	93.98	129.1	271.1	234.4	231.8	214.3
Apr	110.7	110.6	145.7	271.1	234.4	232.1	217.3
May	128	127.8	162.9	271.1	234.4	232.3	220
June	145.8	145.7	180.8	271.1	234.4	232.6	222.4
July	154.7	154.9	190	271.1	234.4	232.7	223.3
Aug	151.2	151.3	186.4	271.1	234.4	232.6	223
Sept	134	133.8	168.9	271.1	234.4	232.4	220.9
Oct	128.4	128.3	163.4	271.1	234.4	232.3	220.1
Nov	101.3	101.1	136.3	271.1	234.4	231.9	215.7
Dec	81.98	81.81	117	271.1	234.4	231.6	211.8
	Entropy (kJ/kg-K)						
State Point	1'	1	2	3	4	4'	5
Jan	0.2865	0.2859	0.2859	0.7902	0.7902	0.7821	0.7963
Feb	0.3162	0.3156	0.3156	0.7902	0.7902	0.7826	0.7955
Mar	0.359	0.3584	0.3584	0.7902	0.7902	0.7833	0.7945
Apr	0.4157	0.4152	0.4152	0.7902	0.7902	0.7841	0.7933
May	0.4732	0.4726	0.4726	0.7902	0.7902	0.7849	0.7925
June	0.5313	0.5308	0.5308	0.7902	0.7902	0.7857	0.7918
July	0.56	0.5595	0.5595	0.7902	0.7902	0.786	0.7916
Aug	0.5487	0.5482	0.5482	0.7902	0.7902	0.7859	0.7917
Sept	0.4929	0.4923	0.4923	0.7902	0.7902	0.7852	0.7922
Oct	0.4748	0.4742	0.4742	0.7902	0.7902	0.785	0.7924
Nov	0.3836	0.383	0.3831	0.7902	0.7902	0.7837	0.7939
Dec	0.3164	0.3157	0.3157	0.7902	0.7902	0.7826	0.7955

Table B-28: Thermodynamic Properties for Direct Single-Loop System Simulations at 3.6km Depth, CO2 Mass Flow Rate of 140kg/s, and Reservoir Temperature of 100°C (DTE=0.85).

Tres	100°C						
Well Depth	3.6 km						
CO2 Mass Flow	140 kg/s						
Pressure (kPa)							
State Point	1'	1	2	3	4	4'	5
Jan	2986	2985	38090	35000	11219	10948	2986
Feb	3286	3285	37780	35000	11219	10948	3286
Mar	3749	3748	37325	35000	11219	10948	3749
Apr	4410	4409	36700	35000	11219	10947	4410
May	5116	5116	36013	35000	11219	10947	5116
June	5837	5836	35212	35000	11219	10947	5837
July	6174	6423	35049	35000	11219	10947	6174
Aug	6046	6195	35120	35000	11219	10947	6046
Sept	5362	5361	35756	35000	11219	10947	5362
Oct	5136	5135	35992	35000	11219	10947	5136
Nov	4030	4029	37059	35000	11219	10948	4030
Dec	3287	3286	37778	35000	11219	10948	3287
Temperature (°C)							
State Point	1'	1	2	3	4	4'	5
Jan	-5.72	-5.73	14.41	100	49.54	48.12	-5.72
Feb	-2.205	-2.214	18.99	100	49.54	48.14	-2.205
Mar	2.782	2.773	25.67	100	49.54	48.17	2.782
Apr	9.167	9.159	34.64	100	49.54	48.2	9.167
May	15.24	15.23	43.82	100	49.54	48.24	15.24
June	20.8	20.79	53.16	100	49.54	48.27	20.8
July	23.21	23.76	57.98	100	49.54	48.29	23.21
Aug	22.31	22.6	56.08	100	49.54	48.28	22.31
Sept	17.2	17.19	46.98	100	49.54	48.25	17.2
Oct	15.4	15.39	44.08	100	49.54	48.24	15.4
Nov	5.592	5.583	29.55	100	49.54	48.18	5.592
Dec	-2.19	-2.199	19.01	100	49.54	48.14	-2.19
Enthalpy (kJ/kg)							
State Point	1'	1	2	3	4	4'	5
Jan	73.61	73.46	108.6	271.1	233.9	231.2	210.2
Feb	81.92	81.77	116.9	271.1	233.9	231.3	212
Mar	94.13	93.98	129.1	271.1	233.9	231.5	214.5
Apr	110.7	110.6	145.7	271.1	233.9	231.7	217.5
May	127.9	127.8	162.9	271.1	233.9	232	220.2
June	145.8	145.7	180.7	271.1	233.9	232.2	222.5
July	154.7	154.9	190	271.1	233.9	232.3	223.5
Aug	151.2	151.3	186.3	271.1	233.9	232.2	223.1
Sept	133.9	133.8	168.9	271.1	233.9	232	221
Oct	128.4	128.3	163.4	271.1	233.9	232	220.3
Nov	101.3	101.1	136.2	271.1	233.9	231.6	215.9
Dec	81.96	81.81	116.9	271.1	233.9	231.3	212
Entropy (kJ/kg-K)							
State Point	1'	1	2	3	4	4'	5
Jan	0.2864	0.2859	0.2859	0.7902	0.7902	0.7834	0.7972
Feb	0.3161	0.3156	0.3156	0.7902	0.7902	0.7838	0.7964
Mar	0.3589	0.3584	0.3584	0.7902	0.7902	0.7844	0.7952
Apr	0.4157	0.4152	0.4152	0.7902	0.7902	0.7851	0.794
May	0.4731	0.4726	0.4726	0.7902	0.7902	0.7858	0.793
June	0.5313	0.5308	0.5308	0.7902	0.7902	0.7865	0.7923
July	0.5599	0.5595	0.5595	0.7902	0.7902	0.7867	0.792
Aug	0.5486	0.5482	0.5482	0.7902	0.7902	0.7866	0.7921
Sept	0.4928	0.4923	0.4923	0.7902	0.7902	0.786	0.7927
Oct	0.4747	0.4742	0.4742	0.7902	0.7902	0.7858	0.793
Nov	0.3836	0.383	0.3831	0.7902	0.7902	0.7847	0.7947
Dec	0.3163	0.3157	0.3157	0.7902	0.7902	0.7838	0.7964

Table B-29: Thermodynamic Properties for Direct Single-Loop System Simulations at 3.6km Depth, CO2 Mass Flow Rate of 70kg/s, and Reservoir Temperature of 125°C (DTE=0.85).

Tres	125°C						
Well Depth	3.6 km						
CO2 Mass Flow	70 kg/s						
Pressure (kPa)							
State Point	1'	1	2	3	4	4'	5
Jan	2986	2985	38160	35000	14306	14047	2986
Feb	3286	3285	37851	35000	14306	14047	3286
Mar	3748	3748	37399	35000	14306	14047	3748
Apr	4410	4409	36777	35000	14306	14047	4410
May	5116	5116	36094	35000	14306	14047	5116
June	5837	5836	35299	35000	14306	14046	5837
July	6173	6423	35139	35000	14306	14046	6173
Aug	6046	6195	35208	35000	14306	14046	6046
Sept	5362	5361	35839	35000	14306	14046	5362
Oct	5136	5135	36073	35000	14306	14047	5136
Nov	4029	4029	37134	35000	14306	14047	4029
Dec	3287	3286	37849	35000	14306	14047	3287
Temperature (°C)							
State Point	1'	1	2	3	4	4'	5
Jan	-5.725	-5.73	14.45	125	71.55	69.05	-5.725
Feb	-2.209	-2.214	19.03	125	71.55	69.11	-2.209
Mar	2.778	2.773	25.71	125	71.55	69.2	2.778
Apr	9.163	9.159	34.69	125	71.55	69.31	9.163
May	15.23	15.23	43.88	125	71.55	69.41	15.23
June	20.79	20.79	53.22	125	71.55	69.5	20.79
July	23.2	23.76	58.05	125	71.55	69.55	23.2
Aug	22.3	22.6	56.15	125	71.55	69.53	22.3
Sept	17.19	17.19	47.04	125	71.55	69.44	17.19
Oct	15.39	15.39	44.13	125	71.55	69.41	15.39
Nov	5.588	5.583	29.59	125	71.55	69.25	5.588
Dec	-2.194	-2.199	19.05	125	71.55	69.11	-2.194
Enthalpy (kJ/kg)							
State Point	1'	1	2	3	4	4'	5
Jan	73.72	73.46	108.7	318.6	281.3	275.8	243.3
Feb	82.03	81.77	117	318.6	281.3	276	245.5
Mar	94.24	93.98	129.2	318.6	281.3	276.3	248.6
Apr	110.8	110.6	145.8	318.6	281.3	276.7	252.3
May	128	127.8	163	318.6	281.3	277.1	255.7
June	145.9	145.7	180.8	318.6	281.3	277.4	258.7
July	154.8	154.9	190.1	318.6	281.3	277.6	259.9
Aug	151.3	151.3	186.4	318.6	281.3	277.5	259.5
Sept	134	133.8	169	318.6	281.3	277.2	256.8
Oct	128.5	128.3	163.5	318.6	281.3	277.1	255.8
Nov	101.4	101.1	136.3	318.6	281.3	276.5	250.2
Dec	82.07	81.81	117	318.6	281.3	276	245.5
Entropy (kJ/kg-K)							
State Point	1'	1	2	3	4	4'	5
Jan	0.2869	0.2859	0.2859	0.9136	0.9137	0.8994	0.9208
Feb	0.3165	0.3156	0.3156	0.9136	0.9137	0.9	0.9199
Mar	0.3593	0.3584	0.3584	0.9136	0.9137	0.9009	0.9186
Apr	0.416	0.4152	0.4152	0.9136	0.9137	0.902	0.9173
May	0.4734	0.4726	0.4726	0.9136	0.9137	0.9031	0.9162
June	0.5316	0.5308	0.5308	0.9136	0.9137	0.9041	0.9153
July	0.5602	0.5595	0.5595	0.9136	0.9137	0.9045	0.915
Aug	0.5489	0.5482	0.5482	0.9136	0.9137	0.9043	0.9151
Sept	0.4931	0.4923	0.4923	0.9136	0.9137	0.9034	0.9158
Oct	0.475	0.4742	0.4742	0.9136	0.9137	0.9031	0.9161
Nov	0.3839	0.383	0.3831	0.9136	0.9137	0.9014	0.918
Dec	0.3167	0.3157	0.3157	0.9136	0.9137	0.9	0.9199

Table B-30: Thermodynamic Properties for Direct Single-Loop System Simulations at 3.6km Depth, CO2 Mass Flow Rate of 90kg/s, and Reservoir Temperature of 125°C (DTE=0.85).

Tres	125°C						
Well Depth	3.6 km						
CO2 Mass Flow	90 kg/s						
	Pressure (kPa)						
State Point	1'	1	2	3	4	4'	5
Jan	2986	2985	38111	35000	13664	13224	2986
Feb	3286	3285	37801	35000	13664	13224	3286
Mar	3749	3748	37348	35000	13664	13224	3749
Apr	4410	4409	36724	35000	13664	13224	4410
May	5116	5116	36037	35000	13664	13223	5116
June	5837	5836	35239	35000	13664	13223	5837
July	6174	6423	35077	35000	13664	13223	6174
Aug	6046	6195	35147	35000	13664	13223	6046
Sept	5362	5361	35781	35000	13664	13223	5362
Oct	5136	5135	36017	35000	13664	13223	5136
Nov	4030	4029	37082	35000	13664	13224	4030
Dec	3287	3286	37800	35000	13664	13224	3287
	Temperature (°C)						
State Point	1'	1	2	3	4	4'	5
Jan	-5.722	-5.73	14.42	125	68.8	65.86	-5.722
Feb	-2.206	-2.214	19	125	68.8	65.91	-2.206
Mar	2.78	2.773	25.68	125	68.8	65.97	2.78
Apr	9.166	9.159	34.65	125	68.8	66.04	9.166
May	15.24	15.23	43.84	125	68.8	66.12	15.24
June	20.8	20.79	53.18	125	68.8	66.19	20.8
July	23.21	23.76	58	125	68.8	66.22	23.21
Aug	22.31	22.6	56.1	125	68.8	66.2	22.31
Sept	17.2	17.19	47	125	68.8	66.14	17.2
Oct	15.4	15.39	44.09	125	68.8	66.12	15.4
Nov	5.591	5.583	29.56	125	68.8	66	5.591
Dec	-2.191	-2.199	19.02	125	68.8	65.91	-2.191
	Enthalpy (kJ/kg)						
State Point	1'	1	2	3	4	4'	5
Jan	73.66	73.46	108.6	318.6	279.9	275.2	244
Feb	81.97	81.77	116.9	318.6	279.9	275.4	246.2
Mar	94.18	93.98	129.1	318.6	279.9	275.6	249.2
Apr	110.8	110.6	145.7	318.6	279.9	275.9	252.9
May	128	127.8	162.9	318.6	279.9	276.2	256.2
June	145.8	145.7	180.8	318.6	279.9	276.5	259.2
July	154.7	154.9	190	318.6	279.9	276.6	260.4
Aug	151.2	151.3	186.4	318.6	279.9	276.5	259.9
Sept	134	133.8	168.9	318.6	279.9	276.3	257.3
Oct	128.5	128.3	163.4	318.6	279.9	276.2	256.3
Nov	101.3	101.1	136.3	318.6	279.9	275.7	250.9
Dec	82.01	81.81	117	318.6	279.9	275.4	246.2
	Entropy (kJ/kg-K)						
State Point	1'	1	2	3	4	4'	5
Jan	0.2866	0.2859	0.2859	0.9136	0.9137	0.9029	0.9235
Feb	0.3163	0.3156	0.3156	0.9136	0.9137	0.9034	0.9224
Mar	0.3591	0.3584	0.3584	0.9136	0.9137	0.9041	0.921
Apr	0.4158	0.4152	0.4152	0.9136	0.9137	0.905	0.9193
May	0.4732	0.4726	0.4726	0.9136	0.9137	0.9058	0.918
June	0.5314	0.5308	0.5308	0.9136	0.9137	0.9066	0.9169
July	0.5601	0.5595	0.5595	0.9136	0.9137	0.9069	0.9165
Aug	0.5488	0.5482	0.5482	0.9136	0.9137	0.9068	0.9167
Sept	0.4929	0.4923	0.4923	0.9136	0.9137	0.9061	0.9176
Oct	0.4748	0.4742	0.4742	0.9136	0.9137	0.9058	0.918
Nov	0.3837	0.383	0.3831	0.9136	0.9137	0.9045	0.9202
Dec	0.3165	0.3157	0.3157	0.9136	0.9137	0.9034	0.9224

Table B-31: Thermodynamic Properties for Direct Single-Loop System Simulations at 3.6km Depth, CO₂

Mass Flow Rate of 120kg/s, and Reservoir Temperature of 125°C (DTE=0.85).

Tres	125°C						
Well Depth	3.6 km						
CO2 Mass Flow	120 kg/s						
Pressure (kPa)							
State Point	1'	1	2	3	4	4'	5
Jan	2986	2985	38129	35000	14414	14184	2986
Feb	3286	3285	37819	35000	14414	14184	3286
Mar	3749	3748	37366	35000	14414	14184	3749
Apr	4410	4409	36742	35000	14414	14184	4410
May	5116	5116	36057	35000	14414	14183	5116
June	5837	5836	35260	35000	14414	14183	5837
July	6173	6423	35098	35000	14414	14183	6173
Aug	6046	6195	35169	35000	14414	14183	6046
Sept	5362	5361	35802	35000	14414	14183	5362
Oct	5136	5135	36037	35000	14414	14183	5136
Nov	4030	4029	37100	35000	14414	14184	4030
Dec	3287	3286	37817	35000	14414	14184	3287
Temperature (°C)							
State Point	1'	1	2	3	4	4'	5
Jan	-5.723	-5.73	14.43	125	72	70.01	-5.723
Feb	-2.207	-2.214	19.01	125	72	70.06	-2.207
Mar	2.779	2.773	25.69	125	72	70.12	2.779
Apr	9.165	9.159	34.67	125	72	70.2	9.165
May	15.24	15.23	43.85	125	72	70.27	15.24
June	20.8	20.79	53.19	125	72	70.34	20.8
July	23.21	23.76	58.02	125	72	70.37	23.21
Aug	22.31	22.6	56.12	125	72	70.36	22.31
Sept	17.2	17.19	47.01	125	72	70.3	17.2
Oct	15.4	15.39	44.11	125	72	70.28	15.4
Nov	5.59	5.583	29.57	125	72	70.15	5.59
Dec	-2.192	-2.199	19.03	125	72	70.06	-2.192
Enthalpy (kJ/kg)							
State Point	1'	1	2	3	4	4'	5
Jan	73.64	73.46	108.6	318.6	281.5	277.5	244.4
Feb	81.94	81.77	116.9	318.6	281.5	277.6	246.6
Mar	94.15	93.98	129.1	318.6	281.5	277.9	249.6
Apr	110.7	110.6	145.7	318.6	281.5	278.1	253.3
May	128	127.8	162.9	318.6	281.5	278.4	256.6
June	145.8	145.7	180.8	318.6	281.5	278.6	259.5
July	154.7	154.9	190	318.6	281.5	278.7	260.8
Aug	151.2	151.3	186.4	318.6	281.5	278.7	260.3
Sept	134	133.8	168.9	318.6	281.5	278.5	257.7
Oct	128.4	128.3	163.4	318.6	281.5	278.4	256.7
Nov	101.3	101.1	136.3	318.6	281.5	278	251.3
Dec	81.98	81.81	117	318.6	281.5	277.6	246.6
Entropy (kJ/kg-K)							
State Point	1'	1	2	3	4	4'	5
Jan	0.2865	0.2859	0.2859	0.9136	0.9137	0.9034	0.9252
Feb	0.3162	0.3156	0.3156	0.9136	0.9137	0.9039	0.9241
Mar	0.359	0.3584	0.3584	0.9136	0.9137	0.9045	0.9225
Apr	0.4157	0.4152	0.4152	0.9136	0.9137	0.9053	0.9208
May	0.4732	0.4726	0.4726	0.9136	0.9137	0.9061	0.9194
June	0.5313	0.5308	0.5308	0.9136	0.9137	0.9068	0.9182
July	0.56	0.5595	0.5595	0.9136	0.9137	0.9071	0.9178
Aug	0.5487	0.5482	0.5482	0.9136	0.9137	0.907	0.9179
Sept	0.4929	0.4923	0.4923	0.9136	0.9137	0.9063	0.919
Oct	0.4748	0.4742	0.4742	0.9136	0.9137	0.9061	0.9193
Nov	0.3836	0.383	0.3831	0.9136	0.9137	0.9049	0.9218
Dec	0.3164	0.3157	0.3157	0.9136	0.9137	0.9039	0.9241

Table B-32: Thermodynamic Properties for Direct Single-Loop System Simulations at 3.6km Depth, CO2 Mass Flow Rate of 140kg/s, and Reservoir Temperature of 125°C (DTE=0.85).

Tres	125°C						
Well Depth	3.6 km						
CO2 Mass Flow	140 kg/s						
	Pressure (kPa)						
State Point	1'	1	2	3	4	4'	5
Jan	2986	2985	38090	35000	14100	13782	2986
Feb	3286	3285	37780	35000	14100	13782	3286
Mar	3749	3748	37325	35000	14100	13782	3749
Apr	4410	4409	36700	35000	14100	13782	4410
May	5116	5116	36013	35000	14100	13782	5116
June	5837	5836	35212	35000	14100	13781	5837
July	6174	6423	35049	35000	14100	13781	6174
Aug	6046	6195	35120	35000	14100	13781	6046
Sept	5362	5361	35756	35000	14100	13782	5362
Oct	5136	5135	35992	35000	14100	13782	5136
Nov	4030	4029	37059	35000	14100	13782	4030
Dec	3287	3286	37778	35000	14100	13782	3287
	Temperature (°C)						
State Point	1'	1	2	3	4	4'	5
Jan	-5.72	-5.73	14.41	125	70.68	68.48	-5.72
Feb	-2.205	-2.214	18.99	125	70.68	68.52	-2.205
Mar	2.782	2.773	25.67	125	70.68	68.57	2.782
Apr	9.167	9.159	34.64	125	70.68	68.64	9.167
May	15.24	15.23	43.82	125	70.68	68.7	15.24
June	20.8	20.79	53.16	125	70.68	68.75	20.8
July	23.21	23.76	57.98	125	70.68	68.78	23.21
Aug	22.31	22.6	56.08	125	70.68	68.77	22.31
Sept	17.2	17.19	46.98	125	70.68	68.72	17.2
Oct	15.4	15.39	44.08	125	70.68	68.7	15.4
Nov	5.592	5.583	29.55	125	70.68	68.6	5.592
Dec	-2.19	-2.199	19.01	125	70.68	68.52	-2.19
	Enthalpy (kJ/kg)						
State Point	1'	1	2	3	4	4'	5
Jan	73.61	73.46	108.6	318.6	280.8	277.2	244.8
Feb	81.92	81.77	116.9	318.6	280.8	277.3	246.9
Mar	94.13	93.98	129.1	318.6	280.8	277.5	249.9
Apr	110.7	110.6	145.7	318.6	280.8	277.7	253.6
May	127.9	127.8	162.9	318.6	280.8	277.9	256.9
June	145.8	145.7	180.7	318.6	280.8	278.1	259.7
July	154.7	154.9	190	318.6	280.8	278.2	261
Aug	151.2	151.3	186.3	318.6	280.8	278.2	260.5
Sept	133.9	133.8	168.9	318.6	280.8	278	257.9
Oct	128.4	128.3	163.4	318.6	280.8	277.9	257
Nov	101.3	101.1	136.2	318.6	280.8	277.6	251.6
Dec	81.96	81.81	116.9	318.6	280.8	277.3	246.9
	Entropy (kJ/kg-K)						
State Point	1'	1	2	3	4	4'	5
Jan	0.2864	0.2859	0.2859	0.9136	0.9137	0.905	0.9264
Feb	0.3161	0.3156	0.3156	0.9136	0.9137	0.9054	0.9252
Mar	0.3589	0.3584	0.3584	0.9136	0.9137	0.9059	0.9236
Apr	0.4157	0.4152	0.4152	0.9136	0.9137	0.9066	0.9217
May	0.4731	0.4726	0.4726	0.9136	0.9137	0.9073	0.9202
June	0.5313	0.5308	0.5308	0.9136	0.9137	0.9079	0.9189
July	0.5599	0.5595	0.5595	0.9136	0.9137	0.9082	0.9184
Aug	0.5486	0.5482	0.5482	0.9136	0.9137	0.9081	0.9186
Sept	0.4928	0.4923	0.4923	0.9136	0.9137	0.9075	0.9197
Oct	0.4747	0.4742	0.4742	0.9136	0.9137	0.9073	0.9201
Nov	0.3836	0.383	0.3831	0.9136	0.9137	0.9062	0.9227
Dec	0.3163	0.3157	0.3157	0.9136	0.9137	0.9054	0.9252

Table B-33: Thermodynamic Properties for Direct Single-Loop System Simulations at 3.6km Depth, CO2 Mass Flow Rate of 70kg/s, and Reservoir Temperature of 150°C (DTE=0.85).

Tres	150°C						
Well Depth	3.6 km						
CO2 Mass Flow	70 kg/s						
	Pressure (kPa)						
State Point	1'	1	2	3	4	4'	5
Jan	2986	2985	38160	35000	16599	16303	2986
Feb	3286	3285	37851	35000	16599	16303	3286
Mar	3748	3748	37399	35000	16599	16303	3748
Apr	4410	4409	36777	35000	16599	16302	4410
May	5116	5116	36094	35000	16599	16302	5116
June	5837	5836	35299	35000	16599	16302	5837
July	6173	6423	35139	35000	16599	16302	6173
Aug	6046	6195	35208	35000	16599	16302	6046
Sept	5362	5361	35839	35000	16599	16302	5362
Oct	5136	5135	36073	35000	16599	16302	5136
Nov	4029	4029	37134	35000	16599	16303	4029
Dec	3287	3286	37849	35000	16599	16303	3287
	Temperature (°C)						
State Point	1'	1	2	3	4	4'	5
Jan	-5.725	-5.73	14.45	150	95.61	91.7	-5.725
Feb	-2.209	-2.214	19.03	150	95.61	91.79	-2.209
Mar	2.778	2.773	25.71	150	95.61	91.91	2.778
Apr	9.163	9.159	34.69	150	95.61	92.06	9.163
May	15.23	15.23	43.88	150	95.61	92.21	15.23
June	20.79	20.79	53.22	150	95.61	92.35	20.79
July	23.2	23.76	58.05	150	95.61	92.4	24.35
Aug	22.3	22.6	56.15	150	95.61	92.38	22.93
Sept	17.19	17.19	47.04	150	95.61	92.26	17.19
Oct	15.39	15.39	44.13	150	95.61	92.21	15.39
Nov	5.588	5.583	29.59	150	95.61	91.98	5.588
Dec	-2.194	-2.199	19.05	150	95.61	91.79	-2.194
	Enthalpy (kJ/kg)						
State Point	1'	1	2	3	4	4'	5
Jan	73.72	73.46	108.7	364.1	326.1	319	274.2
Feb	82.03	81.77	117	364.1	326.1	319.2	276.8
Mar	94.24	93.98	129.2	364.1	326.1	319.5	280.3
Apr	110.8	110.6	145.8	364.1	326.1	319.9	284.6
May	128	127.8	163	364.1	326.1	320.3	288.5
June	145.9	145.7	180.8	364.1	326.1	320.6	292
July	154.8	154.9	190.1	364.1	326.1	320.7	293.5
Aug	151.3	151.3	186.4	364.1	326.1	320.7	292.9
Sept	134	133.8	169	364.1	326.1	320.4	289.8
Oct	128.5	128.3	163.5	364.1	326.1	320.3	288.6
Nov	101.4	101.1	136.3	364.1	326.1	319.7	282.2
Dec	82.07	81.81	117	364.1	326.1	319.2	276.8
	Entropy (kJ/kg-K)						
State Point	1'	1	2	3	4	4'	5
Jan	0.2869	0.2859	0.2859	1.024	1.024	1.007	1.037
Feb	0.3165	0.3156	0.3156	1.024	1.024	1.008	1.035
Mar	0.3593	0.3584	0.3584	1.024	1.024	1.009	1.034
Apr	0.416	0.4152	0.4152	1.024	1.024	1.01	1.032
May	0.4734	0.4726	0.4726	1.024	1.024	1.011	1.03
June	0.5316	0.5308	0.5308	1.024	1.024	1.012	1.029
July	0.5602	0.5595	0.5595	1.024	1.024	1.012	1.028
Aug	0.5489	0.5482	0.5482	1.024	1.024	1.012	1.028
Sept	0.4931	0.4923	0.4923	1.024	1.024	1.011	1.03
Oct	0.475	0.4742	0.4742	1.024	1.024	1.011	1.03
Nov	0.3839	0.383	0.3831	1.024	1.024	1.009	1.033
Dec	0.3167	0.3157	0.3157	1.024	1.024	1.008	1.035

Table B-34: Thermodynamic Properties for Direct Single-Loop System Simulations at 3.6km Depth, CO2 Mass Flow Rate of 90kg/s, and Reservoir Temperature of 150°C (DTE=0.85).

Tres	150°C						
Well Depth	3.6 km						
CO2 Mass Flow	90 kg/s						
Pressure (kPa)							
State Point	1'	1	2	3	4	4'	5
Jan	2986	2985	38111	35000	15856	15352	2986
Feb	3286	3285	37801	35000	15856	15352	3286
Mar	3749	3748	37348	35000	15856	15352	3749
Apr	4410	4409	36724	35000	15856	15351	4410
May	5116	5116	36037	35000	15856	15351	5116
June	5837	5836	35239	35000	15856	15351	5837
July	6174	6423	35077	35000	15856	15351	6174
Aug	6046	6195	35147	35000	15856	15351	6046
Sept	5362	5361	35781	35000	15856	15351	5362
Oct	5136	5135	36017	35000	15856	15351	5136
Nov	4030	4029	37082	35000	15856	15352	4030
Dec	3287	3286	37800	35000	15856	15352	3287
Temperature (°C)							
State Point	1'	1	2	3	4	4'	5
Jan	-5.722	-5.73	14.42	150	92.26	88	-5.722
Feb	-2.206	-2.214	19	150	92.26	88.06	-2.206
Mar	2.78	2.773	25.68	150	92.26	88.16	2.78
Apr	9.166	9.159	34.65	150	92.26	88.27	9.166
May	15.24	15.23	43.84	150	92.26	88.38	15.24
June	20.8	20.79	53.18	150	92.26	88.48	20.8
July	23.21	23.76	58	150	92.26	88.53	24.48
Aug	22.31	22.6	56.1	150	92.26	88.51	23.06
Sept	17.2	17.19	47	150	92.26	88.42	17.2
Oct	15.4	15.39	44.09	150	92.26	88.39	15.4
Nov	5.591	5.583	29.56	150	92.26	88.21	5.591
Dec	-2.191	-2.199	19.02	150	92.26	88.06	-2.191
Enthalpy (kJ/kg)							
State Point	1'	1	2	3	4	4'	5
Jan	73.66	73.46	108.6	364.1	324.2	318.2	275.1
Feb	81.97	81.77	116.9	364.1	324.2	318.3	277.6
Mar	94.18	93.98	129.1	364.1	324.2	318.6	281.1
Apr	110.8	110.6	145.7	364.1	324.2	318.9	285.3
May	128	127.8	162.9	364.1	324.2	319.1	289.2
June	145.8	145.7	180.8	364.1	324.2	319.4	292.6
July	154.7	154.9	190	364.1	324.2	319.5	294.1
Aug	151.2	151.3	186.4	364.1	324.2	319.5	293.5
Sept	134	133.8	168.9	364.1	324.2	319.2	290.4
Oct	128.5	128.3	163.4	364.1	324.2	319.1	289.3
Nov	101.3	101.1	136.3	364.1	324.2	318.7	283
Dec	82.01	81.81	117	364.1	324.2	318.3	277.6
Entropy (kJ/kg-K)							
State Point	1'	1	2	3	4	4'	5
Jan	0.2866	0.2859	0.2859	1.024	1.024	1.011	1.04
Feb	0.3163	0.3156	0.3156	1.024	1.024	1.012	1.038
Mar	0.3591	0.3584	0.3584	1.024	1.024	1.012	1.036
Apr	0.4158	0.4152	0.4152	1.024	1.024	1.013	1.034
May	0.4732	0.4726	0.4726	1.024	1.024	1.014	1.032
June	0.5314	0.5308	0.5308	1.024	1.024	1.015	1.031
July	0.5601	0.5595	0.5595	1.024	1.024	1.015	1.03
Aug	0.5488	0.5482	0.5482	1.024	1.024	1.015	1.03
Sept	0.4929	0.4923	0.4923	1.024	1.024	1.014	1.032
Oct	0.4748	0.4742	0.4742	1.024	1.024	1.014	1.032
Nov	0.3837	0.383	0.3831	1.024	1.024	1.013	1.035
Dec	0.3165	0.3157	0.3157	1.024	1.024	1.012	1.038

Table B-35: Thermodynamic Properties for Direct Single-Loop System Simulations at 3.6km Depth, CO2 Mass Flow Rate of 120kg/s, and Reservoir Temperature of 150°C (DTE=0.85).

Tres	150°C						
Well Depth	3.6 km						
CO2 Mass Flow	120 kg/s						
Pressure (kPa)							
State Point	1'	1	2	3	4	4'	5
Jan	2986	2985	38129	35000	16723	16460	2986
Feb	3286	3285	37819	35000	16723	16460	3286
Mar	3749	3748	37366	35000	16723	16460	3749
Apr	4410	4409	36742	35000	16723	16460	4410
May	5116	5116	36057	35000	16723	16460	5116
June	5837	5836	35260	35000	16723	16459	5837
July	6173	6423	35098	35000	16723	16459	6173
Aug	6046	6195	35169	35000	16723	16459	6046
Sept	5362	5361	35802	35000	16723	16460	5362
Oct	5136	5135	36037	35000	16723	16460	5136
Nov	4030	4029	37100	35000	16723	16460	4030
Dec	3287	3286	37817	35000	16723	16460	3287
Temperature (°C)							
State Point	1'	1	2	3	4	4'	5
Jan	-5.723	-5.73	14.43	150	96.16	93.12	-5.723
Feb	-2.207	-2.214	19.01	150	96.16	93.18	-2.207
Mar	2.779	2.773	25.69	150	96.16	93.27	2.779
Apr	9.165	9.159	34.67	150	96.16	93.38	9.165
May	15.24	15.23	43.85	150	96.16	93.48	15.24
June	20.8	20.79	53.19	150	96.16	93.58	20.8
July	23.21	23.76	58.02	150	96.16	93.62	24.59
Aug	22.31	22.6	56.12	150	96.16	93.61	23.17
Sept	17.2	17.19	47.01	150	96.16	93.52	17.2
Oct	15.4	15.39	44.11	150	96.16	93.49	15.4
Nov	5.59	5.583	29.57	150	96.16	93.31	5.59
Dec	-2.192	-2.199	19.03	150	96.16	93.18	-2.192
Enthalpy (kJ/kg)							
State Point	1'	1	2	3	4	4'	5
Jan	73.64	73.46	108.6	364.1	326.4	321.2	275.7
Feb	81.94	81.77	116.9	364.1	326.4	321.3	278.2
Mar	94.15	93.98	129.1	364.1	326.4	321.5	281.6
Apr	110.7	110.6	145.7	364.1	326.4	321.8	285.9
May	128	127.8	162.9	364.1	326.4	322.1	289.8
June	145.8	145.7	180.8	364.1	326.4	322.3	293.2
July	154.7	154.9	190	364.1	326.4	322.4	294.6
Aug	151.2	151.3	186.4	364.1	326.4	322.4	294.1
Sept	134	133.8	168.9	364.1	326.4	322.2	291
Oct	128.4	128.3	163.4	364.1	326.4	322.1	289.9
Nov	101.3	101.1	136.3	364.1	326.4	321.7	283.5
Dec	81.98	81.81	117	364.1	326.4	321.3	278.2
Entropy (kJ/kg-K)							
State Point	1'	1	2	3	4	4'	5
Jan	0.2865	0.2859	0.2859	1.024	1.024	1.012	1.042
Feb	0.3162	0.3156	0.3156	1.024	1.024	1.012	1.041
Mar	0.359	0.3584	0.3584	1.024	1.024	1.013	1.039
Apr	0.4157	0.4152	0.4152	1.024	1.024	1.014	1.036
May	0.4732	0.4726	0.4726	1.024	1.024	1.014	1.034
June	0.5313	0.5308	0.5308	1.024	1.024	1.015	1.033
July	0.56	0.5595	0.5595	1.024	1.024	1.015	1.032
Aug	0.5487	0.5482	0.5482	1.024	1.024	1.015	1.032
Sept	0.4929	0.4923	0.4923	1.024	1.024	1.015	1.034
Oct	0.4748	0.4742	0.4742	1.024	1.024	1.015	1.034
Nov	0.3836	0.383	0.3831	1.024	1.024	1.013	1.037
Dec	0.3164	0.3157	0.3157	1.024	1.024	1.012	1.041

Table B-36: Thermodynamic Properties for Direct Single-Loop System Simulations at 3.6km Depth, CO2 Mass Flow Rate of 140kg/s, and Reservoir Temperature of 150°C (DTE=0.85).

Tres	150°C						
Well Depth	3.6 km						
CO2 Mass Flow	140 kg/s						
Pressure (kPa)							
State Point	1'	1	2	3	4	4'	5
Jan	2986	2985	38090	35000	16360	15997	2986
Feb	3286	3285	37780	35000	16360	15997	3286
Mar	3749	3748	37325	35000	16360	15997	3749
Apr	4410	4409	36700	35000	16360	15997	4410
May	5116	5116	36013	35000	16360	15997	5116
June	5837	5836	35212	35000	16360	15996	5837
July	6174	6423	35049	35000	16360	15996	6174
Aug	6046	6195	35120	35000	16360	15996	6046
Sept	5362	5361	35756	35000	16360	15996	5362
Oct	5136	5135	35992	35000	16360	15996	5136
Nov	4030	4029	37059	35000	16360	15997	4030
Dec	3287	3286	37778	35000	16360	15997	3287
Temperature (°C)							
State Point	1'	1	2	3	4	4'	5
Jan	-5.72	-5.73	14.41	150	94.55	91.34	-5.72
Feb	-2.205	-2.214	18.99	150	94.55	91.39	-2.205
Mar	2.782	2.773	25.67	150	94.55	91.47	2.782
Apr	9.167	9.159	34.64	150	94.55	91.56	9.167
May	15.24	15.23	43.82	150	94.55	91.65	15.24
June	20.8	20.79	53.16	150	94.55	91.74	20.84
July	23.21	23.76	57.98	150	94.55	91.77	24.65
Aug	22.31	22.6	56.08	150	94.55	91.76	23.23
Sept	17.2	17.19	46.98	150	94.55	91.68	17.2
Oct	15.4	15.39	44.08	150	94.55	91.66	15.4
Nov	5.592	5.583	29.55	150	94.55	91.51	5.592
Dec	-2.19	-2.199	19.01	150	94.55	91.39	-2.19
Enthalpy (kJ/kg)							
State Point	1'	1	2	3	4	4'	5
Jan	73.61	73.46	108.6	364.1	325.5	320.7	276
Feb	81.92	81.77	116.9	364.1	325.5	320.9	278.5
Mar	94.13	93.98	129.1	364.1	325.5	321	282
Apr	110.7	110.6	145.7	364.1	325.5	321.3	286.2
May	127.9	127.8	162.9	364.1	325.5	321.5	290.1
June	145.8	145.7	180.7	364.1	325.5	321.7	293.4
July	154.7	154.9	190	364.1	325.5	321.8	294.9
Aug	151.2	151.3	186.3	364.1	325.5	321.8	294.3
Sept	133.9	133.8	168.9	364.1	325.5	321.6	291.3
Oct	128.4	128.3	163.4	364.1	325.5	321.5	290.2
Nov	101.3	101.1	136.2	364.1	325.5	321.1	283.9
Dec	81.96	81.81	116.9	364.1	325.5	320.9	278.6
Entropy (kJ/kg-K)							
State Point	1'	1	2	3	4	4'	5
Jan	0.2864	0.2859	0.2859	1.024	1.024	1.014	1.043
Feb	0.3161	0.3156	0.3156	1.024	1.024	1.014	1.042
Mar	0.3589	0.3584	0.3584	1.024	1.024	1.015	1.04
Apr	0.4157	0.4152	0.4152	1.024	1.024	1.015	1.037
May	0.4731	0.4726	0.4726	1.024	1.024	1.016	1.035
June	0.5313	0.5308	0.5308	1.024	1.024	1.017	1.034
July	0.5599	0.5595	0.5595	1.024	1.024	1.017	1.033
Aug	0.5486	0.5482	0.5482	1.024	1.024	1.017	1.033
Sept	0.4928	0.4923	0.4923	1.024	1.024	1.016	1.035
Oct	0.4747	0.4742	0.4742	1.024	1.024	1.016	1.035
Nov	0.3836	0.383	0.3831	1.024	1.024	1.015	1.039
Dec	0.3163	0.3157	0.3157	1.024	1.024	1.014	1.042

Table B-37: Thermodynamic Properties for Direct Single-Loop System Simulations at 2.5km Depth, CO2 Mass Flow Rate of 70kg/s, and Reservoir Temperature of 100°C (DTE=0.50).

Tres	100°C						
Well Depth	2.5 km						
CO2 Mass Flow	70 kg/s						
Pressure (kPa)							
State Point	1'	1	2	3	4'	4	5
Jan	2986	2985	27072	25000	11380	11108	2986
Feb	3286	3285	26933	25000	11380	11108	3286
Mar	3749	3748	26736	25000	11380	11108	3749
Apr	4410	4409	26468	25000	11380	11107	4410
May	5117	5116	26164	25000	11380	11107	5117
June	5838	5836	25776	25000	11380	11107	5838
July	6174	6173	25530	25000	11380	11107	6174
Aug	6047	6045	25636	25000	11380	11107	6047
Sept	5362	5361	26044	25000	11380	11107	5362
Oct	5137	5135	26154	25000	11380	11107	5137
Nov	4030	4029	26622	25000	11380	11108	4030
Dec	3288	3286	26932	25000	11380	11108	3288
Temperature (°C)							
State Point	1'	1	2	3	4'	4	5
Jan	-5.717	-5.73	8.958	100	55.9	53.79	-5.717
Feb	-2.201	-2.214	13.29	100	55.9	53.83	-2.201
Mar	2.785	2.773	19.6	100	55.9	53.88	2.785
Apr	9.17	9.159	28.02	100	55.9	53.95	9.17
May	15.24	15.23	36.57	100	55.9	54.02	15.24
June	20.8	20.79	45.18	100	55.9	54.08	20.8
July	23.21	23.2	49.36	100	55.9	54.1	23.21
Aug	22.31	22.3	47.72	100	55.9	54.09	22.31
Sept	17.2	17.19	39.5	100	55.9	54.04	17.2
Oct	15.4	15.39	36.81	100	55.9	54.02	15.4
Nov	5.595	5.583	23.25	100	55.9	53.91	5.595
Dec	-2.186	-2.199	13.32	100	55.9	53.83	-2.186
Enthalpy (kJ/kg)							
State Point	1'	1	2	3	4'	4	5
Jan	73.68	73.46	97.82	291.5	265.4	260.8	245.7
Feb	81.98	81.77	106.1	291.5	265.4	261	247.1
Mar	94.19	93.98	118.3	291.5	265.4	261.3	249
Apr	110.8	110.6	134.9	291.5	265.4	261.7	251.3
May	128	127.8	152.1	291.5	265.4	262.1	253.4
June	145.8	145.7	170	291.5	265.4	262.4	255.2
July	154.8	154.6	178.9	291.5	265.4	262.6	255.9
Aug	151.2	151.1	175.3	291.5	265.4	262.5	255.7
Sept	134	133.8	158.1	291.5	265.4	262.2	254
Oct	128.5	128.3	152.6	291.5	265.4	262.1	253.4
Nov	101.3	101.1	125.5	291.5	265.4	261.5	250
Dec	82.02	81.81	106.2	291.5	265.4	261	247.1
Entropy (kJ/kg-K)							
State Point	1'	1	2	3	4'	4	5
Jan	0.2867	0.2859	0.2859	0.8858	0.8859	0.8738	0.93
Feb	0.3164	0.3156	0.3156	0.8858	0.8859	0.8745	0.9258
Mar	0.3592	0.3584	0.3584	0.8858	0.8859	0.8754	0.9201
Apr	0.4159	0.4152	0.4152	0.8858	0.8859	0.8766	0.9135
May	0.4733	0.4726	0.4726	0.8858	0.8859	0.8777	0.908
June	0.5315	0.5308	0.5308	0.8858	0.8859	0.8787	0.9034
July	0.5601	0.5595	0.5595	0.8858	0.8859	0.8792	0.9015
Aug	0.5488	0.5482	0.5482	0.8858	0.8859	0.879	0.9022
Sept	0.493	0.4923	0.4923	0.8858	0.8859	0.878	0.9063
Oct	0.4749	0.4742	0.4742	0.8858	0.8859	0.8777	0.9078
Nov	0.3838	0.383	0.383	0.8858	0.8859	0.8759	0.9171
Dec	0.3165	0.3157	0.3157	0.8858	0.8859	0.8745	0.9258

Table B-38: Thermodynamic Properties for Direct Single-Loop System Simulations at 2.5km Depth, CO2 Mass Flow Rate of 90kg/s, and Reservoir Temperature of 100°C (DTE=0.50).

Tres	100°C						
Well Depth	2.5 km						
CO2 Mass Flow	90 kg/s						
Pressure (kPa)							
State Point	1'	1	2	3	4'	4	5
Jan	2987	2985	26983	25000	10901	10438	2987
Feb	3287	3285	26843	25000	10901	10438	3287
Mar	3750	3748	26642	25000	10901	10437	3750
Apr	4411	4409	26370	25000	10901	10437	4411
May	5118	5116	26060	25000	10901	10436	5118
June	5839	5836	25665	25000	10901	10436	5839
July	6175	6173	25416	25000	10901	10436	6175
Aug	6048	6045	25523	25000	10901	10436	6048
Sept	5363	5361	25938	25000	10901	10436	5363
Oct	5137	5135	26050	25000	10901	10436	5137
Nov	4031	4029	26527	25000	10901	10437	4031
Dec	3288	3286	26842	25000	10901	10438	3288
Temperature (°C)							
State Point	1'	1	2	3	4'	4	5
Jan	-5.708	-5.73	8.912	100	53.46	50.51	-5.708
Feb	-2.193	-2.214	13.24	100	53.46	50.53	-2.193
Mar	2.793	2.773	19.54	100	53.46	50.57	2.793
Apr	9.177	9.159	27.95	100	53.46	50.62	9.177
May	15.25	15.23	36.49	100	53.46	50.66	15.25
June	20.81	20.79	45.08	100	53.46	50.7	20.81
July	23.22	23.2	49.24	100	53.46	50.72	23.22
Aug	22.32	22.3	47.61	100	53.46	50.71	22.32
Sept	17.21	17.19	39.41	100	53.46	50.67	17.21
Oct	15.41	15.39	36.73	100	53.46	50.66	15.41
Nov	5.602	5.583	23.19	100	53.46	50.59	5.602
Dec	-2.178	-2.199	13.26	100	53.46	50.53	-2.178
Enthalpy (kJ/kg)							
State Point	1'	1	2	3	4'	4	5
Jan	73.63	73.46	97.73	291.5	264.3	260.3	245.9
Feb	81.94	81.77	106	291.5	264.3	260.4	247.2
Mar	94.15	93.98	118.2	291.5	264.3	260.7	249
Apr	110.7	110.6	134.8	291.5	264.3	261	251.2
May	128	127.8	152	291.5	264.3	261.2	253.2
June	145.8	145.7	169.8	291.5	264.3	261.5	255
July	154.7	154.6	178.7	291.5	264.3	261.6	255.7
Aug	151.2	151.1	175.2	291.5	264.3	261.6	255.5
Sept	134	133.8	158	291.5	264.3	261.3	253.9
Oct	128.4	128.3	152.5	291.5	264.3	261.2	253.3
Nov	101.3	101.1	125.4	291.5	264.3	260.8	250
Dec	81.98	81.81	106.1	291.5	264.3	260.4	247.2
Entropy (kJ/kg-K)							
State Point	1'	1	2	3	4'	4	5
Jan	0.2865	0.2859	0.2859	0.8858	0.8859	0.8768	0.9306
Feb	0.3162	0.3156	0.3156	0.8858	0.8859	0.8773	0.9261
Mar	0.359	0.3584	0.3584	0.8858	0.8859	0.8781	0.9202
Apr	0.4157	0.4152	0.4152	0.8858	0.8859	0.879	0.9134
May	0.4731	0.4726	0.4726	0.8858	0.8859	0.8799	0.9076
June	0.5313	0.5308	0.5308	0.8858	0.8859	0.8807	0.9028
July	0.56	0.5595	0.5595	0.8858	0.8859	0.881	0.9008
Aug	0.5487	0.5482	0.5482	0.8858	0.8859	0.8809	0.9016
Sept	0.4928	0.4923	0.4923	0.8858	0.8859	0.8802	0.9058
Oct	0.4747	0.4742	0.4742	0.8858	0.8859	0.8799	0.9074
Nov	0.3836	0.383	0.383	0.8858	0.8859	0.8785	0.9171
Dec	0.3163	0.3157	0.3157	0.8858	0.8859	0.8773	0.9261

Table B-39: Thermodynamic Properties for Direct Single-Loop System Simulations at 2.5km Depth, CO₂

Mass Flow Rate of 120kg/s, and Reservoir Temperature of 100°C (DTE=0.50).

Tres	100°C						
Well Depth	2.5 km						
CO₂ Mass Flow	120 kg/s						
	Pressure (kPa)						
State Point	1'	1	2	3	4'	4	5
Jan	2986	2985	27055	25000	11461	11219	2986
Feb	3286	3285	26917	25000	11461	11219	3286
Mar	3749	3748	26719	25000	11461	11219	3749
Apr	4410	4409	26450	25000	11461	11218	4410
May	5117	5116	26144	25000	11461	11218	5117
June	5838	5836	25755	25000	11461	11218	5838
July	6174	6173	25509	25000	11461	11218	6174
Aug	6047	6045	25615	25000	11461	11218	6047
Sept	5363	5361	26024	25000	11461	11218	5363
Oct	5137	5135	26135	25000	11461	11218	5137
Nov	4030	4029	26605	25000	11461	11219	4030
Dec	3288	3286	26916	25000	11461	11219	3288
	Temperature (°C)						
State Point	1'	1	2	3	4'	4	5
Jan	-5.715	-5.73	8.95	100	56.3	54.55	-5.715
Feb	-2.2	-2.214	13.28	100	56.3	54.57	-2.2
Mar	2.786	2.773	19.59	100	56.3	54.61	2.786
Apr	9.171	9.159	28.01	100	56.3	54.67	9.171
May	15.24	15.23	36.56	100	56.3	54.71	15.24
June	20.8	20.79	45.16	100	56.3	54.76	20.8
July	23.21	23.2	49.34	100	56.3	54.78	23.21
Aug	22.31	22.3	47.7	100	56.3	54.77	22.31
Sept	17.2	17.19	39.48	100	56.3	54.73	17.2
Oct	15.4	15.39	36.8	100	56.3	54.72	15.4
Nov	5.596	5.583	23.24	100	56.3	54.64	5.596
Dec	-2.185	-2.199	13.31	100	56.3	54.57	-2.185
	Enthalpy (kJ/kg)						
State Point	1'	1	2	3	4'	4	5
Jan	73.61	73.46	97.81	291.5	265.6	262.2	246.9
Feb	81.92	81.77	106.1	291.5	265.6	262.3	248.2
Mar	94.13	93.98	118.3	291.5	265.6	262.5	250
Apr	110.7	110.6	134.9	291.5	265.6	262.8	252.2
May	127.9	127.8	152.1	291.5	265.6	263.1	254.2
June	145.8	145.7	169.9	291.5	265.6	263.3	255.9
July	154.7	154.6	178.8	291.5	265.6	263.4	256.6
Aug	151.2	151.1	175.3	291.5	265.6	263.4	256.4
Sept	133.9	133.8	158.1	291.5	265.6	263.2	254.8
Oct	128.4	128.3	152.6	291.5	265.6	263.1	254.2
Nov	101.3	101.1	125.5	291.5	265.6	262.7	251
Dec	81.96	81.81	106.2	291.5	265.6	262.3	248.2
	Entropy (kJ/kg-K)						
State Point	1'	1	2	3	4'	4	5
Jan	0.2865	0.2859	0.2859	0.8858	0.8859	0.8772	0.9344
Feb	0.3161	0.3156	0.3156	0.8858	0.8859	0.8777	0.9298
Mar	0.3589	0.3584	0.3584	0.8858	0.8859	0.8783	0.9238
Apr	0.4157	0.4152	0.4152	0.8858	0.8859	0.8792	0.9168
May	0.4731	0.4726	0.4726	0.8858	0.8859	0.88	0.9108
June	0.5313	0.5308	0.5308	0.8858	0.8859	0.8807	0.9059
July	0.5599	0.5595	0.5595	0.8858	0.8859	0.881	0.9039
Aug	0.5483	0.5482	0.5482	0.8858	0.8859	0.8809	0.9046
Sept	0.4928	0.4923	0.4923	0.8858	0.8859	0.8802	0.909
Oct	0.4747	0.4742	0.4742	0.8858	0.8859	0.88	0.9107
Nov	0.3836	0.383	0.383	0.8858	0.8859	0.8787	0.9206
Dec	0.3163	0.3157	0.3157	0.8858	0.8859	0.8777	0.9298

Table B-40: Thermodynamic Properties for Direct Single-Loop System Simulations at 2.5km Depth, CO₂

Mass Flow Rate of 140kg/s, and Reservoir Temperature of 100°C (DTE=0.50).

Tres	100°C						
Well Depth	2.5 km						
CO₂ Mass Flow	140 kg/s						
	Pressure (kPa)						
State Point	1'	1	2	3	4'	4	5
Jan	2987	2985	27000	25000	11226	10892	2987
Feb	3287	3285	26860	25000	11226	10892	3287
Mar	3750	3748	26661	25000	11226	10892	3750
Apr	4411	4409	26389	25000	11226	10892	4411
May	5117	5116	26080	25000	11226	10892	5117
June	5838	5836	25687	25000	11226	10891	5838
July	6175	6173	25438	25000	11226	10891	6175
Aug	6047	6045	25545	25000	11226	10891	6047
Sept	5363	5361	25959	25000	11226	10891	5363
Oct	5137	5135	26070	25000	11226	10892	5137
Nov	4031	4029	26545	25000	11226	10892	4031
Dec	3288	3286	26859	25000	11226	10892	3288
	Temperature (°C)						
State Point	1'	1	2	3	4'	4	5
Jan	-5.71	-5.73	8.921	100	55.12	52.98	-5.71
Feb	-2.195	-2.214	13.25	100	55.12	53	-2.195
Mar	2.791	2.773	19.55	100	55.12	53.04	2.791
Apr	9.176	9.159	27.97	100	55.12	53.08	9.176
May	15.25	15.23	36.51	100	55.12	53.12	15.25
June	20.81	20.79	45.1	100	55.12	53.15	20.81
July	23.22	23.2	49.27	100	55.12	53.17	23.22
Aug	22.32	22.3	47.64	100	55.12	53.16	22.32
Sept	17.21	17.19	39.43	100	55.12	53.13	17.21
Oct	15.41	15.39	36.74	100	55.12	53.12	15.41
Nov	5.601	5.583	23.2	100	55.12	53.05	5.601
Dec	-2.18	-2.199	13.27	100	55.12	53.01	-2.18
	Enthalpy (kJ/kg)						
State Point	1'	1	2	3	4'	4	5
Jan	73.59	73.46	97.75	291.5	265	261.9	246.9
Feb	81.9	81.77	106.1	291.5	265	262	248.2
Mar	94.11	93.98	118.3	291.5	265	262.2	250
Apr	110.7	110.6	134.8	291.5	265	262.4	252.2
May	127.9	127.8	152	291.5	265	262.7	254.1
June	145.8	145.7	169.9	291.5	265	262.9	255.8
July	154.7	154.6	178.7	291.5	265	262.9	256.5
Aug	151.2	151.1	175.2	291.5	265	262.9	256.3
Sept	133.9	133.8	158	291.5	265	262.7	254.7
Oct	128.4	128.3	152.5	291.5	265	262.7	254.2
Nov	101.3	101.1	125.4	291.5	265	262.3	251
Dec	81.94	81.81	106.1	291.5	265	262	248.2
	Entropy (kJ/kg-K)						
State Point	1'	1	2	3	4'	4	5
Jan	0.2864	0.2859	0.2859	0.8858	0.8859	0.8786	0.9345
Feb	0.316	0.3156	0.3156	0.8858	0.8859	0.879	0.9299
Mar	0.3589	0.3584	0.3584	0.8858	0.8859	0.8796	0.9238
Apr	0.4156	0.4152	0.4152	0.8858	0.8859	0.8803	0.9167
May	0.473	0.4726	0.4726	0.8858	0.8859	0.881	0.9106
June	0.5312	0.5308	0.5308	0.8858	0.8859	0.8816	0.9055
July	0.5599	0.5595	0.5595	0.8858	0.8859	0.8819	0.9035
Aug	0.5484	0.5482	0.5482	0.8858	0.8859	0.8818	0.9043
Sept	0.4927	0.4923	0.4923	0.8858	0.8859	0.8812	0.9088
Oct	0.4746	0.4742	0.4742	0.8858	0.8859	0.881	0.9104
Nov	0.3835	0.383	0.383	0.8858	0.8859	0.8799	0.9206
Dec	0.3162	0.3157	0.3157	0.8858	0.8859	0.879	0.9299

Table B-41: Thermodynamic Properties for Direct Single-Loop System Simulations at 2.5km Depth, CO2 Mass Flow Rate of 70kg/s, and Reservoir Temperature of 125°C (DTE=0.50).

Tres	125°C						
Well Depth	2.5 km						
CO2 Mass Flow	70 kg/s						
Pressure (kPa)							
State Point	1'	1	2	3	4'	4	5
Jan	2986	2985	27072	25000	13488	13158	2986
Feb	3286	3285	26933	25000	13488	13158	3286
Mar	3749	3748	26736	25000	13488	13157	3749
Apr	4410	4409	26468	25000	13488	13157	4410
May	5117	5116	26164	25000	13488	13157	5117
June	5838	5836	25776	25000	13488	13156	5838
July	6174	6173	25530	25000	13488	13156	6174
Aug	6047	6045	25636	25000	13488	13156	6047
Sept	5362	5361	26044	25000	13488	13156	5362
Oct	5137	5135	26154	25000	13488	13157	5137
Nov	4030	4029	26622	25000	13488	13157	4030
Dec	3288	3286	26932	25000	13488	13158	3288
Temperature (°C)							
State Point	1'	1	2	3	4'	4	5
Jan	-5.717	-5.73	8.958	125	80.05	76.32	-5.717
Feb	-2.201	-2.214	13.29	125	80.05	76.39	-2.201
Mar	2.785	2.773	19.6	125	80.05	76.5	2.785
Apr	9.17	9.159	28.02	125	80.05	76.63	9.17
May	15.24	15.23	36.57	125	80.05	76.76	15.24
June	20.8	20.79	45.18	125	80.05	76.87	22.27
July	24.09	23.2	49.36	125	80.05	76.92	26.02
Aug	22.68	22.3	47.72	125	80.05	76.9	24.62
Sept	17.2	17.19	39.5	125	80.05	76.8	17.2
Oct	15.4	15.39	36.81	125	80.05	76.76	15.4
Nov	5.595	5.583	23.25	125	80.05	76.55	5.595
Dec	-2.186	-2.199	13.32	125	80.05	76.39	-2.186
Enthalpy (kJ/kg)							
State Point	1'	1	2	3	4'	4	5
Jan	73.68	73.46	97.82	343.9	317	310.7	288.5
Feb	81.98	81.77	106.1	343.9	317	310.9	290.1
Mar	94.19	93.98	118.3	343.9	317	311.2	292.2
Apr	110.8	110.6	134.9	343.9	317	311.6	295
May	128	127.8	152.1	343.9	317	312	297.4
June	145.8	145.7	170	343.9	317	312.3	299.6
July	154.8	154.6	178.9	343.9	317	312.5	300.5
Aug	151.2	151.1	175.3	343.9	317	312.4	300.2
Sept	134	133.8	158.1	343.9	317	312.1	298.2
Oct	128.5	128.3	152.6	343.9	317	312	297.5
Nov	101.3	101.1	125.5	343.9	317	311.4	293.5
Dec	82.02	81.81	106.2	343.9	317	310.9	290.1
Entropy (kJ/kg-K)							
State Point	1'	1	2	3	4'	4	5
Jan	0.2867	0.2859	0.2859	1.022	1.022	1.007	1.09
Feb	0.3164	0.3156	0.3156	1.022	1.022	1.007	1.084
Mar	0.3592	0.3584	0.3584	1.022	1.022	1.008	1.077
Apr	0.4159	0.4152	0.4152	1.022	1.022	1.009	1.068
May	0.4733	0.4726	0.4726	1.022	1.022	1.01	1.061
June	0.5315	0.5308	0.5308	1.022	1.022	1.011	1.054
July	0.5601	0.5595	0.5595	1.022	1.022	1.012	1.052
Aug	0.5488	0.5482	0.5482	1.022	1.022	1.011	1.053
Sept	0.493	0.4923	0.4923	1.022	1.022	1.011	1.059
Oct	0.4749	0.4742	0.4742	1.022	1.022	1.01	1.061
Nov	0.3838	0.383	0.383	1.022	1.022	1.009	1.073
Dec	0.3165	0.3157	0.3157	1.022	1.022	1.007	1.084

Table B-42: Thermodynamic Properties for Direct Single-Loop System Simulations at 2.5km Depth, CO2 Mass Flow Rate of 90kg/s, and Reservoir Temperature of 125°C (DTE=0.50).

Tres	125°C						
Well Depth	2.5 km						
CO2 Mass Flow	90 kg/s						
	Pressure (kPa)						
State Point	1'	1	2	3	4'	4	5
Jan	2987	2985	26983	25000	12893	12328	2987
Feb	3287	3285	26843	25000	12893	12328	3287
Mar	3750	3748	26642	25000	12893	12328	3750
Apr	4411	4409	26370	25000	12893	12327	4411
May	5118	5116	26060	25000	12893	12327	5118
June	5839	5836	25665	25000	12893	12326	5839
July	6175	6173	25416	25000	12893	12326	6175
Aug	6048	6045	25523	25000	12893	12326	6048
Sept	5363	5361	25938	25000	12893	12326	5363
Oct	5137	5135	26050	25000	12893	12327	5137
Nov	4031	4029	26527	25000	12893	12327	4031
Dec	3288	3286	26842	25000	12893	12328	3288
	Temperature (°C)						
State Point	1'	1	2	3	4'	4	5
Jan	-5.708	-5.73	8.912	125	76.75	72.1	-5.708
Feb	-2.193	-2.214	13.24	125	76.75	72.16	-2.193
Mar	2.793	2.773	19.54	125	76.75	72.23	2.793
Apr	9.177	9.159	27.95	125	76.75	72.33	9.177
May	15.25	15.23	36.49	125	76.75	72.43	15.25
June	20.81	20.79	45.08	125	76.75	72.51	22.22
July	23.22	23.2	49.24	125	76.75	72.55	25.95
Aug	22.32	22.3	47.61	125	76.75	72.54	24.56
Sept	17.21	17.19	39.41	125	76.75	72.46	17.21
Oct	15.41	15.39	36.73	125	76.75	72.43	15.41
Nov	5.602	5.583	23.19	125	76.75	72.28	5.602
Dec	-2.178	-2.199	13.26	125	76.75	72.16	-2.178
	Enthalpy (kJ/kg)						
State Point	1'	1	2	3	4'	4	5
Jan	73.63	73.46	97.73	343.9	315.3	309.7	288.5
Feb	81.94	81.77	106	343.9	315.3	309.9	290
Mar	94.15	93.98	118.2	343.9	315.3	310.1	292.2
Apr	110.7	110.6	134.8	343.9	315.3	310.4	294.8
May	128	127.8	152	343.9	315.3	310.7	297.2
June	145.8	145.7	169.8	343.9	315.3	311	299.3
July	154.7	154.6	178.7	343.9	315.3	311.1	300.2
Aug	151.2	151.1	175.2	343.9	315.3	311	299.9
Sept	134	133.8	158	343.9	315.3	310.8	298
Oct	128.4	128.3	152.5	343.9	315.3	310.7	297.3
Nov	101.3	101.1	125.4	343.9	315.3	310.3	293.4
Dec	81.98	81.81	106.1	343.9	315.3	309.9	290
	Entropy (kJ/kg-K)						
State Point	1'	1	2	3	4'	4	5
Jan	0.2865	0.2859	0.2859	1.022	1.022	1.01	1.09
Feb	0.3162	0.3156	0.3156	1.022	1.022	1.011	1.084
Mar	0.359	0.3584	0.3584	1.022	1.022	1.012	1.077
Apr	0.4157	0.4152	0.4152	1.022	1.022	1.012	1.068
May	0.4731	0.4726	0.4726	1.022	1.022	1.013	1.06
June	0.5313	0.5308	0.5308	1.022	1.022	1.014	1.054
July	0.56	0.5595	0.5595	1.022	1.022	1.014	1.051
Aug	0.5487	0.5482	0.5482	1.022	1.022	1.014	1.052
Sept	0.4928	0.4923	0.4923	1.022	1.022	1.014	1.058
Oct	0.4747	0.4742	0.4742	1.022	1.022	1.013	1.06
Nov	0.3836	0.383	0.383	1.022	1.022	1.012	1.073
Dec	0.3163	0.3157	0.3157	1.022	1.022	1.011	1.084

Table B-43: Thermodynamic Properties for Direct Single-Loop System Simulations at 2.5km Depth, CO2 Mass Flow Rate of 120kg/s, and Reservoir Temperature of 125°C (DTE=0.50).

Tres	125°C						
Well Depth	2.5 km						
CO2 Mass Flow	120 kg/s						
Pressure (kPa)							
State Point	1'	1	2	3	4'	4	5
Jan	2986	2985	27055	25000	13587	13294	2986
Feb	3286	3285	26917	25000	13587	13294	3286
Mar	3749	3748	26719	25000	13587	13294	3749
Apr	4410	4409	26450	25000	13587	13293	4410
May	5117	5116	26144	25000	13587	13293	5117
June	5838	5836	25755	25000	13587	13293	5838
July	6174	6173	25509	25000	13587	13293	6174
Aug	6047	6045	25615	25000	13587	13293	6047
Sept	5363	5361	26024	25000	13587	13293	5363
Oct	5137	5135	26135	25000	13587	13293	5137
Nov	4030	4029	26605	25000	13587	13294	4030
Dec	3288	3286	26916	25000	13587	13294	3288
Temperature (°C)							
State Point	1'	1	2	3	4'	4	5
Jan	-5.715	-5.73	8.95	125	80.59	77.59	-5.715
Feb	-2.2	-2.214	13.28	125	80.59	77.65	-2.2
Mar	2.786	2.773	19.59	125	80.59	77.72	2.786
Apr	9.171	9.159	28.01	125	80.59	77.82	9.171
May	15.24	15.23	36.56	125	80.59	77.91	15.24
June	20.8	20.79	45.16	125	80.59	78	22.58
July	23.21	23.2	49.34	125	80.59	78.03	26.32
Aug	22.31	22.3	47.7	125	80.59	78.02	24.92
Sept	17.2	17.19	39.48	125	80.59	77.94	17.2
Oct	15.4	15.39	36.8	125	80.59	77.91	15.4
Nov	5.596	5.583	23.24	125	80.59	77.76	5.596
Dec	-2.185	-2.199	13.31	125	80.59	77.65	-2.185
Enthalpy (kJ/kg)							
State Point	1'	1	2	3	4'	4	5
Jan	73.61	73.46	97.81	343.9	317.3	312.6	290
Feb	81.92	81.77	106.1	343.9	317.3	312.8	291.5
Mar	94.13	93.98	118.3	343.9	317.3	313	293.7
Apr	110.7	110.6	134.9	343.9	317.3	313.3	296.3
May	127.9	127.8	152.1	343.9	317.3	313.5	298.7
June	145.8	145.7	169.9	343.9	317.3	313.8	300.8
July	154.7	154.6	178.8	343.9	317.3	313.9	301.6
Aug	151.2	151.1	175.3	343.9	317.3	313.8	301.3
Sept	133.9	133.8	158.1	343.9	317.3	313.6	299.4
Oct	128.4	128.3	152.6	343.9	317.3	313.5	298.7
Nov	101.3	101.1	125.5	343.9	317.3	313.1	294.8
Dec	81.96	81.81	106.2	343.9	317.3	312.8	291.5
Entropy (kJ/kg-K)							
State Point	1'	1	2	3	4'	4	5
Jan	0.2865	0.2859	0.2859	1.022	1.022	1.011	1.096
Feb	0.3161	0.3156	0.3156	1.022	1.022	1.011	1.09
Mar	0.3589	0.3584	0.3584	1.022	1.022	1.012	1.082
Apr	0.4157	0.4152	0.4152	1.022	1.022	1.013	1.073
May	0.4731	0.4726	0.4726	1.022	1.022	1.014	1.065
June	0.5313	0.5308	0.5308	1.022	1.022	1.014	1.058
July	0.5599	0.5595	0.5595	1.022	1.022	1.015	1.056
Aug	0.5483	0.5482	0.5482	1.022	1.022	1.014	1.057
Sept	0.4928	0.4923	0.4923	1.022	1.022	1.014	1.063
Oct	0.4747	0.4742	0.4742	1.022	1.022	1.014	1.065
Nov	0.3836	0.383	0.383	1.022	1.022	1.012	1.078
Dec	0.3163	0.3157	0.3157	1.022	1.022	1.011	1.09

Table B-44: Thermodynamic Properties for Direct Single-Loop System Simulations at 2.5km Depth, CO2 Mass Flow Rate of 140kg/s, and Reservoir Temperature of 125°C (DTE=0.50).

Tres	125°C						
Well Depth	2.5 km						
CO2 Mass Flow	140 kg/s						
Pressure (kPa)							
State Point	1'	1	2	3	4'	4	5
Jan	2987	2985	27000	25000	13297	12891	2987
Feb	3287	3285	26860	25000	13297	12891	3287
Mar	3750	3748	26661	25000	13297	12891	3750
Apr	4411	4409	26389	25000	13297	12891	4411
May	5117	5116	26080	25000	13297	12890	5117
June	5838	5836	25687	25000	13297	12890	5838
July	6175	6173	25438	25000	13297	12890	6175
Aug	6047	6045	25545	25000	13297	12890	6047
Sept	5363	5361	25959	25000	13297	12890	5363
Oct	5137	5135	26070	25000	13297	12890	5137
Nov	4031	4029	26545	25000	13297	12891	4031
Dec	3288	3286	26859	25000	13297	12891	3288
Temperature (°C)							
State Point	1'	1	2	3	4'	4	5
Jan	-5.71	-5.73	8.921	125	79.01	75.59	-5.71
Feb	-2.195	-2.214	13.25	125	79.01	75.63	-2.195
Mar	2.791	2.773	19.55	125	79.01	75.7	2.791
Apr	9.176	9.159	27.97	125	79.01	75.78	9.176
May	15.25	15.23	36.51	125	79.01	75.85	15.25
June	20.81	20.79	45.1	125	79.01	75.93	22.55
July	23.22	23.2	49.27	125	79.01	75.96	26.28
Aug	22.32	22.3	47.64	125	79.01	75.95	24.89
Sept	17.21	17.19	39.43	125	79.01	75.88	17.21
Oct	15.41	15.39	36.74	125	79.01	75.86	15.41
Nov	5.601	5.583	23.2	125	79.01	75.73	5.601
Dec	-2.18	-2.199	13.27	125	79.01	75.63	-2.18
Enthalpy (kJ/kg)							
State Point	1'	1	2	3	4'	4	5
Jan	73.59	73.46	97.75	343.9	316.5	312.1	290
Feb	81.9	81.77	106.1	343.9	316.5	312.2	291.5
Mar	94.11	93.98	118.3	343.9	316.5	312.4	293.6
Apr	110.7	110.6	134.8	343.9	316.5	312.7	296.2
May	127.9	127.8	152	343.9	316.5	312.9	298.5
June	145.8	145.7	169.9	343.9	316.5	313.1	300.6
July	154.7	154.6	178.7	343.9	316.5	313.2	301.5
Aug	151.2	151.1	175.2	343.9	316.5	313.1	301.2
Sept	133.9	133.8	158	343.9	316.5	313	299.3
Oct	128.4	128.3	152.5	343.9	316.5	312.9	298.6
Nov	101.3	101.1	125.4	343.9	316.5	312.5	294.7
Dec	81.94	81.81	106.1	343.9	316.5	312.2	291.5
Entropy (kJ/kg-K)							
State Point	1'	1	2	3	4'	4	5
Jan	0.2864	0.2859	0.2859	1.022	1.022	1.013	1.095
Feb	0.316	0.3156	0.3156	1.022	1.022	1.013	1.09
Mar	0.3589	0.3584	0.3584	1.022	1.022	1.014	1.082
Apr	0.4156	0.4152	0.4152	1.022	1.022	1.014	1.073
May	0.473	0.4726	0.4726	1.022	1.022	1.015	1.065
June	0.5312	0.5308	0.5308	1.022	1.022	1.015	1.058
July	0.5599	0.5595	0.5595	1.022	1.022	1.016	1.055
Aug	0.5484	0.5482	0.5482	1.022	1.022	1.016	1.056
Sept	0.4927	0.4923	0.4923	1.022	1.022	1.015	1.062
Oct	0.4746	0.4742	0.4742	1.022	1.022	1.015	1.064
Nov	0.3835	0.383	0.383	1.022	1.022	1.014	1.078
Dec	0.3162	0.3157	0.3157	1.022	1.022	1.013	1.09

Table B-45: Thermodynamic Properties for Direct Single-Loop System Simulations at 2.5km Depth, CO2 Mass Flow Rate of 70kg/s, and Reservoir Temperature of 150°C (DTE=0.50).

Tres	150°C						
Well Depth	2.5 km						
CO2 Mass Flow	70 kg/s						
	Pressure (kPa)						
State Point	1'	1	2	3	4'	4	5
Jan	2986	2985	27072	25000	14868	14484	2986
Feb	3286	3285	26933	25000	14868	14484	3286
Mar	3749	3748	26736	25000	14868	14483	3749
Apr	4410	4409	26468	25000	14868	14483	4410
May	5117	5116	26164	25000	14868	14483	5117
June	5838	5836	25776	25000	14868	14482	5838
July	6174	6173	25530	25000	14868	14482	6174
Aug	6047	6045	25636	25000	14868	14482	6047
Sept	5362	5361	26044	25000	14868	14483	5362
Oct	5137	5135	26154	25000	14868	14483	5137
Nov	4030	4029	26622	25000	14868	14483	4030
Dec	3288	3286	26932	25000	14868	14484	3288
	Temperature (°C)						
State Point	1'	1	2	3	4'	4	5
Jan	-5.717	-5.73	8.958	150	106.2	100.5	-3.009
Feb	-2.201	-2.214	13.29	150	106.2	100.6	2.393
Mar	2.785	2.773	19.6	150	106.2	100.8	10.07
Apr	9.17	9.159	28.02	150	106.2	101	19.91
May	15.24	15.23	36.57	150	106.2	101.1	29.28
June	20.8	20.79	45.18	150	106.2	101.3	37.9
July	23.21	23.2	49.36	150	106.2	101.4	41.66
Aug	22.31	22.3	47.72	150	106.2	101.4	40.25
Sept	17.2	17.19	39.5	150	106.2	101.2	32.32
Oct	15.4	15.39	36.81	150	106.2	101.2	29.53
Nov	5.595	5.583	23.25	150	106.2	100.9	14.4
Dec	-2.186	-2.199	13.32	150	106.2	100.6	2.416
	Enthalpy (kJ/kg)						
State Point	1'	1	2	3	4'	4	5
Jan	73.68	73.46	97.82	390.4	362.6	354.5	325.1
Feb	81.98	81.77	106.1	390.4	362.6	354.7	326.9
Mar	94.19	93.98	118.3	390.4	362.6	355	329.3
Apr	110.8	110.6	134.9	390.4	362.6	355.4	332.4
May	128	127.8	152.1	390.4	362.6	355.7	335.2
June	145.8	145.7	170	390.4	362.6	356.1	337.8
July	154.8	154.6	178.9	390.4	362.6	356.2	338.9
Aug	151.2	151.1	175.3	390.4	362.6	356.2	338.5
Sept	134	133.8	158.1	390.4	362.6	355.8	336.1
Oct	128.5	128.3	152.6	390.4	362.6	355.7	335.3
Nov	101.3	101.1	125.5	390.4	362.6	355.2	330.7
Dec	82.02	81.81	106.2	390.4	362.6	354.7	326.9
	Entropy (kJ/kg-K)						
State Point	1'	1	2	3	4'	4	5
Jan	0.2867	0.2859	0.2859	1.135	1.135	1.117	1.227
Feb	0.3164	0.3156	0.3156	1.135	1.135	1.118	1.22
Mar	0.3592	0.3584	0.3584	1.135	1.135	1.118	1.211
Apr	0.4159	0.4152	0.4152	1.135	1.135	1.119	1.199
May	0.4733	0.4726	0.4726	1.135	1.135	1.12	1.189
June	0.5315	0.5308	0.5308	1.135	1.135	1.121	1.181
July	0.5601	0.5595	0.5595	1.135	1.135	1.122	1.177
Aug	0.5488	0.5482	0.5482	1.135	1.135	1.121	1.179
Sept	0.493	0.4923	0.4923	1.135	1.135	1.121	1.186
Oct	0.4749	0.4742	0.4742	1.135	1.135	1.12	1.189
Nov	0.3838	0.383	0.383	1.135	1.135	1.119	1.206
Dec	0.3165	0.3157	0.3157	1.135	1.135	1.118	1.22

Table B-46: Thermodynamic Properties for Direct Single-Loop System Simulations at 2.5km Depth, CO2 Mass Flow Rate of 90kg/s, and Reservoir Temperature of 150°C (DTE=0.50).

Tres	150°C						
Well Depth	2.5 km						
CO2 Mass Flow	90 kg/s						
	Pressure (kPa)						
State Point	1'	1	2	3	4'	4	5
Jan	2987	2985	26983	25000	14157	13495	2987
Feb	3287	3285	26843	25000	14157	13495	3287
Mar	3750	3748	26642	25000	14157	13494	3750
Apr	4411	4409	26370	25000	14157	13494	4411
May	5118	5116	26060	25000	14157	13493	5118
June	5839	5836	25665	25000	14157	13493	5839
July	6175	6173	25416	25000	14157	13493	6175
Aug	6048	6045	25523	25000	14157	13493	6048
Sept	5363	5361	25938	25000	14157	13493	5363
Oct	5137	5135	26050	25000	14157	13493	5137
Nov	4031	4029	26527	25000	14157	13494	4031
Dec	3288	3286	26842	25000	14157	13495	3288
	Temperature (°C)						
State Point	1'	1	2	3	4'	4	5
Jan	-5.708	-5.73	8.912	150	102.1	95.52	-3.11
Feb	-2.193	-2.214	13.24	150	102.1	95.6	2.274
Mar	2.793	2.773	19.54	150	102.1	95.71	9.924
Apr	9.177	9.159	27.95	150	102.1	95.86	19.73
May	15.25	15.23	36.49	150	102.1	95.99	29.09
June	20.81	20.79	45.08	150	102.1	96.12	37.69
July	23.22	23.2	49.24	150	102.1	96.17	41.43
Aug	22.32	22.3	47.61	150	102.1	96.15	40.03
Sept	17.21	17.19	39.41	150	102.1	96.04	32.12
Oct	15.41	15.39	36.73	150	102.1	96	29.33
Nov	5.602	5.583	23.19	150	102.1	95.78	14.24
Dec	-2.178	-2.199	13.26	150	102.1	95.6	2.297
	Enthalpy (kJ/kg)						
State Point	1'	1	2	3	4'	4	5
Jan	73.63	73.46	97.73	390.4	360.3	352.9	324.9
Feb	81.94	81.77	106	390.4	360.3	353.1	326.7
Mar	94.15	93.98	118.2	390.4	360.3	353.3	329.1
Apr	110.7	110.6	134.8	390.4	360.3	353.6	332.1
May	128	127.8	152	390.4	360.3	353.9	334.8
June	145.8	145.7	169.8	390.4	360.3	354.2	337.4
July	154.7	154.6	178.7	390.4	360.3	354.3	338.5
Aug	151.2	151.1	175.2	390.4	360.3	354.2	338.1
Sept	134	133.8	158	390.4	360.3	354	335.7
Oct	128.4	128.3	152.5	390.4	360.3	353.9	334.9
Nov	101.3	101.1	125.4	390.4	360.3	353.4	330.4
Dec	81.98	81.81	106.1	390.4	360.3	353.1	326.7
	Entropy (kJ/kg-K)						
State Point	1'	1	2	3	4'	4	5
Jan	0.2865	0.2859	0.2859	1.135	1.135	1.121	1.226
Feb	0.3162	0.3156	0.3156	1.135	1.135	1.122	1.219
Mar	0.359	0.3584	0.3584	1.135	1.135	1.123	1.21
Apr	0.4157	0.4152	0.4152	1.135	1.135	1.123	1.198
May	0.4731	0.4726	0.4726	1.135	1.135	1.124	1.188
June	0.5313	0.5308	0.5308	1.135	1.135	1.125	1.179
July	0.56	0.5595	0.5595	1.135	1.135	1.125	1.176
Aug	0.5487	0.5482	0.5482	1.135	1.135	1.125	1.177
Sept	0.4928	0.4923	0.4923	1.135	1.135	1.124	1.185
Oct	0.4747	0.4742	0.4742	1.135	1.135	1.124	1.188
Nov	0.3836	0.383	0.383	1.135	1.135	1.123	1.205
Dec	0.3163	0.3157	0.3157	1.135	1.135	1.122	1.219

Table B-47: Thermodynamic Properties for Direct Single-Loop System Simulations at 2.5km Depth, CO₂

Mass Flow Rate of 120kg/s, and Reservoir Temperature of 150°C (DTE=0.50).

Tres	150°C						
Well Depth	2.5 km						
CO₂ Mass Flow	120 kg/s						
	Pressure (kPa)						
State Point	1'	1	2	3	4'	4	5
Jan	2986	2985	27055	25000	14987	14645	2986
Feb	3286	3285	26917	25000	14987	14645	3286
Mar	3749	3748	26719	25000	14987	14645	3749
Apr	4410	4409	26450	25000	14987	14645	4410
May	5117	5116	26144	25000	14987	14645	5117
June	5838	5836	25755	25000	14987	14644	5838
July	6174	6173	25509	25000	14987	14644	6174
Aug	6047	6045	25615	25000	14987	14644	6047
Sept	5363	5361	26024	25000	14987	14645	5363
Oct	5137	5135	26135	25000	14987	14645	5137
Nov	4030	4029	26605	25000	14987	14645	4030
Dec	3288	3286	26916	25000	14987	14645	3288
	Temperature (°C)						
State Point	1'	1	2	3	4'	4	5
Jan	-5.715	-5.73	8.95	150	106.8	102.4	-1.746
Feb	-2.2	-2.214	13.28	150	106.8	102.5	3.596
Mar	2.786	2.773	19.59	150	106.8	102.6	11.19
Apr	9.171	9.159	28.01	150	106.8	102.7	20.93
May	15.24	15.23	36.56	150	106.8	102.9	30.23
June	20.8	20.79	45.16	150	106.8	103	38.79
July	23.21	23.2	49.34	150	106.8	103	42.51
Aug	22.31	22.3	47.7	150	106.8	103	41.12
Sept	17.2	17.19	39.48	150	106.8	102.9	33.24
Oct	15.4	15.39	36.8	150	106.8	102.9	30.48
Nov	5.596	5.583	23.24	150	106.8	102.7	15.7
Dec	-2.185	-2.199	13.31	150	106.8	102.5	3.619
	Enthalpy (kJ/kg)						
State Point	1'	1	2	3	4'	4	5
Jan	73.61	73.46	97.81	390.4	363	356.9	327
Feb	81.92	81.77	106.1	390.4	363	357.1	328.7
Mar	94.13	93.98	118.3	390.4	363	357.3	331.1
Apr	110.7	110.6	134.9	390.4	363	357.6	334.1
May	127.9	127.8	152.1	390.4	363	357.8	336.9
June	145.8	145.7	169.9	390.4	363	358.1	339.4
July	154.7	154.6	178.8	390.4	363	358.2	340.5
Aug	151.2	151.1	175.3	390.4	363	358.1	340.1
Sept	133.9	133.8	158.1	390.4	363	357.9	337.8
Oct	128.4	128.3	152.6	390.4	363	357.8	336.9
Nov	101.3	101.1	125.5	390.4	363	357.4	332.8
Dec	81.96	81.81	106.2	390.4	363	357.1	328.8
	Entropy (kJ/kg-K)						
State Point	1'	1	2	3	4'	4	5
Jan	0.2865	0.2859	0.2859	1.135	1.135	1.122	1.234
Feb	0.3161	0.3156	0.3156	1.135	1.135	1.123	1.227
Mar	0.3589	0.3584	0.3584	1.135	1.135	1.123	1.217
Apr	0.4157	0.4152	0.4152	1.135	1.135	1.124	1.205
May	0.4731	0.4726	0.4726	1.135	1.135	1.125	1.195
June	0.5313	0.5308	0.5308	1.135	1.135	1.125	1.186
July	0.5599	0.5595	0.5595	1.135	1.135	1.125	1.182
Aug	0.5483	0.5482	0.5482	1.135	1.135	1.125	1.184
Sept	0.4928	0.4923	0.4923	1.135	1.135	1.125	1.192
Oct	0.4747	0.4742	0.4742	1.135	1.135	1.125	1.195
Nov	0.3836	0.383	0.383	1.135	1.135	1.123	1.213
Dec	0.3163	0.3157	0.3157	1.135	1.135	1.123	1.227

Table B-48: Thermodynamic Properties for Direct Single-Loop System Simulations at 2.5km Depth, CO₂

Mass Flow Rate of 140kg/s, and Reservoir Temperature of 150°C (DTE=0.50).

Tres	150°C						
Well Depth	2.5 km						
CO₂ Mass Flow	140 kg/s						
	Pressure (kPa)						
State Point	1'	1	2	3	4'	4	5
Jan	2987	2985	27000	25000	14640	14167	2987
Feb	3287	3285	26860	25000	14640	14167	3287
Mar	3750	3748	26661	25000	14640	14166	3750
Apr	4411	4409	26389	25000	14640	14166	4411
May	5117	5116	26080	25000	14640	14166	5117
June	5838	5836	25687	25000	14640	14166	5838
July	6175	6173	25438	25000	14640	14166	6175
Aug	6047	6045	25545	25000	14640	14166	6047
Sept	5363	5361	25959	25000	14640	14166	5363
Oct	5137	5135	26070	25000	14640	14166	5137
Nov	4031	4029	26545	25000	14640	14166	4031
Dec	3288	3286	26859	25000	14640	14167	3288
	Temperature (°C)						
State Point	1'	1	2	3	4'	4	5
Jan	-5.71	-5.73	8.921	150	104.9	100	-1.817
Feb	-2.195	-2.214	13.25	150	104.9	100.1	3.518
Mar	2.791	2.773	19.55	150	104.9	100.2	11.1
Apr	9.176	9.159	27.97	150	104.9	100.3	20.83
May	15.25	15.23	36.51	150	104.9	100.4	30.12
June	20.81	20.79	45.1	150	104.9	100.5	38.67
July	23.22	23.2	49.27	150	104.9	100.6	42.39
Aug	22.32	22.3	47.64	150	104.9	100.5	41
Sept	17.21	17.19	39.43	150	104.9	100.5	33.13
Oct	15.41	15.39	36.74	150	104.9	100.4	30.36
Nov	5.601	5.583	23.2	150	104.9	100.2	15.38
Dec	-2.18	-2.199	13.27	150	104.9	100.1	3.541
	Enthalpy (kJ/kg)						
State Point	1'	1	2	3	4'	4	5
Jan	73.59	73.46	97.75	390.4	361.9	356.2	326.9
Feb	81.9	81.77	106.1	390.4	361.9	356.3	328.6
Mar	94.11	93.98	118.3	390.4	361.9	356.5	331
Apr	110.7	110.6	134.8	390.4	361.9	356.7	333.9
May	127.9	127.8	152	390.4	361.9	356.9	336.7
June	145.8	145.7	169.9	390.4	361.9	357.1	339.2
July	154.7	154.6	178.7	390.4	361.9	357.2	340.3
Aug	151.2	151.1	175.2	390.4	361.9	357.2	339.9
Sept	133.9	133.8	158	390.4	361.9	357	337.5
Oct	128.4	128.3	152.5	390.4	361.9	356.9	336.7
Nov	101.3	101.1	125.4	390.4	361.9	356.6	332.3
Dec	81.94	81.81	106.1	390.4	361.9	356.3	328.6
	Entropy (kJ/kg-K)						
State Point	1'	1	2	3	4'	4	5
Jan	0.2864	0.2859	0.2859	1.135	1.135	1.124	1.233
Feb	0.316	0.3156	0.3156	1.135	1.135	1.125	1.226
Mar	0.3589	0.3584	0.3584	1.135	1.135	1.125	1.217
Apr	0.4156	0.4152	0.4152	1.135	1.135	1.126	1.205
May	0.473	0.4726	0.4726	1.135	1.135	1.126	1.194
June	0.5312	0.5308	0.5308	1.135	1.135	1.127	1.185
July	0.5599	0.5595	0.5595	1.135	1.135	1.127	1.181
Aug	0.5484	0.5482	0.5482	1.135	1.135	1.127	1.183
Sept	0.4927	0.4923	0.4923	1.135	1.135	1.126	1.191
Oct	0.4746	0.4742	0.4742	1.135	1.135	1.126	1.194
Nov	0.3835	0.383	0.383	1.135	1.135	1.125	1.211
Dec	0.3162	0.3157	0.3157	1.135	1.135	1.125	1.226

Table B-49: Thermodynamic Properties for Direct Single-Loop System Simulations at 3.1km Depth, CO2 Mass Flow Rate of 70kg/s, and Reservoir Temperature of 100°C (DTE=0.50).

Tres	100°C						
Well Depth	3.1 km						
CO2 Mass Flow	70 kg/s						
Pressure (kPa)							
State Point	1'	1	2	3	4'	4	5
Jan	2986	2985	33030	30000	11189	10946	2986
Feb	3286	3285	32796	30000	11189	10946	3286
Mar	3749	3748	32456	30000	11189	10945	3749
Apr	4410	4409	31989	30000	11189	10945	4410
May	5117	5116	31471	30000	11189	10945	5117
June	5838	5836	30853	30000	11189	10944	5838
July	6174	6173	30488	30000	11189	10944	6174
Aug	6047	6045	30641	30000	11189	10944	6047
Sept	5362	5361	31275	30000	11189	10945	5362
Oct	5137	5135	31455	30000	11189	10945	5137
Nov	4030	4029	32257	30000	11189	10945	4030
Dec	3288	3286	32794	30000	11189	10946	3288
Temperature (°C)							
State Point	1'	1	2	3	4'	4	5
Jan	-5.717	-5.73	11.98	100	51.67	49.98	-5.717
Feb	-2.201	-2.214	16.45	100	51.67	50.02	-2.201
Mar	2.785	2.773	22.96	100	51.67	50.07	2.785
Apr	9.17	9.159	31.7	100	51.67	50.13	9.17
May	15.24	15.23	40.6	100	51.67	50.19	15.24
June	20.8	20.79	49.63	100	51.67	50.24	20.8
July	23.21	23.2	54.03	100	51.67	50.26	23.21
Aug	22.31	22.3	52.3	100	51.67	50.25	22.31
Sept	17.2	17.19	43.66	100	51.67	50.2	17.2
Oct	15.4	15.39	40.85	100	51.67	50.19	15.4
Nov	5.595	5.583	26.74	100	51.67	50.09	5.595
Dec	-2.186	-2.199	16.47	100	51.67	50.02	-2.186
Enthalpy (kJ/kg)							
State Point	1'	1	2	3	4'	4	5
Jan	73.68	73.46	103.7	278.9	246.9	242.7	229.4
Feb	81.98	81.77	112	278.9	246.9	242.9	230.6
Mar	94.19	93.98	124.2	278.9	246.9	243.2	232.4
Apr	110.8	110.6	140.8	278.9	246.9	243.6	234.5
May	128	127.8	158	278.9	246.9	244	236.4
June	145.8	145.7	175.8	278.9	246.9	244.3	238.1
July	154.8	154.6	184.7	278.9	246.9	244.4	238.8
Aug	151.2	151.1	181.2	278.9	246.9	244.4	238.5
Sept	134	133.8	164	278.9	246.9	244.1	237
Oct	128.5	128.3	158.4	278.9	246.9	244	236.5
Nov	101.3	101.1	131.3	278.9	246.9	243.4	233.3
Dec	82.02	81.81	112	278.9	246.9	242.9	230.7
Entropy (kJ/kg-K)							
State Point	1'	1	2	3	4'	4	5
Jan	0.2867	0.2859	0.2859	0.8306	0.8306	0.8191	0.8689
Feb	0.3164	0.3156	0.3156	0.8306	0.8306	0.8198	0.8651
Mar	0.3592	0.3584	0.3584	0.8306	0.8306	0.8207	0.86
Apr	0.4159	0.4152	0.4152	0.8306	0.8306	0.8219	0.8541
May	0.4733	0.4726	0.4726	0.8306	0.8306	0.8231	0.8492
June	0.5315	0.5308	0.5308	0.8306	0.8306	0.8241	0.8452
July	0.5601	0.5595	0.5595	0.8306	0.8306	0.8246	0.8437
Aug	0.5488	0.5482	0.5482	0.8306	0.8306	0.8244	0.8442
Sept	0.493	0.4923	0.4923	0.8306	0.8306	0.8234	0.8478
Oct	0.4749	0.4742	0.4742	0.8306	0.8306	0.8231	0.8491
Nov	0.3838	0.383	0.3831	0.8306	0.8306	0.8213	0.8573
Dec	0.3165	0.3157	0.3157	0.8306	0.8306	0.8198	0.865

Table B-50: Thermodynamic Properties for Direct Single-Loop System Simulations at 3.1km Depth, CO2 Mass Flow Rate of 90kg/s, and Reservoir Temperature of 100°C (DTE=0.50).

Tres	100°C						
Well Depth	3.1 km						
CO2 Mass Flow	90 kg/s						
	Pressure (kPa)						
State Point	1'	1	2	3	4'	4	5
Jan	2987	2985	32919	30000	10669	10257	2987
Feb	3287	3285	32683	30000	10669	10257	3287
Mar	3750	3748	32339	30000	10669	10256	3750
Apr	4411	4409	31867	30000	10669	10256	4411
May	5118	5116	31343	30000	10669	10255	5118
June	5839	5836	30716	30000	10669	10255	5839
July	6175	6173	30347	30000	10669	10255	6175
Aug	6048	6045	30502	30000	10669	10255	6048
Sept	5363	5361	31144	30000	10669	10255	5363
Oct	5137	5135	31327	30000	10669	10255	5137
Nov	4031	4029	32138	30000	10669	10256	4031
Dec	3288	3286	32682	30000	10669	10257	3288
	Temperature (°C)						
State Point	1'	1	2	3	4'	4	5
Jan	-5.708	-5.73	11.92	100	49.33	47.01	-5.708
Feb	-2.193	-2.214	16.39	100	49.33	47.03	-2.193
Mar	2.793	2.773	22.9	100	49.33	47.06	2.793
Apr	9.177	9.159	31.62	100	49.33	47.1	9.177
May	15.25	15.23	40.51	100	49.33	47.14	15.25
June	20.81	20.79	49.51	100	49.33	47.17	20.81
July	23.22	23.2	53.9	100	49.33	47.18	23.22
Aug	22.32	22.3	52.18	100	49.33	47.18	22.32
Sept	17.21	17.19	43.56	100	49.33	47.15	17.21
Oct	15.41	15.39	40.76	100	49.33	47.14	15.41
Nov	5.602	5.583	26.67	100	49.33	47.08	5.602
Dec	-2.178	-2.199	16.41	100	49.33	47.03	-2.178
	Enthalpy (kJ/kg)						
State Point	1'	1	2	3	4'	4	5
Jan	73.63	73.46	103.6	278.9	245.8	242.2	229.5
Feb	81.94	81.77	111.9	278.9	245.8	242.4	230.8
Mar	94.15	93.98	124.1	278.9	245.8	242.6	232.4
Apr	110.7	110.6	140.6	278.9	245.8	242.9	234.5
May	128	127.8	157.8	278.9	245.8	243.2	236.3
June	145.8	145.7	175.6	278.9	245.8	243.5	237.9
July	154.7	154.6	184.5	278.9	245.8	243.6	238.6
Aug	151.2	151.1	181	278.9	245.8	243.5	238.4
Sept	134	133.8	163.8	278.9	245.8	243.3	236.9
Oct	128.4	128.3	158.3	278.9	245.8	243.2	236.4
Nov	101.3	101.1	131.2	278.9	245.8	242.7	233.4
Dec	81.98	81.81	111.9	278.9	245.8	242.4	230.8
	Entropy (kJ/kg-K)						
State Point	1'	1	2	3	4'	4	5
Jan	0.2865	0.2859	0.2859	0.8306	0.8306	0.822	0.8694
Feb	0.3162	0.3156	0.3156	0.8306	0.8306	0.8225	0.8654
Mar	0.359	0.3584	0.3584	0.8306	0.8306	0.8233	0.8602
Apr	0.4157	0.4152	0.4152	0.8306	0.8306	0.8242	0.8541
May	0.4731	0.4726	0.4726	0.8306	0.8306	0.8251	0.8489
June	0.5313	0.5308	0.5308	0.8306	0.8306	0.8259	0.8447
July	0.56	0.5595	0.5595	0.8306	0.8306	0.8263	0.843
Aug	0.5487	0.5482	0.5482	0.8306	0.8306	0.8261	0.8436
Sept	0.4928	0.4923	0.4923	0.8306	0.8306	0.8254	0.8474
Oct	0.4747	0.4742	0.4742	0.8306	0.8306	0.8251	0.8488
Nov	0.3836	0.383	0.3831	0.8306	0.8306	0.8237	0.8574
Dec	0.3163	0.3157	0.3157	0.8306	0.8306	0.8225	0.8654

Table B-51: Thermodynamic Properties for Direct Single-Loop System Simulations at 3.1km Depth, CO2 Mass Flow Rate of 120kg/s, and Reservoir Temperature of 100°C (DTE=0.50).

Tres	100°C						
Well Depth	3.1 km						
CO2 Mass Flow	120 kg/s						
Pressure (kPa)							
State Point	1'	1	2	3	4'	4	5
Jan	2986	2985	33009	30000	11276	11060	2986
Feb	3286	3285	32775	30000	11276	11060	3286
Mar	3749	3748	32434	30000	11276	11060	3749
Apr	4410	4409	31966	30000	11276	11060	4410
May	5117	5116	31447	30000	11276	11059	5117
June	5838	5836	30827	30000	11276	11059	5838
July	6174	6173	30462	30000	11276	11059	6174
Aug	6047	6045	30615	30000	11276	11059	6047
Sept	5363	5361	31251	30000	11276	11059	5363
Oct	5137	5135	31431	30000	11276	11059	5137
Nov	4030	4029	32235	30000	11276	11060	4030
Dec	3288	3286	32773	30000	11276	11060	3288
Temperature (°C)							
State Point	1'	1	2	3	4'	4	5
Jan	-5.715	-5.73	11.97	100	52.05	50.65	-5.715
Feb	-2.2	-2.214	16.44	100	52.05	50.68	-2.2
Mar	2.786	2.773	22.95	100	52.05	50.71	2.786
Apr	9.171	9.159	31.68	100	52.05	50.76	9.171
May	15.24	15.23	40.59	100	52.05	50.8	15.24
June	20.8	20.79	49.61	100	52.05	50.84	20.8
July	23.21	23.2	54	100	52.05	50.86	23.21
Aug	22.31	22.3	52.28	100	52.05	50.85	22.31
Sept	17.2	17.19	43.65	100	52.05	50.82	17.2
Oct	15.4	15.39	40.83	100	52.05	50.8	15.4
Nov	5.596	5.583	26.73	100	52.05	50.73	5.596
Dec	-2.185	-2.199	16.46	100	52.05	50.68	-2.185
Enthalpy (kJ/kg)							
State Point	1'	1	2	3	4'	4	5
Jan	73.61	73.46	103.7	278.9	247.1	244	230.5
Feb	81.92	81.77	112	278.9	247.1	244.1	231.7
Mar	94.13	93.98	124.2	278.9	247.1	244.3	233.3
Apr	110.7	110.6	140.7	278.9	247.1	244.6	235.4
May	127.9	127.8	157.9	278.9	247.1	244.9	237.2
June	145.8	145.7	175.8	278.9	247.1	245.1	238.8
July	154.7	154.6	184.7	278.9	247.1	245.2	239.4
Aug	151.2	151.1	181.2	278.9	247.1	245.2	239.2
Sept	133.9	133.8	163.9	278.9	247.1	245	237.8
Oct	128.4	128.3	158.4	278.9	247.1	244.9	237.2
Nov	101.3	101.1	131.3	278.9	247.1	244.5	234.2
Dec	81.96	81.81	112	278.9	247.1	244.1	231.7
Entropy (kJ/kg-K)							
State Point	1'	1	2	3	4'	4	5
Jan	0.2865	0.2859	0.2859	0.8306	0.8306	0.8224	0.8729
Feb	0.3161	0.3156	0.3156	0.8306	0.8306	0.8229	0.8688
Mar	0.3589	0.3584	0.3584	0.8306	0.8306	0.8235	0.8634
Apr	0.4157	0.4152	0.4152	0.8306	0.8306	0.8244	0.8572
May	0.4731	0.4726	0.4726	0.8306	0.8306	0.8252	0.8519
June	0.5313	0.5308	0.5308	0.8306	0.8306	0.8259	0.8476
July	0.5599	0.5595	0.5595	0.8306	0.8306	0.8262	0.8458
Aug	0.5483	0.5482	0.5482	0.8306	0.8306	0.8261	0.8465
Sept	0.4928	0.4923	0.4923	0.8306	0.8306	0.8254	0.8503
Oct	0.4747	0.4742	0.4742	0.8306	0.8306	0.8252	0.8518
Nov	0.3836	0.383	0.3831	0.8306	0.8306	0.8239	0.8606
Dec	0.3163	0.3157	0.3157	0.8306	0.8306	0.8229	0.8688

Table B-52: Thermodynamic Properties for Direct Single-Loop System Simulations at 3.1km Depth, CO2 Mass Flow Rate of 140kg/s, and Reservoir Temperature of 100°C (DTE=0.50).

Tres	100°C						
Well Depth	3.1 km						
CO2 Mass Flow	140 kg/s						
	Pressure (kPa)						
State Point	1'	1	2	3	4'	4	5
Jan	2987	2985	32941	30000	11022	10724	2987
Feb	3287	3285	32705	30000	11022	10724	3287
Mar	3750	3748	32362	30000	11022	10723	3750
Apr	4411	4409	31891	30000	11022	10723	4411
May	5117	5116	31368	30000	11022	10723	5117
June	5838	5836	30743	30000	11022	10723	5838
July	6175	6173	30374	30000	11022	10723	6175
Aug	6047	6045	30529	30000	11022	10723	6047
Sept	5363	5361	31170	30000	11022	10723	5363
Oct	5137	5135	31352	30000	11022	10723	5137
Nov	4031	4029	32161	30000	11022	10723	4031
Dec	3288	3286	32704	30000	11022	10724	3288
	Temperature (°C)						
State Point	1'	1	2	3	4'	4	5
Jan	-5.71	-5.73	11.93	100	50.93	49.23	-5.71
Feb	-2.195	-2.214	16.4	100	50.93	49.25	-2.195
Mar	2.791	2.773	22.91	100	50.93	49.28	2.791
Apr	9.176	9.159	31.63	100	50.93	49.32	9.176
May	15.25	15.23	40.53	100	50.93	49.35	15.25
June	20.81	20.79	49.53	100	50.93	49.38	20.81
July	23.22	23.2	53.92	100	50.93	49.4	23.22
Aug	22.32	22.3	52.2	100	50.93	49.39	22.32
Sept	17.21	17.19	43.58	100	50.93	49.36	17.21
Oct	15.41	15.39	40.78	100	50.93	49.35	15.41
Nov	5.601	5.583	26.68	100	50.93	49.3	5.601
Dec	-2.18	-2.199	16.42	100	50.93	49.25	-2.18
	Enthalpy (kJ/kg)						
State Point	1'	1	2	3	4'	4	5
Jan	73.59	73.46	103.6	278.9	246.6	243.7	230.5
Feb	81.9	81.77	111.9	278.9	246.6	243.8	231.7
Mar	94.11	93.98	124.1	278.9	246.6	244	233.3
Apr	110.7	110.6	140.6	278.9	246.6	244.3	235.3
May	127.9	127.8	157.8	278.9	246.6	244.5	237.1
June	145.8	145.7	175.7	278.9	246.6	244.7	238.7
July	154.7	154.6	184.6	278.9	246.6	244.8	239.3
Aug	151.2	151.1	181.1	278.9	246.6	244.8	239.1
Sept	133.9	133.8	163.8	278.9	246.6	244.6	237.7
Oct	128.4	128.3	158.3	278.9	246.6	244.5	237.2
Nov	101.3	101.1	131.2	278.9	246.6	244.1	234.2
Dec	81.94	81.81	111.9	278.9	246.6	243.8	231.7
	Entropy (kJ/kg-K)						
State Point	1'	1	2	3	4'	4	5
Jan	0.2864	0.2859	0.2859	0.8306	0.8306	0.8237	0.8731
Feb	0.316	0.3156	0.3156	0.8306	0.8306	0.8241	0.8689
Mar	0.3589	0.3584	0.3584	0.8306	0.8306	0.8247	0.8634
Apr	0.4156	0.4152	0.4152	0.8306	0.8306	0.8254	0.8571
May	0.473	0.4726	0.4726	0.8306	0.8306	0.8261	0.8517
June	0.5312	0.5308	0.5308	0.8306	0.8306	0.8267	0.8472
July	0.5599	0.5595	0.5595	0.8306	0.8306	0.827	0.8454
Aug	0.5484	0.5482	0.5482	0.8306	0.8306	0.8269	0.8461
Sept	0.4927	0.4923	0.4923	0.8306	0.8306	0.8263	0.85
Oct	0.4746	0.4742	0.4742	0.8306	0.8306	0.8261	0.8515
Nov	0.3835	0.383	0.3831	0.8306	0.8306	0.825	0.8605
Dec	0.3162	0.3157	0.3157	0.8306	0.8306	0.8241	0.8689

Table B-53: Thermodynamic Properties for Direct Single-Loop System Simulations at 3.1km Depth, CO2 Mass Flow Rate of 70kg/s, and Reservoir Temperature of 125°C (DTE=0.50).

Tres	125°C						
Well Depth	3.1 km						
CO2 Mass Flow	70 kg/s						
	Pressure (kPa)						
State Point	1'	1	2	3	4'	4	5
Jan	2986	2985	33030	30000	13797	13508	2986
Feb	3286	3285	32796	30000	13797	13508	3286
Mar	3749	3748	32456	30000	13797	13508	3749
Apr	4410	4409	31989	30000	13797	13507	4410
May	5117	5116	31471	30000	13797	13507	5117
June	5838	5836	30853	30000	13797	13507	5838
July	6174	6173	30488	30000	13797	13507	6174
Aug	6047	6045	30641	30000	13797	13507	6047
Sept	5362	5361	31275	30000	13797	13507	5362
Oct	5137	5135	31455	30000	13797	13507	5137
Nov	4030	4029	32257	30000	13797	13508	4030
Dec	3288	3286	32794	30000	13797	13508	3288
	Temperature (°C)						
State Point	1'	1	2	3	4'	4	5
Jan	-5.717	-5.73	11.98	125	74.18	71.25	-5.717
Feb	-2.201	-2.214	16.45	125	74.18	71.31	-2.201
Mar	2.785	2.773	22.96	125	74.18	71.4	2.785
Apr	9.17	9.159	31.7	125	74.18	71.52	9.17
May	15.24	15.23	40.6	125	74.18	71.63	15.24
June	20.8	20.79	49.63	125	74.18	71.73	20.8
July	23.21	23.2	54.03	125	74.18	71.77	23.21
Aug	22.31	22.3	52.3	125	74.18	71.76	22.31
Sept	17.2	17.19	43.66	125	74.18	71.66	17.2
Oct	15.4	15.39	40.85	125	74.18	71.63	15.4
Nov	5.595	5.583	26.74	125	74.18	71.45	5.595
Dec	-2.186	-2.199	16.47	125	74.18	71.31	-2.186
	Enthalpy (kJ/kg)						
State Point	1'	1	2	3	4'	4	5
Jan	73.68	73.46	103.7	328.8	296.2	290.4	270.1
Feb	81.98	81.77	112	328.8	296.2	290.6	271.6
Mar	94.19	93.98	124.2	328.8	296.2	290.9	273.7
Apr	110.8	110.6	140.8	328.8	296.2	291.3	276.2
May	128	127.8	158	328.8	296.2	291.7	278.5
June	145.8	145.7	175.8	328.8	296.2	292	280.5
July	154.8	154.6	184.7	328.8	296.2	292.2	281.3
Aug	151.2	151.1	181.2	328.8	296.2	292.1	281
Sept	134	133.8	164	328.8	296.2	291.8	279.2
Oct	128.5	128.3	158.4	328.8	296.2	291.7	278.5
Nov	101.3	101.1	131.3	328.8	296.2	291.1	274.8
Dec	82.02	81.81	112	328.8	296.2	290.6	271.6
	Entropy (kJ/kg-K)						
State Point	1'	1	2	3	4'	4	5
Jan	0.2867	0.2859	0.2859	0.96	0.9601	0.9455	1.021
Feb	0.3164	0.3156	0.3156	0.96	0.9601	0.9461	1.016
Mar	0.3592	0.3584	0.3584	0.96	0.9601	0.947	1.01
Apr	0.4159	0.4152	0.4152	0.96	0.9601	0.9481	1.002
May	0.4733	0.4726	0.4726	0.96	0.9601	0.9491	0.995
June	0.5315	0.5308	0.5308	0.96	0.9601	0.9501	0.9894
July	0.5601	0.5595	0.5595	0.96	0.9601	0.9505	0.9871
Aug	0.5488	0.5482	0.5482	0.96	0.9601	0.9504	0.988
Sept	0.493	0.4923	0.4923	0.96	0.9601	0.9495	0.993
Oct	0.4749	0.4742	0.4742	0.96	0.9601	0.9492	0.9948
Nov	0.3838	0.383	0.3831	0.96	0.9601	0.9475	1.006
Dec	0.3165	0.3157	0.3157	0.96	0.9601	0.9461	1.016

Table B-54: Thermodynamic Properties for Direct Single-Loop System Simulations at 3.1km Depth, CO2 Mass Flow Rate of 90kg/s, and Reservoir Temperature of 125°C (DTE=0.50).

Tres	125°C						
Well Depth	3.1 km						
CO2 Mass Flow	90 kg/s						
Pressure (kPa)							
State Point	1'	1	2	3	4'	4	5
Jan	2987	2985	32919	30000	13175	12683	2987
Feb	3287	3285	32683	30000	13175	12683	3287
Mar	3750	3748	32339	30000	13175	12683	3750
Apr	4411	4409	31867	30000	13175	12682	4411
May	5118	5116	31343	30000	13175	12682	5118
June	5839	5836	30716	30000	13175	12681	5839
July	6175	6173	30347	30000	13175	12681	6175
Aug	6048	6045	30502	30000	13175	12681	6048
Sept	5363	5361	31144	30000	13175	12682	5363
Oct	5137	5135	31327	30000	13175	12682	5137
Nov	4031	4029	32138	30000	13175	12683	4031
Dec	3288	3286	32682	30000	13175	12683	3288
Temperature (°C)							
State Point	1'	1	2	3	4'	4	5
Jan	-5.708	-5.73	11.92	125	71.14	67.55	-5.708
Feb	-2.193	-2.214	16.39	125	71.14	67.6	-2.193
Mar	2.793	2.773	22.9	125	71.14	67.66	2.793
Apr	9.177	9.159	31.62	125	71.14	67.75	9.177
May	15.25	15.23	40.51	125	71.14	67.82	15.25
June	20.81	20.79	49.51	125	71.14	67.9	20.81
July	23.22	23.2	53.9	125	71.14	67.93	23.22
Aug	22.32	22.3	52.18	125	71.14	67.92	22.32
Sept	17.21	17.19	43.56	125	71.14	67.85	17.21
Oct	15.41	15.39	40.76	125	71.14	67.83	15.41
Nov	5.602	5.583	26.67	125	71.14	67.7	5.602
Dec	-2.178	-2.199	16.41	125	71.14	67.6	-2.178
Enthalpy (kJ/kg)							
State Point	1'	1	2	3	4'	4	5
Jan	73.63	73.46	103.6	328.8	294.6	289.6	270.2
Feb	81.94	81.77	111.9	328.8	294.6	289.8	271.7
Mar	94.15	93.98	124.1	328.8	294.6	290	273.7
Apr	110.7	110.6	140.6	328.8	294.6	290.3	276.1
May	128	127.8	157.8	328.8	294.6	290.6	278.3
June	145.8	145.7	175.6	328.8	294.6	290.9	280.3
July	154.7	154.6	184.5	328.8	294.6	291	281.1
Aug	151.2	151.1	181	328.8	294.6	291	280.8
Sept	134	133.8	163.8	328.8	294.6	290.7	279
Oct	128.4	128.3	158.3	328.8	294.6	290.6	278.4
Nov	101.3	101.1	131.2	328.8	294.6	290.2	274.8
Dec	81.98	81.81	111.9	328.8	294.6	289.8	271.7
Entropy (kJ/kg-K)							
State Point	1'	1	2	3	4'	4	5
Jan	0.2865	0.2859	0.2859	0.96	0.9601	0.9491	1.022
Feb	0.3162	0.3156	0.3156	0.96	0.9601	0.9496	1.016
Mar	0.359	0.3584	0.3584	0.96	0.9601	0.9502	1.01
Apr	0.4157	0.4152	0.4152	0.96	0.9601	0.9511	1.002
May	0.4731	0.4726	0.4726	0.96	0.9601	0.952	0.9946
June	0.5313	0.5308	0.5308	0.96	0.9601	0.9527	0.9888
July	0.56	0.5595	0.5595	0.96	0.9601	0.9531	0.9864
Aug	0.5487	0.5482	0.5482	0.96	0.9601	0.9529	0.9873
Sept	0.4928	0.4923	0.4923	0.96	0.9601	0.9522	0.9925
Oct	0.4747	0.4742	0.4742	0.96	0.9601	0.952	0.9944
Nov	0.3836	0.383	0.3831	0.96	0.9601	0.9506	1.006
Dec	0.3163	0.3157	0.3157	0.96	0.9601	0.9496	1.016

Table B-55: Thermodynamic Properties for Direct Single-Loop System Simulations at 3.1km Depth, CO2 Mass Flow Rate of 120kg/s, and Reservoir Temperature of 125°C (DTE=0.50).

Tres	125°C						
Well Depth	3.1 km						
CO2 Mass Flow	120 kg/s						
	Pressure (kPa)						
State Point	1'	1	2	3	4'	4	5
Jan	2986	2985	33009	30000	13901	13644	2986
Feb	3286	3285	32775	30000	13901	13644	3286
Mar	3749	3748	32434	30000	13901	13644	3749
Apr	4410	4409	31966	30000	13901	13644	4410
May	5117	5116	31447	30000	13901	13644	5117
June	5838	5836	30827	30000	13901	13644	5838
July	6174	6173	30462	30000	13901	13644	6174
Aug	6047	6045	30615	30000	13901	13644	6047
Sept	5363	5361	31251	30000	13901	13644	5363
Oct	5137	5135	31431	30000	13901	13644	5137
Nov	4030	4029	32235	30000	13901	13644	4030
Dec	3288	3286	32773	30000	13901	13644	3288
	Temperature (°C)						
State Point	1'	1	2	3	4'	4	5
Jan	-5.715	-5.73	11.97	125	74.68	72.33	-5.715
Feb	-2.2	-2.214	16.44	125	74.68	72.38	-2.2
Mar	2.786	2.773	22.95	125	74.68	72.44	2.786
Apr	9.171	9.159	31.68	125	74.68	72.52	9.171
May	15.24	15.23	40.59	125	74.68	72.6	15.24
June	20.8	20.79	49.61	125	74.68	72.68	20.8
July	23.21	23.2	54	125	74.68	72.71	23.21
Aug	22.31	22.3	52.28	125	74.68	72.7	22.31
Sept	17.2	17.19	43.65	125	74.68	72.63	17.2
Oct	15.4	15.39	40.83	125	74.68	72.61	15.4
Nov	5.596	5.583	26.73	125	74.68	72.48	5.596
Dec	-2.185	-2.199	16.46	125	74.68	72.38	-2.185
	Enthalpy (kJ/kg)						
State Point	1'	1	2	3	4'	4	5
Jan	73.61	73.46	103.7	328.8	296.4	292.2	271.6
Feb	81.92	81.77	112	328.8	296.4	292.3	273
Mar	94.13	93.98	124.2	328.8	296.4	292.5	275
Apr	110.7	110.6	140.7	328.8	296.4	292.8	277.4
May	127.9	127.8	157.9	328.8	296.4	293.1	279.6
June	145.8	145.7	175.8	328.8	296.4	293.3	281.5
July	154.7	154.6	184.7	328.8	296.4	293.4	282.3
Aug	151.2	151.1	181.2	328.8	296.4	293.4	282
Sept	133.9	133.8	163.9	328.8	296.4	293.2	280.3
Oct	128.4	128.3	158.4	328.8	296.4	293.1	279.6
Nov	101.3	101.1	131.3	328.8	296.4	292.7	276
Dec	81.96	81.81	112	328.8	296.4	292.3	273
	Entropy (kJ/kg-K)						
State Point	1'	1	2	3	4'	4	5
Jan	0.2865	0.2859	0.2859	0.96	0.9601	0.9496	1.027
Feb	0.3161	0.3156	0.3156	0.96	0.9601	0.95	1.021
Mar	0.3589	0.3584	0.3584	0.96	0.9601	0.9507	1.014
Apr	0.4157	0.4152	0.4152	0.96	0.9601	0.9515	1.006
May	0.4731	0.4726	0.4726	0.96	0.9601	0.9522	0.9989
June	0.5313	0.5308	0.5308	0.96	0.9601	0.9529	0.993
July	0.5599	0.5595	0.5595	0.96	0.9601	0.9532	0.9906
Aug	0.5483	0.5482	0.5482	0.96	0.9601	0.9531	0.9915
Sept	0.4928	0.4923	0.4923	0.96	0.9601	0.9525	0.9968
Oct	0.4747	0.4742	0.4742	0.96	0.9601	0.9522	0.9988
Nov	0.3836	0.383	0.3831	0.96	0.9601	0.951	1.011
Dec	0.3163	0.3157	0.3157	0.96	0.9601	0.95	1.021

Table B-56: Thermodynamic Properties for Direct Single-Loop System Simulations at 3.1km Depth, CO2 Mass Flow Rate of 140kg/s, and Reservoir Temperature of 125°C (DTE=0.50).

Tres	125°C						
Well Depth	3.1 km						
CO2 Mass Flow	140 kg/s						
	Pressure (kPa)						
State Point	1'	1	2	3	4'	4	5
Jan	2987	2985	32941	30000	13597	13243	2987
Feb	3287	3285	32705	30000	13597	13243	3287
Mar	3750	3748	32362	30000	13597	13242	3750
Apr	4411	4409	31891	30000	13597	13242	4411
May	5117	5116	31368	30000	13597	13242	5117
June	5838	5836	30743	30000	13597	13242	5838
July	6175	6173	30374	30000	13597	13242	6175
Aug	6047	6045	30529	30000	13597	13242	6047
Sept	5363	5361	31170	30000	13597	13242	5363
Oct	5137	5135	31352	30000	13597	13242	5137
Nov	4031	4029	32161	30000	13597	13242	4031
Dec	3288	3286	32704	30000	13597	13243	3288
	Temperature (°C)						
State Point	1'	1	2	3	4'	4	5
Jan	-5.71	-5.73	11.93	125	73.22	70.56	-5.71
Feb	-2.195	-2.214	16.4	125	73.22	70.6	-2.195
Mar	2.791	2.773	22.91	125	73.22	70.66	2.791
Apr	9.176	9.159	31.63	125	73.22	70.73	9.176
May	15.25	15.23	40.53	125	73.22	70.79	15.25
June	20.81	20.79	49.53	125	73.22	70.85	20.81
July	23.22	23.2	53.92	125	73.22	70.88	23.22
Aug	22.32	22.3	52.2	125	73.22	70.87	22.32
Sept	17.21	17.19	43.58	125	73.22	70.81	17.21
Oct	15.41	15.39	40.78	125	73.22	70.79	15.41
Nov	5.601	5.583	26.68	125	73.22	70.69	5.601
Dec	-2.18	-2.199	16.42	125	73.22	70.6	-2.18
	Enthalpy (kJ/kg)						
State Point	1'	1	2	3	4'	4	5
Jan	73.59	73.46	103.6	328.8	295.7	291.8	271.6
Feb	81.9	81.77	111.9	328.8	295.7	291.9	273
Mar	94.11	93.98	124.1	328.8	295.7	292.1	274.9
Apr	110.7	110.6	140.6	328.8	295.7	292.3	277.3
May	127.9	127.8	157.8	328.8	295.7	292.5	279.5
June	145.8	145.7	175.7	328.8	295.7	292.7	281.4
July	154.7	154.6	184.6	328.8	295.7	292.8	282.2
Aug	151.2	151.1	181.1	328.8	295.7	292.8	281.9
Sept	133.9	133.8	163.8	328.8	295.7	292.6	280.2
Oct	128.4	128.3	158.3	328.8	295.7	292.5	279.6
Nov	101.3	101.1	131.2	328.8	295.7	292.2	276
Dec	81.94	81.81	111.9	328.8	295.7	291.9	273
	Entropy (kJ/kg-K)						
State Point	1'	1	2	3	4'	4	5
Jan	0.2864	0.2859	0.2859	0.96	0.9601	0.9512	1.027
Feb	0.316	0.3156	0.3156	0.96	0.9601	0.9516	1.021
Mar	0.3589	0.3584	0.3584	0.96	0.9601	0.9521	1.014
Apr	0.4156	0.4152	0.4152	0.96	0.9601	0.9528	1.006
May	0.473	0.4726	0.4726	0.96	0.9601	0.9535	0.9986
June	0.5312	0.5308	0.5308	0.96	0.9601	0.9541	0.9926
July	0.5599	0.5595	0.5595	0.96	0.9601	0.9543	0.9902
Aug	0.5484	0.5482	0.5482	0.96	0.9601	0.9542	0.9911
Sept	0.4927	0.4923	0.4923	0.96	0.9601	0.9537	0.9965
Oct	0.4746	0.4742	0.4742	0.96	0.9601	0.9535	0.9985
Nov	0.3835	0.383	0.3831	0.96	0.9601	0.9525	1.01
Dec	0.3162	0.3157	0.3157	0.96	0.9601	0.9516	1.021

Table B-57: Thermodynamic Properties for Direct Single-Loop System Simulations at 3.1km Depth, CO2 Mass Flow Rate of 70kg/s, and Reservoir Temperature of 150°C (DTE=0.50).

Tres	150°C						
Well Depth	3.1 km						
CO2 Mass Flow	70 kg/s						
	Pressure (kPa)						
State Point	1'	1	2	3	4'	4	5
Jan	2986	2985	33030	30000	15710	15377	2986
Feb	3286	3285	32796	30000	15710	15377	3286
Mar	3749	3748	32456	30000	15710	15377	3749
Apr	4410	4409	31989	30000	15710	15376	4410
May	5117	5116	31471	30000	15710	15376	5117
June	5838	5836	30853	30000	15710	15376	5838
July	6174	6173	30488	30000	15710	15376	6174
Aug	6047	6045	30641	30000	15710	15376	6047
Sept	5362	5361	31275	30000	15710	15376	5362
Oct	5137	5135	31455	30000	15710	15376	5137
Nov	4030	4029	32257	30000	15710	15377	4030
Dec	3288	3286	32794	30000	15710	15377	3288
	Temperature (°C)						
State Point	1'	1	2	3	4'	4	5
Jan	-5.717	-5.73	11.98	150	99.35	94.78	-5.717
Feb	-2.201	-2.214	16.45	150	99.35	94.88	-2.201
Mar	2.785	2.773	22.96	150	99.35	95.01	2.785
Apr	9.17	9.159	31.7	150	99.35	95.17	10.34
May	15.24	15.23	40.6	150	99.35	95.33	19.93
June	20.8	20.79	49.63	150	99.35	95.48	28.67
July	23.21	23.2	54.03	150	99.35	95.54	32.45
Aug	22.31	22.3	52.3	150	99.35	95.52	31.04
Sept	17.2	17.19	43.66	150	99.35	95.38	23.01
Oct	15.4	15.39	40.85	150	99.35	95.34	20.18
Nov	5.595	5.583	26.74	150	99.35	95.08	5.595
Dec	-2.186	-2.199	16.47	150	99.35	94.88	-2.186
	Enthalpy (kJ/kg)						
State Point	1'	1	2	3	4'	4	5
Jan	73.68	73.46	103.7	375.2	341.8	334.4	306.8
Feb	81.98	81.77	112	375.2	341.8	334.6	308.5
Mar	94.19	93.98	124.2	375.2	341.8	334.9	310.8
Apr	110.8	110.6	140.8	375.2	341.8	335.3	313.7
May	128	127.8	158	375.2	341.8	335.6	316.3
June	145.8	145.7	175.8	375.2	341.8	336	318.6
July	154.8	154.6	184.7	375.2	341.8	336.1	319.6
Aug	151.2	151.1	181.2	375.2	341.8	336.1	319.2
Sept	134	133.8	164	375.2	341.8	335.7	317.1
Oct	128.5	128.3	158.4	375.2	341.8	335.6	316.3
Nov	101.3	101.1	131.3	375.2	341.8	335.1	312.1
Dec	82.02	81.81	112	375.2	341.8	334.6	308.5
	Entropy (kJ/kg-K)						
State Point	1'	1	2	3	4'	4	5
Jan	0.2867	0.2859	0.2859	1.073	1.073	1.056	1.159
Feb	0.3164	0.3156	0.3156	1.073	1.073	1.056	1.152
Mar	0.3592	0.3584	0.3584	1.073	1.073	1.057	1.144
Apr	0.4159	0.4152	0.4152	1.073	1.073	1.058	1.135
May	0.4733	0.4726	0.4726	1.073	1.073	1.059	1.126
June	0.5315	0.5308	0.5308	1.073	1.073	1.06	1.118
July	0.5601	0.5595	0.5595	1.073	1.073	1.06	1.115
Aug	0.5488	0.5482	0.5482	1.073	1.073	1.06	1.116
Sept	0.493	0.4923	0.4923	1.073	1.073	1.059	1.123
Oct	0.4749	0.4742	0.4742	1.073	1.073	1.059	1.126
Nov	0.3838	0.383	0.3831	1.073	1.073	1.057	1.14
Dec	0.3165	0.3157	0.3157	1.073	1.073	1.056	1.152

Table B-58: Thermodynamic Properties for Direct Single-Loop System Simulations at 3.1km Depth, CO2 Mass Flow Rate of 90kg/s, and Reservoir Temperature of 150°C (DTE=0.50).

Tres	150°C						
Well Depth	3.1 km						
CO2 Mass Flow	90 kg/s						
Pressure (kPa)							
State Point	1'	1	2	3	4'	4	5
Jan	2987	2985	32919	30000	14977	14407	2987
Feb	3287	3285	32683	30000	14977	14407	3287
Mar	3750	3748	32339	30000	14977	14407	3750
Apr	4411	4409	31867	30000	14977	14406	4411
May	5118	5116	31343	30000	14977	14406	5118
June	5839	5836	30716	30000	14977	14406	5839
July	6175	6173	30347	30000	14977	14406	6175
Aug	6048	6045	30502	30000	14977	14406	6048
Sept	5363	5361	31144	30000	14977	14406	5363
Oct	5137	5135	31327	30000	14977	14406	5137
Nov	4031	4029	32138	30000	14977	14407	4031
Dec	3288	3286	32682	30000	14977	14407	3288
Temperature (°C)							
State Point	1'	1	2	3	4'	4	5
Jan	-5.708	-5.73	11.92	150	95.61	90.45	-5.708
Feb	-2.193	-2.214	16.39	150	95.61	90.52	-2.193
Mar	2.793	2.773	22.9	150	95.61	90.62	2.793
Apr	9.177	9.159	31.62	150	95.61	90.75	10.29
May	15.25	15.23	40.51	150	95.61	90.87	19.85
June	20.81	20.79	49.51	150	95.61	90.98	28.57
July	23.22	23.2	53.9	150	95.61	91.03	32.35
Aug	22.32	22.3	52.18	150	95.61	91.01	30.94
Sept	17.21	17.19	43.56	150	95.61	90.91	22.93
Oct	15.41	15.39	40.76	150	95.61	90.87	20.1
Nov	5.602	5.583	26.67	150	95.61	90.68	5.602
Dec	-2.178	-2.199	16.41	150	95.61	90.52	-2.178
Enthalpy (kJ/kg)							
State Point	1'	1	2	3	4'	4	5
Jan	73.63	73.46	103.6	375.2	339.7	333.2	306.8
Feb	81.94	81.77	111.9	375.2	339.7	333.4	308.5
Mar	94.15	93.98	124.1	375.2	339.7	333.6	310.7
Apr	110.7	110.6	140.6	375.2	339.7	333.9	313.5
May	128	127.8	157.8	375.2	339.7	334.2	316.1
June	145.8	145.7	175.6	375.2	339.7	334.5	318.3
July	154.7	154.6	184.5	375.2	339.7	334.6	319.3
Aug	151.2	151.1	181	375.2	339.7	334.5	319
Sept	134	133.8	163.8	375.2	339.7	334.3	316.9
Oct	128.4	128.3	158.3	375.2	339.7	334.2	316.1
Nov	101.3	101.1	131.2	375.2	339.7	333.8	312
Dec	81.98	81.81	111.9	375.2	339.7	333.4	308.5
Entropy (kJ/kg-K)							
State Point	1'	1	2	3	4'	4	5
Jan	0.2865	0.2859	0.2859	1.073	1.073	1.06	1.159
Feb	0.3162	0.3156	0.3156	1.073	1.073	1.06	1.152
Mar	0.359	0.3584	0.3584	1.073	1.073	1.061	1.144
Apr	0.4157	0.4152	0.4152	1.073	1.073	1.062	1.134
May	0.4731	0.4726	0.4726	1.073	1.073	1.063	1.125
June	0.5313	0.5308	0.5308	1.073	1.073	1.063	1.117
July	0.56	0.5595	0.5595	1.073	1.073	1.064	1.114
Aug	0.5487	0.5482	0.5482	1.073	1.073	1.064	1.115
Sept	0.4928	0.4923	0.4923	1.073	1.073	1.063	1.122
Oct	0.4747	0.4742	0.4742	1.073	1.073	1.063	1.125
Nov	0.3836	0.383	0.3831	1.073	1.073	1.061	1.139
Dec	0.3163	0.3157	0.3157	1.073	1.073	1.06	1.152

Table B-59: Thermodynamic Properties for Direct Single-Loop System Simulations at 3.1km Depth, CO₂

Mass Flow Rate of 120kg/s, and Reservoir Temperature of 150°C (DTE=0.50).

Tres	150°C						
Well Depth	3.1 km						
CO2 Mass Flow	120 kg/s						
	Pressure (kPa)						
State Point	1'	1	2	3	4'	4	5
Jan	2986	2985	33009	30000	15832	15537	2986
Feb	3286	3285	32775	30000	15832	15537	3286
Mar	3749	3748	32434	30000	15832	15536	3749
Apr	4410	4409	31966	30000	15832	15536	4410
May	5117	5116	31447	30000	15832	15536	5117
June	5838	5836	30827	30000	15832	15536	5838
July	6174	6173	30462	30000	15832	15536	6174
Aug	6047	6045	30615	30000	15832	15536	6047
Sept	5363	5361	31251	30000	15832	15536	5363
Oct	5137	5135	31431	30000	15832	15536	5137
Nov	4030	4029	32235	30000	15832	15536	4030
Dec	3288	3286	32773	30000	15832	15537	3288
	Temperature (°C)						
State Point	1'	1	2	3	4'	4	5
Jan	-5.715	-5.73	11.97	150	99.96	96.39	-5.715
Feb	-2.2	-2.214	16.44	150	99.96	96.45	-2.2
Mar	2.786	2.773	22.95	150	99.96	96.55	2.786
Apr	9.171	9.159	31.68	150	99.96	96.67	11.05
May	15.24	15.23	40.59	150	99.96	96.78	20.58
June	20.8	20.79	49.61	150	99.96	96.89	29.28
July	23.21	23.2	54	150	99.96	96.93	33.05
Aug	22.31	22.3	52.28	150	99.96	96.92	31.64
Sept	17.2	17.19	43.65	150	99.96	96.82	23.65
Oct	15.4	15.39	40.83	150	99.96	96.79	20.83
Nov	5.596	5.583	26.73	150	99.96	96.6	5.596
Dec	-2.185	-2.199	16.46	150	99.96	96.45	-2.185
	Enthalpy (kJ/kg)						
State Point	1'	1	2	3	4'	4	5
Jan	73.61	73.46	103.7	375.2	342.2	336.7	308.6
Feb	81.92	81.77	112	375.2	342.2	336.8	310.3
Mar	94.13	93.98	124.2	375.2	342.2	337	312.5
Apr	110.7	110.6	140.7	375.2	342.2	337.3	315.3
May	127.9	127.8	157.9	375.2	342.2	337.6	317.8
June	145.8	145.7	175.8	375.2	342.2	337.8	320.1
July	154.7	154.6	184.7	375.2	342.2	337.9	321
Aug	151.2	151.1	181.2	375.2	342.2	337.9	320.7
Sept	133.9	133.8	163.9	375.2	342.2	337.6	318.6
Oct	128.4	128.3	158.4	375.2	342.2	337.6	317.9
Nov	101.3	101.1	131.3	375.2	342.2	337.1	313.8
Dec	81.96	81.81	112	375.2	342.2	336.8	310.3
	Entropy (kJ/kg-K)						
State Point	1'	1	2	3	4'	4	5
Jan	0.2865	0.2859	0.2859	1.073	1.073	1.061	1.165
Feb	0.3161	0.3156	0.3156	1.073	1.073	1.061	1.159
Mar	0.3589	0.3584	0.3584	1.073	1.073	1.062	1.15
Apr	0.4157	0.4152	0.4152	1.073	1.073	1.062	1.14
May	0.4731	0.4726	0.4726	1.073	1.073	1.063	1.131
June	0.5313	0.5308	0.5308	1.073	1.073	1.064	1.123
July	0.5599	0.5595	0.5595	1.073	1.073	1.064	1.12
Aug	0.5483	0.5482	0.5482	1.073	1.073	1.064	1.121
Sept	0.4928	0.4923	0.4923	1.073	1.073	1.063	1.128
Oct	0.4747	0.4742	0.4742	1.073	1.073	1.063	1.131
Nov	0.3836	0.383	0.3831	1.073	1.073	1.062	1.146
Dec	0.3163	0.3157	0.3157	1.073	1.073	1.061	1.159

Table B-60: Thermodynamic Properties for Direct Single-Loop System Simulations at 3.1km Depth, CO2 Mass Flow Rate of 140kg/s, and Reservoir Temperature of 150°C (DTE=0.50).

Tres	150°C						
Well Depth	3.1 km						
CO2 Mass Flow	140 kg/s						
	Pressure (kPa)						
State Point	1'	1	2	3	4'	4	5
Jan	2987	2985	32941	30000	15475	15066	2987
Feb	3287	3285	32705	30000	15475	15066	3287
Mar	3750	3748	32362	30000	15475	15065	3750
Apr	4411	4409	31891	30000	15475	15065	4411
May	5117	5116	31368	30000	15475	15065	5117
June	5838	5836	30743	30000	15475	15065	5838
July	6175	6173	30374	30000	15475	15065	6175
Aug	6047	6045	30529	30000	15475	15065	6047
Sept	5363	5361	31170	30000	15475	15065	5363
Oct	5137	5135	31352	30000	15475	15065	5137
Nov	4031	4029	32161	30000	15475	15065	4031
Dec	3288	3286	32704	30000	15475	15066	3288
	Temperature (°C)						
State Point	1'	1	2	3	4'	4	5
Jan	-5.71	-5.73	11.93	150	98.17	94.32	-5.71
Feb	-2.195	-2.214	16.4	150	98.17	94.38	-2.195
Mar	2.791	2.773	22.91	150	98.17	94.46	2.791
Apr	9.176	9.159	31.63	150	98.17	94.56	11.02
May	15.25	15.23	40.53	150	98.17	94.66	20.54
June	20.81	20.79	49.53	150	98.17	94.75	29.22
July	23.22	23.2	53.92	150	98.17	94.79	32.99
Aug	22.32	22.3	52.2	150	98.17	94.77	31.58
Sept	17.21	17.19	43.58	150	98.17	94.69	23.6
Oct	15.41	15.39	40.78	150	98.17	94.66	20.79
Nov	5.601	5.583	26.68	150	98.17	94.5	5.601
Dec	-2.18	-2.199	16.42	150	98.17	94.38	-2.18
	Enthalpy (kJ/kg)						
State Point	1'	1	2	3	4'	4	5
Jan	73.59	73.46	103.6	375.2	341.2	336.1	308.6
Feb	81.9	81.77	111.9	375.2	341.2	336.2	310.2
Mar	94.11	93.98	124.1	375.2	341.2	336.4	312.4
Apr	110.7	110.6	140.6	375.2	341.2	336.6	315.2
May	127.9	127.8	157.8	375.2	341.2	336.8	317.7
June	145.8	145.7	175.7	375.2	341.2	337	319.9
July	154.7	154.6	184.6	375.2	341.2	337.1	320.9
Aug	151.2	151.1	181.1	375.2	341.2	337.1	320.5
Sept	133.9	133.8	163.8	375.2	341.2	336.9	318.5
Oct	128.4	128.3	158.3	375.2	341.2	336.8	317.8
Nov	101.3	101.1	131.2	375.2	341.2	336.5	313.7
Dec	81.94	81.81	111.9	375.2	341.2	336.2	310.2
	Entropy (kJ/kg-K)						
State Point	1'	1	2	3	4'	4	5
Jan	0.2864	0.2859	0.2859	1.073	1.073	1.063	1.165
Feb	0.316	0.3156	0.3156	1.073	1.073	1.063	1.159
Mar	0.3589	0.3584	0.3584	1.073	1.073	1.063	1.15
Apr	0.4156	0.4152	0.4152	1.073	1.073	1.064	1.14
May	0.473	0.4726	0.4726	1.073	1.073	1.065	1.131
June	0.5312	0.5308	0.5308	1.073	1.073	1.065	1.122
July	0.5599	0.5595	0.5595	1.073	1.073	1.065	1.119
Aug	0.5484	0.5482	0.5482	1.073	1.073	1.065	1.12
Sept	0.4927	0.4923	0.4923	1.073	1.073	1.065	1.128
Oct	0.4746	0.4742	0.4742	1.073	1.073	1.065	1.13
Nov	0.3835	0.383	0.3831	1.073	1.073	1.064	1.146
Dec	0.3162	0.3157	0.3157	1.073	1.073	1.063	1.159

Table B-61: Thermodynamic Properties for Direct Single-Loop System Simulations at 3.6km Depth, CO2 Mass Flow Rate of 70kg/s, and Reservoir Temperature of 100°C (DTE=0.50).

Tres	100°C						
Well Depth	3.6 km						
CO2 Mass Flow	70 kg/s						
Pressure (kPa)							
State Point	1'	1	2	3	4'	4	5
Jan	2986	2985	38160	35000	11398	11176	2986
Feb	3286	3285	37851	35000	11398	11176	3286
Mar	3748	3748	37399	35000	11398	11176	3748
Apr	4410	4409	36777	35000	11398	11175	4410
May	5116	5116	36094	35000	11398	11175	5116
June	5837	5836	35299	35000	11398	11175	5837
July	6173	6423	35139	35000	11398	11175	6173
Aug	6046	6195	35208	35000	11398	11175	6046
Sept	5362	5361	35839	35000	11398	11175	5362
Oct	5136	5135	36073	35000	11398	11175	5136
Nov	4029	4029	37134	35000	11398	11175	4029
Dec	3287	3286	37849	35000	11398	11176	3287
Temperature (°C)							
State Point	1'	1	2	3	4'	4	5
Jan	-5.725	-5.73	14.45	100	50.22	48.74	-5.725
Feb	-2.209	-2.214	19.03	100	50.22	48.78	-2.209
Mar	2.778	2.773	25.71	100	50.22	48.83	2.778
Apr	9.163	9.159	34.69	100	50.22	48.89	9.163
May	15.23	15.23	43.88	100	50.22	48.96	15.23
June	20.79	20.79	53.22	100	50.22	49.01	20.79
July	23.2	23.76	58.05	100	50.22	49.04	23.2
Aug	22.3	22.6	56.15	100	50.22	49.03	22.3
Sept	17.19	17.19	47.04	100	50.22	48.98	17.19
Oct	15.39	15.39	44.13	100	50.22	48.96	15.39
Nov	5.588	5.583	29.59	100	50.22	48.86	5.588
Dec	-2.194	-2.199	19.05	100	50.22	48.78	-2.194
Enthalpy (kJ/kg)							
State Point	1'	1	2	3	4'	4	5
Jan	73.72	73.46	108.7	271.1	234.2	230.2	217.7
Feb	82.03	81.77	117	271.1	234.2	230.4	218.9
Mar	94.24	93.98	129.2	271.1	234.2	230.7	220.6
Apr	110.8	110.6	145.8	271.1	234.2	231.1	222.6
May	128	127.8	163	271.1	234.2	231.4	224.4
June	145.9	145.7	180.8	271.1	234.2	231.8	225.9
July	154.8	154.9	190.1	271.1	234.2	231.9	226.6
Aug	151.3	151.3	186.4	271.1	234.2	231.9	226.3
Sept	134	133.8	169	271.1	234.2	231.6	224.9
Oct	128.5	128.3	163.5	271.1	234.2	231.5	224.4
Nov	101.4	101.1	136.3	271.1	234.2	230.9	221.5
Dec	82.07	81.81	117	271.1	234.2	230.4	218.9
Entropy (kJ/kg-K)							
State Point	1'	1	2	3	4'	4	5
Jan	0.2869	0.2859	0.2859	0.7902	0.7902	0.7789	0.8254
Feb	0.3165	0.3156	0.3156	0.7902	0.7902	0.7796	0.8219
Mar	0.3593	0.3584	0.3584	0.7902	0.7902	0.7805	0.8172
Apr	0.416	0.4152	0.4152	0.7902	0.7902	0.7817	0.8119
May	0.4734	0.4726	0.4726	0.7902	0.7902	0.7829	0.8075
June	0.5316	0.5308	0.5308	0.7902	0.7902	0.7839	0.8039
July	0.5602	0.5595	0.5595	0.7902	0.7902	0.7844	0.8025
Aug	0.5489	0.5482	0.5482	0.7902	0.7902	0.7842	0.803
Sept	0.4931	0.4923	0.4923	0.7902	0.7902	0.7833	0.8061
Oct	0.475	0.4742	0.4742	0.7902	0.7902	0.7829	0.8073
Nov	0.3839	0.383	0.3831	0.7902	0.7902	0.7811	0.8148
Dec	0.3167	0.3157	0.3157	0.7902	0.7902	0.7796	0.8218

Table B-62: Thermodynamic Properties for Direct Single-Loop System Simulations at 3.6km Depth, CO2 Mass Flow Rate of 90kg/s, and Reservoir Temperature of 100°C (DTE=0.50).

Tres	100°C						
Well Depth	3.6 km						
CO2 Mass Flow	90 kg/s						
Pressure (kPa)							
State Point	1'	1	2	3	4'	4	5
Jan	2986	2985	38111	35000	10844	10469	2986
Feb	3286	3285	37801	35000	10844	10469	3286
Mar	3749	3748	37348	35000	10844	10468	3749
Apr	4410	4409	36724	35000	10844	10468	4410
May	5116	5116	36037	35000	10844	10468	5116
June	5837	5836	35239	35000	10844	10467	5837
July	6174	6423	35077	35000	10844	10467	6174
Aug	6046	6195	35147	35000	10844	10467	6046
Sept	5362	5361	35781	35000	10844	10468	5362
Oct	5136	5135	36017	35000	10844	10468	5136
Nov	4030	4029	37082	35000	10844	10468	4030
Dec	3287	3286	37800	35000	10844	10469	3287
Temperature (°C)							
State Point	1'	1	2	3	4'	4	5
Jan	-5.722	-5.73	14.42	100	48.06	46.14	-5.722
Feb	-2.206	-2.214	19	100	48.06	46.16	-2.206
Mar	2.78	2.773	25.68	100	48.06	46.19	2.78
Apr	9.166	9.159	34.65	100	48.06	46.24	9.166
May	15.24	15.23	43.84	100	48.06	46.28	15.24
June	20.8	20.79	53.18	100	48.06	46.31	20.8
July	23.21	23.76	58	100	48.06	46.33	23.21
Aug	22.31	22.6	56.1	100	48.06	46.32	22.31
Sept	17.2	17.19	47	100	48.06	46.29	17.2
Oct	15.4	15.39	44.09	100	48.06	46.28	15.4
Nov	5.591	5.583	29.56	100	48.06	46.21	5.591
Dec	-2.191	-2.199	19.02	100	48.06	46.16	-2.191
Enthalpy (kJ/kg)							
State Point	1'	1	2	3	4'	4	5
Jan	73.66	73.46	108.6	271.1	233.2	229.8	217.9
Feb	81.97	81.77	116.9	271.1	233.2	229.9	219.1
Mar	94.18	93.98	129.1	271.1	233.2	230.2	220.6
Apr	110.8	110.6	145.7	271.1	233.2	230.5	222.6
May	128	127.8	162.9	271.1	233.2	230.7	224.3
June	145.8	145.7	180.8	271.1	233.2	231	225.8
July	154.7	154.9	190	271.1	233.2	231.1	226.4
Aug	151.2	151.3	186.4	271.1	233.2	231.1	226.2
Sept	134	133.8	168.9	271.1	233.2	230.8	224.8
Oct	128.5	128.3	163.4	271.1	233.2	230.8	224.3
Nov	101.3	101.1	136.3	271.1	233.2	230.3	221.5
Dec	82.01	81.81	117	271.1	233.2	229.9	219.1
Entropy (kJ/kg-K)							
State Point	1'	1	2	3	4'	4	5
Jan	0.2866	0.2859	0.2859	0.7902	0.7902	0.7817	0.826
Feb	0.3163	0.3156	0.3156	0.7902	0.7902	0.7823	0.8223
Mar	0.3591	0.3584	0.3584	0.7902	0.7902	0.783	0.8175
Apr	0.4158	0.4152	0.4152	0.7902	0.7902	0.7839	0.8119
May	0.4732	0.4726	0.4726	0.7902	0.7902	0.7848	0.8072
June	0.5314	0.5308	0.5308	0.7902	0.7902	0.7857	0.8034
July	0.5601	0.5595	0.5595	0.7902	0.7902	0.786	0.8019
Aug	0.5488	0.5482	0.5482	0.7902	0.7902	0.7859	0.8025
Sept	0.4929	0.4923	0.4923	0.7902	0.7902	0.7851	0.8058
Oct	0.4748	0.4742	0.4742	0.7902	0.7902	0.7849	0.8071
Nov	0.3837	0.383	0.3831	0.7902	0.7902	0.7834	0.8149
Dec	0.3165	0.3157	0.3157	0.7902	0.7902	0.7823	0.8223

Table B-63: Thermodynamic Properties for Direct Single-Loop System Simulations at 3.6km Depth, CO₂

Mass Flow Rate of 120kg/s, and Reservoir Temperature of 100°C (DTE=0.50).

Tres	100°C						
Well Depth	3.6 km						
CO₂ Mass Flow	120 kg/s						
Pressure (kPa)							
State Point	1'	1	2	3	4'	4	5
Jan	2986	2985	38129	35000	11491	11294	2986
Feb	3286	3285	37819	35000	11491	11294	3286
Mar	3749	3748	37366	35000	11491	11294	3749
Apr	4410	4409	36742	35000	11491	11293	4410
May	5116	5116	36057	35000	11491	11293	5116
June	5837	5836	35260	35000	11491	11293	5837
July	6173	6423	35098	35000	11491	11293	6173
Aug	6046	6195	35169	35000	11491	11293	6046
Sept	5362	5361	35802	35000	11491	11293	5362
Oct	5136	5135	36037	35000	11491	11293	5136
Nov	4030	4029	37100	35000	11491	11294	4030
Dec	3287	3286	37817	35000	11491	11294	3287
Temperature (°C)							
State Point	1'	1	2	3	4'	4	5
Jan	-5.723	-5.73	14.43	100	50.57	49.36	-5.723
Feb	-2.207	-2.214	19.01	100	50.57	49.39	-2.207
Mar	2.779	2.773	25.69	100	50.57	49.43	2.779
Apr	9.165	9.159	34.67	100	50.57	49.47	9.165
May	15.24	15.23	43.85	100	50.57	49.52	15.24
June	20.8	20.79	53.19	100	50.57	49.56	20.8
July	23.21	23.76	58.02	100	50.57	49.58	23.21
Aug	22.31	22.6	56.12	100	50.57	49.57	22.31
Sept	17.2	17.19	47.01	100	50.57	49.53	17.2
Oct	15.4	15.39	44.11	100	50.57	49.52	15.4
Nov	5.59	5.583	29.57	100	50.57	49.45	5.59
Dec	-2.192	-2.199	19.03	100	50.57	49.39	-2.192
Enthalpy (kJ/kg)							
State Point	1'	1	2	3	4'	4	5
Jan	73.64	73.46	108.6	271.1	234.4	231.4	218.8
Feb	81.94	81.77	116.9	271.1	234.4	231.6	219.9
Mar	94.15	93.98	129.1	271.1	234.4	231.8	221.5
Apr	110.7	110.6	145.7	271.1	234.4	232.1	223.4
May	128	127.8	162.9	271.1	234.4	232.3	225.1
June	145.8	145.7	180.8	271.1	234.4	232.6	226.6
July	154.7	154.9	190	271.1	234.4	232.7	227.2
Aug	151.2	151.3	186.4	271.1	234.4	232.6	227
Sept	134	133.8	168.9	271.1	234.4	232.4	225.6
Oct	128.4	128.3	163.4	271.1	234.4	232.3	225.1
Nov	101.3	101.1	136.3	271.1	234.4	231.9	222.4
Dec	81.98	81.81	117	271.1	234.4	231.6	219.9
Entropy (kJ/kg-K)							
State Point	1'	1	2	3	4'	4	5
Jan	0.2865	0.2859	0.2859	0.7902	0.7902	0.7821	0.8293
Feb	0.3162	0.3156	0.3156	0.7902	0.7902	0.7826	0.8255
Mar	0.359	0.3584	0.3584	0.7902	0.7902	0.7833	0.8206
Apr	0.4157	0.4152	0.4152	0.7902	0.7902	0.7841	0.8148
May	0.4732	0.4726	0.4726	0.7902	0.7902	0.7849	0.81
June	0.5313	0.5308	0.5308	0.7902	0.7902	0.7857	0.8061
July	0.56	0.5595	0.5595	0.7902	0.7902	0.786	0.8045
Aug	0.5487	0.5482	0.5482	0.7902	0.7902	0.7859	0.8051
Sept	0.4929	0.4923	0.4923	0.7902	0.7902	0.7852	0.8086
Oct	0.4748	0.4742	0.4742	0.7902	0.7902	0.785	0.8099
Nov	0.3836	0.383	0.3831	0.7902	0.7902	0.7837	0.818
Dec	0.3164	0.3157	0.3157	0.7902	0.7902	0.7826	0.8255

Table B-64: Thermodynamic Properties for Direct Single-Loop System Simulations at 3.6km Depth, CO2 Mass Flow Rate of 140kg/s, and Reservoir Temperature of 100°C (DTE=0.50).

Tres	100°C						
Well Depth	3.6 km						
CO2 Mass Flow	140 kg/s						
Pressure (kPa)							
State Point	1'	1	2	3	4'	4	5
Jan	2986	2985	38090	35000	11219	10948	2986
Feb	3286	3285	37780	35000	11219	10948	3286
Mar	3749	3748	37325	35000	11219	10948	3749
Apr	4410	4409	36700	35000	11219	10947	4410
May	5116	5116	36013	35000	11219	10947	5116
June	5837	5836	35212	35000	11219	10947	5837
July	6174	6423	35049	35000	11219	10947	6174
Aug	6046	6195	35120	35000	11219	10947	6046
Sept	5362	5361	35756	35000	11219	10947	5362
Oct	5136	5135	35992	35000	11219	10947	5136
Nov	4030	4029	37059	35000	11219	10948	4030
Dec	3287	3286	37778	35000	11219	10948	3287
Temperature (°C)							
State Point	1'	1	2	3	4'	4	5
Jan	-5.72	-5.73	14.41	100	49.54	48.12	-5.72
Feb	-2.205	-2.214	18.99	100	49.54	48.14	-2.205
Mar	2.782	2.773	25.67	100	49.54	48.17	2.782
Apr	9.167	9.159	34.64	100	49.54	48.2	9.167
May	15.24	15.23	43.82	100	49.54	48.24	15.24
June	20.8	20.79	53.16	100	49.54	48.27	20.8
July	23.21	23.76	57.98	100	49.54	48.29	23.21
Aug	22.31	22.6	56.08	100	49.54	48.28	22.31
Sept	17.2	17.19	46.98	100	49.54	48.25	17.2
Oct	15.4	15.39	44.08	100	49.54	48.24	15.4
Nov	5.592	5.583	29.55	100	49.54	48.18	5.592
Dec	-2.19	-2.199	19.01	100	49.54	48.14	-2.19
Enthalpy (kJ/kg)							
State Point	1'	1	2	3	4'	4	5
Jan	73.61	73.46	108.6	271.1	233.9	231.2	218.9
Feb	81.92	81.77	116.9	271.1	233.9	231.3	220
Mar	94.13	93.98	129.1	271.1	233.9	231.5	221.5
Apr	110.7	110.6	145.7	271.1	233.9	231.7	223.4
May	127.9	127.8	162.9	271.1	233.9	232	225
June	145.8	145.7	180.7	271.1	233.9	232.2	226.5
July	154.7	154.9	190	271.1	233.9	232.3	227.1
Aug	151.2	151.3	186.3	271.1	233.9	232.2	226.9
Sept	133.9	133.8	168.9	271.1	233.9	232	225.6
Oct	128.4	128.3	163.4	271.1	233.9	232	225.1
Nov	101.3	101.1	136.2	271.1	233.9	231.6	222.3
Dec	81.96	81.81	116.9	271.1	233.9	231.3	220
Entropy (kJ/kg-K)							
State Point	1'	1	2	3	4'	4	5
Jan	0.2864	0.2859	0.2859	0.7902	0.7902	0.7834	0.8295
Feb	0.3161	0.3156	0.3156	0.7902	0.7902	0.7838	0.8257
Mar	0.3589	0.3584	0.3584	0.7902	0.7902	0.7844	0.8206
Apr	0.4157	0.4152	0.4152	0.7902	0.7902	0.7851	0.8147
May	0.4731	0.4726	0.4726	0.7902	0.7902	0.7858	0.8098
June	0.5313	0.5308	0.5308	0.7902	0.7902	0.7865	0.8058
July	0.5599	0.5595	0.5595	0.7902	0.7902	0.7867	0.8042
Aug	0.5486	0.5482	0.5482	0.7902	0.7902	0.7866	0.8048
Sept	0.4928	0.4923	0.4923	0.7902	0.7902	0.786	0.8083
Oct	0.4747	0.4742	0.4742	0.7902	0.7902	0.7858	0.8097
Nov	0.3836	0.383	0.3831	0.7902	0.7902	0.7847	0.8179
Dec	0.3163	0.3157	0.3157	0.7902	0.7902	0.7838	0.8257

Table B-65: Thermodynamic Properties for Direct Single-Loop System Simulations at 3.6km Depth, CO2 Mass Flow Rate of 70kg/s, and Reservoir Temperature of 125°C (DTE=0.50).

Tres	125°C						
Well Depth	3.6 km						
CO2 Mass Flow	70 kg/s						
Pressure (kPa)							
State Point	1'	1	2	3	4'	4	5
Jan	2986	2985	38160	35000	14306	14047	2986
Feb	3286	3285	37851	35000	14306	14047	3286
Mar	3748	3748	37399	35000	14306	14047	3748
Apr	4410	4409	36777	35000	14306	14047	4410
May	5116	5116	36094	35000	14306	14047	5116
June	5837	5836	35299	35000	14306	14046	5837
July	6173	6423	35139	35000	14306	14046	6173
Aug	6046	6195	35208	35000	14306	14046	6046
Sept	5362	5361	35839	35000	14306	14046	5362
Oct	5136	5135	36073	35000	14306	14047	5136
Nov	4029	4029	37134	35000	14306	14047	4029
Dec	3287	3286	37849	35000	14306	14047	3287
Temperature (°C)							
State Point	1'	1	2	3	4'	4	5
Jan	-5.725	-5.73	14.45	125	71.55	69.05	-5.725
Feb	-2.209	-2.214	19.03	125	71.55	69.11	-2.209
Mar	2.778	2.773	25.71	125	71.55	69.2	2.778
Apr	9.163	9.159	34.69	125	71.55	69.31	9.163
May	15.23	15.23	43.88	125	71.55	69.41	15.23
June	20.79	20.79	53.22	125	71.55	69.5	20.79
July	23.2	23.76	58.05	125	71.55	69.55	23.2
Aug	22.3	22.6	56.15	125	71.55	69.53	22.3
Sept	17.19	17.19	47.04	125	71.55	69.44	17.19
Oct	15.39	15.39	44.13	125	71.55	69.41	15.39
Nov	5.588	5.583	29.59	125	71.55	69.25	5.588
Dec	-2.194	-2.199	19.05	125	71.55	69.11	-2.194
Enthalpy (kJ/kg)							
State Point	1'	1	2	3	4'	4	5
Jan	73.72	73.46	108.7	318.6	281.3	275.8	256.7
Feb	82.03	81.77	117	318.6	281.3	276	258.1
Mar	94.24	93.98	129.2	318.6	281.3	276.3	260
Apr	110.8	110.6	145.8	318.6	281.3	276.7	262.4
May	128	127.8	163	318.6	281.3	277.1	264.5
June	145.9	145.7	180.8	318.6	281.3	277.4	266.4
July	154.8	154.9	190.1	318.6	281.3	277.6	267.2
Aug	151.3	151.3	186.4	318.6	281.3	277.5	266.9
Sept	134	133.8	169	318.6	281.3	277.2	265.2
Oct	128.5	128.3	163.5	318.6	281.3	277.1	264.6
Nov	101.4	101.1	136.3	318.6	281.3	276.5	261
Dec	82.07	81.81	117	318.6	281.3	276	258.1
Entropy (kJ/kg-K)							
State Point	1'	1	2	3	4'	4	5
Jan	0.2869	0.2859	0.2859	0.9136	0.9137	0.8994	0.971
Feb	0.3165	0.3156	0.3156	0.9136	0.9137	0.9	0.9663
Mar	0.3593	0.3584	0.3584	0.9136	0.9137	0.9009	0.9601
Apr	0.416	0.4152	0.4152	0.9136	0.9137	0.902	0.9528
May	0.4734	0.4726	0.4726	0.9136	0.9137	0.9031	0.9467
June	0.5316	0.5308	0.5308	0.9136	0.9137	0.9041	0.9416
July	0.5602	0.5595	0.5595	0.9136	0.9137	0.9045	0.9395
Aug	0.5489	0.5482	0.5482	0.9136	0.9137	0.9043	0.9402
Sept	0.4931	0.4923	0.4923	0.9136	0.9137	0.9034	0.9448
Oct	0.475	0.4742	0.4742	0.9136	0.9137	0.9031	0.9465
Nov	0.3839	0.383	0.3831	0.9136	0.9137	0.9014	0.9568
Dec	0.3167	0.3157	0.3157	0.9136	0.9137	0.9	0.9662

Table B-66: Thermodynamic Properties for Direct Single-Loop System Simulations at 3.6km Depth, CO2 Mass Flow Rate of 90kg/s, and Reservoir Temperature of 125°C (DTE=0.50).

Tres	125°C						
Well Depth	3.6 km						
CO2 Mass Flow	90 kg/s						
Pressure (kPa)							
State Point	1'	1	2	3	4'	4	5
Jan	2986	2985	38111	35000	13664	13224	2986
Feb	3286	3285	37801	35000	13664	13224	3286
Mar	3749	3748	37348	35000	13664	13224	3749
Apr	4410	4409	36724	35000	13664	13224	4410
May	5116	5116	36037	35000	13664	13223	5116
June	5837	5836	35239	35000	13664	13223	5837
July	6174	6423	35077	35000	13664	13223	6174
Aug	6046	6195	35147	35000	13664	13223	6046
Sept	5362	5361	35781	35000	13664	13223	5362
Oct	5136	5135	36017	35000	13664	13223	5136
Nov	4030	4029	37082	35000	13664	13224	4030
Dec	3287	3286	37800	35000	13664	13224	3287
Temperature (°C)							
State Point	1'	1	2	3	4'	4	5
Jan	-5.722	-5.73	14.42	125	68.8	65.86	-5.722
Feb	-2.206	-2.214	19	125	68.8	65.91	-2.206
Mar	2.78	2.773	25.68	125	68.8	65.97	2.78
Apr	9.166	9.159	34.65	125	68.8	66.04	9.166
May	15.24	15.23	43.84	125	68.8	66.12	15.24
June	20.8	20.79	53.18	125	68.8	66.19	20.8
July	23.21	23.76	58	125	68.8	66.22	23.21
Aug	22.31	22.6	56.1	125	68.8	66.2	22.31
Sept	17.2	17.19	47	125	68.8	66.14	17.2
Oct	15.4	15.39	44.09	125	68.8	66.12	15.4
Nov	5.591	5.583	29.56	125	68.8	66	5.591
Dec	-2.191	-2.199	19.02	125	68.8	65.91	-2.191
Enthalpy (kJ/kg)							
State Point	1'	1	2	3	4'	4	5
Jan	73.66	73.46	108.6	318.6	279.9	275.2	256.8
Feb	81.97	81.77	116.9	318.6	279.9	275.4	258.2
Mar	94.18	93.98	129.1	318.6	279.9	275.6	260.1
Apr	110.8	110.6	145.7	318.6	279.9	275.9	262.4
May	128	127.8	162.9	318.6	279.9	276.2	264.5
June	145.8	145.7	180.8	318.6	279.9	276.5	266.3
July	154.7	154.9	190	318.6	279.9	276.6	267.1
Aug	151.2	151.3	186.4	318.6	279.9	276.5	266.8
Sept	134	133.8	168.9	318.6	279.9	276.3	265.1
Oct	128.5	128.3	163.4	318.6	279.9	276.2	264.5
Nov	101.3	101.1	136.3	318.6	279.9	275.7	261.1
Dec	82.01	81.81	117	318.6	279.9	275.4	258.2
Entropy (kJ/kg-K)							
State Point	1'	1	2	3	4'	4	5
Jan	0.2866	0.2859	0.2859	0.9136	0.9137	0.9029	0.9716
Feb	0.3163	0.3156	0.3156	0.9136	0.9137	0.9034	0.9668
Mar	0.3591	0.3584	0.3584	0.9136	0.9137	0.9041	0.9604
Apr	0.4158	0.4152	0.4152	0.9136	0.9137	0.905	0.9529
May	0.4732	0.4726	0.4726	0.9136	0.9137	0.9058	0.9465
June	0.5314	0.5308	0.5308	0.9136	0.9137	0.9066	0.9412
July	0.5601	0.5595	0.5595	0.9136	0.9137	0.9069	0.939
Aug	0.5488	0.5482	0.5482	0.9136	0.9137	0.9068	0.9398
Sept	0.4929	0.4923	0.4923	0.9136	0.9137	0.9061	0.9446
Oct	0.4748	0.4742	0.4742	0.9136	0.9137	0.9058	0.9463
Nov	0.3837	0.383	0.3831	0.9136	0.9137	0.9045	0.957
Dec	0.3165	0.3157	0.3157	0.9136	0.9137	0.9034	0.9667

Table B-67: Thermodynamic Properties for Direct Single-Loop System Simulations at 3.6km Depth, CO₂

Mass Flow Rate of 120kg/s, and Reservoir Temperature of 125°C (DTE=0.50).

Tres	125°C						
Well Depth	3.6 km						
CO₂ Mass Flow	120 kg/s						
Pressure (kPa)							
State Point	1'	1	2	3	4'	4	5
Jan	2986	2985	38129	35000	14414	14184	2986
Feb	3286	3285	37819	35000	14414	14184	3286
Mar	3749	3748	37366	35000	14414	14184	3749
Apr	4410	4409	36742	35000	14414	14184	4410
May	5116	5116	36057	35000	14414	14183	5116
June	5837	5836	35260	35000	14414	14183	5837
July	6173	6423	35098	35000	14414	14183	6173
Aug	6046	6195	35169	35000	14414	14183	6046
Sept	5362	5361	35802	35000	14414	14183	5362
Oct	5136	5135	36037	35000	14414	14183	5136
Nov	4030	4029	37100	35000	14414	14184	4030
Dec	3287	3286	37817	35000	14414	14184	3287
Temperature (°C)							
State Point	1'	1	2	3	4'	4	5
Jan	-5.723	-5.73	14.43	125	72	70.01	-5.723
Feb	-2.207	-2.214	19.01	125	72	70.06	-2.207
Mar	2.779	2.773	25.69	125	72	70.12	2.779
Apr	9.165	9.159	34.67	125	72	70.2	9.165
May	15.24	15.23	43.85	125	72	70.27	15.24
June	20.8	20.79	53.19	125	72	70.34	20.8
July	23.21	23.76	58.02	125	72	70.37	23.21
Aug	22.31	22.6	56.12	125	72	70.36	22.31
Sept	17.2	17.19	47.01	125	72	70.3	17.2
Oct	15.4	15.39	44.11	125	72	70.28	15.4
Nov	5.59	5.583	29.57	125	72	70.15	5.59
Dec	-2.192	-2.199	19.03	125	72	70.06	-2.192
Enthalpy (kJ/kg)							
State Point	1'	1	2	3	4'	4	5
Jan	73.64	73.46	108.6	318.6	281.5	277.5	258
Feb	81.94	81.77	116.9	318.6	281.5	277.6	259.4
Mar	94.15	93.98	129.1	318.6	281.5	277.9	261.3
Apr	110.7	110.6	145.7	318.6	281.5	278.1	263.5
May	128	127.8	162.9	318.6	281.5	278.4	265.6
June	145.8	145.7	180.8	318.6	281.5	278.6	267.4
July	154.7	154.9	190	318.6	281.5	278.7	268.2
Aug	151.2	151.3	186.4	318.6	281.5	278.7	267.9
Sept	134	133.8	168.9	318.6	281.5	278.5	266.2
Oct	128.4	128.3	163.4	318.6	281.5	278.4	265.7
Nov	101.3	101.1	136.3	318.6	281.5	278	262.3
Dec	81.98	81.81	117	318.6	281.5	277.6	259.4
Entropy (kJ/kg-K)							
State Point	1'	1	2	3	4'	4	5
Jan	0.2865	0.2859	0.2859	0.9136	0.9137	0.9034	0.9761
Feb	0.3162	0.3156	0.3156	0.9136	0.9137	0.9039	0.9712
Mar	0.359	0.3584	0.3584	0.9136	0.9137	0.9045	0.9646
Apr	0.4157	0.4152	0.4152	0.9136	0.9137	0.9053	0.957
May	0.4732	0.4726	0.4726	0.9136	0.9137	0.9061	0.9504
June	0.5313	0.5308	0.5308	0.9136	0.9137	0.9068	0.945
July	0.56	0.5595	0.5595	0.9136	0.9137	0.9071	0.9428
Aug	0.5487	0.5482	0.5482	0.9136	0.9137	0.907	0.9436
Sept	0.4929	0.4923	0.4923	0.9136	0.9137	0.9063	0.9485
Oct	0.4748	0.4742	0.4742	0.9136	0.9137	0.9061	0.9503
Nov	0.3836	0.383	0.3831	0.9136	0.9137	0.9049	0.9612
Dec	0.3164	0.3157	0.3157	0.9136	0.9137	0.9039	0.9712

Table B-68: Thermodynamic Properties for Direct Single-Loop System Simulations at 3.6km Depth, CO₂

Mass Flow Rate of 140kg/s, and Reservoir Temperature of 125°C (DTE=0.50).

Tres	125°C						
Well Depth	3.6 km						
CO₂ Mass Flow	140 kg/s						
	Pressure (kPa)						
State Point	1'	1	2	3	4'	4	5
Jan	2986	2985	38090	35000	14100	13782	2986
Feb	3286	3285	37780	35000	14100	13782	3286
Mar	3749	3748	37325	35000	14100	13782	3749
Apr	4410	4409	36700	35000	14100	13782	4410
May	5116	5116	36013	35000	14100	13782	5116
June	5837	5836	35212	35000	14100	13781	5837
July	6174	6423	35049	35000	14100	13781	6174
Aug	6046	6195	35120	35000	14100	13781	6046
Sept	5362	5361	35756	35000	14100	13782	5362
Oct	5136	5135	35992	35000	14100	13782	5136
Nov	4030	4029	37059	35000	14100	13782	4030
Dec	3287	3286	37778	35000	14100	13782	3287
	Temperature (°C)						
State Point	1'	1	2	3	4'	4	5
Jan	-5.72	-5.73	14.41	125	70.68	68.48	-5.72
Feb	-2.205	-2.214	18.99	125	70.68	68.52	-2.205
Mar	2.782	2.773	25.67	125	70.68	68.57	2.782
Apr	9.167	9.159	34.64	125	70.68	68.64	9.167
May	15.24	15.23	43.82	125	70.68	68.7	15.24
June	20.8	20.79	53.16	125	70.68	68.75	20.8
July	23.21	23.76	57.98	125	70.68	68.78	23.21
Aug	22.31	22.6	56.08	125	70.68	68.77	22.31
Sept	17.2	17.19	46.98	125	70.68	68.72	17.2
Oct	15.4	15.39	44.08	125	70.68	68.7	15.4
Nov	5.592	5.583	29.55	125	70.68	68.6	5.592
Dec	-2.19	-2.199	19.01	125	70.68	68.52	-2.19
	Enthalpy (kJ/kg)						
State Point	1'	1	2	3	4'	4	5
Jan	73.61	73.46	108.6	318.6	280.8	277.2	258.1
Feb	81.92	81.77	116.9	318.6	280.8	277.3	259.4
Mar	94.13	93.98	129.1	318.6	280.8	277.5	261.3
Apr	110.7	110.6	145.7	318.6	280.8	277.7	263.5
May	127.9	127.8	162.9	318.6	280.8	277.9	265.5
June	145.8	145.7	180.7	318.6	280.8	278.1	267.3
July	154.7	154.9	190	318.6	280.8	278.2	268.1
Aug	151.2	151.3	186.3	318.6	280.8	278.2	267.8
Sept	133.9	133.8	168.9	318.6	280.8	278	266.2
Oct	128.4	128.3	163.4	318.6	280.8	277.9	265.6
Nov	101.3	101.1	136.2	318.6	280.8	277.6	262.3
Dec	81.96	81.81	116.9	318.6	280.8	277.3	259.4
	Entropy (kJ/kg-K)						
State Point	1'	1	2	3	4'	4	5
Jan	0.2864	0.2859	0.2859	0.9136	0.9137	0.905	0.9763
Feb	0.3161	0.3156	0.3156	0.9136	0.9137	0.9054	0.9713
Mar	0.3589	0.3584	0.3584	0.9136	0.9137	0.9059	0.9647
Apr	0.4157	0.4152	0.4152	0.9136	0.9137	0.9066	0.9569
May	0.4731	0.4726	0.4726	0.9136	0.9137	0.9073	0.9503
June	0.5313	0.5308	0.5308	0.9136	0.9137	0.9079	0.9447
July	0.5599	0.5595	0.5595	0.9136	0.9137	0.9082	0.9425
Aug	0.5486	0.5482	0.5482	0.9136	0.9137	0.9081	0.9433
Sept	0.4928	0.4923	0.4923	0.9136	0.9137	0.9075	0.9482
Oct	0.4747	0.4742	0.4742	0.9136	0.9137	0.9073	0.9501
Nov	0.3836	0.383	0.3831	0.9136	0.9137	0.9062	0.9612
Dec	0.3163	0.3157	0.3157	0.9136	0.9137	0.9054	0.9713

Table B-69: Thermodynamic Properties for Direct Single-Loop System Simulations at 3.6km Depth, CO2 Mass Flow Rate of 70kg/s, and Reservoir Temperature of 150°C (DTE=0.50).

Tres	150°C						
Well Depth	3.6 km						
CO2 Mass Flow	70 kg/s						
Pressure (kPa)							
State Point	1'	1	2	3	4'	4	5
Jan	2986	2985	38160	35000	16599	16303	2986
Feb	3286	3285	37851	35000	16599	16303	3286
Mar	3748	3748	37399	35000	16599	16303	3748
Apr	4410	4409	36777	35000	16599	16302	4410
May	5116	5116	36094	35000	16599	16302	5116
June	5837	5836	35299	35000	16599	16302	5837
July	6173	6423	35139	35000	16599	16302	6173
Aug	6046	6195	35208	35000	16599	16302	6046
Sept	5362	5361	35839	35000	16599	16302	5362
Oct	5136	5135	36073	35000	16599	16302	5136
Nov	4029	4029	37134	35000	16599	16303	4029
Dec	3287	3286	37849	35000	16599	16303	3287
Temperature (°C)							
State Point	1'	1	2	3	4'	4	5
Jan	-5.725	-5.73	14.45	150	95.61	91.7	-5.725
Feb	-2.209	-2.214	19.03	150	95.61	91.79	-2.209
Mar	2.778	2.773	25.71	150	95.61	91.91	2.778
Apr	9.163	9.159	34.69	150	95.61	92.06	9.163
May	15.23	15.23	43.88	150	95.61	92.21	15.23
June	20.79	20.79	53.22	150	95.61	92.35	23.42
July	23.2	23.76	58.05	150	95.61	92.4	27.17
Aug	22.3	22.6	56.15	150	95.61	92.38	25.77
Sept	17.19	17.19	47.04	150	95.61	92.26	17.78
Oct	15.39	15.39	44.13	150	95.61	92.21	15.39
Nov	5.588	5.583	29.59	150	95.61	91.98	5.588
Dec	-2.194	-2.199	19.05	150	95.61	91.79	-2.194
Enthalpy (kJ/kg)							
State Point	1'	1	2	3	4'	4	5
Jan	73.72	73.46	108.7	364.1	326.1	319	292.7
Feb	82.03	81.77	117	364.1	326.1	319.2	294.3
Mar	94.24	93.98	129.2	364.1	326.1	319.5	296.4
Apr	110.8	110.6	145.8	364.1	326.1	319.9	299.1
May	128	127.8	163	364.1	326.1	320.3	301.6
June	145.9	145.7	180.8	364.1	326.1	320.6	303.8
July	154.8	154.9	190.1	364.1	326.1	320.7	304.7
Aug	151.3	151.3	186.4	364.1	326.1	320.7	304.4
Sept	134	133.8	169	364.1	326.1	320.4	302.4
Oct	128.5	128.3	163.5	364.1	326.1	320.3	301.7
Nov	101.4	101.1	136.3	364.1	326.1	319.7	297.6
Dec	82.07	81.81	117	364.1	326.1	319.2	294.3
Entropy (kJ/kg-K)							
State Point	1'	1	2	3	4'	4	5
Jan	0.2869	0.2859	0.2859	1.024	1.024	1.007	1.106
Feb	0.3165	0.3156	0.3156	1.024	1.024	1.008	1.1
Mar	0.3593	0.3584	0.3584	1.024	1.024	1.009	1.092
Apr	0.416	0.4152	0.4152	1.024	1.024	1.01	1.083
May	0.4734	0.4726	0.4726	1.024	1.024	1.011	1.075
June	0.5316	0.5308	0.5308	1.024	1.024	1.012	1.069
July	0.5602	0.5595	0.5595	1.024	1.024	1.012	1.066
Aug	0.5489	0.5482	0.5482	1.024	1.024	1.012	1.067
Sept	0.4931	0.4923	0.4923	1.024	1.024	1.011	1.073
Oct	0.475	0.4742	0.4742	1.024	1.024	1.011	1.075
Nov	0.3839	0.383	0.3831	1.024	1.024	1.009	1.088
Dec	0.3167	0.3157	0.3157	1.024	1.024	1.008	1.1

Table B-70: Thermodynamic Properties for Direct Single-Loop System Simulations at 3.6km Depth, CO2 Mass Flow Rate of 90kg/s, and Reservoir Temperature of 150°C (DTE=0.50).

Tres	150°C						
Well Depth	3.6 km						
CO2 Mass Flow	90 kg/s						
Pressure (kPa)							
State Point	1'	1	2	3	4'	4	5
Jan	2986	2985	38111	35000	15856	15352	2986
Feb	3286	3285	37801	35000	15856	15352	3286
Mar	3749	3748	37348	35000	15856	15352	3749
Apr	4410	4409	36724	35000	15856	15351	4410
May	5116	5116	36037	35000	15856	15351	5116
June	5837	5836	35239	35000	15856	15351	5837
July	6174	6423	35077	35000	15856	15351	6174
Aug	6046	6195	35147	35000	15856	15351	6046
Sept	5362	5361	35781	35000	15856	15351	5362
Oct	5136	5135	36017	35000	15856	15351	5136
Nov	4030	4029	37082	35000	15856	15352	4030
Dec	3287	3286	37800	35000	15856	15352	3287
Temperature (°C)							
State Point	1'	1	2	3	4'	4	5
Jan	-5.722	-5.73	14.42	150	92.26	88	-5.722
Feb	-2.206	-2.214	19	150	92.26	88.06	-2.206
Mar	2.78	2.773	25.68	150	92.26	88.16	2.78
Apr	9.166	9.159	34.65	150	92.26	88.27	9.166
May	15.24	15.23	43.84	150	92.26	88.38	15.24
June	20.8	20.79	53.18	150	92.26	88.48	23.38
July	23.21	23.76	58	150	92.26	88.53	27.13
Aug	22.31	22.6	56.1	150	92.26	88.51	25.74
Sept	17.2	17.19	47	150	92.26	88.42	17.76
Oct	15.4	15.39	44.09	150	92.26	88.39	15.4
Nov	5.591	5.583	29.56	150	92.26	88.21	5.591
Dec	-2.191	-2.199	19.02	150	92.26	88.06	-2.191
Enthalpy (kJ/kg)							
State Point	1'	1	2	3	4'	4	5
Jan	73.66	73.46	108.6	364.1	324.2	318.2	292.8
Feb	81.97	81.77	116.9	364.1	324.2	318.3	294.4
Mar	94.18	93.98	129.1	364.1	324.2	318.6	296.5
Apr	110.8	110.6	145.7	364.1	324.2	318.9	299.1
May	128	127.8	162.9	364.1	324.2	319.1	301.5
June	145.8	145.7	180.8	364.1	324.2	319.4	303.7
July	154.7	154.9	190	364.1	324.2	319.5	304.6
Aug	151.2	151.3	186.4	364.1	324.2	319.5	304.2
Sept	134	133.8	168.9	364.1	324.2	319.2	302.3
Oct	128.5	128.3	163.4	364.1	324.2	319.1	301.6
Nov	101.3	101.1	136.3	364.1	324.2	318.7	297.7
Dec	82.01	81.81	117	364.1	324.2	318.3	294.4
Entropy (kJ/kg-K)							
State Point	1'	1	2	3	4'	4	5
Jan	0.2866	0.2859	0.2859	1.024	1.024	1.011	1.106
Feb	0.3163	0.3156	0.3156	1.024	1.024	1.012	1.1
Mar	0.3591	0.3584	0.3584	1.024	1.024	1.012	1.092
Apr	0.4158	0.4152	0.4152	1.024	1.024	1.013	1.083
May	0.4732	0.4726	0.4726	1.024	1.024	1.014	1.075
June	0.5314	0.5308	0.5308	1.024	1.024	1.015	1.068
July	0.5601	0.5595	0.5595	1.024	1.024	1.015	1.065
Aug	0.5488	0.5482	0.5482	1.024	1.024	1.015	1.066
Sept	0.4929	0.4923	0.4923	1.024	1.024	1.014	1.073
Oct	0.4748	0.4742	0.4742	1.024	1.024	1.014	1.075
Nov	0.3837	0.383	0.3831	1.024	1.024	1.013	1.088
Dec	0.3165	0.3157	0.3157	1.024	1.024	1.012	1.1

Table B-71: Thermodynamic Properties for Direct Single-Loop System Simulations at 3.6km Depth, CO₂

Mass Flow Rate of 120kg/s, and Reservoir Temperature of 150°C (DTE=0.50).

Tres	150°C						
Well Depth	3.6 km						
CO₂ Mass Flow	120 kg/s						
	Pressure (kPa)						
State Point	1'	1	2	3	4'	4	5
Jan	2986	2985	38129	35000	16723	16460	2986
Feb	3286	3285	37819	35000	16723	16460	3286
Mar	3749	3748	37366	35000	16723	16460	3749
Apr	4410	4409	36742	35000	16723	16460	4410
May	5116	5116	36057	35000	16723	16460	5116
June	5837	5836	35260	35000	16723	16459	5837
July	6173	6423	35098	35000	16723	16459	6173
Aug	6046	6195	35169	35000	16723	16459	6046
Sept	5362	5361	35802	35000	16723	16460	5362
Oct	5136	5135	36037	35000	16723	16460	5136
Nov	4030	4029	37100	35000	16723	16460	4030
Dec	3287	3286	37817	35000	16723	16460	3287
	Temperature (°C)						
State Point	1'	1	2	3	4'	4	5
Jan	-5.723	-5.73	14.43	150	96.16	93.12	-5.723
Feb	-2.207	-2.214	19.01	150	96.16	93.18	-2.207
Mar	2.779	2.773	25.69	150	96.16	93.27	2.779
Apr	9.165	9.159	34.67	150	96.16	93.38	9.165
May	15.24	15.23	43.85	150	96.16	93.48	15.24
June	20.8	20.79	53.19	150	96.16	93.58	23.84
July	23.21	23.76	58.02	150	96.16	93.62	27.59
Aug	22.31	22.6	56.12	150	96.16	93.61	26.19
Sept	17.2	17.19	47.01	150	96.16	93.52	18.21
Oct	15.4	15.39	44.11	150	96.16	93.49	15.4
Nov	5.59	5.583	29.57	150	96.16	93.31	5.59
Dec	-2.192	-2.199	19.03	150	96.16	93.18	-2.192
	Enthalpy (kJ/kg)						
State Point	1'	1	2	3	4'	4	5
Jan	73.64	73.46	108.6	364.1	326.4	321.2	294.4
Feb	81.94	81.77	116.9	364.1	326.4	321.3	296
Mar	94.15	93.98	129.1	364.1	326.4	321.5	298.1
Apr	110.7	110.6	145.7	364.1	326.4	321.8	300.7
May	128	127.8	162.9	364.1	326.4	322.1	303.1
June	145.8	145.7	180.8	364.1	326.4	322.3	305.2
July	154.7	154.9	190	364.1	326.4	322.4	306.1
Aug	151.2	151.3	186.4	364.1	326.4	322.4	305.7
Sept	134	133.8	168.9	364.1	326.4	322.2	303.8
Oct	128.4	128.3	163.4	364.1	326.4	322.1	303.1
Nov	101.3	101.1	136.3	364.1	326.4	321.7	299.2
Dec	81.98	81.81	117	364.1	326.4	321.3	296
	Entropy (kJ/kg-K)						
State Point	1'	1	2	3	4'	4	5
Jan	0.2865	0.2859	0.2859	1.024	1.024	1.012	1.112
Feb	0.3162	0.3156	0.3156	1.024	1.024	1.012	1.106
Mar	0.359	0.3584	0.3584	1.024	1.024	1.013	1.098
Apr	0.4157	0.4152	0.4152	1.024	1.024	1.014	1.089
May	0.4732	0.4726	0.4726	1.024	1.024	1.014	1.08
June	0.5313	0.5308	0.5308	1.024	1.024	1.015	1.073
July	0.56	0.5595	0.5595	1.024	1.024	1.015	1.07
Aug	0.5487	0.5482	0.5482	1.024	1.024	1.015	1.071
Sept	0.4929	0.4923	0.4923	1.024	1.024	1.015	1.078
Oct	0.4748	0.4742	0.4742	1.024	1.024	1.015	1.08
Nov	0.3836	0.383	0.3831	1.024	1.024	1.013	1.094
Dec	0.3164	0.3157	0.3157	1.024	1.024	1.012	1.106

Table B-72: Thermodynamic Properties for Direct Single-Loop System Simulations at 3.6km Depth, CO₂

Mass Flow Rate of 140kg/s, and Reservoir Temperature of 150°C (DTE=0.50).

Tres	150°C						
Well Depth	3.6 km						
CO₂ Mass Flow	140 kg/s						
Pressure (kPa)							
State Point	1'	1	2	3	4'	4	5
Jan	2986	2985	38090	35000	16360	15997	2986
Feb	3286	3285	37780	35000	16360	15997	3286
Mar	3749	3748	37325	35000	16360	15997	3749
Apr	4410	4409	36700	35000	16360	15997	4410
May	5116	5116	36013	35000	16360	15997	5116
June	5837	5836	35212	35000	16360	15996	5837
July	6174	6423	35049	35000	16360	15996	6174
Aug	6046	6195	35120	35000	16360	15996	6046
Sept	5362	5361	35756	35000	16360	15996	5362
Oct	5136	5135	35992	35000	16360	15996	5136
Nov	4030	4029	37059	35000	16360	15997	4030
Dec	3287	3286	37778	35000	16360	15997	3287
Temperature (°C)							
State Point	1'	1	2	3	4'	4	5
Jan	-5.72	-5.73	14.41	150	94.55	91.34	-5.72
Feb	-2.205	-2.214	18.99	150	94.55	91.39	-2.205
Mar	2.782	2.773	25.67	150	94.55	91.47	2.782
Apr	9.167	9.159	34.64	150	94.55	91.56	9.167
May	15.24	15.23	43.82	150	94.55	91.65	15.24
June	20.8	20.79	53.16	150	94.55	91.74	23.81
July	23.21	23.76	57.98	150	94.55	91.77	27.56
Aug	22.31	22.6	56.08	150	94.55	91.76	26.16
Sept	17.2	17.19	46.98	150	94.55	91.68	18.19
Oct	15.4	15.39	44.08	150	94.55	91.66	15.4
Nov	5.592	5.583	29.55	150	94.55	91.51	5.592
Dec	-2.19	-2.199	19.01	150	94.55	91.39	-2.19
Enthalpy (kJ/kg)							
State Point	1'	1	2	3	4'	4	5
Jan	73.61	73.46	108.6	364.1	325.5	320.7	294.4
Feb	81.92	81.77	116.9	364.1	325.5	320.9	296
Mar	94.13	93.98	129.1	364.1	325.5	321	298.1
Apr	110.7	110.6	145.7	364.1	325.5	321.3	300.7
May	127.9	127.8	162.9	364.1	325.5	321.5	303
June	145.8	145.7	180.7	364.1	325.5	321.7	305.1
July	154.7	154.9	190	364.1	325.5	321.8	306
Aug	151.2	151.3	186.3	364.1	325.5	321.8	305.6
Sept	133.9	133.8	168.9	364.1	325.5	321.6	303.8
Oct	128.4	128.3	163.4	364.1	325.5	321.5	303.1
Nov	101.3	101.1	136.2	364.1	325.5	321.1	299.2
Dec	81.96	81.81	116.9	364.1	325.5	320.9	296
Entropy (kJ/kg-K)							
State Point	1'	1	2	3	4'	4	5
Jan	0.2864	0.2859	0.2859	1.024	1.024	1.014	1.112
Feb	0.3161	0.3156	0.3156	1.024	1.024	1.014	1.106
Mar	0.3589	0.3584	0.3584	1.024	1.024	1.015	1.098
Apr	0.4157	0.4152	0.4152	1.024	1.024	1.015	1.088
May	0.4731	0.4726	0.4726	1.024	1.024	1.016	1.08
June	0.5313	0.5308	0.5308	1.024	1.024	1.017	1.073
July	0.5599	0.5595	0.5595	1.024	1.024	1.017	1.07
Aug	0.5486	0.5482	0.5482	1.024	1.024	1.017	1.071
Sept	0.4928	0.4923	0.4923	1.024	1.024	1.016	1.078
Oct	0.4747	0.4742	0.4742	1.024	1.024	1.016	1.08
Nov	0.3836	0.383	0.3831	1.024	1.024	1.015	1.094
Dec	0.3163	0.3157	0.3157	1.024	1.024	1.014	1.106

Appendix C: Binary ORC System Simulation Results

C.1: Binary ORC System Monthly Average Power Production Tables

Table C-1: Binary ORC System Monthly Average Power Production at 2.5km Depth

Binary ORC System Power Production					
Well Depth	2.5km				
CO2 Mass Flow	70 kg/s	90 kg/s	120 kg/s	140 kg/s	
Tres	100°C				
Jan	725.4 kW	919.3 kW	1262 kW	1461 kW	
Feb	648.6 kW	819.0 kW	1129 kW	1305 kW	
Mar	546.4 kW	685.6 kW	951.3 kW	1097 kW	
Apr	427.1 kW	530.1 kW	744.5 kW	853.8 kW	
May	325.8 kW	398.0 kW	568.9 kW	647.7 kW	
June	243.5 kW	290.3 kW	426.5 kW	480.8 kW	
July	204.9 kW	240.2 kW	359.7 kW	402.2 kW	
Aug	216.9 kW	255.8 kW	389.8 kW	426.4 kW	
Sept	295.6 kW	358.8 kW	516.7 kW	586.4 kW	
Oct	323.3 kW	394.8 kW	564.5 kW	642.7 kW	
Nov	492.3 kW	615.0 kW	857.5 kW	986.6 kW	
Dec	648.3 kW	818.5 kW	1128 kW	1304 kW	
Total Power	5098 kW	6325 kW	8898 kW	10193 kW	
Tres	125°C				
Jan	1124 kW	1410 kW	1958 kW	2256 kW	
Feb	1025 kW	1278 kW	1785 kW	2051 kW	
Mar	889.5 kW	1103 kW	1552 kW	1778 kW	
Apr	731.0 kW	896.1 kW	1276 kW	1455 kW	
May	594.1 kW	717.7 kW	1039 kW	1177 kW	
June	481.0 kW	570.9 kW	843.1 kW	947.7 kW	
July	435.7 kW	512.3 kW	764.7 kW	856.1 kW	
Aug	452.3 kW	533.7 kW	793.4 kW	889.7 kW	
Sept	552.8 kW	664.1 kW	967.5 kW	1093 kW	
Oct	590.6 kW	713.3 kW	1033 kW	1170 kW	
Nov	818.0 kW	1010 kW	1427 kW	1632 kW	
Dec	1024 kW	1278 kW	1784 kW	2050 kW	
Total Power	8717 kW	10688 kW	15221 kW	17357 kW	
Tres	150°C				
Jan	1501 kW	1851 kW	2619 kW	2994 kW	
Feb	1381 kW	1694 kW	2412 kW	2752 kW	
Mar	1222 kW	1487 kW	2134 kW	2426 kW	
Apr	1034 kW	1240 kW	1806 kW	2043 kW	
May	868.5 kW	1029 kW	1524 kW	1711 kW	
June	735.2 kW	854.8 kW	1290 kW	1439 kW	
July	679.1 kW	785.6 kW	1196 kW	1333 kW	
Aug	699.1 kW	811.0 kW	1231 kW	1373 kW	
Sept	819.3 kW	965.3 kW	1442 kW	1612 kW	
Oct	864.4 kW	1024 kW	1517 kW	1704 kW	
Nov	1136 kW	1376 kW	1987 kW	2253 kW	
Dec	1381 kW	1694 kW	2411 kW	2750 kW	
Total Power	12322 kW	14813 kW	21570 kW	24391 kW	

Table C-2: Binary ORC System Monthly Average Power Production at 3.1km Depth

Binary ORC System Power Production					
Well Depth	3.1km				
CO2 Mass Flow		70 kg/s	90 kg/s	120 kg/s	140 kg/s
Tres		100°C			
Jan		600.0 kW	760.7 kW	1044 kW	1211 kW
Feb		532.7 kW	672.9 kW	927.8 kW	1073 kW
Mar		443.6 kW	556.8 kW	773.3 kW	891.4 kW
Apr		340.7 kW	422.8 kW	594.5 kW	681.7 kW
May		254.3 kW	310.3 kW	444.5 kW	505.8 kW
June		179.7 kW	212.9 kW	323.8 kW	354.5 kW
July		152.4 kW	178.0 kW	268.1 kW	299.1 kW
Aug		162.4 kW	190.9 kW	285.3 kW	319.3 kW
Sept		228.7 kW	277.2 kW	400.3 kW	454.1 kW
Oct		252.1 kW	307.5 kW	440.7 kW	501.5 kW
Nov		396.8 kW	495.8 kW	691.9 kW	796.0 kW
Dec		532.4 kW	672.5 kW	927.3 kW	1072 kW
Total Power		4076 kW	5058 kW	7122 kW	8159 kW
Tres		125°C			
Jan		976.3 kW	1230 kW	1701 kW	1964 kW
Feb		887.3 kW	1113 kW	1546 kW	1783 kW
Mar		768.3 kW	958.3 kW	1340 kW	1540 kW
Apr		628.0 kW	775.7 kW	1096 kW	1255 kW
May		507.6 kW	619.2 kW	887.5 kW	1010 kW
June		408.4 kW	490.5 kW	715.5 kW	808.5 kW
July		368.6 kW	439.2 kW	646.7 kW	728.1 kW
Aug		383.1 kW	458.0 kW	671.9 kW	757.6 kW
Sept		471.3 kW	572.2 kW	824.8 kW	936.4 kW
Oct		504.6 kW	615.3 kW	882.3 kW	1004 kW
Nov		704.8 kW	875.7 kW	1230 kW	1411 kW
Dec		886.9 kW	1113 kW	1545 kW	1782 kW
Total Power		7495 kW	9259 kW	13088 kW	14979 kW
Tres		150°C			
Jan		1377 kW	1716 kW	2402 kW	2760 kW
Feb		1268 kW	1574 kW	2215 kW	2539 kW
Mar		1122 kW	1385 kW	1961 kW	2243 kW
Apr		950.2 kW	1161 kW	1662 kW	1897 kW
May		800.6 kW	967.1 kW	1403 kW	1589 kW
June		677.9 kW	808.4 kW	1187 kW	1340 kW
July		625.9 kW	742.0 kW	1100 kW	1239 kW
Aug		646.0 kW	765.6 kW	1132 kW	1276 kW
Sept		755.4 kW	908.7 kW	1328 kW	1498 kW
Oct		797.0 kW	962.2 kW	1397 kW	1581 kW
Nov		1045 kW	1284 kW	1827 kW	2085 kW
Dec		1268 kW	1574 kW	2214 kW	2539 kW
Total Power		11333 kW	13848 kW	19828 kW	22588 kW

Table C-3: Binary ORC System Monthly Average Power Production at 3.6km Depth

Binary ORC System Power Production					
Well Depth	3.6km				
CO2 Mass Flow	70 kg/s	90 kg/s	120 kg/s	140 kg/s	
Tres	100°C				
Jan	520.2 kW	659.4 kW	906.7 kW	1051 kW	
Feb	459.6 kW	580.5 kW	801.3 kW	926.5 kW	
Mar	379.8 kW	476.7 kW	662.6 kW	763.8 kW	
Apr	288.3 kW	357.7 kW	503.5 kW	577.3 kW	
May	212.3 kW	259.1 kW	371.5 kW	422.8 kW	
June	147.3 kW	174.9 kW	258.8 kW	290.9 kW	
July	123.9 kW	144.8 kW	218.1 kW	243.4 kW	
Aug	132.4 kW	155.7 kW	233.0 kW	260.7 kW	
Sept	190.0 kW	230.3 kW	332.9 kW	377.7 kW	
Oct	210.4 kW	256.7 kW	368.3 kW	419.0 kW	
Nov	338.1 kW	422.4 kW	590.1 kW	678.8 kW	
Dec	459.3 kW	580.2 kW	800.8 kW	926.0 kW	
Total Power	3462 kW	4298 kW	6048 kW	6938 kW	
Tres	125°C				
Jan	870.9 kW	1099 kW	1519 kW	1756 kW	
Feb	790.0 kW	994.7 kW	1378 kW	1591 kW	
Mar	682.2 kW	854.3 kW	1191 kW	1371 kW	
Apr	555.8 kW	689.9 kW	971.0 kW	1114 kW	
May	447.6 kW	549.6 kW	782.9 kW	893.5 kW	
June	358.7 kW	434.6 kW	628.7 kW	713.1 kW	
July	323.4 kW	388.9 kW	567.1 kW	641.1 kW	
Aug	336.3 kW	405.7 kW	589.7 kW	667.6 kW	
Sept	415.2 kW	507.6 kW	726.6 kW	827.6 kW	
Oct	444.8 kW	546.0 kW	778.3 kW	888.0 kW	
Nov	625.0 kW	779.9 kW	1091 kW	1255 kW	
Dec	789.7 kW	993.7 kW	1377 kW	1590 kW	
Total Power	6640 kW	8244 kW	11600 kW	13308 kW	
Tres	150°C				
Jan	1271 kW	1594 kW	2218 kW	2557 kW	
Feb	1172 kW	1465 kW	2045 kW	2353 kW	
Mar	1037 kW	1290 kW	1812 kW	2081 kW	
Apr	880.2 kW	1084 kW	1536 kW	1762 kW	
May	740.6 kW	905.9 kW	1297 kW	1481 kW	
June	627.3 kW	757.7 kW	1101 kW	1244 kW	
July	579.3 kW	699.7 kW	1016 kW	1153 kW	
Aug	597.9 kW	720.0 kW	1046 kW	1188 kW	
Sept	698.8 kW	852.1 kW	1228 kW	1393 kW	
Oct	737.1 kW	901.4 kW	1291 kW	1475 kW	
Nov	965.4 kW	1197 kW	1687 kW	1934 kW	
Dec	1171 kW	1464 kW	2044 kW	2353 kW	
Total Power	10477 kW	12931 kW	18322 kW	20974 kW	

C.2 Binary ORC System Monthly Average System Efficiency

Table C-4: Binary ORC System Monthly Average System Efficiency at 2.5km Depth

Binary ORC System Efficiency					
Well Depth 2.5km					
CO2 Mass Flow		70 kg/s	90 kg/s	120 kg/s	140 kg/s
Tres		100°C			
Jan		0.05868	0.05795	0.05950	0.05912
Feb		0.05508	0.05424	0.05586	0.05542
Mar		0.05006	0.04904	0.05078	0.05027
Apr		0.04378	0.04247	0.04444	0.04381
May		0.03799	0.03647	0.03862	0.03786
June		0.03291	0.03110	0.03351	0.03262
July		0.03080	0.02885	0.03139	0.03044
Aug		0.03158	0.02968	0.03218	0.03124
Sept		0.03617	0.03456	0.03679	0.03599
Oct		0.03784	0.03632	0.03847	0.03771
Nov		0.04727	0.04616	0.04797	0.04740
Dec		0.05507	0.05422	0.05584	0.05540
Tres		125°C			
Jan		0.06528	0.06362	0.06630	0.06546
Feb		0.06154	0.05973	0.06252	0.06160
Mar		0.05632	0.05431	0.05729	0.05628
Apr		0.04996	0.04761	0.05086	0.04970
May		0.04424	0.04155	0.04512	0.04380
June		0.03949	0.03643	0.04038	0.03889
July		0.03770	0.03445	0.03860	0.03702
Aug		0.03832	0.03515	0.03921	0.03767
Sept		0.04250	0.03968	0.04338	0.04201
Oct		0.04410	0.04140	0.04498	0.04366
Nov		0.05349	0.05133	0.05442	0.05334
Dec		0.06152	0.05971	0.06251	0.06159
Tres		150°C			
Jan		0.07327	0.07028	0.07457	0.07308
Feb		0.06941	0.06621	0.07069	0.06912
Mar		0.06412	0.06070	0.06537	0.06368
Apr		0.05782	0.05392	0.05891	0.05707
May		0.05206	0.04794	0.05328	0.05128
June		0.04763	0.04305	0.04876	0.04659
July		0.04585	0.04123	0.04711	0.04498
Aug		0.04643	0.04187	0.04768	0.04558
Sept		0.05037	0.04614	0.05173	0.04955
Oct		0.05192	0.04779	0.05314	0.05114
Nov		0.06122	0.05766	0.06247	0.06071
Dec		0.06940	0.06619	0.07067	0.06910

Table C-5: Binary ORC System Monthly Average System Efficiency at 3.1km Depth

Binary ORC System Efficiency					
Well Depth 3.1km					
CO2 Mass Flow		70 kg/s	90 kg/s	120 kg/s	140 kg/s
Tres		100°C			
Jan		0.04893	0.04821	0.04968	0.04931
Feb		0.04560	0.04477	0.04632	0.04589
Mar		0.04097	0.03996	0.04165	0.04113
Apr		0.03523	0.03397	0.03586	0.03522
May		0.03004	0.02848	0.03063	0.02986
June		0.02491	0.02291	0.02617	0.02453
July		0.02312	0.02096	0.02372	0.02265
Aug		0.02375	0.02167	0.02433	0.02332
Sept		0.02844	0.02677	0.02902	0.02819
Oct		0.02991	0.02834	0.03049	0.02972
Nov		0.03842	0.03730	0.03907	0.03850
Dec		0.04558	0.04476	0.04631	0.04587
Tres		125°C			
Jan		0.06196	0.06066	0.06297	0.06230
Feb		0.05847	0.05704	0.05944	0.05871
Mar		0.05364	0.05201	0.05457	0.05375
Apr		0.04772	0.04581	0.04859	0.04764
May		0.04245	0.04024	0.04329	0.04221
June		0.03814	0.03559	0.03897	0.03772
July		0.03655	0.03383	0.03740	0.03606
Aug		0.03709	0.03444	0.03794	0.03664
Sept		0.04086	0.03854	0.04170	0.04056
Oct		0.04232	0.04011	0.04316	0.04207
Nov		0.05099	0.04925	0.05190	0.05102
Dec		0.05846	0.05702	0.05943	0.05869
Tres		150°C			
Jan		0.07244	0.07017	0.07373	0.07259
Feb		0.06884	0.06643	0.07010	0.06889
Mar		0.06390	0.06127	0.06512	0.06381
Apr		0.05790	0.05498	0.05908	0.05777
May		0.05265	0.04943	0.05381	0.05223
June		0.04856	0.04501	0.04959	0.04798
July		0.04693	0.04323	0.04810	0.04641
Aug		0.04756	0.04381	0.04861	0.04695
Sept		0.05108	0.04776	0.05237	0.05061
Oct		0.05252	0.04929	0.05368	0.05209
Nov		0.06121	0.05846	0.06240	0.06104
Dec		0.06883	0.06642	0.07009	0.06888

Table C-6: Binary ORC System Monthly Average System Efficiency at 3.6km Depth

Binary ORC System Efficiency					
Well Depth 3.6km					
CO2 Mass Flow	70 kg/s	90 kg/s	120 kg/s	140 kg/s	
Tres		100°C			
Jan	0.04573	0.04510	0.04652	0.04617	
Feb	0.04257	0.04184	0.04332	0.04293	
Mar	0.03821	0.03732	0.03891	0.03844	
Apr	0.03283	0.03171	0.03348	0.03289	
May	0.02802	0.02662	0.02864	0.02792	
June	0.02328	0.02152	0.02389	0.02301	
July	0.02172	0.01976	0.02234	0.02136	
Aug	0.02226	0.02038	0.02288	0.02193	
Sept	0.02655	0.02506	0.02717	0.02641	
Oct	0.02790	0.02650	0.02851	0.02779	
Nov	0.03581	0.03482	0.03649	0.03597	
Dec	0.04256	0.04183	0.04331	0.04292	
Tres		125°C			
Jan	0.05925	0.05818	0.06026	0.05970	
Feb	0.05596	0.05478	0.05693	0.05633	
Mar	0.05144	0.05009	0.05236	0.05167	
Apr	0.04593	0.04433	0.04679	0.04599	
May	0.04108	0.03922	0.04191	0.04098	
June	0.03719	0.03503	0.03800	0.03694	
July	0.03583	0.03350	0.03665	0.03550	
Aug	0.03629	0.03403	0.03710	0.03598	
Sept	0.03963	0.03767	0.04045	0.03948	
Oct	0.04096	0.03909	0.04179	0.04086	
Nov	0.04897	0.04752	0.04986	0.04913	
Dec	0.05595	0.05477	0.05692	0.05631	
Tres		150°C			
Jan	0.07109	0.06933	0.07238	0.07149	
Feb	0.06771	0.06583	0.06896	0.06801	
Mar	0.06307	0.06101	0.06428	0.06324	
Apr	0.05760	0.05516	0.05863	0.05761	
May	0.05261	0.05004	0.05374	0.05259	
June	0.04891	0.04593	0.05002	0.04849	
July	0.04747	0.04458	0.04858	0.04723	
Aug	0.04802	0.04496	0.04902	0.04769	
Sept	0.05118	0.04851	0.05242	0.05098	
Oct	0.05249	0.04991	0.05362	0.05247	
Nov	0.06056	0.05839	0.06174	0.06065	
Dec	0.06770	0.06581	0.06895	0.06800	

C.3 Binary ORC System Monthly Average Power Production Plots

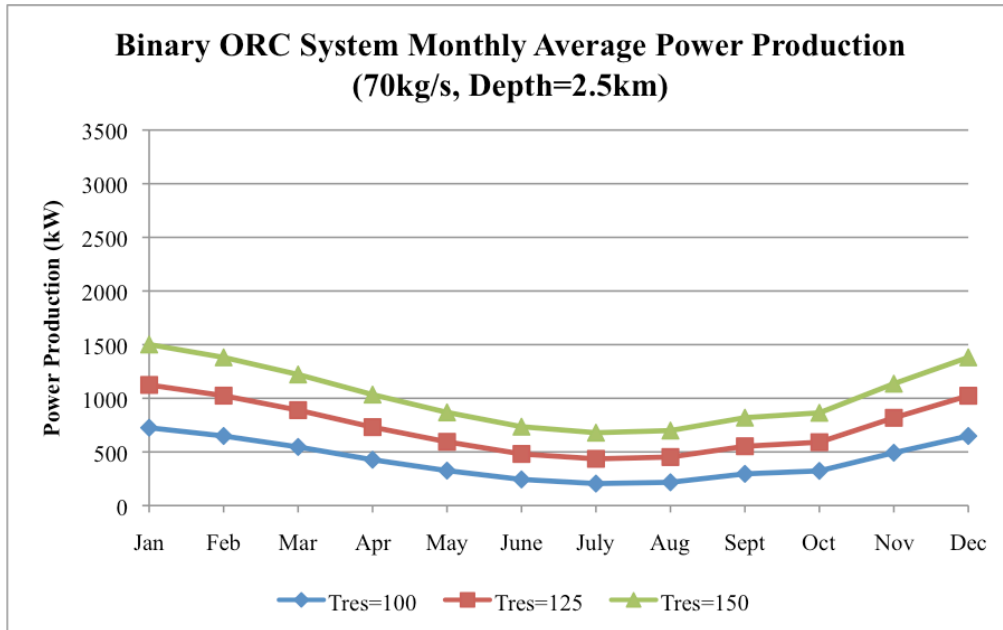


Figure C-1: Binary ORC System monthly average power production simulation results at 2.5km depth with a CO₂ mass flow rate of 70kg/s for various reservoir temperatures.

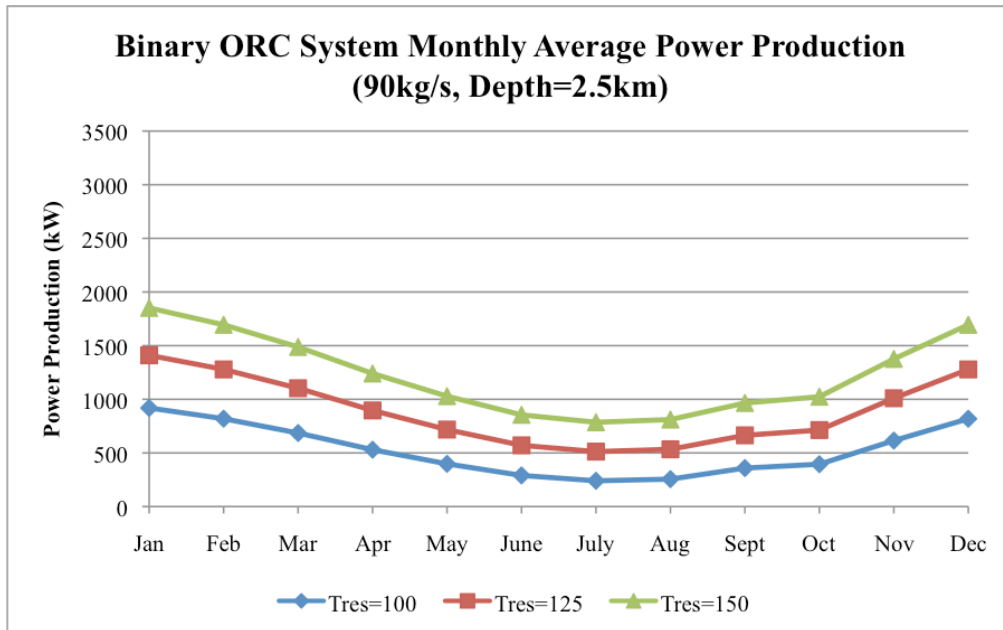


Figure C-2: Binary ORC System monthly average power production simulation results at 2.5km depth with a CO₂ mass flow rate of 90kg/s for various reservoir temperatures.

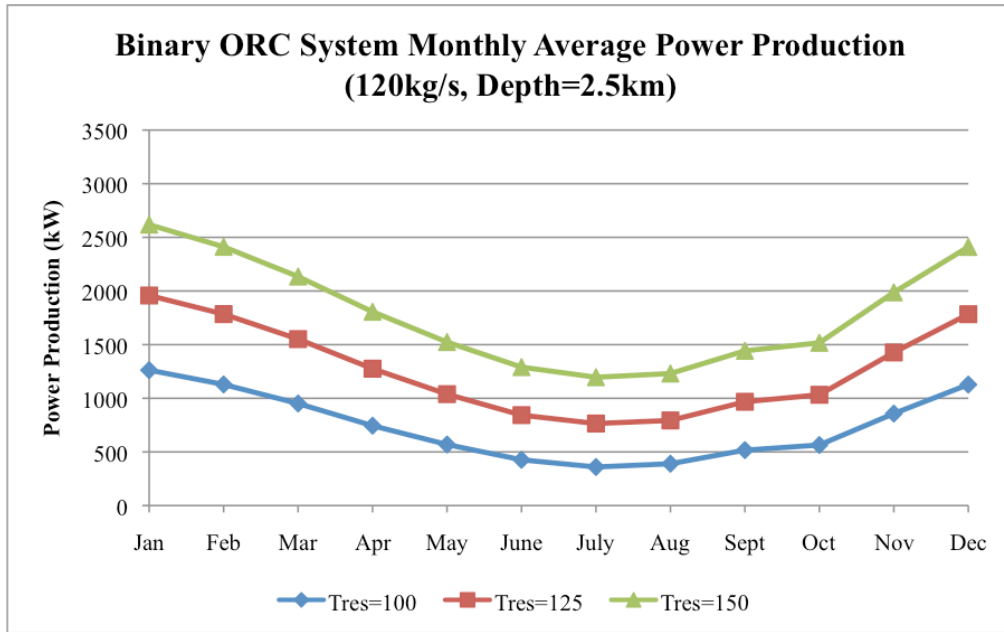


Figure C-3: Binary ORC System monthly average power production simulation results at 2.5km depth with a CO₂ mass flow rate of 120kg/s for various reservoir temperatures.

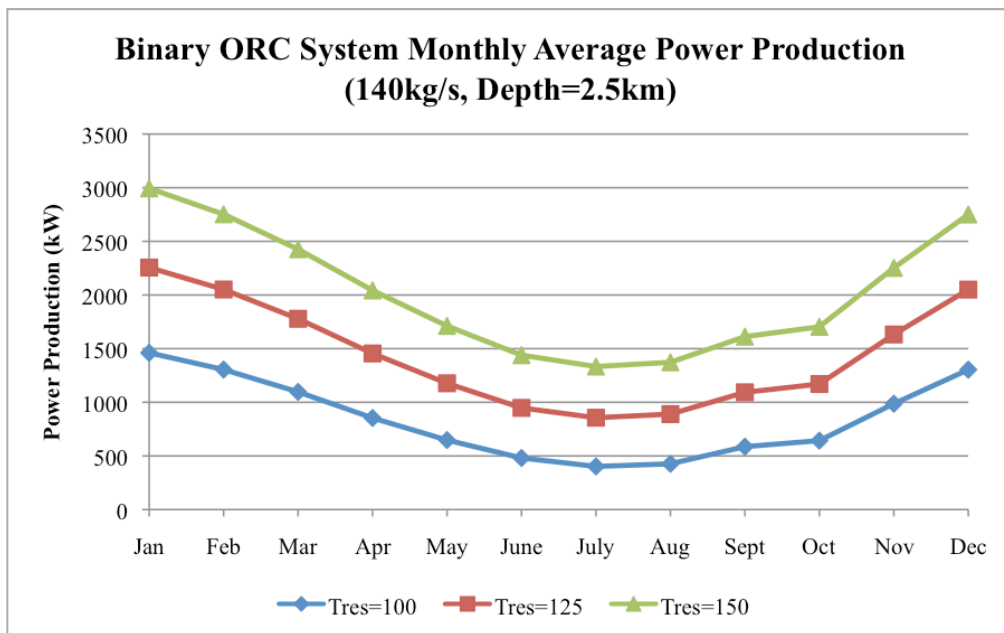


Figure C-4: Binary ORC System monthly average power production simulation results at 2.5km depth with a CO₂ mass flow rate of 140kg/s for various reservoir temperatures.

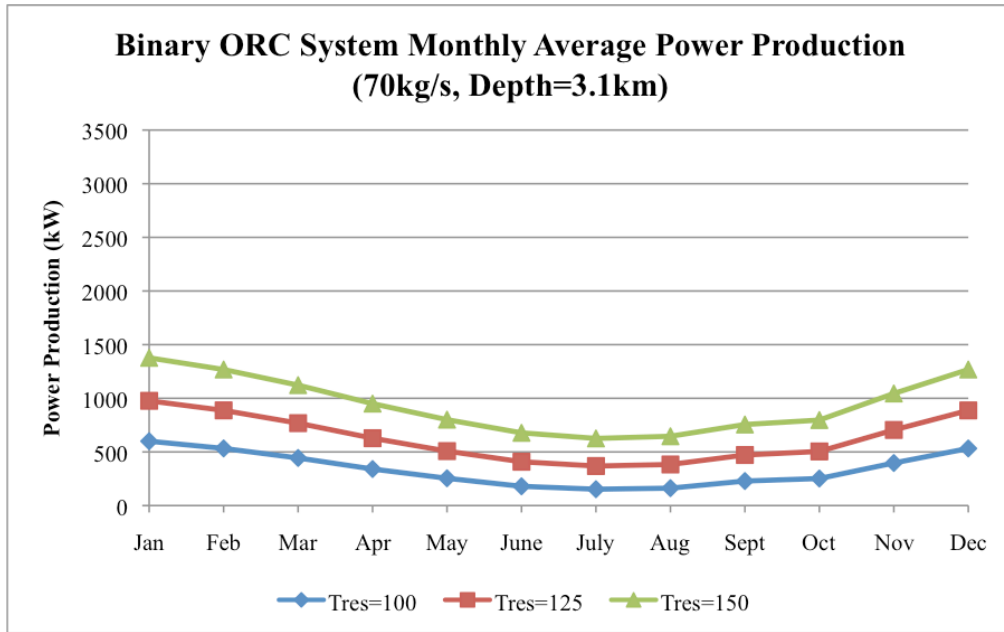


Figure C-5: Binary ORC System monthly average power production simulation results at 3.1km depth with a CO2 mass flow rate of 70kg/s for various reservoir temperatures.

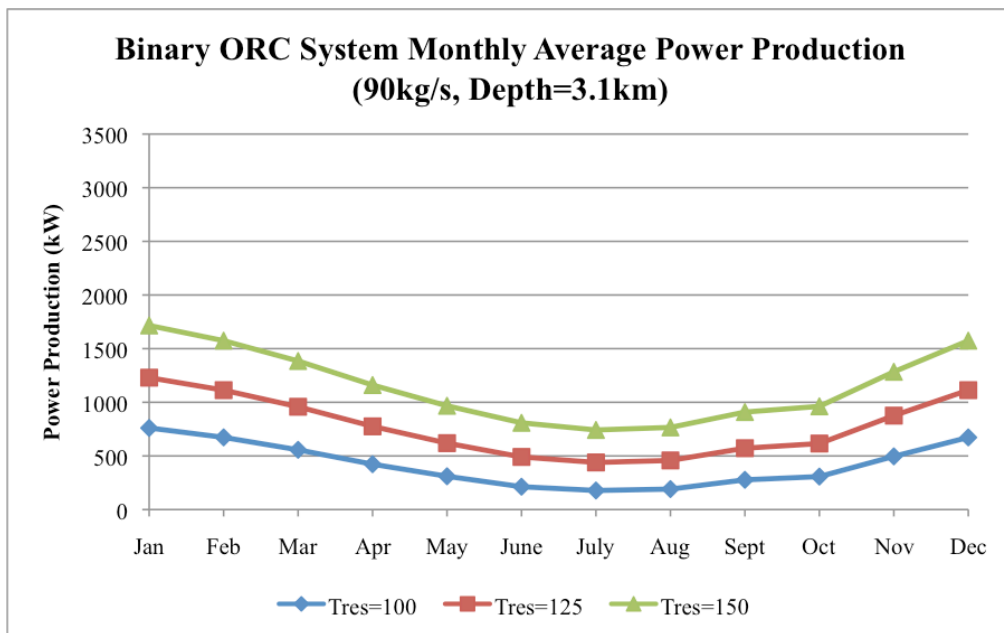


Figure C-6: Binary ORC System monthly average power production simulation results at 3.1km depth with a CO2 mass flow rate of 90kg/s for various reservoir temperatures.

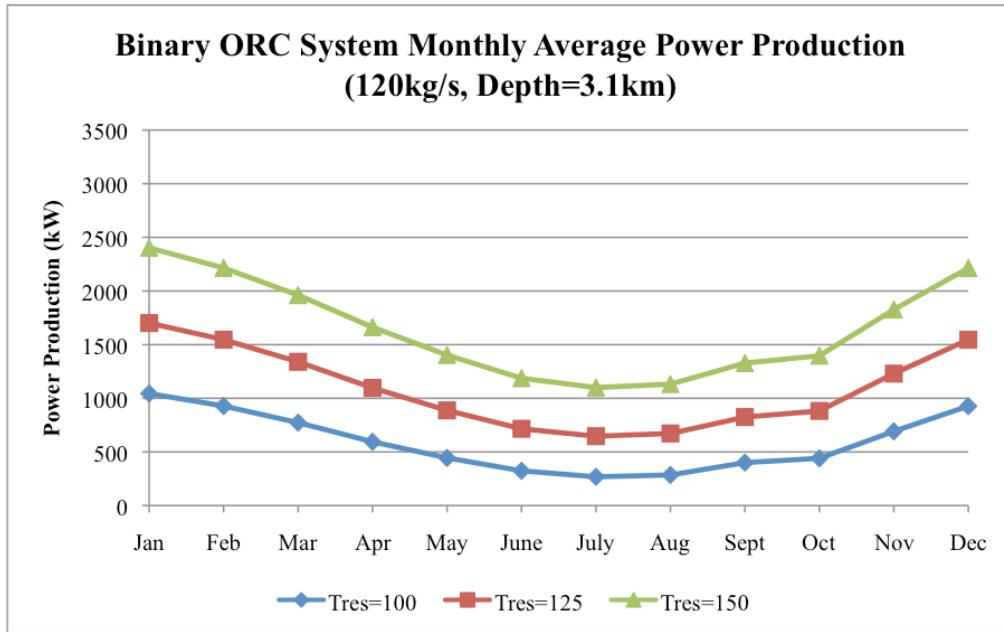


Figure C-7: Binary ORC System monthly average power production simulation results at 3.1km depth with a CO2 mass flow rate of 120kg/s for various reservoir temperatures.

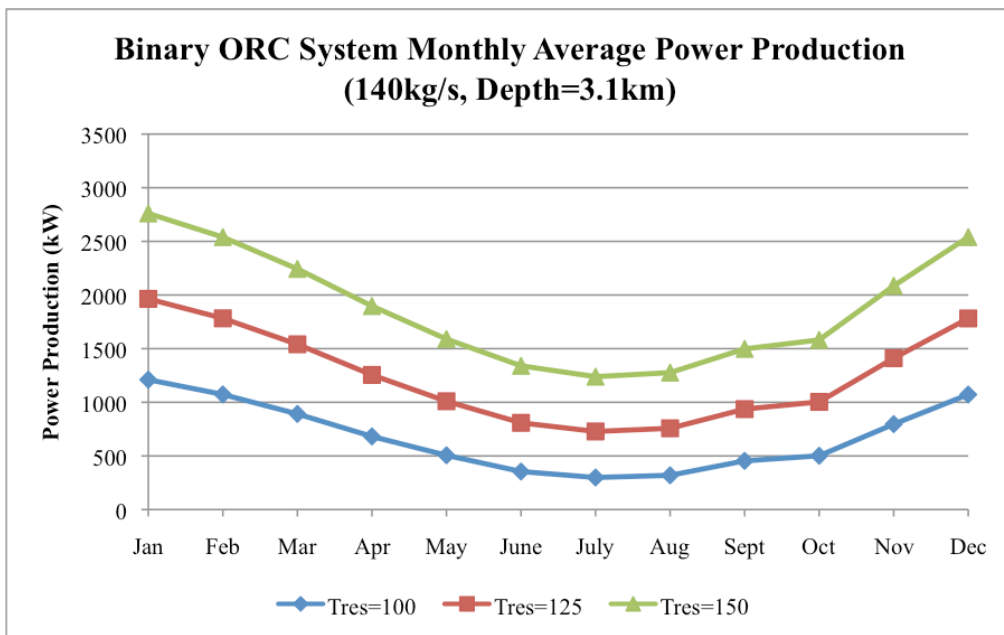


Figure C-8: Binary ORC System monthly average power production simulation results at 3.1km depth with a CO2 mass flow rate of 140kg/s for various reservoir temperatures.

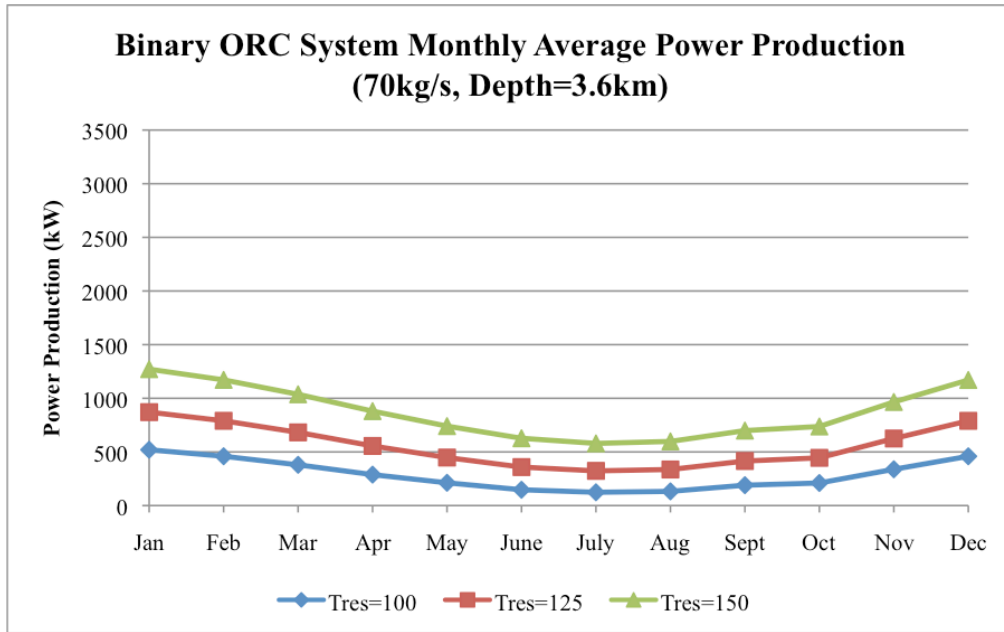


Figure C-9: Binary ORC System monthly average power production simulation results at 3.6km depth with a CO₂ mass flow rate of 70kg/s for various reservoir temperatures.

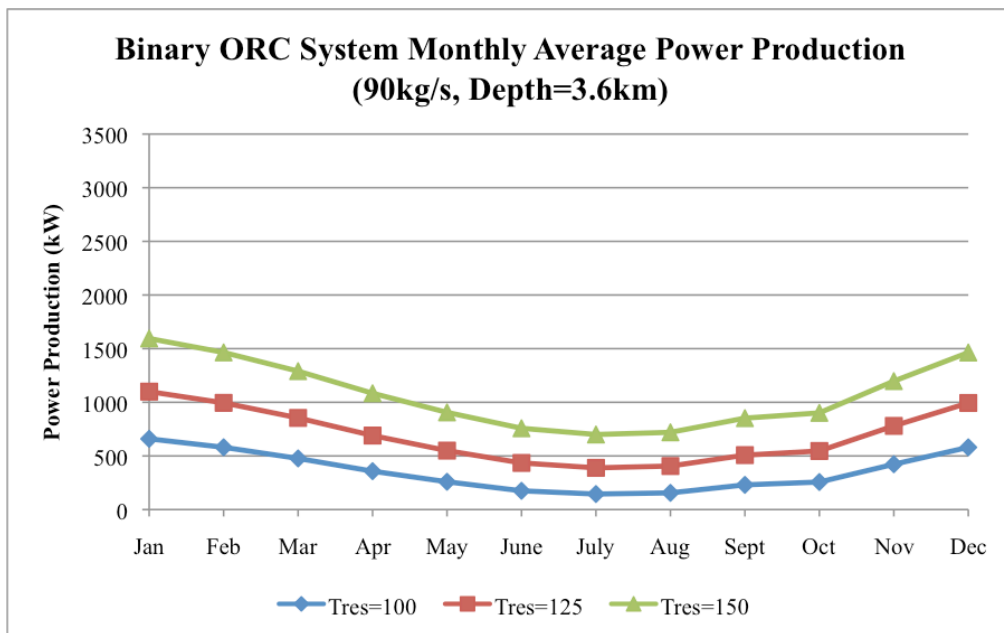


Figure C-10: Binary ORC System monthly average power production simulation results at 3.6km depth with a CO₂ mass flow rate of 90kg/s for various reservoir temperatures.

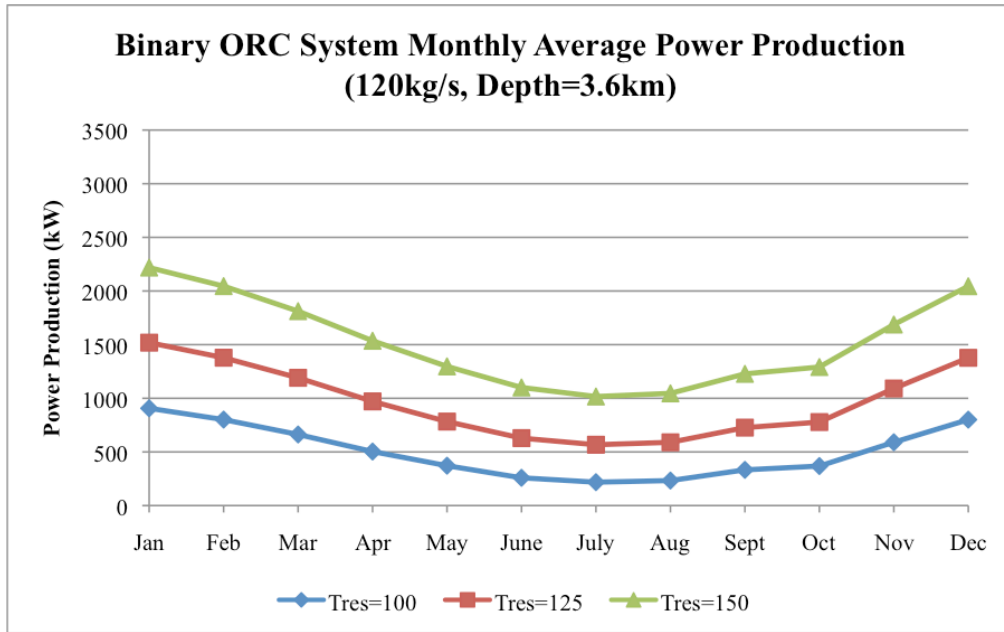


Figure C-11: Binary ORC System monthly average power production simulation results at 3.6km depth with a CO2 mass flow rate of 120kg/s for various reservoir temperatures.

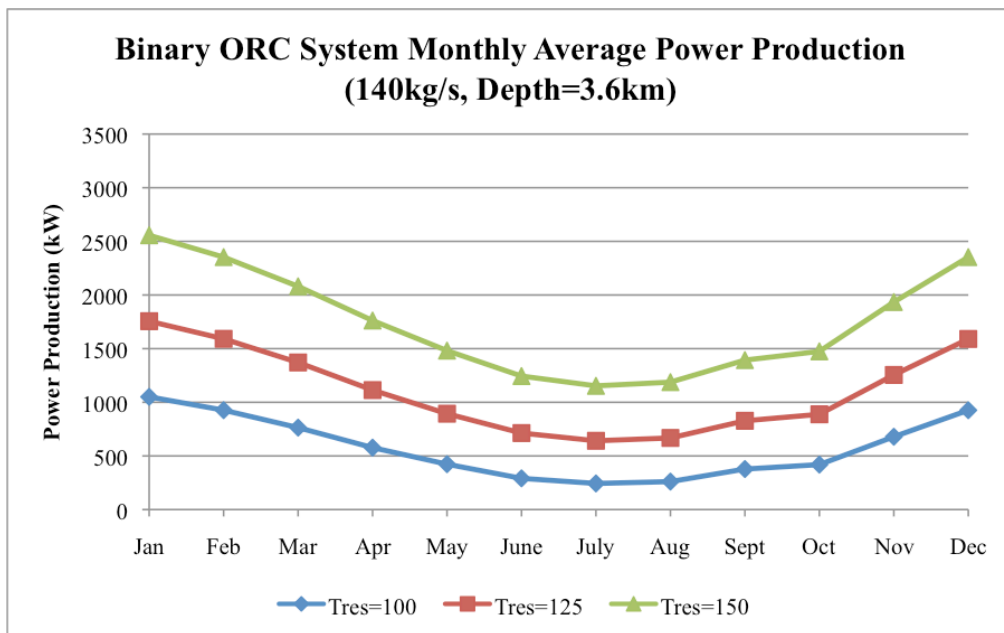


Figure C-12: Binary ORC System monthly average power production simulation results at 3.6km depth with a CO2 mass flow rate of 140kg/s for various reservoir temperatures.

Appendix D: Binary ORC System Thermodynamic Property Tables

The state points listed in the tables refer to those labeled in figure 3-10.

Table D-1: Thermodynamic properties for Binary ORC System simulations at 2.5km depth with a CO₂ mass flow rate of 70kg/s and a reservoir temperature of 100°C.

Well Temp	100°C											
Well Depth	2.5 km											
CO₂ Mass Flow	70 kg/s											
	Pressure (kPa)											
State Point	1	1'	2	3	4	4'	5	5'	6	7	8	9
Jan	2985	2986	27072	25000	11380	11108	11108	2986	404.5	404.5	127.2	127.2
Feb	3285	3286	26933	25000	11380	11108	11108	3286	416	416	144.7	144.7
Mar	3748	3749	26736	25000	11380	11108	11108	3749	439.7	439.7	172.7	172.7
Apr	4409	4410	26468	25000	11380	11107	11107	4410	470.8	470.8	214.3	214.3
May	5116	5117	26164	25000	11380	11107	11107	5117	496.9	496.9	260.6	260.6
June	5836	5838	25776	25000	11380	11107	11107	5838	523.9	523.9	309.3	309.3
July	6173	6174	25530	25000	11380	11107	11107	6174	537.9	537.9	332.3	332.3
Aug	6045	6047	25636	25000	11380	11107	11107	6047	530.9	530.9	323.6	323.6
Sept	5361	5362	26044	25000	11380	11107	11107	5362	503.5	503.5	277	277
Oct	5135	5137	26154	25000	11380	11107	11107	5137	496.9	496.9	261.9	261.9
Nov	4029	4030	26622	25000	11380	11108	11108	4030	452	452	190.2	190.2
Dec	3286	3288	26932	25000	11380	11108	11108	3288	416	416	144.8	144.8
	Temperature (°C)											
State Point	1	1'	2	3	4	4'	5	5'	6	7	8	9
Jan	-5.73	-5.72	8.958	100	55.9	53.79	26.86	-5.72	-5.57	30	0.757	-5.73
Feb	-2.21	-2.2	13.29	100	55.9	53.83	28.56	-2.2	-2.07	31	4.026	-2.21
Mar	2.773	2.785	19.6	100	55.9	53.88	31.41	2.785	2.89	33	8.725	2.773
Apr	9.159	9.17	28.02	100	55.9	53.95	34.87	9.17	9.236	35.5	14.61	9.159
May	15.23	15.24	36.57	100	55.9	54.02	37.65	15.24	15.26	37.5	20	15.23
June	20.79	20.8	45.18	100	55.9	54.08	40.19	20.8	20.78	39.5	24.91	20.79
July	23.2	23.21	49.36	100	55.9	54.1	41.37	23.21	23.3	40.5	27.05	23.2
Aug	22.3	22.31	47.72	100	55.9	54.09	40.83	22.31	22.4	40	26.22	22.3
Sept	17.19	17.2	39.5	100	55.9	54.04	38.38	17.2	17.21	38	21.69	17.19
Oct	15.39	15.4	36.81	100	55.9	54.02	37.67	15.4	15.42	37.5	20.13	15.39
Nov	5.583	5.595	23.25	100	55.9	53.91	32.87	5.595	5.683	34	11.31	5.583
Dec	-2.2	-2.19	13.32	100	55.9	53.83	28.56	-2.19	-2.06	31	4.038	-2.2
	Enthalpy (kJ/kg)											
State Point	1	1'	2	3	4	4'	5	5'	6	7	8	9
Jan	73.46	73.68	97.82	291.5	265.4	260.8	146.1	146.1	74.99	482.5	445.3	74.57
Feb	81.77	81.98	106.1	291.5	265.4	261	150.8	150.8	82.96	483.9	449.7	82.54
Mar	93.98	94.19	118.3	291.5	265.4	261.3	159.2	159.2	94.38	486.5	456.1	93.96
Apr	110.6	110.8	134.9	291.5	265.4	261.7	170.1	170.1	109.2	489.9	464.1	108.8
May	127.8	128	152.1	291.5	265.4	262.1	179.7	179.7	123.5	492.5	471.3	123.1
June	145.7	145.8	170	291.5	265.4	262.4	189.3	189.3	136.8	495.2	477.8	136.4
July	154.6	154.8	178.9	291.5	265.4	262.6	194.1	194.1	143	496.5	480.6	142.3
Aug	151.1	151.2	175.3	291.5	265.4	262.5	191.9	191.9	140.8	495.8	479.5	140.1
Sept	133.8	134	158.1	291.5	265.4	262.2	182.3	182.3	128.1	493.2	473.5	127.8
Oct	128.3	128.5	152.6	291.5	265.4	262.1	179.7	179.7	123.9	492.5	471.5	123.5
Nov	101.1	101.3	125.5	291.5	265.4	261.5	163.7	163.7	100.9	487.9	459.6	100.5
Dec	81.81	82.02	106.2	291.5	265.4	261	150.9	150.9	82.99	483.9	449.7	82.57
	Entropy (kJ/kg-K)											
State Point	1	1'	2	3	4	4'	5	5'	6	7	8	9
Jan	0.286	0.287	0.286	0.886	0.886	0.874	0.51	0.558	0.297	1.659	1.683	0.297
Feb	0.316	0.316	0.316	0.886	0.886	0.875	0.526	0.571	0.327	1.66	1.682	0.327
Mar	0.358	0.359	0.358	0.886	0.886	0.875	0.553	0.595	0.368	1.661	1.681	0.368
Apr	0.415	0.416	0.415	0.886	0.886	0.877	0.589	0.626	0.421	1.664	1.68	0.421
May	0.473	0.473	0.473	0.886	0.886	0.878	0.62	0.652	0.471	1.666	1.678	0.471
June	0.531	0.532	0.531	0.886	0.886	0.879	0.651	0.679	0.517	1.667	1.678	0.517
July	0.56	0.56	0.56	0.886	0.886	0.879	0.666	0.693	0.536	1.668	1.678	0.536
Aug	0.548	0.549	0.548	0.886	0.886	0.879	0.659	0.686	0.529	1.668	1.678	0.529
Sept	0.492	0.493	0.492	0.886	0.886	0.878	0.628	0.659	0.487	1.666	1.678	0.487
Oct	0.474	0.475	0.474	0.886	0.886	0.878	0.62	0.653	0.472	1.666	1.678	0.473
Nov	0.383	0.384	0.383	0.886	0.886	0.876	0.568	0.607	0.392	1.662	1.68	0.392
Dec	0.316	0.317	0.316	0.886	0.886	0.875	0.526	0.571	0.327	1.66	1.682	0.327

Table D-2: Thermodynamic properties for Binary ORC System simulations at 2.5km depth with a CO2 mass flow rate of 90kg/s and a reservoir temperature of 100°C.

Well Temp	100°C											
Well Depth	2.5 km											
CO2 Mass Flow	90 kg/s											
	Pressure (kPa)											
State Point	1	1'	2	3	4	4'	5	5'	6	7	8	9
Jan	2985	2987	26983	25000	10901	10438	10438	2987	393.2	393.2	127.2	127.2
Feb	3285	3287	26843	25000	10901	10438	10438	3287	404.5	404.5	144.7	144.7
Mar	3748	3750	26642	25000	10901	10437	10437	3750	427.7	427.7	172.7	172.7
Apr	4409	4411	26370	25000	10901	10437	10437	4411	452	452	214.3	214.3
May	5116	5118	26060	25000	10901	10436	10436	5118	477.2	477.2	260.6	260.6
June	5836	5839	25665	25000	10901	10436	10436	5839	510.3	510.3	309.3	309.3
July	6173	6175	25416	25000	10901	10436	10436	6175	517.1	517.1	332.3	332.3
Aug	6045	6048	25523	25000	10901	10436	10436	6048	510.3	510.3	323.6	323.6
Sept	5361	5363	25938	25000	10901	10436	10436	5363	483.7	483.7	277	277
Oct	5135	5137	26050	25000	10901	10436	10436	5137	477.2	477.2	261.9	261.9
Nov	4029	4031	26527	25000	10901	10437	10437	4031	433.7	433.7	190.2	190.2
Dec	3286	3288	26842	25000	10901	10438	10438	3288	404.5	404.5	144.8	144.8
	Temperature (°C)											
State Point	1	1'	2	3	4	4'	5	5'	6	7	8	9
Jan	-5.73	-5.71	8.912	100	53.46	50.51	25.78	-5.71	-5.57	29	0.517	-5.73
Feb	-2.21	-2.19	13.24	100	53.46	50.53	27.48	-2.19	-2.07	30	3.785	-2.21
Mar	2.773	2.793	19.54	100	53.46	50.57	30.36	2.793	2.886	32	8.482	2.773
Apr	9.159	9.177	27.95	100	53.46	50.62	33.37	9.177	9.229	34	14.24	9.159
May	15.23	15.25	36.49	100	53.46	50.66	36.14	15.25	15.26	36	19.64	15.23
June	20.79	20.81	45.08	100	53.46	50.7	39.12	20.81	20.78	38.5	24.66	20.79
July	23.2	23.22	49.24	100	53.46	50.72	39.84	23.22	23.3	39	26.68	23.2
Aug	22.3	22.32	47.61	100	53.46	50.71	39.3	22.32	22.4	38.5	25.85	22.3
Sept	17.19	17.21	39.41	100	53.46	50.67	36.87	17.21	17.2	36.5	21.32	17.19
Oct	15.39	15.41	36.73	100	53.46	50.66	36.16	15.41	15.42	36	19.76	15.39
Nov	5.583	5.602	23.19	100	53.46	50.59	31.35	5.602	5.676	32.5	10.94	5.583
Dec	-2.2	-2.18	13.26	100	53.46	50.53	27.49	-2.18	-2.06	30	3.798	-2.2
	Enthalpy (kJ/kg)											
State Point	1	1'	2	3	4	4'	5	5'	6	7	8	9
Jan	73.46	73.63	97.73	291.5	264.3	260.3	144.6	144.6	74.97	481.2	444.9	74.57
Feb	81.77	81.94	106	291.5	264.3	260.4	149.5	149.5	82.94	482.5	449.3	82.54
Mar	93.98	94.15	118.2	291.5	264.3	260.7	158.2	158.2	94.36	485.2	455.7	93.96
Apr	110.6	110.7	134.8	291.5	264.3	261	168.1	168.1	109.2	487.9	463.5	108.8
May	127.8	128	152	291.5	264.3	261.2	178.1	178.1	123.5	490.5	470.7	123.1
June	145.7	145.8	169.8	291.5	264.3	261.5	190.3	190.3	136.7	493.8	477.3	136.4
July	154.6	154.7	178.7	291.5	264.3	261.6	193.6	193.6	143	494.5	479.9	142.3
Aug	151.1	151.2	175.2	291.5	264.3	261.6	191.1	191.1	140.8	493.8	478.8	140.1
Sept	133.8	134	158	291.5	264.3	261.3	180.9	180.9	128.1	491.2	472.9	127.8
Oct	128.3	128.4	152.5	291.5	264.3	261.2	178.2	178.2	123.8	490.5	470.8	123.5
Nov	101.1	101.3	125.4	291.5	264.3	260.8	161.4	161.4	100.8	485.9	459	100.5
Dec	81.81	81.98	106.1	291.5	264.3	260.4	149.6	149.6	82.97	482.5	449.3	82.57
	Entropy (kJ/kg-K)											
State Point	1	1'	2	3	4	4'	5	5'	6	7	8	9
Jan	0.286	0.287	0.286	0.886	0.886	0.877	0.508	0.552	0.297	1.658	1.682	0.297
Feb	0.316	0.316	0.316	0.886	0.886	0.877	0.524	0.566	0.327	1.659	1.68	0.327
Mar	0.358	0.359	0.358	0.886	0.886	0.878	0.553	0.591	0.368	1.661	1.679	0.368
Apr	0.415	0.416	0.415	0.886	0.886	0.879	0.585	0.619	0.421	1.662	1.677	0.421
May	0.473	0.473	0.473	0.886	0.886	0.88	0.618	0.647	0.471	1.664	1.676	0.471
June	0.531	0.531	0.531	0.886	0.886	0.881	0.657	0.683	0.517	1.666	1.676	0.517
July	0.56	0.56	0.56	0.886	0.886	0.881	0.668	0.691	0.536	1.667	1.676	0.536
Aug	0.548	0.549	0.548	0.886	0.886	0.881	0.66	0.684	0.529	1.666	1.675	0.529
Sept	0.492	0.493	0.492	0.886	0.886	0.88	0.627	0.654	0.487	1.665	1.676	0.487
Oct	0.474	0.475	0.474	0.886	0.886	0.88	0.618	0.647	0.472	1.664	1.676	0.473
Nov	0.383	0.384	0.383	0.886	0.886	0.879	0.563	0.599	0.392	1.661	1.678	0.392
Dec	0.316	0.316	0.316	0.886	0.886	0.877	0.524	0.566	0.327	1.659	1.68	0.327

Table D-3: Thermodynamic properties for Binary ORC System simulations at 2.5km depth with a CO2 mass flow rate of 120kg/s and a reservoir temperature of 100°C.

Well Temp	100°C											
Well Depth	2.5 km											
CO2 Mass Flow	120 kg/s											
	Pressure (kPa)											
State Point	1	1'	2	3	4	4'	5	5'	6	7	8	9
Jan	2985	2986	27055	25000	11461	11219	11219	2986	410.2	410.2	127.2	127.2
Feb	3285	3286	26917	25000	11461	11219	11219	3286	421.8	421.8	144.7	144.7
Mar	3748	3749	26719	25000	11461	11219	11219	3749	445.8	445.8	172.7	172.7
Apr	4409	4410	26450	25000	11461	11218	11218	4410	470.8	470.8	214.3	214.3
May	5116	5117	26144	25000	11461	11218	11218	5117	496.9	496.9	260.6	260.6
June	5836	5838	25755	25000	11461	11218	11218	5838	523.9	523.9	309.3	309.3
July	6173	6174	25509	25000	11461	11218	11218	6174	545	545	332.3	332.3
Aug	6045	6047	25615	25000	11461	11218	11218	6047	545	545	323.6	323.6
Sept	5361	5363	26024	25000	11461	11218	11218	5363	510.3	510.3	277	277
Oct	5135	5137	26135	25000	11461	11218	11218	5137	496.9	496.9	261.9	261.9
Nov	4029	4030	26605	25000	11461	11219	11219	4030	452	452	190.2	190.2
Dec	3286	3288	26916	25000	11461	11219	11219	3288	421.8	421.8	144.8	144.8
	Temperature (°C)											
State Point	1	1'	2	3	4	4'	5	5'	6	7	8	9
Jan	-5.73	-5.72	8.95	100	56.3	54.55	27.29	-5.72	-5.56	30.5	0.877	-5.73
Feb	-2.21	-2.2	13.28	100	56.3	54.57	29	-2.2	-2.07	31.5	4.147	-2.21
Mar	2.773	2.786	19.59	100	56.3	54.61	31.87	2.786	2.892	33.5	8.847	2.773
Apr	9.159	9.171	28.01	100	56.3	54.67	34.88	9.171	9.236	35.5	14.61	9.159
May	15.23	15.24	36.56	100	56.3	54.71	37.67	15.24	15.26	37.5	20	15.23
June	20.79	20.8	45.16	100	56.3	54.76	40.22	20.8	20.78	39.5	24.91	20.79
July	23.2	23.21	49.34	100	56.3	54.78	41.85	23.21	23.3	41	27.17	23.2
Aug	22.3	22.31	47.7	100	56.3	54.77	41.73	22.31	22.29	41	26.46	22.3
Sept	17.19	17.2	39.48	100	56.3	54.73	38.85	17.2	17.21	38.5	21.81	17.19
Oct	15.39	15.4	36.8	100	56.3	54.72	37.7	15.4	15.42	37.5	20.13	15.39
Nov	5.583	5.596	23.24	100	56.3	54.64	32.87	5.596	5.683	34	11.31	5.583
Dec	-2.2	-2.19	13.31	100	56.3	54.57	29	-2.19	-2.05	31.5	4.159	-2.2
	Enthalpy (kJ/kg)											
State Point	1	1'	2	3	4	4'	5	5'	6	7	8	9
Jan	73.46	73.61	97.81	291.5	265.6	262.2	147	147	75	483.2	445.5	74.57
Feb	81.77	81.92	106.1	291.5	265.6	262.3	151.8	151.8	82.97	484.5	449.9	82.54
Mar	93.98	94.13	118.3	291.5	265.6	262.5	160.2	160.2	94.39	487.2	456.3	93.96
Apr	110.6	110.7	134.9	291.5	265.6	262.8	169.7	169.7	109.2	489.9	464.1	108.8
May	127.8	127.9	152.1	291.5	265.6	263.1	179.1	179.1	123.5	492.5	471.3	123.1
June	145.7	145.8	169.9	291.5	265.6	263.3	188.6	188.6	136.8	495.2	477.8	136.4
July	154.6	154.7	178.8	291.5	265.6	263.4	195.2	195.2	143	497.1	480.8	142.3
Aug	151.1	151.2	175.3	291.5	265.6	263.4	194.7	194.7	140.4	497.1	479.9	140.1
Sept	133.8	133.9	158.1	291.5	265.6	263.2	183.4	183.4	128.2	493.8	473.7	127.8
Oct	128.3	128.4	152.6	291.5	265.6	263.1	179.2	179.2	123.9	492.5	471.5	123.5
Nov	101.1	101.3	125.5	291.5	265.6	262.7	163.3	163.3	100.9	487.9	459.6	100.5
Dec	81.81	81.96	106.2	291.5	265.6	262.3	151.8	151.8	83	484.5	449.9	82.57
	Entropy (kJ/kg-K)											
State Point	1	1'	2	3	4	4'	5	5'	6	7	8	9
Jan	0.286	0.287	0.286	0.886	0.886	0.877	0.513	0.561	0.297	1.659	1.684	0.297
Feb	0.316	0.316	0.316	0.886	0.886	0.878	0.529	0.574	0.327	1.66	1.682	0.327
Mar	0.358	0.359	0.358	0.886	0.886	0.878	0.556	0.599	0.368	1.662	1.681	0.368
Apr	0.415	0.416	0.415	0.886	0.886	0.879	0.587	0.625	0.421	1.664	1.68	0.421
May	0.473	0.473	0.473	0.886	0.886	0.88	0.618	0.651	0.471	1.666	1.678	0.471
June	0.531	0.531	0.531	0.886	0.886	0.881	0.648	0.677	0.517	1.667	1.678	0.517
July	0.56	0.56	0.56	0.886	0.886	0.881	0.669	0.697	0.536	1.669	1.678	0.536
Aug	0.548	0.548	0.548	0.886	0.886	0.881	0.667	0.696	0.529	1.669	1.679	0.529
Sept	0.492	0.493	0.492	0.886	0.886	0.88	0.631	0.663	0.487	1.666	1.679	0.487
Oct	0.474	0.475	0.474	0.886	0.886	0.88	0.618	0.651	0.472	1.666	1.678	0.473
Nov	0.383	0.384	0.383	0.886	0.886	0.879	0.566	0.606	0.392	1.662	1.68	0.392
Dec	0.316	0.316	0.316	0.886	0.886	0.878	0.529	0.574	0.327	1.66	1.682	0.327

Table D-4: Thermodynamic properties for Binary ORC System simulations at 2.5km depth with a CO2 mass flow rate of 140kg/s and a reservoir temperature of 100°C.

Well Temp	100°C											
Well Depth	2.5 km											
CO2 Mass Flow	140 kg/s											
	Pressure (kPa)											
State Point	1	1'	2	3	4	4'	5	5'	6	7	8	9
Jan	2985	2987	27000	25000	11226	10892	10892	2987	404.5	404.5	127.2	127.2
Feb	3285	3287	26860	25000	11226	10892	10892	3287	416	416	144.7	144.7
Mar	3748	3750	26661	25000	11226	10892	10892	3750	439.7	439.7	172.7	172.7
Apr	4409	4411	26389	25000	11226	10892	10892	4411	464.5	464.5	214.3	214.3
May	5116	5117	26080	25000	11226	10892	10892	5117	490.3	490.3	260.6	260.6
June	5836	5838	25687	25000	11226	10891	10891	5838	517.1	517.1	309.3	309.3
July	6173	6175	25438	25000	11226	10891	10891	6175	530.9	530.9	332.3	332.3
Aug	6045	6047	25545	25000	11226	10891	10891	6047	523.9	523.9	323.6	323.6
Sept	5361	5363	25959	25000	11226	10891	10891	5363	496.9	496.9	277	277
Oct	5135	5137	26070	25000	11226	10892	10892	5137	490.3	490.3	261.9	261.9
Nov	4029	4031	26545	25000	11226	10892	10892	4031	445.8	445.8	190.2	190.2
Dec	3286	3288	26859	25000	11226	10892	10892	3288	416	416	144.8	144.8
	Temperature (°C)											
State Point	1	1'	2	3	4	4'	5	5'	6	7	8	9
Jan	-5.73	-5.71	8.921	100	55.12	52.98	26.77	-5.71	-5.57	30	0.757	-5.73
Feb	-2.21	-2.2	13.25	100	55.12	53	28.48	-2.2	-2.07	31	4.026	-2.21
Mar	2.773	2.791	19.55	100	55.12	53.04	31.35	2.791	2.89	33	8.725	2.773
Apr	9.159	9.176	27.97	100	55.12	53.08	34.37	9.176	9.234	35	14.49	9.159
May	15.23	15.25	36.51	100	55.12	53.12	37.16	15.25	15.26	37	19.88	15.23
June	20.79	20.81	45.1	100	55.12	53.15	39.7	20.81	20.78	39	24.78	20.79
July	23.2	23.22	49.27	100	55.12	53.17	40.88	23.22	23.3	40	26.92	23.2
Aug	22.3	22.32	47.64	100	55.12	53.16	40.34	22.32	22.4	39.5	26.09	22.3
Sept	17.19	17.21	39.43	100	55.12	53.13	37.89	17.21	17.21	37.5	21.57	17.19
Oct	15.39	15.41	36.74	100	55.12	53.12	37.18	15.41	15.42	37	20.01	15.39
Nov	5.583	5.601	23.2	100	55.12	53.05	32.35	5.601	5.681	33.5	11.18	5.583
Dec	-2.2	-2.18	13.27	100	55.12	53.01	28.48	-2.18	-2.06	31	4.038	-2.2
	Enthalpy (kJ/kg)											
State Point	1	1'	2	3	4	4'	5	5'	6	7	8	9
Jan	73.46	73.59	97.75	291.5	265	261.9	146.3	146.3	74.99	482.5	445.3	74.57
Feb	81.77	81.9	106.1	291.5	265	262	151.2	151.2	82.96	483.9	449.7	82.54
Mar	93.98	94.11	118.3	291.5	265	262.2	159.7	159.7	94.38	486.5	456.1	93.96
Apr	110.6	110.7	134.8	291.5	265	262.4	169.4	169.4	109.2	489.2	463.9	108.8
May	127.8	127.9	152	291.5	265	262.7	179.1	179.1	123.5	491.8	471.1	123.1
June	145.7	145.8	169.9	291.5	265	262.9	188.9	188.9	136.8	494.5	477.5	136.4
July	154.6	154.7	178.7	291.5	265	262.9	193.9	193.9	143	495.8	480.4	142.3
Aug	151.1	151.2	175.2	291.5	265	262.9	191.6	191.6	140.8	495.2	479.3	140.1
Sept	133.8	133.9	158	291.5	265	262.7	181.8	181.8	128.1	492.5	473.3	127.8
Oct	128.3	128.4	152.5	291.5	265	262.7	179.2	179.2	123.9	491.8	471.2	123.5
Nov	101.1	101.3	125.4	291.5	265	262.3	162.9	162.9	100.9	487.2	459.4	100.5
Dec	81.81	81.94	106.1	291.5	265	262	151.2	151.2	82.99	483.9	449.7	82.57
	Entropy (kJ/kg-K)											
State Point	1	1'	2	3	4	4'	5	5'	6	7	8	9
Jan	0.286	0.286	0.286	0.886	0.886	0.879	0.512	0.558	0.297	1.659	1.683	0.297
Feb	0.316	0.316	0.316	0.886	0.886	0.879	0.528	0.572	0.327	1.66	1.682	0.327
Mar	0.358	0.359	0.358	0.886	0.886	0.88	0.556	0.597	0.368	1.661	1.681	0.368
Apr	0.415	0.416	0.415	0.886	0.886	0.88	0.588	0.624	0.421	1.663	1.679	0.421
May	0.473	0.473	0.473	0.886	0.886	0.881	0.619	0.651	0.471	1.665	1.678	0.471
June	0.531	0.531	0.531	0.886	0.886	0.882	0.651	0.678	0.517	1.667	1.677	0.517
July	0.56	0.56	0.56	0.886	0.886	0.882	0.666	0.692	0.536	1.668	1.677	0.536
Aug	0.548	0.548	0.548	0.886	0.886	0.882	0.659	0.685	0.529	1.667	1.677	0.529
Sept	0.492	0.493	0.492	0.886	0.886	0.881	0.628	0.658	0.487	1.666	1.677	0.487
Oct	0.474	0.475	0.474	0.886	0.886	0.881	0.619	0.651	0.472	1.665	1.677	0.473
Nov	0.383	0.384	0.383	0.886	0.886	0.88	0.566	0.605	0.392	1.662	1.679	0.392
Dec	0.316	0.316	0.316	0.886	0.886	0.879	0.528	0.572	0.327	1.66	1.682	0.327

Table D-5: Thermodynamic properties for Binary ORC System simulations at 2.5km depth with a CO2 mass flow rate of 70kg/s and a reservoir temperature of 125°C.

Well Temp	125°C											
Well Depth	2.5 km											
CO2 Mass Flow	70 kg/s											
	Pressure (kPa)											
State Point	1	1'	2	3	4	4'	5	5'	6	7	8	9
Jan	2985	2986	27072	25000	13488	13158	13158	2986	503.5	503.5	127.2	127.2
Feb	3285	3286	26933	25000	13488	13158	13158	3286	523.9	523.9	144.7	144.7
Mar	3748	3749	26736	25000	13488	13157	13157	3749	537.9	537.9	172.7	172.7
Apr	4409	4410	26468	25000	13488	13157	13157	4410	581.4	581.4	214.3	214.3
May	5116	5117	26164	25000	13488	13157	13157	5117	619.5	619.5	260.6	260.6
June	5836	5838	25776	25000	13488	13156	13156	5838	651.4	651.4	309.3	309.3
July	6173	6174	25530	25000	13488	13156	13156	6174	667.7	667.7	332.3	332.3
Aug	6045	6047	25636	25000	13488	13156	13156	6047	659.5	659.5	323.6	323.6
Sept	5361	5362	26044	25000	13488	13156	13156	5362	627.4	627.4	277	277
Oct	5135	5137	26154	25000	13488	13157	13157	5137	619.5	619.5	261.9	261.9
Nov	4029	4030	26622	25000	13488	13157	13157	4030	559.3	559.3	190.2	190.2
Dec	3286	3288	26932	25000	13488	13158	13158	3288	523.9	523.9	144.8	144.8
	Temperature (°C)											
State Point	1	1'	2	3	4	4'	5	5'	6	7	8	9
Jan	-5.73	-5.72	8.958	125	80.05	76.32	33.09	-5.72	-5.54	38	2.749	-5.73
Feb	-2.21	-2.2	13.29	125	80.05	76.39	35.56	-2.2	-2.03	39.5	6.15	-2.21
Mar	2.773	2.785	19.6	125	80.05	76.5	37.9	2.785	2.924	40.5	10.6	2.773
Apr	9.159	9.17	28.02	125	80.05	76.63	42.31	9.17	9.278	43.5	16.62	9.159
May	15.23	15.24	36.57	125	80.05	76.76	45.95	15.24	15.31	46	22.15	15.23
June	20.79	20.8	45.18	125	80.05	76.87	48.81	20.8	20.84	48	27.05	20.79
July	23.2	23.21	49.36	125	80.05	76.92	50.11	23.21	23.23	49	29.18	23.2
Aug	22.3	22.31	47.72	125	80.05	76.9	49.52	22.31	22.34	48.5	28.35	22.3
Sept	17.19	17.2	39.5	125	80.05	76.8	46.8	17.2	17.26	46.5	23.83	17.19
Oct	15.39	15.4	36.81	125	80.05	76.76	45.98	15.4	15.47	46	22.27	15.39
Nov	5.583	5.595	23.25	125	80.05	76.55	40.03	5.595	5.722	42	13.31	5.583
Dec	-2.2	-2.19	13.32	125	80.05	76.39	35.56	-2.19	-2.02	39.5	6.162	-2.2
	Enthalpy (kJ/kg)											
State Point	1	1'	2	3	4	4'	5	5'	6	7	8	9
Jan	73.46	73.68	97.82	343.9	317	310.7	158.4	158.4	75.14	493.2	448.5	74.57
Feb	81.77	81.98	106.1	343.9	317	310.9	165.2	165.2	83.12	495.2	453.2	82.54
Mar	93.98	94.19	118.3	343.9	317	311.2	171.9	171.9	94.53	496.5	459.3	93.96
Apr	110.6	110.8	134.9	343.9	317	311.6	185.2	185.2	109.4	500.4	467.5	108.8
May	127.8	128	152.1	343.9	317	312	197.2	197.2	123.7	503.7	475	123.1
June	145.7	145.8	170	343.9	317	312.3	207.4	207.4	137	506.3	481.6	136.4
July	154.6	154.8	178.9	343.9	317	312.5	212.2	212.2	142.8	507.6	484.4	142.3
Aug	151.1	151.2	175.3	343.9	317	312.4	210	210	140.6	507	483.3	140.1
Sept	133.8	134	158.1	343.9	317	312.1	200.2	200.2	128.3	504.4	477.3	127.8
Oct	128.3	128.5	152.6	343.9	317	312	197.3	197.3	124.1	503.7	475.2	123.5
Nov	101.1	101.3	125.5	343.9	317	311.4	178.2	178.2	101	498.5	463	100.5
Dec	81.81	82.02	106.2	343.9	317	310.9	165.2	165.2	83.16	495.2	453.2	82.57
	Entropy (kJ/kg-K)											
State Point	1	1'	2	3	4	4'	5	5'	6	7	8	9
Jan	0.286	0.287	0.286	1.022	1.022	1.007	0.542	0.604	0.297	1.666	1.695	0.297
Feb	0.316	0.316	0.316	1.022	1.022	1.007	0.564	0.624	0.327	1.667	1.694	0.327
Mar	0.358	0.359	0.358	1.022	1.022	1.008	0.586	0.641	0.368	1.668	1.692	0.368
Apr	0.415	0.416	0.415	1.022	1.022	1.009	0.629	0.68	0.421	1.671	1.691	0.421
May	0.473	0.473	0.473	1.022	1.022	1.01	0.666	0.713	0.471	1.674	1.691	0.471
June	0.531	0.532	0.531	1.022	1.022	1.011	0.698	0.741	0.516	1.676	1.691	0.517
July	0.56	0.56	0.56	1.022	1.022	1.012	0.713	0.754	0.536	1.677	1.691	0.536
Aug	0.548	0.549	0.548	1.022	1.022	1.011	0.706	0.748	0.529	1.676	1.69	0.529
Sept	0.492	0.493	0.492	1.022	1.022	1.011	0.676	0.721	0.487	1.674	1.691	0.487
Oct	0.474	0.475	0.474	1.022	1.022	1.01	0.667	0.714	0.472	1.674	1.691	0.473
Nov	0.383	0.384	0.383	1.022	1.022	1.009	0.606	0.66	0.392	1.67	1.692	0.392
Dec	0.316	0.317	0.316	1.022	1.022	1.007	0.564	0.624	0.327	1.667	1.694	0.327

Table D-6: Thermodynamic properties for Binary ORC System simulations at 2.5km depth with a CO2 mass flow rate of 90kg/s and a reservoir temperature of 125°C.

Well Temp	125°C											
Well Depth	2.5 km											
CO2 Mass Flow	90 kg/s											
	Pressure (kPa)											
State Point	1	1'	2	3	4	4'	5	5'	6	7	8	9
Jan	2985	2987	26983	25000	12893	12328	12328	2987	483.7	483.7	127.2	127.2
Feb	3285	3287	26843	25000	12893	12328	12328	3287	496.9	496.9	144.7	144.7
Mar	3748	3750	26642	25000	12893	12328	12328	3750	517.1	517.1	172.7	172.7
Apr	4409	4411	26370	25000	12893	12327	12327	4411	552.1	552.1	214.3	214.3
May	5116	5118	26060	25000	12893	12327	12327	5118	581.4	581.4	260.6	260.6
June	5836	5839	25665	25000	12893	12326	12326	5839	611.8	611.8	309.3	309.3
July	6173	6175	25416	25000	12893	12326	12326	6175	627.4	627.4	332.3	332.3
Aug	6045	6048	25523	25000	12893	12326	12326	6048	619.5	619.5	323.6	323.6
Sept	5361	5363	25938	25000	12893	12326	12326	5363	596.4	596.4	277	277
Oct	5135	5137	26050	25000	12893	12327	12327	5137	581.4	581.4	261.9	261.9
Nov	4029	4031	26527	25000	12893	12327	12327	4031	530.9	530.9	190.2	190.2
Dec	3286	3288	26842	25000	12893	12328	12328	3288	496.9	496.9	144.8	144.8
	Temperature (°C)											
State Point	1	1'	2	3	4	4'	5	5'	6	7	8	9
Jan	-5.73	-5.71	8.912	125	76.75	72.1	31.96	-5.71	-5.54	36.5	2.367	-5.73
Feb	-2.21	-2.19	13.24	125	76.75	72.16	33.96	-2.19	-2.04	37.5	5.638	-2.21
Mar	2.773	2.793	19.54	125	76.75	72.23	36.79	2.793	2.917	39	10.22	2.773
Apr	9.159	9.177	27.95	125	76.75	72.33	40.77	9.177	9.267	41.5	16.11	9.159
May	15.23	15.25	36.49	125	76.75	72.43	43.94	15.25	15.3	43.5	21.51	15.23
June	20.79	20.81	45.08	125	76.75	72.51	46.78	20.81	20.82	45.5	26.41	20.79
July	23.2	23.22	49.24	125	76.75	72.55	48.05	23.22	23.21	46.5	28.55	23.2
Aug	22.3	22.32	47.61	125	76.75	72.54	47.47	22.32	22.32	46	27.72	22.3
Sept	17.19	17.21	39.41	125	76.75	72.46	45.23	17.21	17.25	44.5	23.32	17.19
Oct	15.39	15.41	36.73	125	76.75	72.43	43.97	15.41	15.46	43.5	21.63	15.39
Nov	5.583	5.602	23.19	125	76.75	72.28	38.47	5.602	5.711	40	12.8	5.583
Dec	-2.2	-2.18	13.26	125	76.75	72.16	33.97	-2.18	-2.03	37.5	5.651	-2.2
	Enthalpy (kJ/kg)											
State Point	1	1'	2	3	4	4'	5	5'	6	7	8	9
Jan	73.46	73.63	97.73	343.9	315.3	309.7	157.3	157.3	75.11	491.2	447.9	74.57
Feb	81.77	81.94	106	343.9	315.3	309.9	163	163	83.08	492.5	452.4	82.54
Mar	93.98	94.15	118.2	343.9	315.3	310.1	171.4	171.4	94.5	494.5	458.6	93.96
Apr	110.6	110.7	134.8	343.9	315.3	310.4	184	184	109.3	497.8	466.7	108.8
May	127.8	128	152	343.9	315.3	310.7	195.1	195.1	123.6	500.4	473.9	123.1
June	145.7	145.8	169.8	343.9	315.3	311	206	206	136.9	503.1	480.5	136.4
July	154.6	154.7	178.7	343.9	315.3	311.1	211.2	211.2	142.7	504.4	483.3	142.3
Aug	151.1	151.2	175.2	343.9	315.3	311	208.8	208.8	140.6	503.7	482.2	140.1
Sept	133.8	134	158	343.9	315.3	310.8	200	200	128.3	501.8	476.4	127.8
Oct	128.3	128.4	152.5	343.9	315.3	310.7	195.2	195.2	124	500.4	474.1	123.5
Nov	101.1	101.3	125.4	343.9	315.3	310.3	176.6	176.6	101	495.8	462.2	100.5
Dec	81.81	81.98	106.1	343.9	315.3	309.9	163	163	83.12	492.5	452.4	82.57
	Entropy (kJ/kg-K)											
State Point	1	1'	2	3	4	4'	5	5'	6	7	8	9
Jan	0.286	0.287	0.286	1.022	1.022	1.01	0.542	0.599	0.297	1.665	1.693	0.297
Feb	0.316	0.316	0.316	1.022	1.022	1.011	0.561	0.615	0.327	1.666	1.691	0.327
Mar	0.358	0.359	0.358	1.022	1.022	1.012	0.588	0.639	0.368	1.667	1.689	0.368
Apr	0.415	0.416	0.415	1.022	1.022	1.012	0.628	0.675	0.421	1.669	1.688	0.421
May	0.473	0.473	0.473	1.022	1.022	1.013	0.664	0.706	0.471	1.671	1.687	0.471
June	0.531	0.531	0.531	1.022	1.022	1.014	0.698	0.736	0.516	1.673	1.687	0.517
July	0.56	0.56	0.56	1.022	1.022	1.014	0.714	0.75	0.536	1.674	1.687	0.536
Aug	0.548	0.549	0.548	1.022	1.022	1.014	0.706	0.744	0.529	1.674	1.687	0.529
Sept	0.492	0.493	0.492	1.022	1.022	1.014	0.679	0.72	0.487	1.672	1.688	0.487
Oct	0.474	0.475	0.474	1.022	1.022	1.013	0.664	0.706	0.472	1.671	1.687	0.473
Nov	0.383	0.384	0.383	1.022	1.022	1.012	0.605	0.654	0.392	1.668	1.689	0.392
Dec	0.316	0.316	0.316	1.022	1.022	1.011	0.561	0.615	0.327	1.666	1.691	0.327

Table D-7: Thermodynamic properties for Binary ORC System simulations at 2.5km depth with a CO2 mass flow rate of 120kg/s and a reservoir temperature of 125°C.

Well Temp	125°C											
Well Depth	2.5 km											
CO2 Mass Flow	120 kg/s											
	Pressure (kPa)											
State Point	1	1'	2	3	4	4'	5	5'	6	7	8	9
Jan	2985	2986	27055	25000	13587	13294	13294	2986	510.3	510.3	127.2	127.2
Feb	3285	3286	26917	25000	13587	13294	13294	3286	530.9	530.9	144.7	144.7
Mar	3748	3749	26719	25000	13587	13294	13294	3749	552.1	552.1	172.7	172.7
Apr	4409	4410	26450	25000	13587	13293	13293	4410	588.9	588.9	214.3	214.3
May	5116	5117	26144	25000	13587	13293	13293	5117	627.4	627.4	260.6	260.6
June	5836	5838	25755	25000	13587	13293	13293	5838	659.5	659.5	309.3	309.3
July	6173	6174	25509	25000	13587	13293	13293	6174	676	676	332.3	332.3
Aug	6045	6047	25615	25000	13587	13293	13293	6047	667.7	667.7	323.6	323.6
Sept	5361	5363	26024	25000	13587	13293	13293	5363	635.3	635.3	277	277
Oct	5135	5137	26135	25000	13587	13293	13293	5137	627.4	627.4	261.9	261.9
Nov	4029	4030	26605	25000	13587	13294	13294	4030	566.6	566.6	190.2	190.2
Dec	3286	3288	26916	25000	13587	13294	13294	3288	530.9	530.9	144.8	144.8
	Temperature (°C)											
State Point	1	1'	2	3	4	4'	5	5'	6	7	8	9
Jan	-5.73	-5.72	8.95	125	80.59	77.59	33.5	-5.72	-5.53	38.5	2.878	-5.73
Feb	-2.21	-2.2	13.28	125	80.59	77.65	35.97	-2.2	-2.03	40	6.279	-2.21
Mar	2.773	2.786	19.59	125	80.59	77.72	38.79	2.786	2.929	41.5	10.86	2.773
Apr	9.159	9.171	28.01	125	80.59	77.82	42.75	9.171	9.281	44	16.75	9.159
May	15.23	15.24	36.56	125	80.59	77.91	46.39	15.24	15.32	46.5	22.27	15.23
June	20.79	20.8	45.16	125	80.59	78	49.26	20.8	20.84	48.5	27.17	20.79
July	23.2	23.21	49.34	125	80.59	78.03	50.56	23.21	23.24	49.5	29.31	23.2
Aug	22.3	22.31	47.7	125	80.59	78.02	49.97	22.31	22.34	49	28.48	22.3
Sept	17.19	17.2	39.48	125	80.59	77.94	47.24	17.2	17.26	47	23.96	17.19
Oct	15.39	15.4	36.8	125	80.59	77.91	46.42	15.4	15.48	46.5	22.4	15.39
Nov	5.583	5.596	23.24	125	80.59	77.76	40.47	5.596	5.724	42.5	13.44	5.583
Dec	-2.2	-2.19	13.31	125	80.59	77.65	35.98	-2.19	-2.02	40	6.291	-2.2
	Enthalpy (kJ/kg)											
State Point	1	1'	2	3	4	4'	5	5'	6	7	8	9
Jan	73.46	73.61	97.81	343.9	317.3	312.6	159.2	159.2	75.15	493.8	448.7	74.57
Feb	81.77	81.92	106.1	343.9	317.3	312.8	166	166	83.14	495.8	453.4	82.54
Mar	93.98	94.13	118.3	343.9	317.3	313	174	174	94.56	497.8	459.7	93.96
Apr	110.6	110.7	134.9	343.9	317.3	313.3	186	186	109.4	501.1	467.8	108.8
May	127.8	127.9	152.1	343.9	317.3	313.5	197.9	197.9	123.7	504.4	475.3	123.1
June	145.7	145.8	169.9	343.9	317.3	313.8	208	208	137	507	481.8	136.4
July	154.6	154.7	178.8	343.9	317.3	313.9	212.8	212.8	142.8	508.3	484.7	142.3
Aug	151.1	151.2	175.3	343.9	317.3	313.8	210.6	210.6	140.6	507.6	483.6	140.1
Sept	133.8	133.9	158.1	343.9	317.3	313.6	200.9	200.9	128.4	505	477.5	127.8
Oct	128.3	128.4	152.6	343.9	317.3	313.5	198.1	198.1	124.1	504.4	475.4	123.5
Nov	101.1	101.3	125.5	343.9	317.3	313.1	179	179	101.1	499.1	463.2	100.5
Dec	81.81	81.96	106.2	343.9	317.3	312.8	166	166	83.17	495.8	453.4	82.57
	Entropy (kJ/kg-K)											
State Point	1	1'	2	3	4	4'	5	5'	6	7	8	9
Jan	0.286	0.287	0.286	1.022	1.022	1.011	0.544	0.607	0.297	1.666	1.696	0.297
Feb	0.316	0.316	0.316	1.022	1.022	1.011	0.566	0.626	0.327	1.668	1.695	0.327
Mar	0.358	0.359	0.358	1.022	1.022	1.012	0.592	0.649	0.368	1.669	1.693	0.368
Apr	0.415	0.416	0.415	1.022	1.022	1.013	0.63	0.682	0.421	1.672	1.692	0.421
May	0.473	0.473	0.473	1.022	1.022	1.014	0.668	0.716	0.471	1.674	1.692	0.471
June	0.531	0.531	0.531	1.022	1.022	1.014	0.699	0.743	0.516	1.676	1.691	0.517
July	0.56	0.56	0.56	1.022	1.022	1.015	0.714	0.756	0.536	1.678	1.691	0.536
Aug	0.548	0.548	0.548	1.022	1.022	1.014	0.707	0.75	0.529	1.677	1.691	0.529
Sept	0.492	0.493	0.492	1.022	1.022	1.014	0.677	0.723	0.487	1.675	1.691	0.487
Oct	0.474	0.475	0.474	1.022	1.022	1.014	0.668	0.716	0.472	1.674	1.692	0.473
Nov	0.383	0.384	0.383	1.022	1.022	1.012	0.608	0.663	0.392	1.67	1.693	0.392
Dec	0.316	0.316	0.316	1.022	1.022	1.011	0.566	0.627	0.327	1.668	1.695	0.327

Table D-8: Thermodynamic properties for Binary ORC System simulations at 2.5km depth with a CO2 mass flow rate of 140kg/s and a reservoir temperature of 125°C.

Well Temp	125°C											
Well Depth	2.5 km											
CO2 Mass Flow	140 kg/s											
	Pressure (kPa)											
State Point	1	1'	2	3	4	4'	5	5'	6	7	8	9
Jan	2985	2987	27000	25000	13297	12891	12891	2987	496.9	496.9	127.2	127.2
Feb	3285	3287	26860	25000	13297	12891	12891	3287	510.3	510.3	144.7	144.7
Mar	3748	3750	26661	25000	13297	12891	12891	3750	537.9	537.9	172.7	172.7
Apr	4409	4411	26389	25000	13297	12891	12891	4411	573.9	573.9	214.3	214.3
May	5116	5117	26080	25000	13297	12890	12890	5117	611.8	611.8	260.6	260.6
June	5836	5838	25687	25000	13297	12890	12890	5838	643.3	643.3	309.3	309.3
July	6173	6175	25438	25000	13297	12890	12890	6175	659.5	659.5	332.3	332.3
Aug	6045	6047	25545	25000	13297	12890	12890	6047	651.4	651.4	323.6	323.6
Sept	5361	5363	25959	25000	13297	12890	12890	5363	619.5	619.5	277	277
Oct	5135	5137	26070	25000	13297	12890	12890	5137	611.8	611.8	261.9	261.9
Nov	4029	4031	26545	25000	13297	12891	12891	4031	552.1	552.1	190.2	190.2
Dec	3286	3288	26859	25000	13297	12891	12891	3288	510.3	510.3	144.8	144.8
	Temperature (°C)											
State Point	1	1'	2	3	4	4'	5	5'	6	7	8	9
Jan	-5.73	-5.71	8.921	125	79.01	75.59	32.71	-5.71	-5.54	37.5	2.621	-5.73
Feb	-2.21	-2.2	13.25	125	79.01	75.63	34.72	-2.2	-2.04	38.5	5.893	-2.21
Mar	2.773	2.791	19.55	125	79.01	75.7	38.02	2.791	2.924	40.5	10.6	2.773
Apr	9.159	9.176	27.97	125	79.01	75.78	41.99	9.176	9.275	43	16.5	9.159
May	15.23	15.25	36.51	125	79.01	75.85	45.63	15.25	15.31	45.5	22.02	15.23
June	20.79	20.81	45.1	125	79.01	75.93	48.48	20.81	20.83	47.5	26.92	20.79
July	23.2	23.22	49.27	125	79.01	75.96	49.76	23.22	23.23	48.5	29.05	23.2
Aug	22.3	22.32	47.64	125	79.01	75.95	49.18	22.32	22.33	48	28.23	22.3
Sept	17.19	17.21	39.43	125	79.01	75.88	46.47	17.21	17.26	46	23.7	17.19
Oct	15.39	15.41	36.74	125	79.01	75.86	45.66	15.41	15.47	45.5	22.14	15.39
Nov	5.583	5.601	23.2	125	79.01	75.73	39.7	5.601	5.719	41.5	13.19	5.583
Dec	-2.2	-2.18	13.27	125	79.01	75.63	34.72	-2.18	-2.02	38.5	5.906	-2.2
	Enthalpy (kJ/kg)											
State Point	1	1'	2	3	4	4'	5	5'	6	7	8	9
Jan	73.46	73.59	97.75	343.9	316.5	312.1	158	158	75.13	492.5	448.3	74.57
Feb	81.77	81.9	106.1	343.9	316.5	312.2	163.6	163.6	83.1	493.8	452.8	82.54
Mar	93.98	94.11	118.3	343.9	316.5	312.4	173.1	173.1	94.53	496.5	459.3	93.96
Apr	110.6	110.7	134.8	343.9	316.5	312.7	185.4	185.4	109.4	499.8	467.3	108.8
May	127.8	127.9	152	343.9	316.5	312.9	197.7	197.7	123.7	503.1	474.8	123.1
June	145.7	145.8	169.9	343.9	316.5	313.1	208.1	208.1	137	505.7	481.4	136.4
July	154.6	154.7	178.7	343.9	316.5	313.2	213	213	142.8	507	484.2	142.3
Aug	151.1	151.2	175.2	343.9	316.5	313.1	210.7	210.7	140.6	506.3	483.1	140.1
Sept	133.8	133.9	158	343.9	316.5	313	200.7	200.7	128.3	503.7	477.1	127.8
Oct	128.3	128.4	152.5	343.9	316.5	312.9	197.8	197.8	124.1	503.1	475	123.5
Nov	101.1	101.3	125.4	343.9	316.5	312.5	178.2	178.2	101	497.8	462.8	100.5
Dec	81.81	81.94	106.1	343.9	316.5	312.2	163.6	163.6	83.14	493.8	452.8	82.57
	Entropy (kJ/kg-K)											
State Point	1	1'	2	3	4	4'	5	5'	6	7	8	9
Jan	0.286	0.286	0.286	1.022	1.022	1.013	0.542	0.602	0.297	1.666	1.694	0.297
Feb	0.316	0.316	0.316	1.022	1.022	1.013	0.56	0.618	0.327	1.666	1.693	0.327
Mar	0.358	0.359	0.358	1.022	1.022	1.014	0.591	0.645	0.368	1.668	1.692	0.368
Apr	0.415	0.416	0.415	1.022	1.022	1.014	0.63	0.68	0.421	1.671	1.691	0.421
May	0.473	0.473	0.473	1.022	1.022	1.015	0.669	0.715	0.471	1.673	1.69	0.471
June	0.531	0.531	0.531	1.022	1.022	1.015	0.701	0.743	0.516	1.675	1.69	0.517
July	0.56	0.56	0.56	1.022	1.022	1.016	0.717	0.757	0.536	1.676	1.69	0.536
Aug	0.548	0.548	0.548	1.022	1.022	1.016	0.71	0.75	0.529	1.676	1.69	0.529
Sept	0.492	0.493	0.492	1.022	1.022	1.015	0.678	0.723	0.487	1.674	1.69	0.487
Oct	0.474	0.475	0.474	1.022	1.022	1.015	0.669	0.715	0.472	1.673	1.69	0.473
Nov	0.383	0.384	0.383	1.022	1.022	1.014	0.607	0.66	0.392	1.669	1.691	0.392
Dec	0.316	0.316	0.316	1.022	1.022	1.013	0.56	0.618	0.327	1.666	1.693	0.327

Table D-9: Thermodynamic properties for Binary ORC System simulations at 2.5km depth with a CO2 mass flow rate of 70kg/s and a reservoir temperature of 150°C.

Well Temp	150°C											
Well Depth	2.5 km											
CO2 Mass Flow	70 kg/s											
	Pressure (kPa)											
State Point	1	1'	2	3	4	4'	5	5'	6	7	8	9
Jan	2985	2986	27072	25000	14868	14484	14484	2986	596.4	596.4	127.2	127.2
Feb	3285	3286	26933	25000	14868	14484	14484	3286	627.4	627.4	144.7	144.7
Mar	3748	3749	26736	25000	14868	14483	14483	3749	651.4	651.4	172.7	172.7
Apr	4409	4410	26468	25000	14868	14483	14483	4410	701.4	701.4	214.3	214.3
May	5116	5117	26164	25000	14868	14483	14483	5117	754.2	754.2	260.6	260.6
June	5836	5838	25776	25000	14868	14482	14482	5838	800.3	800.3	309.3	309.3
July	6173	6174	25530	25000	14868	14482	14482	6174	829	829	332.3	332.3
Aug	6045	6047	25636	25000	14868	14482	14482	6047	819.4	819.4	323.6	323.6
Sept	5361	5362	26044	25000	14868	14483	14483	5362	772.4	772.4	277	277
Oct	5135	5137	26154	25000	14868	14483	14483	5137	754.2	754.2	261.9	261.9
Nov	4029	4030	26622	25000	14868	14483	14483	4030	684.4	684.4	190.2	190.2
Dec	3286	3288	26932	25000	14868	14484	14484	3288	627.4	627.4	144.8	144.8
	Temperature (°C)											
State Point	1	1'	2	3	4	4'	5	5'	6	7	8	9
Jan	-5.73	-5.72	8.958	150	106.2	100.5	38.84	-5.72	-5.51	44.5	4.446	-5.73
Feb	-2.21	-2.2	13.29	150	106.2	100.6	41.96	-2.2	-2	46.5	7.983	-2.21
Mar	2.773	2.785	19.6	150	106.2	100.8	44.98	2.785	2.964	48	12.56	2.773
Apr	9.159	9.17	28.02	150	106.2	101	49.46	9.17	9.323	51	18.58	9.159
May	15.23	15.24	36.57	150	106.2	101.1	53.74	15.24	15.37	54	24.23	15.23
June	20.79	20.8	45.18	150	106.2	101.3	56.99	20.8	20.9	56.5	29.25	20.79
July	23.2	23.21	49.36	150	106.2	101.4	58.79	23.21	23.3	58	31.51	23.2
Aug	22.3	22.31	47.72	150	106.2	101.4	58.2	22.31	22.41	57.5	30.68	22.3
Sept	17.19	17.2	39.5	150	106.2	101.2	55.04	17.2	17.32	55	26.04	17.19
Oct	15.39	15.4	36.81	150	106.2	101.2	53.78	15.4	15.53	54	24.36	15.39
Nov	5.583	5.595	23.25	150	106.2	100.9	47.65	5.595	5.767	50	15.41	5.583
Dec	-2.2	-2.19	13.32	150	106.2	100.6	41.97	-2.19	-1.99	46.5	7.996	-2.2
	Enthalpy (kJ/kg)											
State Point	1	1'	2	3	4	4'	5	5'	6	7	8	9
Jan	73.46	73.68	97.82	390.4	362.6	354.5	170.8	170.8	75.28	501.8	451.3	74.57
Feb	81.77	81.98	106.1	390.4	362.6	354.7	179.4	179.4	83.28	504.4	456.2	82.54
Mar	93.98	94.19	118.3	390.4	362.6	355	188.1	188.1	94.71	506.3	462.5	93.96
Apr	110.6	110.8	134.9	390.4	362.6	355.4	201.8	201.8	109.6	510.2	470.9	108.8
May	127.8	128	152.1	390.4	362.6	355.7	215.8	215.8	123.9	514.1	478.7	123.1
June	145.7	145.8	170	390.4	362.6	356.1	227.1	227.1	137.2	517.3	485.6	136.4
July	154.6	154.8	178.9	390.4	362.6	356.2	233.5	233.5	143.1	519.2	488.7	142.3
Aug	151.1	151.2	175.3	390.4	362.6	356.2	231.4	231.4	140.9	518.6	487.5	140.1
Sept	133.8	134	158.1	390.4	362.6	355.8	220.3	220.3	128.6	515.4	481.2	127.8
Oct	128.3	128.5	152.6	390.4	362.6	355.7	215.9	215.9	124.3	514.1	478.9	123.5
Nov	101.1	101.3	125.5	390.4	362.6	355.2	196.2	196.2	101.2	508.9	466.6	100.5
Dec	81.81	82.02	106.2	390.4	362.6	354.7	179.4	179.4	83.32	504.4	456.2	82.57
	Entropy (kJ/kg-K)											
State Point	1	1'	2	3	4	4'	5	5'	6	7	8	9
Jan	0.286	0.287	0.286	1.135	1.135	1.117	0.577	0.65	0.297	1.672	1.705	0.297
Feb	0.316	0.316	0.316	1.135	1.135	1.118	0.604	0.676	0.327	1.674	1.705	0.327
Mar	0.358	0.359	0.358	1.135	1.135	1.118	0.632	0.7	0.368	1.676	1.703	0.368
Apr	0.415	0.416	0.415	1.135	1.135	1.119	0.675	0.738	0.421	1.679	1.703	0.421
May	0.473	0.473	0.473	1.135	1.135	1.12	0.718	0.778	0.471	1.682	1.703	0.471
June	0.531	0.532	0.531	1.135	1.135	1.121	0.752	0.808	0.516	1.685	1.704	0.517
July	0.56	0.56	0.56	1.135	1.135	1.122	0.771	0.826	0.536	1.687	1.704	0.536
Aug	0.548	0.549	0.548	1.135	1.135	1.121	0.765	0.82	0.529	1.686	1.704	0.529
Sept	0.492	0.493	0.492	1.135	1.135	1.121	0.731	0.79	0.487	1.683	1.704	0.487
Oct	0.474	0.475	0.474	1.135	1.135	1.12	0.718	0.778	0.472	1.682	1.703	0.473
Nov	0.383	0.384	0.383	1.135	1.135	1.119	0.657	0.724	0.391	1.678	1.704	0.392
Dec	0.316	0.317	0.316	1.135	1.135	1.118	0.604	0.676	0.327	1.674	1.705	0.327

Table D-10: Thermodynamic properties for Binary ORC System simulations at 2.5km depth with a CO2 mass flow rate of 90kg/s and a reservoir temperature of 150°C.

Well Temp	150°C											
Well Depth	2.5 km											
CO2 Mass Flow	90 kg/s											
Pressure (kPa)												
State Point	1	1'	2	3	4	4'	5	5'	6	7	8	9
Jan	2985	2987	26983	25000	14157	13495	13495	2987	552.1	552.1	127.2	127.2
Feb	3285	3287	26843	25000	14157	13495	13495	3287	588.9	588.9	144.7	144.7
Mar	3748	3750	26642	25000	14157	13494	13494	3750	604	604	172.7	172.7
Apr	4409	4411	26370	25000	14157	13494	13494	4411	643.3	643.3	214.3	214.3
May	5116	5118	26060	25000	14157	13493	13493	5118	692.9	692.9	260.6	260.6
June	5836	5839	25665	25000	14157	13493	13493	5839	736.3	736.3	309.3	309.3
July	6173	6175	25416	25000	14157	13493	13493	6175	763.2	763.2	332.3	332.3
Aug	6045	6048	25523	25000	14157	13493	13493	6048	754.2	754.2	323.6	323.6
Sept	5361	5363	25938	25000	14157	13493	13493	5363	710	710	277	277
Oct	5135	5137	26050	25000	14157	13493	13493	5137	692.9	692.9	261.9	261.9
Nov	4029	4031	26527	25000	14157	13494	13494	4031	619.5	619.5	190.2	190.2
Dec	3286	3288	26842	25000	14157	13495	13495	3288	588.9	588.9	144.8	144.8
Temperature (°C)												
State Point	1	1'	2	3	4	4'	5	5'	6	7	8	9
Jan	-5.73	-5.71	8.912	150	102.1	95.53	37.13	-5.71	-5.52	41.5	3.656	-5.73
Feb	-2.21	-2.19	13.24	150	102.1	95.61	40.81	-2.19	-2.01	44	7.322	-2.21
Mar	2.773	2.793	19.54	150	102.1	95.72	43.34	2.793	2.947	45	11.77	2.773
Apr	9.159	9.177	27.95	150	102.1	95.86	47.48	9.177	9.301	47.5	17.66	9.159
May	15.23	15.25	36.49	150	102.1	96	51.61	15.25	15.34	50.5	23.31	15.23
June	20.79	20.81	45.08	150	102.1	96.12	54.87	20.81	20.87	53	28.34	20.79
July	23.2	23.22	49.24	150	102.1	96.18	56.53	23.22	23.27	54.5	30.6	23.2
Aug	22.3	22.32	47.61	150	102.1	96.16	55.97	22.32	22.38	54	29.77	22.3
Sept	17.19	17.21	39.41	150	102.1	96.04	52.89	17.21	17.29	51.5	25.12	17.19
Oct	15.39	15.41	36.73	150	102.1	96	51.65	15.41	15.5	50.5	23.44	15.39
Nov	5.583	5.602	23.19	150	102.1	95.78	45.11	5.602	5.743	46	14.35	5.583
Dec	-2.2	-2.18	13.26	150	102.1	95.61	40.81	-2.18	-2	44	7.334	-2.2
Enthalpy (kJ/kg)												
State Point	1	1'	2	3	4	4'	5	5'	6	7	8	9
Jan	73.46	73.63	97.73	390.4	360.3	352.9	168.7	168.7	75.22	497.8	450	74.57
Feb	81.77	81.94	106	390.4	360.3	353.1	179.3	179.3	83.23	501.1	455.1	82.54
Mar	93.98	94.15	118.2	390.4	360.3	353.3	187	187	94.64	502.4	461.2	93.96
Apr	110.6	110.7	134.8	390.4	360.3	353.6	200.5	200.5	109.5	505.7	469.3	108.8
May	127.8	128	152	390.4	360.3	353.9	215.2	215.2	123.8	509.6	477.1	123.1
June	145.7	145.8	169.8	390.4	360.3	354.2	227.6	227.6	137.1	512.8	483.9	136.4
July	154.6	154.7	178.7	390.4	360.3	354.3	234.2	234.2	143	514.7	487	142.3
Aug	151.1	151.2	175.2	390.4	360.3	354.2	231.9	231.9	140.8	514.1	485.9	140.1
Sept	133.8	134	158	390.4	360.3	354	220	220	128.5	510.9	479.6	127.8
Oct	128.3	128.4	152.5	390.4	360.3	353.9	215.3	215.3	124.2	509.6	477.3	123.5
Nov	101.1	101.3	125.4	390.4	360.3	353.5	192.7	192.7	101.1	503.7	464.8	100.5
Dec	81.81	81.98	106.1	390.4	360.3	353.1	179.3	179.3	83.26	501.1	455.1	82.57
Entropy (kJ/kg-K)												
State Point	1	1'	2	3	4	4'	5	5'	6	7	8	9
Jan	0.286	0.287	0.286	1.135	1.135	1.121	0.574	0.642	0.297	1.669	1.7	0.297
Feb	0.316	0.316	0.316	1.135	1.135	1.122	0.608	0.676	0.327	1.672	1.701	0.327
Mar	0.358	0.359	0.358	1.135	1.135	1.123	0.633	0.696	0.368	1.673	1.699	0.368
Apr	0.415	0.416	0.415	1.135	1.135	1.123	0.675	0.734	0.421	1.675	1.698	0.421
May	0.473	0.473	0.473	1.135	1.135	1.124	0.721	0.776	0.471	1.679	1.698	0.471
June	0.531	0.531	0.531	1.135	1.135	1.125	0.759	0.81	0.516	1.681	1.698	0.517
July	0.56	0.56	0.56	1.135	1.135	1.125	0.779	0.828	0.536	1.683	1.699	0.536
Aug	0.548	0.549	0.548	1.135	1.135	1.125	0.772	0.822	0.529	1.682	1.699	0.529
Sept	0.492	0.493	0.492	1.135	1.135	1.124	0.735	0.789	0.487	1.68	1.698	0.487
Oct	0.474	0.475	0.474	1.135	1.135	1.124	0.721	0.776	0.472	1.679	1.698	0.473
Nov	0.383	0.384	0.383	1.135	1.135	1.123	0.651	0.711	0.392	1.674	1.698	0.392
Dec	0.316	0.316	0.316	1.135	1.135	1.122	0.608	0.676	0.327	1.672	1.701	0.327

Table D-11: Thermodynamic properties for Binary ORC System simulations at 2.5km depth with a CO2 mass flow rate of 120kg/s and a reservoir temperature of 150°C.

Well Temp	150°C											
Well Depth	2.5 km											
CO2 Mass Flow	120 kg/s											
	Pressure (kPa)											
State Point	1	1'	2	3	4	4'	5	5'	6	7	8	9
Jan	2985	2986	27055	25000	14987	14645	14645	2986	611.8	611.8	127.2	127.2
Feb	3285	3286	26917	25000	14987	14645	14645	3286	635.3	635.3	144.7	144.7
Mar	3748	3749	26719	25000	14987	14645	14645	3749	667.7	667.7	172.7	172.7
Apr	4409	4410	26450	25000	14987	14645	14645	4410	718.7	718.7	214.3	214.3
May	5116	5117	26144	25000	14987	14645	14645	5117	763.2	763.2	260.6	260.6
June	5836	5838	25755	25000	14987	14644	14644	5838	819.4	819.4	309.3	309.3
July	6173	6174	25509	25000	14987	14644	14644	6174	848.5	848.5	332.3	332.3
Aug	6045	6047	25615	25000	14987	14644	14644	6047	838.7	838.7	323.6	323.6
Sept	5361	5363	26024	25000	14987	14645	14645	5363	781.6	781.6	277	277
Oct	5135	5137	26135	25000	14987	14645	14645	5137	763.2	763.2	261.9	261.9
Nov	4029	4030	26605	25000	14987	14645	14645	4030	684.4	684.4	190.2	190.2
Dec	3286	3288	26916	25000	14987	14645	14645	3288	635.3	635.3	144.8	144.8
	Temperature (°C)											
State Point	1	1'	2	3	4	4'	5	5'	6	7	8	9
Jan	-5.73	-5.72	8.95	150	106.8	102.4	39.66	-5.72	-5.5	45.5	4.712	-5.73
Feb	-2.21	-2.2	13.28	150	106.8	102.5	42.3	-2.2	-2	47	8.116	-2.21
Mar	2.773	2.786	19.59	150	106.8	102.6	45.78	2.786	2.969	49	12.83	2.773
Apr	9.159	9.171	28.01	150	106.8	102.7	50.35	9.171	9.329	52	18.85	9.159
May	15.23	15.24	36.56	150	106.8	102.9	54.09	15.24	15.37	54.5	24.36	15.23
June	20.79	20.8	45.16	150	106.8	103	57.84	20.8	20.91	57.5	29.51	20.79
July	23.2	23.21	49.34	150	106.8	103	59.54	23.21	23.31	59	31.77	23.2
Aug	22.3	22.31	47.7	150	106.8	103	58.96	22.31	22.41	58.5	30.94	22.3
Sept	17.19	17.2	39.48	150	106.8	102.9	55.3	17.2	17.32	55.5	26.17	17.19
Oct	15.39	15.4	36.8	150	106.8	102.9	54.13	15.4	15.53	54.5	24.49	15.39
Nov	5.583	5.596	23.24	150	106.8	102.7	47.55	5.596	5.767	50	15.41	5.583
Dec	-2.2	-2.19	13.31	150	106.8	102.5	42.31	-2.19	-1.98	47	8.129	-2.2
	Enthalpy (kJ/kg)											
State Point	1	1'	2	3	4	4'	5	5'	6	7	8	9
Jan	73.46	73.61	97.81	390.4	363	356.9	172.6	172.6	75.31	503.1	451.7	74.57
Feb	81.77	81.92	106.1	390.4	363	357.1	179.9	179.9	83.3	505	456.4	82.54
Mar	93.98	94.13	118.3	390.4	363	357.3	189.9	189.9	94.74	507.6	463	93.96
Apr	110.6	110.7	134.9	390.4	363	357.6	203.8	203.8	109.6	511.5	471.4	108.8
May	127.8	127.9	152.1	390.4	363	357.8	216	216	123.9	514.7	478.9	123.1
June	145.7	145.8	169.9	390.4	363	358.1	228.8	228.8	137.2	518.6	486	136.4
July	154.6	154.7	178.8	390.4	363	358.2	234.8	234.8	143.1	520.5	489.1	142.3
Aug	151.1	151.2	175.3	390.4	363	358.1	232.8	232.8	140.9	519.8	488	140.1
Sept	133.8	133.9	158.1	390.4	363	357.9	220.1	220.1	128.6	516	481.4	127.8
Oct	128.3	128.4	152.6	390.4	363	357.8	216.1	216.1	124.3	514.7	479.1	123.5
Nov	101.1	101.3	125.5	390.4	363	357.4	195.2	195.2	101.2	508.9	466.6	100.5
Dec	81.81	81.96	106.2	390.4	363	357.1	179.9	179.9	83.33	505	456.5	82.57
	Entropy (kJ/kg-K)											
State Point	1	1'	2	3	4	4'	5	5'	6	7	8	9
Jan	0.286	0.287	0.286	1.135	1.135	1.122	0.582	0.657	0.297	1.673	1.706	0.297
Feb	0.316	0.316	0.316	1.135	1.135	1.123	0.605	0.678	0.327	1.675	1.706	0.327
Mar	0.358	0.359	0.358	1.135	1.135	1.123	0.637	0.706	0.368	1.677	1.705	0.368
Apr	0.415	0.416	0.415	1.135	1.135	1.124	0.68	0.746	0.421	1.68	1.705	0.421
May	0.473	0.473	0.473	1.135	1.135	1.125	0.718	0.778	0.471	1.683	1.704	0.471
June	0.531	0.531	0.531	1.135	1.135	1.125	0.757	0.814	0.516	1.686	1.705	0.517
July	0.56	0.56	0.56	1.135	1.135	1.125	0.775	0.83	0.536	1.688	1.706	0.536
Aug	0.548	0.548	0.548	1.135	1.135	1.125	0.768	0.825	0.529	1.687	1.706	0.529
Sept	0.492	0.493	0.492	1.135	1.135	1.125	0.73	0.789	0.487	1.684	1.704	0.487
Oct	0.474	0.475	0.474	1.135	1.135	1.125	0.718	0.779	0.472	1.683	1.704	0.473
Nov	0.383	0.384	0.383	1.135	1.135	1.123	0.653	0.72	0.391	1.678	1.704	0.392
Dec	0.316	0.316	0.316	1.135	1.135	1.123	0.605	0.678	0.327	1.675	1.706	0.327

Table D-12: Thermodynamic properties for Binary ORC System simulations at 2.5km depth with a CO2 mass flow rate of 140kg/s and a reservoir temperature of 150°C.

Well Temp	150°C											
Well Depth	2.5 km											
CO2 Mass Flow	140 kg/s											
	Pressure (kPa)											
State Point	1	1'	2	3	4	4'	5	5'	6	7	8	9
Jan	2985	2987	27000	25000	14640	14167	14167	2987	588.9	588.9	127.2	127.2
Feb	3285	3287	26860	25000	14640	14167	14167	3287	611.8	611.8	144.7	144.7
Mar	3748	3750	26661	25000	14640	14166	14166	3750	643.3	643.3	172.7	172.7
Apr	4409	4411	26389	25000	14640	14166	14166	4411	684.4	684.4	214.3	214.3
May	5116	5117	26080	25000	14640	14166	14166	5117	736.3	736.3	260.6	260.6
June	5836	5838	25687	25000	14640	14166	14166	5838	790.9	790.9	309.3	309.3
July	6173	6175	25438	25000	14640	14166	14166	6175	809.8	809.8	332.3	332.3
Aug	6045	6047	25545	25000	14640	14166	14166	6047	800.3	800.3	323.6	323.6
Sept	5361	5363	25959	25000	14640	14166	14166	5363	754.2	754.2	277	277
Oct	5135	5137	26070	25000	14640	14166	14166	5137	736.3	736.3	261.9	261.9
Nov	4029	4031	26545	25000	14640	14166	14166	4031	659.5	659.5	190.2	190.2
Dec	3286	3288	26859	25000	14640	14167	14167	3288	611.8	611.8	144.8	144.8
	Temperature (°C)											
State Point	1	1'	2	3	4	4'	5	5'	6	7	8	9
Jan	-5.73	-5.71	8.921	150	104.9	100	38.83	-5.71	-5.51	44	4.314	-5.73
Feb	-2.21	-2.2	13.25	150	104.9	100.1	41.49	-2.2	-2.01	45.5	7.718	-2.21
Mar	2.773	2.791	19.55	150	104.9	100.2	44.99	2.791	2.961	47.5	12.43	2.773
Apr	9.159	9.176	27.97	150	104.9	100.3	49.12	9.176	9.316	50	18.32	9.159
May	15.23	15.25	36.51	150	104.9	100.4	53.26	15.25	15.36	53	23.97	15.23
June	20.79	20.81	45.1	150	104.9	100.5	56.96	20.81	20.9	56	29.12	20.79
July	23.2	23.22	49.27	150	104.9	100.6	58.17	23.22	23.29	57	31.25	23.2
Aug	22.3	22.32	47.64	150	104.9	100.5	57.59	22.32	22.4	56.5	30.42	22.3
Sept	17.19	17.21	39.43	150	104.9	100.5	54.55	17.21	17.31	54	25.78	17.19
Oct	15.39	15.41	36.74	150	104.9	100.4	53.3	15.41	15.52	53	24.09	15.39
Nov	5.583	5.601	23.2	150	104.9	100.2	46.75	5.601	5.758	48.5	15.01	5.583
Dec	-2.2	-2.18	13.27	150	104.9	100.1	41.5	-2.18	-1.99	45.5	7.73	-2.2
	Enthalpy (kJ/kg)											
State Point	1	1'	2	3	4	4'	5	5'	6	7	8	9
Jan	73.46	73.59	97.75	390.4	361.9	356.2	171.6	171.6	75.27	501.1	451	74.57
Feb	81.77	81.9	106.1	390.4	361.9	356.3	179	179	83.26	503.1	455.8	82.54
Mar	93.98	94.11	118.3	390.4	361.9	356.5	189.3	189.3	94.7	505.7	462.3	93.96
Apr	110.6	110.7	134.8	390.4	361.9	356.7	202.3	202.3	109.5	508.9	470.5	108.8
May	127.8	127.9	152	390.4	361.9	356.9	216.2	216.2	123.9	512.8	478.3	123.1
June	145.7	145.8	169.9	390.4	361.9	357.1	229.5	229.5	137.2	516.7	485.3	136.4
July	154.6	154.7	178.7	390.4	361.9	357.2	234	234	143	517.9	488.2	142.3
Aug	151.1	151.2	175.2	390.4	361.9	357.2	231.8	231.8	140.8	517.3	487.1	140.1
Sept	133.8	133.9	158	390.4	361.9	357	220.8	220.8	128.6	514.1	480.7	127.8
Oct	128.3	128.4	152.5	390.4	361.9	356.9	216.4	216.4	124.3	512.8	478.4	123.5
Nov	101.1	101.3	125.4	390.4	361.9	356.6	194.8	194.8	101.2	507	465.9	100.5
Dec	81.81	81.94	106.1	390.4	361.9	356.3	179.1	179.1	83.29	503.1	455.8	82.57
	Entropy (kJ/kg-K)											
State Point	1	1'	2	3	4	4'	5	5'	6	7	8	9
Jan	0.286	0.286	0.286	1.135	1.135	1.124	0.581	0.653	0.297	1.672	1.704	0.297
Feb	0.316	0.316	0.316	1.135	1.135	1.125	0.605	0.675	0.327	1.673	1.703	0.327
Mar	0.358	0.359	0.358	1.135	1.135	1.125	0.637	0.704	0.368	1.675	1.702	0.368
Apr	0.415	0.416	0.415	1.135	1.135	1.126	0.678	0.74	0.421	1.678	1.701	0.421
May	0.473	0.473	0.473	1.135	1.135	1.126	0.721	0.779	0.471	1.681	1.702	0.471
June	0.531	0.531	0.531	1.135	1.135	1.127	0.761	0.816	0.516	1.684	1.703	0.517
July	0.56	0.56	0.56	1.135	1.135	1.127	0.775	0.827	0.536	1.686	1.703	0.536
Aug	0.548	0.548	0.548	1.135	1.135	1.127	0.768	0.822	0.529	1.685	1.703	0.529
Sept	0.492	0.493	0.492	1.135	1.135	1.126	0.735	0.792	0.487	1.682	1.702	0.487
Oct	0.474	0.475	0.474	1.135	1.135	1.126	0.721	0.78	0.472	1.681	1.702	0.473
Nov	0.383	0.384	0.383	1.135	1.135	1.125	0.654	0.719	0.391	1.676	1.702	0.392
Dec	0.316	0.316	0.316	1.135	1.135	1.125	0.605	0.675	0.327	1.673	1.703	0.327

Table D-13: Thermodynamic properties for Binary ORC System simulations at 3.1km depth with a CO2 mass flow rate of 70kg/s and a reservoir temperature of 100°C.

Well Temp	100°C											
Well Depth	3.1 km											
CO2 Mass Flow	70 kg/s											
	Pressure (kPa)											
State Point	1	1'	2	3	4	4'	5	5'	6	7	8	9
Jan	2985	2986	33030	30000	11189	10946	10946	2986	376.7	376.7	127.2	127.2
Feb	3285	3286	32796	30000	11189	10946	10946	3286	393.2	393.2	144.7	144.7
Mar	3748	3749	32456	30000	11189	10945	10945	3749	416	416	172.7	172.7
Apr	4409	4410	31989	30000	11189	10945	10945	4410	439.7	439.7	214.3	214.3
May	5116	5117	31471	30000	11189	10945	10945	5117	470.8	470.8	260.6	260.6
June	5836	5838	30853	30000	11189	10944	10944	5838	503.5	503.5	309.3	309.3
July	6173	6174	30488	30000	11189	10944	10944	6174	517.1	517.1	332.3	332.3
Aug	6045	6047	30641	30000	11189	10944	10944	6047	510.3	510.3	323.6	323.6
Sept	5361	5362	31275	30000	11189	10945	10945	5362	477.2	477.2	277	277
Oct	5135	5137	31455	30000	11189	10945	10945	5137	470.8	470.8	261.9	261.9
Nov	4029	4030	32257	30000	11189	10945	10945	4030	427.7	427.7	190.2	190.2
Dec	3286	3288	32794	30000	11189	10946	10946	3288	393.2	393.2	144.8	144.8
	Temperature (°C)											
State Point	1	1'	2	3	4	4'	5	5'	6	7	8	9
Jan	-5.73	-5.72	11.98	100	51.67	49.98	25.31	-5.72	-5.58	27.5	0.162	-5.73
Feb	-2.21	-2.2	16.45	100	51.67	50.02	27.33	-2.2	-2.08	29	3.547	-2.21
Mar	2.773	2.785	22.96	100	51.67	50.07	30.01	2.785	2.881	31	8.242	2.773
Apr	9.159	9.17	31.7	100	51.67	50.13	32.82	9.17	9.225	33	14	9.159
May	15.23	15.24	40.6	100	51.67	50.19	35.86	15.24	15.25	35.5	19.52	15.23
June	20.79	20.8	49.63	100	51.67	50.24	38.71	20.8	20.89	38	24.54	20.79
July	23.2	23.21	54.03	100	51.67	50.26	39.81	23.21	23.3	39	26.68	23.2
Aug	22.3	22.31	52.3	100	51.67	50.25	39.3	22.31	22.4	38.5	25.85	22.3
Sept	17.19	17.2	43.66	100	51.67	50.2	36.54	17.2	17.2	36	21.2	17.19
Oct	15.39	15.4	40.85	100	51.67	50.19	35.88	15.4	15.41	35.5	19.64	15.39
Nov	5.583	5.595	26.74	100	51.67	50.09	31.37	5.595	5.674	32	10.82	5.583
Dec	-2.2	-2.19	16.47	100	51.67	50.02	27.33	-2.19	-2.06	29	3.56	-2.2
	Enthalpy (kJ/kg)											
State Point	1	1'	2	3	4	4'	5	5'	6	7	8	9
Jan	73.46	73.68	103.7	278.9	246.9	242.7	142.2	142.2	74.95	479.2	444.3	74.57
Feb	81.77	81.98	112	278.9	246.9	242.9	147.8	147.8	82.92	481.2	448.9	82.54
Mar	93.98	94.19	124.2	278.9	246.9	243.2	155.5	155.5	94.34	483.9	455.3	93.96
Apr	110.6	110.8	140.8	278.9	246.9	243.6	164.1	164.1	109.2	486.5	463.1	108.8
May	127.8	128	158	278.9	246.9	244	174.2	174.2	123.5	489.9	470.4	123.1
June	145.7	145.8	175.8	278.9	246.9	244.3	184.6	184.6	137.2	493.2	477.1	136.4
July	154.6	154.8	184.7	278.9	246.9	244.4	189	189	143	494.5	479.9	142.3
Aug	151.1	151.2	181.2	278.9	246.9	244.4	186.9	186.9	140.8	493.8	478.8	140.1
Sept	133.8	134	164	278.9	246.9	244.1	176.6	176.6	128.1	490.5	472.6	127.8
Oct	128.3	128.5	158.4	278.9	246.9	244	174.3	174.3	123.8	489.9	470.6	123.5
Nov	101.1	101.3	131.3	278.9	246.9	243.4	159.6	159.6	100.8	485.2	458.8	100.5
Dec	81.81	82.02	112	278.9	246.9	242.9	147.8	147.8	82.96	481.2	449	82.57
	Entropy (kJ/kg-K)											
State Point	1	1'	2	3	4	4'	5	5'	6	7	8	9
Jan	0.286	0.287	0.286	0.831	0.831	0.819	0.498	0.543	0.297	1.657	1.68	0.297
Feb	0.316	0.316	0.316	0.831	0.831	0.82	0.516	0.559	0.327	1.658	1.679	0.327
Mar	0.358	0.359	0.358	0.831	0.831	0.821	0.542	0.582	0.368	1.66	1.678	0.368
Apr	0.415	0.416	0.415	0.831	0.831	0.822	0.57	0.605	0.421	1.661	1.676	0.421
May	0.473	0.473	0.473	0.831	0.831	0.823	0.603	0.634	0.471	1.664	1.675	0.471
June	0.531	0.532	0.531	0.831	0.831	0.824	0.636	0.663	0.516	1.666	1.676	0.517
July	0.56	0.56	0.56	0.831	0.831	0.825	0.65	0.676	0.536	1.667	1.676	0.536
Aug	0.548	0.549	0.548	0.831	0.831	0.824	0.644	0.67	0.529	1.666	1.675	0.529
Sept	0.492	0.493	0.492	0.831	0.831	0.823	0.611	0.64	0.487	1.664	1.675	0.487
Oct	0.474	0.475	0.474	0.831	0.831	0.823	0.603	0.634	0.472	1.664	1.675	0.473
Nov	0.383	0.384	0.383	0.831	0.831	0.821	0.555	0.593	0.392	1.661	1.677	0.392
Dec	0.316	0.317	0.316	0.831	0.831	0.82	0.516	0.559	0.327	1.658	1.679	0.327

Table D-14: Thermodynamic properties for Binary ORC System simulations at 3.1km depth with a CO2 mass flow rate of 90kg/s and a reservoir temperature of 100°C.

Well Temp	100°C											
Well Depth	3.1 km											
CO2 Mass Flow	90 kg/s											
	Pressure (kPa)											
State Point	1	1'	2	3	4	4'	5	5'	6	7	8	9
Jan	2985	2987	32919	30000	10669	10257	10257	2987	366	366	127.2	127.2
Feb	3285	3287	32683	30000	10669	10257	10257	3287	382.1	382.1	144.7	144.7
Mar	3748	3750	32340	30000	10669	10256	10256	3750	404.5	404.5	172.7	172.7
Apr	4409	4411	31867	30000	10669	10256	10256	4411	427.7	427.7	214.3	214.3
May	5116	5118	31343	30000	10669	10255	10255	5118	452	452	260.6	260.6
June	5836	5839	30716	30000	10669	10255	10255	5839	490.3	490.3	309.3	309.3
July	6173	6175	30347	30000	10669	10255	10255	6175	496.9	496.9	332.3	332.3
Aug	6045	6048	30502	30000	10669	10255	10255	6048	490.3	490.3	323.6	323.6
Sept	5361	5363	31144	30000	10669	10255	10255	5363	464.5	464.5	277	277
Oct	5135	5137	31327	30000	10669	10255	10255	5137	452	452	261.9	261.9
Nov	4029	4031	32138	30000	10669	10256	10256	4031	416	416	190.2	190.2
Dec	3286	3288	32682	30000	10669	10257	10257	3288	382.1	382.1	144.8	144.8
	Temperature (°C)											
State Point	1	1'	2	3	4	4'	5	5'	6	7	8	9
Jan	-5.73	-5.71	11.92	100	49.33	47.01	24.21	-5.71	-5.58	26.5	-0.07	-5.73
Feb	-2.21	-2.19	16.39	100	49.33	47.03	26.24	-2.19	-2.08	28	3.311	-2.21
Mar	2.773	2.793	22.9	100	49.33	47.06	28.93	2.793	2.877	30	8.004	2.773
Apr	9.159	9.177	31.62	100	49.33	47.1	31.73	9.177	9.22	32	13.76	9.159
May	15.23	15.25	40.51	100	49.33	47.14	34.33	15.25	15.25	34	19.15	15.23
June	20.79	20.81	49.51	100	49.33	47.17	37.6	20.81	20.89	37	24.3	20.79
July	23.2	23.22	53.9	100	49.33	47.18	38.26	23.22	23.3	37.5	26.32	23.2
Aug	22.3	22.32	52.18	100	49.33	47.18	37.74	22.32	22.4	37	25.49	22.3
Sept	17.19	17.21	43.56	100	49.33	47.15	35.44	17.21	17.19	35	20.96	17.19
Oct	15.39	15.41	40.76	100	49.33	47.14	34.35	15.41	15.4	34	19.28	15.39
Nov	5.583	5.602	26.67	100	49.33	47.08	30.29	5.602	5.67	31	10.58	5.583
Dec	-2.2	-2.18	16.41	100	49.33	47.03	26.24	-2.18	-2.07	28	3.324	-2.2
	Enthalpy (kJ/kg)											
State Point	1	1'	2	3	4	4'	5	5'	6	7	8	9
Jan	73.46	73.63	103.6	278.9	245.8	242.2	140.7	140.7	74.93	477.8	443.9	74.57
Feb	81.77	81.94	111.9	278.9	245.8	242.4	146.4	146.4	82.91	479.8	448.6	82.54
Mar	93.98	94.15	124.1	278.9	245.8	242.6	154.4	154.4	94.33	482.5	454.9	93.96
Apr	110.6	110.7	140.6	278.9	245.8	242.9	163.4	163.4	109.1	485.2	462.7	108.8
May	127.8	128	157.8	278.9	245.8	243.2	172.4	172.4	123.4	487.9	469.8	123.1
June	145.7	145.8	175.6	278.9	245.8	243.5	185.3	185.3	137.2	491.8	476.7	136.4
July	154.6	154.7	184.5	278.9	245.8	243.6	188.1	188.1	143	492.5	479.3	142.3
Aug	151.1	151.2	181	278.9	245.8	243.5	185.9	185.9	140.8	491.8	478.2	140.1
Sept	133.8	134	163.8	278.9	245.8	243.3	176.5	176.5	128.1	489.2	472.2	127.8
Oct	128.3	128.4	158.3	278.9	245.8	243.2	172.5	172.5	123.8	487.9	470	123.5
Nov	101.1	101.3	131.2	278.9	245.8	242.7	158.7	158.7	100.8	483.9	458.4	100.5
Dec	81.81	81.98	111.9	278.9	245.8	242.4	146.4	146.4	82.94	479.8	448.6	82.57
	Entropy (kJ/kg-K)											
State Point	1	1'	2	3	4	4'	5	5'	6	7	8	9
Jan	0.286	0.287	0.286	0.831	0.831	0.822	0.495	0.537	0.297	1.656	1.678	0.297
Feb	0.316	0.316	0.316	0.831	0.831	0.823	0.515	0.554	0.327	1.657	1.677	0.327
Mar	0.358	0.359	0.358	0.831	0.831	0.823	0.541	0.577	0.368	1.659	1.676	0.368
Apr	0.415	0.416	0.415	0.831	0.831	0.824	0.571	0.602	0.421	1.661	1.675	0.421
May	0.473	0.473	0.473	0.831	0.831	0.825	0.6	0.627	0.471	1.662	1.673	0.471
June	0.531	0.531	0.531	0.831	0.831	0.826	0.642	0.666	0.516	1.665	1.674	0.517
July	0.56	0.56	0.56	0.831	0.831	0.826	0.651	0.673	0.536	1.666	1.673	0.536
Aug	0.548	0.549	0.548	0.831	0.831	0.826	0.644	0.666	0.529	1.665	1.673	0.529
Sept	0.492	0.493	0.492	0.831	0.831	0.825	0.614	0.64	0.487	1.663	1.673	0.487
Oct	0.474	0.475	0.474	0.831	0.831	0.825	0.6	0.627	0.472	1.662	1.673	0.473
Nov	0.383	0.384	0.383	0.831	0.831	0.824	0.555	0.59	0.392	1.66	1.676	0.392
Dec	0.316	0.316	0.316	0.831	0.831	0.823	0.515	0.554	0.327	1.657	1.677	0.327

Table D-15: Thermodynamic properties for Binary ORC System simulations at 3.1km depth with a CO2 mass flow rate of 120kg/s and a reservoir temperature of 100°C.

Well Temp	100°C											
Well Depth	3.1 km											
CO2 Mass Flow	120 kg/s											
	Pressure (kPa)											
State Point	1	1'	2	3	4	4'	5	5'	6	7	8	9
Jan	2985	2986	33009	30000	11276	11060	11060	2986	376.7	376.7	127.2	127.2
Feb	3285	3286	32775	30000	11276	11060	11060	3286	393.2	393.2	144.7	144.7
Mar	3748	3749	32434	30000	11276	11060	11060	3749	416	416	172.7	172.7
Apr	4409	4410	31966	30000	11276	11060	11060	4410	445.8	445.8	214.3	214.3
May	5116	5117	31447	30000	11276	11059	11059	5117	470.8	470.8	260.6	260.6
June	5836	5838	30828	30000	11276	11059	11059	5838	510.3	510.3	309.3	309.3
July	6173	6174	30462	30000	11276	11059	11059	6174	517.1	517.1	332.3	332.3
Aug	6045	6047	30615	30000	11276	11059	11059	6047	510.3	510.3	323.6	323.6
Sept	5361	5363	31251	30000	11276	11059	11059	5363	483.7	483.7	277	277
Oct	5135	5137	31431	30000	11276	11059	11059	5137	470.8	470.8	261.9	261.9
Nov	4029	4030	32235	30000	11276	11060	11060	4030	427.7	427.7	190.2	190.2
Dec	3286	3288	32773	30000	11276	11060	11060	3288	393.2	393.2	144.8	144.8
	Temperature (°C)											
State Point	1	1'	2	3	4	4'	5	5'	6	7	8	9
Jan	-5.73	-5.72	11.97	100	52.05	50.65	25.29	-5.72	-5.58	27.5	0.162	-5.73
Feb	-2.21	-2.2	16.44	100	52.05	50.68	27.32	-2.2	-2.08	29	3.547	-2.21
Mar	2.773	2.786	22.95	100	52.05	50.71	30.02	2.786	2.881	31	8.242	2.773
Apr	9.159	9.171	31.68	100	52.05	50.76	33.27	9.171	9.227	33.5	14.12	9.159
May	15.23	15.24	40.59	100	52.05	50.8	35.89	15.24	15.25	35.5	19.52	15.23
June	20.79	20.8	49.61	100	52.05	50.84	39.16	20.8	20.78	38.5	24.66	20.79
July	23.2	23.21	54	100	52.05	50.86	39.86	23.21	23.3	39	26.68	23.2
Aug	22.3	22.31	52.28	100	52.05	50.85	39.34	22.31	22.4	38.5	25.85	22.3
Sept	17.19	17.2	43.65	100	52.05	50.82	37.01	17.2	17.2	36.5	21.32	17.19
Oct	15.39	15.4	40.83	100	52.05	50.8	35.91	15.4	15.41	35.5	19.64	15.39
Nov	5.583	5.596	26.73	100	52.05	50.73	31.38	5.596	5.674	32	10.82	5.583
Dec	-2.2	-2.19	16.46	100	52.05	50.68	27.32	-2.19	-2.06	29	3.56	-2.2
	Enthalpy (kJ/kg)											
State Point	1	1'	2	3	4	4'	5	5'	6	7	8	9
Jan	73.46	73.61	103.7	278.9	247.1	244	141.9	141.9	74.95	479.2	444.3	74.57
Feb	81.77	81.92	112	278.9	247.1	244.1	147.5	147.5	82.92	481.2	448.9	82.54
Mar	93.98	94.13	124.2	278.9	247.1	244.3	155.2	155.2	94.34	483.9	455.3	93.96
Apr	110.6	110.7	140.7	278.9	247.1	244.6	165.1	165.1	109.2	487.2	463.3	108.8
May	127.8	127.9	157.9	278.9	247.1	244.9	173.7	173.7	123.5	489.9	470.4	123.1
June	145.7	145.8	175.8	278.9	247.1	245.1	185.6	185.6	136.7	493.8	477.3	136.4
July	154.6	154.7	184.7	278.9	247.1	245.2	188.3	188.3	143	494.5	479.9	142.3
Aug	151.1	151.2	181.2	278.9	247.1	245.2	186.3	186.3	140.8	493.8	478.8	140.1
Sept	133.8	133.9	163.9	278.9	247.1	245	177.6	177.6	128.1	491.2	472.9	127.8
Oct	128.3	128.4	158.4	278.9	247.1	244.9	173.8	173.8	123.8	489.9	470.6	123.5
Nov	101.1	101.3	131.3	278.9	247.1	244.5	159.3	159.3	100.8	485.2	458.8	100.5
Dec	81.81	81.96	112	278.9	247.1	244.1	147.5	147.5	82.96	481.2	449	82.57
	Entropy (kJ/kg-K)											
State Point	1	1'	2	3	4	4'	5	5'	6	7	8	9
Jan	0.286	0.287	0.286	0.831	0.831	0.822	0.496	0.542	0.297	1.657	1.68	0.297
Feb	0.316	0.316	0.316	0.831	0.831	0.823	0.515	0.558	0.327	1.658	1.679	0.327
Mar	0.358	0.359	0.358	0.831	0.831	0.824	0.54	0.58	0.368	1.66	1.678	0.368
Apr	0.415	0.416	0.415	0.831	0.831	0.824	0.573	0.608	0.421	1.662	1.677	0.421
May	0.473	0.473	0.473	0.831	0.831	0.825	0.601	0.632	0.471	1.664	1.675	0.471
June	0.531	0.531	0.531	0.831	0.831	0.826	0.639	0.667	0.517	1.666	1.676	0.517
July	0.56	0.56	0.56	0.831	0.831	0.826	0.648	0.673	0.536	1.667	1.676	0.536
Aug	0.548	0.548	0.548	0.831	0.831	0.826	0.641	0.667	0.529	1.666	1.675	0.529
Sept	0.492	0.493	0.492	0.831	0.831	0.825	0.614	0.643	0.487	1.665	1.676	0.487
Oct	0.474	0.475	0.474	0.831	0.831	0.825	0.601	0.632	0.472	1.664	1.675	0.473
Nov	0.383	0.384	0.383	0.831	0.831	0.824	0.554	0.592	0.392	1.661	1.677	0.392
Dec	0.316	0.316	0.316	0.831	0.831	0.823	0.515	0.558	0.327	1.658	1.679	0.327

Table D-16: Thermodynamic properties for Binary ORC System simulations at 3.1km depth with a CO2 mass flow rate of 140kg/s and a reservoir temperature of 100°C.

Well Temp	100°C											
Well Depth	3.1 km											
CO2 Mass Flow	140 kg/s											
	Pressure (kPa)											
State Point	1	1'	2	3	4	4'	5	5'	6	7	8	9
Jan	2985	2987	32941	30000	11022	10724	10724	2987	376.7	376.7	127.2	127.2
Feb	3285	3287	32705	30000	11022	10724	10724	3287	387.6	387.6	144.7	144.7
Mar	3748	3750	32362	30000	11022	10723	10723	3750	410.2	410.2	172.7	172.7
Apr	4409	4411	31891	30000	11022	10723	10723	4411	439.7	439.7	214.3	214.3
May	5116	5117	31368	30000	11022	10723	10723	5117	464.5	464.5	260.6	260.6
June	5836	5838	30743	30000	11022	10723	10723	5838	496.9	496.9	309.3	309.3
July	6173	6175	30374	30000	11022	10723	10723	6175	510.3	510.3	332.3	332.3
Aug	6045	6047	30529	30000	11022	10723	10723	6047	503.5	503.5	323.6	323.6
Sept	5361	5363	31170	30000	11022	10723	10723	5363	477.2	477.2	277	277
Oct	5135	5137	31352	30000	11022	10723	10723	5137	464.5	464.5	261.9	261.9
Nov	4029	4031	32161	30000	11022	10723	10723	4031	421.8	421.8	190.2	190.2
Dec	3286	3288	32704	30000	11022	10724	10724	3288	387.6	387.6	144.8	144.8
	Temperature (°C)											
State Point	1	1'	2	3	4	4'	5	5'	6	7	8	9
Jan	-5.73	-5.71	11.93	100	50.93	49.23	25.2	-5.71	-5.58	27.5	0.162	-5.73
Feb	-2.21	-2.2	16.4	100	50.93	49.25	26.79	-2.2	-2.08	28.5	3.428	-2.21
Mar	2.773	2.791	22.91	100	50.93	49.28	29.49	2.791	2.879	30.5	8.123	2.773
Apr	9.159	9.176	31.63	100	50.93	49.32	32.75	9.176	9.225	33	14	9.159
May	15.23	15.25	40.53	100	50.93	49.35	35.36	15.25	15.25	35	19.39	15.23
June	20.79	20.81	49.53	100	50.93	49.38	38.21	20.81	20.89	37.5	24.42	20.79
July	23.2	23.22	53.92	100	50.93	49.4	39.31	23.22	23.3	38.5	26.56	23.2
Aug	22.3	22.32	52.2	100	50.93	49.39	38.79	22.32	22.4	38	25.73	22.3
Sept	17.19	17.21	43.58	100	50.93	49.36	36.48	17.21	17.2	36	21.2	17.19
Oct	15.39	15.41	40.78	100	50.93	49.35	35.38	15.41	15.41	35	19.52	15.39
Nov	5.583	5.601	26.68	100	50.93	49.3	30.85	5.601	5.672	31.5	10.7	5.583
Dec	-2.2	-2.18	16.42	100	50.93	49.25	26.79	-2.18	-2.06	28.5	3.441	-2.2
	Enthalpy (kJ/kg)											
State Point	1	1'	2	3	4	4'	5	5'	6	7	8	9
Jan	73.46	73.59	103.6	278.9	246.6	243.7	142.4	142.4	74.95	479.2	444.3	74.57
Feb	81.77	81.9	111.9	278.9	246.6	243.8	146.8	146.8	82.91	480.5	448.7	82.54
Mar	93.98	94.11	124.1	278.9	246.6	244	154.6	154.6	94.33	483.2	455.1	93.96
Apr	110.6	110.7	140.6	278.9	246.6	244.3	164.8	164.8	109.2	486.5	463.1	108.8
May	127.8	127.9	157.8	278.9	246.6	244.5	173.6	173.6	123.4	489.2	470.2	123.1
June	145.7	145.8	175.7	278.9	246.6	244.7	184.2	184.2	137.2	492.5	476.9	136.4
July	154.6	154.7	184.6	278.9	246.6	244.8	188.7	188.7	143	493.8	479.7	142.3
Aug	151.1	151.2	181.1	278.9	246.6	244.8	186.5	186.5	140.8	493.2	478.6	140.1
Sept	133.8	133.9	163.8	278.9	246.6	244.6	177.6	177.6	128.1	490.5	472.6	127.8
Oct	128.3	128.4	158.3	278.9	246.6	244.5	173.6	173.6	123.8	489.2	470.4	123.5
Nov	101.1	101.3	131.2	278.9	246.6	244.1	158.8	158.8	100.8	484.5	458.6	100.5
Dec	81.81	81.94	111.9	278.9	246.6	243.8	146.8	146.8	82.95	480.5	448.8	82.57
	Entropy (kJ/kg-K)											
State Point	1	1'	2	3	4	4'	5	5'	6	7	8	9
Jan	0.286	0.286	0.286	0.831	0.831	0.824	0.499	0.544	0.297	1.657	1.68	0.297
Feb	0.316	0.316	0.316	0.831	0.831	0.824	0.514	0.556	0.327	1.658	1.678	0.327
Mar	0.358	0.359	0.358	0.831	0.831	0.825	0.54	0.578	0.368	1.659	1.677	0.368
Apr	0.415	0.416	0.415	0.831	0.831	0.825	0.573	0.607	0.421	1.661	1.676	0.421
May	0.473	0.473	0.473	0.831	0.831	0.826	0.602	0.631	0.471	1.663	1.675	0.471
June	0.531	0.531	0.531	0.831	0.831	0.827	0.636	0.662	0.516	1.666	1.675	0.517
July	0.56	0.56	0.56	0.831	0.831	0.827	0.65	0.675	0.536	1.666	1.675	0.536
Aug	0.548	0.548	0.548	0.831	0.831	0.827	0.644	0.668	0.529	1.666	1.675	0.529
Sept	0.492	0.493	0.492	0.831	0.831	0.826	0.615	0.643	0.487	1.664	1.675	0.487
Oct	0.474	0.475	0.474	0.831	0.831	0.826	0.602	0.631	0.472	1.663	1.675	0.473
Nov	0.383	0.384	0.383	0.831	0.831	0.825	0.554	0.59	0.392	1.66	1.676	0.392
Dec	0.316	0.316	0.316	0.831	0.831	0.824	0.514	0.556	0.327	1.658	1.678	0.327

Table D-17: Thermodynamic properties for Binary ORC System simulations at 3.1km depth with a CO2 mass flow rate of 70kg/s and a reservoir temperature of 125°C.

Well Temp	125°C											
Well Depth	3.1 km											
CO2 Mass Flow	70 kg/s											
	Pressure (kPa)											
State Point	1	1'	2	3	4	4'	5	5'	6	7	8	9
Jan	2985	2986	33030	30000	13797	13508	13508	2986	490.3	490.3	127.2	127.2
Feb	3285	3286	32796	30000	13797	13508	13508	3286	503.5	503.5	144.7	144.7
Mar	3748	3749	32456	30000	13797	13508	13508	3749	530.9	530.9	172.7	172.7
Apr	4409	4410	31989	30000	13797	13507	13507	4410	566.6	566.6	214.3	214.3
May	5116	5117	31471	30000	13797	13507	13507	5117	604	604	260.6	260.6
June	5836	5838	30853	30000	13797	13507	13507	5838	635.3	635.3	309.3	309.3
July	6173	6174	30488	30000	13797	13507	13507	6174	651.4	651.4	332.3	332.3
Aug	6045	6047	30641	30000	13797	13507	13507	6047	651.4	651.4	323.6	323.6
Sept	5361	5362	31275	30000	13797	13507	13507	5362	611.8	611.8	277	277
Oct	5135	5137	31455	30000	13797	13507	13507	5137	604	604	261.9	261.9
Nov	4029	4030	32257	30000	13797	13508	13508	4030	545	545	190.2	190.2
Dec	3286	3288	32794	30000	13797	13508	13508	3288	503.5	503.5	144.8	144.8
	Temperature (°C)											
State Point	1	1'	2	3	4	4'	5	5'	6	7	8	9
Jan	-5.73	-5.72	11.98	125	74.18	71.25	32.42	-5.72	-5.54	37	2.494	-5.73
Feb	-2.21	-2.2	16.45	125	74.18	71.31	34.28	-2.2	-2.04	38	5.766	-2.21
Mar	2.773	2.785	22.96	125	74.18	71.4	37.36	2.785	2.922	40	10.47	2.773
Apr	9.159	9.17	31.7	125	74.18	71.52	41.11	9.17	9.272	42.5	16.37	9.159
May	15.23	15.24	40.6	125	74.18	71.63	44.6	15.24	15.31	45	21.89	15.23
June	20.79	20.8	49.63	125	74.18	71.73	47.38	20.8	20.83	47	26.79	20.79
July	23.2	23.21	54.03	125	74.18	71.77	48.65	23.21	23.22	48	28.93	23.2
Aug	22.3	22.31	52.3	125	74.18	71.76	48.5	22.31	22.33	48	28.23	22.3
Sept	17.19	17.2	43.66	125	74.18	71.66	45.42	17.2	17.25	45.5	23.57	17.19
Oct	15.39	15.4	40.85	125	74.18	71.63	44.63	15.4	15.47	45	22.02	15.39
Nov	5.583	5.595	26.74	125	74.18	71.45	38.94	5.595	5.716	41	13.06	5.583
Dec	-2.2	-2.19	16.47	125	74.18	71.31	34.28	-2.19	-2.03	38	5.778	-2.2
	Enthalpy (kJ/kg)											
State Point	1	1'	2	3	4	4'	5	5'	6	7	8	9
Jan	73.46	73.68	103.7	328.8	296.2	290.4	155.9	155.9	75.12	491.8	448.1	74.57
Feb	81.77	81.98	112	328.8	296.2	290.6	160.8	160.8	83.09	493.2	452.6	82.54
Mar	93.98	94.19	124.2	328.8	296.2	290.9	169.3	169.3	94.52	495.8	459.1	93.96
Apr	110.6	110.8	140.8	328.8	296.2	291.3	180.2	180.2	109.4	499.1	467.1	108.8
May	127.8	128	158	328.8	296.2	291.7	190.9	190.9	123.7	502.4	474.6	123.1
June	145.7	145.8	175.8	328.8	296.2	292	200.1	200.1	137	505	481.1	136.4
July	154.6	154.8	184.7	328.8	296.2	292.2	204.4	204.4	142.8	506.3	484	142.3
Aug	151.1	151.2	181.2	328.8	296.2	292.1	203.9	203.9	140.6	506.3	483.1	140.1
Sept	133.8	134	164	328.8	296.2	291.8	193.6	193.6	128.3	503.1	476.8	127.8
Oct	128.3	128.5	158.4	328.8	296.2	291.7	191	191	124	502.4	474.8	123.5
Nov	101.1	101.3	131.3	328.8	296.2	291.1	173.8	173.8	101	497.1	462.6	100.5
Dec	81.81	82.02	112	328.8	296.2	290.6	160.8	160.8	83.13	493.2	452.6	82.57
	Entropy (kJ/kg-K)											
State Point	1	1'	2	3	4	4'	5	5'	6	7	8	9
Jan	0.286	0.287	0.286	0.96	0.96	0.946	0.533	0.594	0.297	1.665	1.693	0.297
Feb	0.316	0.316	0.316	0.96	0.96	0.946	0.549	0.607	0.327	1.666	1.692	0.327
Mar	0.358	0.359	0.358	0.96	0.96	0.947	0.576	0.631	0.368	1.668	1.691	0.368
Apr	0.415	0.416	0.415	0.96	0.96	0.948	0.611	0.662	0.421	1.67	1.69	0.421
May	0.473	0.473	0.473	0.96	0.96	0.949	0.645	0.692	0.471	1.673	1.69	0.471
June	0.531	0.532	0.531	0.96	0.96	0.95	0.674	0.716	0.516	1.675	1.689	0.517
July	0.56	0.56	0.56	0.96	0.96	0.951	0.687	0.728	0.536	1.676	1.689	0.536
Aug	0.548	0.549	0.548	0.96	0.96	0.95	0.686	0.727	0.529	1.676	1.69	0.529
Sept	0.492	0.493	0.492	0.96	0.96	0.95	0.653	0.698	0.487	1.673	1.689	0.487
Oct	0.474	0.475	0.474	0.96	0.96	0.949	0.645	0.692	0.472	1.673	1.689	0.473
Nov	0.383	0.384	0.383	0.96	0.96	0.948	0.591	0.644	0.392	1.669	1.69	0.392
Dec	0.316	0.317	0.316	0.96	0.96	0.946	0.549	0.607	0.327	1.666	1.692	0.327

Table D-18: Thermodynamic properties for Binary ORC System simulations at 3.1km depth with a CO2 mass flow rate of 90kg/s and a reservoir temperature of 125°C.

Well Temp	125°C											
Well Depth	3.1 km											
CO2 Mass Flow	90 kg/s											
	Pressure (kPa)											
State Point	1	1'	2	3	4	4'	5	5'	6	7	8	9
Jan	2985	2987	32919	30000	13175	12683	12683	2987	470.8	470.8	127.2	127.2
Feb	3285	3287	32683	30000	13175	12683	12683	3287	483.7	483.7	144.7	144.7
Mar	3748	3750	32340	30000	13175	12683	12683	3750	510.3	510.3	172.7	172.7
Apr	4409	4411	31867	30000	13175	12682	12682	4411	537.9	537.9	214.3	214.3
May	5116	5118	31343	30000	13175	12682	12682	5118	573.9	573.9	260.6	260.6
June	5836	5839	30716	30000	13175	12681	12681	5839	604	604	309.3	309.3
July	6173	6175	30347	30000	13175	12681	12681	6175	619.5	619.5	332.3	332.3
Aug	6045	6048	30502	30000	13175	12681	12681	6048	611.8	611.8	323.6	323.6
Sept	5361	5363	31144	30000	13175	12682	12682	5363	581.4	581.4	277	277
Oct	5135	5137	31327	30000	13175	12682	12682	5137	573.9	573.9	261.9	261.9
Nov	4029	4031	32138	30000	13175	12683	12683	4031	523.9	523.9	190.2	190.2
Dec	3286	3288	32682	30000	13175	12683	12683	3288	483.7	483.7	144.8	144.8
	Temperature (°C)											
State Point	1	1'	2	3	4	4'	5	5'	6	7	8	9
Jan	-5.73	-5.71	11.92	125	71.14	67.55	31.16	-5.71	35.5	2.114	-5.73	-5.73
Feb	-2.21	-2.19	16.39	125	71.14	67.6	33.02	-2.19	36.5	5.385	-2.21	-2.21
Mar	2.773	2.793	22.9	125	71.14	67.66	36.12	2.793	38.5	10.09	2.773	2.773
Apr	9.159	9.177	31.62	125	71.14	67.75	39.42	9.177	40.5	15.86	9.159	9.159
May	15.23	15.25	40.51	125	71.14	67.82	42.91	15.25	43	21.38	15.23	15.23
June	20.79	20.81	49.51	125	71.14	67.9	45.66	20.81	45	26.28	20.79	20.79
July	23.2	23.22	53.9	125	71.14	67.93	46.92	23.22	46	28.42	23.2	23.2
Aug	22.3	22.32	52.18	125	71.14	67.92	46.34	22.32	45.5	27.59	22.3	22.3
Sept	17.19	17.21	43.56	125	71.14	67.85	43.72	17.21	43.5	23.06	17.19	17.19
Oct	15.39	15.41	40.76	125	71.14	67.83	42.94	15.41	43	21.51	15.39	15.39
Nov	5.583	5.602	26.67	125	71.14	67.7	37.71	5.602	39.5	12.68	5.583	5.583
Dec	-2.2	-2.18	16.41	125	71.14	67.6	33.03	-2.18	36.5	5.398	-2.2	-2.2
	Enthalpy (kJ/kg)											
State Point	1	1'	2	3	4	4'	5	5'	6	7	8	9
Jan	73.46	73.63	103.6	328.8	294.6	289.6	154.3	154.3	75.09	489.9	447.5	74.57
Feb	81.77	81.94	111.9	328.8	294.6	289.8	159.4	159.4	83.06	491.2	451.9	82.54
Mar	93.98	94.15	124.1	328.8	294.6	290	168.2	168.2	94.49	493.8	458.4	93.96
Apr	110.6	110.7	140.6	328.8	294.6	290.3	178.1	178.1	109.3	496.5	466.2	108.8
May	127.8	128	157.8	328.8	294.6	290.6	189.4	189.4	123.6	499.8	473.7	123.1
June	145.7	145.8	175.6	328.8	294.6	290.9	199.1	199.1	136.9	502.4	480.2	136.4
July	154.6	154.7	184.5	328.8	294.6	291	203.7	203.7	142.7	503.7	483.1	142.3
Aug	151.1	151.2	181	328.8	294.6	291	201.6	201.6	140.5	503.1	482	140.1
Sept	133.8	134	163.8	328.8	294.6	290.7	192.2	192.2	128.3	500.4	475.9	127.8
Oct	128.3	128.4	158.3	328.8	294.6	290.6	189.5	189.5	124	499.8	473.9	123.5
Nov	101.1	101.3	131.2	328.8	294.6	290.2	172.9	172.9	101	495.2	461.9	100.5
Dec	81.81	81.98	111.9	328.8	294.6	289.8	159.4	159.4	83.1	491.2	452	82.57
	Entropy (kJ/kg-K)											
State Point	1	1'	2	3	4	4'	5	5'	6	7	8	9
Jan	0.286	0.287	0.286	0.96	0.96	0.949	0.531	0.588	0.297	1.664	1.691	0.297
Feb	0.316	0.316	0.316	0.96	0.96	0.95	0.547	0.602	0.327	1.665	1.69	0.327
Mar	0.358	0.359	0.358	0.96	0.96	0.95	0.576	0.627	0.368	1.666	1.689	0.368
Apr	0.415	0.416	0.415	0.96	0.96	0.951	0.608	0.655	0.421	1.668	1.687	0.421
May	0.473	0.473	0.473	0.96	0.96	0.952	0.644	0.686	0.471	1.671	1.687	0.471
June	0.531	0.531	0.531	0.96	0.96	0.953	0.674	0.713	0.516	1.673	1.686	0.517
July	0.56	0.56	0.56	0.96	0.96	0.953	0.689	0.725	0.536	1.674	1.686	0.536
Aug	0.548	0.549	0.548	0.96	0.96	0.953	0.682	0.719	0.529	1.673	1.686	0.529
Sept	0.492	0.493	0.492	0.96	0.96	0.952	0.653	0.693	0.487	1.671	1.686	0.487
Oct	0.474	0.475	0.474	0.96	0.96	0.952	0.644	0.687	0.472	1.671	1.686	0.473
Nov	0.383	0.384	0.383	0.96	0.96	0.951	0.591	0.641	0.392	1.667	1.688	0.392
Dec	0.316	0.316	0.316	0.96	0.96	0.95	0.547	0.602	0.327	1.665	1.69	0.327

Table D-19: Thermodynamic properties for Binary ORC System simulations at 3.1km depth with a CO2 mass flow rate of 120kg/s and a reservoir temperature of 125°C.

Well Temp	125°C											
Well Depth	3.1 km											
CO2 Mass Flow	120 kg/s											
	Pressure (kPa)											
State Point	1	1'	2	3	4	4'	5	5'	6	7	8	9
Jan	2985	2986	33009	30000	13901	13644	13644	2986	496.9	496.9	127.2	127.2
Feb	3285	3286	32775	30000	13901	13644	13644	3286	510.3	510.3	144.7	144.7
Mar	3748	3749	32434	30000	13901	13644	13644	3749	537.9	537.9	172.7	172.7
Apr	4409	4410	31966	30000	13901	13644	13644	4410	573.9	573.9	214.3	214.3
May	5116	5117	31447	30000	13901	13644	13644	5117	611.8	611.8	260.6	260.6
June	5836	5838	30828	30000	13901	13644	13644	5838	643.3	643.3	309.3	309.3
July	6173	6174	30462	30000	13901	13644	13644	6174	659.5	659.5	332.3	332.3
Aug	6045	6047	30615	30000	13901	13644	13644	6047	651.4	651.4	323.6	323.6
Sept	5361	5363	31251	30000	13901	13644	13644	5363	619.5	619.5	277	277
Oct	5135	5137	31431	30000	13901	13644	13644	5137	611.8	611.8	261.9	261.9
Nov	4029	4030	32235	30000	13901	13644	13644	4030	552.1	552.1	190.2	190.2
Dec	3286	3288	32773	30000	13901	13644	13644	3288	510.3	510.3	144.8	144.8
	Temperature (°C)											
State Point	1	1'	2	3	4	4'	5	5'	6	7	8	9
Jan	-5.73	-5.72	11.97	125	74.68	72.33	32.81	-5.72	-5.54	37.5	2.621	-5.73
Feb	-2.21	-2.2	16.44	125	74.68	72.38	34.68	-2.2	-2.04	38.5	5.893	-2.21
Mar	2.773	2.786	22.95	125	74.68	72.44	37.77	2.786	2.924	40.5	10.6	2.773
Apr	9.159	9.171	31.68	125	74.68	72.52	41.53	9.171	9.275	43	16.5	9.159
May	15.23	15.24	40.59	125	74.68	72.6	45.03	15.24	15.31	45.5	22.02	15.23
June	20.79	20.8	49.61	125	74.68	72.68	47.82	20.8	20.83	47.5	26.92	20.79
July	23.2	23.21	54	125	74.68	72.71	49.09	23.21	23.23	48.5	29.05	23.2
Aug	22.3	22.31	52.28	125	74.68	72.7	48.51	22.31	22.33	48	28.23	22.3
Sept	17.19	17.2	43.65	125	74.68	72.63	45.85	17.2	17.26	46	23.7	17.19
Oct	15.39	15.4	40.83	125	74.68	72.61	45.06	15.4	15.47	45.5	22.14	15.39
Nov	5.583	5.596	26.73	125	74.68	72.48	39.36	5.596	5.719	41.5	13.19	5.583
Dec	-2.2	-2.19	16.46	125	74.68	72.38	34.68	-2.19	-2.02	38.5	5.906	-2.2
	Enthalpy (kJ/kg)											
State Point	1	1'	2	3	4	4'	5	5'	6	7	8	9
Jan	73.46	73.61	103.7	328.8	296.4	292.2	156.6	156.6	75.13	492.5	448.3	74.57
Feb	81.77	81.92	112	328.8	296.4	292.3	161.6	161.6	83.1	493.8	452.8	82.54
Mar	93.98	94.13	124.2	328.8	296.4	292.5	170.1	170.1	94.53	496.5	459.3	93.96
Apr	110.6	110.7	140.7	328.8	296.4	292.8	180.9	180.9	109.4	499.8	467.3	108.8
May	127.8	127.9	157.9	328.8	296.4	293.1	191.7	191.7	123.7	503.1	474.8	123.1
June	145.7	145.8	175.8	328.8	296.4	293.3	200.8	200.8	137	505.7	481.4	136.4
July	154.6	154.7	184.7	328.8	296.4	293.4	205.1	205.1	142.8	507	484.2	142.3
Aug	151.1	151.2	181.2	328.8	296.4	293.4	203.2	203.2	140.6	506.3	483.1	140.1
Sept	133.8	133.9	163.9	328.8	296.4	293.2	194.3	194.3	128.3	503.7	477.1	127.8
Oct	128.3	128.4	158.4	328.8	296.4	293.1	191.8	191.8	124.1	503.1	475	123.5
Nov	101.1	101.3	131.3	328.8	296.4	292.7	174.6	174.6	101	497.8	462.8	100.5
Dec	81.81	81.96	112	328.8	296.4	292.3	161.6	161.6	83.14	493.8	452.8	82.57
	Entropy (kJ/kg-K)											
State Point	1	1'	2	3	4	4'	5	5'	6	7	8	9
Jan	0.286	0.287	0.286	0.96	0.96	0.95	0.534	0.597	0.297	1.666	1.694	0.297
Feb	0.316	0.316	0.316	0.96	0.96	0.95	0.551	0.61	0.327	1.666	1.693	0.327
Mar	0.358	0.359	0.358	0.96	0.96	0.951	0.578	0.634	0.368	1.668	1.692	0.368
Apr	0.415	0.416	0.415	0.96	0.96	0.952	0.613	0.664	0.421	1.671	1.691	0.421
May	0.473	0.473	0.473	0.96	0.96	0.952	0.647	0.694	0.471	1.673	1.69	0.471
June	0.531	0.531	0.531	0.96	0.96	0.953	0.675	0.718	0.516	1.675	1.69	0.517
July	0.56	0.56	0.56	0.96	0.96	0.953	0.689	0.73	0.536	1.676	1.69	0.536
Aug	0.548	0.548	0.548	0.96	0.96	0.953	0.683	0.725	0.529	1.676	1.69	0.529
Sept	0.492	0.493	0.492	0.96	0.96	0.953	0.655	0.701	0.487	1.674	1.69	0.487
Oct	0.474	0.475	0.474	0.96	0.96	0.952	0.647	0.694	0.472	1.673	1.69	0.473
Nov	0.383	0.384	0.383	0.96	0.96	0.951	0.593	0.647	0.392	1.669	1.691	0.392
Dec	0.316	0.316	0.316	0.96	0.96	0.95	0.551	0.61	0.327	1.666	1.693	0.327

Table D-20: Thermodynamic properties for Binary ORC System simulations at 3.1km depth with a CO2 mass flow rate of 140kg/s and a reservoir temperature of 125°C.

Well Temp	125°C											
Well Depth	3.1 km											
CO2 Mass Flow	140 kg/s											
	Pressure (kPa)											
State Point	1	1'	2	3	4	4'	5	5'	6	7	8	9
Jan	2985	2987	32941	30000	13597	13243	13243	2987	483.7	483.7	127.2	127.2
Feb	3285	3287	32705	30000	13597	13243	13243	3287	496.9	496.9	144.7	144.7
Mar	3748	3750	32362	30000	13597	13242	13242	3750	523.9	523.9	172.7	172.7
Apr	4409	4411	31891	30000	13597	13242	13242	4411	559.3	559.3	214.3	214.3
May	5116	5117	31368	30000	13597	13242	13242	5117	596.4	596.4	260.6	260.6
June	5836	5838	30743	30000	13597	13242	13242	5838	627.4	627.4	309.3	309.3
July	6173	6175	30374	30000	13597	13242	13242	6175	643.3	643.3	332.3	332.3
Aug	6045	6047	30529	30000	13597	13242	13242	6047	635.3	635.3	323.6	323.6
Sept	5361	5363	31170	30000	13597	13242	13242	5363	604	604	277	277
Oct	5135	5137	31352	30000	13597	13242	13242	5137	596.4	596.4	261.9	261.9
Nov	4029	4031	32161	30000	13597	13242	13242	4031	537.9	537.9	190.2	190.2
Dec	3286	3288	32704	30000	13597	13243	13243	3288	496.9	496.9	144.8	144.8
	Temperature (°C)											
State Point	1	1'	2	3	4	4'	5	5'	6	7	8	9
Jan	-5.73	-5.71	11.93	125	73.22	70.56	31.97	-5.71	-5.54	36.5	2.367	-5.73
Feb	-2.21	-2.2	16.4	125	73.22	70.6	33.84	-2.2	-2.04	37.5	5.638	-2.21
Mar	2.773	2.791	22.91	125	73.22	70.66	36.94	2.791	2.919	39.5	10.35	2.773
Apr	9.159	9.176	31.63	125	73.22	70.73	40.7	9.176	9.27	42	16.24	9.159
May	15.23	15.25	40.53	125	73.22	70.79	44.2	15.25	15.3	44.5	21.76	15.23
June	20.79	20.81	49.53	125	73.22	70.85	46.98	20.81	20.83	46.5	26.66	20.79
July	23.2	23.22	53.92	125	73.22	70.88	48.24	23.22	23.22	47.5	28.8	23.2
Aug	22.3	22.32	52.2	125	73.22	70.87	47.66	22.32	22.33	47	27.97	22.3
Sept	17.19	17.21	43.58	125	73.22	70.81	45.02	17.21	17.25	45	23.44	17.19
Oct	15.39	15.41	40.78	125	73.22	70.79	44.23	15.41	15.46	44.5	21.89	15.39
Nov	5.583	5.601	26.68	125	73.22	70.69	38.53	5.601	5.714	40.5	12.93	5.583
Dec	-2.2	-2.18	16.42	125	73.22	70.6	33.84	-2.18	-2.03	37.5	5.651	-2.2
	Enthalpy (kJ/kg)											
State Point	1	1'	2	3	4	4'	5	5'	6	7	8	9
Jan	73.46	73.59	103.6	328.8	295.7	291.8	155.2	155.2	75.11	491.2	447.9	74.57
Feb	81.77	81.9	111.9	328.8	295.7	291.9	160.2	160.2	83.08	492.5	452.4	82.54
Mar	93.98	94.11	124.1	328.8	295.7	292.1	168.9	168.9	94.51	495.2	458.8	93.96
Apr	110.6	110.7	140.6	328.8	295.7	292.3	179.9	179.9	109.3	498.5	466.9	108.8
May	127.8	127.9	157.8	328.8	295.7	292.5	190.9	190.9	123.7	501.8	474.4	123.1
June	145.7	145.8	175.7	328.8	295.7	292.7	200.3	200.3	136.9	504.4	480.9	136.4
July	154.6	154.7	184.6	328.8	295.7	292.8	204.7	204.7	142.8	505.7	483.8	142.3
Aug	151.1	151.2	181.1	328.8	295.7	292.8	202.7	202.7	140.6	505	482.6	140.1
Sept	133.8	133.9	163.8	328.8	295.7	292.6	193.6	193.6	128.3	502.4	476.6	127.8
Oct	128.3	128.4	158.3	328.8	295.7	292.5	191	191	124	501.8	474.5	123.5
Nov	101.1	101.3	131.2	328.8	295.7	292.2	173.4	173.4	101	496.5	462.4	100.5
Dec	81.81	81.94	111.9	328.8	295.7	291.9	160.3	160.3	83.12	492.5	452.4	82.57
	Entropy (kJ/kg-K)											
State Point	1	1'	2	3	4	4'	5	5'	6	7	8	9
Jan	0.286	0.286	0.286	0.96	0.96	0.951	0.532	0.592	0.297	1.665	1.693	0.297
Feb	0.316	0.316	0.316	0.96	0.96	0.952	0.548	0.605	0.327	1.666	1.691	0.327
Mar	0.358	0.359	0.358	0.96	0.96	0.952	0.576	0.63	0.368	1.667	1.69	0.368
Apr	0.415	0.416	0.415	0.96	0.96	0.953	0.611	0.661	0.421	1.67	1.689	0.421
May	0.473	0.473	0.473	0.96	0.96	0.954	0.646	0.691	0.471	1.672	1.689	0.471
June	0.531	0.531	0.531	0.96	0.96	0.954	0.675	0.717	0.516	1.674	1.688	0.517
July	0.56	0.56	0.56	0.96	0.96	0.954	0.689	0.729	0.536	1.675	1.688	0.536
Aug	0.548	0.548	0.548	0.96	0.96	0.954	0.683	0.723	0.529	1.675	1.688	0.529
Sept	0.492	0.493	0.492	0.96	0.96	0.954	0.655	0.698	0.487	1.673	1.688	0.487
Oct	0.474	0.475	0.474	0.96	0.96	0.954	0.646	0.692	0.472	1.672	1.689	0.473
Nov	0.383	0.384	0.383	0.96	0.96	0.953	0.591	0.643	0.392	1.668	1.69	0.392
Dec	0.316	0.316	0.316	0.96	0.96	0.952	0.548	0.605	0.327	1.666	1.691	0.327

Table D-21: Thermodynamic properties for Binary ORC System simulations at 3.1km depth with a CO2 mass flow rate of 70kg/s and a reservoir temperature of 150°C.

Well Temp	150°C											
Well Depth	3.1 km											
CO2 Mass Flow	70 kg/s											
	Pressure (kPa)											
State Point	1	1'	2	3	4	4'	5	5'	6	7	8	9
Jan	2985	2986	33030	30000	15710	15377	15377	2986	604	604	127.2	127.2
Feb	3285	3286	32796	30000	15710	15377	15377	3286	627.4	627.4	144.7	144.7
Mar	3748	3749	32456	30000	15710	15377	15377	3749	659.5	659.5	172.7	172.7
Apr	4409	4410	31989	30000	15710	15376	15376	4410	710	710	214.3	214.3
May	5116	5117	31471	30000	15710	15376	15376	5117	754.2	754.2	260.6	260.6
June	5836	5838	30853	30000	15710	15376	15376	5838	800.3	800.3	309.3	309.3
July	6173	6174	30488	30000	15710	15376	15376	6174	819.4	819.4	332.3	332.3
Aug	6045	6047	30641	30000	15710	15376	15376	6047	809.8	809.8	323.6	323.6
Sept	5361	5362	31275	30000	15710	15376	15376	5362	772.4	772.4	277	277
Oct	5135	5137	31455	30000	15710	15376	15376	5137	754.2	754.2	261.9	261.9
Nov	4029	4030	32257	30000	15710	15377	15377	4030	676	676	190.2	190.2
Dec	3286	3288	32794	30000	15710	15377	15377	3288	627.4	627.4	144.8	144.8
	Temperature (°C)											
State Point	1	1'	2	3	4	4'	5	5'	6	7	8	9
Jan	-5.73	-5.72	11.98	150	99.35	94.78	38.2	-5.72	-5.5	45	4.579	-5.73
Feb	-2.21	-2.2	16.45	150	99.35	94.88	40.73	-2.2	-2	46.5	7.983	-2.21
Mar	2.773	2.785	22.96	150	99.35	95.01	44.1	2.785	2.966	48.5	12.69	2.773
Apr	9.159	9.17	31.7	150	99.35	95.17	48.61	9.17	9.326	51.5	18.72	9.159
May	15.23	15.24	40.6	150	99.35	95.33	52.38	15.24	15.37	54	24.23	15.23
June	20.79	20.8	49.63	150	99.35	95.48	55.72	20.8	20.9	56.5	29.25	20.79
July	23.2	23.21	54.03	150	99.35	95.54	57.19	23.21	23.3	57.5	31.38	23.2
Aug	22.3	22.31	52.3	150	99.35	95.52	56.48	22.31	22.4	57	30.55	22.3
Sept	17.19	17.2	43.66	150	99.35	95.38	53.71	17.2	17.32	55	26.04	17.19
Oct	15.39	15.4	40.85	150	99.35	95.34	52.42	15.4	15.53	54	24.36	15.39
Nov	5.583	5.595	26.74	150	99.35	95.08	45.83	5.595	5.764	49.5	15.28	5.583
Dec	-2.2	-2.19	16.47	150	99.35	94.88	40.73	-2.19	-1.99	46.5	7.996	-2.2
	Enthalpy (kJ/kg)											
State Point	1	1'	2	3	4	4'	5	5'	6	7	8	9
Jan	73.46	73.68	103.7	375.2	341.8	334.4	167	167	75.3	502.4	451.5	74.57
Feb	81.77	81.98	112	375.2	341.8	334.6	173.6	173.6	83.28	504.4	456.2	82.54
Mar	93.98	94.19	124.2	375.2	341.8	334.9	182.7	182.7	94.72	507	462.8	93.96
Apr	110.6	110.8	140.8	375.2	341.8	335.3	195.4	195.4	109.6	510.9	471.1	108.8
May	127.8	128	158	375.2	341.8	335.6	206.6	206.6	123.9	514.1	478.7	123.1
June	145.7	145.8	175.8	375.2	341.8	336	217.1	217.1	137.2	517.3	485.6	136.4
July	154.6	154.8	184.7	375.2	341.8	336.1	221.7	221.7	143	518.6	488.4	142.3
Aug	151.1	151.2	181.2	375.2	341.8	336.1	219.5	219.5	140.9	517.9	487.3	140.1
Sept	133.8	134	164	375.2	341.8	335.7	210.7	210.7	128.6	515.4	481.2	127.8
Oct	128.3	128.5	158.4	375.2	341.8	335.6	206.8	206.8	124.3	514.1	478.9	123.5
Nov	101.1	101.3	131.3	375.2	341.8	335.1	187.5	187.5	101.2	508.3	466.3	100.5
Dec	81.81	82.02	112	375.2	341.8	334.6	173.6	173.6	83.32	504.4	456.2	82.57
	Entropy (kJ/kg-K)											
State Point	1	1'	2	3	4	4'	5	5'	6	7	8	9
Jan	0.286	0.287	0.286	1.073	1.073	1.056	0.561	0.636	0.297	1.673	1.706	0.297
Feb	0.316	0.316	0.316	1.073	1.073	1.056	0.582	0.655	0.327	1.674	1.705	0.327
Mar	0.358	0.359	0.358	1.073	1.073	1.057	0.611	0.68	0.368	1.676	1.704	0.368
Apr	0.415	0.416	0.415	1.073	1.073	1.058	0.651	0.716	0.421	1.68	1.704	0.421
May	0.473	0.473	0.473	1.073	1.073	1.059	0.686	0.746	0.471	1.682	1.703	0.471
June	0.531	0.532	0.531	1.073	1.073	1.06	0.717	0.774	0.516	1.685	1.704	0.517
July	0.56	0.56	0.56	1.073	1.073	1.06	0.732	0.786	0.536	1.686	1.704	0.536
Aug	0.548	0.549	0.548	1.073	1.073	1.06	0.725	0.78	0.529	1.686	1.703	0.529
Sept	0.492	0.493	0.492	1.073	1.073	1.059	0.698	0.757	0.487	1.683	1.704	0.487
Oct	0.474	0.475	0.474	1.073	1.073	1.059	0.686	0.746	0.472	1.682	1.703	0.473
Nov	0.383	0.384	0.383	1.073	1.073	1.057	0.626	0.693	0.391	1.678	1.703	0.392
Dec	0.316	0.317	0.316	1.073	1.073	1.056	0.582	0.655	0.327	1.674	1.705	0.327

Table D-22: Thermodynamic properties for Binary ORC System simulations at 3.1km depth with a CO2 mass flow rate of 90kg/s and a reservoir temperature of 150°C.

Well Temp	150°C											
Well Depth	3.1 km											
CO2 Mass Flow	90 kg/s											
Pressure (kPa)												
State Point	1	1'	2	3	4	4'	5	5'	6	7	8	9
Jan	2985	2987	32919	30000	14977	14407	14407	2987	573.9	573.9	127.2	127.2
Feb	3285	3287	32683	30000	14977	14407	14407	3287	588.9	588.9	144.7	144.7
Mar	3748	3750	32340	30000	14977	14407	14407	3750	619.5	619.5	172.7	172.7
Apr	4409	4411	31867	30000	14977	14406	14406	4411	659.5	659.5	214.3	214.3
May	5116	5118	31343	30000	14977	14406	14406	5118	710	710	260.6	260.6
June	5836	5839	30716	30000	14977	14406	14406	5839	745.2	745.2	309.3	309.3
July	6173	6175	30347	30000	14977	14406	14406	6175	772.4	772.4	332.3	332.3
Aug	6045	6048	30502	30000	14977	14406	14406	6048	754.2	754.2	323.6	323.6
Sept	5361	5363	31144	30000	14977	14406	14406	5363	718.7	718.7	277	277
Oct	5135	5137	31327	30000	14977	14406	14406	5137	710	710	261.9	261.9
Nov	4029	4031	32138	30000	14977	14407	14407	4031	635.3	635.3	190.2	190.2
Dec	3286	3288	32682	30000	14977	14407	14407	3288	588.9	588.9	144.8	144.8
Temperature (°C)												
State Point	1	1'	2	3	4	4'	5	5'	6	7	8	9
Jan	-5.73	-5.71	11.92	150	95.61	90.45	37.11	-5.71	-5.51	43	4.05	-5.73
Feb	-2.21	-2.19	16.39	150	95.61	90.52	39.2	-2.19	-2.01	44	7.322	-2.21
Mar	2.773	2.793	22.9	150	95.61	90.62	42.59	2.793	2.953	46	12.03	2.773
Apr	9.159	9.177	31.62	150	95.61	90.75	46.67	9.177	9.307	48.5	17.93	9.159
May	15.23	15.25	40.51	150	95.61	90.87	50.84	15.25	15.35	51.5	23.57	15.23
June	20.79	20.81	49.51	150	95.61	90.98	53.73	20.81	20.88	53.5	28.47	20.79
July	23.2	23.22	53.9	150	95.61	91.03	55.56	23.22	23.28	55	30.73	23.2
Aug	22.3	22.32	52.18	150	95.61	91.01	54.55	22.32	22.38	54	29.77	22.3
Sept	17.19	17.21	43.56	150	95.61	90.91	51.73	17.21	17.3	52	25.25	17.19
Oct	15.39	15.41	40.76	150	95.61	90.87	50.88	15.41	15.51	51.5	23.7	15.39
Nov	5.583	5.602	26.67	150	95.61	90.68	44.32	5.602	5.749	47	14.62	5.583
Dec	-2.2	-2.18	16.41	150	95.61	90.52	39.2	-2.18	-2	44	7.334	-2.2
Enthalpy (kJ/kg)												
State Point	1	1'	2	3	4	4'	5	5'	6	7	8	9
Jan	73.46	73.63	103.6	375.2	339.7	333.2	166.3	166.3	75.25	499.8	450.6	74.57
Feb	81.77	81.94	111.9	375.2	339.7	333.4	171.9	171.9	83.23	501.1	455.1	82.54
Mar	93.98	94.15	124.1	375.2	339.7	333.6	181.4	181.4	94.66	503.7	461.7	93.96
Apr	110.6	110.7	140.6	375.2	339.7	333.9	193.5	193.5	109.5	507	469.8	108.8
May	127.8	128	157.8	375.2	339.7	334.2	206.6	206.6	123.8	510.9	477.6	123.1
June	145.7	145.8	175.6	375.2	339.7	334.5	216.3	216.3	137.1	513.5	484.2	136.4
July	154.6	154.7	184.5	375.2	339.7	334.6	222.6	222.6	143	515.4	487.2	142.3
Aug	151.1	151.2	181	375.2	339.7	334.5	219.1	219.1	140.8	514.1	485.9	140.1
Sept	133.8	134	163.8	375.2	339.7	334.3	209.6	209.6	128.5	511.5	479.8	127.8
Oct	128.3	128.4	158.3	375.2	339.7	334.2	206.8	206.8	124.2	510.9	477.7	123.5
Nov	101.1	101.3	131.2	375.2	339.7	333.8	186.4	186.4	101.2	505	465.2	100.5
Dec	81.81	81.98	111.9	375.2	339.7	333.4	172	172	83.26	501.1	455.1	82.57
Entropy (kJ/kg-K)												
State Point	1	1'	2	3	4	4'	5	5'	6	7	8	9
Jan	0.286	0.287	0.286	1.073	1.073	1.06	0.563	0.633	0.297	1.671	1.702	0.297
Feb	0.316	0.316	0.316	1.073	1.073	1.06	0.581	0.648	0.327	1.672	1.701	0.327
Mar	0.358	0.359	0.358	1.073	1.073	1.061	0.611	0.675	0.368	1.674	1.7	0.368
Apr	0.415	0.416	0.415	1.073	1.073	1.062	0.649	0.709	0.421	1.676	1.699	0.421
May	0.473	0.473	0.473	1.073	1.073	1.063	0.69	0.746	0.471	1.68	1.7	0.471
June	0.531	0.531	0.531	1.073	1.073	1.063	0.72	0.771	0.516	1.682	1.699	0.517
July	0.56	0.56	0.56	1.073	1.073	1.064	0.739	0.789	0.536	1.683	1.7	0.536
Aug	0.548	0.549	0.548	1.073	1.073	1.064	0.728	0.779	0.529	1.682	1.699	0.529
Sept	0.492	0.493	0.492	1.073	1.073	1.063	0.699	0.753	0.487	1.68	1.699	0.487
Oct	0.474	0.475	0.474	1.073	1.073	1.063	0.69	0.746	0.472	1.68	1.699	0.473
Nov	0.383	0.384	0.383	1.073	1.073	1.061	0.627	0.689	0.392	1.675	1.699	0.392
Dec	0.316	0.316	0.316	1.073	1.073	1.06	0.581	0.648	0.327	1.672	1.701	0.327

Table D-23: Thermodynamic properties for Binary ORC System simulations at 3.1km depth with a CO2 mass flow rate of 120kg/s and a reservoir temperature of 150°C.

Well Temp	150°C											
Well Depth	3.1 km											
CO2 Mass Flow	120 kg/s											
	Pressure (kPa)											
State Point	1	1'	2	3	4	4'	5	5'	6	7	8	9
Jan	2985	2986	33009	30000	15832	15537	15537	2986	619.5	619.5	127.2	127.2
Feb	3285	3286	32775	30000	15832	15537	15537	3286	643.3	643.3	144.7	144.7
Mar	3748	3749	32434	30000	15832	15536	15536	3749	667.7	667.7	172.7	172.7
Apr	4409	4410	31966	30000	15832	15536	15536	4410	718.7	718.7	214.3	214.3
May	5116	5117	31447	30000	15832	15536	15536	5117	763.2	763.2	260.6	260.6
June	5836	5838	30828	30000	15832	15536	15536	5838	819.4	819.4	309.3	309.3
July	6173	6174	30462	30000	15832	15536	15536	6174	838.7	838.7	332.3	332.3
Aug	6045	6047	30615	30000	15832	15536	15536	6047	829	829	323.6	323.6
Sept	5361	5363	31251	30000	15832	15536	15536	5363	781.6	781.6	277	277
Oct	5135	5137	31431	30000	15832	15536	15536	5137	763.2	763.2	261.9	261.9
Nov	4029	4030	32235	30000	15832	15536	15536	4030	684.4	684.4	190.2	190.2
Dec	3286	3288	32773	30000	15832	15537	15537	3288	643.3	643.3	144.8	144.8
	Temperature (°C)											
State Point	1	1'	2	3	4	4'	5	5'	6	7	8	9
Jan	-5.73	-5.72	11.97	150	99.96	96.39	38.96	-5.72	-5.5	46	4.845	-5.73
Feb	-2.21	-2.2	16.44	150	99.96	96.45	41.49	-2.2	-1.99	47.5	8.249	-2.21
Mar	2.773	2.786	22.95	150	99.96	96.55	44.43	2.786	2.969	49	12.83	2.773
Apr	9.159	9.171	31.68	150	99.96	96.67	48.95	9.171	9.329	52	18.85	9.159
May	15.23	15.24	40.59	150	99.96	96.78	52.73	15.24	15.37	54.5	24.36	15.23
June	20.79	20.8	49.61	150	99.96	96.89	56.59	20.8	20.91	57.5	29.51	20.79
July	23.2	23.21	54	150	99.96	96.93	57.95	23.21	23.31	58.5	31.64	23.2
Aug	22.3	22.31	52.28	150	99.96	96.92	57.35	22.31	22.41	58	30.81	22.3
Sept	17.19	17.2	43.65	150	99.96	96.82	53.96	17.2	17.32	55.5	26.17	17.19
Oct	15.39	15.4	40.83	150	99.96	96.79	52.77	15.4	15.53	54.5	24.49	15.39
Nov	5.583	5.596	26.73	150	99.96	96.6	46.17	5.596	5.767	50	15.41	5.583
Dec	-2.2	-2.19	16.46	150	99.96	96.45	41.5	-2.19	-1.98	47.5	8.262	-2.2
	Enthalpy (kJ/kg)											
State Point	1	1'	2	3	4	4'	5	5'	6	7	8	9
Jan	73.46	73.61	103.7	375.2	342.2	336.7	168.7	168.7	75.32	503.7	451.9	74.57
Feb	81.77	81.92	112	375.2	342.2	336.8	175.3	175.3	83.31	505.7	456.7	82.54
Mar	93.98	94.13	124.2	375.2	342.2	337	183.1	183.1	94.74	507.6	463	93.96
Apr	110.6	110.7	140.7	375.2	342.2	337.3	195.8	195.8	109.6	511.5	471.4	108.8
May	127.8	127.9	157.9	375.2	342.2	337.6	207	207	123.9	514.7	478.9	123.1
June	145.7	145.8	175.8	375.2	342.2	337.8	218.9	218.9	137.2	518.6	486	136.4
July	154.6	154.7	184.7	375.2	342.2	337.9	223.3	223.3	143.1	519.8	488.9	142.3
Aug	151.1	151.2	181.2	375.2	342.2	337.9	221.3	221.3	140.9	519.2	487.8	140.1
Sept	133.8	133.9	163.9	375.2	342.2	337.6	210.7	210.7	128.6	516	481.4	127.8
Oct	128.3	128.4	158.4	375.2	342.2	337.6	207.1	207.1	124.3	514.7	479.1	123.5
Nov	101.1	101.3	131.3	375.2	342.2	337.1	187.9	187.9	101.2	508.9	466.6	100.5
Dec	81.81	81.96	112	375.2	342.2	336.8	175.3	175.3	83.34	505.7	456.7	82.57
	Entropy (kJ/kg-K)											
State Point	1	1'	2	3	4	4'	5	5'	6	7	8	9
Jan	0.286	0.287	0.286	1.073	1.073	1.061	0.566	0.642	0.297	1.674	1.707	0.297
Feb	0.316	0.316	0.316	1.073	1.073	1.061	0.587	0.661	0.327	1.675	1.706	0.327
Mar	0.358	0.359	0.358	1.073	1.073	1.062	0.612	0.682	0.368	1.677	1.705	0.368
Apr	0.415	0.416	0.415	1.073	1.073	1.062	0.651	0.717	0.421	1.68	1.705	0.421
May	0.473	0.473	0.473	1.073	1.073	1.063	0.686	0.747	0.471	1.683	1.704	0.471
June	0.531	0.531	0.531	1.073	1.073	1.064	0.722	0.78	0.516	1.686	1.705	0.517
July	0.56	0.56	0.56	1.073	1.073	1.064	0.735	0.791	0.536	1.687	1.705	0.536
Aug	0.548	0.548	0.548	1.073	1.073	1.064	0.73	0.786	0.529	1.687	1.705	0.529
Sept	0.492	0.493	0.492	1.073	1.073	1.063	0.697	0.757	0.487	1.684	1.704	0.487
Oct	0.474	0.475	0.474	1.073	1.073	1.063	0.686	0.747	0.472	1.683	1.704	0.473
Nov	0.383	0.384	0.383	1.073	1.073	1.062	0.627	0.695	0.391	1.678	1.704	0.392
Dec	0.316	0.316	0.316	1.073	1.073	1.061	0.587	0.661	0.327	1.675	1.706	0.327

Table D-24: Thermodynamic properties for Binary ORC System simulations at 3.1km depth with a CO2 mass flow rate of 140kg/s and a reservoir temperature of 150°C.

Well Temp	150°C											
Well Depth	3.1 km											
CO2 Mass Flow	140 kg/s											
	Pressure (kPa)											
State Point	1	1'	2	3	4	4'	5	5'	6	7	8	9
Jan	2985	2987	32941	30000	15475	15066	15066	2987	596.4	596.4	127.2	127.2
Feb	3285	3287	32705	30000	15475	15066	15066	3287	619.5	619.5	144.7	144.7
Mar	3748	3750	32362	30000	15475	15065	15065	3750	651.4	651.4	172.7	172.7
Apr	4409	4411	31891	30000	15475	15065	15065	4411	701.4	701.4	214.3	214.3
May	5116	5117	31368	30000	15475	15065	15065	5117	736.3	736.3	260.6	260.6
June	5836	5838	30743	30000	15475	15065	15065	5838	781.6	781.6	309.3	309.3
July	6173	6175	30374	30000	15475	15065	15065	6175	809.8	809.8	332.3	332.3
Aug	6045	6047	30529	30000	15475	15065	15065	6047	800.3	800.3	323.6	323.6
Sept	5361	5363	31170	30000	15475	15065	15065	5363	754.2	754.2	277	277
Oct	5135	5137	31352	30000	15475	15065	15065	5137	736.3	736.3	261.9	261.9
Nov	4029	4031	32161	30000	15475	15065	15065	4031	676	676	190.2	190.2
Dec	3286	3288	32704	30000	15475	15066	15066	3288	619.5	619.5	144.8	144.8
	Temperature (°C)											
State Point	1	1'	2	3	4	4'	5	5'	6	7	8	9
Jan	-5.73	-5.71	11.93	150	98.17	94.32	37.98	-5.71	-5.51	44.5	4.446	-5.73
Feb	-2.21	-2.2	16.4	150	98.17	94.38	40.53	-2.2	-2	46	7.85	-2.21
Mar	2.773	2.791	22.91	150	98.17	94.46	43.91	2.791	2.964	48	12.56	2.773
Apr	9.159	9.176	31.63	150	98.17	94.56	48.32	9.176	9.323	51	18.58	9.159
May	15.23	15.25	40.53	150	98.17	94.66	51.77	15.25	15.36	53	23.97	15.23
June	20.79	20.81	49.53	150	98.17	94.75	55.11	20.81	20.89	55.5	28.99	20.79
July	23.2	23.22	53.92	150	98.17	94.79	56.87	23.22	23.29	57	31.25	23.2
Aug	22.3	22.32	52.2	150	98.17	94.77	56.27	22.32	22.4	56.5	30.42	22.3
Sept	17.19	17.21	43.58	150	98.17	94.69	53.1	17.21	17.31	54	25.78	17.19
Oct	15.39	15.41	40.78	150	98.17	94.67	51.81	15.41	15.52	53	24.09	15.39
Nov	5.583	5.601	26.68	150	98.17	94.5	46.09	5.601	5.764	49.5	15.28	5.583
Dec	-2.2	-2.18	16.42	150	98.17	94.38	40.53	-2.18	-1.99	46	7.863	-2.2
	Enthalpy (kJ/kg)											
State Point	1	1'	2	3	4	4'	5	5'	6	7	8	9
Jan	73.46	73.59	103.6	375.2	341.2	336.1	167.1	167.1	75.28	501.8	451.3	74.57
Feb	81.77	81.9	111.9	375.2	341.2	336.2	173.8	173.8	83.27	503.7	456	82.54
Mar	93.98	94.11	124.1	375.2	341.2	336.4	183.1	183.1	94.71	506.3	462.5	93.96
Apr	110.6	110.7	140.6	375.2	341.2	336.6	195.8	195.8	109.6	510.2	470.9	108.8
May	127.8	127.9	157.8	375.2	341.2	336.8	206.2	206.2	123.9	512.8	478.3	123.1
June	145.7	145.8	175.7	375.2	341.2	337	216.8	216.8	137.2	516	485.1	136.4
July	154.6	154.7	184.6	375.2	341.2	337.1	222.6	222.6	143	517.9	488.2	142.3
Aug	151.1	151.2	181.1	375.2	341.2	337.1	220.6	220.6	140.8	517.3	487.1	140.1
Sept	133.8	133.9	163.8	375.2	341.2	336.9	210.4	210.4	128.6	514.1	480.7	127.8
Oct	128.3	128.4	158.3	375.2	341.2	336.8	206.3	206.3	124.3	512.8	478.4	123.5
Nov	101.1	101.3	131.2	375.2	341.2	336.5	189.3	189.3	101.2	508.3	466.3	100.5
Dec	81.81	81.94	111.9	375.2	341.2	336.2	173.9	173.9	83.31	503.7	456	82.57
	Entropy (kJ/kg-K)											
State Point	1	1'	2	3	4	4'	5	5'	6	7	8	9
Jan	0.286	0.286	0.286	1.073	1.073	1.063	0.563	0.636	0.297	1.672	1.705	0.297
Feb	0.316	0.316	0.316	1.073	1.073	1.063	0.584	0.655	0.327	1.674	1.704	0.327
Mar	0.358	0.359	0.358	1.073	1.073	1.063	0.614	0.681	0.368	1.676	1.703	0.368
Apr	0.415	0.416	0.415	1.073	1.073	1.064	0.653	0.717	0.421	1.679	1.703	0.421
May	0.473	0.473	0.473	1.073	1.073	1.065	0.686	0.745	0.471	1.681	1.702	0.471
June	0.531	0.531	0.531	1.073	1.073	1.065	0.718	0.773	0.516	1.684	1.702	0.517
July	0.56	0.56	0.56	1.073	1.073	1.065	0.736	0.789	0.536	1.686	1.703	0.536
Aug	0.548	0.548	0.548	1.073	1.073	1.065	0.73	0.784	0.529	1.685	1.703	0.529
Sept	0.492	0.493	0.492	1.073	1.073	1.065	0.698	0.756	0.487	1.682	1.702	0.487
Oct	0.474	0.475	0.474	1.073	1.073	1.065	0.686	0.745	0.472	1.681	1.702	0.473
Nov	0.383	0.384	0.383	1.073	1.073	1.064	0.633	0.699	0.391	1.678	1.703	0.392
Dec	0.316	0.316	0.316	1.073	1.073	1.063	0.584	0.655	0.327	1.674	1.704	0.327

Table D-25: Thermodynamic properties for Binary ORC System simulations at 3.6km depth with a CO2 mass flow rate of 70kg/s and a reservoir temperature of 100°C.

Well Temp	100°C											
Well Depth	3.6 km											
CO2 Mass Flow	70 kg/s											
	Pressure (kPa)											
State Point	1	1'	2	3	4	4'	5	5'	6	7	8	9
Jan	2985	2986	38160	35000	11398	11176	11176	2986	360.8	360.8	127.2	127.2
Feb	3285	3286	37851	35000	11398	11176	11176	3286	376.7	376.7	144.7	144.7
Mar	3748	3748	37399	35000	11398	11176	11176	3749	398.8	398.8	172.7	172.7
Apr	4409	4410	36777	35000	11398	11175	11175	4410	427.7	427.7	214.3	214.3
May	5116	5116	36094	35000	11398	11175	11175	5117	458.2	458.2	260.6	260.6
June	5836	5837	35299	35000	11398	11175	11175	5838	490.3	490.3	309.3	309.3
July	6423	6173	35139	35000	11398	11175	11175	6174	503.5	503.5	332.3	332.3
Aug	6195	6046	35208	35000	11398	11175	11175	6047	496.9	496.9	323.6	323.6
Sept	5361	5362	35839	35000	11398	11175	11175	5362	464.5	464.5	277	277
Oct	5135	5136	36073	35000	11398	11175	11175	5137	458.2	458.2	261.9	261.9
Nov	4029	4029	37134	35000	11398	11175	11175	4030	410.2	410.2	190.2	190.2
Dec	3286	3287	37849	35000	11398	11176	11176	3288	376.7	376.7	144.8	144.8
	Temperature (°C)											
State Point	1	1'	2	3	4	4'	5	5'	6	7	8	9
Jan	-5.73	-5.73	14.45	100	50.22	48.74	24.57	-5.72	-5.58	26	-0.19	-5.73
Feb	-2.21	-2.21	19.03	100	50.22	48.78	26.5	-2.2	-2.08	27.5	3.194	-2.21
Mar	2.773	2.778	25.71	100	50.22	48.83	29.07	2.785	2.875	29.5	7.885	2.773
Apr	9.159	9.163	34.69	100	50.22	48.89	32.18	9.17	9.22	32	13.76	9.159
May	15.23	15.23	43.88	100	50.22	48.96	35.11	15.24	15.25	34.5	19.27	15.23
June	20.79	20.79	53.22	100	50.22	49.01	37.85	20.8	20.89	37	24.3	20.79
July	23.76	23.2	58.05	100	50.22	49.04	38.93	23.21	23.3	38	26.44	23.2
Aug	22.6	22.3	56.15	100	50.22	49.03	38.42	22.31	22.4	37.5	25.61	22.3
Sept	17.19	17.19	47.04	100	50.22	48.98	35.76	17.2	17.19	35	20.96	17.19
Oct	15.39	15.39	44.13	100	50.22	48.96	35.12	15.4	15.41	34.5	19.4	15.39
Nov	5.583	5.588	29.59	100	50.22	48.86	30.37	5.595	5.668	30.5	10.46	5.583
Dec	-2.2	-2.19	19.05	100	50.22	48.78	26.51	-2.19	-2.07	27.5	3.207	-2.2
	Enthalpy (kJ/kg)											
State Point	1	1'	2	3	4	4'	5	5'	6	7	8	9
Jan	73.46	73.72	108.7	271.1	234.2	230.2	139.8	139.8	74.92	477.2	443.8	74.57
Feb	81.77	82.03	117	271.1	234.2	230.4	145	145	82.9	479.2	448.4	82.54
Mar	93.98	94.24	129.2	271.1	234.2	230.7	152.1	152.1	94.32	481.9	454.7	93.96
Apr	110.6	110.8	145.8	271.1	234.2	231.1	161.3	161.3	109.1	485.2	462.7	108.8
May	127.8	128	163	271.1	234.2	231.4	170.6	170.6	123.4	488.5	470	123.1
June	145.7	145.9	180.8	271.1	234.2	231.8	180	180	137.2	491.8	476.7	136.4
July	154.9	154.8	190.1	271.1	234.2	231.9	183.9	183.9	143	493.2	479.5	142.3
Aug	151.3	151.3	186.4	271.1	234.2	231.9	182.1	182.1	140.8	492.5	478.4	140.1
Sept	133.8	134	169	271.1	234.2	231.6	172.7	172.7	128.1	489.2	472.2	127.8
Oct	128.3	128.5	163.5	271.1	234.2	231.5	170.6	170.6	123.8	488.5	470.2	123.5
Nov	101.1	101.4	136.3	271.1	234.2	230.9	155.9	155.9	100.8	483.2	458.2	100.5
Dec	81.81	82.07	117	271.1	234.2	230.4	145	145	82.93	479.2	448.4	82.57
	Entropy (kJ/kg-K)											
State Point	1	1'	2	3	4	4'	5	5'	6	7	8	9
Jan	0.286	0.287	0.286	0.79	0.79	0.779	0.489	0.534	0.297	1.656	1.678	0.297
Feb	0.316	0.317	0.316	0.79	0.79	0.78	0.506	0.549	0.327	1.657	1.677	0.327
Mar	0.358	0.359	0.358	0.79	0.79	0.781	0.53	0.569	0.368	1.658	1.676	0.368
Apr	0.415	0.416	0.415	0.79	0.79	0.782	0.56	0.595	0.421	1.661	1.675	0.421
May	0.473	0.473	0.473	0.79	0.79	0.783	0.59	0.621	0.471	1.663	1.674	0.471
June	0.531	0.532	0.531	0.79	0.79	0.784	0.621	0.648	0.516	1.665	1.674	0.517
July	0.56	0.56	0.56	0.79	0.79	0.784	0.633	0.659	0.536	1.666	1.674	0.536
Aug	0.548	0.549	0.548	0.79	0.79	0.784	0.627	0.653	0.529	1.666	1.674	0.529
Sept	0.492	0.493	0.492	0.79	0.79	0.783	0.597	0.626	0.487	1.663	1.673	0.487
Oct	0.474	0.475	0.474	0.79	0.79	0.783	0.59	0.621	0.472	1.663	1.674	0.473
Nov	0.383	0.384	0.383	0.79	0.79	0.781	0.542	0.58	0.392	1.659	1.675	0.392
Dec	0.316	0.317	0.316	0.79	0.79	0.78	0.506	0.549	0.327	1.657	1.677	0.327

Table D-26: Thermodynamic properties for Binary ORC System simulations at 3.6km depth with a CO2 mass flow rate of 90kg/s and a reservoir temperature of 100°C.

Well Temp	100°C											
Well Depth	3.6 km											
CO2 Mass Flow	90 kg/s											
	Pressure (kPa)											
State Point	1	1'	2	3	4	4'	5	5'	6	7	8	9
Jan	2985	2986	38111	35000	10844	10469	10469	2986	355.6	355.6	127.2	127.2
Feb	3285	3286	37801	35000	10844	10469	10469	3286	366	366	144.7	144.7
Mar	3748	3749	37348	35000	10844	10468	10468	3749	387.6	387.6	172.7	172.7
Apr	4409	4410	36724	35000	10844	10468	10468	4410	416	416	214.3	214.3
May	5116	5116	36037	35000	10844	10468	10468	5116	445.8	445.8	260.6	260.6
June	5836	5837	35239	35000	10844	10467	10467	5837	477.2	477.2	309.3	309.3
July	6423	6174	35077	35000	10844	10467	10467	6174	483.7	483.7	332.3	332.3
Aug	6195	6046	35147	35000	10844	10467	10467	6046	483.7	483.7	323.6	323.6
Sept	5361	5362	35781	35000	10844	10468	10468	5362	452	452	277	277
Oct	5135	5136	36017	35000	10844	10468	10468	5136	445.8	445.8	261.9	261.9
Nov	4029	4030	37082	35000	10844	10468	10468	4030	398.8	398.8	190.2	190.2
Dec	3286	3287	37800	35000	10844	10469	10469	3287	366	366	144.8	144.8
	Temperature (°C)											
State Point	1	1'	2	3	4	4'	5	5'	6	7	8	9
Jan	-5.73	-5.72	14.42	100	48.06	46.14	23.93	-5.72	-5.58	25.5	-0.3	-5.73
Feb	-2.21	-2.21	19	100	48.06	46.16	25.44	-2.21	-2.09	26.5	2.961	-2.21
Mar	2.773	2.78	25.68	100	48.06	46.19	28.01	2.78	2.872	28.5	7.651	2.773
Apr	9.159	9.166	34.65	100	48.06	46.24	31.11	9.166	9.216	31	13.53	9.159
May	15.23	15.24	43.84	100	48.06	46.28	34.03	15.24	15.24	33.5	19.03	15.23
June	20.79	20.8	53.18	100	48.06	46.31	36.75	20.8	20.89	36	24.06	20.79
July	23.76	23.21	58	100	48.06	46.33	37.39	23.21	23.3	36.5	26.08	23.2
Aug	22.6	22.31	56.1	100	48.06	46.32	37.31	22.31	22.4	36.5	25.37	22.3
Sept	17.19	17.2	47	100	48.06	46.29	34.67	17.2	17.19	34	20.72	17.19
Oct	15.39	15.4	44.09	100	48.06	46.28	34.04	15.4	15.4	33.5	19.16	15.39
Nov	5.583	5.591	29.56	100	48.06	46.21	29.31	5.591	5.664	29.5	10.23	5.583
Dec	-2.2	-2.19	19.02	100	48.06	46.16	25.44	-2.19	-2.07	26.5	2.974	-2.2
	Enthalpy (kJ/kg)											
State Point	1	1'	2	3	4	4'	5	5'	6	7	8	9
Jan	73.46	73.66	108.6	271.1	233.2	229.8	139.5	139.5	74.92	476.5	443.6	74.57
Feb	81.77	81.97	116.9	271.1	233.2	229.9	143.6	143.6	82.88	477.8	448	82.54
Mar	93.98	94.18	129.1	271.1	233.2	230.2	151	151	94.3	480.5	454.3	93.96
Apr	110.6	110.8	145.7	271.1	233.2	230.5	160.5	160.5	109.1	483.9	462.2	108.8
May	127.8	128	162.9	271.1	233.2	230.7	170.2	170.2	123.4	487.2	469.6	123.1
June	145.7	145.8	180.8	271.1	233.2	231	180.2	180.2	137.2	490.5	476.2	136.4
July	154.9	154.7	190	271.1	233.2	231.1	182.7	182.7	143	491.2	478.8	142.3
Aug	151.3	151.2	186.4	271.1	233.2	231.1	182.4	182.4	140.8	491.2	477.9	140.1
Sept	133.8	134	168.9	271.1	233.2	230.8	172.5	172.5	128.1	487.9	471.8	127.8
Oct	128.3	128.5	163.4	271.1	233.2	230.8	170.3	170.3	123.8	487.2	469.8	123.5
Nov	101.1	101.3	136.3	271.1	233.2	230.3	154.9	154.9	100.8	481.9	457.8	100.5
Dec	81.81	82.01	117	271.1	233.2	229.9	143.6	143.6	82.92	477.8	448	82.57
	Entropy (kJ/kg-K)											
State Point	1	1'	2	3	4	4'	5	5'	6	7	8	9
Jan	0.286	0.287	0.286	0.79	0.79	0.782	0.49	0.533	0.297	1.655	1.677	0.297
Feb	0.316	0.316	0.316	0.79	0.79	0.782	0.504	0.544	0.327	1.656	1.675	0.327
Mar	0.358	0.359	0.358	0.79	0.79	0.783	0.529	0.565	0.368	1.658	1.674	0.368
Apr	0.415	0.416	0.415	0.79	0.79	0.784	0.56	0.592	0.421	1.66	1.673	0.421
May	0.473	0.473	0.473	0.79	0.79	0.785	0.592	0.62	0.471	1.662	1.673	0.471
June	0.531	0.531	0.531	0.79	0.79	0.786	0.625	0.648	0.516	1.664	1.673	0.517
July	0.56	0.56	0.56	0.79	0.79	0.786	0.633	0.655	0.536	1.665	1.672	0.536
Aug	0.548	0.549	0.548	0.79	0.79	0.786	0.632	0.654	0.529	1.665	1.672	0.529
Sept	0.492	0.493	0.492	0.79	0.79	0.785	0.599	0.626	0.487	1.662	1.672	0.487
Oct	0.474	0.475	0.474	0.79	0.79	0.785	0.592	0.62	0.472	1.662	1.672	0.473
Nov	0.383	0.384	0.383	0.79	0.79	0.783	0.542	0.576	0.392	1.658	1.674	0.392
Dec	0.316	0.317	0.316	0.79	0.79	0.782	0.504	0.544	0.327	1.656	1.675	0.327

Table D-27: Thermodynamic properties for Binary ORC System simulations at 3.6km depth with a CO2 mass flow rate of 120kg/s and a reservoir temperature of 100°C.

Well Temp	100°C											
Well Depth	3.6 km											
CO2 Mass Flow	120 kg/s											
	Pressure (kPa)											
State Point	1	1'	2	3	4	4'	5	5'	6	7	8	9
Jan	2985	2986	38129	35000	11491	11294	11294	2986	366	366	127.2	127.2
Feb	3285	3286	37819	35000	11491	11294	11294	3286	376.7	376.7	144.7	144.7
Mar	3748	3749	37366	35000	11491	11294	11294	3749	404.5	404.5	172.7	172.7
Apr	4409	4410	36742	35000	11491	11293	11293	4410	433.7	433.7	214.3	214.3
May	5116	5116	36057	35000	11491	11293	11293	5116	458.2	458.2	260.6	260.6
June	5836	5837	35260	35000	11491	11293	11293	5837	490.3	490.3	309.3	309.3
July	6423	6173	35098	35000	11491	11293	11293	6173	510.3	510.3	332.3	332.3
Aug	6195	6046	35169	35000	11491	11293	11293	6046	503.5	503.5	323.6	323.6
Sept	5361	5362	35802	35000	11491	11293	11293	5362	470.8	470.8	277	277
Oct	5135	5136	36037	35000	11491	11293	11293	5136	458.2	458.2	261.9	261.9
Nov	4029	4030	37100	35000	11491	11294	11294	4030	416	416	190.2	190.2
Dec	3286	3287	37817	35000	11491	11294	11294	3287	376.7	376.7	144.8	144.8
	Temperature (°C)											
State Point	1	1'	2	3	4	4'	5	5'	6	7	8	9
Jan	-5.73	-5.72	14.43	100	50.57	49.36	24.98	-5.72	-5.58	26.5	-0.07	-5.73
Feb	-2.21	-2.21	19.01	100	50.57	49.39	26.5	-2.21	-2.08	27.5	3.194	-2.21
Mar	2.773	2.779	25.69	100	50.57	49.43	29.51	2.779	2.877	30	8.004	2.773
Apr	9.159	9.165	34.67	100	50.57	49.47	32.63	9.165	9.222	32.5	13.88	9.159
May	15.23	15.24	43.85	100	50.57	49.52	35.14	15.24	15.25	34.5	19.27	15.23
June	20.79	20.8	53.19	100	50.57	49.56	37.9	20.8	20.89	37	24.3	20.79
July	23.76	23.21	58.02	100	50.57	49.58	39.39	23.21	23.3	38.5	26.56	23.2
Aug	22.6	22.31	56.12	100	50.57	49.57	38.89	22.31	22.4	38	25.73	22.3
Sept	17.19	17.2	47.01	100	50.57	49.53	36.22	17.2	17.2	35.5	21.08	17.19
Oct	15.39	15.4	44.11	100	50.57	49.52	35.16	15.4	15.41	34.5	19.4	15.39
Nov	5.583	5.59	29.57	100	50.57	49.45	30.82	5.59	5.67	31	10.58	5.583
Dec	-2.2	-2.19	19.03	100	50.57	49.39	26.5	-2.19	-2.07	27.5	3.207	-2.2
	Enthalpy (kJ/kg)											
State Point	1	1'	2	3	4	4'	5	5'	6	7	8	9
Jan	73.46	73.64	108.6	271.1	234.4	231.4	140.6	140.6	74.93	477.8	443.9	74.57
Feb	81.77	81.94	116.9	271.1	234.4	231.6	144.7	144.7	82.9	479.2	448.4	82.54
Mar	93.98	94.15	129.1	271.1	234.4	231.8	153.1	153.1	94.33	482.5	454.9	93.96
Apr	110.6	110.7	145.7	271.1	234.4	232.1	162.3	162.3	109.1	485.9	462.9	108.8
May	127.8	128	162.9	271.1	234.4	232.3	170.2	170.2	123.4	488.5	470	123.1
June	145.7	145.8	180.8	271.1	234.4	232.6	179.5	179.5	137.2	491.8	476.7	136.4
July	154.9	154.7	190	271.1	234.4	232.7	184.9	184.9	143	493.8	479.7	142.3
Aug	151.3	151.2	186.4	271.1	234.4	232.6	183.1	183.1	140.8	493.2	478.6	140.1
Sept	133.8	134	168.9	271.1	234.4	232.4	173.7	173.7	128.1	489.9	472.4	127.8
Oct	128.3	128.4	163.4	271.1	234.4	232.3	170.2	170.2	123.8	488.5	470.2	123.5
Nov	101.1	101.3	136.3	271.1	234.4	231.9	156.9	156.9	100.8	483.9	458.4	100.5
Dec	81.81	81.98	117	271.1	234.4	231.6	144.7	144.7	82.93	479.2	448.4	82.57
	Entropy (kJ/kg-K)											
State Point	1	1'	2	3	4	4'	5	5'	6	7	8	9
Jan	0.286	0.287	0.286	0.79	0.79	0.782	0.491	0.537	0.297	1.656	1.678	0.297
Feb	0.316	0.316	0.316	0.79	0.79	0.783	0.505	0.548	0.327	1.657	1.677	0.327
Mar	0.358	0.359	0.358	0.79	0.79	0.783	0.532	0.573	0.368	1.659	1.676	0.368
Apr	0.415	0.416	0.415	0.79	0.79	0.784	0.563	0.598	0.421	1.661	1.675	0.421
May	0.473	0.473	0.473	0.79	0.79	0.785	0.588	0.62	0.471	1.663	1.674	0.471
June	0.531	0.531	0.531	0.79	0.79	0.786	0.619	0.646	0.516	1.665	1.674	0.517
July	0.56	0.56	0.56	0.79	0.79	0.786	0.636	0.662	0.536	1.666	1.675	0.536
Aug	0.548	0.549	0.548	0.79	0.79	0.786	0.63	0.657	0.529	1.666	1.675	0.529
Sept	0.492	0.493	0.492	0.79	0.79	0.785	0.6	0.63	0.487	1.664	1.674	0.487
Oct	0.474	0.475	0.474	0.79	0.79	0.785	0.589	0.62	0.472	1.663	1.674	0.473
Nov	0.383	0.384	0.383	0.79	0.79	0.784	0.545	0.583	0.392	1.66	1.676	0.392
Dec	0.316	0.316	0.316	0.79	0.79	0.783	0.505	0.548	0.327	1.657	1.677	0.327

Table D-28: Thermodynamic properties for Binary ORC System simulations at 3.6km depth with a CO2 mass flow rate of 140kg/s and a reservoir temperature of 100°C.

Well Temp	100°C											
Well Depth	3.6 km											
CO2 Mass Flow	140 kg/s											
	Pressure (kPa)											
State Point	1	1'	2	3	4	4'	5	5'	6	7	8	9
Jan	2985	2986	38090	35000	11219	10948	10948	2986	360.8	360.8	127.2	127.2
Feb	3285	3286	37780	35000	11219	10948	10948	3286	376.7	376.7	144.7	144.7
Mar	3748	3749	37325	35000	11219	10948	10948	3749	398.8	398.8	172.7	172.7
Apr	4409	4410	36700	35000	11219	10947	10947	4410	427.7	427.7	214.3	214.3
May	5116	5116	36013	35000	11219	10947	10947	5116	452	452	260.6	260.6
June	5836	5837	35212	35000	11219	10947	10947	5837	483.7	483.7	309.3	309.3
July	6423	6174	35049	35000	11219	10947	10947	6174	496.9	496.9	332.3	332.3
Aug	6195	6046	35120	35000	11219	10947	10947	6046	496.9	496.9	323.6	323.6
Sept	5361	5362	35756	35000	11219	10947	10947	5362	464.5	464.5	277	277
Oct	5135	5136	35992	35000	11219	10947	10947	5136	452	452	261.9	261.9
Nov	4029	4030	37059	35000	11219	10948	10948	4030	410.2	410.2	190.2	190.2
Dec	3286	3287	37778	35000	11219	10948	10948	3287	376.7	376.7	144.8	144.8
	Temperature (°C)											
State Point	1	1'	2	3	4	4'	5	5'	6	7	8	9
Jan	-5.73	-5.72	14.41	100	49.54	48.12	24.46	-5.72	-5.58	26	-0.19	-5.73
Feb	-2.21	-2.21	18.99	100	49.54	48.14	26.41	-2.21	-2.08	27.5	3.194	-2.21
Mar	2.773	2.782	25.67	100	49.54	48.17	28.99	2.782	2.875	29.5	7.885	2.773
Apr	9.159	9.167	34.64	100	49.54	48.2	32.11	9.167	9.22	32	13.76	9.159
May	15.23	15.24	43.82	100	49.54	48.24	34.61	15.24	15.25	34	19.15	15.23
June	20.79	20.8	53.16	100	49.54	48.27	37.36	20.8	20.89	36.5	24.18	20.79
July	23.76	23.21	57.98	100	49.54	48.29	38.43	23.21	23.3	37.5	26.32	23.2
Aug	22.6	22.31	56.08	100	49.54	48.28	38.35	22.31	22.4	37.5	25.61	22.3
Sept	17.19	17.2	46.98	100	49.54	48.25	35.69	17.2	17.19	35	20.96	17.19
Oct	15.39	15.4	44.08	100	49.54	48.24	34.63	15.4	15.4	34	19.28	15.39
Nov	5.583	5.592	29.55	100	49.54	48.18	30.3	5.592	5.668	30.5	10.46	5.583
Dec	-2.2	-2.19	19.01	100	49.54	48.14	26.41	-2.19	-2.07	27.5	3.207	-2.2
	Enthalpy (kJ/kg)											
State Point	1	1'	2	3	4	4'	5	5'	6	7	8	9
Jan	73.46	73.61	108.6	271.1	233.9	231.2	139.9	139.9	74.92	477.2	443.8	74.57
Feb	81.77	81.92	116.9	271.1	233.9	231.3	145.2	145.2	82.9	479.2	448.4	82.54
Mar	93.98	94.13	129.1	271.1	233.9	231.5	152.5	152.5	94.32	481.9	454.7	93.96
Apr	110.6	110.7	145.7	271.1	233.9	231.7	161.9	161.9	109.1	485.2	462.7	108.8
May	127.8	127.9	162.9	271.1	233.9	232	169.9	169.9	123.4	487.9	469.8	123.1
June	145.7	145.8	180.7	271.1	233.9	232.2	179.5	179.5	137.2	491.2	476.5	136.4
July	154.9	154.7	190	271.1	233.9	232.3	183.5	183.5	143	492.5	479.3	142.3
Aug	151.3	151.2	186.3	271.1	233.9	232.2	183.2	183.2	140.8	492.5	478.4	140.1
Sept	133.8	133.9	168.9	271.1	233.9	232	173.6	173.6	128.1	489.2	472.2	127.8
Oct	128.3	128.4	163.4	271.1	233.9	232	170	170	123.8	487.9	470	123.5
Nov	101.1	101.3	136.2	271.1	233.9	231.6	156.4	156.4	100.8	483.2	458.2	100.5
Dec	81.81	81.96	116.9	271.1	233.9	231.3	145.2	145.2	82.93	479.2	448.4	82.57
	Entropy (kJ/kg-K)											
State Point	1	1'	2	3	4	4'	5	5'	6	7	8	9
Jan	0.286	0.286	0.286	0.79	0.79	0.783	0.49	0.534	0.297	1.656	1.678	0.297
Feb	0.316	0.316	0.316	0.79	0.79	0.784	0.508	0.55	0.327	1.657	1.677	0.327
Mar	0.358	0.359	0.358	0.79	0.79	0.784	0.532	0.571	0.368	1.658	1.676	0.368
Apr	0.415	0.416	0.415	0.79	0.79	0.785	0.563	0.597	0.421	1.661	1.675	0.421
May	0.473	0.473	0.473	0.79	0.79	0.786	0.589	0.619	0.471	1.662	1.673	0.471
June	0.531	0.531	0.531	0.79	0.79	0.787	0.62	0.646	0.516	1.665	1.673	0.517
July	0.56	0.56	0.56	0.79	0.79	0.787	0.633	0.657	0.536	1.666	1.673	0.536
Aug	0.548	0.549	0.548	0.79	0.79	0.787	0.632	0.657	0.529	1.666	1.674	0.529
Sept	0.492	0.493	0.492	0.79	0.79	0.786	0.601	0.629	0.487	1.663	1.673	0.487
Oct	0.474	0.475	0.474	0.79	0.79	0.786	0.589	0.619	0.472	1.662	1.673	0.473
Nov	0.383	0.384	0.383	0.79	0.79	0.785	0.545	0.581	0.392	1.659	1.675	0.392
Dec	0.316	0.316	0.316	0.79	0.79	0.784	0.508	0.55	0.327	1.657	1.677	0.327

Table D-29: Thermodynamic properties for Binary ORC System simulations at 3.6km depth with a CO2 mass flow rate of 70kg/s and a reservoir temperature of 125°C.

Well Temp	125°C											
Well Depth	3.6 km											
CO2 Mass Flow	70 kg/s											
	Pressure (kPa)											
State Point	1	1'	2	3	4	4'	5	5'	6	7	8	9
Jan	2985	2986	38160	35000	14306	14047	14047	2986	477.2	477.2	127.2	127.2
Feb	3285	3286	37851	35000	14306	14047	14047	3286	490.3	490.3	144.7	144.7
Mar	3748	3748	37399	35000	14306	14047	14047	3748	517.1	517.1	172.7	172.7
Apr	4409	4410	36777	35000	14306	14047	14047	4410	552.1	552.1	214.3	214.3
May	5116	5116	36094	35000	14306	14047	14047	5116	588.9	588.9	260.6	260.6
June	5836	5837	35299	35000	14306	14046	14046	5837	627.4	627.4	309.3	309.3
July	6423	6173	35139	35000	14306	14046	14046	6173	643.3	643.3	332.3	332.3
Aug	6195	6046	35208	35000	14306	14046	14046	6046	635.3	635.3	323.6	323.6
Sept	5361	5362	35839	35000	14306	14046	14046	5362	604	604	277	277
Oct	5135	5136	36073	35000	14306	14047	14047	5136	588.9	588.9	261.9	261.9
Nov	4029	4029	37134	35000	14306	14047	14047	4029	537.9	537.9	190.2	190.2
Dec	3286	3287	37849	35000	14306	14047	14047	3287	490.3	490.3	144.8	144.8
	Temperature (°C)											
State Point	1	1'	2	3	4	4'	5	5'	6	7	8	9
Jan	-5.73	-5.73	14.45	125	71.55	69.05	31.97	-5.73	-5.54	36	2.24	-5.73
Feb	-2.21	-2.21	19.03	125	71.55	69.11	33.73	-2.21	-2.05	37	5.511	-2.21
Mar	2.773	2.778	25.71	125	71.55	69.2	36.67	2.778	2.917	39	10.22	2.773
Apr	9.159	9.163	34.69	125	71.55	69.31	40.26	9.163	9.267	41.5	16.11	9.159
May	15.23	15.23	43.88	125	71.55	69.41	43.63	15.23	15.3	44	21.63	15.23
June	20.79	20.79	53.22	125	71.55	69.5	46.76	20.79	20.83	46.5	26.66	20.79
July	23.76	23.2	57.8	125	71.55	69.55	48.01	23.2	23.22	47.5	28.8	23.2
Aug	22.6	22.3	56.01	125	71.55	69.53	47.44	22.3	22.33	47	27.97	22.3
Sept	17.19	17.19	47.04	125	71.55	69.44	44.85	17.19	17.25	45	23.44	17.19
Oct	15.39	15.39	44.13	125	71.55	69.41	43.66	15.39	15.46	44	21.76	15.39
Nov	5.583	5.588	29.59	125	71.55	69.25	38.62	5.588	5.714	40.5	12.93	5.583
Dec	-2.2	-2.19	19.05	125	71.55	69.11	33.74	-2.19	-2.03	37	5.524	-2.2
	Enthalpy (kJ/kg)											
State Point	1	1'	2	3	4	4'	5	5'	6	7	8	9
Jan	73.46	73.72	108.7	318.6	281.3	275.8	153.6	153.6	75.1	490.5	447.7	74.57
Feb	81.77	82.03	117	318.6	281.3	276	158.2	158.2	83.07	491.8	452.2	82.54
Mar	93.98	94.24	129.2	318.6	281.3	276.3	166	166	94.5	494.5	458.6	93.96
Apr	110.6	110.8	145.8	318.6	281.3	276.7	175.9	175.9	109.3	497.8	466.7	108.8
May	127.8	128	163	318.6	281.3	277.1	185.7	185.7	123.6	501.1	474.1	123.1
June	145.7	145.9	180.8	318.6	281.3	277.4	195.3	195.3	136.9	504.4	480.9	136.4
July	154.9	154.8	190.1	318.6	281.3	277.6	199.3	199.3	142.8	505.7	483.8	142.3
Aug	151.3	151.3	186.4	318.6	281.3	277.5	197.5	197.5	140.6	505	482.6	140.1
Sept	133.8	134	169	318.6	281.3	277.2	189.4	189.4	128.3	502.4	476.6	127.8
Oct	128.3	128.5	163.5	318.6	281.3	277.1	185.8	185.8	124	501.1	474.3	123.5
Nov	101.1	101.4	136.3	318.6	281.3	276.5	171.3	171.3	101	496.5	462.4	100.5
Dec	81.81	82.07	117	318.6	281.3	276	158.2	158.2	83.11	491.8	452.2	82.57
	Entropy (kJ/kg-K)											
State Point	1	1'	2	3	4	4'	5	5'	6	7	8	9
Jan	0.286	0.287	0.286	0.914	0.914	0.899	0.523	0.586	0.297	1.664	1.692	0.297
Feb	0.316	0.317	0.316	0.914	0.914	0.9	0.538	0.598	0.327	1.665	1.69	0.327
Mar	0.358	0.359	0.358	0.914	0.914	0.901	0.563	0.619	0.368	1.667	1.689	0.368
Apr	0.415	0.416	0.415	0.914	0.914	0.902	0.595	0.647	0.421	1.669	1.688	0.421
May	0.473	0.473	0.473	0.914	0.914	0.903	0.626	0.674	0.471	1.672	1.688	0.471
June	0.531	0.532	0.531	0.914	0.914	0.904	0.656	0.7	0.516	1.674	1.688	0.517
July	0.56	0.56	0.56	0.914	0.914	0.905	0.669	0.71	0.536	1.675	1.688	0.536
Aug	0.548	0.549	0.548	0.914	0.914	0.904	0.663	0.705	0.529	1.675	1.688	0.529
Sept	0.492	0.493	0.492	0.914	0.914	0.903	0.638	0.684	0.487	1.673	1.688	0.487
Oct	0.474	0.475	0.474	0.914	0.914	0.903	0.627	0.674	0.472	1.672	1.688	0.473
Nov	0.383	0.384	0.383	0.914	0.914	0.901	0.58	0.635	0.392	1.668	1.69	0.392
Dec	0.316	0.317	0.316	0.914	0.914	0.9	0.538	0.598	0.327	1.665	1.69	0.327

Table D-30: Thermodynamic properties for Binary ORC System simulations at 3.6km depth with a CO2 mass flow rate of 90kg/s and a reservoir temperature of 125°C.

Well Temp	125°C											
Well Depth	3.6 km											
CO2 Mass Flow	90 kg/s											
	Pressure (kPa)											
State Point	1	1'	2	3	4	4'	5	5'	6	7	8	9
Jan	2985	2986	38111	35000	13664	13224	13224	2986	458.2	458.2	127.2	127.2
Feb	3285	3286	37801	35000	13664	13224	13224	3286	477.2	477.2	144.7	144.7
Mar	3748	3749	37348	35000	13664	13224	13224	3749	503.5	503.5	172.7	172.7
Apr	4409	4410	36724	35000	13664	13224	13224	4410	537.9	537.9	214.3	214.3
May	5116	5116	36037	35000	13664	13223	13223	5116	566.6	566.6	260.6	260.6
June	5836	5837	35239	35000	13664	13223	13223	5837	604	604	309.3	309.3
July	6423	6174	35077	35000	13664	13223	13223	6174	619.5	619.5	332.3	332.3
Aug	6195	6046	35147	35000	13664	13223	13223	6046	611.8	611.8	323.6	323.6
Sept	5361	5362	35781	35000	13664	13223	13223	5362	581.4	581.4	277	277
Oct	5135	5136	36017	35000	13664	13223	13223	5136	566.6	566.6	261.9	261.9
Nov	4029	4030	37082	35000	13664	13224	13224	4030	517.1	517.1	190.2	190.2
Dec	3286	3287	37800	35000	13664	13224	13224	3287	477.2	477.2	144.8	144.8
	Temperature (°C)											
State Point	1	1'	2	3	4	4'	5	5'	6	7	8	9
Jan	-5.73	-5.72	14.42	125	68.8	65.86	30.66	-5.72	-5.55	34.5	1.862	-5.73
Feb	-2.21	-2.21	19	125	68.8	65.91	32.88	-2.21	-2.05	36	5.259	-2.21
Mar	2.773	2.78	25.68	125	68.8	65.97	35.83	2.78	2.912	38	9.966	2.773
Apr	9.159	9.166	34.65	125	68.8	66.04	39.41	9.166	9.262	40.5	15.86	9.159
May	15.23	15.24	43.84	125	68.8	66.12	42.33	15.24	15.29	42.5	21.25	15.23
June	20.79	20.8	53.18	125	68.8	66.19	45.44	20.8	20.82	45	26.28	20.79
July	23.76	23.21	58	125	68.8	66.22	46.67	23.21	23.21	46	28.42	23.2
Aug	22.6	22.31	56.1	125	68.8	66.2	46.1	22.31	22.32	45.5	27.59	22.3
Sept	17.19	17.2	47	125	68.8	66.14	43.55	17.2	17.24	43.5	23.06	17.19
Oct	15.39	15.4	44.09	125	68.8	66.12	42.36	15.4	15.45	42.5	21.38	15.39
Nov	5.583	5.591	29.56	125	68.8	66	37.33	5.591	5.706	39	12.55	5.583
Dec	-2.2	-2.19	19.02	125	68.8	65.91	32.88	-2.19	-2.03	36	5.272	-2.2
	Enthalpy (kJ/kg)											
State Point	1	1'	2	3	4	4'	5	5'	6	7	8	9
Jan	73.46	73.66	108.6	318.6	279.9	275.2	151.8	151.8	75.07	488.5	447.1	74.57
Feb	81.77	81.97	116.9	318.6	279.9	275.4	157.7	157.7	83.05	490.5	451.7	82.54
Mar	93.98	94.18	129.1	318.6	279.9	275.6	165.8	165.8	94.48	493.2	458.2	93.96
Apr	110.6	110.8	145.7	318.6	279.9	275.9	176.1	176.1	109.3	496.5	466.2	108.8
May	127.8	128	162.9	318.6	279.9	276.2	185	185	123.6	499.1	473.5	123.1
June	145.7	145.8	180.8	318.6	279.9	276.5	195.1	195.1	136.9	502.4	480.2	136.4
July	154.9	154.7	190	318.6	279.9	276.6	199.3	199.3	142.7	503.7	483.1	142.3
Aug	151.3	151.2	186.4	318.6	279.9	276.5	197.4	197.4	140.5	503.1	482	140.1
Sept	133.8	134	168.9	318.6	279.9	276.3	188.9	188.9	128.3	500.4	475.9	127.8
Oct	128.3	128.5	163.4	318.6	279.9	276.2	185.1	185.1	124	499.1	473.6	123.5
Nov	101.1	101.3	136.3	318.6	279.9	275.7	170	170	101	494.5	461.7	100.5
Dec	81.81	82.01	117	318.6	279.9	275.4	157.7	157.7	83.09	490.5	451.8	82.57
	Entropy (kJ/kg-K)											
State Point	1	1'	2	3	4	4'	5	5'	6	7	8	9
Jan	0.286	0.287	0.286	0.914	0.914	0.903	0.52	0.579	0.297	1.663	1.69	0.297
Feb	0.316	0.316	0.316	0.914	0.914	0.903	0.54	0.596	0.327	1.664	1.689	0.327
Mar	0.358	0.359	0.358	0.914	0.914	0.904	0.566	0.619	0.368	1.666	1.688	0.368
Apr	0.415	0.416	0.415	0.914	0.914	0.905	0.599	0.647	0.421	1.668	1.687	0.421
May	0.473	0.473	0.473	0.914	0.914	0.906	0.628	0.671	0.471	1.67	1.686	0.471
June	0.531	0.531	0.531	0.914	0.914	0.907	0.659	0.699	0.516	1.673	1.686	0.517
July	0.56	0.56	0.56	0.914	0.914	0.907	0.673	0.71	0.536	1.674	1.686	0.536
Aug	0.548	0.549	0.548	0.914	0.914	0.907	0.667	0.705	0.529	1.673	1.686	0.529
Sept	0.492	0.493	0.492	0.914	0.914	0.906	0.64	0.682	0.487	1.671	1.686	0.487
Oct	0.474	0.475	0.474	0.914	0.914	0.906	0.628	0.671	0.472	1.67	1.686	0.473
Nov	0.383	0.384	0.383	0.914	0.914	0.905	0.58	0.63	0.392	1.667	1.687	0.392
Dec	0.316	0.317	0.316	0.914	0.914	0.903	0.54	0.596	0.327	1.664	1.689	0.327

Table D-31: Thermodynamic properties for Binary ORC System simulations at 3.6km depth with a CO2 mass flow rate of 120kg/s and a reservoir temperature of 125°C.

Well Temp	125°C											
Well Depth	3.6 km											
CO2 Mass Flow	120 kg/s											
	Pressure (kPa)											
State Point	1	1'	2	3	4	4'	5	5'	6	7	8	9
Jan	2985	2986	38129	35000	14414	14184	14184	2986	483.7	483.7	127.2	127.2
Feb	3285	3286	37819	35000	14414	14184	14184	3286	496.9	496.9	144.7	144.7
Mar	3748	3749	37366	35000	14414	14184	14184	3749	523.9	523.9	172.7	172.7
Apr	4409	4410	36742	35000	14414	14184	14184	4410	559.3	559.3	214.3	214.3
May	5116	5116	36057	35000	14414	14183	14183	5116	596.4	596.4	260.6	260.6
June	5836	5837	35260	35000	14414	14183	14183	5837	635.3	635.3	309.3	309.3
July	6423	6173	35098	35000	14414	14183	14183	6173	651.4	651.4	332.3	332.3
Aug	6195	6046	35169	35000	14414	14183	14183	6046	643.3	643.3	323.6	323.6
Sept	5361	5362	35802	35000	14414	14183	14183	5362	611.8	611.8	277	277
Oct	5135	5136	36037	35000	14414	14183	14183	5136	596.4	596.4	261.9	261.9
Nov	4029	4030	37100	35000	14414	14184	14184	4030	537.9	537.9	190.2	190.2
Dec	3286	3287	37817	35000	14414	14184	14184	3287	496.9	496.9	144.8	144.8
	Temperature (°C)											
State Point	1	1'	2	3	4	4'	5	5'	6	7	8	9
Jan	-5.73	-5.72	14.43	125	72	70.01	32.34	-5.72	-5.54	36.5	2.367	-5.73
Feb	-2.21	-2.21	19.01	125	72	70.06	34.12	-2.21	-2.04	37.5	5.638	-2.21
Mar	2.773	2.779	25.69	125	72	70.12	37.07	2.779	2.919	39.5	10.35	2.773
Apr	9.159	9.165	34.67	125	72	70.2	40.67	9.165	9.27	42	16.24	9.159
May	15.23	15.24	43.85	125	72	70.27	44.06	15.24	15.3	44.5	21.76	15.23
June	20.79	20.8	53.19	125	72	70.34	47.2	20.8	20.83	47	26.79	20.79
July	23.76	23.21	58.02	125	72	70.37	48.45	23.21	23.22	48	28.93	23.2
Aug	22.6	22.31	56.12	125	72	70.36	47.88	22.31	22.33	47.5	28.1	22.3
Sept	17.19	17.2	47.01	125	72	70.3	45.28	17.2	17.25	45.5	23.57	17.19
Oct	15.39	15.4	44.11	125	72	70.28	44.09	15.4	15.46	44.5	21.89	15.39
Nov	5.583	5.59	29.57	125	72	70.15	38.59	5.59	5.714	40.5	12.93	5.583
Dec	-2.2	-2.19	19.03	125	72	70.06	34.12	-2.19	-2.03	37.5	5.651	-2.2
	Enthalpy (kJ/kg)											
State Point	1	1'	2	3	4	4'	5	5'	6	7	8	9
Jan	73.46	73.64	108.6	318.6	281.5	277.5	154.3	154.3	75.11	491.2	447.9	74.57
Feb	81.77	81.94	116.9	318.6	281.5	277.6	158.9	158.9	83.08	492.5	452.4	82.54
Mar	93.98	94.15	129.1	318.6	281.5	277.9	166.7	166.7	94.51	495.2	458.8	93.96
Apr	110.6	110.7	145.7	318.6	281.5	278.1	176.7	176.7	109.3	498.5	466.9	108.8
May	127.8	128	162.9	318.6	281.5	278.4	186.5	186.5	123.7	501.8	474.4	123.1
June	145.7	145.8	180.8	318.6	281.5	278.6	196.1	196.1	137	505	481.1	136.4
July	154.9	154.7	190	318.6	281.5	278.7	200	200	142.8	506.3	484	142.3
Aug	151.3	151.2	186.4	318.6	281.5	278.7	198.2	198.2	140.6	505.7	482.9	140.1
Sept	133.8	134	168.9	318.6	281.5	278.5	190.2	190.2	128.3	503.1	476.8	127.8
Oct	128.3	128.4	163.4	318.6	281.5	278.4	186.6	186.6	124	501.8	474.5	123.5
Nov	101.1	101.3	136.3	318.6	281.5	278	170.9	170.9	101	496.5	462.4	100.5
Dec	81.81	81.98	117	318.6	281.5	277.6	158.9	158.9	83.12	492.5	452.4	82.57
	Entropy (kJ/kg-K)											
State Point	1	1'	2	3	4	4'	5	5'	6	7	8	9
Jan	0.286	0.287	0.286	0.914	0.914	0.903	0.525	0.588	0.297	1.665	1.693	0.297
Feb	0.316	0.316	0.316	0.914	0.914	0.904	0.54	0.6	0.327	1.666	1.691	0.327
Mar	0.358	0.359	0.358	0.914	0.914	0.905	0.565	0.622	0.368	1.667	1.69	0.368
Apr	0.415	0.416	0.415	0.914	0.914	0.905	0.597	0.649	0.421	1.67	1.689	0.421
May	0.473	0.473	0.473	0.914	0.914	0.906	0.628	0.676	0.471	1.672	1.689	0.471
June	0.531	0.531	0.531	0.914	0.914	0.907	0.658	0.702	0.516	1.675	1.689	0.517
July	0.56	0.56	0.56	0.914	0.914	0.907	0.67	0.713	0.536	1.676	1.689	0.536
Aug	0.548	0.549	0.548	0.914	0.914	0.907	0.665	0.708	0.529	1.675	1.689	0.529
Sept	0.492	0.493	0.492	0.914	0.914	0.906	0.64	0.686	0.487	1.673	1.689	0.487
Oct	0.474	0.475	0.474	0.914	0.914	0.906	0.628	0.676	0.472	1.672	1.689	0.473
Nov	0.383	0.384	0.383	0.914	0.914	0.905	0.578	0.633	0.392	1.668	1.69	0.392
Dec	0.316	0.316	0.316	0.914	0.914	0.904	0.54	0.6	0.327	1.666	1.691	0.327

Table D-32: Thermodynamic properties for Binary ORC System simulations at 3.6km depth with a CO2 mass flow rate of 140kg/s and a reservoir temperature of 125°C.

Well Temp	125°C											
Well Depth	3.6 km											
CO2 Mass Flow	140 kg/s											
	Pressure (kPa)											
State Point	1	1'	2	3	4	4'	5	5'	6	7	8	9
Jan	2985	2986	38090	35000	14100	13782	13782	2986	470.8	470.8	127.2	127.2
Feb	3285	3286	37780	35000	14100	13782	13782	3286	490.3	490.3	144.7	144.7
Mar	3748	3749	37325	35000	14100	13782	13782	3749	517.1	517.1	172.7	172.7
Apr	4409	4410	36700	35000	14100	13782	13782	4410	552.1	552.1	214.3	214.3
May	5116	5116	36013	35000	14100	13782	13782	5116	588.9	588.9	260.6	260.6
June	5836	5837	35212	35000	14100	13781	13781	5837	619.5	619.5	309.3	309.3
July	6423	6174	35049	35000	14100	13781	13781	6174	635.3	635.3	332.3	332.3
Aug	6195	6046	35120	35000	14100	13781	13781	6046	627.4	627.4	323.6	323.6
Sept	5361	5362	35756	35000	14100	13782	13782	5362	596.4	596.4	277	277
Oct	5135	5136	35992	35000	14100	13782	13782	5136	588.9	588.9	261.9	261.9
Nov	4029	4030	37059	35000	14100	13782	13782	4030	530.9	530.9	190.2	190.2
Dec	3286	3287	37778	35000	14100	13782	13782	3287	490.3	490.3	144.8	144.8
	Temperature (°C)											
State Point	1	1'	2	3	4	4'	5	5'	6	7	8	9
Jan	-5.73	-5.72	14.41	125	70.68	68.48	31.48	-5.72	-5.55	35.5	2.114	-5.73
Feb	-2.21	-2.21	18.99	125	70.68	68.52	33.7	-2.21	-2.05	37	5.511	-2.21
Mar	2.773	2.782	25.67	125	70.68	68.57	36.66	2.782	2.917	39	10.22	2.773
Apr	9.159	9.167	34.64	125	70.68	68.64	40.26	9.167	9.267	41.5	16.11	9.159
May	15.23	15.24	43.82	125	70.68	68.7	43.64	15.24	15.3	44	21.63	15.23
June	20.79	20.8	53.16	125	70.68	68.75	46.34	20.8	20.82	46	26.53	20.79
July	23.76	23.21	57.98	125	70.68	68.78	47.58	23.21	23.22	47	28.67	23.2
Aug	22.6	22.31	56.08	125	70.68	68.77	47.01	22.31	22.32	46.5	27.84	22.3
Sept	17.19	17.2	46.98	125	70.68	68.72	44.43	17.2	17.25	44.5	23.32	17.19
Oct	15.39	15.4	44.08	125	70.68	68.7	43.67	15.4	15.46	44	21.76	15.39
Nov	5.583	5.592	29.55	125	70.68	68.6	38.18	5.592	5.711	40	12.8	5.583
Dec	-2.2	-2.19	19.01	125	70.68	68.52	33.7	-2.19	-2.03	37	5.524	-2.2
	Enthalpy (kJ/kg)											
State Point	1	1'	2	3	4	4'	5	5'	6	7	8	9
Jan	73.46	73.61	108.6	318.6	280.8	277.2	152.9	152.9	75.09	489.9	447.5	74.57
Feb	81.77	81.92	116.9	318.6	280.8	277.3	158.7	158.7	83.07	491.8	452.2	82.54
Mar	93.98	94.13	129.1	318.6	280.8	277.5	166.6	166.6	94.5	494.5	458.6	93.96
Apr	110.6	110.7	145.7	318.6	280.8	277.7	176.7	176.7	109.3	497.8	466.7	108.8
May	127.8	127.9	162.9	318.6	280.8	277.9	186.8	186.8	123.6	501.1	474.1	123.1
June	145.7	145.8	180.7	318.6	280.8	278.1	195.2	195.2	136.9	503.7	480.7	136.4
July	154.9	154.7	190	318.6	280.8	278.2	199.3	199.3	142.7	505	483.5	142.3
Aug	151.3	151.2	186.3	318.6	280.8	278.2	197.4	197.4	140.6	504.4	482.4	140.1
Sept	133.8	133.9	168.9	318.6	280.8	278	189.2	189.2	128.3	501.8	476.4	127.8
Oct	128.3	128.4	163.4	318.6	280.8	277.9	186.9	186.9	124	501.1	474.3	123.5
Nov	101.1	101.3	136.2	318.6	280.8	277.6	170.8	170.8	101	495.8	462.2	100.5
Dec	81.81	81.96	116.9	318.6	280.8	277.3	158.7	158.7	83.11	491.8	452.2	82.57
	Entropy (kJ/kg-K)											
State Point	1	1'	2	3	4	4'	5	5'	6	7	8	9
Jan	0.286	0.286	0.286	0.914	0.914	0.905	0.522	0.583	0.297	1.664	1.691	0.297
Feb	0.316	0.316	0.316	0.914	0.914	0.905	0.541	0.599	0.327	1.665	1.69	0.327
Mar	0.358	0.359	0.358	0.914	0.914	0.906	0.566	0.622	0.368	1.667	1.689	0.368
Apr	0.415	0.416	0.415	0.914	0.914	0.907	0.599	0.65	0.421	1.669	1.688	0.421
May	0.473	0.473	0.473	0.914	0.914	0.907	0.631	0.677	0.471	1.672	1.688	0.471
June	0.531	0.531	0.531	0.914	0.914	0.908	0.657	0.699	0.516	1.674	1.687	0.517
July	0.56	0.56	0.56	0.914	0.914	0.908	0.67	0.71	0.536	1.675	1.688	0.536
Aug	0.548	0.549	0.548	0.914	0.914	0.908	0.664	0.705	0.529	1.674	1.687	0.529
Sept	0.492	0.493	0.492	0.914	0.914	0.908	0.638	0.683	0.487	1.672	1.688	0.487
Oct	0.474	0.475	0.474	0.914	0.914	0.907	0.631	0.677	0.472	1.672	1.688	0.473
Nov	0.383	0.384	0.383	0.914	0.914	0.906	0.58	0.633	0.392	1.668	1.689	0.392
Dec	0.316	0.316	0.316	0.914	0.914	0.905	0.541	0.599	0.327	1.665	1.69	0.327

Table D-33: Thermodynamic properties for Binary ORC System simulations at 3.6km depth with a CO2 mass flow rate of 70kg/s and a reservoir temperature of 150°C.

Well Temp	150°C											
Well Depth	3.6 km											
CO2 Mass Flow	70 kg/s											
	Pressure (kPa)											
State Point	1	1'	2	3	4	4'	5	5'	6	7	8	9
Jan	2985	2986	38160	35000	16599	16303	16303	2986	611.8	611.8	127.2	127.2
Feb	3285	3286	37851	35000	16599	16303	16303	3286	627.4	627.4	144.7	144.7
Mar	3748	3748	37399	35000	16599	16303	16303	3748	659.5	659.5	172.7	172.7
Apr	4409	4410	36777	35000	16599	16302	16302	4410	701.4	701.4	214.3	214.3
May	5116	5116	36094	35000	16599	16302	16302	5116	754.2	754.2	260.6	260.6
June	5836	5837	35299	35000	16599	16302	16302	5837	800.3	800.3	309.3	309.3
July	6423	6173	35139	35000	16599	16302	16302	6173	819.4	819.4	332.3	332.3
Aug	6195	6046	35208	35000	16599	16302	16302	6046	809.8	809.8	323.6	323.6
Sept	5361	5362	35839	35000	16599	16302	16302	5362	772.4	772.4	277	277
Oct	5135	5136	36073	35000	16599	16302	16302	5136	754.2	754.2	261.9	261.9
Nov	4029	4029	37134	35000	16599	16303	16303	4029	684.4	684.4	190.2	190.2
Dec	3286	3287	37849	35000	16599	16303	16303	3287	627.4	627.4	144.8	144.8
	Temperature (°C)											
State Point	1	1'	2	3	4	4'	5	5'	6	7	8	9
Jan	-5.73	-5.73	14.45	150	95.61	91.7	38.35	-5.73	-5.5	45.5	4.712	-5.73
Feb	-2.21	-2.21	19.03	150	95.61	91.79	40.34	-2.21	-2	46.5	7.983	-2.21
Mar	2.773	2.778	25.71	150	95.61	91.91	43.6	2.778	2.966	48.5	12.69	2.773
Apr	9.159	9.163	34.69	150	95.61	92.06	47.46	9.163	9.323	51	18.58	9.159
May	15.23	15.23	43.88	150	95.61	92.21	51.72	15.23	15.37	54	24.23	15.23
June	20.79	20.79	53.22	150	95.61	92.35	55.05	20.79	20.9	56.5	29.25	20.79
July	23.76	23.2	58.05	150	95.61	92.4	56.52	23.2	23.3	57.5	31.38	23.2
Aug	22.6	22.3	56.15	150	95.61	92.38	55.82	22.3	22.4	57	30.55	22.3
Sept	17.19	17.19	47.04	150	95.61	92.26	53.04	17.19	17.32	55	26.04	17.19
Oct	15.39	15.39	44.13	150	95.61	92.21	51.76	15.39	15.53	54	24.36	15.39
Nov	5.583	5.588	29.59	150	95.61	91.98	45.71	5.588	5.767	50	15.41	5.583
Dec	-2.2	-2.19	19.05	150	95.61	91.79	40.35	-2.19	-1.99	46.5	7.996	-2.2
	Enthalpy (kJ/kg)											
State Point	1	1'	2	3	4	4'	5	5'	6	7	8	9
Jan	73.46	73.72	108.7	364.1	326.1	319	165.6	165.6	75.31	503.1	451.7	74.57
Feb	81.77	82.03	117	364.1	326.1	319.2	170.6	170.6	83.28	504.4	456.2	82.54
Mar	93.98	94.24	129.2	364.1	326.1	319.5	178.9	178.9	94.72	507	462.8	93.96
Apr	110.6	110.8	145.8	364.1	326.1	319.9	189.2	189.2	109.6	510.2	470.9	108.8
May	127.8	128	163	364.1	326.1	320.3	200.9	200.9	123.9	514.1	478.7	123.1
June	145.7	145.9	180.8	364.1	326.1	320.6	210.6	210.6	137.2	517.3	485.6	136.4
July	154.9	154.8	190.1	364.1	326.1	320.7	214.9	214.9	143	518.6	488.4	142.3
Aug	151.3	151.3	186.4	364.1	326.1	320.7	212.8	212.8	140.9	517.9	487.3	140.1
Sept	133.8	134	169	364.1	326.1	320.4	204.7	204.7	128.6	515.4	481.2	127.8
Oct	128.3	128.5	163.5	364.1	326.1	320.3	201.1	201.1	124.3	514.1	478.9	123.5
Nov	101.1	101.4	136.3	364.1	326.1	319.7	184.5	184.5	101.2	508.9	466.6	100.5
Dec	81.81	82.07	117	364.1	326.1	319.2	170.6	170.6	83.32	504.4	456.2	82.57
	Entropy (kJ/kg-K)											
State Point	1	1'	2	3	4	4'	5	5'	6	7	8	9
Jan	0.286	0.287	0.286	1.024	1.024	1.007	0.553	0.631	0.297	1.673	1.706	0.297
Feb	0.316	0.317	0.316	1.024	1.024	1.008	0.569	0.643	0.327	1.674	1.705	0.327
Mar	0.358	0.359	0.358	1.024	1.024	1.009	0.595	0.666	0.368	1.676	1.704	0.368
Apr	0.415	0.416	0.415	1.024	1.024	1.01	0.628	0.694	0.421	1.679	1.703	0.421
May	0.473	0.473	0.473	1.024	1.024	1.011	0.664	0.726	0.471	1.682	1.703	0.471
June	0.531	0.532	0.531	1.024	1.024	1.012	0.693	0.752	0.516	1.685	1.704	0.517
July	0.56	0.56	0.56	1.024	1.024	1.012	0.707	0.763	0.536	1.686	1.704	0.536
Aug	0.548	0.549	0.548	1.024	1.024	1.012	0.7	0.757	0.529	1.686	1.703	0.529
Sept	0.492	0.493	0.492	1.024	1.024	1.011	0.676	0.737	0.487	1.683	1.704	0.487
Oct	0.474	0.475	0.474	1.024	1.024	1.011	0.664	0.726	0.472	1.682	1.703	0.473
Nov	0.383	0.384	0.383	1.024	1.024	1.009	0.613	0.682	0.391	1.678	1.704	0.392
Dec	0.316	0.317	0.316	1.024	1.024	1.008	0.569	0.644	0.327	1.674	1.705	0.327

Table D-34: Thermodynamic properties for Binary ORC System simulations at 3.6km depth with a CO2 mass flow rate of 90kg/s and a reservoir temperature of 150°C.

Well Temp	150°C											
Well Depth	3.6 km											
CO2 Mass Flow	90 kg/s											
	Pressure (kPa)											
State Point	1	1'	2	3	4	4'	5	5'	6	7	8	9
Jan	2985	2986	38111	35000	15856	15352	15352	2986	573.9	573.9	127.2	127.2
Feb	3285	3286	37801	35000	15856	15352	15352	3286	596.4	596.4	144.7	144.7
Mar	3748	3749	37348	35000	15856	15352	15352	3749	627.4	627.4	172.7	172.7
Apr	4409	4410	36724	35000	15856	15351	15351	4410	667.7	667.7	214.3	214.3
May	5116	5116	36037	35000	15856	15351	15351	5116	718.7	718.7	260.6	260.6
June	5836	5837	35239	35000	15856	15351	15351	5837	754.2	754.2	309.3	309.3
July	6423	6174	35077	35000	15856	15351	15351	6174	781.6	781.6	332.3	332.3
Aug	6195	6046	35147	35000	15856	15351	15351	6046	772.4	772.4	323.6	323.6
Sept	5361	5362	35781	35000	15856	15351	15351	5362	727.4	727.4	277	277
Oct	5135	5136	36017	35000	15856	15351	15351	5136	718.7	718.7	261.9	261.9
Nov	4029	4030	37082	35000	15856	15352	15352	4030	651.4	651.4	190.2	190.2
Dec	3286	3287	37800	35000	15856	15352	15352	3287	596.4	596.4	144.8	144.8
	Temperature (°C)											
State Point	1	1'	2	3	4	4'	5	5'	6	7	8	9
Jan	-5.73	-5.72	14.42	150	92.26	88	36.63	-5.72	-5.51	43	4.05	-5.73
Feb	-2.21	-2.21	19	150	92.26	88.06	39.08	-2.21	-2.01	44.5	7.453	-2.21
Mar	2.773	2.78	25.68	150	92.26	88.16	42.35	2.78	2.955	46.5	12.17	2.773
Apr	9.159	9.166	34.65	150	92.26	88.27	46.32	9.166	9.31	49	18.06	9.159
May	15.23	15.24	43.84	150	92.26	88.38	50.44	15.24	15.35	52	23.71	15.23
June	20.79	20.8	53.18	150	92.26	88.48	53.42	20.8	20.88	54	28.6	20.79
July	23.76	23.21	58	150	92.26	88.53	55.1	23.21	23.28	55.5	30.86	23.2
Aug	22.6	22.31	56.1	150	92.26	88.51	54.58	22.31	22.39	55	30.03	22.3
Sept	17.19	17.2	47	150	92.26	88.42	51.33	17.2	17.3	52.5	25.38	17.19
Oct	15.39	15.4	44.09	150	92.26	88.39	50.48	15.4	15.51	52	23.83	15.39
Nov	5.583	5.591	29.56	150	92.26	88.21	44.47	5.591	5.755	48	14.88	5.583
Dec	-2.2	-2.19	19.02	150	92.26	88.06	39.08	-2.19	-2	44.5	7.466	-2.2
	Enthalpy (kJ/kg)											
State Point	1	1'	2	3	4	4'	5	5'	6	7	8	9
Jan	73.46	73.66	108.6	364.1	324.2	318.2	163.1	163.1	75.25	499.8	450.6	74.57
Feb	81.77	81.97	116.9	364.1	324.2	318.3	169.4	169.4	83.24	501.8	455.3	82.54
Mar	93.98	94.18	129.1	364.1	324.2	318.6	178	178	94.67	504.4	461.9	93.96
Apr	110.6	110.8	145.7	364.1	324.2	318.9	188.9	188.9	109.5	507.6	470	108.8
May	127.8	128	162.9	364.1	324.2	319.1	200.9	200.9	123.8	511.5	477.8	123.1
June	145.7	145.8	180.8	364.1	324.2	319.4	209.9	209.9	137.1	514.1	484.4	136.4
July	154.9	154.7	190	364.1	324.2	319.5	215.2	215.2	143	516	487.5	142.3
Aug	151.3	151.2	186.4	364.1	324.2	319.5	213.6	213.6	140.8	515.4	486.4	140.1
Sept	133.8	134	168.9	364.1	324.2	319.2	203.6	203.6	128.5	512.2	480	127.8
Oct	128.3	128.5	163.4	364.1	324.2	319.1	201	201	124.2	511.5	478	123.5
Nov	101.1	101.3	136.3	364.1	324.2	318.7	183.8	183.8	101.2	506.3	465.7	100.5
Dec	81.81	82.01	117	364.1	324.2	318.3	169.4	169.4	83.27	501.8	455.4	82.57
	Entropy (kJ/kg-K)											
State Point	1	1'	2	3	4	4'	5	5'	6	7	8	9
Jan	0.286	0.287	0.286	1.024	1.024	1.011	0.549	0.621	0.297	1.671	1.702	0.297
Feb	0.316	0.316	0.316	1.024	1.024	1.012	0.569	0.639	0.327	1.672	1.702	0.327
Mar	0.358	0.359	0.358	1.024	1.024	1.012	0.596	0.663	0.368	1.674	1.701	0.368
Apr	0.415	0.416	0.415	1.024	1.024	1.013	0.631	0.693	0.421	1.677	1.7	0.421
May	0.473	0.473	0.473	1.024	1.024	1.014	0.668	0.726	0.471	1.68	1.7	0.471
June	0.531	0.531	0.531	1.024	1.024	1.015	0.696	0.75	0.516	1.682	1.7	0.517
July	0.56	0.56	0.56	1.024	1.024	1.015	0.712	0.764	0.536	1.684	1.701	0.536
Aug	0.548	0.549	0.548	1.024	1.024	1.015	0.707	0.76	0.529	1.683	1.7	0.529
Sept	0.492	0.493	0.492	1.024	1.024	1.014	0.676	0.733	0.487	1.681	1.7	0.487
Oct	0.474	0.475	0.474	1.024	1.024	1.014	0.668	0.726	0.472	1.68	1.7	0.473
Nov	0.383	0.384	0.383	1.024	1.024	1.013	0.615	0.68	0.391	1.676	1.701	0.392
Dec	0.316	0.317	0.316	1.024	1.024	1.012	0.569	0.639	0.327	1.672	1.702	0.327

Table D-35: Thermodynamic properties for Binary ORC System simulations at 3.6km depth with a CO2 mass flow rate of 120kg/s and a reservoir temperature of 150°C.

Well Temp	150°C											
Well Depth	3.6 km											
CO2 Mass Flow	120 kg/s											
	Pressure (kPa)											
State Point	1	1'	2	3	4	4'	5	5'	6	7	8	9
Jan	2985	2986	38129	35000	16723	16460	16460	2986	611.8	611.8	127.2	127.2
Feb	3285	3286	37819	35000	16723	16460	16460	3286	643.3	643.3	144.7	144.7
Mar	3748	3749	37366	35000	16723	16460	16460	3749	676	676	172.7	172.7
Apr	4409	4410	36742	35000	16723	16460	16460	4410	718.7	718.7	214.3	214.3
May	5116	5116	36057	35000	16723	16460	16460	5116	763.2	763.2	260.6	260.6
June	5836	5837	35260	35000	16723	16459	16459	5837	809.8	809.8	309.3	309.3
July	6423	6173	35098	35000	16723	16459	16459	6173	829	829	332.3	332.3
Aug	6195	6046	35169	35000	16723	16459	16459	6046	829	829	323.6	323.6
Sept	5361	5362	35802	35000	16723	16460	16460	5362	781.6	781.6	277	277
Oct	5135	5136	36037	35000	16723	16460	16460	5136	763.2	763.2	261.9	261.9
Nov	4029	4030	37100	35000	16723	16460	16460	4030	692.9	692.9	190.2	190.2
Dec	3286	3287	37817	35000	16723	16460	16460	3287	643.3	643.3	144.8	144.8
	Temperature (°C)											
State Point	1	1'	2	3	4	4'	5	5'	6	7	8	9
Jan	-5.73	-5.72	14.43	150	96.16	93.12	38.2	-5.72	-5.5	45.5	4.712	-5.73
Feb	-2.21	-2.21	19.01	150	96.16	93.18	41.08	-2.21	-1.99	47.5	8.249	-2.21
Mar	2.773	2.779	25.69	150	96.16	93.27	44.35	2.779	2.972	49.5	12.96	2.773
Apr	9.159	9.165	34.67	150	96.16	93.38	48.33	9.165	9.329	52	18.85	9.159
May	15.23	15.24	43.85	150	96.16	93.48	52.06	15.24	15.37	54.5	24.36	15.23
June	20.79	20.8	53.19	150	96.16	93.58	55.41	20.8	20.9	57	29.38	20.79
July	23.76	23.21	58.02	150	96.16	93.62	56.89	23.21	23.3	58	31.51	23.2
Aug	22.6	22.31	56.12	150	96.16	93.61	56.68	22.31	22.41	58	30.81	22.3
Sept	17.19	17.2	47.01	150	96.16	93.52	53.29	17.2	17.32	55.5	26.17	17.19
Oct	15.39	15.4	44.11	150	96.16	93.49	52.11	15.4	15.53	54.5	24.49	15.39
Nov	5.583	5.59	29.57	150	96.16	93.31	46.04	5.59	5.77	50.5	15.54	5.583
Dec	-2.2	-2.19	19.03	150	96.16	93.18	41.08	-2.19	-1.98	47.5	8.262	-2.2
	Enthalpy (kJ/kg)											
State Point	1	1'	2	3	4	4'	5	5'	6	7	8	9
Jan	73.46	73.64	108.6	364.1	326.4	321.2	165	165	75.31	503.1	451.7	74.57
Feb	81.77	81.94	116.9	364.1	326.4	321.3	172.1	172.1	83.31	505.7	456.7	82.54
Mar	93.98	94.15	129.1	364.1	326.4	321.5	180.5	180.5	94.75	508.3	463.2	93.96
Apr	110.6	110.7	145.7	364.1	326.4	321.8	191.1	191.1	109.6	511.5	471.4	108.8
May	127.8	128	162.9	364.1	326.4	322.1	201.4	201.4	123.9	514.7	478.9	123.1
June	145.7	145.8	180.8	364.1	326.4	322.3	210.9	210.9	137.2	517.9	485.8	136.4
July	154.9	154.7	190	364.1	326.4	322.4	215.3	215.3	143.1	519.2	488.7	142.3
Aug	151.3	151.2	186.4	364.1	326.4	322.4	214.6	214.6	140.9	519.2	487.8	140.1
Sept	133.8	134	168.9	364.1	326.4	322.2	204.8	204.8	128.6	516	481.4	127.8
Oct	128.3	128.4	163.4	364.1	326.4	322.1	201.5	201.5	124.3	514.7	479.1	123.5
Nov	101.1	101.3	136.3	364.1	326.4	321.7	184.9	184.9	101.3	509.6	466.8	100.5
Dec	81.81	81.98	117	364.1	326.4	321.3	172.2	172.2	83.34	505.7	456.7	82.57
	Entropy (kJ/kg-K)											
State Point	1	1'	2	3	4	4'	5	5'	6	7	8	9
Jan	0.286	0.287	0.286	1.024	1.024	1.012	0.55	0.628	0.297	1.673	1.706	0.297
Feb	0.316	0.316	0.316	1.024	1.024	1.012	0.573	0.649	0.327	1.675	1.706	0.327
Mar	0.358	0.359	0.358	1.024	1.024	1.013	0.6	0.672	0.368	1.678	1.706	0.368
Apr	0.415	0.416	0.415	1.024	1.024	1.014	0.633	0.7	0.421	1.68	1.705	0.421
May	0.473	0.473	0.473	1.024	1.024	1.014	0.665	0.728	0.471	1.683	1.704	0.471
June	0.531	0.531	0.531	1.024	1.024	1.015	0.694	0.753	0.516	1.686	1.704	0.516
July	0.56	0.56	0.56	1.024	1.024	1.015	0.707	0.764	0.536	1.687	1.704	0.536
Aug	0.548	0.549	0.548	1.024	1.024	1.015	0.705	0.763	0.529	1.687	1.705	0.529
Sept	0.492	0.493	0.492	1.024	1.024	1.015	0.675	0.737	0.487	1.684	1.704	0.487
Oct	0.474	0.475	0.474	1.024	1.024	1.015	0.665	0.728	0.472	1.683	1.704	0.473
Nov	0.383	0.384	0.383	1.024	1.024	1.013	0.614	0.684	0.391	1.679	1.705	0.392
Dec	0.316	0.316	0.316	1.024	1.024	1.012	0.573	0.649	0.327	1.675	1.706	0.327

Table D-36: Thermodynamic properties for Binary ORC System simulations at 3.6km depth with a CO2 mass flow rate of 140kg/s and a reservoir temperature of 150°C.

Well Temp	150°C											
Well Depth	3.6 km											
CO2 Mass Flow	140 kg/s											
	Pressure (kPa)											
State Point	1	1'	2	3	4	4'	5	5'	6	7	8	9
Jan	2985	2986	38090	35000	16360	15997	15997	2986	604	604	127.2	127.2
Feb	3285	3286	37780	35000	16360	15997	15997	3286	627.4	627.4	144.7	144.7
Mar	3748	3749	37325	35000	16360	15997	15997	3749	659.5	659.5	172.7	172.7
Apr	4409	4410	36700	35000	16360	15997	15997	4410	701.4	701.4	214.3	214.3
May	5116	5116	36013	35000	16360	15997	15997	5116	745.2	745.2	260.6	260.6
June	5836	5837	35212	35000	16360	15996	15996	5837	790.9	790.9	309.3	309.3
July	6423	6174	35049	35000	16360	15996	15996	6174	809.8	809.8	332.3	332.3
Aug	6195	6046	35120	35000	16360	15996	15996	6046	800.3	800.3	323.6	323.6
Sept	5361	5362	35756	35000	16360	15996	15996	5362	763.2	763.2	277	277
Oct	5135	5136	35992	35000	16360	15996	15996	5136	745.2	745.2	261.9	261.9
Nov	4029	4030	37059	35000	16360	15997	15997	4030	676	676	190.2	190.2
Dec	3286	3287	37778	35000	16360	15997	15997	3287	627.4	627.4	144.8	144.8
	Temperature (°C)											
State Point	1	1'	2	3	4	4'	5	5'	6	7	8	9
Jan	-5.73	-5.72	14.41	150	94.55	91.34	38.02	-5.72	-5.5	45	4.579	-5.73
Feb	-2.21	-2.21	18.99	150	94.55	91.39	40.47	-2.21	-2	46.5	7.983	-2.21
Mar	2.773	2.782	25.67	150	94.55	91.47	43.74	2.782	2.966	48.5	12.69	2.773
Apr	9.159	9.167	34.64	150	94.55	91.56	47.61	9.167	9.323	51	18.58	9.159
May	15.23	15.24	43.82	150	94.55	91.65	51.34	15.24	15.36	53.5	24.1	15.23
June	20.79	20.8	53.16	150	94.55	91.74	54.86	20.8	20.9	56	29.12	20.79
July	23.76	23.21	57.98	150	94.55	91.77	56.14	23.21	23.29	57	31.25	23.2
Aug	22.6	22.31	56.08	150	94.55	91.76	55.53	22.31	22.4	56.5	30.42	22.3
Sept	17.19	17.2	46.98	150	94.55	91.68	52.76	17.2	17.32	54.5	25.91	17.19
Oct	15.39	15.4	44.08	150	94.55	91.66	51.38	15.4	15.52	53.5	24.23	15.39
Nov	5.583	5.592	29.55	150	94.55	91.51	45.42	5.592	5.764	49.5	15.28	5.583
Dec	-2.2	-2.19	19.01	150	94.55	91.39	40.47	-2.19	-1.99	46.5	7.996	-2.2
	Enthalpy (kJ/kg)											
State Point	1	1'	2	3	4	4'	5	5'	6	7	8	9
Jan	73.46	73.61	108.6	364.1	325.5	320.7	165.4	165.4	75.3	502.4	451.5	74.57
Feb	81.77	81.92	116.9	364.1	325.5	320.9	171.5	171.5	83.28	504.4	456.2	82.54
Mar	93.98	94.13	129.1	364.1	325.5	321	180.1	180.1	94.72	507	462.8	93.96
Apr	110.6	110.7	145.7	364.1	325.5	321.3	190.5	190.5	109.6	510.2	470.9	108.8
May	127.8	127.9	162.9	364.1	325.5	321.5	201	201	123.9	513.5	478.5	123.1
June	145.7	145.8	180.7	364.1	325.5	321.7	211.3	211.3	137.2	516.7	485.3	136.4
July	154.9	154.7	190	364.1	325.5	321.8	215.2	215.2	143	517.9	488.2	142.3
Aug	151.3	151.2	186.3	364.1	325.5	321.8	213.3	213.3	140.8	517.3	487.1	140.1
Sept	133.8	133.9	168.9	364.1	325.5	321.6	205.1	205.1	128.6	514.7	481	127.8
Oct	128.3	128.4	163.4	364.1	325.5	321.5	201.1	201.1	124.3	513.5	478.6	123.5
Nov	101.1	101.3	136.2	364.1	325.5	321.1	184.6	184.6	101.2	508.3	466.3	100.5
Dec	81.81	81.96	116.9	364.1	325.5	320.9	171.6	171.6	83.32	504.4	456.2	82.57
	Entropy (kJ/kg-K)											
State Point	1	1'	2	3	4	4'	5	5'	6	7	8	9
Jan	0.286	0.286	0.286	1.024	1.024	1.014	0.553	0.63	0.297	1.673	1.706	0.297
Feb	0.316	0.316	0.316	1.024	1.024	1.014	0.573	0.647	0.327	1.674	1.705	0.327
Mar	0.358	0.359	0.358	1.024	1.024	1.015	0.6	0.67	0.368	1.676	1.704	0.368
Apr	0.415	0.416	0.415	1.024	1.024	1.015	0.633	0.698	0.421	1.679	1.703	0.421
May	0.473	0.473	0.473	1.024	1.024	1.016	0.665	0.726	0.471	1.682	1.703	0.471
June	0.531	0.531	0.531	1.024	1.024	1.017	0.697	0.754	0.516	1.684	1.703	0.517
July	0.56	0.56	0.56	1.024	1.024	1.017	0.709	0.764	0.536	1.686	1.703	0.536
Aug	0.548	0.549	0.548	1.024	1.024	1.017	0.703	0.759	0.529	1.685	1.703	0.529
Sept	0.492	0.493	0.492	1.024	1.024	1.016	0.678	0.738	0.487	1.683	1.703	0.487
Oct	0.474	0.475	0.474	1.024	1.024	1.016	0.666	0.727	0.472	1.682	1.703	0.473
Nov	0.383	0.384	0.383	1.024	1.024	1.015	0.614	0.682	0.391	1.678	1.703	0.392
Dec	0.316	0.316	0.316	1.024	1.024	1.014	0.573	0.647	0.327	1.674	1.705	0.327

Appendix E: Supplemental Diagrams

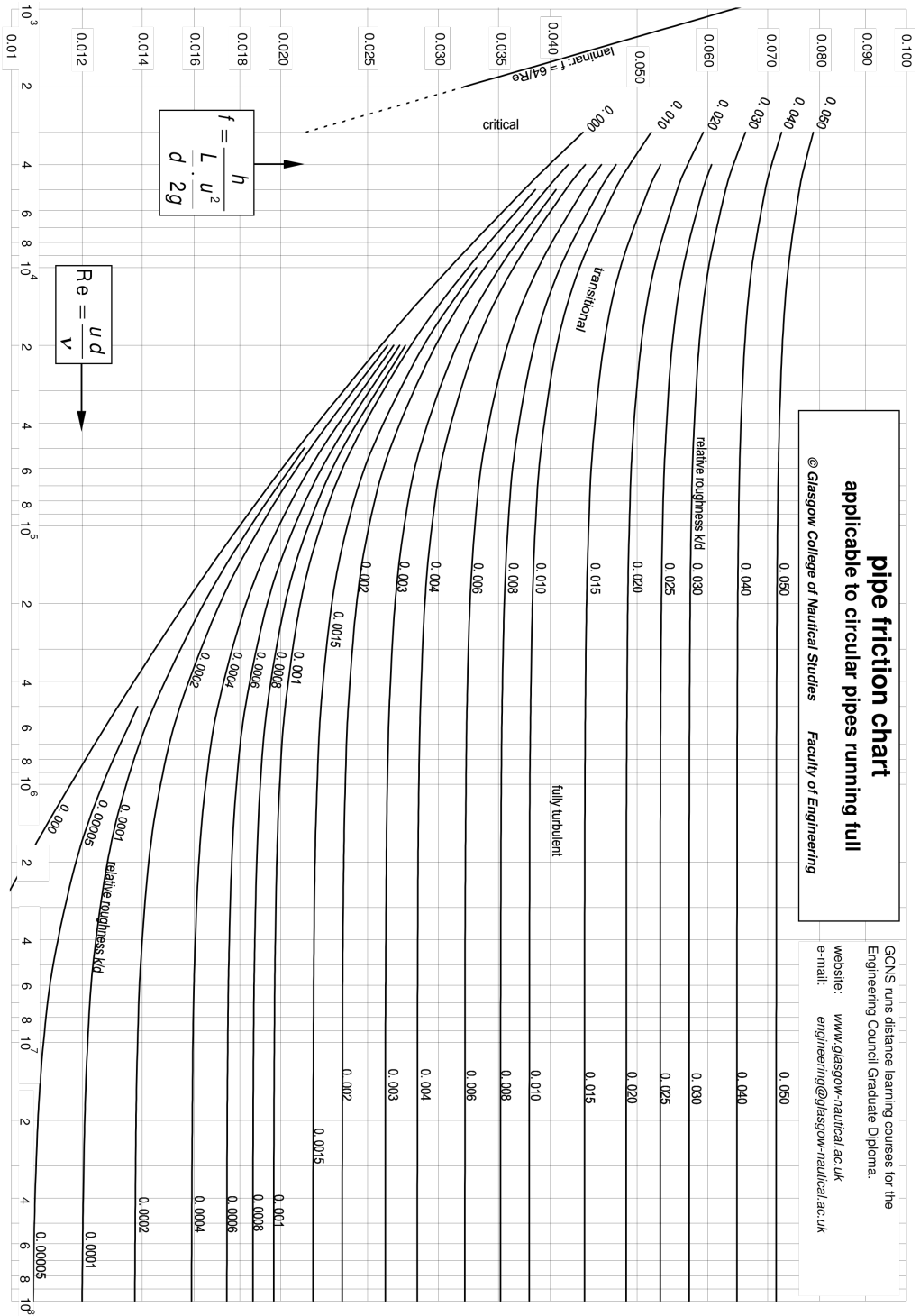


Figure E-1: Moody Diagram [27] relating friction factor to Reynolds number for various ratios of pipe roughness coefficient to pipe diameter.

Appendix F: EES Codes for System Simulations

Direct Single-Loop System Code

{CO2 Direct Single-Loop Geothermal Power Cycle}

{headloss in the injection pipe, Depth in meters equal to 10 times number of intervals }

PROCEDURE

Injectionpipe(L,ffact,D,g,massflow,P11,Den11,H11,T11,S11,V11:P[1..250],rho[1..250],H[1..250],T[1..250],S[1..250],V[1..250])

\$COMMON L,ffact,D,g,massflow,P11,Den11,H11,T11,S11,V11

\$REFERENCE R744 ASH

i:=0

P[i]:=P11

rho[i]:=Den11

H[i]:=H11

T[i]:=T11

S[i]:=S11

V[i]:=V11

REPEAT

i:=i+1

{headloss through the pipe due to frictional effects}

headloss:=(8*L*ffact*massflow^2)/(g*rho[i-1]^2*Pi^2*D^5)

{Pressure change through a segment of pipe due to hydrostatic and frictional headloss}

P[i]:=P[i-1]+rho[i-1]*g*L/1000-rho[i-1]*g*headloss/1000

{Change in Enthalpy through a segment of pipe relative to change in pressure}

H[i]:=((P[i]-P[i-1])/rho[i-1])+H[i-1]

T[i]:=Temperature(R744,H=H[i],P=P[i])

rho[i]:=Density(R744,H=H[i],P=P[i])

S[i]:=Entropy(R744,H=H[i],P=P[i])

```

V[i]:=massflow/(rho[i]*Pi*(D/2)^2)

UNTIL(i=250)

END

{headloss in the riser pipe, Depth in meters equal to 10 times number of intervals}

PROCEDURE

Riserpipe(L,ffact,Driser,g,massflow,P3,Den3,H3,T3,S3,V3:P4[1..250],rho4[1..250],H4[1..250],T4[1..250],
S4[1..250],V4[1..250])

$COMMON L,ffact,Driser,g,massflow,P3,Den3,H3,T3,S3,V3

$REFERENCE R744 ASH

i:=0

P4[i]:=P3

rho4[i]:=Den3

H4[i]:=H3

T4[i]:=T3

S4[i]:=S3

V4[i]:=V3

REPEAT

i:=i+1

{headloss through the pipe due to frictional effects}

headloss:=(8*L*ffact*massflow^2)/(g*rho4[i-1]^2*Pi^2*Driser^5)

{Pressure change through a segment of pipe due to hydrostatic and frictional headloss}

P4[i]:=P4[i-1]-rho4[i-1]*g*L/1000-rho4[i-1]*g*headloss/1000

{Change in Enthalpy through a segment of pipe relative to change in pressure}

H4[i]:=((P4[i]-P4[i-1])/rho4[i-1])+H4[i-1]

T4[i]:=Temperature(R744,H=H4[i],P=P4[i])

rho4[i]:=Density(R744,H=H4[i],P=P4[i])

S4[i]:=Entropy(R744,H=H4[i],P=P4[i])

```

```

V4[i]:=massflow/(rho4[i]*Pi*(Driser/2)^2)

UNTIL(i=250)

END

{headloss in the supply line, length of pipe equal to 10 times number of intervals}

PROCEDURE

supplyline(L,ffact,Driser,delt_ins,g,massflow,Pa,To,P4,Den4,H4,T4,S4,V4,Ts4:P4a[1..69],rho4a[1..69],H4a[1..69],T4a[1..69],S4a[1..69],V4a[1..69],qamb4a[1..69],qins4a[1..69],Ts4_insa[1..69])

$COMMON L,ffact,Driser,delt_ins,g,massflow,Pa,To,P4,Den4,H4,T4,S4,V4,Ts4

$REFERENCE R744 ASH

i:=0

P4a[i]:=P4

rho4a[i]:=Den4

H4a[i]:=H4

T4a[i]:=T4

S4a[i]:=S4

V4a[i]:=V4

Ts4_insa[i]:=Ts4

qamb4a[i]:=0

qins4a[i]:=0

REPEAT

i:=i+1

Ts=Ts4+i*delt_ins {Change in surface temperature of the supply line}

Tavg=(Ts+To)/2 {Averaging ambient and surface temperatures}

Pr=Prandtl(Air_ha,T=Tavg,P=Pa)

Beta=VolExpCoef(Air_ha,T=Tavg,P=Pa)

mu=Viscosity(Air_ha,T=Tavg,P=Pa)

k=Conductivity(Air_ha,T=Tavg,P=Pa)

```

```

Gr=(g*Beta*(Ts-To)*Driser^3)/((mu/rho4a[i-1])^2)

Ra=Gr*Pr

Nu=(0.60+(.387*Ra^(1/6))/(1+(.559/Pr)^(9/16))^(8/27))^2

hcoef=k*Nu/Driser

{convective and radiation heat losses to the ambient}

qamb:=hcoef*2*Pi*(Driser/2+0.05)*(Ts-To)+0.9*2*Pi*(Driser/2+0.05)*(5.67*10^(-
8))*((Ts+273)^4-(To+273)^4)

{conductive heat losses through insulation}

qins:=2*Pi*0.42*(T4a[i-1]-Ts)/ln((Driser/2+0.05)/(Driser/2))

{headloss through the pipe due to frictional effects}

headloss:=(8*L*ffact*massflow^2)/(g*rho4a[i-1]^2*Pi^2*Driser^5)

{Pressure change through a segment of pipe due to frictional headloss}

P4a[i]:=P4a[i-1]-rho4a[i-1]*g*headloss/1000

{Change in Enthalpy through relative to change in pressure and thermal losses}

H4a[i]:=((P4a[i]-P4a[i-1])/rho4a[i-1])+H4a[i-1]-qins*L/(massflow*1000)

T4a[i]:=Temperature(R744,H=H4a[i],P=P4a[i])

rho4a[i]:=Density(R744,H=H4a[i],P=P4a[i])

S4a[i]:=Entropy(R744,H=H4a[i],P=P4a[i])

V4a[i]:=massflow/(rho4a[i]*Pi*(Driser/2)^2)

qamb4a[i]:=qamb

qins4a[i]:=qins

Ts4_insa[i]:=Ts

UNTIL(i=69)

END

{headloss in the return line, length of pipe equal to 10 times number of intervals}

PROCEDURE

returnline(L,ffact,D,g,massflow,Pa,P1,Den1,H1,To,T1,S1,V1:P1a[1..2],rho1a[1..2],H1a[1..2],T1a[1..2],S1a
[1..2],V1a[1..2])

```

\$COMMON L,ffact,D,g,massflow,Pa,P1,Den1,H1,To,T1,S1,V1

\$REFERENCE R744 ASH

i:=0

P1a[i]:=P1

rho1a[i]:=Den1

H1a[i]:=H1

T1a[i]:=T1

S1a[i]:=S1

V1a[i]:=V1

REPEAT

i:=i+1

Ts=T1a[i-1]

Tavg=(T1a[i-1]+To)/2 {Averaging ambient and surface temperatures}

Pr=Prandtl(Air_ha,T=Tavg,P=Pa)

Beta=VolExpCoef(Air_ha,T=Tavg,P=Pa)

mu=Viscosity(Air_ha,T=Tavg,P=Pa)

k=Conductivity(Air_ha,T=Tavg,P=Pa)

Gr=(g*Beta*(T1a[i-1]-To)*D^3)/((mu/rho1a[i-1])^2)

Ra=Gr*Pr

Nu=(0.60+(.387*Ra^(1/6))/(1+(.559/Pr)^(9/16))^(8/27))^2

hcoef=k*Nu/D

{convective and radiation heat losses to the ambient}

qamb=hcoef*Pi*D*(Ts-To)+0.9*Pi*D*(5.67*10^(-8))*((Ts+273)^4-(To+273)^4)

{headloss through the pipe due to frictional effects}

headloss:=(8*L*ffact*massflow^2)/(g*rho1a[i-1]^2*Pi^2*D^5)

{Pressure change through a segment of pipe due to frictional headloss}

P1a[i]:=P1a[i-1]+(rho1a[i-1]*g*headloss/1000)

{Change in Enthalpy relative to change in pressure and thermal losses}

$H1a[i]:=H1a[i-1]-((P1a[i-1]-P1a[i])/rho1a[i-1])+L*qamb/(massflow*1000)$

$T1a[i]:=Temperature(R744,H=H1a[i],P=P1a[i])$

$rho1a[i]:=Density(R744,H=H1a[i],P=P1a[i])$

$S1a[i]:=Entropy(R744,H=H1a[i],P=P1a[i])$

$V1a[i]:=massflow/(rho1a[i]*Pi*(D/2)^2)$

UNTIL(i=2)

END

{L = length of pipe segment}

L=10.0

{ffact = friction factor in pipe}

ffact=0.014

{D = diameter of pipe}

D=0.254

{Driser = diameter of production pipe {m}}

Driser=0.20

{g = gravitational constant}

g=9.8

{T1 sets condensing temperature (C)}

T1=Tamb+5

{P3 sets the reservoir pressure (kPa)}

P3=25000

{T3 sets the reservoir temperature (C)}

T3=100

{Turbeff sets turbine isentropic efficiency}

Turbeff=0.85

{Pumpeff sets pump isentropic efficiency}

Pumpeff=0.90

{P11 sets the pressure leaving the pump (kPa)}

P11=P1+Ppump {Ppump is the pressure change across the pump}

{mass flow rates for the CO2 through the power system (massflow) and for the CO2 through the compression cycle (M) (kg/s)}

massflow=70

M=10.0

{Mass sets amount of CO2 to be sequestered (kg)}

Mass=1000000000.0

{State a, CO2 supplied at sea level pressure and ambient temperature=T1}

Pa=101.3

{Intermediate pressure for two phase compression}

Pint=(Pa*P1)^(1/2)

{P-v diagram intermediate pressures}

Pad=(Pint+Pa)/2

Pcd=(P1+Pint)/2

\$REFERENCE R744 ASH

{work per unit mass to isentropically compress CO2 gas to saturated vapor at T1}

{wcomp=Hc-Ha} {single isentropic compression process}

wcomp=(Hd-Ha)+(Hf-He) {isentropic compression with intercooling}

{Reference state values}

To=Tamb

Ho=Enthalpy(R744,T=To,P=Pa)

So=Entropy(R744,T=To,P=Pa)

{State a: CO2 at ambient conditions entering compressor}

$$S_a = \text{Entropy}(\text{R744}, T=T_1, P=P_a)$$

$$H_a = \text{Enthalpy}(\text{R744}, T=T_1, P=P_a)$$

$$v_a = \text{Volume}(\text{R744}, T=T_1, P=P_a)$$

$$T_a = T_{amb}$$

{State b: saturated CO2 vapor entering condenser} {a-b is an isothermal process}

$$T_b = T_{amb}$$

$$P_b = P_1$$

$$H_b = \text{Enthalpy}(\text{R744}, T=T_b, x=1.0)$$

$$S_b = \text{Entropy}(\text{R744}, T=T_b, x=1.0)$$

{state c: compressed CO2 gas entering condenser} {a-c is a single stage isentropic compression process}

$$H_c = \text{Enthalpy}(\text{R744}, S=S_a, P=P_1)$$

$$v_c = \text{Volume}(\text{R744}, S=S_a, P=P_1)$$

$$P_c = P_1$$

$$S_c = S_a$$

$$T_c = \text{Temperature}(\text{R744}, S=S_a, P=P_1)$$

{state d: compressed CO2 entering inter-cooler} {a-d is the first stage isentropic compression of a compression cycle with intercooling}

$$H_d = \text{Enthalpy}(\text{R744}, S=S_a, P=P_{int})$$

$$v_d = \text{Volume}(\text{R744}, P=P_{int}, S=S_a)$$

$$S_d = S_a$$

$$P_d = P_{int}$$

$$T_d = \text{Temperature}(\text{R744}, P=P_{int}, S=S_d)$$

{d-e is intercooling condensing process}

{state e: CO2 gas entering secondary compression cycle} {e-f is the second stage isentropic compression of a compression cycle with intercooling}

$$H_e = \text{Enthalpy}(\text{R744}, T=T1, P=P_{int})$$

$$v_e = \text{Volume}(\text{R744}, P=P_{int}, T=T1)$$

$$T_e = T_{amb}$$

$$P_e = P_{int}$$

$$S_e = \text{Entropy}(\text{R744}, T=T1, P=P_{int})$$

{state f: CO2 gas entering final condenser} {f-b is the final condensing process of the intercooling compression cycle}

$$H_f = \text{Enthalpy}(\text{R744}, S=S_e, P=P1)$$

$$v_f = \text{Volume}(\text{R744}, P=P1, S=S_e)$$

$$P_f = P1$$

$$S_f = S_e$$

$$T_f = \text{Temperature}(\text{R744}, P=P_f, S=S_f)$$

{Intermediate Specific Volumes for p-v diagram}

$$v_{ad} = \text{Volume}(\text{R744}, P=P_{ad}, S=S_a)$$

$$v_{cd} = \text{Volume}(\text{R744}, S=S_a, P=P_{cd})$$

$$v_{ef} = \text{Volume}(\text{R744}, P=P_{cd}, S=S_e)$$

{Compressor power requirement (kW)}

$$\text{CompPower} = w_{\text{comp}} * M$$

{Time required for Mass Injection(days)}

$$\text{InjectionTime} = (\text{Mass}/M)/3600/24$$

$$\text{Time} = \text{Month} \text{ \{number of days in a given month\}}$$

{Energy required to compress injected mass (kJ)}

$$E = \text{CompPower} * \text{Time} * 3600 * 24$$

{state1a:saturated liquid CO2 leaving condenser}

CALL

returnline(L,ffact,D,g,massflow,Pa,P1,Den1,H1,To,T1,S1,V1:P1a[1..2],rho1a[1..2],H1a[1..2],T1a[1..2],S1a[1..2],V1a[1..2])

S1a=S1a[2]

P1a=P1a[2]

T1a=T1a[2]

H1a=H1a[2]

Den1a=rho1a[2]

V1a=V1a[2]

ef1a=H1a-Ho-(To+273)*(S1a-So) {flow exergy of CO2 leaving the condenser}

{state 1: saturated liquid CO2 entering injection pipe}

Tts[1]=T1

Sts[1]=S1

P1=Pressure(R744,x=0,T=T1)

S1=Entropy(R744,x=0,T=T1)

H1=Enthalpy(R744,x=0,T=T1)

Den1=Density(R744,x=0,T=T1)

V1=massflow/(Den1*Pi*(D/2)^2)

mu1=Viscosity(R744,x=0.0,T=T1)

Re1=(4*massflow)/(Pi*D*mu1)

ef1=H1-Ho-(To+273)*(S1-So) {flow exergy of CO2 entering the injection pipe}

{state 11: liquid CO2 leaving the pump}

S11=S1

H11=H1+((P11-P1)/Den1)

T11=Temperature(R744,H=H11,P=P11)

Den11=Density(R744,H=H11,P=P11)

V11=massflow/(Den11*Pi*(D/2)^2)

{state 2: CO2 at bottom of injection pipe}

CALL

Injectionpipe(L,ffact,D,g,massflow,P11,Den11,H11,T11,S11,V11:P[1..250],rho[1..250],H[1..250],T[1..250],S[1..250],V[1..250])

S2=S[250]

P2=P[250]

T2=T[250]

H2=H[250]

Den2=rho[250]

mu2=Viscosity(R744,T=T2,P=P2)

Re2=(4*massflow)/(Pi*D*mu2)

Tts[2]=T2

Sts[2]=S2

ef2=H2-Ho-(To+273)*(S2-So) {flow exergy of CO2 exiting the injection pipe}

{state 3: superheated CO2 entering bottom of riser pipe}

S3=Entropy(R744,P=P3,T=T3)

H3=Enthalpy(R744,P=P3,T=T3)

Den3=Density(R744,P=P3,T=T3)

V3=massflow/(Den3*Pi*(D/2)^2)

mu3=Viscosity(R744,T=T3,P=P3)

Re3=(4*massflow)/(Pi*Driser*mu3)

Tts[3]=T3

Sts[3]=S3

ef3=H3-Ho-(To+273)*(S3-So) {flow exergy of CO2 entering the production pipe}

{state 4: superheated CO2 exiting riser pipe}

CALL

Riserpipe(L,ffact,Driser,g,massflow,P3,Den3,H3,T3,S3,V3:P4[1..250],rho4[1..250],H4[1..250],T4[1..250],S4[1..250],V4[1..250])

S4=S4[250]

P4=P4[250]

T4=T4[250]

H4=H4[250]

Den4=rho4[250]

V4=V4[250]

Ts4=Tsrf {initial surface temperature of supply line}

delt_ins=deltins {change in surface temperature along a segment of piping}

mu4=Viscosity(R744,T=T4,P=P4)

Re4=(4*massflow)/(Pi*Driser*mu4)

ef4=H4-Ho-(To+273)*(S4-So) {flow exergy exiting the production pipe}

{state 4a: superheated CO2 entering turbine}

CALL

supplyline(L,ffact,Driser,delt_ins,g,massflow,Pa,To,P4,Den4,H4,T4,S4,V4,Ts4:P4a[1..69],rho4a[1..69],H4a[1..69],T4a[1..69],S4a[1..69],V4a[1..69],qamb4a[1..69],qins4a[1..69],Ts4_insa[1..69])

S4a=S4a[69]

P4a=P4a[69]

T4a=T4a[69]

H4a=H4a[69]

Den4a=rho4a[69]

V4a=V4a[69]

mu4a=Viscosity(R744,T=T4a,P=P4a)

Re4a=(4*massflow)/(Pi*Driser*mu4a)

Ts4_insa=Ts4_insa[69]

$$q_{amb4a} = q_{amb4a}[69]$$

$$q_{ins4a} = q_{ins4a}[69]$$

$$T_{ts[4]} = T_{4a}$$

$$S_{ts[4]} = S_{4a}$$

$$ef_{4a} = H_{4a} - H_o - (T_o + 273) * (S_{4a} - S_o) \text{ \{flow exergy entering the turbine\}}$$

{state 5s: CO2 leaving isentropic turbine}

$$P_5 = P_{1a}$$

$$S_{5s} = S_{4a}$$

$$H_{5s} = \text{Enthalpy}(R744, S=S_{5s}, P=P_5)$$

{state 5: CO2 leaving real turbine}

$$H_5 = H_{4a} - (H_{4a} - H_{5s}) * \text{Turbeff}$$

$$T_5 = \text{Temperature}(R744, H=H_5, P=P_5)$$

$$\text{Den}_5 = \text{Density}(R744, P=P_5, H=H_5)$$

$$S_5 = \text{Entropy}(R744, P=P_5, H=H_5)$$

$$T_{ts[5]} = T_5$$

$$S_{ts[5]} = S_5$$

$$ef_5 = H_5 - H_o - (T_o + 273) * (S_5 - S_o) \text{ \{flow exergy exiting the turbine\}}$$

{T-s diagram state points}

$$T_{ts[6]} = T_1$$

$$S_{ts[6]} = \text{Entropy}(R744, P=P_5, x=1.0)$$

$$T_{ts[7]} = T_1$$

$$S_{ts[7]} = S_1$$

{Efficiency = cycle thermal efficiency}

$$\text{Efficiency} = ((H_{4a} - H_5) - (H_{11} - H_1)) / (H_3 - H_2)$$

{Wturb = Work done by the Turbine}

$$W_{turb} = \text{massflow} * (H_{4a} - H_5)$$

{WNet = Net Energy Production}

$$W_{net} = W_{turb} - W_{pump}$$

{Wpump = Work required to run pump}

$$W_{pump} = \text{massflow} * (H_{11} - H_1)$$

{Time for turbine energy output to equal compressor energy requirement (days)}

$$\text{Days} = E / W_{turb} / 3600 / 24$$

{Vol4 = volumetric flow rate out of turbine(cubic m/s)}

$$\text{Vol}_5 = \text{massflow} / \text{Den}_5$$

{Vol1 = volumetric flow rate into pump(cubic m/s)}

$$\text{Vol}_1 = \text{massflow} / \text{Den}_1$$

{Vol3a = volumetric flow rate into vapor column(cubic m/s)}

$$\text{Vol}_3 = \text{massflow} / \text{Den}_3$$

{Qin = the input heat rate (kW)}

$$Q_{in} = \text{massflow} * (H_3 - H_2)$$

{Qout = Heat out of the condenser {kW} }

$$Q_{out} = \text{massflow} * (H_5 - H_1)$$

Binary ORC System Code

{CO2 Binary ORC Geothermal Power Cycle}

{headloss in the injection pipe, Depth in meters equal to 10 times number of intervals }

PROCEDURE

Injectionpipe(L,ffact,D,g,mdot1,P1,Den1,H1,T1,S1,V1:P[1..250],rho[1..250],H[1..250],T[1..250],S[1..250],V[1..250])

\$COMMON L,ffact,D,g,mdot1,P1,Den1,H1,T1,S1,V1

\$REFERENCE R744 ASH

i:=0

P[i]:=P1

rho[i]:=Den1

H[i]:=H1

T[i]:=T1

S[i]:=S1

V[i]:=V1

REPEAT

i:=i+1

{headloss through the pipe due to frictional effects}

headloss:=(8*L*ffact*mdot1^2)/(g*rho[i-1]^2*Pi^2*D^5)

{Pressure change through a segment of pipe due to hydrostatic and frictional headloss}

P[i]:=P[i-1]+rho[i-1]*g*L/1000-rho[i-1]*g*headloss/1000

{Change in Enthalpy through a segment of pipe relative to change in pressure}

H[i]:=((P[i]-P[i-1])/rho[i-1])+H[i-1]

T[i]:=Temperature(R744,H=H[i],P=P[i])

rho[i]:=Density(R744,H=H[i],P=P[i])

S[i]:=Entropy(R744,H=H[i],P=P[i])

V[i]:=mdot1/(rho[i]*Pi*(D/2)^2)

UNTIL(i=250)

END

{headloss in the riser pipe, Depth in meters equal to 10 times number of intervals}

PROCEDURE

Riserpipe(L,ffact,Driser,g,mdot1,P3,Den3,H3,T3,S3,V3:P4[1..250],rho4[1..250],H4[1..250],T4[1..250],S4[1..250],V4[1..250])

\$COMMON L,ffact,Driser,g,mdot1,P3,Den3,H3,T3,S3,V3

\$REFERENCE R744 ASH

i:=0

P4[i]:=P3

rho4[i]:=Den3

H4[i]:=H3

T4[i]:=T3

S4[i]:=S3

V4[i]:=V3

REPEAT

i:=i+1

{headloss through the pipe due to frictional effects}

headloss:=(8*L*ffact*mdot1^2)/(g*rho4[i-1]^2*Pi^2*Driser^5)

{Pressure change through a segment of pipe due to hydrostatic and frictional headloss}

P4[i]:=P4[i-1]-rho4[i-1]*g*L/1000-rho4[i-1]*g*headloss/1000

{Change in Enthalpy through a segment of pipe relative to change in pressure}

H4[i]:=((P4[i]-P4[i-1])/rho4[i-1])+H4[i-1]

T4[i]:=Temperature(R744,H=H4[i],P=P4[i])

rho4[i]:=Density(R744,H=H4[i],P=P4[i])

S4[i]:=Entropy(R744,H=H4[i],P=P4[i])

V4[i]:=mdot1/(rho4[i]*Pi*(Driser/2)^2)

UNTIL(i=250)

END

{headloss in the supply line, length of pipe equal to 10 times number of intervals}

PROCEDURE

supplyline(L,ffact,Driser,delt_ins,g,mdot1,Pa,To,P4,Den4,H4,T4,S4,V4,Ts4:P4a[1..69],rho4a[1..69],H4a[1..69],T4a[1..69],S4a[1..69],V4a[1..69],qamb4a[1..69],qins4a[1..69],Ts4_insa[1..69])

\$COMMON L,ffact,Driser,delt_ins,g,mdot1,Pa,To,P4,Den4,H4,T4,S4,V4,Ts4

\$REFERENCE R744 ASH

i:=0

P4a[i]:=P4

rho4a[i]:=Den4

H4a[i]:=H4

T4a[i]:=T4

S4a[i]:=S4

V4a[i]:=V4

Ts4_insa[i]:=Ts4

qamb4a[i]:=0

qins4a[i]:=0

REPEAT

i:=i+1

Ts=Ts4+i*delt_ins {Change in surface temperature of the supply line}

Tavg=(Ts+To)/2 {Averaging ambient and surface temperatures}

Pr=Prandtl(Air_ha,T=Tavg,P=Pa)

Beta=VolExpCoef(Air_ha,T=Tavg,P=Pa)

mu=Viscosity(Air_ha,T=Tavg,P=Pa)

k=Conductivity(Air_ha,T=Tavg,P=Pa)

Gr=(g*Beta*(Ts-To)*Driser^3)/((mu/rho4a[i-1])^2)

Ra=Gr*Pr

```

Nu=(0.60+(.387*Ra^(1/6))/(1+(.559/Pr)^(9/16))^(8/27))^2
hcoef=k*Nu/Driser
{convective and radiation heat losses to the ambient}
qamb:=hcoef*2*Pi*(Driser/2+0.05)*(Ts-To)+0.9*2*Pi*(Driser/2+0.05)*(5.67*10^(-
8))*((Ts+273)^4-(To+273)^4)
{conductive heat losses through insulation}
qins:=2*Pi*0.42*(T4a[i-1]-Ts)/ln((Driser/2+0.05)/(Driser/2))
{headloss through the pipe due to frictional effects}
headloss:=(8*L*ffact*mdot1^2)/(g*rho4a[i-1]^2*Pi^2*Driser^5)
{Pressure change through a segment of pipe due to frictional headloss}
P4a[i]:=P4a[i-1]-rho4a[i-1]*g*headloss/1000
{Change in Enthalpy relative to change in pressure and thermal losses}
H4a[i]:=((P4a[i]-P4a[i-1])/rho4a[i-1])+H4a[i-1]-qins*L/(mdot1*1000)
T4a[i]:=Temperature(R744,H=H4a[i],P=P4a[i])
rho4a[i]:=Density(R744,H=H4a[i],P=P4a[i])
S4a[i]:=Entropy(R744,H=H4a[i],P=P4a[i])
V4a[i]:=mdot1/(rho4a[i]*Pi*(Driser/2)^2)
qamb4a[i]:=qamb
qins4a[i]:=qins
Ts4_insa[i]:=Ts
UNTIL(i=69)
END

{headloss in the return line, length of pipe equal to 10 times number of intervals}
PROCEDURE
returnline(L,ffact,D,g,mdot1,Pa,P1,Den1,H1,To,T1,S1,V1:P1a[1..2],rho1a[1..2],H1a[1..2],T1a[1..2],S1a[1..
2],V1a[1..2])
$COMMON L,ffact,D,g,mdot1,Pa,P1,Den1,H1,To,T1,S1,V1
$REFERENCE R744 ASH

```

```

i:=0

P1a[i]:=P1

rho1a[i]:=Den1

H1a[i]:=H1

T1a[i]:=T1

S1a[i]:=S1

V1a[i]:=V1

REPEAT

    i:=i+1

    Ts=T1a[i-1]

    Tavg=(T1a[i-1]+To)/2 {Averaging ambient and surface temperatures}

    Pr=Prandtl(Air_ha,T=Tavg,P=Pa)

    Beta=VolExpCoef(Air_ha,T=Tavg,P=Pa)

    mu=Viscosity(Air_ha,T=Tavg,P=Pa)

    k=Conductivity(Air_ha,T=Tavg,P=Pa)

    Gr=(g*Beta*(T1a[i-1]-To)*D^3)/((mu/rho1a[i-1])^2)

    Ra=Gr*Pr

    Nu=(0.60+(.387*Ra^(1/6))/(1+(.559/Pr)^(9/16))^(8/27))^2

    hcoef=k*Nu/D

    {convective and radiation heat losses to the ambient}

    qamb=hcoef*Pi*D*(Ts-To)+0.9*Pi*D*(5.67*10^(-8))*((Ts+273)^4-(To+273)^4)

    {headloss through the pipe due to frictional effects}

    headloss:=(8*L*ffact*mdot1^2)/(g*rho1a[i-1]^2*Pi^2*D^5)

    {Pressure change through a segment of pipe due to frictional headloss}

    P1a[i]:=P1a[i-1]+(rho1a[i-1]*g*headloss/1000)

    {Change in Enthalpy relative to change in pressure and thermal losses}

    H1a[i]:=H1a[i-1]-((P1a[i-1]-P1a[i])/rho1a[i-1])+L*qamb/(mdot1*1000)

    T1a[i]:=Temperature(R744,H=H1a[i],P=P1a[i])

```

$\rho_{1a}[i] := \text{Density}(\text{R744}, \text{H}=\text{H1a}[i], \text{P}=\text{P1a}[i])$

$S_{1a}[i] := \text{Entropy}(\text{R744}, \text{H}=\text{H1a}[i], \text{P}=\text{P1a}[i])$

$V_{1a}[i] := \dot{m} / (\rho_{1a}[i] * \text{Pi} * (\text{D}/2)^2)$

UNTIL(i=2)

END

{L = length of pipe segment {m}}

L=10.0

{ffact = friction factor in pipe}

ffact=0.014

{D = diameter of injection pipe {m}}

D=0.254

{Driser = diameter of production pipe {m}}

Driser=0.20

{g = gravitational constant {kg/s²}

g=9.8

{T9 sets condensing temperature (C) of the condenser in the ORC loop}

T9=T1

{P3 sets the reservoir pressure (kPa)}

P3=25000

{T3 sets the reservoir temperature (C)}

T3=100

{Turbeff sets turbine isentropic efficiency}

Turbeff=0.85

{expeff sets the expansion turbine efficiency}

expeff=0.85

{Pumpeff sets the pump efficiency}

Pumpeff=0.90

{mass flowrates for the CO2 loop and the ORC loop, mdot1 is the mass flowrate in the CO2 loop, mdot2 is the mass flowrate in the ORC loop}

mdot2=Qboiler/(H7-H6b)

mdot1=70

{Heat Exchanger Effectiveness}

e=0.8

{Boiler NTU}

NTU=-ln(1-e)

\$REFERENCE R744 ASH

\$REFERENCE ISOBUTANE ASH

{state 9: saturated liquid isobutane leaving condenser}

P9=Pressure(ISOBUTANE,x=0,T=T9)

S9=Entropy(ISOBUTANE,x=0,T=T9)

H9=Enthalpy(ISOBUTANE,x=0,T=T9)

Den9=Density(ISOBUTANE,x=0,T=T9)

ef9=H9-Ho_rfg-(To+273)*(S9-So_rfg) {flow exergy value of the Isobutane exiting the condenser}

{state 6s: isobutane leaving ideal pump}

S6s=S9

H6s=Enthalpy(ISOBUTANE,P=P6,S=S6s)

{state 6: isobutane entering preheater}

P6=P6b

H6=H9-(H9-H6s)*Pumpeff

T6=Temperature(ISOBUTANE,H=H6,P=P6)

Den6=Density(ISOBUTANE,H=H6,P=P6)

S6=Entropy(ISOBUTANE,P=P6,H=H6)

Cp6=(H6b-H6)/(T6b-T6)

ef6=H6-Ho_rfg-(To+273)*(S6-So_rfg) {flow exergy value of the Isobutane entering the heat exchanger}

{state 6b: saturated isobutane entering boiler}

T6b=Tsixb {Boiling temperature of isobutane}

P6b=Pressure(ISOBUTANE,T=T6b,x=0.0)

H6b=Enthalpy(ISOBUTANE,P=P6b,x=0.0)

S6b=Entropy(ISOBUTANE,P=P6b,x=0.0)

{state 7: saturated isobutane exiting heat exchanger}

H7=Enthalpy(ISOBUTANE,T=T7,x=1.0)

P7=P6b

T7=T6b

S7=Entropy(ISOBUTANE,T=T7,x=1.0)

ef7=H7-Ho_rfg-(To+273)*(S7-So_rfg) {flow exergy value of the Isobutane exiting the heat exchanger/entering the turbine}

{state 8s: isobutane leaving isentropic turbine}

P8=P9

S8s=S7

H8s=Enthalpy(ISOBUTANE,S=S8s,P=P8)

{state 8: isobutane leaving real turbine/entering the condenser}

H8=H7-(H7-H8s)*Turbeff

T8=Temperature(ISOBUTANE,H=H8,P=P8)

Den8=Density(ISOBUTANE,P=P8,H=H8)

S8=Entropy(ISOBUTANE,P=P8,H=H8)

Cp8=Cp(ISOBUTANE,P=P8,x=0.0)

ef8=H8-Ho_rfg-(To+273)*(S8-So_rfg) {flow exergy value of the Isobutane leaving the turbine/entering the condenser}

{state 3: superheated CO2 entering bottom of riser pipe}

S3=Entropy(R744,P=P3,T=T3)

H3=Enthalpy(R744,P=P3,T=T3)

Den3=Density(R744,P=P3,T=T3)

V3=mdot1/(Den3*Pi*(D/2)^2)

ef3=H3-Ho-(To+273)*(S3-So) {flow exergy value of the CO2 entering the riserpipe}

{state 4: superheated CO2 exiting riser pipe}

CALL

Riserpipe(L,ffact,Driser,g,mdot1,P3,Den3,H3,T3,S3,V3:P4[1..250],rho4[1..250],H4[1..250],T4[1..250],S4[1..250],V4[1..250])

S4=S4[250]

P4=P4[250]

T4=T4[250]

H4=H4[250]

Den4=rho4[250]

V4=V4[250]

Ts4=Ts surf {initial surface temperature of supply line}

delt_ins=deltins {change in surface temperature along a segment of piping}

ef4=H4-Ho-(To+273)*(S4-So) {flow exergy value of the CO2 exiting the riserpipe}

{state 4a: superheated CO2 entering boiler}

CALL

supplyline(L,ffact,Driser,delt_ins,g,mdot1,Pa,To,P4,Den4,H4,T4,S4,V4,Ts4:P4a[1..69],rho4a[1..69],H4a[1..69],T4a[1..69],S4a[1..69],V4a[1..69],qamb4a[1..69],qins4a[1..69],Ts4_insa[1..69])

S4a=S4a[69]

P4a=P4a[69]

T4a=T4a[69]

H4a=H4a[69]

Den4a=rho4a[69]

V4a=V4a[69]

Ts4_insa=Ts4_insa[69]

qamb4a=qamb4a[69]

qins4a=qins4a[69]

Tts[4]=T4a

Sts[4]=S4a

ef4a=H4a-Ho-(To+273)*(S4a-So) {flow exergy value of the CO2 entering the heat exchanger}

{state 4b: superheated CO2 entering preheater}

T4b=T4a-e*(T4a-T6b)

P4b=P4a

H4b=Enthalpy(R744,T=T4b,P=P4b)

S4b=Entropy(R744,T=T4b,P=P4b)

Cp4b=(H4b-H5)/(T4b-T5)

{state 5: CO2 leaving the HX}

H5=H4b-Qprehtr/mdot1

P5=P4b

T5=Temperature(R744,P=P5,H=H5)

S5=Entropy(R744,P=P5,H=H5)

Den5=Density(R744,P=P5,H=H5)

ef5=H5-Ho-(To+273)*(S5-So) {flow exergy value of the CO2 exiting the heat exchanger}

{state 5p: CO2 leaving the expansion turbine} {For use in place of an expansion valve if additional energy production is desired}

{S5exp=S5

T5exp=T1

H5exp=Enthalpy(R744,T=T5exp,S=S5exp)

P5exp=Pressure(R744,T=T5exp,H=H5exp)

Den5exp=Density(R744,H=H5exp,P=P5exp)

Tts[6]=T5exp

Sts[6]=S5exp

ef5exp=H5exp-Ho-(To+273)*(S5exp-So) {flow exergy value of the CO2 exiting the expansion turbine}

{State5p: CO2 leaving expansion valve}

H5exp=H5

P5exp=P1a

T5exp=Temperature(R744,P=P5exp,H=H5exp)

S5exp=Entropy(R744,T=T5exp,H=H5exp)

Den5exp=Density(R744,T=T5exp,H=H5exp)

ef5exp=H5exp-Ho-(To+273)*(S5exp-So) {flow exergy value of the CO2 exiting the expansion valve/entering the condenser}

{state1a: saturated liquid CO2 leaving condenser}

CALL

returnline(L,ffact,D,g,mdot1,Pa,P1,Den1,H1,To,T1,S1,V1:P1a[1..2],rho1a[1..2],H1a[1..2],T1a[1..2],S1a[1..2],V1a[1..2])

S1a=S1a[2]

$$P1a=P1a[2]$$

$$T1a=T1a[2]$$

$$H1a=H1a[2]$$

$$\text{Den1a}=\text{rho1a}[2]$$

$$V1a=V1a[2]$$

$$ef1a=H1a-Ho-(To+273)*(S1a-So) \text{ \{flow exergy value of the CO2 exiting the condenser\}}$$

{state 1: saturated liquid CO2 entering injection pipe}

$$T1=To+\text{DelT} \text{ \{DelT is the change in temperature between the CO2 and the ambient\}}$$

$$P1=\text{Pressure}(\text{R744},T=T1,x=0)$$

$$H1=\text{Enthalpy}(\text{R744},T=T1,x=0)$$

$$S1=\text{Entropy}(\text{R744},T=T1,x=0)$$

$$\text{Den1}=\text{Density}(\text{R744},T=T1,x=0)$$

$$V1=\text{mdot1}/(\text{Den1}*\text{Pi}*(D/2)^2)$$

$$ef1=H1-Ho-(To+273)*(S1-So) \text{ \{flow exergy value of the CO2 entering the injection pipe\}}$$

{state 2: CO2 at bottom of injection pipe}

CALL

$$\text{Injectionpipe}(L,\text{ffact},D,g,\text{mdot1},P1,\text{Den1},H1,T1,S1,V1:\text{P}[1..250],\text{rho}[1..250],\text{H}[1..250],\text{T}[1..250],\text{S}[1..250],\text{V}[1..250])$$

$$S2=S[250]$$

$$P2=P[250]$$

$$T2=T[250]$$

$$H2=H[250]$$

$$\text{Den2}=\text{rho}[250]$$

$$ef2=H2-Ho-(To+273)*(S2-So) \text{ \{flow exergy value of the CO2 exiting the injection pipe/entering the reservoir\}}$$

{T-s Diagram closing points}

$$\{Tts[7]=T1$$

$$Sts[7]=S1$$

$$Tts2[5]=T9$$

$$Sts2[5]=S9\}$$

{Boiler Calculations}

$$Qboiler=e*\dot{m}1*Cp_co2*(T4a-T6b)$$

$$Qbcheck=\dot{m}1*(H4a-H4b)$$

$$Qbcheck2=\dot{m}2*(H7-H6b)$$

$$Cp_co2=(H4a-H4b)/(T4a-T4b)$$

$$UA_boiler=\dot{m}1*Cp_co2*NTU$$

$$LMTD_boiler=((T4a-T7)-(T4b-T6b))/LN((T4a-T7)/(T4b-T6b))$$

{Preheater Calculations}

$$e_prehtr=0.8$$

$$Qprehtr=\dot{m}2*(H6b-H6)$$

$$F=((e_prehtr*Cr-1)/(e_prehtr-1))\^{(1/2)}$$

$$el=(F-1)/(F-Cr)$$

$$E_cap=(2/el-(1+Cr))/(1+Cr^2)\^{(1/2)}$$

$$NTU_prehtr=-((1+Cr^2)\^{-1/2})*LN((E_cap-1)/(E_cap+1)) \text{ {for a shell and tube heat exchanger}}$$

$$\{NTU_prehtr=(1/(Cr-1))*LN((e_prehtr-1)/(e_prehtr*Cr-1))\} \text{ {for a counterflow heat exchanger}}$$

$$UA_prehtr=Cc*NTU_prehtr$$

{heat capacity rates}

$$Ch=\dot{m}1*Cp4b$$

$$Cc=\dot{m}2*Cp6$$

$$Cr=Cc/Ch$$

{exergy reference states at ambient conditions}

$$P_a=101.3$$

$T_o=T_{amb}$ {monthly average ambient temperature}

$$H_o=\text{Enthalpy}(R744, T=T_o, P=P_a)$$

$$S_o=\text{Entropy}(R744, T=T_o, P=P_a)$$

$$H_{o_rfg}=\text{Enthalpy}(\text{ISOBUTANE}, T=T_o, P=P_a)$$

$$S_{o_rfg}=\text{Entropy}(\text{ISOBUTANE}, T=T_o, P=P_a)$$

{exergy destruction of some key components of the Binary ORC System}

$$E_{d_turb}=\dot{m}_2(e_{f7}-e_{f8})-W_{turb}$$

$$I_{d_co2}=\dot{m}_1(e_{f4a}-e_{f5})$$

$$I_{d_refhx}=\dot{m}_2(e_{f7}-e_{f6})$$

$$E_{d_hx}=I_{d_co2}-I_{d_refhx}$$

$$E_{d_exp}=\dot{m}_1(e_{f5}-e_{f5exp})$$

$$E_{d_pump}=\dot{m}_2(e_{f6}-e_{f9})-W_{pump}$$

$$E_{d_supply}=\dot{m}_1(e_{f4}-e_{f4a})$$

$$E_{d_return}=\dot{m}_1(e_{f1a}-e_{f1})$$

$$E_{d_total}=E_{d_turb}+E_{d_hx}+E_{d_exp}+E_{d_pump}+E_{d_supply}+E_{d_return}$$

{ Q_{in} = Heat into the system through reservoir (kW)}

$$Q_{in}=\dot{m}_1(H_3-H_2)$$

{ W_{exp} = power required to run the expander}

$$W_{exp}=\frac{e_{f5}-e_{f5exp}}{\eta_{exp}}\dot{m}_1(H_5-H_{5exp})$$

{ W_{pump} = power required to run the pump}

$$W_{pump}=\dot{m}_2(H_6-H_9)$$

{ W_{turb} = power output from Turbine}

$$W_{turb}=\dot{m}_2(H_7-H_8)$$

{ W_{net} = Net Work}

$$W_{net} = W_{turb} - W_{pump}$$

{Efficiency = Total system efficiency}

$$\text{Efficiency} = (W_{turb} - W_{pump} + W_{exp}) / Q_{in}$$

{Qout = Heat out of the ORC}

$$Q_{out} = \dot{m} (H_8 - H_9)$$